

**The development of a novel therapeutic strategy for the
treatment of prostate cancer by targeting metabolic
signalling**

Amna Allafi

**A thesis submitted for the degree of Doctor of Philosophy in
Molecular Medicine**

School of Biological Sciences

University of Essex

Date of submission April 2018

Statement of Originality

I clarify that the content of this thesis is the result of my own work. All sources and previously published material used are acknowledged accordingly in the text. I further confirm that this work has not been previously used for the award of any degree.

Amna Allafi
2018

Abstract

Prostate cancer is one of the most prevalent cancers worldwide. The early stages of prostate cancer (PCa) are highly dependent on the androgen receptor (AR) pathway and hence therapies target this signalling axis. This approach is successful initially but invariably fails and the tumours progress to castration resistant prostate cancer (CRPC), for which few therapeutic options exist. Therefore, there is a great need to identify and characterize novel therapeutic targets for this stage of the disease.

Cancer cells undergo alterations that allow them to survive and proliferate, and metabolic reprogramming is one of the most important manifestations in cancer progression. Therefore, targeting tumour metabolism is an attractive approach to treat cancer. Screening for novel metabolic targets was performed using an siRNA library. 26 metabolic factors were identified to affect proliferation and/or migration, and these were found to be involved in essential pathways including lipogenesis, heme-biosynthesis, redox homeostasis, and glycolysis. The lead targets were validated in a range of cell lines and additional assays performed to investigate the effect upon cell cycle and cell death.

UROS, the fourth step of heme synthesis, was further investigated and depletion of this enzyme significantly inhibited prostate cancer proliferation and migration, promoted cell cycle arrest and induced cell death. Further, inhibition of heme synthesis using the inhibitor succinylacetone was found to significantly induce caspase-independent cell death and to sensitise cells to ROS. Importantly, the inhibitory activity of succinylacetone in combination with ROS showed specificity for cancer cell lines. Targeting heme synthesis therefore represents a novel targeted treatment option for prostate cancer and further work is needed to develop this into a therapeutic strategy.

Acknowledgements

First of all, I would like to thank my husband, Hisain Abdalla, for his continued support, generosity, and all help he offered me throughout my PhD from the start to this point. I also hold in my heart loads of appreciation to my beloved parents, my sisters, and my brother for their encouragement, inspiration, and emotional and personal support at all critical times of my life. I especially thank my angels, Fatima, Zain, and Alia, their smiles always pushed me a step ahead for being better.

Next, I would like to thank my PhD supervisors, Dr Greg Brooke and Dr Philippe Laissue, for all their guidance and support in every way throughout my course. I am again grateful to Dr Greg Brooke for his patience and the continued high level of supervision he offered in all aspects of this work. I also thank Dr Ralf Zwacka for his help, guidance, and contributions as an advisor. I would like next to thank the other members of the Molecular Oncology Lab that I worked with, Dr Rosie Bryan, Mila Pavlova, Mohammad Alkheilewi, Dr Svetlana Gretton, Angela Pine, Ana Mary Isac, and Eleanor Rees, for their help and personal support throughout my study. I thank my previous colleague Rana Alghamti for her help and support at the beginning of my PhD journey. I am also grateful to the graduate administrator Emma Revill for all support and guidance throughout my course. I would like next to give a special mention to Dr Andrea Mohr for her valuable advices and technical support she offered throughout my PhD. Finally, I would like to acknowledge the Libyan embassy for their financial contribution and the scholarship they awarded me to carry out this work, and I am grateful to my academic advisor Hosam Ounalla for all the advices and instructions he offered.

Amna Allafi
2018

Abbreviations

γ -GCS: Gamma-Glutamylcysteine Synthetase

1°: Primary Antibody

2D: Two-Dimensional

2°: Secondary Antibody

A: Absorbance

ABLM: Activated Bleomycin

ACACA: Acetyl-CoA Carboxylase Alpha (α)

Acetyl-CoA: Acetyl-Coenzyme A

ACLY: ATP Citrate Lyase

ACSL1: Acyl-CoA Synthetases 1

ACSL3: Acyl-CoA Synthetases 3

ACSL5: Acyl-CoA Synthetases 5

ACSM1: Acyl-CoA Synthetase Medium Chain family member1

AD: Androstenedione

ADT: Androgen Deprivation Therapies

AIF: Apoptosis-Inducing Factor

Akt: Alpha Serine-Threonine Kinase

ALA: 5-Aminolevulinic Acid

ALAD: δ - Aminolevulinic Acid Dehydratase

ALDOA: Aldolase A, fructose-bisphosphate A

AMACR: α -Methylacyl-CoA Racemase

AMPK: 5' Adenosine Monophosphate-activated protein Kinase

AP-1: Activator Protein-1

APCs: Antigen-Presenting Cells

APS: Ammonium Persulfate

AR-Vs: AR Splice Variants

AR: Androgen Receptor

AREs: Androgen Receptor Elements

AS: Active Surveillance

ASCO: The American Society of Clinical Oncology

ASCT2: Alanine, Serine, Cysteine-preferring Transporter 2

ASS: Argininosuccinate Synthetase

B-Me: Beta-Mercaptoethanol

BCL2: B-Cell CLL/Lymphoma 2

BLM: Bleomycin Sulfate

BMI: Body Mass Index

BPH: Benign Prostatic Hyperplasia

BRCA2: Breast Cancer 2, Early Onset

BSA: Bovine Serum Albumin

CEP: Congenital Erythropoietic Porphyria

cIAP1: Cellular Inhibitor of Apoptosis 1

CLYD: Clyndromatosis

CO₂: Carbon Dioxide

CPA: Cyproterone Acetate

CRPC: Castration Resistant Prostate Cancer

CRUK: Cancer Research UK

CV: Crystal Violet

CYP17: Cytochrome P450 17 alpha-hydroxylase

DC: Detergent Compatible

DCA: Dichloroacetate

DHEA: Dehydroepiandrosterone

DHT: Dihydrotestosterone

DISC: Death-Inducing Signalling Complex

DMSO Dimethyl Sulfoxide

DNA: Deoxyribonucleic Acid

DOC: Docetaxel

dsRNAs: Double-stranded RNAs

ED: Erectile Dysfunction

EDTA: Ethylenediaminetetraacetic Acid

EMT: Epithelial-Mesenchymal Transition

ERK: Extracellular signal-Regulated Kinase

ERM: Ezrin/Radixin/Moesin

ETS: E26 Transformation-Specific

FADD: Fas -Associated Death Domain

FASN: Fatty Acid Synthase

FasR: First Apoptosis Signal Receptor

FBS: Fetal Bovine Serum,

FDA: Food and Drug Administration

FDPS: Farnesyl Diphosphate Synthase

FECH: Ferrochelatase

FKBP11: FK506 binding protein 11

FKBP9L: FK506 Binding Protein 9 pseudogene 1

FLIP: FLICE Inhibitory Protein

FSH: Follicle Stimulating Hormone

GCAT: Glycine C-acetyltransferase (2-amino-3-ketobutyrate coenzyme A ligase)

GCLC: Glutamate-Cysteine Ligase Catalytic subunit, gamma-Glutamylcysteine Synthetase

GEO: Gene Expression Omnibus

GFP: Green Fluorescent Protein

GnRH: Gonadotropin Releasing Hormone

GPX4: Glutathione Peroxidase

GSPT1: Glutathione-S-transferase P1

H&M: Haematoxylin-Eosin

H₂O₂: Hydrogen Peroxide

HA: Hyaluronan

HAS3: Hyaluronan Synthase 3

HDRB: High Dose-Rate Brachytherapy

HFD: High-Fat Diet

HGF: Hepatocyte Growth Factor Receptor

HIF-1: Hypoxia-Inducible Factor-1

HK: Hexokinases

HMGC2S: 3-Hydroxy-3-Methylglutaryl-CoA Synthase 2

HNE: 4-Hydroxy-2-Nonenal

HSP: Heat Shock Protein

HUVECs: Human Umbilical Vein Endothelial Cells

IAP: Inhibitor of Apoptosis

IPTG: Isopropyl-B-D-Thiogalactoside

ISUP: International Society of Urological Pathology

KLF6: Kruppel-Like zinc Finger transcription factor 6

KLKs: Kallikriens

LARS2: Leucyl-tRNA Synthetase 2

LATs: L-type Amino acids Transporters

LDRB: Low Dose-Rate Brachytherapy

LFD: Low-Fat Diet

LH: Luteinizing Hormon

LHRH: Luteinizing Hormone Releasing Hormone

LL: Lymphoblastic Leukaemia

LLGL2: Scribble Cell Polarity Complex component

LUTS: Lower Urinary Track Symptoms

MAB: Maximum Androgens Blocked

Malonyl-CoA: Malonyl-Coenzyme A

MARS: Methionyl-tRNA Synthetase

mCRPC: Metastatic Castration Resistant Prostate Cancer

MDA: Malondialdehyde

MDSCs: Myeloid-Derived Suppressor Cells

MeOH: Methanol

Met: Methionine

MGC26963: Sphingomyelin Synthase 2

MMP: Mitochondrial Membrane Potential

MMP9: Matrix Metalloproteinase-9

MPT: Mitochondrial Permeability Transition

mTOR: Mammalian Target Of Rapamycin

N.A: Numerical Aperture

NaCl: Sodium Chloride

NCBI: National Centre for Biotechnology Information

NF- κ B: Nuclear Factor- κ B

NOS3: Nitric Oxide Synthase 3

NPC: Nasopharyngeal Carcinoma

NRF2: Nuclear Factor Erythroid 2-Related Factor 2

NSAAs: Non-Steroidal Anti-Androgens

NSCLC: Non-Small Cell Lung Cancer

NSF: N-Ethylmaleimide-Sensitive Factor

ODX: Osteodex

ONOO⁻: Oxidant Peroxynitrite

OS: Overall Survival

OTOP: Otopetrin 3

PAF: Platelet Activating Factor

PAFAH2: Platelet Activating Factor Acetyl-Hydrolase 2

PAP: Prostatic Acid Phosphatase

PARP: Poly-Adenosine Diphosphate-Ribose Polymerase

PBG: Porphobilinogen

PBGD: Porphobilinogen Deaminase

PBGS: Porphobilinogen Synthase

PBS: Phosphate-Buffered Saline

PCa: Prostate Cancer

PCR: Polymerase Chain Reaction

PDK: Pyruvate Dehydrogenase Kinase

PDT: Photodynamic Therapy

PFA: Paraformaldehyde

PFK: Phosphofructokinase

PFS: Progression-free Survival

PI: Propodeum Iodide

PI3K: Phosphoinositide 3-Kinase

PIA: Proliferative Inflammatory Atrophy

PIN: Premalignant Prostatic Intraepithelial Neoplasia

PKC β : Protein Kinase C beta

PLK1: Polo-Like Kinase 1

PMSF: Phenylmethanesulphonyl Fluoride

PSA: Prostate Specific Antigen

PSG: Penicillin-Streptomycin-Glutamine

PTEN: Phosphate and Tensin homologue

qPCR: Quantitative PCR

R223: Radium-223 Dichloride

RCD: Regulated Cell Death

RIP1: Receptor Interacting Protein-1

RIPA: Radioimmunoprecipitation Assay Buffer

RISC: RNA-Induced Silencing Complex

RNA: Ribonucleic Acid

RNAi: RNA Interference

ROS: Reactive Oxygen Species

RP: Radical Prostatectomy

RPMI: Roswell Park Memorial Institute

RT: Radiation Therapy

SA: Succinylacetone

SDS: Sodium Dodecyl Sulphate

SEER: Surveillance, Epidemiology and End Results

SFCS: Charcoal Stripped Foetal Calf Serum

SHBG: Steroid Hormone Binding Globulin

siRNA Small Interfering RNA

SLC27A1: Solute Carrier family 27 member 1

SLC27A5: Solute Carrier family 27 member 5

SMAC/Diablo: Second Mitochondria-derived Activator of Caspases/Direct

SNAP: NSF Attachment Proteins

SNAREs: NSF Attachment Protein Receptors

SREBPs: Sterol Response Element-Binding Proteins

STX1A: Syntaxin 1A

T: Testosterone

TCA: Tricarboxylic Acid Cycle

TCR: T-Cells Receptor

TE: Thioesterase

TEMED: Tetramethylethylenediamine

TNF: Tumour Necrosis Factor

TNF- α : Tumour Necrotic Factor - α

TNFR: Tumour Necrotic Factor Receptors

TRADD: TNFR-Associated Death Domain

TRAF2: TNFR-Associated Factor 2

TRAIL: TNF-Related Apoptosis Inducing Ligand

Tregs: Regulatory T Cells

tRNA: Transfer RNA

TXNDC13: TMX4, thioredoxin related transmembrane protein 4

TYMS: Thymidylate Synthetase

UGS: Urogenital Sinus

UROGEN: Uroporphyrinogen III

UROS: Uroporphyrinogen III synthase

VEGF: Vascular Endothelial Growth Factor

WHO: World Health Organization

WW: Watchful Waiting

X-gal: 5-Bromo-4-Chloro-3-Indolyl β -D-Galactopyranoside

1 Table of Contents

STATEMENT OF ORIGINALITY	2
ABSTRACT.....	3
ACKNOWLEDGEMENTS.....	4
ABBREVIATIONS	5
LIST OF FIGURES	17
LIST OF TABLES	19
1 CHAPTER 1 INTRODUCTION	20
1.1 PROSTATE GLAND DEVELOPMENT AND STRUCTURE	20
1.2 FUNCTIONS AND DISEASES OF THE PROSTATE.....	26
1.3 PROSTATE CANCER.....	27
1.3.1 <i>Aetiology and molecular biology of the disease</i>	28
1.3.2 <i>Epidemiology</i>	32
1.3.3 <i>Risk Factors</i>	35
1.3.4 <i>Symptoms and diagnosis/detection of prostate cancer</i>	37
1.3.5 <i>Histology and grading</i>	41
1.4 PROSTATE CANCER TREATMENTS.....	45
1.4.1 <i>Current therapies</i>	45
1.5 HORMONE THERAPY FAILURE AND PROGRESSION TO CRPC	55
1.5.1 <i>Molecular pathways that could be essential for prostate cancer progression</i>	57
1.5.2 <i>Chemotherapies</i>	58
1.6 NOVEL AND TARGETED THERAPIES	63
1.6.1 <i>Androgen-targeted new therapies</i>	64
1.6.2 <i>Cytotoxic and pathway-based agents</i>	66
1.7 METABOLISM OF CANCER AS A THERAPEUTIC WINDOW	73
1.7.1 <i>Metabolism in normal and tumour cells</i>	74
1.7.2 <i>Metabolic pathways as novel therapeutic targets</i>	77
1.7.3 <i>The potential side-effects of metabolism inhibition</i>	79
1.7.4 <i>Metabolism of normal prostate</i>	81
1.7.5 <i>Metabolic alterations in prostate cancer</i>	84
1.7.6 <i>Targeting novel metabolic reprogramming in CRPC</i>	86
1.8 INDUCTION OF TUMOUR CELL DEATH.....	87
1.8.1 <i>Defective apoptosis and cancer</i>	88
1.8.2 <i>Non-apoptotic cell death pathways</i>	91
1.9 NOVEL DRUG TARGETS IDENTIFICATION	94
1.9.1 <i>Drug target screening using RNA interference</i>	95
1.9.2 <i>Targets characterization/validation</i>	97
1.10 AIMS OF THE PROJECT	98
2 CHAPTER 2: MATERIAL AND METHODS	100
2.1 siRNAs, REAGENTS AND BUFFERS	100
2.1.1 <i>Reagents and kits</i>	100
2.1.2 <i>Solutions and buffers</i>	103
2.2 CELL CULTURE	106
2.2.1 <i>Passaging cells</i>	106
2.2.2 <i>Cell counting and plating</i>	106
AN ANDROGEN-INDEPENDENT CELL LINE MODEL THAT WAS ESTABLISHED FROM A HUMAN PCA METASTATIC TO THE BONE.	107
2.2.3 <i>Defrosting/freezing cells</i>	108
2.3 TRANSFECTION BY siRNAs	108
2.3.1 <i>Proliferation assay for siRNA screening</i>	110
2.3.2 <i>Migration assay for siRNA screening</i>	110

2.3.3	<i>Statistical analysis</i>	113
2.3.4	<i>Wound healing assays after siRNA knockdowns</i>	114
2.4	HEME DEPLETION AND HEME-SYNTHESIS INHIBITION	118
2.4.1	<i>Heme-depleted media preparation</i>	118
2.4.2	<i>Succinylacetone dose-treatments for proliferation assays</i>	118
2.4.3	<i>Succinylacetone dose treatment for cells migration assays</i>	119
2.5	COMBINATIONS OF HEME BIOSYNTHESIS INHIBITION WITH CHEMOTHERAPEUTICS AND ROS ENHANCING AGENTS	119
2.5.1	<i>Treatments of cells with succinylacetone and docetaxel</i>	120
2.5.2	<i>Treatments of cells with succinylacetone and bleomycin sulfate (BLM) doses</i>	120
2.5.3	<i>Treatments of cells with succinylacetone and hydrogen peroxide doses</i>	120
2.6	FLOW CYTOMETRIC ASSAYS.....	121
2.6.1	<i>Treatments</i>	121
2.6.2	<i>Flow Cytometric Measurement of Apoptotic and Necrotic Cells</i>	121
2.6.3	<i>Flow cytometric analysis of cell cycle</i>	122
2.6.4	<i>Flow cytometric analysis of mitochondrial membrane potential</i>	122
2.7	MEASUREMENT OF CELLULAR HEME CONTENT	123
2.8	REAL-TIME QUANTITATIVE PCR	123
2.8.1	<i>Cells preparations</i>	124
2.8.2	<i>RNA extraction</i>	124
2.8.3	<i>DNase treatment of RNAs and cDNA synthesis</i>	125
2.8.4	<i>Real time QPCR</i>	125
2.9	PROTEIN IMMUNOBLOTTING.....	125
2.9.1	<i>Preparing cell lysate and protein quantification</i>	127
2.9.2	<i>SDS polyacrylamide gel electrophoresis</i>	127
2.9.3	<i>Immunoblotting</i>	128
2.10	CLONING DNA SITES OF LEAD TARGETS	128
2.10.1	<i>PCR amplification and gel extraction DNA sites</i>	130
2.10.2	<i>Ligation into pGEM T-easy vector and transformation</i>	130
2.10.3	<i>Plasmid DNA extraction and sequencing</i>	133
2.10.4	<i>Re-cloning into pEGFP-c1 vector</i>	133
2.10.5	<i>DNA transient transfection of UROS and ALDOA containing pEGFP-C1 vectors into PC3 cells</i>	135
2.11	CELL FIXATION AND IMMUNOFLUORESCENT PROBING	136
2.11.1	<i>Laser scanning confocal microscopy for proteins localization</i>	136
3	CHAPTER 3 RESULTS I.....	138
3	SCREENING FOR NOVEL THERAPEUTIC TARGETS THAT REGULATE PROSTATE CANCER PROLIFERATION AND MIGRATION	138
3.1	IDENTIFICATION OF METABOLIC FACTORS AFFECTING PCA CELL PROLIFERATION	139
3.1.1	<i>Screening for metabolic factors that regulate PC3 proliferation</i>	139
3.1.2	<i>Validation of lead targets implicated in PCa proliferation</i>	142
3.2	IDENTIFICATION OF METABOLIC FACTORS AFFECTING PCA MIGRATION	146
3.2.1	<i>Optimization of single cell tracking</i>	146
3.2.2	<i>The effect of Radixin knockdown on motility</i>	147
3.2.3	<i>Tracking analysis automation</i>	151
3.2.4	<i>Screening for the identification of metabolic targets regulating prostate cancer motility</i>	153
3.2.5	<i>Validating targets that significantly affect PCa cell migration</i>	159
3.3	BIOINFORMATICS ANALYSIS AND LEAD TARGETS	170
3.3.1	<i>Bioinformatics analysis of hit targets</i>	170
3.3.2	<i>Lead targets</i>	177
3.4	THE EFFECT OF siRNA DEPLETION OF THE LEAD TARGETS UPON APOPTOSIS AND CELL CYCLE	180
3.5	DISCUSSION	183
3.5.1	<i>Lipogenesis and prostate cancer progression</i>	184
3.5.2	<i>Heme-biosynthesis and prostate cancer progression</i>	190
3.5.3	<i>Glycolysis-related factors in prostate cancer</i>	195
3.5.4	<i>Amino acids and protein biosynthesis</i>	197
3.5.5	<i>Nucleic acids biosynthesis</i>	199

3.5.6	<i>Free-radicals and redox status regulators</i>	200
3.5.7	<i>Other identified metabolic factors/pathways</i>	202
3.5.8	<i>Summary</i>	205
4	CHAPTER 4 RESULTS II	208
4	FURTHER VALIDATIONS AND INVESTIGATION INTO UROS AND ALDOA	208
4.1	VALIDATION OF UROS AND ALDOA KNOCKDOWNS.....	210
4.2	INVESTIGATION OF UROS AND ALDOA BASAL LEVELS IN CANCEROUS AND NONCANCEROUS CELLS.....	212
4.3	UROS AND ALDOA LOCALISATION IN PC3 CELLS.....	216
4.4	VALIDATION OF UROS AND ALDOA IMPLICATION IN PC3 MIGRATION BY WOUND HEALING ASSAYS.....	219
4.4.1	<i>Knockdown of Radixin reduces PC3 population cell motility</i>	219
4.4.2	<i>Investigation of the effect of UROS and ALDOA knockdown upon PC3 migration</i>	221
4.5	DISCUSSION.....	223
4.5.1	<i>The effect of UROS depletion upon prostate cancer</i>	223
4.5.2	<i>Investigations of ALDOA in prostate cancer</i>	224
4.5.3	<i>Summary</i>	226
5	CHAPTER 5 RESULTS III	227
5	HEME-BIOSYNTHESIS INHIBITION: A THERAPEUTIC APPROACH TO INHIBIT PROSTATE CANCER PROGRESSION	227
5.1	REDUCTION OF CELLULAR HEME CONTENT INHIBITS PROLIFERATION OF PCA CELLS.....	228
5.2	INHIBITION OF HEME SYNTHESIS REDUCES THE METASTATIC POTENTIAL OF PCA CELLS.....	233
5.3	INHIBITION OF HEME SYNTHESIS BLOCKS CELL CYCLE PROGRESSION AND ENHANCES NECROTIC AND APOPTOTIC CELL DEATH IN PCA CELLS.....	236
5.4	INHIBITION OF HEME SYNTHESIS SENSITIZES PROSTATE CANCER CELLS TO ROS DAMAGE AND ENHANCES NECROTIC CELL DEATH.....	239
5.4.1	<i>ROS potently inhibits prostate cancer proliferation following heme synthesis inhibition</i>	239
5.4.2	<i>Necrotic-like cell death of PCa cells following heme synthesis inhibition in combination with ROS</i> <i>242</i>	242
5.4.3	<i>Succinylacetone induces caspase-independent cell death</i>	246
5.4.4	<i>Bleomycin shows no additive effect in combination with heme synthesis inhibition</i>	250
5.4.5	<i>Docetaxel shows no additive effect in combination with heme synthesis inhibition</i>	251
5.5	DISCUSSION.....	254
5.5.1	<i>Heme biosynthesis inhibition impairs prostate cancer progression</i>	254
5.5.2	<i>Intracellular heme depletion induces necrotic-like cell death</i>	255
5.5.3	<i>H₂O₂ treatment of heme biosynthesis-inhibited prostate cancer cells further halted proliferation</i> <i>260</i>	260
5.5.4	<i>H₂O₂ enhances SA-induced caspase-independent cell death</i>	262
5.5.5	<i>Chemotherapeutic treatments did not enhance the efficacy of heme biosynthesis inhibition in prostate cancer cells</i>	263
5.5.6	<i>Summary</i>	264
6	CHAPTER 6 FINAL DISCUSSION	266
6.1	METABOLIC FEATURES OF PROSTATE CANCER IN RELATION TO SCREENING OUTCOMES.....	266
6.2	INHIBITION OF HEME BIOSYNTHESIS IN COMBINATION WITH ELEVATED OXIDATIVE STRESS AS A NOVEL APPROACH TO TREAT PROSTATE CANCER.....	271
6.3	FINAL CONCLUSION.....	276
6.4	FUTURE WORK.....	277
7	REFERENCES	280
8	APPENDIX	329

List of Figures

FIGURE 1.1 THE PROSTATE GLAND LOCATION IN THE MALE REPRODUCTIVE SYSTEM.....	21
FIGURE 1.2 THE ANATOMY OF PROSTATE GLAND.....	22
FIGURE 1.3 SCHEMATIC SHOWING THE DEVELOPMENT OF THE PROSTATE GLAND.....	23
FIGURE 1.4 CELL TYPES OF THE ADULT HUMAN PROSTATE.	25
FIGURE 1.5 THE ANDROGEN RECEPTOR SIGNALLING AXIS.....	29
FIGURE 1.6 THE UK INCIDENCE AND DEATHS RATES.....	33
FIGURE 1.7 USA INCIDENCE AND DEATHS RATES FROM 1975 TO 2014.....	34
FIGURE 1.8 BLACK VERSUS WHITE MALES' INCIDENCE AND MORTALITY RATES IN THE USA FROM 1975-2014.	36
FIGURE 1.9 DETECTION/STAGING OF PCA USING DIFFERENT IMAGING MODALITIES.....	40
FIGURE 1.10 THE GLEASON GRADING SYSTEM.....	44
FIGURE 1.11 ENDOCRINE CONTROL OF PROSTATIC GROWTH.....	51
FIGURE 1.12 METABOLISM OF NORMAL CELL VERSUS CANCER CELL.....	75
FIGURE 1.13 REGULATION AND MAINTENANCE OF SPECIFIC METABOLIC SIGNALLING IN NORMAL/BENIGN PROSTATIC CELLS.....	83
FIGURE 1.14 INTRINSIC AND EXTRINSIC APOPTOSIS PATHWAYS.....	89
FIGURE 1.15 THE SIGNALLING PATHWAYS OF CELL SURVIVAL, APOPTOSIS, AND NECROPTOSIS (INTERCONNECTION BETWEEN CELL DEATH PATHWAYS).....	93
FIGURE 1.16 THE MECHANISM OF siRNA GENE KNOCKDOWN IN MAMMALIAN CELLS.....	96
FIGURE 1.17 SCHEMATIC ILLUSTRATION TO SHOW THE AIM, METHODS USED AND GENERAL OUTCOMES OF THIS STUDY.....	99
FIGURE 2.1 ILLUSTRATION FOR THE PROCESSING STEPS APPLIED FOR CELL SEGMENTATION OF TIME-LAPSE SEQUENCES.....	112
FIGURE 2.2 THE MAIN METHOD OF PERFORMING SCRATCHES ON CELL MONOLAYERS.....	115
FIGURE 2.3 MENISCUS EFFECT ON IMAGING CELLS IN 96-WELL PLATE USING 2 X OBJECTIVES ON NIKON TI WIDEFIELD MICROSCOPE.....	115
FIGURE 2.4 SOBEL FILTER WAS USED TO FIND AND ENHANCE THE SCRATCH EDGES.....	117
FIGURE 2.5 MAP OF pGEM-T EASY VECTOR. TAKEN FROM: PROMEGA.CO.UK.....	132
FIGURE 2.6 PLASMID MAP OF pEGFP-C1 VECTOR (DESIGNED BY SNAPGENE SOFTWARE).....	134
FIGURE 3.1 AN siRNA SCREEN TO EVALUATE THE IMPACT OF DEPLETION OF METABOLIC AND CELL TRAFFIC FACTORS ON PC3 GROWTH.....	140
FIGURE 3.2 A HEAT MAP REPRESENTING THE FOLD CHANGE OF PC3 CELL PROLIFERATION WHEN TRANSFECTED AGAINST 40 METABOLIC RELATED FACTORS BY siRNA.....	141
FIGURE 3.3 VALIDATION GROWTH ASSAYS OF 14 HITS IN PROSTATE CANCER (PC) CELL LINES AND BPH1 CELLS.....	145
FIGURE 3.4 CONFIRMATION OF RADIXIN KNOCKDOWN AT THE RNA AND PROTEIN LEVELS.....	148
FIGURE 3.5 MEAN VELOCITY (MICRON/FRAME) OF CELLS FOLLOWING DEPLETION OF RADIXIN.....	149
FIGURE 3.6 QUANTIFICATION OF PC3-GFP MOTILITY USING A SEMI-AUTOMATED ALGORITHM (TRACKMATE).....	150
FIGURE 3.7 QUANTIFICATION OF PC3-GFP CELL SPEED USING BATCH MODE BASED PRE-PROCESSING MACROS AND AN AUTOMATED TRACKING ALGORITHM (ADAPT) VERSUS RESULTS OF THE SEMI-AUTOMATED METHOD.....	152
FIGURE 3.8 AN siRNA SCREEN TO IDENTIFY METABOLIC AND CELL TRAFFIC FACTORS THAT AFFECT CELL MOTILITY.....	154
FIGURE 3.9 HEAT MAP OF LEAD TARGETS AFFECTING PC3 CELL MIGRATION.....	155
FIGURE 3.10 QUANTIFICATION OF THE EFFECT OF ALDOA KNOCKDOWN UPON SINGLE CELL TRACKING IN GFP-PC3 CELLS.....	160
FIGURE 3.11 QUANTIFICATION OF THE EFFECT OF UROS KNOCKDOWN UPON SINGLE CELL TRACKING IN GFP-PC3 CELLS.....	161
FIGURE 3.12 QUANTIFICATION OF THE EFFECT OF FDPS KNOCKDOWN UPON SINGLE CELL TRACKING IN GFP-PC3 CELLS.....	162
FIGURE 3.13 QUANTIFICATION OF THE EFFECT OF FECH KNOCKDOWN UPON SINGLE CELL TRACKING IN GFP-PC3 CELLS.....	163
FIGURE 3.14 QUANTIFICATION OF THE EFFECT OF NOS3 KNOCKDOWN UPON SINGLE CELL TRACKING IN GFP-PC3 CELLS.....	164
FIGURE 3.15 QUANTIFICATION OF THE EFFECT OF FKBP11 KNOCKDOWN UPON SINGLE CELL TRACKING IN GFP-PC3 CELLS.....	165
FIGURE 3.16 QUANTIFICATION OF THE EFFECT OF MGC26963 KNOCKDOWN UPON SINGLE CELL TRACKING IN GFP-PC3 CELLS.....	166
FIGURE 3.17 QUANTIFICATION OF THE EFFECT OF LLGL2 KNOCKDOWN UPON SINGLE CELL TRACKING IN GFP-PC3 CELLS.....	167
FIGURE 3.18 QUANTIFICATION OF THE EFFECT OF TXNDC13 KNOCKDOWN UPON SINGLE CELL TRACKING IN GFP-PC3 CELLS.....	168
FIGURE 3.19 QUANTIFICATION OF THE EFFECT OF HMGCS2 KNOCKDOWN UPON SINGLE CELL TRACKING IN GFP-PC3 CELLS.....	169
FIGURE 3.20 GENE EXPRESSION ANALYSIS OF PROLIFERATION LEAD TARGETS USING GENE EXPRESSION OMNIBUS (GEO) DATABASE.....	171
FIGURE 3.21 GENE EXPRESSION ANALYSIS OF MIGRATION LEAD TARGETS USING GENE EXPRESSION OMNIBUS (GEO) DATABASE.....	172
FIGURE 3.22 HUMAN PROTEIN ATLAS BASED ANALYSIS OF PROTEIN EXPRESSION LEVELS OF PROLIFERATION HITS IN NORMAL PROSTATE VERSUS LOW- AND HIGH-GRADE PROSTATIC CANCER TISSUES.....	174
FIGURE 3.23 HUMAN PROTEIN ATLAS BASED ANALYSIS OF PROTEIN EXPRESSION LEVELS OF MIGRATION HITS IN NORMAL PROSTATE VERSUS LOW- AND HIGH-GRADE PROSTATIC CANCER TISSUES.....	176

FIGURE 3.24 INVESTIGATION OF THE EFFECTS OF siRNA DEPLETION OF THE LEAD TARGETS UPON CELL DEATH.	181
FIGURE 3.25 INVESTIGATION OF THE EFFECTS OF siRNA DEPLETION OF THE LEAD TARGETS UPON CELL CYCLE.	182
FIGURE 3.26 FATTY ACIDS <i>DE NOVO</i> BIOSYNTHESIS PATHWAY.	186
FIGURE 3.27 CHOLESTEROL BIOSYNTHESIS THROUGH THE MEVALONATE PATHWAY.	189
FIGURE 3.28 HEME-BIOSYNTHESIS PATHWAY IN MAMMALIAN CELLS.	191
FIGURE 3.29 THE EFFECT OF OTHER HEME-BIOSYNTHESIS GENES KNOCKDOWNS ON PC3 CELL PROLIFERATION AND MIGRATION.	194
FIGURE 3.30 THE ROLE OF ALDOA IN THE GLYCOLYSIS PATHWAY.	196
FIGURE 3.31 OVERALL KEY METABOLIC ALTERATIONS AND THEIR PARTICIPATION IN PROSTATE CANCER METABOLISM.	207
FIGURE 4.1 QPCR AND WESTERN BLOTTING TO CONFIRM UROS AND ALDOA KNOCKDOWNS.	211
FIGURE 4.2 TRANSCRIPT LEVELS OF UROS AND ALDOA IN PCA CELL LINES (PC3, LNCAP AND DU145) AND A NON-CANCEROUS CELL LINE BPH1.	213
FIGURE 4.3 UROS PROTEIN LEVELS IN PCA CELL LINES AND NON-TUMORIGENIC CONTROLS.	214
FIGURE 4.4 ALDOA PROTEIN LEVELS IN PCA CELL LINES AND NON-TUMORIGENIC CONTROLS.	215
FIGURE 4.5 CONFOCAL MICROSCOPE IMAGES TO SHOW ALDOA LOCALIZATION IN PC3.	217
FIGURE 4.6 CONFOCAL MICROSCOPE IMAGES TO SHOW UROS LOCALIZATION IN PC3.	218
FIGURE 4.7 INHIBITION OF PC3 CELL MIGRATION IN RESPONSE TO RADIXIN KNOCKDOWN.	220
FIGURE 4.8 INHIBITION OF PC3 CELL MIGRATION IN RESPONSE TO ALDOA AND UROS KNOCKDOWN.	222
FIGURE 5.1 TIME-COURSE TREATMENT OF PROSTATE CANCER CELL LINES WITH SUCCINYLACETONE (SA).	229
FIGURE 5.2 HEME CONTENT OF PC3 CELLS TREATED WITH SUCCINYLACETONE (SA).	231
FIGURE 5.3 HEME-DEPLETION AND SUCCINYLACETONE (SA) TREATMENTS UPON THE PROLIFERATION OF PROSTATE CANCER CELL LINES AND BPH1 CELLS.	232
FIGURE 5.4 SUCCINYLACETONE (SA) INHIBITION OF THE POPULATION MOTILITY OF PC3 CELLS.	234
FIGURE 5.5 EVALUATION OF THE EFFECT OF SUCCINYLACETONE (SA) ON SINGLE CELL MIGRATION OF PC3 CELLS.	235
FIGURE 5.6 FLOW CYTOMETRY ANALYSIS OF PC3 CELLS TREATED WITH SUCCINYLACETONE (SA).	237
FIGURE 5.7 CELL DEATH ANALYSIS BY FLOW CYTOMETRY OF SUCCINYLACETONE (SA) TREATED DU145 AND LNCAP CELLS.	238
FIGURE 5.8 INHIBITION OF PROSTATE CANCER CELL PROLIFERATION BY SUCCINYLACETONE (SA) IN COMBINATION WITH DOSE-TREATMENT OF HYDROGEN PEROXIDE (H ₂ O ₂).	240
FIGURE 5.9 INHIBITION OF PROSTATE CANCER CELL PROLIFERATION WITH A HIGH DOSE OF SUCCINYLACETONE (SA) IN COMBINATION WITH HYDROGEN PEROXIDE (H ₂ O ₂).	241
FIGURE 5.10 INDUCTION OF NECROTIC-LIKE CELL DEATH OF PROSTATE CANCER CELL LINES BY A SUB-LETHAL DOSE OF SUCCINYLACETONE (SA) IN COMBINATION WITH HYDROGEN PEROXIDE (H ₂ O ₂).	243
FIGURE 5.11 INDUCTION OF NECROTIC-LIKE CELL DEATH OF PROSTATE CANCER CELL LINES WITH A HIGH DOSE OF SUCCINYLACETONE (SA) IN COMBINATION WITH HYDROGEN PEROXIDE (H ₂ O ₂).	244
FIGURE 5.12 CELL CYCLE ANALYSIS OF PC3 CELLS TREATED WITH SUCCINYLACETONE (SA) AND HYDROGEN PEROXIDE (H ₂ O ₂).	245
FIGURE 5.13 SUCCINYLACETONE (SA) AND HYDROGEN PEROXIDE (H ₂ O ₂) PROMOTE CASPASE-INDEPENDENT CELL DEATH.	247
FIGURE 5.14 ANALYSIS OF MITOCHONDRIAL MEMBRANE DEPOLARIZATION (MMD) OF CELLS TREATED WITH SUCCINYLACETONE (SA) AND HYDROGEN PEROXIDE (H ₂ O ₂).	249
FIGURE 5.15 INDUCTION OF PC3 AND BPH1 CELL DEATH BY SUCCINYLACETONE (SA) AND BLEOMYCIN SULFATE (BLM) COMBINATION.	252
FIGURE 5.16 DOCETAXEL DOES NOT ENHANCE THE INHIBITORY ACTION OF SUCCINYLACETONE (SA).	253
FIGURE 5.17 THE FORMATION OF ROS SPECIES UPON Fe ⁺² AND HYDROGEN PEROXIDE (H ₂ O ₂) REACTION (FENTON REACTION).	257
FIGURE 5.18 THE PROPOSED ACCUMULATION OF IRON DUE TO SA INHIBITION OF HEME BIOSYNTHESIS LEADS TO ACCUMULATION OF LIPID-ROS AND CELL DEATH BY FERROPTOSIS.	259
FIGURE 6.1 THE ALTERATIONS OF CITRATE METABOLISM IN PROSTATE CANCER CELLS.	267
FIGURE 6.2 SCHEMATIC REPRESENTATION OF THE NECROSIS/NECROPTOSIS FEED-FORWARD MECHANISM.	273
FIGURE 6.3 RATIONALE FOR THE COMBINATION OF HEME SYNTHESIS INHIBITION WITH IMMUNE CHECKPOINT INHIBITION.	275
FIGURE 6.4 INHIBITION OF PC3 CELL MIGRATION IN RESPONSE TO LARS2, FDPS, AND ACSM1 KNOCKDOWN.	278
FIGURE 6.5 QPCR TO CONFIRM LARS2 AND FDPS KNOCKDOWNS.	279

List of Tables

TABLE 1.1 THE GLEASON STAGING SYSTEM OF PROSTATE CANCER TUMOURS ACCORDING TO THE MOST TWO PREDOMINANT HISTOLOGICAL PATTERNS.	43
TABLE 1.2 LIST OF FIRST LINE/SECOND LINE CURRENT DRUG OPTIONS USED FOR HORMONE THERAPY.....	52
TABLE 1.3 DOCETAXEL-BASED TREATMENT OF CASTRATION RESISTANCE PROSTATE CANCER: A SUMMARY OF SINGLE-AGENT STUDIES. D = DOCETAXEL, NR=NOT REPORTED.	60
TABLE 1.4 DOCETAXEL-BASED TREATMENT OF CASTRATION RESISTANCE PROSTATE CANCER: A SUMMARY OF COMBINATION STUDIES. D=DOCETAXEL, E=ESTRAMUSTINE, H=HYDROCORTISONE, NR=NOT REPORTED.	61
TABLE 1.5 NOVEL ANDROGENS TARGETED DUGS.	65
TABLE 1.6 ON-GOING PROSTVAC PHASE III CLINICAL STUDIES.	68
TABLE 2.1 REAGENTS AND COMMERCIALY AVAILABLE KITS.	100
TABLE 2.2 BUFFERS AND SOLUTIONS USED.	103
TABLE 2.3 MAMMALIAN CELL LINES MODELS USED IN THIS STUDY.	107
TABLE 2.4 siRNA TRANSFECTION REAGENTS VOLUMES AND CONCENTRATIONS.....	109
TABLE 2.5 SEQUENCES OF PRIMERS USED TO AMPLIFY TARGETS' DNA SEQUENCES BY QPCR.	126
TABLE 2.6 ANTIBODIES.	129
TABLE 2.7 PRIMERS' SEQUENCES USED TO AMPLIFY STUDIED DNA SITES AND ADD RESTRICTION SITES.	131
TABLE 2.8 PRIMERS USED FOR SEQUENCING OF UROS AND ALDOA INSERTS.	134
TABLE 3.1 SUMMARY OF THE LEAD TARGETS IDENTIFIED IN THE siRNA SCREEN TO REDUCE PROLIFERATION.	143
TABLE 3.2 SUMMARY OF THE LEAD TARGETS IDENTIFIED IN THE siRNA SCREEN TO SIGNIFICANTLY REDUCE CELL MOTILITY.	156
TABLE 3.3 SUMMARY OF THE LEAD TARGETS.	178
TABLE 7.1 SUMMARY OF THE TARGETS IDENTIFIED IN THE siRNA SCREEN TO ELEVATE PC3 PROLIFERATION.	329
TABLE 7.2 SUMMARY OF EXTRA 37 TARGETS IDENTIFIED IN THE siRNA SCREEN TO SIGNIFICANTLY REDUCE CELL MOTILITY.	332

1 Chapter 1 Introduction

1.1 Prostate gland development and Structure

The prostate gland is an essential part of the male reproductive system. This secretory gland forms a small acorn-shaped tissue with ductal features (Abate-Shen & Shen 2000), and it surrounds the urethra under the neck of the bladder anterior to the rectum (Figure 1.1). In humans and other mammals, the prostate develops as a single organ consisting of glandular regions that become histologically distinct after sexual maturity (Meeks & Schaeffer 2011). The secretions of the prostate play an important part in male fertility; contributing important factors to the seminal fluid (Hoover & Naz 2012).

Structurally, the prostate is formed of two main compartments, the stroma and epithelium. The epithelial tissue forms the inside layer of the prostate ducts which are enclosed by stroma (Aaron et al. 2016). The anatomy of the prostate as stated in Verze et al. (2016) is described as having three main zones: the central zone which surrounds the ejaculatory ducts and projects under the bladder base, the transition zone which encloses the urethra, and the peripheral zone making the apical, posterior and lateral parts of the prostate (Figure 1.2) (Verze et al. 2016). The importance of this anatomical structure comes from its relationship to prostatic diseases, where for example the Benign Prostatic Hyperplasia (BPH), a non-malignant growth, occurs in the transition zone, while 70-80 % of Prostatic Carcinoma (PCa) usually arise in the peripheral zone (Abate-Shen & Shen 2000; Sinnott et al. 2015).

Prostate gland development can be divided into five stages including determination, initiation or budding, branching morphogenesis, differentiation, and maturation (Prins & Putz 2008). The human prostate initially develops during the foetal stages from the urogenital sinus (UGS) (Figure 1.3), a hindgut endodermal structure, that produces 5 α -reductase, an enzyme that converts testosterone to dihydrotestosterone (DHT) (Marker et al. 2003). The production of

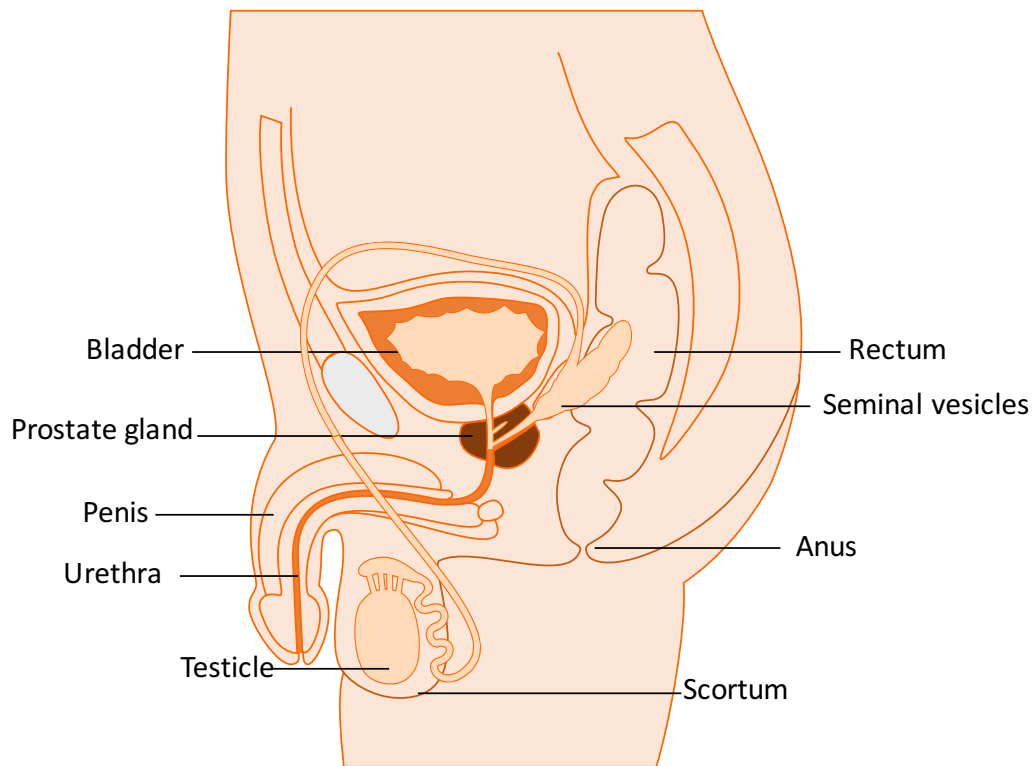


Figure 1.1 The prostate gland location in the male reproductive system.

The prostate is located under the neck of the bladder and anterior to the rectum.

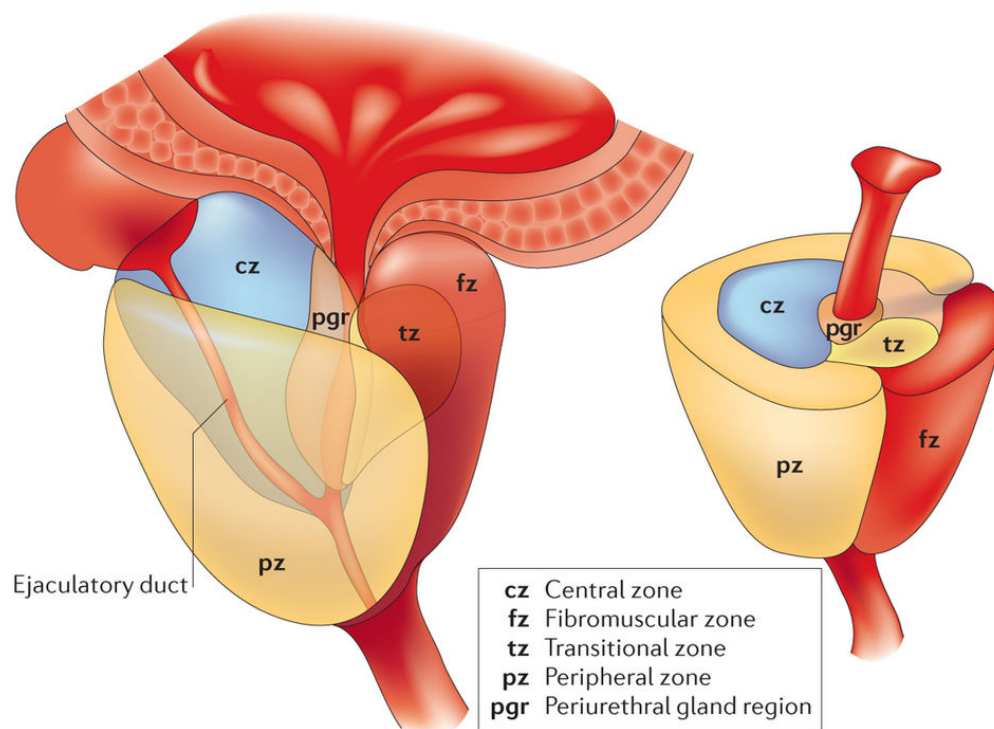


Figure 1.2 The anatomy of prostate gland.

Anatomical illustration of the prostate gland highlighting the main zones of the prostate gland. The central zone forms a cone shape surrounding the ejaculatory ducts and stretches to the bladder's base and contributes 20-25% of the glandular tissue of the prostate. The transition zone is separated from the other glandular compartments by a fibromuscular band of tissue and it forms 5-10% of the glandular tissue of the prostate. The fibromuscular zone is a thick band of muscle fibres and fibrous connective tissues forming the apex of the prostate. The peripheral zone accounts for most of the glandular tissue of the prostate (70%) and forms the posterior and lateral aspects of the gland. The Periurethral gland region forms a narrow area that consists of short ducts close to the urethra. [Illustration taken from Vertez et al, 2016].

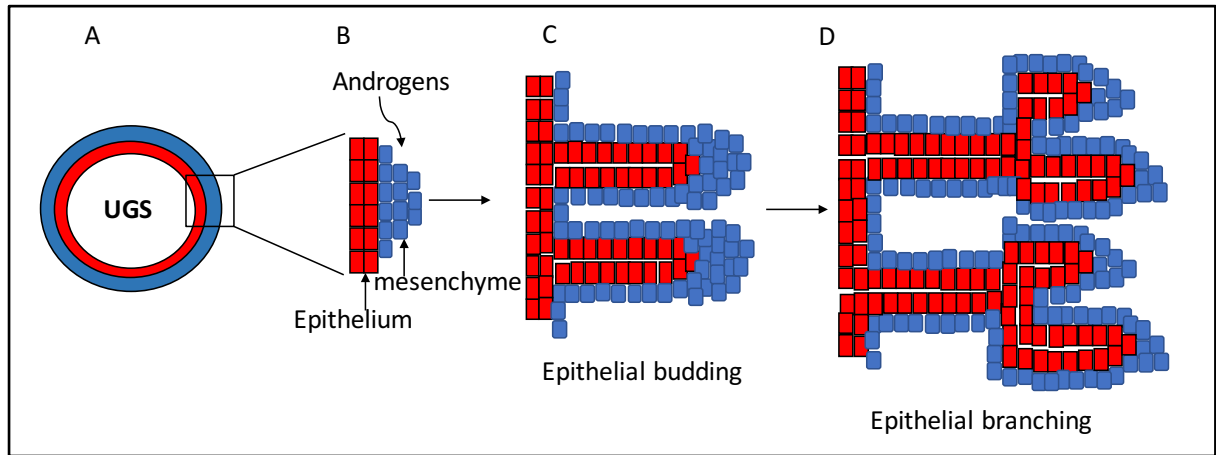


Figure 1.3 Schematic showing the development of the prostate gland.

A: The urogenital sinus (UGS) is the main endodermal structure from where the prostate develops in foetal stages. The UGS is composed of epithelium (red) and mesenchyme (blue). B: The binding of androgens to AR in the mesenchyme stimulates the epithelial budding. C: Elongation of epithelial buds into solid cords of tissues that then forms ducts. D: Later development phase of prostate stimulates branching of epithelial tissues.

androgens (from leydig cells) then stimulates the UGS to develop into epithelial buds, ducts and branching (Meeks & Schaeffer 2011; Nieto et al. 2014). Paracrine signalling is suggested to be responsible for the early development of the prostate where the mesenchymal AR signals induces the growth, invasion and differentiation of the epithelial tissue into prostatic ducts (Cunha 1975). This process occurs as early as 10 weeks' gestation in humans (Meeks & Schaeffer 2011). The development and proliferation induced by this mesenchymal AR signalling occurs only in early development, but it can be reactivated later in life, leading to disease occurrence. In contrast, AR signalling in the epithelium is required later in development and initiates the production of prostatic secretions that initiate cell type differentiation, ductal morphogenesis and prostate maturation during puberty (Schaeffer et al. 2008).

The prostate develops as a result of signalling between the mesenchyme and epithelium (Peng & Joyner 2015). Experiments have shown that the absence of the former causes prostatic formation to fail, demonstrating the importance of signalling coming from the stroma to the epithelium during embryonic prostatic development (Cunha 1994). However, this vital signalling does not only maintain the normal prostatic development and homeostasis, but can also lead to tumour formation (Peng & Joyner 2015).

The epithelium consists of three distinct cell types (Figure 1.4). These, as described by Abate-Shen & Shen (2000), include secretory luminal cells, which exhibit androgen-sensitivity and produce prostatic secretory proteins and are characterized by the expression of the androgen receptor, cytokeratins 8 and 18 and the CD57 cell surface marker. The second type of prostatic epithelial cells are the basal cells that are embedded between the luminal cells and the basement membrane; these cells show low levels of AR and express cytokeratins 5 and 14 and CD44 (Abate-Shen & Shen 2000). The third type of prostatic epithelial cells are the neuroendocrine cells that forms the minority of epithelial cells and they are androgen-independent and thought

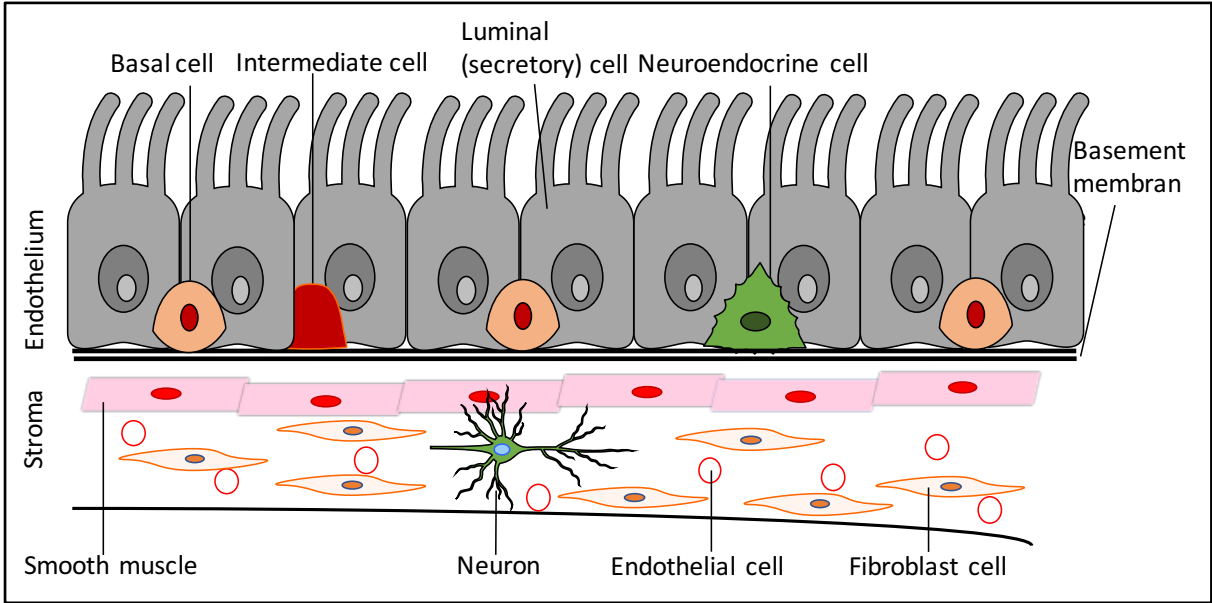


Figure 1.4 Cell types of the adult human prostate.

The endothelium of the prostate composed of secretory luminal cells, basal cells, neuroendocrine cells, and rarely some intermediate cells. The endothelium is separated from stromal part by a basement membrane, and the stroma consists of smooth muscle cells, endothelial cells, fibroblast cells, and neurons.

to produce paracrine signals that help development of the luminal cells (Abate-Shen & Shen 2000).

1.2 Functions and diseases of the prostate

The prostate plays an essential role in male reproduction and is responsible for secreting enzymes, lipids, amines and metal ions that are required for maintaining the normal function of the prostate and spermatozoa (Kumar & Majumder 1995). Prostatic secretions are normally produced by the epithelial compartment and they account for one-fifth to one-third of the whole ejaculation fluid (Nieto et al. 2014). The factors produced by the prostatic epithelium include kallikreins (KLKs), for example the serine protease prostate specific antigen (PSA, KLK3), citrate, which is an intermediate metabolite implicated in the Krebs Cycle, and Zn^{+2} , a trace element found in the cytoplasm of the prostatic epithelium (Franklin et al. 2005; Medrano et al. 2006; Franz et al. 2013; Verze et al. 2016). Zn^{+2} accumulation in prostatic cells is vital for its role in citrate production and secretion, and the prostatic fluid enriched in Zn^{+2} , citrate and kallikreins is important for the molecular synchronization of the functional pathways stimulated by the ejaculatory stimuli (Verze et al. 2016). The accumulation of Zn^{+2} and subsequent production of citrate is found to be lost in prostate malignancy and this loss is regarded as an important characteristic of PCa (Franklin et al. 2005). The epithelial cells of the prostate gland are the only human cells that rely on energy production using aerobic glycolysis by the conversion of glucose into lactic acid rather than its complete oxidation through the Krebs Cycle, and this phenotype is also a hallmark of cancerous cells (Verze et al. 2016).

After maturity the prostate gland stops growing, however, androgens continue to play a vital role in maintaining its normal function (Brooke & Bevan 2009). In some cases, an abnormal growth of the prostate occurs resulting in conditions including benign prostatic hyperplasia (BPH), and premalignant prostatic intraepithelial neoplasia (PIN) or prostate cancer (PCa) (Brooke & Bevan 2009). Another disease called prostatitis (inflammation of prostate)

occurs in 11-13 % of adult men. This condition is predominantly caused by bacterial infection and the resulting inflammation can have a significant impact upon quality of life (Roberts et al. 1997; Wagenlehner et al. 2013). The inflammation of the prostate is believed to result in high damage in prostatic epithelial tissues. BPH is a benign condition affecting males over 50 years, and it is characterized by prostatic cell proliferation, enlargement of the prostate and urethral obstruction leading to lower urinary tract symptoms (Skinder et al. 2016). The risk of BPH development correlates with age where the prevalence increases by 8%, 50%, and 80% in the 4th, 6th, and 9th decades of life, respectively (Lim 2017). BPH occurs in the transition zone where epithelial and stromal cells of the prostate meet (Figure 1.2). This growth is driven by altered androgen levels, specifically dihydrotestosterone (DHT) levels. This has been supported by the fact that BPH patients show a decrease in symptoms when treated with orchiectomy or 5 α -reductase inhibitors, which aim to block the conversion of testosterone to DHT (Homma et al. 2011; Skinder et al. 2016). Further, DHT levels have been found to be higher in BPH patients compared with men with a normal prostate (Ho & Habib 2011).

1.3 Prostate Cancer

PCa is regarded as the most common cancer in Western male populations and forms the second leading cause of cancer-related deaths in men worldwide (Williams & Naz 2010; Kumar & Lupold 2016). It is believed to develop from damaged epithelial foci which is characterized as proliferative inflammatory atrophy (PIA) and/or prostatic intraepithelial neoplasia (Kumar & Lupold 2016). It is indicated that 80% of PCa cases originate as adenocarcinomas that arise from the secretory epithelial cells in the peripheral zone of the prostate (Franz et al. 2013). The risk of the disease increases with age (Brooke & Bevan 2009). Prostate tumours growth is almost always driven by the androgen-signalling axis (Brooke & Bevan 2009; Brooke et al. 2014). Androgens, including testosterone and 5-alpha dihydrotestosterone, act through binding to the androgen receptor (AR) which then regulates the expression of downstream genes

involved in prostate cancer progression (Hirawat et al. 2003) (Figure 1.5). Androgen-dependent transcriptional activation is initiated by androgen binding to the AR which leads to dissociation of the HSP (heat shock protein) complex that holds the receptor in a ligand-binding competent state. Activated AR travels to the nucleus where it dimerizes and binds to AREs in the genome, subsequently regulating the expression of target genes (Heinlein & Chang 2004). The development of the prostate in human and rodent foetuses is largely based on androgen signalling because androgen ablation in early embryogenesis leads to inhibition of prostate development. Further, reduced prostate development is also seen in human and mice with complete AR dysfunction (Prins & Putz 2008).

1.3.1 Aetiology and molecular biology of the disease

PCa aetiology is not completely understood. However, genetic events are directly linked to this disease. Aberrant methylation of genes has been implicated in prostate cancer development (Donkena et al. 2010). For example, the hyper-methylation of tumour suppressor genes that are usually unmethylated could lead to tumour development (Woodson et al. 2003). For example, Woodson et al. (2003) demonstrated that *GSTP1*; a gene encoding the enzyme glutathione-S-transferase P1 (GSTP1), that catalyses the transfer of protons from the reduced glutathione to oxidants, is found to be hypermethylated in PIN and PCa: 70% of PIN lesions and 90% of prostate cancer tumours were found to have hypermethylation of *GSTP1* whereas no methylation was detected in BPH or normal prostatic samples.

Approximately 5-10% of prostate cancers are hereditary and several loci have been implicated in this increased risk (Shand & Gelmann 2006). The number of genetic variations associated with PCa has been increased as a result of the development of genome-wide association study (GWAS) and sharing of large-scale genotype data (Lim 2017). PCa is highly heterogeneous disease in terms of genetic changes, although it has been found that the prostate epithelial cells demonstrate some common genetic changes when the transformation occurs.

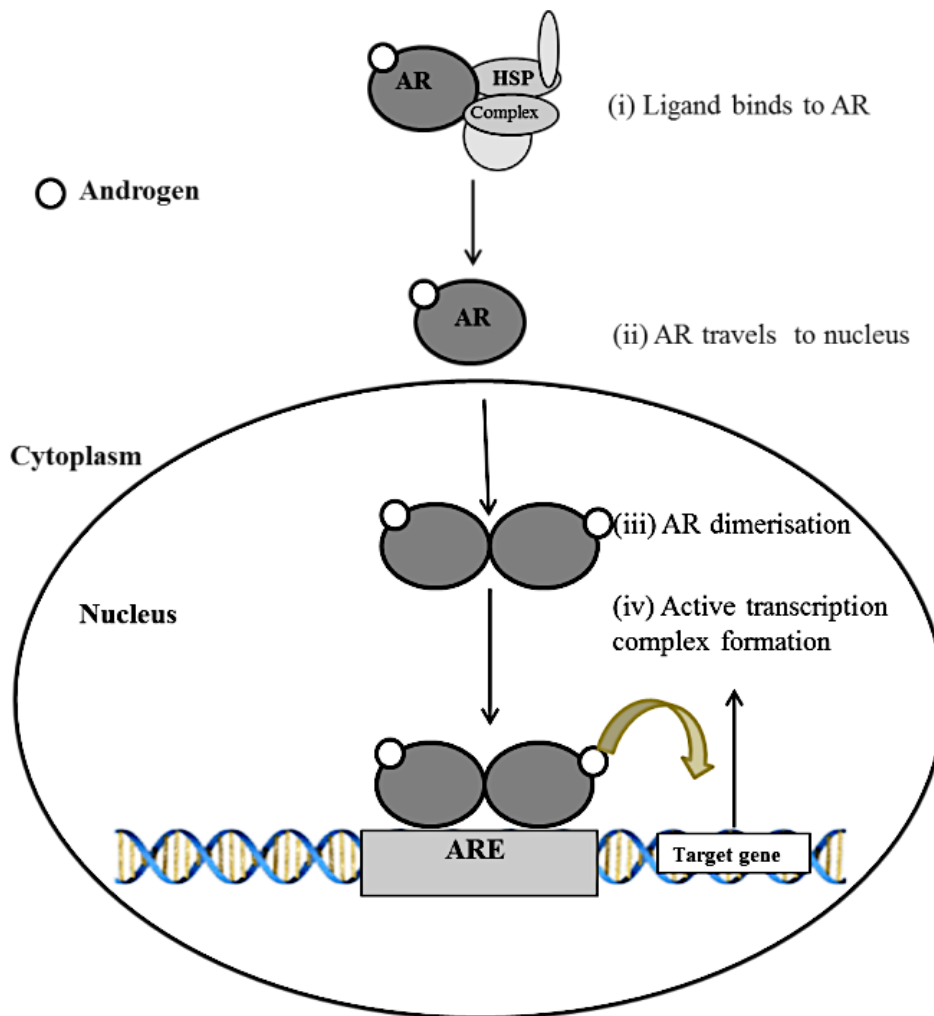


Figure 1.5 The Androgen Receptor signalling axis.

The androgen signalling cascade is activated by androgen binding to the Androgen Receptor (AR), resulting in dissociation of the Heat Shock Proteins (HSP) complex that keeps the receptor in a ligand-binding competent state. Activated AR travels to the nucleus where it dimerizes and binds to Androgen Response Elements (AREs) in the genome and activates target gene expression.

Large genome-based studies led to subgrouping of prostate cancers according to the common genetic modifications which included alterations in the *ERG*, *ETV1*, *ETV4*, *FLI1*, *SPOP*, *FOXA1*, *IDH1*, and *SPINK1* genes (Johnson et al. 2016; Wedge et al. 2018). *ERG*, *ETVs* and *FLI1* are ETS (E26 transformation-specific) transcription factors that are commonly over-expressed in some cases and involved in gene fusions (Tomlins et al. 2005; Paulo et al. 2012). In addition, the promoter of the androgen-regulated prostate-specific serine protease, *TMPRSS2* (transmembrane protease serine 2), has been found to be fused upstream of ETS family members, most commonly *ERG*. The resulting *TMPRSS2:ERG* gene fusion has been found in 50 % of PCa patients, and more than 90 % of *ERG*-positive prostate cancers possess *TMPRSS2-ERG* fusions (Tomlins et al. 2008). There are over 20 *TMPRSS2-ERG* fusion variants and the protein products of the fusion genes and their phenotypic implications in PCa still unclear, however, the presence of such rearrangements is correlated with poor cancer-related survival (Narod et al. 2008).

SPOP point mutations are one of the most common mutations in PCa and are detected in 10% of primary and metastatic tumours (Blattner et al. 2017). *SPINK1* overexpression was also detected in more than 10% of PCa patients as shown by a recent study conducted by Johnson et al. (2016). *DHI* mutations were also reported in prostate cancers, although their occurrence is rare compared to other alterations. Therapeutics targeting such alterations would therefore only benefit a small group of patients (Flaherty et al. 2014; Hinsch et al. 2018). Other common mutations in tumour suppressor and oncogenes have also been reported in PCa such as *TP53*, *PTEN*, *RB1*, *PIK3CA*, *KRAS* and *BRAF* (Wedge et al. 2018).

AR, *TP53*, and *Bcl2* are implicated in progression and metastasis of PCa (Benedettini et al. 2008). The anti-apoptotic factor *Bcl2* has been found to be upregulated in androgen-independent prostate cancer cells and its silencing resulted in enhanced cell death and suppression of growth (Catz & Johnson 2003). Further, Lin et al. (2007) demonstrated that *Bcl2*

is required for the transition from androgen-dependence to androgen-independence. This transition was halted when the Bcl2 antagonist, Bax, was expressed or when Bcl2-shRNA was used (Lin et al. 2007). Other tumour suppressors like the transcription factor TP53 has also been found to be mutated in prostate cancer. Mutations in the *TP53* DNA-binding domain inhibit its ability to bind to target gene promoters and hence it loses its activity in cell cycle regulation (Chappell et al. 2012). A study on 90 tumour tissue samples obtained by radical prostatectomy showed that *TP53* mutations were detected in 32 out of 90 patients (35.6%), and 40.6% of the patients with mutated *TP53* exhibited tumour progression after 25 months while only 9% of wild-type *TP53* patients showed tumour progression, but over a longer period of time (40 months) (Ecke et al. 2010).

AR drives PCa development and progression in several ways which results in alteration of PCa cells responsiveness to androgens. For example, somatic mutations can alter AR ligand specificity resulting in a receptor that is not only responsive to androgens but also to estrogens, progesterone, dehydroepiandrosterone, or even antiandrogens (Veldscholte et al. 1990). Additionally, AR splicing can result in constitutively active receptors that lack the ligand binding domain (Watson et al. 2010). Another mechanism that can alter androgen signalling is *AR* overexpression which makes tumour cells more sensitive to residual levels of androgens or other signals (Eisermann et al. 2013). However, some prostate carcinomas (particularly metastatic tumours) do not express AR as it is silenced by promoter hypermethylation and signalling for survival and growth is assumed to occur through peptide growth factors (Jarrard et al. 1998).

New regions of genetic aberrations have also been found in PCa such as the identification of 8q24 as a significant prostate cancer risk region and the identification of the missense G84E variant in HOXB13 (Lim 2017). The former was regarded as non-coding with little or no transcriptional activity (Wallis & Nam 2015). However, recent studies have shown

that this region is involved in PCa progression through, for example, enhancers involved in the regulation of *MYC* which is located downstream of 8q24 region (Wasserman et al. 2010). Further, two metastatic PCa associated polymorphisms (rs4242382 and rs6983267) were found in this region (Ahn et al. 2011).

1.3.2 Epidemiology

PCa is one of the most prevalent cancers in males, with an expectation of 160,000 cases to be diagnosed in 2017 in the United States plus 3.3 million existing survivors (Miller et al. 2016; Litwin & Tan 2017). Men have a 1:7 risk of developing PCa in their life (Siegel et al. 2016). It is estimated that the global number of new cases will increase to 1.7 million cases and 477,000 deaths by 2030 due to population growth and aging (Ferlay et al. 2010). In Europe, PCa incidence have been increasing, but mortality rates have decreased significantly and this has been attributed to improved prognosis through PSA screening and the availability of imaging techniques in these countries (Crocetti 2015). In the UK (Figure 1.6), there was an apparent increase in the incidence rates since 1993, but the mortality data demonstrated about 20% declined in the time between 1990-2014. (Cancer Research UK 2014). In the USA, both the incidence and death rates of all races and ages (during 1975 to 2014) demonstrated more significant decline over the period of the past 20 years (Figure 1.7).

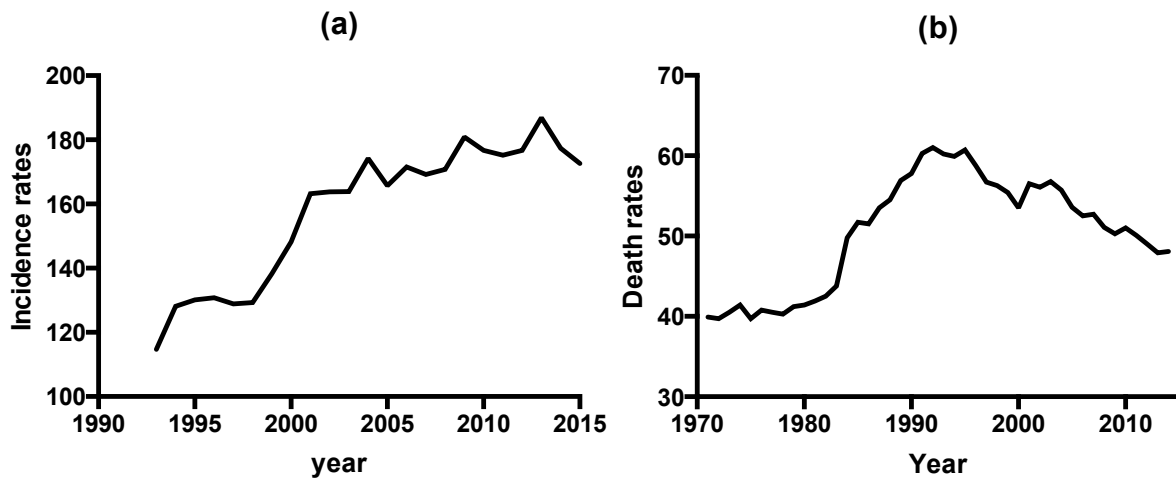


Figure 1.6 The UK incidence and deaths rates.

(a) The incidence rates of PCa from 1993-2015, (b) PCa death rates from 1971-2014. Date is age-standardised and per 100,000 males and adapted from CRUK (Cancer Research UK 2014).

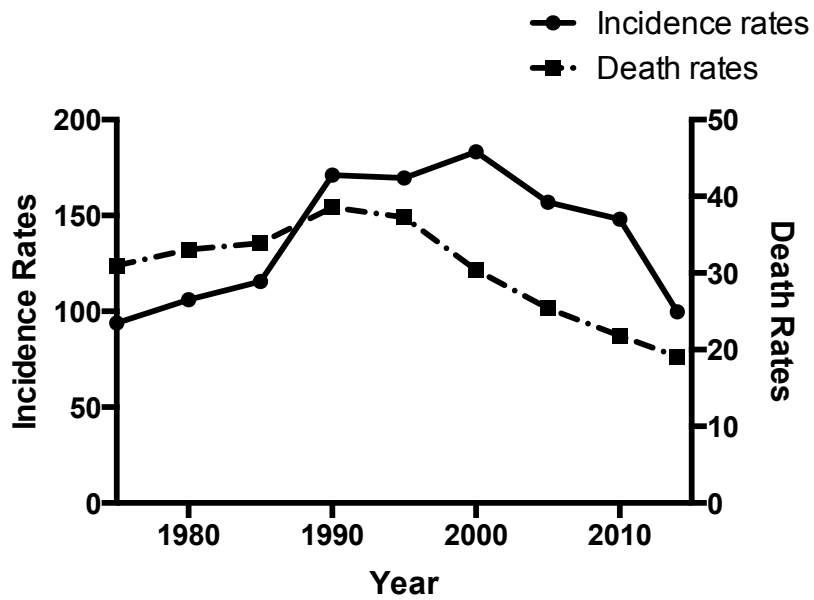


Figure 1.7 USA incidence and deaths rates from 1975 to 2014.

Rates are per 100,000 people (All races males) and are age-adjusted. Data from the SEER Cancer Statistics Review 1975-2014.

1.3.3 Risk Factors

To date, research could not link the occurrence of PCa to any lifestyle choices, however there still some risk factors that can be associated with the increased likelihood of developing the disease; these mainly include increasing age, ethnicity, and genetics (Strief 2007).

Males over 60 years are regarded to be at greater risk of developing PCa than other ages; 80% of cases are of ages over 60 years (Bostwick et al. 2004). Between 2007-2011 (in the USA), only 0.6% of prostate cancer cases were diagnosed between 35 and 44; 9.7% between 45 and 54; 32.7% between 55 and 64; 36.3% between 65 and 74; 16.8% between 75 and 84; and 3.8% for 85 years or older (Bashir 2015). The strong correlation between aging and PCa progression might be explained by the low proliferation rate of the prostatic epithelium, and the subsequent longer periods required for cells' transformation to occur (Abate-Shen & Shen 2000).

In addition, the incident of this disease is the highest in African-American males and Caucasians, with lower rates in Americans of Asian ancestry or white Americans; these racial differences might be due to exogenous factors such as dietary differences or endogenous factors which include the genetic differences (Johns & Houlston 2003; Zeigler-Johnson et al. 2008). The incidence of PCa was more than 60 % higher in African-black men than white men in the USA between 1975-2014; the average incidence of black men was 223.7 per 100,000 men while white men had an incidence of 135.5 per 100,000 men (Figure 1.8) (SEER Cancer Statistics Review 2014). The mortality was also higher in black males according to SEER Cancer Statistics Review 1975-2014 (Figure 1.8).

The genetic or familial risk is higher four times in first-degree relatives than that for the other general population, and it has been found that 50 % higher risk involved with monozygotic twins than dizygotic twins (Grönberg et al. 1994; Hemminki & Vaitinen 1998). In addition, as mentioned earlier, some rare mutations (e.g. rare BRCA2 mutations associated with breast and ovarian cancers) might mark a higher risk of PCa.

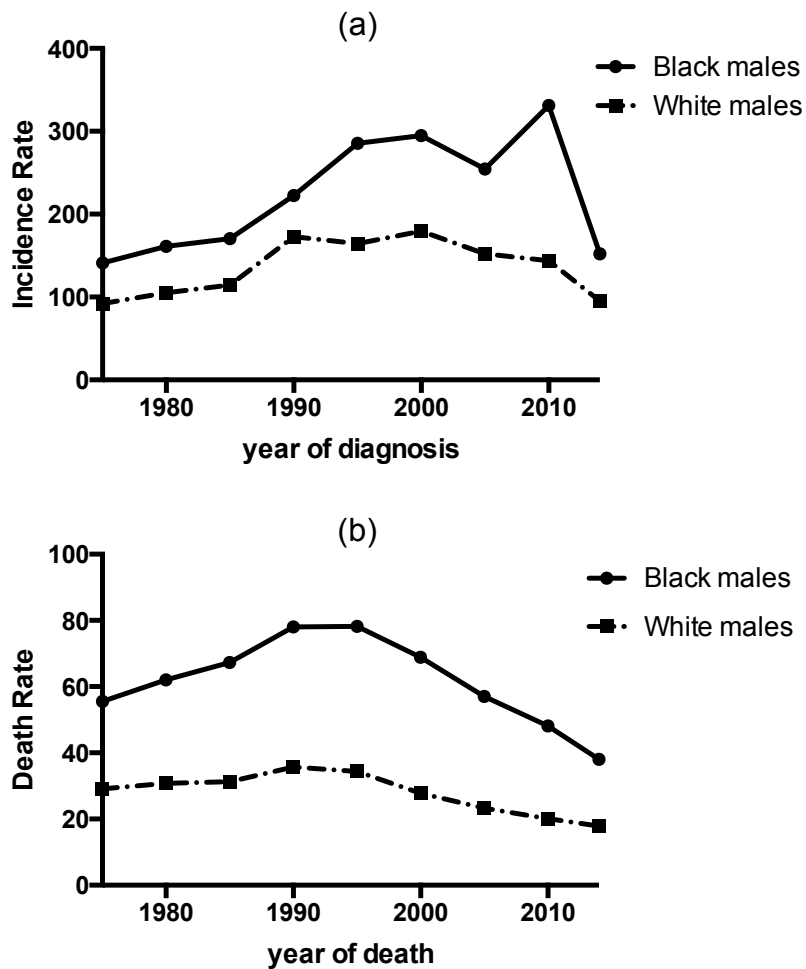


Figure 1.8 Black versus white males' incidence and mortality rates in the USA from 1975-2014.

Rates are per 100,000 people (All races males) and are age-adjusted. Data from the SEER Cancer Statistics Review 1975-2014 (SEER Cancer Statistics Review 2014).

High body mass index (BMI) or gaining weight is believed to increase the risk of dying from PCa (Wright et al. 2007). Western lifestyle was thought to be promoting PCa development. Western diet that is low in protective factors such as antioxidants, micronutrients, and vitamins and high in red meat, fatty food, and dairy products is thought to increase risk but there is still not enough data and evidence to support this (Masko et al. 2013)

In addition to diet, the exogenous factors include the exposure to environmental agents that cause hormonal disruption; one example of these agents is endocrine disrupting chemicals (EDCs) that can enter human body through food ingestion, water or inhalation. EDCs result in hormone activity alteration and hence affect reproduction, development and carcinogenesis (Bostwick et al. 2004). An example of these chemicals is vinclozolin which is an antagonist of androgen and binds to AR and leads to decreased expression of androgen-regulated genes (Euling & Kimmel 2001).

1.3.4 Symptoms and diagnosis/detection of prostate cancer

The early stages of PCa are often symptomless. Patients might show lower urinary track symptoms (LUTS) if the tumour reaches the urethra and/or the neck of the bladder leading to obstructive voiding symptoms (Pentyala et al. 2016). LUTS might include urgency, frequency, poor urinary stream, hesitancy, leakage, and erectile dysfunction (hematospermia and/or reduced ejaculatory volume due to ejaculatory duct obstruction) (Hamilton & Sharp 2004; Pentyala et al. 2016).

Comparative studies of symptoms between control and PCa patients have demonstrated that LUTS symptoms are not a sufficient indicator for PCa diagnosis and detection because such symptoms exist more commonly due to other benign conditions (Hamilton & Sharp 2004; Young et al. 2015). The LUTS are more specific to BPH than PCa (Strief 2007). Therefore, other diagnostic approaches are required to detect the disease.

The discovery of the biomarker prostate-specific antigen (PSA) has aided in PCa detection (Stephan et al. 2014). Serum levels of PSA are usually increased in response to abnormal prostate growth, however the diagnostic properties of PSA can be misleading as it can increase in non-tumour conditions and the levels cannot be detected in early stages of PCa (Wang et al. 1981; Williams & Naz 2010). It is estimated that the use of 4 ng/ml PSA as a cut-off demonstrates only 21% sensitivity to detect PCa and this increases into 51% when higher-grade PCa is present (Adhyam & Gupta 2012). In addition, PSA levels may not be a valid indicator of some rare prostatic carcinomas such as in the case of neuroendocrine PCa (anaplastic or small-cell carcinoma), which accounts for approximately 25 % of late stage tumours, that manifests low or undetectable PSA levels (Caubet et al. 2015).

Digital rectal examination (DRE) is another routine examination performed by physicians to aid PCa detection. However, recent studies demonstrated that the use of DRE exhibits low specificity and sensitivity with or without the use of PSA screening so there have been no evidence to support the DRE efficacy in detecting PCa (Djulgovic et al. 2010; Naji et al. 2018). Therefore, it has been recommended against the use of this routine in the primary care settings (Naji et al. 2018).

Biopsy examination via microscopic techniques is argued to be the first choice that can give adequate details about the tissue state and hence precise staging of the cancer (Kumar et al. 2015). Biopsies of the prostate usually involves the collection of 10-12 tissue samples by transrectal ultrasound and a pathologist examines the samples and gives two Gleason scores (see Section 1.3.5) (Litwin & Tan 2017).

The use of PSA, DRE, and biopsy examination might help in local PCa detection/staging; however, they cannot detect metastasis (Mapelli & Picchio 2015). Imaging modalities are therefore commonly used in PCa diagnosis and staging (Harvey & deSouza 2016). Several imaging techniques are utilized, such as the morphological imaging modalities

which include MRI (magnetic resonance imaging), CT (computerised topography), and transrectal ultrasonography (TRUS) (Mapelli & Picchio 2015). All of these methods though have some limitations, for example CT imaging (Figure 1.9 (a)) relies on the size of the tumour and does not differentiate cancer from benign tumours, and both CT and MRI usually under-stage metastasis. Further, lesions smaller than 8-10 mm are usually missed (Mapelli & Picchio 2015; Li et al. 2018). However, some recent studies investigating MRI for PCa bone metastasis detection demonstrated high sensitivity and specificity (>90%) and excellent diagnostic performance (Woo et al. 2016).

Other promising alternatives of the mentioned PCa imaging modalities are the nuclear medicine techniques such as PET/CT (positron emission tomography/computed tomography) and PET/MRI that merges anatomic CT or MRI sequential images with a superimposed functional image demonstrating the distribution of a radiotracer or positron emitter (Rakheja et al. 2013; Ehman et al. 2017). An example of the latter is ^{18}F -NaF (^{18}F -sodium fluoride) which has high affinity for proliferating bones, and was demonstrated to be better in visualising both lytic and blastic lesions and small lesions compared to whole body bone scans due to the higher resolution of the sectional images and the enhanced target/background ratio (Araz et al. 2015; Harmon et al. 2018). In addition, measurements of standardised uptake values (SUV) of the radiotracer can give information to differentiate malignant from benign lesions, however standard values of the normal and/or benign tissues uptake need to be evaluated first and there have been no enough studies demonstrating the utility of the recent radiotracers (such as ^{18}F -NaF) especially in PCa (Oldan et al. 2016).

Radiolabelled precursors targeted to tumour biological processes such as metabolism, cellular proliferation and receptor binding have also been used in PET/CT and MRI to further stage PCa and investigate into the biochemical features of tumours after therapy failure or metastases (Sarkar & Das 2016). An example of that is the use of radiolabelled choline which

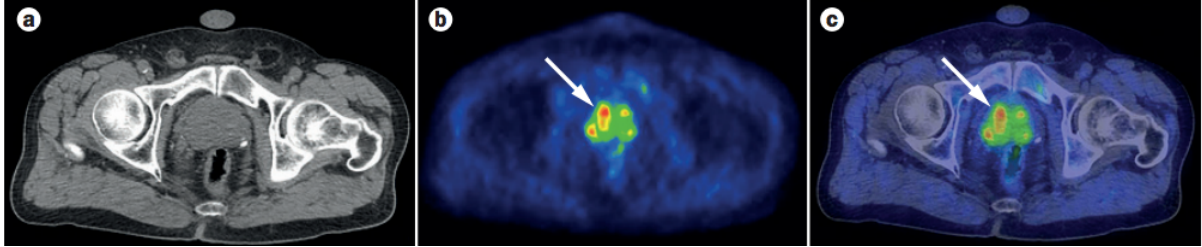


Figure 1.9 Detection/staging of PCa using different imaging modalities.

(a): Transaxial CT. (b): Transaxial ¹¹C-choline-PET. (c): Transaxial PET/CT where a prostate tumour shows a higher uptake. Adapted from (Mapelli & Picchio 2015).

forms the most investigated functional imaging modality for PCa evaluation (Mapelli & Picchio 2015). Choline is a constituent of cell membranes and as PCa induces membranes formation so the uptake of this tracer is higher in PCa tissues relative to normal prostatic tissues (Sarkar & Das 2016). Figure 1.9 (b)-(c) shows higher ^{11}C -choline uptake by PCa tumour in a 70 year old man with stage 7 PCa (Mapelli & Picchio 2015). Other tracers related to other biological processes are reviewed in: (Araz et al. 2015; Mapelli & Picchio 2015; Oldan et al. 2016; Woo et al. 2016; Sarkar & Das 2016; Harmon et al. 2018; Li et al. 2018), and the use of such techniques has been shown to improve the specificity and sensitivity of PCa detection and staging but some limitations and conflicting results regarding their performance have been noted.

1.3.5 Histology and grading

Analysis of PCa foci from small lesions, with similar phenotypes, revealed that they harbour different genotype which indicates that they evolve independently from each other (Macintosh et al. 1998). Previous studies outlined that PIN foci also arise independently in the same prostate, suggesting that PIN might be the origin of multi-focality or heterogeneity of prostate tumours (Bostwick et al. 1998). The heterogeneous and multi-focal nature of prostate tumours makes it difficult for prognostic studies and optimal treatments decisions. To assist, the Gleason grading system was developed and is used as prognostic indicator.

Gleason grading uses needle biopsy that have been stained with Haematoxylin-Eosin (H&M), and lower magnification light microscopy (typically 4x or 10x) is employed to examine the tissues (Gordetsky & Epstein 2016). The decision on grading is based on the differentiation degree and architecture of the neoplastic cells (Humphrey 2004). The PCa staging according to Gleason system adds the most common pattern score, primary pattern (for example 2) to the score of the second most prevalent morphology of prostate neoplastic cells, secondary pattern (for example 3) to give one score (2+3=5). The scale of Gleason scores ranges from 2 to 10; 2

forms the most differentiated adenocarcinoma and as the Gleason score increases tumour cells so does the degree of de-differentiation (Table 1.1, Figure 1.10).

The original system used for grading suffers from deficiencies that make it poor in differentiating between different grades of cancer. For example, it gives a Gleason score of 7 for both 3+4 (mostly well differentiated cancer with smaller portion of poorly differentiated cancer) and 4+3 (mostly poorly differentiated proportion and less of well differentiated cancer) grades, however these are prognostically very different (Epstein et al. 2016). In addition, the lowest score used in practice is 6 although it is on a scale of 2-10 which leads to the incorrect thought that the patient is on the middle stage of the disease, which might result in unnecessary overtreatments (Epstein et al. 2016). Further, risk stratification or staging of patients after radical treatments using models like the D'Amico model (which stages non-metastatic PCa patients into either low, intermediate or high risk of biochemical recurrence after surgery according to their pre-treatment PSA level, clinical TNM-stage and Gleason score) suffered from weaknesses due to inaccuracy of Gleason scoring (Hernandez et al. 2007; Rodrigues et al. 2012).

Therefore, the grading system was revised to minimize confusion and is now graded on a scale of 1-5; where grade 1 represents Gleason scores of ≤ 6 , grade 2 assigned to 3+4 Gleason score, grade 3 for 4+3 Gleason score, grade 4 for 8 Gleason scores, and grade 5 for 9-10 Gleason scores (Epstein et al. 2016; Litwin & Tan 2017). This new grading scheme was introduced since the 2014 International Society of Urological Pathology (ISUP) Consensus Conference on Gleason Grading of Prostatic Carcinoma and the update shows more accurate grading stratification with the aim of reducing overtreatment (Pierorazio et al. 2013). This new system was also included in the 2016 World Health Organization (WHO) classification of tumours and validated as an international standard for pathologists (Epstein et al. 2016).

Table 1.1 The Gleason staging system of prostate cancer tumours according to the most two predominant histological patterns.

Gleason's Pattern	Gleason's Score	Histologic Grade
1, 2	2, 3, 4	I. Well-differentiated
3	5, 6	II. Moderately differentiated
4, 5	7, 8,9,10	III. Poorly Differentiated

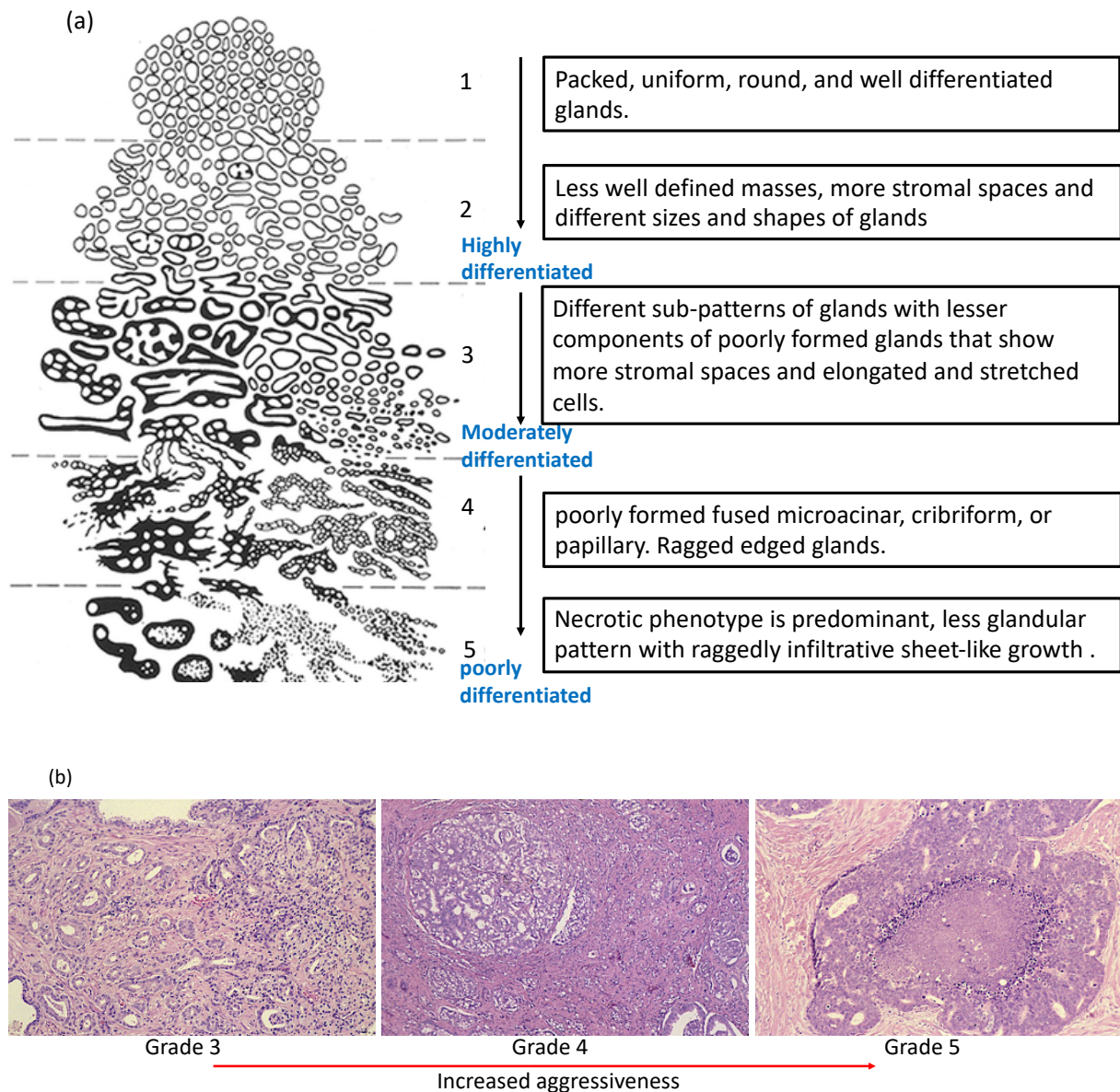


Figure 1.10 The Gleason Grading system.

(a): Gleason scoring according to glandular architecture and patterns. Grade number 1 shows Packed, uniform, round, and well differentiated glands, number 2 glands exhibit less well defined masses, more stromal spaces and different sizes and shapes of glands, number 3 shows different sub-patterns of glands with lesser components of poorly formed glands that show more stromal spaces and elongated and stretched cells, number 4 glands seem to have ragged edges and poorly fused microacinar, cribriform, or papillary, and in number 5 necrotic phenotype is predominant, less glandular pattern with raggedly infiltrative sheet-like growth. (b): Gleason histological patterns and features of grades 3, 4, and 5. The drawing and images are adapted from (Humphrey 2004) and (Epstein et al. 2016).

1.4 Prostate cancer treatments

1.4.1 Current therapies

Treatments for localized PCa include therapies that target AR signalling, hormone therapy, brachytherapy, radical prostatectomy, or external beam radiation therapy (Duchesne 2011). These management options have led to an increase in overall survival of patients with organ confined disease and locally advanced disease, however they can have a significant impact on quality of life for the patient and are not effective after relapse (Verze et al. 2016).

The side effects of radical treatments, radical prostatectomy and radiotherapy, can include urinary symptoms and/or bowel toxicity, erectile dysfunction and haematuria (Keyes et al. 2013; Skowronek 2013). Hot flushes, loss of sex drive, weight increase and fatigue are commonly reported in the case of hormonal therapy (Mohile et al. 2009; Boccon-Gibod et al. 2011; Helsen et al. 2014; Gilson et al. 2015). There is limited evidence as to which of the treatment options have the best harm-benefit balance for patients and the decision on therapy will usually be according to preferences of a particular doctor and patient, symptoms, potential side effects, and economic considerations (Denis & Griffiths 2000). However, the overdiagnosis of insignificant disease, because of PSA screening, and the unnecessary treatments led to the development of some conservative management options (watchful waiting and active surveillance) which are advised to follow prior to treatments.

1.4.1.1 Watchful waiting and active surveillance

Screening for PCa has increased survival rates, but at the price of over-diagnosis and unnecessary treatment of patients with nonthreatening disease. As a result, 2 conservative management options were developed, active surveillance (AS) and watchful waiting (WW), to reduce unnecessary actions (Kakehi 2003; Adolfsson 2008). WW is based on cancer monitoring and deferral of treatments until symptoms appear, it is the most suitable option for

patients with other health issues and/or elderly patients with localized disease to improve their quality of life with no curative intent (Keyes et al. 2013). AS also aims to delay active treatment and the associated side-effects of treatments when the disease is unthreatening. It is often used when patients are predicted to live for a long time (Lund et al. 2014). AS includes more frequent monitoring of disease progression indicators including PSA levels, Gleason score, the development of metastases and increased tumour volume (Cooperberg et al. 2011; Tosoian et al. 2016). AS will be followed by active/curative treatment when cancer progression is reported (Xu et al. 2012). AS was shown to extend survival more than WW (Loeb et al. 2017).

The American Society of Clinical Oncology (ASCO) has recommended that patients with local disease that manifests low- (Gleason score ≤ 6) and intermediate-risk (Gleason score $3+4=7$) should be managed by AS, but other factors such as age, tumour volume, and ethnicity should also be taken into account (Chen et al. 2016). However, there is no clinical or biological strategy that can stratify patients into those that are at low or high risk of disease progression and hence the AS strategy should be personalised according to the risk level based upon routine examinations (Tosoian et al. 2016).

Recent studies comparing RP (radical prostatectomy) to AS demonstrated that radical therapies benefit only a sub-group of patients (Hadjipavlou et al. 2015). Other studies showed that there is a significant positive correlation between RP and survival and metastasis-free disease compared to AS (Bill-Axelson et al. 2014). WW and AS both include the close monitoring of disease progression to proceed to a palliative or active treatment when the disease becomes symptomatic or shows progression (Xu et al. 2012). Such strategies aim firstly to reduce overtreatment associated mortality and reduce the costs of therapies that might not benefit survival and quality of life, however some patients might opt for curative treatment options such as RP or RT to ease the anxiety associated with being diagnosed with cancer (Corcoran et al. 2010).

1.4.1.2 Radiation therapy

Radiotherapy (RT) aims to kill cancer cells with little effect upon adjacent tissues. The approach is based on concentrating a beam of radiation on the tumour tissues which can be performed using an external source of radiation (external beam radiotherapy) or internally through what is called brachytherapy (Sadeghi et al. 2010). The latter involves the implantation of radioactive seeds that can emit radiation simultaneously for short-term; high dose-rate brachytherapy (HDRB), or long-term; low dose-rate brachytherapy (LDRB), according to the doses required (Skowronek 2013). This method generally is dependent on the detailed anatomy of the prostate, and the number of seeds injected is dependent on the area and size of the prostate where physicians are more conservative in areas close to other organs, such as the rectum and bladder to prevent unwanted tissue damage (Cesaretti et al. 2007).

Treatment using radiation is generally offered to patients with clinically localised disease and used in combination with hormonal therapies in locally advanced PCa (Stein et al. 2007). Like RP, this option shows side-effects, mainly minimum urinary symptoms and rectal toxicity (Keyes et al. 2013). Previous research work presented by Potosky et al. (2004), investigated follow-up data for PCa patient with localised disease treated with either RP or RT for five years. Their analysis showed that both RT or RP resulted in overall reduced sexual function, although erectile dysfunction was more frequent in RP-treated patients and only 5 % of RT patients developed incontinence compared to 14-16 % of RP patients. Further, the RT group demonstrated more frequency of bowel urgency and haemorrhoids than the RP group of patients (Potosky et al. 2004). To date, few comparable studies exist and hence it is difficult to conclude which of these therapies is the best option to treat localised PCa patients; each of these options affect the overall life quality of patients and the survival benefits of these therapies are not clear, but a recent analysis concluded that radiotherapy is correlated with higher mortality rates compared to RP (Wallis et al. 2016).

In addition to the typical side effects; including urinary incontinence and erectile dysfunction, radiotherapy has also been linked to the risk of inducing secondary malignancies as adjacent non-malignant tissues might receive genetic alterations without direct exposure to radiation because of the raised levels of reactive oxygen species (ROS) (Wallis et al. 2016). However, this is still uncertain because of the limited amount of data available, which mainly show a low rate of the risk of secondary tumours in close organs such as the bladder, rectum, and colon (Jao et al. 1987; Neugut et al. 1997; Sountoulides et al. 2010).

1.4.1.3 Radical prostatectomy

RP is the surgical removal of the prostate and it is used as a first line treatment option for PCa patients with organ-confined disease. RP has been used to control local PCa for 100 years (Walsh 2000). It was discussed by Hugosson et al. (2011) that in most patients RP cures the disease, and with the improved surgical techniques the pre-operative mortality rate has dropped to 0.1 %. They also added that improvements in surgery have led to reduced incontinence, but 30 % of patients do claim light incontinence post RP. Further the risk of stricture of vesico-urethral anastomosis has decreased from 10-20 % to only 2-9 % (Hugosson et al. 2011).

RP is often offered to patients with localised tumours who are expected to live at least 10 years (Lepor 2000). RP is mainly performed by either open (retropubic or perineal) or laparoscopic approaches (Salomon et al. 2004). The severity of the complications associated with retrotropic or perineal surgical approaches are mainly related to the individual's anatomy, age, the surgical techniques used, and the experience and skills of the surgeon (McCullough 2005). Comparisons between the open and laparoscopic techniques showed that they result in similar functional outcomes (erectile dysfunction and incontinence) (Damber & Khatami 2005). Recently a type of laparoscopic prostatectomy called Da Vinci, robotic-assisted prostatectomy, has been claimed to be a better option for its benefits over the traditional surgical approaches

in terms of intraoperative and postoperative outcomes (Seo et al. 2016). A recent comparison study by Niklas et al. (2016) demonstrated that robotic-assisted RP compared to open RP is exhibiting reduced surgical margins, reduced need for intraoperative blood transfusions, less catheter duration, less post-operative complications, and overall shorter hospitalisation time and hence reduced care costs. However, the intraoperative complications were similar in both groups but the operation time of robotic-assisted RP is longer than open RP (Niklas et al. 2016).

1.4.1.4 Androgen deprivation hormonal therapies and antiandrogens

Therapeutics for localized/metastatic PCa usually target the AR pathway to prevent AR-dependent gene transcription (Karantanos et al. 2013). This is achieved by using drugs like luteinizing hormone releasing hormone (LHRH) (also known as gonadotropin-releasing hormone (GnRH)) analogues (Helsen et al. 2014), and recently GnRH antagonists (Cook & Sheridan 2000), and anti-androgens (Chen et al. 2009).

Hormonal therapies form an important side of treatment of symptomatic metastatic PCa (Crawford 2004). However, hormone-based therapies are used in other different settings. They are used as a primary treatment option for localised PCa instead of surgery or radiotherapy, and in combination with surgery or radiotherapy or after biochemical reoccurrence (PSA increase) (Isbarn et al. 2009). AR-targeting therapies are highly successful at early stages of the disease, although most patients ultimately relapse after an average of 2-3 years and tumours progress to the more aggressive stage, CRPC (Karantanos et al. 2013).

Hormonal therapies work by the inhibition of androgens produced by adrenal glands, testes and tumour cells, or inhibiting the AR itself (Potter et al. 1995). Androgen castration can be achieved by surgical orchiectomy or androgen reducing drugs like estrogens (previously) or GnRH analogues; with or without anti-androgens (Crawford 2004; Duchesne 2011). GnRH agonists work by downregulating the GnRH receptors in the pituitary gland which regulates the

luteinizing hormone (LH) secretion and hence blocking testicular production of testosterone and DHT (Figure 1.11) (Debruyne 2004; Karantanos et al. 2013). The GnRH initially leads to a transient rise in serum LH levels and thus increasing testosterone serum levels, known as the testosterone surge (T surge). This in turn delays the desired suppression of testosterone production and can lead to clinical exacerbation of symptoms in advanced PCa patients, termed the “clinical flare” (Boccon-Gibod et al. 2011). The flare can be minimized by the use of antiandrogens (Table 1.2) to lessen the effect of the T surge.

A trial study using one of the GnRH agonist goserelin (Table 1.2) demonstrated that T surge occurred in 22.6 % of patients after repeated injections of 3.6 or 10.8 mg of the drug, although none of the patients with T surge showed any tumour flare (Zinner et al. 2004). Another study, by Lundström et al. (2009), was conducted on 120 patients in South Africa using two injections of Triptoline 6 months’ formulation (22.5 mg). The study showed that 97.5 % of the patients achieved a castrate testosterone level (≤ 50 ng/dL) by 29 days and 93 % maintained castrate level in 2-12 months. Further, 98.3 % of patients demonstrated no LH after the second dose of the drug. Triptoline treatment was also found to decrease testosterone levels to less than 20 ng/dL after 6 months in 94 % of the patients, 92.2 % at 9 months, and 91.3 % at 12 months (Lundström et al. 2009).

More recently, GnRH antagonists were demonstrated to be much more potent than the GnRH agonists as they do not cause the initial T surge (Crawford 2004). Degarelix is the most studied GnRH antagonist, it has been shown to have better clinical outcomes than leuprolide and has been shown to delay progression to CRPC (Shore 2013). In addition, the use of GnRH antagonists does not require the use of adjuvant anti-androgenic agents, therefore avoiding the adverse effects associated with these drugs (Boccon-Gibod et al. 2011).

As mentioned, an additive treatment to the hormonal or surgical castration (androgen deprivation therapies; ADT) is the use of anti-androgens to achieve maximal androgens

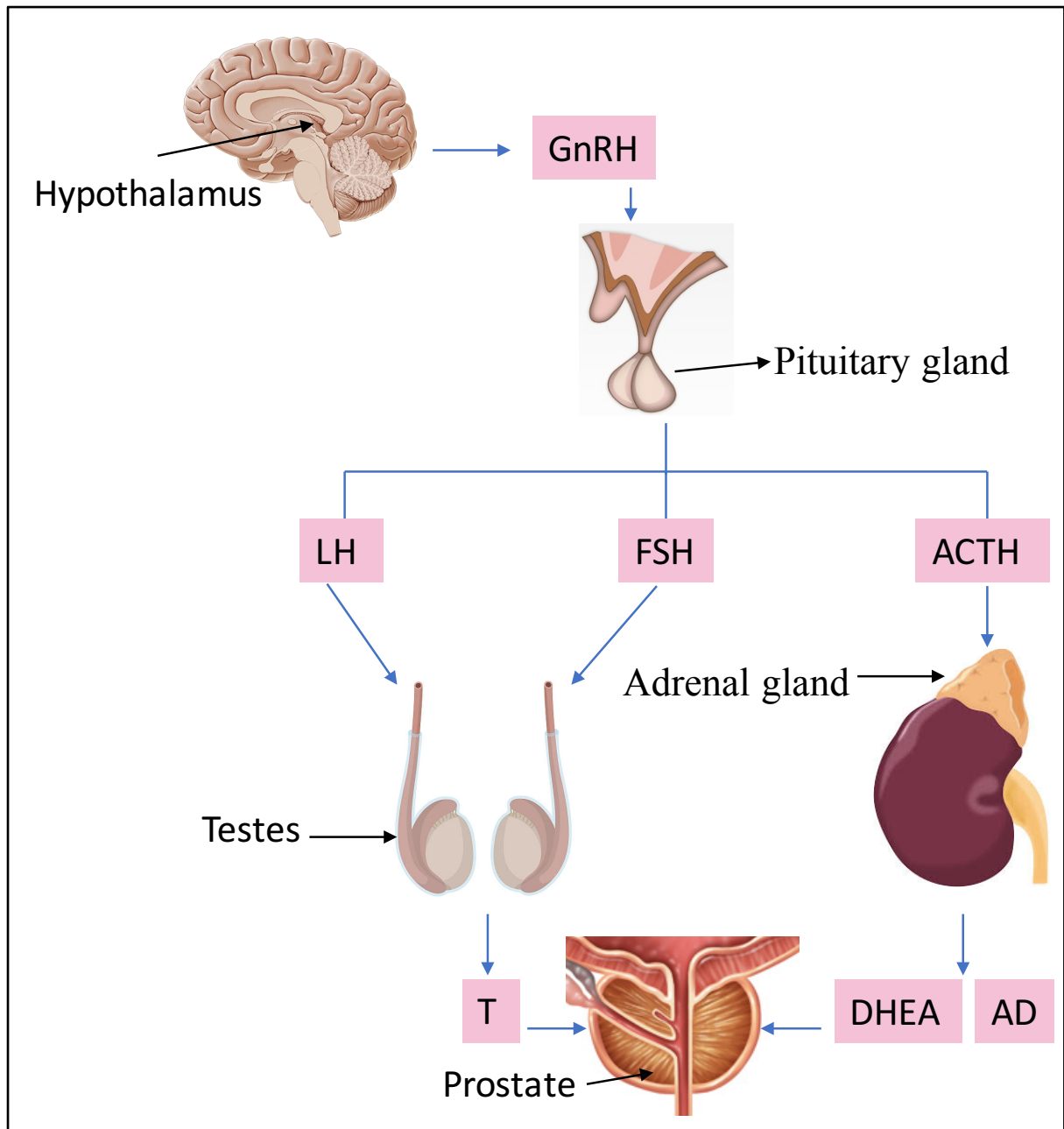


Figure 1.11 Endocrine control of prostatic growth.

Normal prostate development and function requires AR signalling which is controlled by the binding of androgens which in turn are regulated by hypothalamic–pituitary–adrenal/gonadal axis. Synthesis of Androgens [testosterone (T), androstenedione (AD), dehydroepiandrosterone (DHEA)] and other steroids occurs in the testes or adrenal glands. Steroids (T, AD, and DHEA) release into the circulation is stimulated by specific hormonal signals including follicle stimulating hormone (FSH), gonadotropin releasing hormone (GnRH), luteinizing hormone (LH), luteinizing hormone releasing hormone (LHRH). Steroid hormone binding globulin (SHBG) transports testosterone to the prostate where it is converted by 5 α -reductase to its active form (5 α -dihydrotestosterone, DHT). The pituitary releases the adrenocorticotropic hormone (ACTH) which stimulates adrenals to produce AD and DHEA.

Table 1.2 List of first line/second line current drug options used for hormone therapy.

Drug name	Mechanism of action	Reference
Leuprolide	A GnRH agonist works by desensitizing GnRH receptors. T flare occurs.	(Tunn et al. 2013)
Bruserelin	a synthetic nonapeptide analogue of native LHRH. T flare initiated.	(Soloway 1988)
Abarelix	A peptide antagonist of GnRH receptor. No T flare initiation.	(Kirby et al. 2009)
Degarelix	A peptide antagonist of GnRH receptor. No T flare initiation.	(Kirby et al. 2009)
Goserelin (Zoladex)	A GnRH agonist, T flare initiated.	(Zinner et al. 2004)
Triptorelin	A GnRH agonist, T flare initiated.	(Ploussard & Mongiat-Artus 2013)
Abiraterone acetate	Steroidal anti-androgen, and irreversible inhibitor of CYP17.	(Rehman & Rosenberg 2012)
Cyproterone acetate (CPA)	Steroidal anti-androgen.	(Goldenberg & Bruchofsky 1991)
Mifepristone (RU486)	Steroidal anti-androgens, progesterone analogue.	(Terakawa et al. 1988), (Hazra & Pore 2001)
Spirolactone	Steroidal anti-androgens, Inhibition of cytochrome P450.	(Walsh & Siiteri 1975),(Sundar & Dickinson 2012)
Galeterone (VN/124-1)	Steroidal anti-androgen	(Njar & Brodie 2015)
Flutamide	Non-steroidal anti-androgen	(Goldspiel & Kohler 1990)

Nilutamide	Non-steroidal anti-androgen	(Kassouf et al. 2003)
Bicalutamide	Non-steroidal anti-androgen	(Goa & Spencer 1998)
Enzalutamide (MDV3100)	Non-steroidal anti-androgen; androgen receptor antagonist.	(Scher et al. 2010)

blockade (MAB) (Klotz 2008). According to their chemical structures antiandrogens are of two classes; steroidal or non-steroidal (Table 1.2) (Akakura et al. 1998). The former works by blocking the production of androgens from adrenals, tumour cells, and tumour microenvironment by inhibiting an enzyme called cytochrome P-450-c17 (CYP17) (Karantanos et al. 2013). An example of steroidal antiandrogens is abiraterone acetate, which was shown to enhance the overall survival of metastatic CRPC patients who previously received chemotherapy (de Bono et al. 2011). The administration of steroidal antiandrogens, however, usually result in sexual dysfunction, and their steroidal nature explains the associated cardiovascular symptoms and fluid retentions (Mohile et al. 2009). This highlights the reason of the preference and tolerability of non-steroidal anti-androgens (NSAAs) over steroidal agents (Chen et al. 2009). NSAAs anti-androgens work by competing with endogenous androgens to bind to the AR ligand binding pocket, resulting in a conformational change in the receptor that promotes transcriptional silencing (Chen et al. 2009). NSAAs are pure anti-androgens; they do not interact with other steroid receptors, and as opposed to the steroidal anti-androgens they inhibit the negative feedback of androgens activity, and in consequence they increase LH and hence raise testosterone levels, however, this rise in androgens has no effect because of their AR inhibitory effect (Akakura et al. 1998; Kolvenbag & Furr 2009). NSAAs in clinical use include flutamide, nilutamide, and bicalutamide (Table 1.2); they all work as competitive inhibitors of androgens to AR and the antagonist-bound AR stays associated with heat shock factors in the cytoplasm or form transcriptionally inactive complex with DNA (Scher et al. 2010).

The symptoms associated with the non-steroidal AR antagonists include hot flushes, gastrointestinal symptoms, diarrhoea, and hepatotoxicity, reduction in haemoglobin, and increased levels of aminotransferases (McLeod 1997). The application of NSAAs as a single therapy has been preferred by young patients over the LHRH-targeted agents because they

preserve the sexual potency, however it can be less effective (Pope & Abel 2010). In respect to survival rates, available data shows that antiandrogens effect on survival rates is significant. For example, a new antiandrogen called enzalutamide has been shown to decrease PSA levels and improve the overall survival of patients with CRPC after chemotherapy (Dhingra et al. 2013). In addition, a phase 3 study compared 800 patients treated with enzalutamide (daily doses of 160 mg) to 399 males treated with placebo found that the median overall survival was 18.4 months in first group versus 13.6 months in the placebo group, and the decrease of PSA level by 50% or more was 54 % in the enzalutamide group compared to only 2 % in the placebo group, however an increased frequency of side effects was reported in the enzalutamide group (Scher et al. 2012).

Hormone therapies are usually used for organ-confined or locally advanced PCa as adjuvant therapies, after a prior therapy (radiation therapy or prostatectomy), when reoccurrence is expected (Payne & Mason 2011). It was demonstrated that the use of hormonal drugs as adjuvant therapy improves the disease-free survival after prostatectomy and can even increase the overall survival if applied after radiotherapy (Kumar et al. 2006). Hormonal therapies can also be used as neo-adjuvant therapy, before or during radiotherapy, and this regimen was shown to improve the overall survival and reduce mortality of PCa patients (Jones et al. 2011). Hormonal therapies can be utilized as a single palliative therapy in cases when other primary therapies with curative intent cannot be performed (Studer et al. 2006).

1.5 Hormone therapy failure and progression to CRPC

Hormonal therapies are highly successful at early stages of the disease, although most patients ultimately relapse after an average of 2-3 years and the tumours progress to the more aggressive stage, termed CRPC which is associated with poor prognosis and lower survival rates (Karantanos et al. 2013). The survival for CRPC patients has a median of only 1-2 years

(Brooke et al. 2008; Mostaghel et al. 2010). CRPC was previously known as “hormone-refractory” or “androgen-independent” PCa, but these terms are not precise as recent evidence has demonstrated that advanced/metastatic PCa is not “hormone-refractory” nor “androgen-independent” (Foley & Mitsiades 2016). Androgen receptor signalling is believed to drive all stages of the disease (Coutinho et al. 2016). As discussed, the principle treatment for locally advanced PCa is hormone therapy which causes remission of the disease, but patients with castrate resistant disease no longer respond to such therapy regardless of testosterone levels (Karantanos et al. 2013). Until recently, the only therapeutic option for CRPC was chemotherapeutics, typically docetaxel, with ADT and/or antiandrogens (Hotte & Saad 2010). Several therapies targeting the AR pathway, such as abiraterone acetate and enzalutamide (Section 1.4.5), have entered the clinic because it is well accepted that androgen signalling drives CRPC. However, still no treatment could cure this stage of prostate cancer and the current regimens are only palliative.

Multiple mechanisms have been proposed to explain how AR signalling drives CRPC, including AR amplification and mutations, modifications of AR coregulator expression (leading to enhancement of AR signal transduction), protein kinase alterations, steroid metabolism perturbations, and crosstalk with other signalling axes with the AR pathway (Heinlein & Chang 2004; Chang 2007; Mostaghel et al. 2010). Previous studies have demonstrated that mutations of the AR, common in CRPC, result in reduced ligand specificity allowing the receptor to be activated in response to other ligands, including antiandrogens and other hormones (Heinlein & Chang 2004; Brooke & Bevan 2009). More recently, it has been also demonstrated that constitutively active AR splice variants (AR-Vs) are up-regulated in CRPC. These variants lack the ligand binding domain and are therefore able to circumvent antiandrogenic agents (Cao et al. 2014). The failure of current treatments for CRPC has led to a large volume of research on the subject, to understand different factors and pathways that

regulate and lead to tumour progression.

1.5.1 Molecular pathways that could be essential for prostate cancer progression

Many pathways have been suggested to enhance PCa proliferation and migration. Several of these pathways, as mentioned before, are AR-regulated and others are AR independent oncogenic and tumour suppressor pathways. For example, the PI3K-Akt-mTOR pathway promotes PCa survival, growth, migration, metabolism, angiogenesis, and differentiation (Bitting & Armstrong 2013). This pathway is often constitutively active in PCa as a result of inactivation of its negative regulator PTEN (Phin et al. 2013). However, targeting this pathway with single agents was not found to result in significant clinical activity in castration resistant disease, and hence it has been proposed that dual targeting will improve efficacy (Saad & Eisenberger 2014). The *TP53* tumour suppressor gene is also commonly mutated in PCa, however the frequency of this alteration is still low in the disease (5 % of PCa patients) compared to its existence in other cancers. Further, alterations in *TP53* do not clearly correlate with disease grading and staging (Ecke et al. 2010; Kluth et al. 2014).

There is significant evidence to suggest that CRPC proliferation is still under the regulation of AR or via cross-talk with androgen signalling (Hoang et al. 2017). One such pathway is Wnt/ β -catenin and genomic alterations of this pathway have been detected in CRPC but not in hormone naïve prostate cancer. Further, Hoang et al. (2017) demonstrated that β -catenin is found to colocalise with the nuclear AR more commonly in CRPC than in primary PCa. This data suggest that AR and β -catenin interact and may cooperate to control the expression of target genes in CRPC, promoting survival and drug resistance (Yokoyama et al. 2014).

The mentioned signalling pathways form only the most common alterations found in PCa. However, none of the pathways were frequently altered to the extent that could suggest

they are major causes of PCa. The heterogeneity of the molecular alterations in PCa suggests that targeting a common downstream signalling pathway (e.g. metabolic signalling) could be a viable strategy to treat CRPC.

1.5.2 Chemotherapies

The majority of patients will respond to ADT and antiandrogens, however these therapies will invariably fail and the tumours will progress to CRPC (Deshayes et al. 2017). Since the 1990s, several chemotherapeutics have been introduced for the treatment of CRPC. Mitoxantrone was approved by the United States Food and Drug Administration (FDA) for CRPC in 1999, although other drugs like 5-fluorouracil and cyclophosphamide were already established and shown to have a palliative effect on CRPC patients (Sundararajan & Vogelzang 2014). Several randomized trials using mitoxantrone in combination with other treatments (such as prednisone and hydrocortisone) have shown that this chemo-drug has a palliative effect on patients (mainly reduced bone pain), however it did not show any enhancement on overall survival (Tannock et al. 1996; Kantoff et al. 1999; Berry et al. 2002). This drug is not currently in common use as it has been replaced with newer agents that show better efficacy in CRPC patients. However, it might be used as a third or fourth-line treatment when other drugs such as Radium-223, docetaxel, and cabazitaxel have failed/cannot be administered (Sundararajan & Vogelzang 2014).

The first taxane agent introduced for CRPC was paclitaxel, which was introduced in the early 1990s. It is believed that taxanes block cell cycle progression due to their effect on microtubule disassembly, leading to cell cycle arrest in G2/M phase (Schiff & Horwitz 1980; Caplows et al. 1994). Taxanes are also proposed to deactivate the anti-apoptotic activity of Bcl2 proteins, consequently inducing apoptosis (Li et al. 2004). These drugs have been shown to reduce PSA levels, improve symptoms, and increase survival time (Dayyani et al. 2011).

Paclitaxel (taxol) was initially reported in a randomized phase 2 trial study; using a 24-hour infusion doses of 135-170 mg/m² every three weeks, which was found to be ineffective as a treatment for CRPC (Roth et al. 1993). A following trial study using weekly treatment of 24-hour infusion taxol at a dose of 150 mg/m² showed that 39 % of patients exhibited a decline in their PSA levels, but toxicity was also high (35%) (Trivedi et al. 2000). Several other phase 1 and 2 trial studies combined paclitaxel with estramustine (an antitumor agent which also affects microtubules assembly leading to growth inhibition) and concluded that the addition of microtubules targeted agents enhanced PSA response, quality of life, and somewhat prolonged survival time (Hudes et al. 1997; Smith et al. 1999; Haas et al. 2001; Kelly et al. 2001). However, the small number of patients included in these studies made it difficult to draw a final conclusions and again, the treatment regime was associated with significant side-effect including fatigue, diarrhoea, hepatotoxicity, anaemia, leukopenia, nausea, fluid retention, hyperglycaemia, hypophosphatemia, leukopenia, thrombocytopenia, and peripheral neuropathy (Hudes et al. 1997; Smith et al. 1999; Haas et al. 2001; Kelly et al. 2001). Docetaxel was subsequently found to show better efficacy compared to paclitaxel, as confirmed by cell culture studies (Kreis et al. 1997), and in xenograft tumours in nude mice (Vanhoefer et al. 1997). In addition, it is demonstrated that docetaxel is twice as effective as paclitaxel in microtubules destabilisation (Williams et al. 2000). Several randomized trials were conducted using docetaxel as a single agent or in combinations as shown in Tables 1.3 and 1.4. Overall, docetaxel, with or without other agents, is moderately tolerated by patients in phase 1 and 2 studies at doses of less than 80 mg/m², but a greater decrease in PSA levels were seen in the combination studies (Table 1.4). Docetaxel as a single agent and in combined treatments was also reported to enhance survival and provide symptomatic relief (Beer et al. 2001; Berry et al. 2001; Berthold et al. 2008). Toxicity was mostly mild to moderate in these studies and included hematologic and non-hematologic toxicities. Hematologic toxicities like neutropenia, anaemia

Table 1.3 Docetaxel-Based Treatment of Castration Resistance Prostate Cancer: A Summary of Single-Agent studies. D = docetaxel, NR=not reported.

<i>Reference</i>	No. of patients	Study Phase	Doses and timing	>50 % PSA decline (%)	survival (Months)
(Beer et al. 2001)	25	II	D 36 mg/m ² x 6 weeks.	46	9
(Picus & Schultz 1999)	35	II	D 75 mg/m ² /3weeks.	46	12
(Friedland et al. 1999)	21	II	D 75 mg/m ² /3weeks.	38	NR
(Gravis et al. 2003)	30	II	D 35 mg/m ² /week for 24 weeks, 2 weeks intervals every 6 weeks.	48	20
(Berry et al. 2001)	60	II	D 36 mg/m ² /week for 6 weeks, 3 cycles with 2 weeks intervals between each.	41	9.4

Table 1.4 Docetaxel-Based Treatment of Castration Resistance Prostate Cancer: A Summary of combination studies. D=docetaxel, E=Estramustine, H=hydrocortisone, NR=not reported.

<i>Reference</i>	No. of patients	Study Phase	Doses and timing	>50 % PSA decline (%)	survival (Months)
(Petrylak et al. 1999)	34	I	E 280 mg 1- 5 days + D 40 or 80 mg/m ² on day2. Repeated every 3 weeks.	63	NR
(Kreis et al. 1999)	17	I	D 40-80 mg/m ² /3weeks + E 14 mg/kg/ dpo.	82	NR
(Oh et al. 2005)	30	I	D ≤ 34 mg/m ² on days 2,6,9 of 28-day cycles + E 140 mg 3x/day on days 1-5,8-12, & 15-19+ C on day2.	63	14.6
(Chittoor et al. 2006)	58	II	D 25 mg/m ² on days 2,9,16 of 28-dyas cycles + E 140 mg 2x/day on days 1-3, 8-10, & 15-17.	68	5.3
(Savarese et al. 2001)	47	II	D 70 mg/m ² on days2/3weeks + E 10 mg/kg/dpo days 1-5 + H 40 mg/day.	68	20
(Sinibaldi et al. 2002)	40	II	D 70 mg/m ² + E 280 mg/6hours/3 weeks up to 6 cycles.	45	13.5

(Picus & Schultz 1999; Savarese et al. 2001; Gravis et al. 2003), grade 3/4 granulocytopenia (Petrylak et al. 1999; Savarese et al. 2001), and grade 3 and 4 myelosuppression (Sinibaldi et al. 2002; Oh et al. 2005) were reported. Other adverse effects reported in the phase 1 and 2 trials included hyperglycaemia, grade 1 or 2 hypocalcaemia, hypophosphatemia, dermatitis, myalgia, nausea, emesis, fatigue, edema, diarrhoea, anorexia, myalgias, and mild alopecia (Kreis et al. 1997; Picus & Schultz 1999; Savarese et al. 2001; Sinibaldi et al. 2002; Gravis et al. 2003). Due to the side-effects associated with these therapies, the docetaxel regimens are only now applied to patients with CRPC (Puente et al. 2017).

The current standard treatment of CRPC consists of a combination of docetaxel chemotherapy (75 mg/m² every three weeks) with continued androgens suppression plus 10 mg/day of prednisone (DeLongchamps 2014). The latter is a corticosteroid that is administered to manage the excessive mineralocorticoids-related side effects which arise because of CYP17A1 inhibition (Vasaitis et al. 2011). A study demonstrated by Sweeney et al. (2015) followed 790 patients with CRPC and showed that the combination of docetaxel (75 mg/m²) every three weeks with ADT treatment significantly prolonged the survival of patients by 13.6 months compared with ADT alone, and the median time of biochemical, symptomatic or radiographic progression was 20.2 months in the combination group and only 11.8 months in ADT-alone group. In addition, the docetaxel plus ADT treatment group exhibited 27.7 % decrease in PSA levels to less than 0.2 ng/mL compared to 16.8 % in the ADT only group (Sweeney et al. 2015).

As discussed by Sundararajan and Vogelzang (2014), several subsequent phase 3 studies were conducted using docetaxel in combination with other agents, such as immune modulators, vascular endothelial growth factor receptor inhibitors, monoclonal antibodies, and tyrosine kinase inhibitors, none of which showed any improvement in the overall survival rates compared to the standard treatment using docetaxel and prednisone. One of these studies was

conducted by treating 1059 patients with docetaxel and prednisone in combination with lenalidomide or placebo (NCT00988208), the addition of lenalidomide did not demonstrate any improvement in overall survival and led to greater toxicity levels (Sundararajan & Vogelzang 2014).

The standard treatment used to treat patients with progressed CRPC after docetaxel treatment is cabazitaxel (25 mg/m² every 3 weeks) in combination with ADT agents such as abiraterone acetate or enzalutamide (Nakouzi et al. 2015; Omlin et al. 2014; Sonpavde et al. 2015). This second-generation taxane was proven by phase 1 and 2 trials that it has anti-tumour activity and increases overall survival, although toxicity is still considerable. Many patients required the cabazitaxel dose to less than 25 mg/m² in the trials (Pivot et al. 2008; Mita et al. 2009; Massard et al. 2017). De Bono et al. (2010), in a randomized phase 3 study comparing prednisone plus cabazitaxel to mitoxantrone in 755 males, demonstrated that overall survival was longer in cabazitaxel treated group than the mitoxantrone arm. However, the study also demonstrated that 82% of cabazitaxel treated males exhibited neutropenia compared to 53% in the other group (de Bono et al. 2010). These results demonstrated the efficacy of cabazitaxel but at the price of increased levels of toxicity and adverse side effects compared to other agents and combinations. CRPC is still regarded as incurable and toxicity associated with chemotherapy agents results in poor quality of life (Hotte & Saad 2010). These reasons stress the urgent need for alternative approaches to treat PCa that confer less toxicity and more efficacy than chemotherapy drugs.

1.6 Novel and targeted therapies

Improvements in our biological and molecular knowledge of prostate cancer progression have transformed the way CRPC is managed, improving survival times and reducing unwanted side-effects (Macfarlane & Chi 2010).

1.6.1 Androgen-targeted new therapies

CRPC is believed to be still driven by AR signalling and hence targeting this axis remains an important window for new therapies. For example, previous in situ hybridisation studies reported that 20–30% of androgen-independent prostatic tumours exhibit *AR* gene amplification (Koivisto et al. 1997; Linja et al. 2001) and most of which showed an average of 6-fold higher expression than that of androgen-dependent tumours or BPH (Linja et al. 2001). This is thought to hypersensitise the pathway to the residual low levels of androgens that are synthesised by the adrenal gland and intra-tumoural steroid production (Osanto & Van Poppel 2012). For this reason, several AR targeting agents are in clinical use for the treatment of CRPC. For example, CYP17 inhibitors (inhibition of adrenal androgen production, Table 1.2 and 1.5) have been shown to be effective in CRPC (Sternberg 2012). Abiraterone acetate, for instance, has been demonstrated to improve the survival of CRPC patients that had experienced docetaxel failure (Altavilla et al. 2012). This family of inhibitors (e.g. abiraterone acetate and Orteronel) are still under investigation and on-going clinical trials are assessing their efficacy in combination with chemotherapies (Yoo et al. 2016).

Orteronel inhibits the 17,20 lyase activity of the enzyme CYP17A1, which forms an important step of androgen synthesis in the testes, adrenal glands and prostate cancer cells (Van Hook et al. 2014). Orteronel possess greater specificity for 17,20 lyase over 17 hydroxylase and therefore appears to be more specific compared to abiraterone acetate (Alex et al. 2016). Phase 3 studies have shown that this inhibitor increases progression-free survival (PFS) and reduces PSA levels, however, it did not enhance the overall survival when combined with chemotherapeutics (Fizazi et al. 2015).

Other examples of newly developed ADT agents are Seviteronel (VT464) and Galeterone (Imamura & Sadar 2016). Seviteronel is a novel non-steroidal CYP17 inhibitor and AR-antagonist, it targets 17,20 lyase over 17 α hydroxylase and blocks the AR variants F877L

Table 1.5 Novel androgens targeted drugs.

Drug name	Mechanism of action	Status
Abiraterone acetate	Irreversible inhibitor of CYP17.	Under clinical phase II study with apalutamide (NCT03360721).
Orteronel (TAK-700)	Inhibits the 17,20 lyase activity of the enzyme CYP17A1.	Phase III double blind study with prednisone was completed in 2016 (NCT01193244).
Seviteronel (VT464)	CYP17 inhibitor, AR antagonist, and reduces the intratumoral androgen levels.	Multiple phase I/II and II studies. (NCT02012920), (NCT02445976), (NCT02130700).
Galeteron (VN/124-1, TOK-001)	CYP17 inhibitor, AR antagonist, and decreases intratumoral androgen levels.	Phase III compared to enzalutamide was terminated 2017 (NCT02438007).
Apalutamide (ARN-509)	AR antagonist targets the AR ligand-binding domain and prevents AR nuclear translocation.	Under clinical phase II with abiraterone acetate (NCT03360721).
CFG920	CYP17A1 inhibitor.	I/II phase studies completed, no further studies.

and T878A, which were shown to be correlated with resistance to enzalutamide and abiraterone acetate, respectively (Alex et al. 2016). Galeterone exerts a similar mechanism of action as Seviteronel, both have no inhibitory effect on 17 α hydroxylase and hence have reduced side effects (Imamura & Sadar 2016). These and other ADP-based newly developed drugs are still under investigations and clinical trials, and they might be approved in future by FDA (Table 1.5).

In addition to new ADTs, new antiandrogens are also being developed. AR-antagonists such as apalutamide and PAY1841788 (ODM-201) are new AR-targeting drugs that bind to the ligand binding domain of the AR and inhibit its nuclear translocation and hence halt the transcription of AR-target genes (Yoo et al. 2016). These new AR-antagonists were shown to have a good safety profile, antitumour activity and to reduce PSA levels (Smith et al. 2016; Shore 2017). These drugs are currently in clinical trials to elucidate their efficacy for CRPC.

1.6.2 Cytotoxic and pathway-based agents

ADT agents and third generation antiandrogens have proved to be effective for CRPC; however, resistance will occur in most cases (Madan et al. 2011; Karantanos et al. 2013). For this reason, novel therapeutic strategies that do not target the AR pathway are needed. These include immunologic/vaccine therapies such as sipuleucel-T, ipilimumab and Prostavac, antiangiogenic molecules such as cabozantinib and tasquinimod, and cytotoxic agents such as platinum-based drugs (Mehta & Armstrong 2016).

1.6.2.1 Novel vaccines and immunotherapies

Vaccines and immunotherapies aim to utilise the hosts immune system to recognize and destroy cancer cells (Schweizer & Drake 2014). For example, the recently approved (2010) sipuleucel-T targets antigen-presenting cells (dendritic cells, APCs), on the basis of stimulating a T-cell immune response targeted against prostatic acid phosphatase (PAP), an antigen that is

highly expressed in most prostate cancer cells (Anassi & Ndefo 2011). Sipuleucel-T is specifically used to treat asymptomatic or minimally symptomatic CRPC without visceral metastasis, and several on-going clinical trials are investigating the efficacy of Sipuleucel-T with other agents (Wei et al. 2015). For example, an on-going phase 2 clinical study is investigating sipuleucel-T in combination with R223 for the treatment of asymptomatic or minimally symptomatic CRPC (NCT02463799). Sipuleucel-T-based therapy was found to increase the median survival by 4.1 months in non-visceral CRPC patients when compared to placebo (Nussbaum et al. 2016). This is currently the only vaccine for PCa approved by the FDA, however an additional vaccine is also under development. The Prostavac vaccine is composed of vectors containing PSA and other T-cell stimulatory molecules (Singh et al. 2015) and it is in phase 3 clinical trials (Table 1.6).

Immune checkpoint inhibitors, such as ipilimumab (an IgG antibody that binds to cytotoxic T-lymphocyte antigen 4 (CTLA-4) and increases anti-tumour T-cell responses (Festino et al. 2018)) have also been trialled in PCa. Ipilimumab was shown to improve progression-free survival and reduce PSA levels, however it did not meet the endpoint of improved overall survival rates (Beer et al. 2017). Therefore, some phase 3 studies of ipilimumab were recently terminated (CA184095).

1.6.2.2 Targeted alpha and beta-particle therapies

Radioisotopes or radionuclides are particles emitting energy that can cause damage, so they are delivered to tumour cells to enhance their destruction (Waldmann 2003). Antibodies have been utilized to deliver alpha and beta-emitting isotopes specifically to tumour tissues (Brechtel 2007). Targeted alpha and beta-particle therapies form the new era of radio-immunotherapies for the treatment of PCa and other cancers. Wild et al (2011) discussed that several antibodies labelled with beta-emitting isotopes have been evaluated in PCa and limited success rates were reported. Due to lower energy and high travelling distances, more

Table 1.6 On-going PROSTVAC phase III clinical studies.

Phase study code	Drug name	Study design	Status
NCT01322490	PROSTVAC	Double blinded phase III of Prostvac +/- GMC-SF in CRPC.	Completed December 2017, no results released.
NCT02326805	PROSTVAC	Phase II Randomised, Placebo-controlled trial of Prostvac.	Not recruiting yet.
NCT02933255	PROSTVAC	phase II/I of Prostvac +/- Nivolumab.	Recruiting.

damaging/cytotoxic effects occur when a beta-emitter is used. Therefore, alpha-emitters have been recognised as a better alternative due to advantages such as higher linear energy transfer, minimum dependence on oxygen availability in tumour tissues, their shorter path length and ability to overcome radio-and chemo-resistance (Wild et al. 2011).

Several alpha-emitters have emerged over last few decades (Kozempel et al. 2018). A radioactive isotope called radium-223 dichloride (R223) is an example of an alpha-emitter. R223 was recently approved (2013) by the FDA for its benefit in increasing the overall survival of CRPC patients in the ALSYMPCA study (Hoskin et al. 2014). R223 is a calcium mimetic absorbed by bones that emits radiation to adjacent tissues and hence it is used to kill tumour cells in bone metastasises (Deshayes et al. 2017). The beneficial effect of this alpha-therapy was established by phase I, II, and III trial studies (Vogelzang 2017) and R223 was shown to enhance CRPC survival regardless of prior docetaxel use (Hoskin et al. 2014).

1.6.2.3 Cytotoxic chemotherapies

Since docetaxel's introduction in 2004, research has aimed to improve the efficacy of chemotherapeutics for the treatment of PCa. Several cytotoxic chemotherapeutics emerged and are currently under clinical investigations (Yoo et al. 2016). Cytotoxic agents like carboplatin (a platinum-based drug) have been under clinical investigation. Carboplatin is an analogue of cisplatin which is suggested to act by inducing DNA damage through interaction with purine bases of the DNA, and hence stimulate apoptosis (Dasari & Tchounwou 2014). This drug was shown to led to a decrease in PSA levels, in 18% of patients, when combined with docetaxel in tumours that progressed after prior docetaxel treatment (Ross et al. 2007). However, elevated toxicity was also reported when carboplatin was combined with docetaxel in other studies (Bouman-Wammes et al. 2017). Minimal clinical efficacy was obtained when carboplatin was used in combination with the mTOR inhibitor everolimus in a phase II study (Vaishampayan et al. 2015). Other studies are currently on-going (NCT02311764, NCT01505868, and

NCT02598895) to evaluate its efficacious and anti-tumoural profile as a single and combined therapy.

Another novel cytotoxic drug is osteodex (ODX), which is a bone-targeting polybisphosphonate used against metastatic CRPC. ODX was shown to have well tolerated toxicity and promising efficacy levels (Thellenberg-Karlsson et al. 2016). This drug is also under clinical phase 2 studies for further investigations of its efficacious properties and tolerability (NCT02825628).

1.6.2.4 Gene-based and personalised therapies

The anatomy of the prostate, the natural history of the disease, and the increased volume of knowledge in relation to the molecular basis of prostate cancer rendered it an attractive target for gene-based therapy (Patel et al. 2004). Several genes, that have been found to be up/down-regulated or mutated in prostate cancer cell lines and tumour tissues, are regarded as potential therapeutic targets for alternative novel therapies. An example of these is the gene *TP53* which was found to be mutated in a subgroup of PCa patients (Heidenberg et al. 1995). The potent tumour suppressor activity of *TP53* has made restoration of the wild-type function a promising anti-tumour approach for various cancers (Martinez 2010). Chen et al. (2014) discussed that several clinical trials were conducted using restoration of *TP53* function and utilised a recombinant human serotype5 adenovirus to insert the wild-type *TP53* gene to tumour cells. Gendicine was the first vector-based agent (Avp53) approved for clinical use of this strategy. These studies were carried out in several inactivated *TP53* cancers and demonstrated that ectopic expression of *TP53* wild-type led to induction of cell death and cell cycle arrest (Chen et al. 2014). In addition to *TP53*, a large number of other suppressor/activator mutations were associated with prostate cancer progression and could offer various strategies for novel therapeutics (Robbins et al. 2011; Taylor et al. 2010; Kan et al. 2010).

1.6.2.5 Alternative targets and pathways

As mentioned above, inhibitors are being developed to target AR-independent pathways that have been shown to be critical for PCa progression. For example, antiangiogenic molecules such as cabozantinib and tasquinimod (Brower 2016; Patnaik et al. 2017), and signal transduction targeted agents such as everolimus (an mTOR inhibitor) (Templeton et al. 2013), are being developed. mTOR (target of rapamycin) is a serine-threonine kinase down-stream of PI3K (Laplane & Sabatini 2012; Soliman 2013). mTOR is implicated in signalling of protein synthesis, cell growth, proliferation, angiogenesis, and survival through the action of its complexes including mTORC1 and mTORC2 (Kaur & Sharma 2017). This signalling pathway is believed to be upregulated in CRPC and is hence a potential therapeutic target for progressive prostate cancer (Bitting & Armstrong 2013). However, inhibition of this pathway with everolimus was found to have a minimal effect on CRPC and led to an upregulation of AR-signalling. For this reason, everolimus was subsequently combined with ADT/antiandrogens (Wang et al. 2008). For example, combination of this everolimus with the AR-antagonist bicalutamide, in a phase 2 study in bicalutamide-naïve CRPC patients, led to a significant PSA decrease ($\geq 50\%$) in 62.5% of patients with a median overall survival of 28 months, but adverse grade 3 and 4 events such as anaemia, hyperglycaemia, anorexia, abdominal pain, and nausea were reported in 58% of the patients (Chow et al. 2016). Combination of everolimus with docetaxel and bevacizumab was found to have similar outcomes to the bicalutamide study; the PSA decrease ($\geq 50\%$) was detected in 74 % of patients, overall survival was 21.9 months and adverse side effects were reported (Gross et al. 2018). The overall survival is higher in the latter combination study compared to docetaxel monotherapy (17-19 months) as shown in a separate study (Tannock et al. 2004).

Tasquinimod is another therapeutic that is being developed for the treatment of PCa that has a unique mechanism of action. Tasquinimod targets specific immunosuppressive and pro-

angiogenic cells called the myeloid-derived suppressor cells (MDSCs) and inhibits their immune and angiogenic properties (Mehta & Armstrong 2016). This therapeutic inhibits the immunosuppressive properties of the tumour microenvironment by modulating specific interactions between MDSCs and the tumour cells (reviewed in (Raymond et al. 2014)). The preclinical studies of this agent demonstrated its success in exerting immunomodulatory and anti-angiogenic activity against CRPC, hence it has been in the final stages of clinical development for the treatment of this disease (Gupta et al. 2014). A double blinded global phase III study of this agent compared to placebo demonstrated improved progression-free survival (PFS) (median of 7 months and 4.4 months, respectively) in chemotherapy-naïve men with metastatic CRPC, however no benefit in overall survival was observed and significant side-effects were again described (Sternberg et al. 2016).

Cabozantinib is a tyrosine kinase inhibitor and regarded as a novel anti-angiogenic agent for CRPC that is currently still under investigation (Patnaik et al. 2017). This drug blocks several growth associated kinases, including hepatocyte growth factor receptor (HGF) and vascular endothelial growth factor (VEGF), that were demonstrated to be associated with PCa progression and bone metastasis (Fay et al. 2015). This novel approach of inhibiting these signalling pathways is based on the rationale that therapy resistance in metastatic cancer induces hypoxia, which in turn upregulates HGF and VEGF levels resulting in angiogenesis and stimulation of invasion (Vaishampayan 2014). Phase II trial studies in CRPC patients demonstrated that cabozantinib enhanced PFS and showed other encouraging anti-tumoural activity (Smith et al. 2013; Smith et al. 2014). However, a recent phase III study investigating the efficacy of this agent in chemotherapy-naïve CRPC patients demonstrated that the agent improved PFS but did not improve the PSA decline or overall survival in comparison with prednisone (Smith et al. 2016). Another phase III study of this agent combined with docetaxel and prednisone is on-going (NCT01683994).

More recently, a new poly-adenosine diphosphate-ribose polymerase (PARP)-inhibitor called olaparib, which was approved by FDA for certain ovarian and breast cancers with BRCA1/2 mutations (DNA repair aberrations) (Kim et al. 2015; Robson et al. 2017), have been in phase II/III clinical trials (NCT0347135, NCT0239893917, NCT02987543) to evaluate its anti-tumour activity in metastatic CRPC. A recent study by Mateo et al. (2015) showed that this agent induced a high response rate (33 %) in CRPC patients, and next-generation sequencing demonstrated that this response was associated with deleterious mutations in the *BRCA1/2* genes. These results are promising as this gene-targeted therapeutic approach could offer sustained responses for the right subgroup of patients, according to their genetic profiling, but this approach would be made more beneficial if incorporated with precise biomarkers that can identify such genetic alterations (Mateo et al. 2015).

1.7 Metabolism of cancer as a therapeutic window

An emerging field for novel cancer treatment strategies is tumour metabolism which is regarded as a hallmark of cancer (Kroemer & Pouyssegur 2008; Deberardinis et al. 2008; Hanahan & Weinberg 2011; Ros et al. 2012; Vander Heiden 2013; The Deberardinis 2014; Yizhak et al. 2014). The survival of cancer cells can be linked directly to altered metabolism for example by increasing aerobic glycolysis and lipogenesis (Costello & Franklin 2000; Benedettini et al. 2008; Ward & Thompson 2012; Wu et al. 2014). Several decades ago Otto Warburg observed that cancer cells convert pyruvate into lactic acid even in the presence of oxygen (termed the Warburg effect) (Warburg 1956). This switch to aerobic glycolysis sustains high energy levels in cancer cells as it makes 100 times more ATP than mitochondrial respiration, but this is associated with higher glucose consumption (Valvona et al. 2016). Oxidative phosphorylation generate 36 ATP molecules per one molecule of glucose, whereas aerobic glycolysis generates two ATP molecules per one glucose molecule (Vander Heiden et al. 2009). Such metabolic alterations could be seen as consequences of the genetic aberrations

that arise sporadically or as a result of harsh tumour microenvironment conditions such as hypoxia and poor nutrient availability (Cutruzzolà et al. 2017). Understanding the basis of metabolic alterations in relation to tumorigenesis and metastasis have made cancer metabolism an attractive area of research in cancer biology and drug discovery. Generally, how metabolic reprogramming occurs, which pathways are altered, and how they can be exploited for the invention of novel and beneficial cancer therapeutics form the main questions in the current research.

Drugs targeting altered cellular metabolism in cancer is not a new approach. Many metabolic reprogramming strategies have been translated into successful treatment regimens. For example, asparaginase, an enzyme that converts asparagine to aspartic acid and degrades glutamine (DeBerardinis & Chandel 2016), is a therapeutic target for lymphoblastic leukaemia (LL) and other types of lymphomas (Salzer et al. 2017). Inhibitors of this enzyme have been shown to improve event-free survival in children with ALL, which relies on asparagine for its high rate of protein synthesis and growth (Clavell et al. 1986).

1.7.1 Metabolism in normal and tumour cells

Metabolism has been an attractive axis to treat cancers because metabolic pathways are significantly altered in tumours to suit tumour growth and survival (Figure 1.12) (Vander Heiden 2013). However, cancer cell metabolism is altered in a heterogeneous manner according to several factors including tumour type, conditions inside the tumour, and nutrients available (Vander Heiden 2011). Therefore, therapeutics that target a metabolic pathway in one cancer may not work in others. Normal non-replicating cells maintain low ATP production via glycolysis (oxidative phosphorylation) to sustain homeostatic processes, however, proliferating cells would require energy not only for the replication process but further to support the anabolic requirements for macromolecule biosynthesis as well as to maintain cellular redox homeostasis to neutralize the toxic effect of reactive oxygen species (ROS) generated

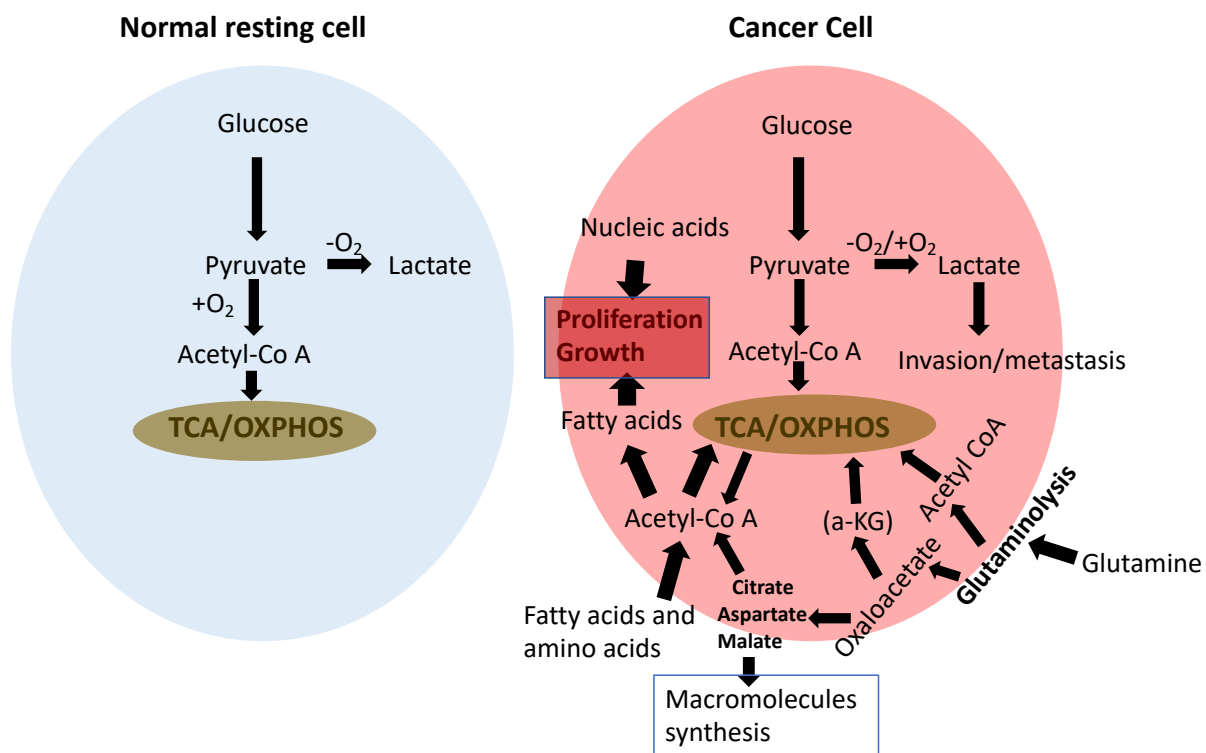


Figure 1.12 Metabolism of normal cell versus cancer cell.

Schematic shows the metabolic remodelling of cancer cells to maintain their growth and survival. Normal cells (blue) usually perform complete breakdown of glucose in presence of oxygen (O₂) into acetyl-CoA that enters the mitochondria for the respiratory cycle and ATP synthesis. Cancer cells (red) attenuate the conversion of pyruvate into acetyl-CoA in presence and absence of oxygen and instead produce lactate. Cancer cells use other sources for biosynthetic precursors such as glutamine, fatty acids, and other non-essential amino acids to maintain the tricarboxylic acid (TCA) cycle for ATP and macromolecule synthesis.

(Cantor & Sabatini 2012).

One of the best-known modifications in cancer metabolism, observed in 1920 by Warburg, is aerobic glycolysis (DeBerardinis & Chandel 2016). Aerobic glycolysis is associated with increased lactate production, regardless of the amount of oxygen available, which normally only occurs in hypoxic conditions in normal cells (Koppenol et al. 2011). Tumour cells convert glucose to lactate despite the fact that this process is far less efficient in energy production (ATP) compared to typical oxidation of glucose to pyruvate (Vander Heiden et al. 2009). The glycolytic use of glucose provides cancer cells with essential glycolytic intermediates that feed the metabolic demands of tumours (Lunt & Vander Heiden 2011).

Glycolysis is induced to meet the ATP required by cancer cells, and glycolysis' carbon forms the main resource of building blocks for fatty acid and nucleotide biosynthesis (Romero-Garcia et al. 2011). Therefore, the switch of cancer cells to fermentative metabolism of glucose was suggested to predominantly support the accumulation of biomass and maintenance of redox state (Cantor & Sabatini 2012).

Reprogramming of glucose metabolism is not sufficient to explain all of the alterations required for cancer cell survival and growth. For example, increased glutamine metabolism and elevated fatty acids synthesis are additional alterations associated with tumour metabolic reprogramming (Zhao et al. 2013). Cancer cells utilise nitrogen derived from glutamine to generate nucleotides, non-essential amino acids, and hexoamines (Zhu et al. 2017). Further, as the tricarboxylic acid (TCA) cycle provides several intermediates that can be redirected to biosynthetic and NADPH-generating pathways, proliferating cells are able to utilise these intermediates and maintain TCA through glutamine anaplerosis (Wise & Thompson 2010). The latter occurs through either glutamine conversion to glutamate which enters TCA cycle as α -ketoglutarate (α -KG) or via the carboxylation of pyruvate derived from glycolysis into oxaloacetate (Figure 1.11) (Cantor & Sabatini 2012; DeBerardinis & Chandel 2016).

An increase in metabolite flux in tumours can occur as a result of the oncogenic activation or loss of several suppressors of specific genes, especially those affecting glucose and glutamine uptake and catabolism, including mutations in *MYC*, *HIF1a*, *TP53*, the Ras-related oncogenes, and the LKB1-AMP kinase (AMPK), and PI3 kinase (PI3K) signalling pathways (Wu et al. 2015; Boroughs & DeBerardinis 2015). One of the most important signalling pathways associated with metabolism is the PI3K-Akt-mTOR pathway, which is frequently altered in malignancies (Dienstmann et al. 2014). This pathway is triggered by growth factors that stimulate PI3K (phosphatidylinositol 3-kinase) and downstream Akt (Alpha Serine-Threonine Kinase) and mTOR (mammalian target of rapamycin) pathways, which in turn initiate anabolic processes including increased glycolytic flux and fatty acid production following activation of HIF-1 (hypoxia-inducible factor-1) and SREBP (sterol regulatory element-binding protein), respectively (Dibble & Manning 2013). The PI3K-Akt-mTOR pathway is vital for cell survival in stress conditions, and as cancer cells emerge under such conditions, this pathway appears crucial for metabolic reprogramming in tumours (Porta et al. 2014). Activation of this cascade has been found to enhance the expression of *GLUT1*, a glucose transporter, and translocation of its encoded protein to the plasma membrane (Wieman et al. 2007). In addition, Akt also promotes the activity of hexokinases (HK) which phosphorylate glucose to abrogate its extracellular efflux (Elstrom et al. 2004; Engelman et al. 2006; Porta et al. 2014). Further, exogenous expression of constitutively active Akt was found to promote cell survival and maintain growth and homeostasis in growth factor deprived medium (Plas et al. 2001).

1.7.2 Metabolic pathways as novel therapeutic targets

As described above, metabolism is known to be distorted in malignant cells and therefore suggested to be a novel therapeutic approach to inhibit cancer cell proliferation with minimal effects upon normal cells. Inhibitors for several metabolic pathways are already in

development/clinical trials.

1.7.2.1 Targeting glucose and glutamine

Metabolic alterations are heterogeneous and occur according to the tumour microenvironment and nutrient availability. However, there are some common metabolic features shared between most cancers such as the alterations in glucose, glutamine, and mitochondrial metabolism (Kishton & Rathmell 2015). These hallmarks may provide targeting strategies to halt cancer proliferation and survival. Cancer genes can drive metabolic reprogramming in malignant cells, also several essential enzymes/proteins that regulate these metabolic pathways are found to be overexpressed/mutated in such cells (Dang 2012). For example, the glucose transporters GLUT1 and GLUT3 are found to be oncogenically mutated to allow high glucose uptake for cancer cells (Ganapathy-Kanniappan 2013), and other factors, such as those in the PI3K-Akt-mTOR pathway, are also mutated to further stimulate glucose consumption in malignant cells (Chen et al. 2016). Importantly, inhibition of factors involved in glucose or glutamine metabolism does attenuate the proliferation of cancer cells (Liu et al. 2012).

Various glutamine metabolism targeting agents have been investigated, however, similar to glycolysis inhibitors, the majority of compounds were found to have significant effects upon non-tumorigenic cells and hence only preclinical testing was performed (Ganapathy-Kanniappan 2013; Altman et al. 2016). Despite this, many other metabolic inhibitors have been approved for cancer treatment or are under clinical trials. For example, the glutamine metabolism inhibitor CB-839 (targeting the glutaminase enzyme which converts glutamine to glutamate) has been shown to have anti-tumour activity in several cancers (Gross et al. 2014; Jacque et al. 2015; Biancur et al. 2017), and is under clinical trials for further validation for solid tumours, lymphoid, and myeloid malignancies (NCT02071862, NCT02071888 and NCT02071927) (Fung & Chan 2017).

1.7.2.2 Targeting macromolecules synthesis and specific genetic alterations

Apart from targeting glucose and glutamine, other metabolic targeting strategies include inhibition of macromolecule synthesis, such as inhibition of nucleotide and fatty acid synthesis (Nishi et al. 2016; Shuvalov et al. 2017). Nucleotide synthesis forms an important part of cell division and proliferation, hence it gained interest as a potential novel strategy to halt cancer growth. The inhibition of enzymes implicated in nucleotide base synthesis by small molecules that mimic nucleotide metabolites (antimetabolites) has been a successful strategy to treat cancer for many years (Farber et al. 1948). Recent examples of such antimetabolite molecules are gemcitabine and cytarabine, which inhibit DNA-polymerase activity and these are currently being utilized to treat several cancers (Luengo et al. 2017).

An example of successful inhibitors that halt fatty acid synthesis is the fatty acid synthase (FASN)-inhibitor (TVB-2640) that is currently under clinical trials (NCT02980029, NCT03032484, NCT03179904) (Alwarawrah et al. 2016). FASN is over-expressed in cancer and its inhibition selectively induced apoptosis and abrogated growth and viability in xenograft tumour models (Heuer et al. 2017). In addition to these therapeutics, mitochondrial complex, asparagine synthesis and glutamine synthesis inhibitors are also under investigation (Luengo et al. 2017).

1.7.3 The potential side-effects of metabolism inhibition

Most of the currently used chemotherapeutics and radiation-based therapies result in cytotoxicity to normal cells as well as to cancer cells (Kalyanaraman 2017), which results in acute side effects that affect the patient's quality of life. This highlights the need for therapeutics that are selective for cancer cells with minimal effects on normal tissues. Using metabolic inhibition as strategy to treat cancers has proven to be effective, however toxicity is common with such agents because of the shared pathways and signalling between cancer and normal tissues (DeBerardinis & Chandel 2016). For example, inhibition of Pyruvate Dehydrogenase

Kinase 1 (PDK1), an enzyme commonly activated in solid tumours that deactivates the mitochondrial pyruvate dehydrogenase complex and thereby decreases the flow of pyruvate used by the TCA cycle, by the PDK-inhibitor dichloroacetate (DCA), was demonstrated to have good therapeutic activity against some cases of brain cancer. However, nerve toxicity was reported in some studies and the use of the therapy has therefore been restricted to selected patients (Muñoz-Pinedo et al. 2012).

Another example is L-asparaginase, which resulted in significant toxicity when it was used to treat pancreatic cancer patients (Lessner et al. 1980). Glutamine inhibition also exhibited a toxicity profile. For example, phase I study on relapsed leukaemia patients demonstrated that the glutaminase inhibitor CB-839, that shows a potent anti-tumour activity as indicated earlier, is associated with grade 1 and 2 toxicities such as transaminitis, thrombocytopenia, gastrointestinal events, and fatigue and one third of patients showed grade 3/4 toxicities like hematologic cytopenia (Wang et al. 2015). However, CB-839 combination with paclitaxel showed tolerable side effects in triple negative breast cancer patients (Fung & Chan 2017).

In addition, several agents that target the Warburg effect/glycolysis and lipogenesis have been established but none have reached the clinic due to their off-target effects. These side-effects including significant weight loss and were also found to have reduced efficacy *in vivo* (Muñoz-Pinedo et al. 2012). It was discussed by Pelicano et al. (2006) that it has proved difficult to predict the side-effects of glycolytic inhibitors especially in tissues that rely upon glucose as a main energy source such as the brain, testis, and retinae. The utilization of alternative sources such as amino acids and fatty acids by such tissues when glycolytic pathway is impaired remains unknown and warrants further investigation (Pelicano et al. 2006). Therefore, the specificity of the chosen pathways to be inhibited should be restricted to those that are crucial for the proliferation of cancer cells but not normal cells. This can be challenging

as different tumours and different foci of the same tumour can have different adaptations to suit their survival.

Minimisation of side-effects might be achieved through the use of combinational therapeutic strategies; the standard therapy (chemotherapy) plus metabolic inhibition might form an important rationale to maximize efficacy of such treatments and minimize the associated toxicity to normal cells (Kalyanaraman 2017). In addition, the heterogeneity in genetic and epigenetic changes that occur in the tumour cell population, which changes over time because of genetic instability, also provides a rationale for targeting multiple genes/pathways found to be altered in a given tumour (Pelicano et al. 2006). It is therefore important that customized treatments regimens, adjusted according to the type and the stage of the tumour and the common genetic/pathways reprogramming to eradicate all malignant cells with minimum off-target effects, are developed.

1.7.4 Metabolism of normal prostate

Typically, in normal mammalian cells, the complete oxidation of glucose or fats occurs by generating citrate that enters the Krebs cycle for ATP synthesis and this is coupled to the generation of various Krebs cycle intermediates which are employed in biosynthetic pathways (Costello & Franklin 2000). In prostate tissues (especially epithelial cells in the peripheral zone) this is different. Prostate epithelial cells synthesise citrate and do not oxidise it; instead accumulation of citrate take place in these cells as high citrate levels are a constituent of semen (Dakubo et al. 2006). The increased levels of citrate is also accompanied with zinc accumulation (Figure 1.12) (Costello et al. 2004). Zinc is transported to the cells from the extracellular space by the ZIP family of plasma membrane transporters, and distributed to different organelles via the ZnT (slc30A) intracellular transporters (Costello & Franklin 2016).

The accumulation of zinc in prostatic tissues have an essential role in inhibiting the enzyme aconitase that catalyses the oxidation of citrate into isocitrate to complete the Krebs

cycle energy production process (Figure 1.12) (Eidelman et al. 2017). However, as discussed by Costello and Franklin (2000) the cells of the central zone of the prostate do not accumulate zinc and still carry out the citrate-oxidation like other mammalian cells.

In other mammalian cells, enzymes such as phosphofructokinase (PFK) are inhibited by high concentrations of citrate and hence glycolysis is halted in a negative feedback loop. However, this is also different in the prostatic glandular cells, which retain high citrate levels but still demonstrate high glycolysis levels (Costello & Franklin 2000). This may be explained by the utilization of aerobic glycolysis (Figure 1.13) (Wu et al. 2014). Costello and Franklin (2016) indicated that citrate and zinc levels in prostatic epithelial tissues are significantly greater than other soft tissues, 30-80 and 10-20-fold respectively. The synthesis of citrate and zinc does occur in all other types of cells, however citrate is predominantly produced in mitochondria and used in the Krebs cycle or delivered to the cytosol and converted to acetyl-CoA for lipid synthesis, but accumulations of these ions are only seen in prostatic tissues (Costello & Franklin 2016). More interestingly, the peripheral zone where citrate and zinc are accumulated is where prostatic cancers usually develop (Sinnott et al. 2015; Wernert et al. 2011). These observations demonstrate that the prostatic tissues harbour unique metabolic modifications to maintain their secretory functions, however the role of citrate in prostatic cells and prostatic secretions is not completely understood.

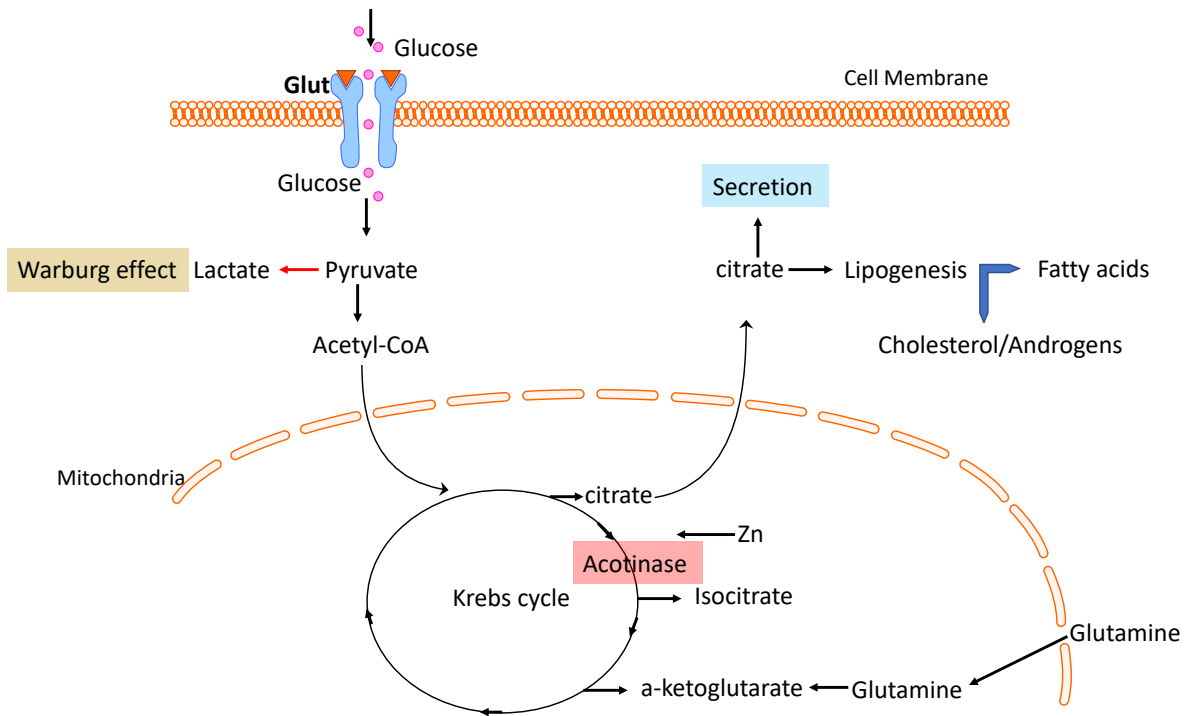


Figure 1.13 Regulation and maintenance of specific metabolic signalling in normal/benign prostatic cells.

The secretory function of epithelial cells in the peripheral zone requires adaptive metabolic modification to suit their roles. The citrate formed in Krebs cycle is not completely oxidised and instead it is accumulated and secreted into cytosol to be used in lipogenesis or to be a part of the prostatic fluids. This is regulated by increased zinc concentrations which deactivate *acotinase* enzyme that perform citrate oxidation in the Krebs cycle.

1.7.5 Metabolic alterations in prostate cancer

1.7.5.1 Citrate metabolism and aerobic glycolysis in prostatic carcinomas

As discussed, prostatic epithelial cells in the peripheral zone of the prostate accumulate zinc and citrate. However, in prostate cancer it is reported that zinc levels are reduced, and this is associated with citrate oxidation and Krebs cycle progression to supply malignant cells with energy (Franz et al. 2013). The expression of zinc transporters (e.g. ZIP1) are also down-regulated in prostatic adenocarcinomas compared to intact prostatic tissues (Franklin et al. 2005; Costello et al. 2011). This phenotype (citrate complete oxidation through the Krebs cycle and a reduction of zinc levels) is seen in prostate cancer cells, especially in the early stages, rather than the Warburg effect (Zadra et al. 2013; Sadeghi et al. 2015; Twum-Ampofo et al. 2016) which is present in most other cancers (Ganapathy-Kanniappan & Geschwind 2013; Deberardinis 2014; Kishton & Rathmell 2015). Therefore, most early prostatic cancers do not rely on aerobic glycolysis for energy and biomass production, instead they use citrate oxidation in the Krebs cycle and resumed oxidative phosphorylation as well as fatty acids and protein catabolism, however, late stages of PCa, when large numbers of mutations and modifications take place, utilise the Warburg effect (aerobic glycolysis) (Eidelman et al. 2017).

1.7.5.2 Amino acids in prostate cancer

As discussed above, glutamine forms an essential fuel for many cancers and PCa is known to utilise amino acids for ATP and macromolecule biosynthesis. Further, the expression of glutaminase-1, an enzyme that carries out glutaminolysis, is found to correlate with PCa progression (Pan et al. 2015). The glutamine transporter ASCT2 (Alanine, serine, cysteine-preferring transporter 2) is also over-expressed in PCa, and the inhibition of this protein was associated with reduction of glutamine intake and cell cycle progression *in vitro* and decreased PC-3 xenografts growth and metastasis *in vivo* (Wang et al. 2015). In addition, other amino

acids might be important for PCa growth. For example, arginine was proposed as a potential target for the treatment of PCa since this strategy had been shown to be effective in inhibiting other cancers (Eidelman et al. 2017). However, its depletion did not show a significant induction of apoptosis in PCa cell lines (Kang et al. 2000; Hsueh et al. 2012). This may be explained by the fact that these cell lines express argininosuccinate synthetase (ASS), which carries out the *de novo* conversion of citrulline into arginine. Hence, arginine depletion might be more effective in tumours lacking ASS expression (Feun et al. 2008). In addition, transporters of amino acids such as L-type amino acids transporters (LATs) are over-expressed in all stages of PCa and their knockdown inhibits cell growth, cell cycle progression, and metastasis *in vivo* (Wang et al. 2013). This suggests the importance of the alteration of amino acid metabolism in PCa progression.

1.7.5.3 Lipids metabolism and prostate cancer progression

Another essential cellular energy source utilized by PCa cells is lipids. PCa cells regulate lipids synthesis and/or uptake by androgens (Butler et al. 2016). However, at some stages (CRPC) PCa cells are able to synthesize lipids independently from androgens probably through the reactivation of AR-signalling by elevated expression of AR splice variants (Han et al. 2018). The latter is linked to poor prognosis in prostatic carcinomas and other cancers (Butler et al. 2016). *De novo* lipid synthesis is correlated with the over-expression of certain lipogenic enzymes (probably due to oncogenic aberrations) such as fatty acid synthase (FASN) and α -methylacyl-CoA racemase (AMACR), which convert long branched fatty acids to a form that facilitates β -oxidation (Wu et al. 2014). In addition, androgens are suggested to enhance fatty acid synthesis by increasing the activity of lipogenic enzymes (Swinnen et al. 1997). It was also found that the expression of multiple factors involved in lipid synthesis (ATP citrate lyase (ACLY), acetyl-CoA carboxylase α (ACACA), FASN, long chain fatty acyl-CoA synthetases

1, 3 and 5 (ACSL1, ACSL3, ACSL5) and sterol regulatory binding protein 1 (SREBP1)) are increased in PCa (Wu et al. 2014).

Alterations in the synthesis and metabolism of lipids can occur as a consequence of several oncogenic events including deactivation or loss of *PTEN*, *Akt* activation, loss or mutation of *TP53* or *BRCA1*, steroid hormone action, and intra-tumoural hypoxic conditions (Butler et al. 2016). Lipids in PCa cells undergo β -oxidation for energy production, stored as intracellular lipid droplets, or form phospholipids for membrane synthesis supporting cell growth and survival (Butler et al. 2016).

An important type of lipid for prostatic cell growth is cholesterol, which is an essential precursor of androgens synthesis as well. The accumulation of cholesterol has also been linked to the aggressiveness of PCa (Pelton et al. 2012). For example, Yue et al. (2014) found that high-grade PCa cells were found to have an increase in lipid droplets consisting of esterified cholesterol and this increase was linked to stimulation of the PI3K-Akt pathway and loss of PTEN activity; the latter is a tumour suppressor found to be commonly deleted/mutated in PCa and is associated with disease progression and poor prognosis (Geybels et al. 2017). Additionally, the depletion of esterified cholesterol led to a reduction in cell proliferation, invasion and the growth of mouse tumour models (Yue et al. 2014). These data suggest that lipids including cholesterol and fatty acids form an important energetic source for PCa (Liu 2006) suggesting that they might be good targets for novel therapies and many may be useful prognostic biomarkers.

1.7.6 Targeting novel metabolic reprogramming in CRPC

Several attempts have been made to target metabolic signalling in advanced prostate cancer. For instance, fatty acids synthesis factors were targeted to enhance the sensitivity of PCa to conventional therapies such as AR-antagonism. An example is a study conducted by Shah et al. (2016) which demonstrated that inhibition of ATP-citrate lyase (ACTL), an enzyme

implicated in fatty acids synthesis, decreased AR levels, inhibited proliferation, and promoted apoptosis of PCa cells when used with AR-antagonists. More recently, a model of invasive and metastatic PCa cells (PC3) was used to measure the accumulation and metabolism of long chain fatty acids. The study showed that these cells had enhanced metabolism and transport of the long chain fatty acids into the mitochondria. Further, inhibition of this transportation into the mitochondria inhibited PC3 proliferation (Marín de Mas et al. 2018).

Apart from targeting lipids biosynthesis, amino acids essential for PCa such as glutamine are also still under investigation. A recent study demonstrated that inhibition of the glutamine transporter ASTC2 led to glutamine uptake inhibition, mTOR pathway deactivation, and growth inhibition of PC3 xenografts (Wang et al. 2014). This suggests that metabolism of fatty acids, amino acids and other metabolic factors are potential therapeutic targets for CRPC that warrant further investigation.

1.8 Induction of tumour cell death

Targeted therapies for the treatment of cancer usually arise from the investigation of the molecular pathways implicated in cell growth and cell death (Ricci & Zong 2006). Tumours are treated with agents that enhance cell death, and the mechanism by which cancer cells die does not strictly mean apoptosis or programmed cell death. Chemotherapeutics, for example, can promote cell death through several mechanisms including necrosis, autophagy, and mitotic catastrophe (Ricci & Zong 2006). In normal cells, the decision on which of these cell death pathways will be used is linked to many factors such as the type of tissue, physiological nature, developmental stage and the type of death signal (Elmore 2007). However, in the case of cancer, apoptosis is defective and therefore unfavoured conditions such as metabolic stress or hypoxia often cannot induce the apoptotic cascade. This can therefore lead to therapy resistance (Jin et al. 2007). Inhibition of apoptotic pathways is a general phenomenon by which most cancers

promote their survival, and targeting pro-apoptotic factors is a strategy to overcome tumour cell survival and resistance to anti-cancer drugs (Rivera et al. 2017).

1.8.1 Defective apoptosis and cancer

Apoptosis is a well characterised form of programmed cell death (Rastogi et al. 2009). The process can be defined as a series of events that result in phenotypical changes including cell membrane blebbing, cell shrinkage, chromatin condensation, DNA fragmentation, loss of adhesion to other cells or the extracellular matrix and finally formation of apoptotic bodies which are engulfed by macrophages or neighbouring cells (Ouyang et al. 2012). There are two pathways that can induce apoptosis: the intrinsic and extrinsic pathways (Figure 1.14). The former take place as a result of intracellular stimuli, such as DNA damage and oxidative stress, where pro-apoptotic bcl2 factors (such as Bax, Bak, and Bid) initiate the permeabilisation of mitochondrial membranes which in turn results in the release of apoptotic proteins including cytochrome c, Smac/DIABLO, Omi/HtrA2, apoptosis-inducing factor (AIF) and endonuclease G. The latter proteins induce either caspase-dependent or caspase-independent cell death effectors (Fulda & Debatin 2006).

In the case of caspase-dependent apoptosis, caspase 3 is activated by the formation of the cytochrome c/ABAF-1/caspase 9 apoptosome complex, which subsequently cleaves several substrates leading to apoptotic cell death (Figure 1.14). Saelens et al. (2004) stated that the caspase-independent pathway occurs through the nuclear translocation of AIF and endonuclease G, which mediate DNA-fragmentation. SMAC/Diablo and Omi/HtrA2 are suggested to play roles in caspase-dependent apoptosis, and may induce caspase-independent cell death (Saelens et al. 2004). SMAC/Diablo is found to be released under conditions that induce apoptosis which suggests that it is required in this cell death modality (Maycotte et al. 2008). It is a positive regulator of apoptosis by activating caspases and by inhibiting IAPs. A recent work by Paul et al. (2017) demonstrated that SMAC/Diablo has implicated in lipid

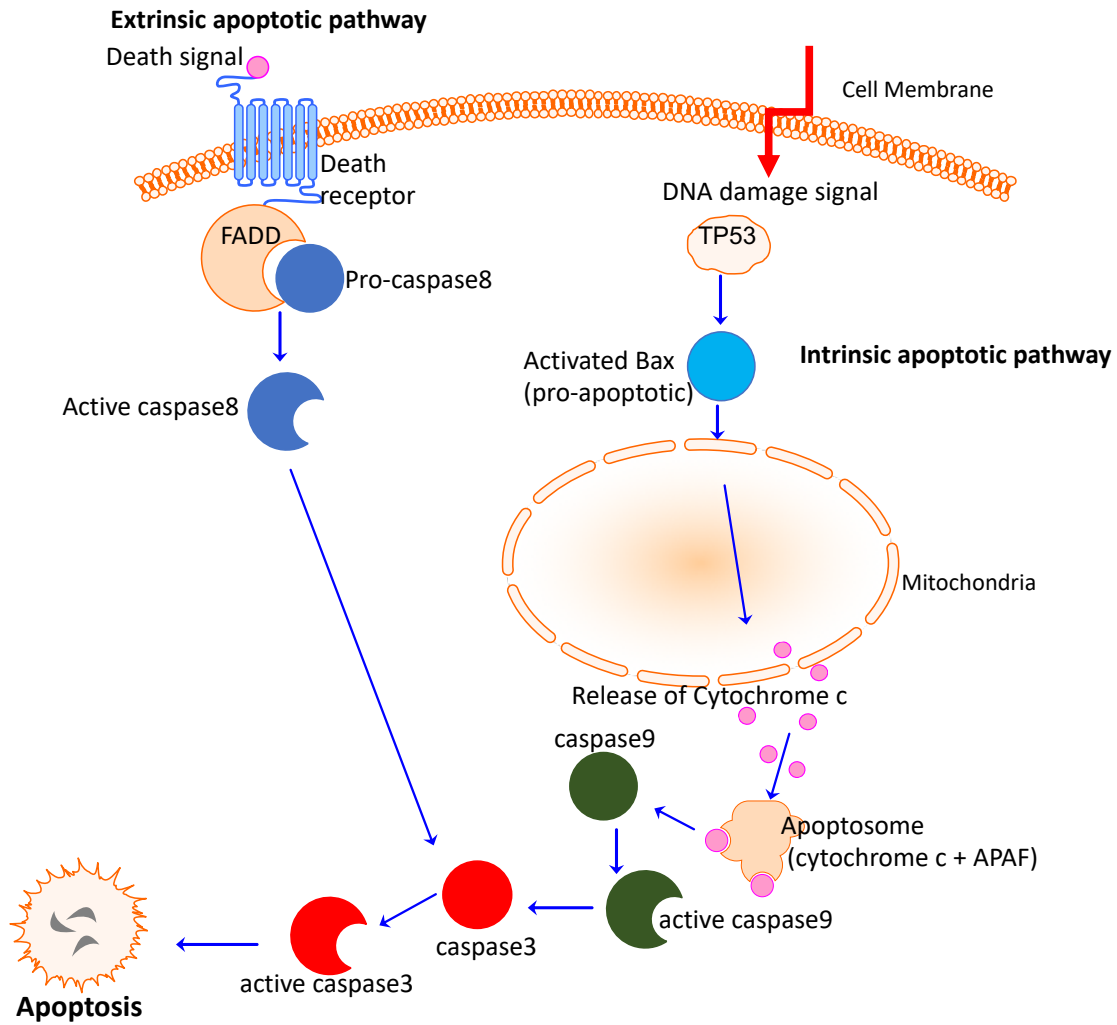


Figure 1.14 Intrinsic and extrinsic apoptosis pathways.

Apoptosis can occur in two ways according to the type of stimuli. Intrinsic pathway is initiated by intracellular stimuli like DNA damage which triggers TP53 apoptotic activity and caspase cascade take place. The other type of apoptotic pathways is the extrinsic cascade which is stimulated upon death signal that enhance ligands to bind to death receptors leading to recruit adaptor molecules such as Fas-associated death domain (FADD) followed by caspase 8 and caspase 3 cleavage and activation.

biosynthesis when silenced by siRNAs, it led to reduction of phospholipids and next generation sequencing analysis of SMAC/Diablo silenced tumour tissues was associated with altered expression of genes related to cellular membrane and extracellular matrix of genes associated with lipid, metabolite, and ion transport. These findings suggested non-apoptotic functions for SMAC/Diablo; it is essential for lipid biosynthesis and cancer cell progression which also could explain its overexpression profile in tumours (Paul et al. 2017).

Extrinsic apoptosis (Figure 1.14), as explained by Fulda and Debatin (2006), is induced by extracellular stimuli such as tumour necrotic factor- α (TNF α), first-apoptotic signal receptors (FasR) ligands e.g. CD95/APO1, or TRAIL (TNF related apoptosis inducing ligand) which bind to death receptors of the tumour necrotic factor receptors (TNFR) superfamily. TNFR, following ligand binding, form dimers activating the death domains, which in turn recruit adaptor molecules such as Fas-associated death domain (FADD) (Su et al. 2015). The latter then recruits procaspase-8/10 to form the death inducing signalling complex (DISC) leading to caspase-8 activation which in turn cleaves caspase-3 and the rest of apoptotic pathway (Fulda & Debatin 2006).

Genetic aberrations in several pro-apoptotic or anti-apoptotic factors is a hallmark of carcinogenesis (Fernald & Kurokawa 2013), for example mutations in *TP53* (Lowe & Lin 2000). It was explained by Fridman and Lowe (2003) that cellular stresses such as DNA damage, hypoxia, or aberrant oncogene expression promote *TP53* activity which can block cell-cycle progression and promote DNA repair, cellular senescence, or apoptosis according to the damage level. Therefore, defective *TP53* can result in checkpoint defects, genomic instability and abnormal survival, resulting in the uncontrolled proliferation and evasion of apoptosis (Fridman & Lowe 2003). *TP53* regulates the transcriptional activity of a number of pro-apoptotic factors including Puma, Noxa, Bim, Bid, Bik, Bak, Bax, Apaf-1, Bmf, Hrk, Pag608, Drs, Fas and Gadd45, and is therefore directly linked to the activation of

mitochondrial membranes to release apoptotic factors and hence induce apoptosis (Rastogi et al. 2009; Miyashita et al. 1994).

Genetic alterations resulting in over-expression of anti-apoptotic proteins or down-regulation of pro-apoptotic factors are also directly related to impaired apoptosis (Placzek et al. 2010; Ionov et al. 2000). The anti-apoptotic phenotype of tumours then can be a result of the deregulation of apoptotic gene expression which might occur downstream of cell checkpoints like *TP53* or other genes that could induce the release of these factors by affecting mitochondrial membrane integrity (Rastogi et al. 2009). These genetic alterations affect cell fate not only in the development of neoplastic cell populations but also in drug-resistance phenotypes.

1.8.2 Non-apoptotic cell death pathways

Necrosis is a non-apoptotic form of cell death that occurs as a result of irreversible injury as a consequence of pathogens or extreme conditions such as hypoxia, heat, or radiation (Adigun & Bhimji 2017). Necrosis manifests phenotypic changes that include cytoplasmic swelling, irreversible plasma membrane injury, organelle damage and random degradation of DNA (Festjens et al. 2006). This type of cell death is usually accompanied with the release of the cells contents together with cytokines, resulting in inflammation (Kanduc et al. 2002). Importantly, it has been suggested that necrotic cell death could be exploited as a therapeutic strategy to kill cancer cells when apoptotic cascades are deactivated (Festjens et al. 2006).

Necrosis is known to be caspase-independent because treatment of cells with $\text{TNF}\alpha$, a cytokine produced by macrophages that induces apoptosis, resulted in necrosis induction when caspases were inhibited in embryonic fibroblasts (Lin et al. 2004). Similarly, inhibition of caspases also enhanced $\text{TNF}\alpha$ -induced necrosis in L929 fibrosarcoma cells (Vercammen et al. 1998). Further, FasR ligand in caspase 8 deficient Jurkat cells also promoted necrosis

(Kawahara et al. 1998). Therefore, death receptors (like TNFR, FasR, and TRAILR) have been demonstrated to regulate necrosis (Nikoletopoulou et al. 2013). However, it has now become clear that multiple non-apoptotic pathways exist such as necroptosis, autophagy, and pyroptosis (Tait et al. 2014). Furthermore, programmed cell death does not strictly mean apoptosis and cross-talk between cell death pathways has been described (Figure 1.15) (Conrad et al. 2016).

Necrosis has recently been proposed to occur in a controlled and regulated manner and it has been suggested that the term should encompass all forms of caspase-independent death pathways including necroptosis, parthanatos, ferroptosis or oxytosis mitochondrial permeability transition (MPT)-dependent necrosis, pyroptosis and pyronecrosis, and cell death associated with the release of (neutrophil) extracellular traps, that is defined as NETosis or ETosis (Pasparakis & Vandenabeele 2015). However, some non-apoptotic cell death mechanisms such as pyroptosis and autophagy lack the clear necrotic phenotypic characteristics associated with necrosis (Conrad et al. 2016). Among all these mechanisms (reviewed in (Pasparakis & Vandenabeele 2015)) necroptosis is the most characterised mechanism of caspase-independent cell death.

The process of necroptosis (Figure 1.15) as described by Vanlangenakker et al. (2011) occurs upon ligand (TNF/TNF α) binding to death receptors (TNFR) which leads to the recruitment of several factors, including TNFR-associated death domain (TRADD), receptor interacting protein-1 (RIP1), cellular inhibitor of apoptosis 1 (cIAP1), cIAP2, TNFR-associated factor 2 (TRAF2) and TRAF5, to the cytoplasmic part of the receptor dimers and this big structure is termed as complex I. At this point several signalling pathways including NF- κ B signalling, cell survival signals, and cell-death-inducing cascades are initiated as a result of ubiquitylation and deubiquitylation (Conrad et al. 2016). The polyubiquitination of RIP1 by cIAP2 activates NF- κ B pathways through TRAF2/5 and promoting cell survival. NF- κ B signalling also leads to FLIP (FLICE inhibitory protein) inhibition of caspase 8 cleavage and

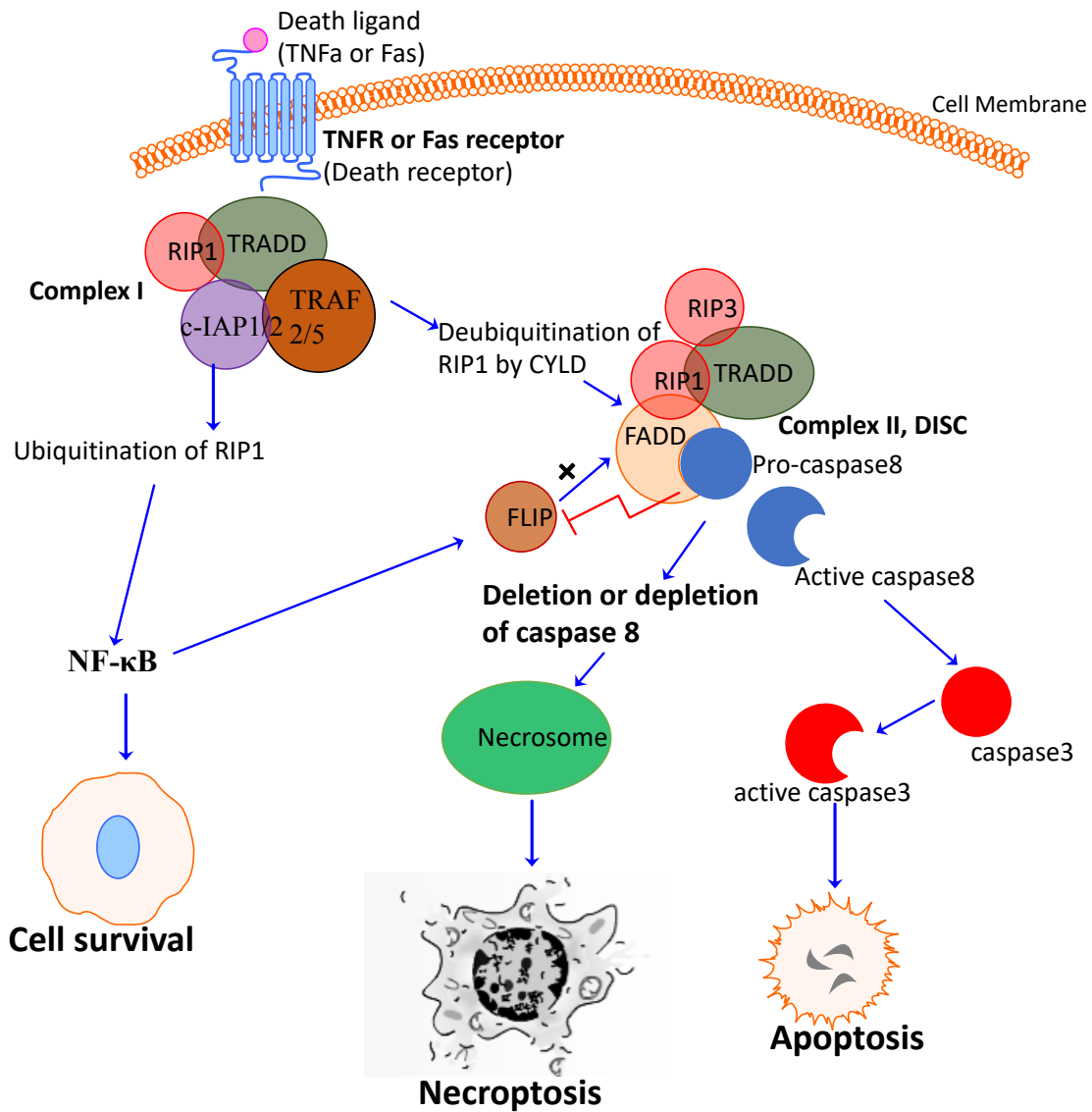


Figure 1.15 The signalling pathways of cell survival, apoptosis, and necroptosis (interconnection between cell death pathways).

Caspase-dependant and independent pathways are believed to cross-talk through tumour necrotic factor (TNF) or death receptor pathways. Death receptor activation results in the recruitment of several factors including TRADD, RIP1, TRAF2/5, and cAIP1. Ubiquitination of RIP1 by cAIP1 promotes cell survival, while its deubiquitination by CYLD results in the recruitment of FADD, RIP3, and caspase 8 to the TRADD complex to form complex II or DISC. The latter activates caspase 8 cleavage and leads to apoptosis. Necroptosis is believed to occur as a result of deletion or depletion of caspase 8.

apoptosis therefore promoting cell survival (Micheau & Tschopp 2003; Vanlangenakker et al. 2011). In contrast, the deubiquitination of RIP1 by cylindromatosis (CYLD) promotes the formation of complex II, or cytosolic death-inducing signalling complex (DISC), which consists of TRADD, FADD (Fas-associated protein with death domain), RIP1, RIP3, and caspase-8. This complex induces apoptotic cell death, but in the case of deletion or depletion of caspase 8 complex II will lead to necrosome complex formation leading to necroptotic cell death (Figure 1.15) (Micheau & Tschopp 2003).

1.9 Novel drug targets identification

Target identification attempts to find factors which significantly induce or inhibit disease progression (Lindsay 2003). A drug target can be defined as a specific molecule or binding site, which plays an important role in signalling pathways or metabolism of a particular disease, in which a drug can bind and exerts its activity *in vivo* (Chen & Du 2007). In spite of developments in the pharmaceutical industry, as a result of e.g. advancements in molecular biology and the completion of human genome project, the rate of new drug approvals has remained relatively constant. In 2017, there were 46 new drugs approvals by FDA which is still not exceed the record of 53 approvals in 1996 (U.S. Food and Drug Administration 2017).

Novel target identification is an important step in the drug discovery process and can be carried out by different methods including phenotypic approaches which are associated with the examination of the expression of mRNA/protein levels and whether their expression is linked to disease progression. A second method is the use of bioinformatic approaches which utilise available data sources including patients information, genomics, proteomics, transgenic phenotyping and compound profiling (Sioud 2007). Another method is the use of genetic associations, for example, determining whether the presence of a particular polymorphism or mutation is correlated with disease development and progression (Hughes et al. 2011). All of

these approaches have resulted in a significant increase in the number of targets that have been identified.

1.9.1 Drug target screening using RNA interference

Various techniques can be applied to identify targets; these generally include forward and reverse genetic approaches. Forward genetics looks initially at the phenotype and then works out its genotype by genetic mapping, while reverse genetics deals with the manipulation of a particular gene expression and observing its resulted phenotype (Desselberger 2017). Reverse genetics through RNA interference (RNAi) has become a promising tool in the drug discovery process because it gives direct insights into the role of individual genes (Kroenke et al. 2004). RNAi was initially characterized in the nematode worm *Caenorhabditis elegans* by Fire and colleagues, who found that double stranded RNAs (dsRNAs) are more efficient in introducing sequence-specific silencing of a particular mRNA than a single stranded antisense RNA, which were originally used for target knockdowns (Fire et al. 1998; Sledz & Williams 2005). However, RNAi was originally defined in plants as an immune response to viral infection in 1928 (Sledz & Williams 2005). The upper leaves of a tobacco plant which was infected with ringspot virus showed resistance to the viral infection and this correlated with activation of RNAi machinery. More specifically, the dsRNA intermediates produced during the viral infection, led to silencing of the complementary viral genes (Ratcliff et al. 1997; Covey et al. 1997).

RNAi-based gene silencing is an evolutionary process which depends on using small double-stranded RNA molecules (20-25 base pairs with two nucleotide 3' overhangs) complementary to the targeted mRNA sequence, these RNAs then bind to the mRNA and cause its degradation hence reducing target protein levels inside the cell (Figure 1.16) (Kroenke et al. 2004). The siRNA approach works through the association of the antisense strand of the siRNA

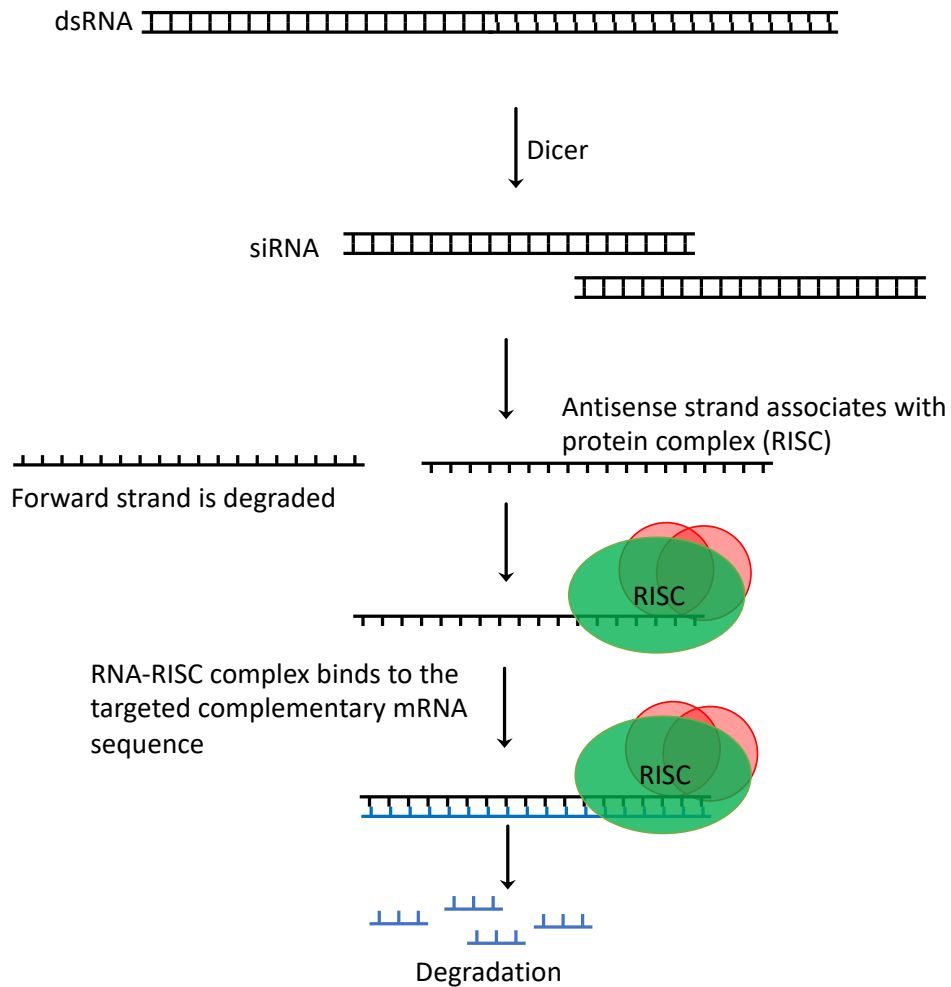


Figure 1.16 The mechanism of siRNA gene knockdown in mammalian cells.

The mechanism of siRNA gene silencing is initiated by the presence of double stranded (ds)-RNAs that are cleaved with an enzyme called dicer forming 21-23 fragments of siRNAs. The latter unwinds and the antisense strand associates with protein components of the RNA-Induced Silencing Complex (RISC). The activated complex of RNA-RISC binds to the complementary mRNA inducing its degradation.

with the protein components of the RNA-Induced Silencing Complex (RISC). The RNA/RISC binds to the complementary mRNA region, resulting in its degradation and hence a subsequent decrease in the level of the corresponding protein (Zeng & Cullen 2002; Kroenke et al. 2004; Sledz & Williams 2005; Singh et al. 2016).

For research purposes, siRNA libraries are now available that target the whole genome or a particular subset of genes; such as kinases, metabolic factors, or phosphatases, allowing large-scale phenotypic screening (Campeau & Gobeil 2011). Therefore, RNAi-based gene silencing has facilitated the identification of a large number of therapeutic targets (Perrimon et al. 2010). After targets are identified by screening, further validation and characterization can follow. If a target is validated, then it can be tested further to determine whether it can be bound by drug molecules or not; small molecule library screens can then be performed to identify leads that exhibit activity upon the target protein (Hughes et al. 2011).

1.9.2 Targets characterization/validation

The validation of targets that harbour potential therapeutic characteristics is a crucial step in the discovery of new drugs (Chen & Du 2007), and several methods can be used to obtain adequate information to validate the importance of a target to disease development and progression (Chen & Du 2007). RNAi can be also be used to validate targets, e.g. as a direct method to study a target's role in proliferation using live cell line models or transgenic animals (Hughes et al. 2011). However, the off-target effects of approaches such as RNAi can lead to false-positive results and limit the confidence needed for validation. The application of inactive derivatives as negative controls will enhance the confidence that the associated phenotypic changes are not due to nonspecific effects (Jones 2016).

The design of experiments to elucidate the biological activity of a target will depend on what the target does (Chen & Du 2007). Phenotypic investigations of a drug target in patient-derived cell-line models, representing the disease state, are seen as a valid method to provide

confidence of the association of the target or pathway with disease progression and the results can be translated into clinical studies (Vincent et al. 2015). However, such models are limited due to the lack of e.g. the tumour micro-environment which is known to have a significant impact upon tumours (Goodspeed et al. 2016). Therefore, the use of cell-lines models for screening and validation proposes forms only a step into the drug discovery process as further preclinical investigations, for example using transgenic animals, will follow such studies (Kanade et al. 2011).

1.10 Aims of the project

Therapies for non-organ confined PCa usually target the AR signalling pathway. These are initially successful in the majority of patients, but invariably fail and the tumour progresses to CRPC. Few options exist for this stage of the disease and hence there is a great need to identify novel therapeutic targets. It is well known that metabolism is altered in cancer and is seen as its Achilles' heel. The hypothesis of this study was that metabolic factors are potential therapeutic targets for prostate cancer and I therefore sought to identify metabolic vulnerabilities in prostate cancer, which could be exploited for therapeutic gain. A flow diagram summarising the study is provided in Figure 1.17.

Aims:

- i.** to carry out an siRNA screen targeting 217 metabolic and cell traffic factors, and study the effect of knocking down each factor on PCa cell proliferation and migration to identify novel metabolic genes and pathways that play critical roles in PCa progression.
- ii.** to validate potential targets across a range of prostate cancer cell lines using different functional assays.
- iii.** to further characterise and validate UROS as a novel therapeutic target for the treatment of PCa.

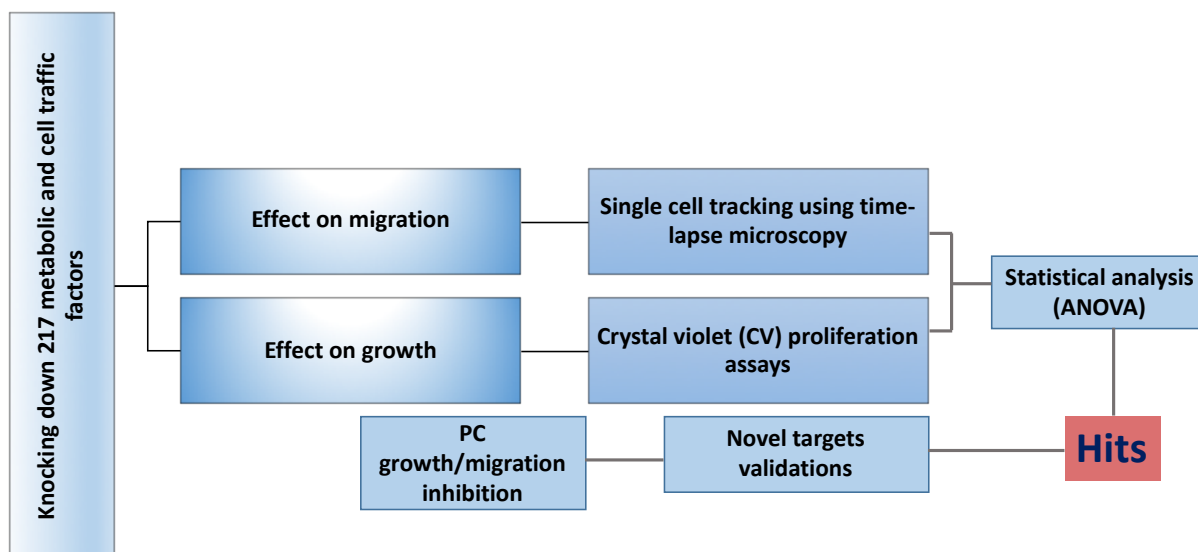


Figure 1.17 Schematic illustration to show the aim, methods used and general outcomes of this study.

siRNA screening was conducted to identify metabolic factors that affect cell growth and migration using crystal violet (CV) proliferation assay and single cell tracking assays respectively. Potential hits were identified using statistical analysis. Hits were further assessed to elucidate their role in PCa and to validate them as drug targets for PCa.

2 Chapter 2: Material and methods

2.1 siRNAs, Reagents and Buffers

2.1.1 Reagents and kits

The siRNA library used in this work was kindly provided by Dr Greg Brooke (Sigma-Aldrich, Cat. No SI10100-1SET). The library consisted of 3 individual siRNA duplexes against each target gene (217 genes), and all were designed by Rosetta Inpharmatics' design algorithm. The siRNAs are 21 nucleotides duplexes with dTdT overhangs.

The siRNA sequences were supplied dry with a final quantity of 1 nmol per duplex in 96-well microplates with 80 duplexes per plate. Positive control sequences were included in all plates. Plate maps, target genes list and full siRNA sequences information were included.

The details of all other reagents and kits used in this work are in the following table (Table 2.1), otherwise stated accordingly in the text.

Table 2.1 Reagents and commercially available kits.

Reagent/kit	Supplier
Acrylamide	Sigma-Aldrich
Agar	Fisher Scientific
Agarose	Fisher Scientific
APS (Ammonium persulfate)	Sigma-Aldrich
Bleomycin Sulfate (BLM)	Sigma-Aldrich (Cat. No. B1141000)
Bovine serum albumin (BSA)	Sigma-Aldrich
Crystal violet (CV) stain	Sigma-Aldrich
DC assay kit	Bio-Rad
DiCO6(3) (3,3'-Dihexyloxycarbocyanine Iodide).	Sigma-Aldrich
Dimethyl sulfoxide (DMSO)	Sigma-Aldrich
Docetaxel	Sigma-Aldrich
DNA-Free™ Kit	Thermo Scientific, Leicestershire, UK

EDTA	Sigma-Aldrich
Ethidium bromide	Sigma-Aldrich
Fast Ion™ Plasmid Midi Advanced Kit	RBCBiosciences (Cat. No. YPMI-25)
Fetal bovine serum, FBS	SLS (Cat. No. HYC85)
GeneJET Gel Extraction Kit	Thermo-Fisher Scientific
GeneJET Miniprep Kit	Thermo-Fisher Scientific
Glucose	Thermo-Fisher Scientific
Glycine	Thermo-Fisher Scientific
Glycogen blue	Thermo-Fisher Scientific
Halt™ phosphate inhibitor cocktail	Thermo-Fisher Scientific
Hydrogen peroxide (30%) solution	Sigma-Aldrich
IPTG (Isopropyl-B-D-thiogalactoside)	Sigma-Aldrich
Kanamycin	Sigma-Aldrich
L-Ascorbic acid	Sigma-Aldrich (Cat. No. A92902)
Lipofectamine® RNAiMAX Transfection Reagent	Thermo-Fisher Scientific (Cat. No. 13778075)
Luria Broth (LB)	(Lennox, larger granules, Fisher Scientific)
Luria Broth (LB) Agar	Sigma-Aldrich
NaCl	Sigma-Aldrich
Opti-MEM I reduced serum medium	Thermo-Fisher Scientific
PageRuler™ Plus Prestained Protein Ladder	Thermo-Fisher Scientific
Penicillin-Streptomycin-Glutamine (PSG)	Sigma-Aldrich
Phenol red-free RPMI-1640	SLS
phosphate-buffered saline (PBS) tablets	Sigma-Aldrich
PMSF (Phenylmethylsulfonyl fluoride)	Sigma-Aldrich
Propodeum iodide (PI) 1 mg/ml staining solution	Sigma Aldrich (Cat. No. P4864-10ML)
PureLink™ RNase A (20 mg/mL)	Thermo-Fisher Scientific (Cat.No.12091021)
REDTaq ReadyMix™ PCR Reaction Mix	Sigma-Aldrich

RPMI-1640	SLS (Cat. No. LZBE04-558F)
Sodium citrate	Sigma-Aldrich
Sodium deoxycholate	Sigma-Aldrich
Specta/Por Dialysis Membrane6MW CO:2000	Sigma-Aldrich
SYPR-Green	Bio-Rad
TEMED (Tetramethylethylenediamine)	Sigma-Aldrich
Transcriptor First Strand cDNA synthesis kit	Roche
Succinylacetone (SA)	Sigma-Aldrich
Tris	Sigma-Aldrich
TRI-Sure reagent	Bioline, Taunton, MA
Triton X-100	Sigma-Aldrich
Trypsin/EDTA	Sigma-Aldrich
Tryptone	Oxoid
Tween® 20	Sigma-Aldrich
Xgal	Sigma-Aldrich
Yeast extract	Oxoid
4X Laemmli loading buffer	Bio-Rad
Sodium dodecyl sulphate (SDS)	Fisher Scientific

2.1.2 Solutions and buffers

The details of all buffers and solutions used in this study are provided in the following table (Table 2.2).

Table 2.2 Buffers and solutions used.

Name	Description	Sterilization and storage
------	-------------	---------------------------

Western blotting

RIPA (Radioimmunoprecipitation) cell lysis buffer	0.5 ml of 1 mM Tris-Cl (pH 8.0), 1 mM of EDTA (20 mg), 1% Triton X-100 (0.0 ml), 0.1% sodium deoxycholate (50 mg), 0.1% SDS, 140 mM NaCl, protease inhibitors (added in time of experiment).	Autoclaved and stored at 4 °C.
10x Running buffer	30.3g of Tris, 144g of Glycine, 100 ml of 10% SDS, ddH ₂ O to make up 1000 ml.	Autoclaved and stored at room temperature.
1x Running buffer	100 ml of 10x running buffer, 900 ml of ddH ₂ O.	Autoclaved and stored at 4 °C.
Transfer Buffer	22.52g of Glycine, 4.88g of Tris, 400ml of methanol, made up to 2 L by ddH ₂ O.	Autoclaved and stored at room temperature.
10% acrylamide gel	3.3ml of acrylamide, 2.5ml of 1.5M Tris pH 8.9, 4ml of ddH ₂ O, 100µl of 10% SDS, 100µl of 10% APS, 10µl TEMED (Tetramethylethylenediamine).	Prepared fresh every time.
Stacking Gel	0.85ml acrylamide, 1.25ml of 1.5M Tris pH 6.8, 2.8ml of ddH ₂ O, 50µl of 10% SDS, 50µl of 10% APS, 5µl of TEMED.	Prepared fresh every time.

10 % SDS	50 g of SDS dissolved in a total of 500 mL ddH ₂ O.	Stored at RT.
----------	--	---------------

Cloning

Luria Broth (LB)	10 g of LB dissolved in 500 ml of ddH ₂ O and autoclaved prior to use; 50 µg/ml of Kanamycin added if needed.	Autoclaved and stored at room temperature.
Luria Broth Agar (LB Agar)	35 g of LB agar added to 1 L of ddH ₂ O. Stock was then autoclaved, warmed, and supplemented with antibiotics (50 µg/ml of ampicillin or kanamycin) before pouring into plates. 4 µL IPTG (200 mg/mL) and 40 µL Xgal (20 mg/mL) were spread on the surface of each plate before use.	Autoclaved and stored at room temperature, antibiotics and Xgal/IPTG mix added before use.
Super Optimal broth with Catabolite repression (SOC) Medium	2% tryptone, 0.5% yeast extract, 10 mM NaCl, 2.5 mM KCl, 10 mM MgCl ₂ , 10 mM MgSO ₄ , and 20 mM glucose, made up in 1 L of ddH ₂ O.	Autoclaved and stored at room temperature.
Agarose Gel (1%)	1 g agarose was added to 100 ml of Tris acetic acid EDTA (TAE) (1x) buffer and heated until boiling. 5µl of ethidium bromide (10 mg/ml) were added to the gel solution.	Stored at room temperature.
Tris acetic acid EDTA (TAE) (1x) buffer	40 mM Tris base, 1.114 mL glacial acetic acid, and 1 mM EDTA in a total of 1 L ddH ₂ O.	Autoclaved and stored at room temperature.

Flow cytometry (FACS) buffers

Nicolletti buffer	10 g of Sodium citrate, 10 ml triton (100x), diluted to 1000 ml of ddH ₂ O.	Stored at 4 °C.
PI staining solution for apoptosis measurements	200µl PI (1 mg/ml), 5ml Nicolletti buffer.	Stored at 4 °C.
PI staining solution for cell cycle measurements	1ml PBS, 20µl RNase (10 mg/ml), 10µl PI (1 mg/ml in).	Freshly prepared.

Drugs

Docetaxel (Doc)	Dissolved in DMSO.	Kept at -20 °C.
Succinylacetone (SA)	Dissolved in ddH ₂ O, 0.5 mM stocks.	Kept at -20 °C.
Bleomycin (BLM)	Dissolved in DMSO, 20 mM stocks.	Kept at -20 °C.

2.2 Cell culture

Human prostate cancer cells (PC3, LNCaP, DU145, 22RV1, C42, and C42B) and the benign normal prostatic cell lines (BPH1, PNT1A) (Table 2.3), were all provided by Dr. Greg N Brooke, University of Essex. They were maintained in 1640 RPMI supplemented with 10 % fetal bovine serum (FBS). The RPMI media was also supplemented with Penicillin-Streptomycin-Glutamine (PSG); 5 ml PSG per 500 ml RPMI. Cell culture was performed using standard tissue culture techniques under sterile conditions and cells were incubated in humidified air containing 5% CO₂ at 37 °C.

2.2.1 Passaging cells

Cells were passaged every time they reach 70-80% confluency by removing the old medium and washing cells for few minutes with PBS. Cells then were incubated for 3-5 minutes with trypsin/EDTA to detach them. Trypsinized cells were resuspended with 4.5 or 9.5 ml of fresh RPMI depending on flask size, and the desired volume was transferred into a new flask containing warm 10 % FBS-RPMI, normally 1×10^5 cells/75 cm² flasks or 0.5×10^5 cells/25cm² flasks (Nunclon™ Delta Surface, Thermo Scientific).

2.2.2 Cell counting and plating

To count cells, 10 µl of cell suspension; 1:10 dilution from the main flask, was placed in a haemocytometer and 10 squares were counted and averaged. The number of cells in the whole flask was estimated by making the number $\times 10^6$. To find number of cells per ml, it was further divided by the volume of RPMI used to resuspend cells (10 or 5 ml). Normally, 1×10^5 cells/ml stocks were prepared to allow further dilution of cells for plating according to plate size and experimental design.

Table 2.3 Mammalian cell line models used in this study.

CELL LINE	DESCRIPTION	MEDIA
PC3	an androgen-independent cell line model that was established from a human PCa metastatic to the bone.	RPMI-1640
PC3-GFP	PC3 cell that were stably transfected with GFP.	RPMI-1640
LNCAP	A hormone-sensitive cell line originated from a metastatic lesion of PCa grew in a lymph node of a patient that developed CRPC after ADT.	RPMI-1640
DU145	A model of castration resistant prostate cancer (like PC3) that derived from a central nervous system metastasis.	RPMI-1640
C42	A metastatic cell line derived from LNCaP-C4 sub-cell line that was co-injected with fibroblasts into castrated mice.	RPMI-1640
C42B	A bone metastatic cell line derived after injecting the sub-cell line C42 into castrated mice.	RPMI-1640
22RV1	Derived from an androgen-dependent PCa xenograft line (CWR22R).	RPMI-1640
BPH1	A benign hyperplastic prostatic epithelial cell line.	RPMI-1640
PNTA1	Normal prostatic epithelial cells that were immortalised with SV40.	RPMI-1640

2.2.3 Defrosting/freezing cells

For defrosting cells that have been stored in liquid nitrogen, stocks were firstly kept on dry ice and rapidly defrosted using a warm water bath. Cell suspensions were transferred to a flask containing 10 ml of fresh 10 % FBS-RPMI and left overnight in the incubator. The following day medium was aspirated, and cells were washed once with warm PBS. 20 ml of RPMI was added to the cells and allowed to reach confluency. Fresh cells were passaged at least twice before using in experiments.

To freeze down cells, confluent cultures were detached by trypsin as described in Section 2.2.1. Cells suspensions was then collected in 15 ml tubes and centrifuged at 1500 rpm for 3-5 minutes. Media was aspirated off and pellets were resuspended in freezing medium; 10% Dimethyl Sulphoxide (DMSO) and 90 % FBS. Cell suspension was transferred to a cryotube (1.5-2 ml each), wrapped in insulating material and stored at -80 °C at least 24 hours before transferring into liquid nitrogen.

2.3 Transfection by siRNAs

Cells were transfected 24 hours post seeding using about 11-17 nM of siRNAs diluted in Opti-MEM reduced serum medium and mixed with Lipofectamine RNAiMAX transfection reagent as indicated in Table 2.4. The siRNA-lipid complex solutions were incubated for 5 minutes before applying to the cells. 10-15 hours post treatments culture medium was replaced with fresh RPMI-1640 medium, cells were then incubated for 72 hours for transfection process, and phenotype quantification was followed as required. Details of cell numbers and plate types used depended on each experiment, and they are generally as indicated in Table 2.4 or accordingly in the following methods sections if different.

Table 2.4 siRNA transfection reagents volumes and concentrations.

Component	96-well	12-well	6-well
Number of cells per well	1-6x10 ³	1 x10 ⁵	2-4 x10 ⁵
Opti-MEM	24.8125 µl	100 µl	150 µl
Lipofectamine RNAMAX	0.1875 µl	3 µl	4.5 µl
Opti-MEM	24.5 µl	100 µl	150 µl
siRNA (10 µM)	0.5 µl	2 µl	3 µl
Diluted Lipofectamine iRNAMAX	25 µl	103 µl	154.5 µl
Diluted siRNA	25 µl	102 µl	153 µl
Final transfection mix volume	50 µl	205	307.5 µl
Volume of siRNA-lipid complex per well	20 µl	125 µl	250 µl
siRNA concentration per well	≈17 nM	≈11 nM	≈11 nM

2.3.1 Proliferation assay for siRNA screening

Crystal violet staining (CV) was used as a main experiment to determine the effect of siRNA transfections and drugs treatments on cell proliferation of PCa cells. The dye works by staining the protein content and DNA of all cells; viable and dead cells equally. Using the fact that dead cells will lose their adherence, only viable adherent cells will stay reducing the staining levels in treated cells compared to controls which in theory should maintain all cells (Feoktistova et al. 2016).

Cells were seeded in 96 well plates in complete RPMI-1640 at a final volume of 100 μ l (1.0 -2.0 x 10³ cell/ well for PC3 and DU145, 6.0 x 10³ cell/well for LNCaP, and 6.0-8.0x10³ cell/well for BPH1) and maintained at 37 °C for 24 hours prior to treatments. The medium was refreshed 10-15 hours post-treatment and left to grow 6 days for screening plates or as indicated for drug treatments, explained later in this chapter. After treatments incubations, 100 μ l of 4% paraformaldehyde (PFA) was added to each well and incubated at room temperature (RT) for one hour. Plates then were washed three times using phosphate-buffered saline (PBS) and left to dry at RT. Cells then were incubated for one hour in 50 μ l of 0.04 % crystal violet stain, washed three times with distilled H₂O and allowed to dry. Finally, 100 μ l of acetic acid (10 %) was added to all wells and left for one hour on a shaker. Plates were read using spectrophotometer microplate reader (FLUOstar Omrega, BMG LABTECH, UK) at 490 nm wavelength.

2.3.2 Migration assay for siRNA screening

GFP-tagged PC3 cells were seeded on 96-well plates (500-1,000 cell/well) 24 hours prior to treatments. Treatment with siRNAs was followed and incubated for 72 hours. Media was replaced with phenol red-free RPMI (5% SFCS, Charcoal Stripped Foetal Calf Serum) 10-

15 hours after treatments; to reduce cell growth as cell density is an important factor when taking images. Media then switched back to 10 % FBS RPMI 1640 24 hours before imaging.

2.3.2.1 Single cell tracking and image acquisition by widefield microscopy

Widefield microscope (Eclipse Ti; Nikon) with a motorized stage and humidified chamber (Model: H301, OkoLab, Italy), 37 °C in 5 % CO₂ conditions, was set to acquire images using 10X 0.3 N.A objective lens using 20-30 % illumination and 3-5 seconds exposure. GFP was excited using blue light 470 nm via a CoolLED pE excitation system. Two-dimensional (2D) time series frames were captured with an Andor camera (Model: Luca-R DL-626, Andor Technology, UK) using NIS-Elements AR 4.13.04 (Build 925) software every 15 minutes for 24 hours in multiple locations in every well, 3-4 fields minimum per well. Resulted image sequences were pre-processed and analysed as described in the following section.

2.3.2.2 Image pre-processing and automated quantification of PC3 cell speed

High resolution time-lapse image sequences were captured and used to analyse the trajectories and the speed of single PC3 cells. Analysis was carried out by a semi-automated method using the *ADAPT* algorithm (Barry et al. 2015). For cell segmentation, multiple manual processing steps were required to make the objects in a form that *ADAPT* algorithm can easily and precisely detect and track. The pre-processing steps were background subtraction, contrast adjusting and thresholding (Figure 2.1). These steps are labour intensive when dealing with large sets of images as in this study. Therefore, the pre-processing steps were gathered in one macro using existing ImageJ plugins in a batch process to accelerate the pre-processing of image datasets. The Macro used to convert ICS files into TIFF files is as the following:

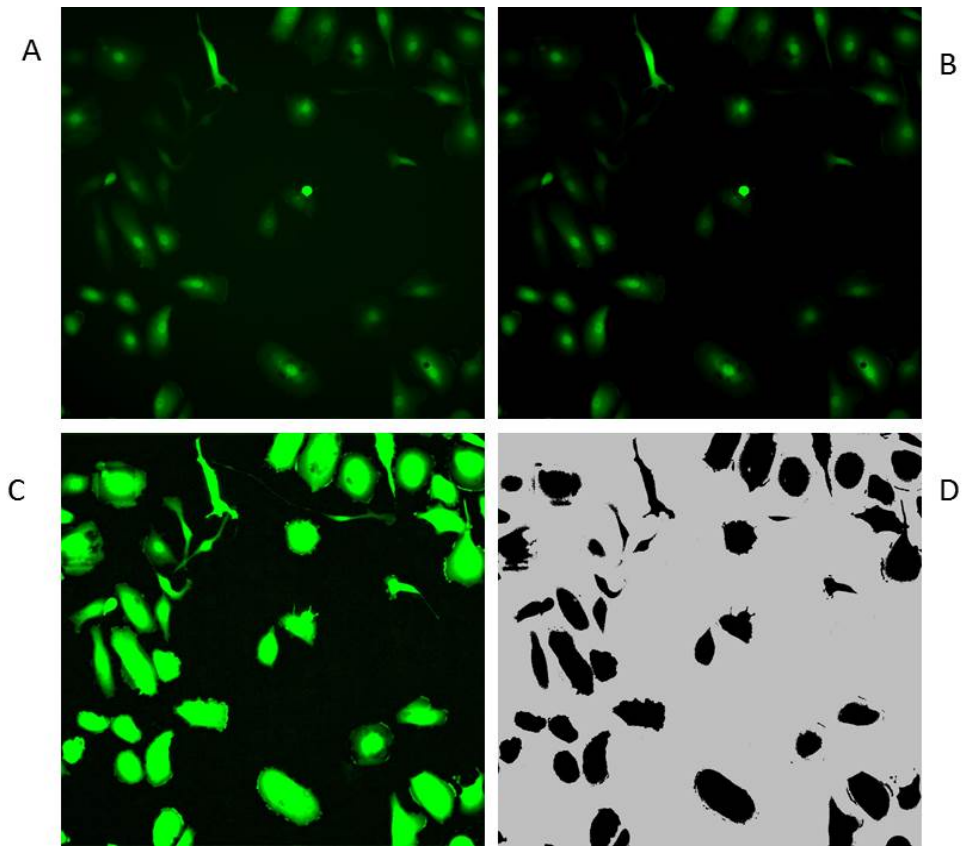


Figure 2.1 Illustration for the processing steps applied for cell segmentation of time-lapse sequences.

The background of the original image (A) was firstly subtracted (B), contrast was then adjusted (C) and finally images were thresholded manually to the point that cells are clear enough for the detection process (D).

```

macro "tracking images preprocessing" {
  dir1 = getDirectory("Choose Source Directory ");
  dir2 = getDirectory("Choose Destination Directory ");
  images = getFileList(dir1);
  setBatchMode(true);
  for(i=0; i<images.length; i++) {
  open(dir1 + images[i]);
  run("8-bit");
  saveAs("Tiff", dir2 + images[i]);
  close();
  }
}

```

The routine used to pre-process the images in a batch mode is:

```

macro "tracking images preprocessing" {
  dir1 = getDirectory("Choose Source Directory ");
  dir2 = getDirectory("Choose Destination Directory ");
  images = getFileList(dir1);
  setBatchMode(true);
  for(i=0; i<images.length; i++) {
  open(dir1 + images[i]);

  run("Subtract Background...", "rolling=50 stack");
  setAutoThreshold("Default dark");
  //run("Threshold...");
  setAutoThreshold("Default dark");
  run("Convert to Mask", "method=Default background=Default");
  saveAs("Tiff", dir2 + images[i]);
  close();
  }
}

```

2.3.3 *Statistical analysis*

One-way ANOVA was used to determine the statistical difference between treated cells and negative control (NTC) experiments including proliferation assays and wound healing migration assays. For proliferation screen, all 3 siRNA treatments for each target were combined and compared to NTC-siRNA transfection control using ANOVA followed by Fisher's LSD (least significance difference) post hoc. Validation growth assays and wound healing assays were analysed by ANOVA using Dunnett's post hoc test.

Non-parametric Kruskal-Wallis test using Dunn's post hoc test was applied to for single cells migration screen comparisons where each siRNA was compared individually to NTC and targets with all three significant siRNA results were marked as hits and showed in the heat map. A P value of < 0.01 (95 % confidence interval) was used to decide on significance.

2.3.4 Wound healing assays after siRNA knockdowns

1.0-2.0 x 10⁵ cells/well or 2.0-4.0 x 10⁵ cells/well of PC3 were seeded in 12 or 6 well plates, respectively, 24 hours prior to siRNA based transfections. 10-15 hours after siRNA treatments (as indicated in Table 2.4), media was changed to fresh 10 % FBS RPMI and cells left to reach required confluency. Cells were left 72 hours in total after transfection, and 24 hours before making scratches medium was switched to 5% SFCS phenol red-free RPMI (1% Penicillin- Streptomycin-Glutamine) to minimize cell proliferation that can interfere with population cell migration. Monolayers were then wounded using 200 μ l pipette tip; the tip was used to make multiple scratches in each well by gently removing a patch of cells (Figure 2.2). After wounding, cells were gently washed twice with PBS to remove cell debris, fresh medium was applied, and imaging was followed as in the next section.

2.3.4.1 Imaging scratch assays using widefield Ti Nikon microscope

Nikon Eclipse Ti widefield microscope was used to capture large scale images of the whole plates. Images were captured at the start of the experiment (zero hour) and at different time intervals to determine the time point which allow seeing the difference in the closure speed between the treated and untreated cells. Large scale images of the whole plate were taken by brightfield using 2X objective without binning. Uneven illumination (Figure 2.3) was the main problem when using smaller well plates because of the meniscus effect of the liquid which

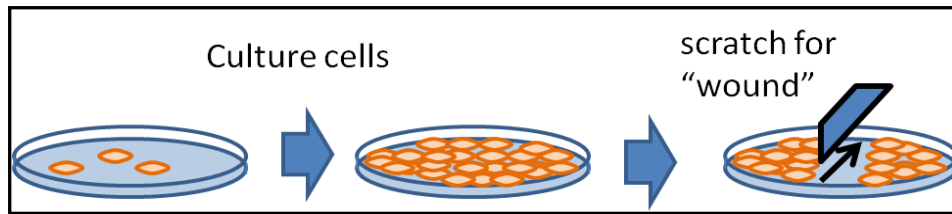


Figure 2.2 The main method of performing scratches on cell monolayers.

Taken from: Bise et al. (2011).

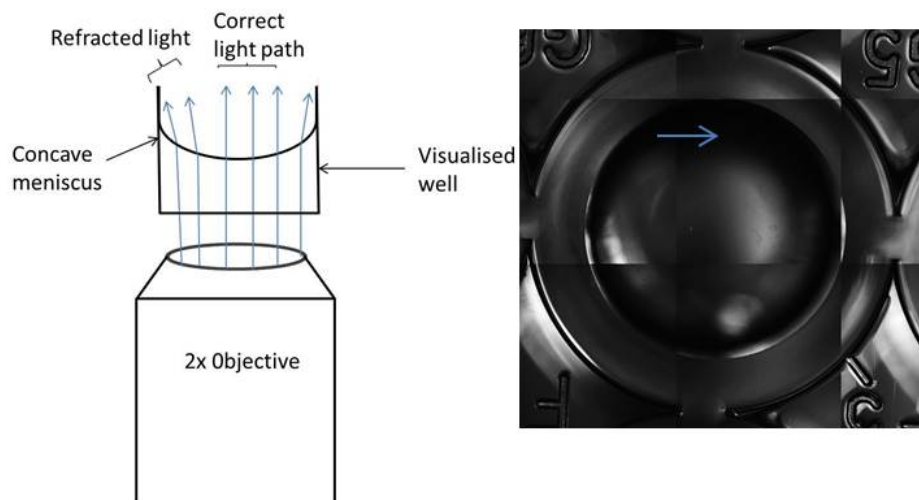


Figure 2.3 Meniscus effect on imaging cells in 96-well plate using 2 x objectives on Nikon Ti widefield microscope.

Left: Light is diffracted when it gets close well edges as surface is not flat. Right: The small size of the wells of 96-well plate cause to further increase the meniscus of residual medium which in turn increase the shading effect (dark regions, arrow).

results in shaded areas of the well, and hence wider wells-plates, which display less meniscus effect, were preferred to perform the assay. Also, binning of pixels, combining signals from adjacent pixels together, when taking the image increases signal to noise ratio and reduces image-acquisition time in the cost of spatial resolution; which is not critical in scratch imaging that does not seek cells details. Uneven illumination can also be further reduced by simply acquiring a bright image of an empty field, then divide the original image by this image or by convolving the image with a low pass filter such as Gaussian (Leong et al. 2003), also other specialized algorithms for shading correction are available in most software packages like ImageJ (Bolte & Cordelières 2006).

2.3.4.2 Semi-automated quantification of scratch assay images

Image analysis of scratches was carried out using NIS-elements software (Nikon). The rate of scratch closure was found by calculating the difference between the open area of each scratch at 0 hours and at 24 hours. The area of each wound was determined using a method similar to that presented by Treloar & co-workers (2013) (Figure 2.4) which depends mainly on using an edge detection algorithm called Sobel that convolves images with horizontal and vertical edge detection kernels and results in increasing the contrast between dark and bright areas which makes the area's detection easy and concise (Treloar & Simpson 2013). More sharpening was also used to further increase the brightness difference along the edges in the image.

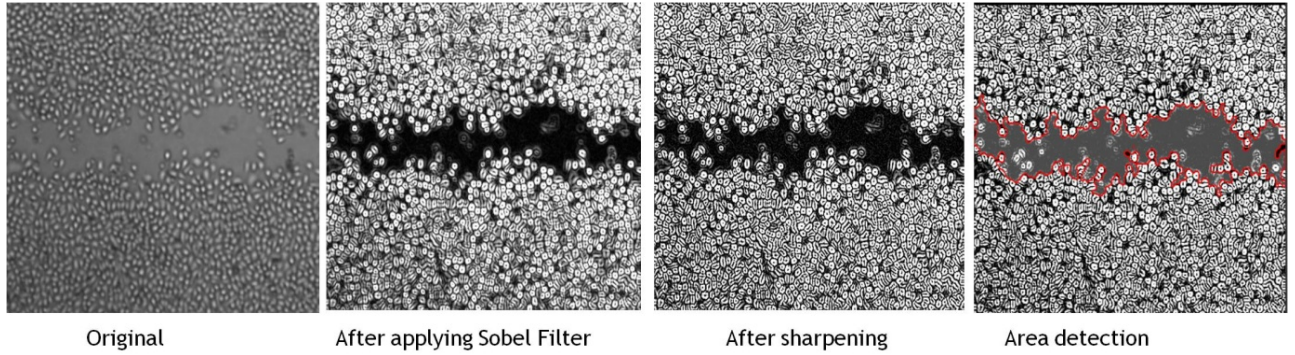


Figure 2.4 Sobel filter was used to find and enhance the scratch edges.

Sobel filter was used to find and enhance the scratch edges which then can be sharpened to increase the contrast between the dark and white areas. This method helps to easily detect the wound area. However, some randomly moved cells in the open area of scratches could not be detected precisely.

2.4 Heme depletion and heme-synthesis inhibition

As our lead target (UROS) is implicated in heme-synthesis pathway, we decided to abolish heme from the medium and further halt the intracellular production of heme by using succinylacetone (SA) inhibitor, which targets the *ALAD* gene that works upstream of *UROS* gene. The next sections explain the recipe of how heme content was reduced from the serum and the dose-based SA treatments used to stop the *de novo* heme biosynthesis in PCa cell lines.

2.4.1 Heme-depleted media preparation

To remove heme from FBS, the initial absorbance (A) of the serum was measured as 405 nm. Then, ascorbic acid was added to the FBS at a concentration of 10 mM and serum was placed in a water bath (37 °C). Absorbance was recorded every 60 minutes intervals until it reached half of the initial reading. FBS was then placed in a dialysis bag (Specta/Por Dialysis Membrane 6 MWCO:2000) under sterile conditions and dialyzed against 10 times the volume of PBS for 3-4 hours. Then, PBS was changed and dialyzed overnight. The next day, again PBS was changed and dialyzed for 3-4 hour. All dialysis was carried out with continuous stirring of PBS at 4 °C, and then serum was filtered in the tissue culture hood and stored the aliquots in -20 °C. This serum was then added to RPMI media at 5 % concentration to form heme-depleted RPMI medium for use as required in experiments.

2.4.2 Succinylacetone dose-treatments for proliferation assays

For heme biosynthesis inhibition, SA inhibitor was used as doses between 0 and 1000 μ M. PC3, DU145, LNCaP, and BPH1 cells were seeded in 96 well plates (1000, 2000, 6000, and 6000-8000 cell/well, respectively) using 5% heme-depleted or 5% typical FBS 24 hours prior to the SA dose-treatments. Cells were left for either 2, 4, or 6 days to allow growth. CV growth assays as explained in Section 2.3.1 was carried out to determine the effect of SA doses on proliferation of PCa cell lines. At 2 and 4 days, there was an initial effect of the

inhibitor doses on PC3 cell growth, but the effect was clearer at 6 days' treatments. Therefore, the 6 days' dose treatment was extended to other experiments.

2.4.3 Succinylacetone dose treatment for cells migration assays

To investigate if SA doses inhibits PC3 cell migration, cells were seeded in 5 % RPMI at either 96 well plates (500 cell/well) or 12 well plates (100,000 cell /well) 24 hours before SA doses addition. Cells in 96 well plates were left 3 days, and on day 4 images were acquired as explained above (Section 2.3.2.1) using widefield Nikon microscope every 20 minutes over 24 hours. Images were analysed as in Section 2.3.2.2.

12 well plates were also left 3 days to allow them to form a confluent monolayer. On day 4, cells were washed once with PBS and media was changed to fresh 5 % SFCS phenol red-free RMPI. 6 hours later, wounds were introduced as explained before and cells washed with PBS to remove cell debris. Fresh 5 % SFCS phenol red-free RMPI was added and cells were retreated with SA doses. A big scale image of the whole plate was acquired using widefield inverted microscope via brightfield and 2x objectives (no binning was needed, and objective calibration was applied before imaging). 24 hours another image was acquired similarly, and scratch analysis was carried out as explained in Section 2.3.4.2.

2.5 Combinations of heme biosynthesis inhibition with chemotherapeutics and ROS enhancing agents

To investigate if cellular stress brought about by heme biosynthesis inhibition will have additive effects to the existing chemotherapeutics and whether the reactive oxygen species (ROS) generated by SA sensitise PCa cells to other treatments, the inhibitor in low doses was combined with other drugs including docetaxel (DOC) and bleomycin (BLM). In addition, doses of fresh H₂O₂ were applied as an artificial ROS that is proposed to be generated by cancer cells when under great amount of stress. The following sections explains methods of these

combinations in details. Cell numbers of $1.0 - 2.0 \times 10^3$ cell/ well for PC3 and DU145, 6.0×10^3 cell/well for LNCaP, and $6.0 - 8.0 \times 10^3$ cell/well for BPH1 were used for all experiments. All experiments were conducted 24 hours post-seeding.

2.5.1 Treatments of cells with succinylacetone and docetaxel

1 nM of DOC was added to PC3, DU145, LNCaP and BPH1 that were initially treated with SA doses (0-1000 μ M) in 96 well plates. Cells were allowed to grow over 6 days and on day 7 they were fixed, CV assay was followed and absorbance was read at 490 nm.

2.5.2 Treatments of cells with succinylacetone and bleomycin sulfate (BLM) doses

Cells were treated with a sub-lethal concentration of SA (50 μ M) 24 hours post-seeding. Few hours after SA treatment, cells were treated with BLM doses (0-10 nM) and allowed to grow for 6 days. Then, cell fixation and CV staining were followed, and absorbance was read at 490 nm.

2.5.3 Treatments of cells with succinylacetone and hydrogen peroxide doses

PCa cell lines and PBH1 cells were seeded 24 hours before treatments in correct numbers as indicated before. For each cell line, cells were either treated or untreated with 50 μ M or 500 μ M of SA inhibitor and left to grow over 5 days. On day 6, cells were treated with H₂O₂ doses of 100-500 μ M and left 24 hours. Control cells that were untreated, only SA treated, or only H₂O₂ treated were included in all experiments. Cells were then fixed with 4% PFA and CV assays was followed to determine cell viability (Section 2.3.1).

2.6 Flow cytometric assays

2.6.1 Treatments

For siRNA knockdowns assays, cells were seeded in either 6 or 12 well plates and treated as presented in Table 2.4. Cells were left 72 hours and harvested on day 4 for corresponding flow cytometric analysis as explained in the next sections.

For SA flow cytometric experiments, in 12 well plates, 1×10^4 , 2×10^4 , 4×10^4 and 5×10^4 cell/well of PC3, DU145, LNCaP, and BPH, respectively, were seeded 24 hours prior to treatments. Cells then were either treated with SA doses and incubated for 6 days or treated with a single dose of SA (50 or 500 μM) and incubated for 5 days followed by H_2O_2 dose treatments that lasts for 24 hours.

For the experiment included the caspase inhibitor, PC3 cells were treated with 10 μM of the caspase inhibitor ZVAD-FMK 20 minutes prior to SA treatments. H_2O_2 was added on day 5 and left 24 hours before analysis.

After incubations cells were trypsinised and collected for flow cytometric analysis. Most experiments included a minimum of 10,000 cells per sample in the analysis except the apoptotic measurements which included 1000 cells per sample.

2.6.2 Flow Cytometric Measurement of Apoptotic and Necrotic Cells

For apoptosis measurements, control and treated cells were harvested by collecting medium in 1.5 ml tubes, cells then were washed with 500 μl of PBS which was transferred to the same tube. 100 μl of trypsin was then added to cells and incubated for few minutes to allow cells dissociation. 500 μl of the collected media and PBS mixture was added to cells and pipetted gently up and down and transferred to the corresponding tube. Cell suspensions were centrifuged for 2 minutes at 5000 rpm. Pellets were then suspended in 200 μl of PI (Propodeum

iodide) staining buffer; Section 2.1.2. Percentage of apoptotic cells were analysed and measured by flow cytometry using Accuri C6 software.

Necrosis was determined by measuring the number of PI positive cells using flow cytometry. Briefly, cells harvested with its medium, stained with 20 µg/ml of PI and immediately assessed by flow cytometry after a gentle vortex. Percentage of necrotic cells were then measured by flow cytometry using Accuri C6.

2.6.3 Flow cytometric analysis of cell cycle

Media was collected in clean 2 ml tube and cells were washed with 500 µl of PBS which then was transferred to the same tube. 100 µl of trypsin was added to cells and incubated for a few minutes to allow cell dissociation. 500 µl of the collected media and PBS mixture was added to cells and pipetted up and down. Cell suspension was transferred back to the 2 ml tube and centrifuged at 5500 rpm for 5 minutes. Media was discarded, and pellets were resuspended in 50 µl PBS. Cells were fixed by dropwise addition of 500 µl of 70 % ethanol with gentle vortex. Cells were stored at 4 °C. In analysis time, cells were pelleted at 5500 rpm for 5 minutes and ethanol was aspirated off. Pellets were resuspended in 200 µl of PI staining solution containing RNase A, Section 2.1.2. 10,000 cells per sample were analysed and quantified by Accuri C6.

2.6.4 Flow cytometric analysis of mitochondrial membrane potential

In 12 well plates, 10,000, 20,000, 40,000 and 50,000 cell/well of PC3, DU145, LNCaP, and BPH1, respectively, were seeded 24 hours before treatments. Cells were treated with/without SA (50 µM or 100 µM) and incubated. On day 3, cells were treated with/without 300 µM H₂O₂ and left 24 hours. On days 4, cells were harvested and washed with pre-warmed PBS, then labelled with 40 nM DIOC6(3) at 37 °C for 15 minutes. The mitochondrial

membrane depolarisation was measured using flow cytometric analysis using Accuri C6. A minimum of 10,000 cells per sample were acquired and analysed.

2.7 Measurement of Cellular Heme Content

In 6 well plates, 20,000, 40,000, 80,000 and 60,000 cell/well of PC3, DU145, LNCaP, and BPH1, respectively, were seeded 24 hours before treatments. Cells were treated with 0-1000 μ M doses of SA and left for 6 days. Cells then were harvested and counted, and the same number of cells was pelleted in 1.5 tubes; the number of cells was made relative to the control sample in each single experiment. The protocol presented by Sinclair et al. (2001) was followed for heme content analysis. Briefly, pellets were resuspended in 2M solution of oxalic acid and kept 30 minutes in a heating block at 100 °C. Controls of unheated suspensions of pellets were included for blank readings in order to subtract the background fluorescence. 200 μ l of each sample was loaded into a white polystyrene flat-bottom microplate (Sigma Aldrich) and the fluorescence of porphyrin was read at 400 nm excitation and 662 nm emission by plate reader (CLARIOstar, BMG LABTECH, UK). Data was made relative to untreated control cells.

2.8 Real-Time Quantitative PCR

Quantitative PCR (qPCR) has been employed in this work to quantify the efficiency of targets knockdowns by siRNA transfections as well as to assess the transcript levels of UROS and ALDOA in different cell lines. Validation of targets knockdowns was performed by comparing the levels of transcripts of interest in treated samples with mock transfected and NTC-treated control samples. The principle behind qPCR is briefly the detection of fluorescence produced by the SYBR-Green dye when it binds to the double stranded DNA produced during the amplification time. SYBR-Green dye conformation changes when it binds to double helix DNA and produces more fluorescence that is collected by a detector and displayed in real time. Melt curves displayed will give an overview of the amplification efficiency of the target DNA.

2.8.1 Cells preparations

After transfections or required treatments, cells were firstly washed with cold PBS; 1 ml of cold PBS was added and pipetted up and down to detach cells with help of a scrapper. Cells were transferred into pre-chilled 1.5 ml tubes, then pelleted at 4 °C (5000 rpm) for 5 minutes and kept on ice. PBS was discarded, and pellets were either snap frozen (in dry ice ethanol path) and stored at -80 °C or proceeded directly into RNA extraction (Section 2.8.2).

2.8.2 RNA extraction

RNA extraction was performed in a fume hood and only filtered tips were used to avoid any spontaneous contamination. Cell pellets were lysed in 1 ml of TRI-Sure reagent and incubated for 5 minutes at RT. 200 µl of chloroform was added, and tubes were vortexed for 15 second and kept at RT for 5 minutes. Centrifugation at 4 °C and maximum speed for 15 minutes was followed and the aqueous clear part (contains RNAs) was transferred into fresh 1.5 ml tubes. 500 µl of isopropanol and 1 µl of Glycoblue (Ambion) was added, mixed by inversion, and incubated 5 minutes at RT. Tubes were then centrifuged at full speed for 15 minutes at 4°C and carefully the supernatant was removed by pipetting. A pulse spin was followed to ensure that all liquid was removed. 1 ml of 75 % ethanol was added and tubes vortexed and centrifuged at 7500 g at 4°C for 5-10 minutes. Supernatants were removed with pipetting and pellets were air-dried for 10 minutes. Dry pellets were finally resuspended in 30 µl of sterile RNase-Free water and kept on ice. RNAs concentration was measured using NanoDrop® ND-1000 UV/VIS Spectrophotometer (Nanodrop, Thermo Scientific).

2.8.3 DNase treatment of RNAs and cDNA synthesis

A DNase step was performed before cDNA synthesis to remove any DNA contaminations in RNA stocks. DNA-Free™ Kit was used according to manufacturer's instructions. T100 Thermal Cycler (Bio-Rad) was employed to perform reverse transcription to generate cDNAs from RNA templates by PCR Transcriptor First Strand cDNA synthesis kit (Roche) according to the manufacturer's protocol. The concentrations of cDNAs were quantified using NanoDrop® ND-1000 UV/VIS Spectrophotometer (Nanodrop, Thermo Scientific). All samples were stored at -20 until the qPCR experiment time.

2.8.4 Real time QPCR

Roche LightCycler 96, Roche, was used to quantify alterations in gene of interest expression using SYPR-Green. All cDNA stocks were diluted using 60 µl of RNase-free water before using. QPCR mix consists from 2 µl of cDNA, 5 µl SYPR-Green, 0.5 µl of forward primer, F (10 µM), 0.5 µl of reverse primer, R (10 µM) and 2 µl RNase-free. Gene expression was normalised by the *RPL19 ribosomal protein (L19)* reference gene. Primers used in this study were all purchased from Sigma-Aldrich (Table 2.5).

2.9 Protein immunoblotting

Protein immunoblotting is a basic technique that allows the semi-quantification and analysis of proteins levels in tissues and cells. An antibody will bind specifically to the protein of interest which then is conjugated to a secondary antibody that carries a fluorophore; which in turn will allow detection. The detection was through the measurement of chemiluminescence using Fusion FX (VILBER LOURMAT). Protein immunoblotting was employed in this work to validate the knockdowns efficiency at protein levels as well as to access lead targets proteins levels in PCa cell lines.

Table 2.5 Sequences of primers used to amplify targets' DNA sequences by QPCR.

<i>Primer Name</i>	<i>Sequence</i>
L19_F	GCAGCCGGCGCAAA
L19_R	GCGGAAGGGTACAGCCAAT
RDX_F (Radixin)	TATGCTGTCCAAGCCAAGTATG
RDX_R (Radixin)	CGCTGGGGTAGGAGTCTATCA
UROS_var2F	GTCCTCAGCACTGCCTCTTC
UROS_var2R	TGGGTGTGCAACTGTCTGAT
ALDOA_F	ATGCCCTACCAATATCCAGCA
ALDOA_R	GCTCCCAGTGGACTCATCTG
FDPS_F	CCAAGAAAAGCAGGATTTTCG
FDPS_R	TCCCGGAATGCTACTACCAC
LARS_F	GCGACACCATAGCACGGTT
LARS_R	TGTGGATGTAGATTCCTCTCGAC

2.9.1 Preparing cell lysate and protein quantification

After treatments and incubations as required, cells were washed in PBS and harvested by cell scraping. Cells were then pelleted at 1200 rpm for 4 min, lysed by sonicating (2 cycles on 'high' of 30 secs on and 30 secs off using Biorupter® Plus, Diagenode) in RIPA buffer containing protease inhibitors (10 µl Halt phosphate inhibitor cocktail, 5 µl PMSF per 1 ml of RIPA buffer, Section 2.1.2). Lysates were centrifuged at maximum speed for 10 minutes at 4 °C. Clear supernatants were transferred to clean microcentrifuge tubes and kept on ice or - 80 °C until further analysis. Proteins concentrations were determined using Protein Detergent Compatible (DC) assay kit according to manufacturer's instructions. Briefly, 5 µl of each sample was used against a series of standard concentrations of BSA as a reference. Protein concentrations were detected at absorbance (A) of 750 nm using the FLUOstar Omega plate reader (BMG LABTECH). Protein volumes were made equal in each experiment; 10 µg per 10 µl of each sample, by diluting them accordingly with the lysis buffer (RIPA).

2.9.2 SDS polyacrylamide gel electrophoresis

10 % SDS polyacrylamide gel was prepared briefly by pouring 4-5 ml of 10% acrylamide gel (Section 2.1.2) between a sandwich of two glass plates and was topped up with 1 ml of H₂O and left to set before adding the stacking buffer (Section 2.1.2). Proteins stocks were heated to 95 °C for 5-10 minutes. Samples then were immediately placed on ice for 2 minutes and then mixed up with 4x Laemmli loading buffer containing Beta-mercaptoethanol (B-Me). A total of 25-30 µg of proteins were loaded together with 5 µl of PageRuler™ Plus Prestained Protein Ladder (Bio-Rad) and run in 1x running buffer (Section 2.1.2) at 120 V for 1.5-2.0 hours.

2.9.3 Immunoblotting

Gels then were hydrated with 100 % methanol (Sigma-Aldrich) and then washed with pre-made transfer buffer (Section 2.1.2). Proteins were transferred into a soaked polyvinylidene fluoride (PVDF) membrane (Sigma Aldrich) over two hours (15 mA, and 100 V) using semi-dry electro blotting apparatus (Bio-Rad). Membranes were then washed with PBS and blocked with 5% Milk PBS-T (0.1% Tween) on rotator for 30 minutes. Membranes were then incubated with the required primary antibodies (1^o) diluted in 5% Milk PBS-T for one hour at RT or overnight at 4 °C with rotation. Antibodies and concentration details used to probe the membranes are shown in Table 2.6. After primary antibody incubation, membranes were washed quickly 2 times with PBS-T followed with 3 washes with PBS-T for 5 minutes each with rotation. Re-blocking with Milk- PBS-T for 15 minutes was followed and respective secondary antibodies (2^o) diluted in Milk- PBS-T (1:2000) were added and incubated for an hour at RT with rotation. Protein bands were visualized by LuminataTM Forte Western HRP Substrate (Millipore) using Fusion FX (VILBER LOURMAT) equipped with Fusion analysis software. The molecular weights of the proteins were estimated in respect to PageRulerTM Plus Prestained Protein Ladder used.

2.10 Cloning DNA sites of lead targets

DNA sites of lead targets were cloned for further investigation into their localization to give more indications into their related signalling and functions. DNA sites were firstly amplified by PCR, digested and ligated into pGEM as it has more efficiency. They were then cut and re-ligated into pEGFP-C1 vector and transit transfection was used to allow their GFP signal visualization by widefield microscope.

Table 2.6 Antibodies.**(a) Immunoblotting**

Protein	Primary antibody	Secondary antibody
Radixin	anti-Radixin (Abcam, ab52495), 1:500 dilution.	Anti-Rabbit IgG (whole molecule)-Peroxidase (Sigma-Aldrich, 1:2000 dilution)
UROS	anti-UROS (Sigma-Aldrich, HPA044038) 1:100 dilution.	Anti-Rabbit IgG (whole molecule)-Peroxidase (Sigma-Aldrich), 1:2000 dilution.
ALDOA	anti-ALDOA (Abnova, H00000226-MO2), anti-ALDOA (Santa Cruz Biotechnology, sc390733) 1:500 dilution.	Anti-Mouse IgG (whole molecule)-Peroxidase (Sigma-Aldrich), 1:2000 dilution.
α-Tubulin	anti- α -Tubulin (Sigma Aldrich, T5168), 1:1000 dilution.	Anti-Mouse IgG (whole molecule)-Peroxidase (Sigma-Aldrich), 1:2000 dilution.

(b) Confocal microscopy

Protein	Primary antibody	Secondary antibody
UROS	anti-UROS (Santa Cruz Biotechnology, sc-365120), 1:50 dilution.	Goat anti-Mouse IgG H&L (Alexa Fluor® 568), 1:1000 dilution.
ALDOA	anti-ALDOA (Santa Cruz Biotechnology, sc390733), 1:200 dilution.	Goat anti-Mouse IgG H&L (Alexa Fluor® 488), 1:1000 dilution.

2.10.1 PCR amplification and gel extraction DNA sites

For the amplification DNA sites of UROS and ALDOA, REDTaq® ReadyMix™ PCR Reaction Mix (Sigma-Aldrich) was used and primers were designed to add *Bgl*III and *Eco*RI restriction sites as shown below in Table 2.6. Each reaction consisted of 5 µl of both primers (forward and reverse), 2 µl of cDNA, 25 µl of RedTaq and 13 µl of ddH₂O. The cDNAs used were generated from untreated PC3-GFP cells as explained in Section 2.8.3. Several PCR reactions were run at a series of temperatures and amplified DNAs were all run on 1 % agarose gel in 1x TAE buffer (Section 2.1.2) to access their quality and lengths. Gels were visualized using the AlphaImager EP MultiImage I system (Alpha Innotech).

For gel extraction of DNAs, bands were visualized using a UV box to help cut them precisely. The cut bands were placed in 1.5 ml tubes. DNA was extracted using GeneJET Gel Extraction Kit by following the manufacturer's protocol.

2.10.2 Ligation into pGEM T-easy vector and transformation

DNA fragments were ligated into pGEM T-easy vector (Promega) (Figure 2.5) according to the kit's guidelines. The reaction consisted of 1 µl (50 ng) of pGEM vector, 2 µl of DNA, 2 µl of 10x Ligase buffer, 14 µl of ddH₂O and 1 µl of Ligase enzyme. The reaction was incubated overnight at 4 °C.

Vectors were then transformed into *Escherichia coli* XL-1 competent cells (Promega). In brief, 1 µl of the ligation reaction was added to 50 µl of competent cells that has been defrosted on ice. Reactions were incubated for 30 minutes on ice before heat shocking them for 45 seconds at 42 °C. Reactions were then placed on ice for 2 minutes and 450 µl of SOC medium (Section 2.1.2) was added and left shaking for 1 hour at 37 °C. In a fume hood, 200 µl

Table 2.7 Primers' sequences used to amplify studied DNA sites and add restriction sites.

<i>Primer Name</i>	<i>Sequence (5'-3')</i>
ALDOAFBgIII	AGATCTATGCCCTACCAATATCCAGC
ALDOAREcoRI	GAATTCTTAATAGGCGTGGTTAGAGACGA
UROSFBgIII	AGATCTATGAAGGTTCTTTTACTGAAGGATG
UOSREcoRI	GAATTCTCAGCAGCAGCCATGG

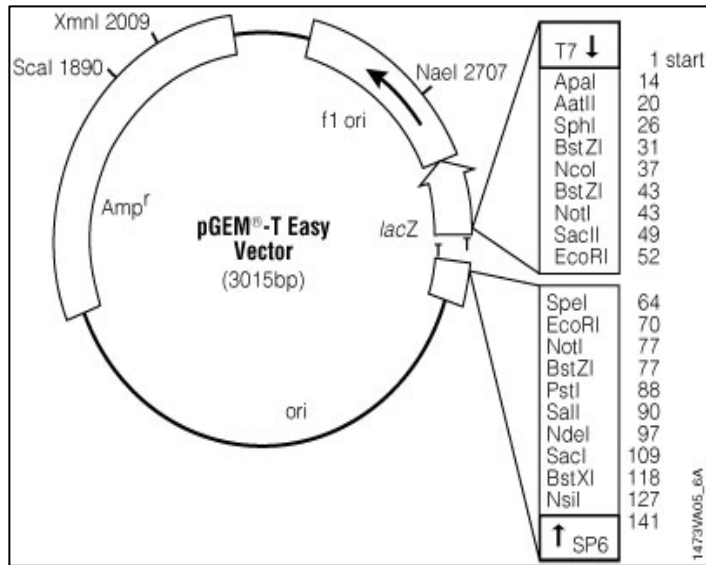


Figure 2.5 Map of pGEM-T Easy vector. Taken from: Promega.co.uk

of the reaction was spread on a LB agar plate supplemented with 50 µg/ml ampicillin (Sigma-Aldrich) on which a mixture of 4 µl IPTG (Isopropyl-B-D-thiogalactoside) and 40 µl Xgal was spread on the surface. Plates were left overnight at 37 °C. After incubating plates overnight for white-blue colonies screening, single white colonies were picked carefully each by a sterile tip and inoculated into 5 ml of LB broth containing 50 µg/ml ampicillin (Table 2.2). Cultures were incubated at 37 °C overnight in a shaking incubator. 4.5 ml of each culture was centrifuged at 8000 rpm for 1 minute at RT, pellets were used for the following plasmid extraction.

2.10.3 Plasmid DNA extraction and sequencing

Pellets from the previous section were used to extract the plasmid DNAs using GeneJET Miniprep Kit (Thermo Scientific) by following the manufacturer's guidelines. DNA yield was measured using a NanoDrop® ND-1000 UV/VIS Spectrophotometer (Nanodrop, Thermo Scientific). Samples were digested using *BglII* and *EcoRI* and run on 1% agarose gel together with uncut pGEM vector containing the corresponding DNA insert for size conformation. Sequencing (Biosciences) confirmed that all sequences were efficiently ligated into the pGEM vector. Primers used are shown in Table 2.8.

2.10.4 Re-cloning into pEGFP-c1 vector

After cloning the sites efficiently into pGEM T-easy vector, digestion with the corresponding restriction enzymes was followed and samples were separated on 1 % agarose gel together with pEGFP-c1 vector sample (Figure 2.6). Gel extraction of DNA, ligation, and transformation steps were followed as explained in cloning into pGEM T-easy vector above. Colonies were grown on a larger scale by adding 500 µl of grown competent cells to 200 ml of LB broth containing 50 µg/ml kanamycin (Sigma-Aldrich). Cultures were left to grow overnight in a shaking incubator at 37 °C and harvested by centrifugation at 6000 rpm at 4 °C for 15

Table 2.8 Primers used for sequencing of UROS and ALDOA inserts.

Description	Sequence
pGEM F	GTAAAACGACGGCCAGT
pGEM R	CATGGTCATAGCTGTTTCC
EGFP-C F	CATGGTCCTGCTGGAGTTCGTG
EGFP-C R	GTTCAGGGGGAGGTGTG

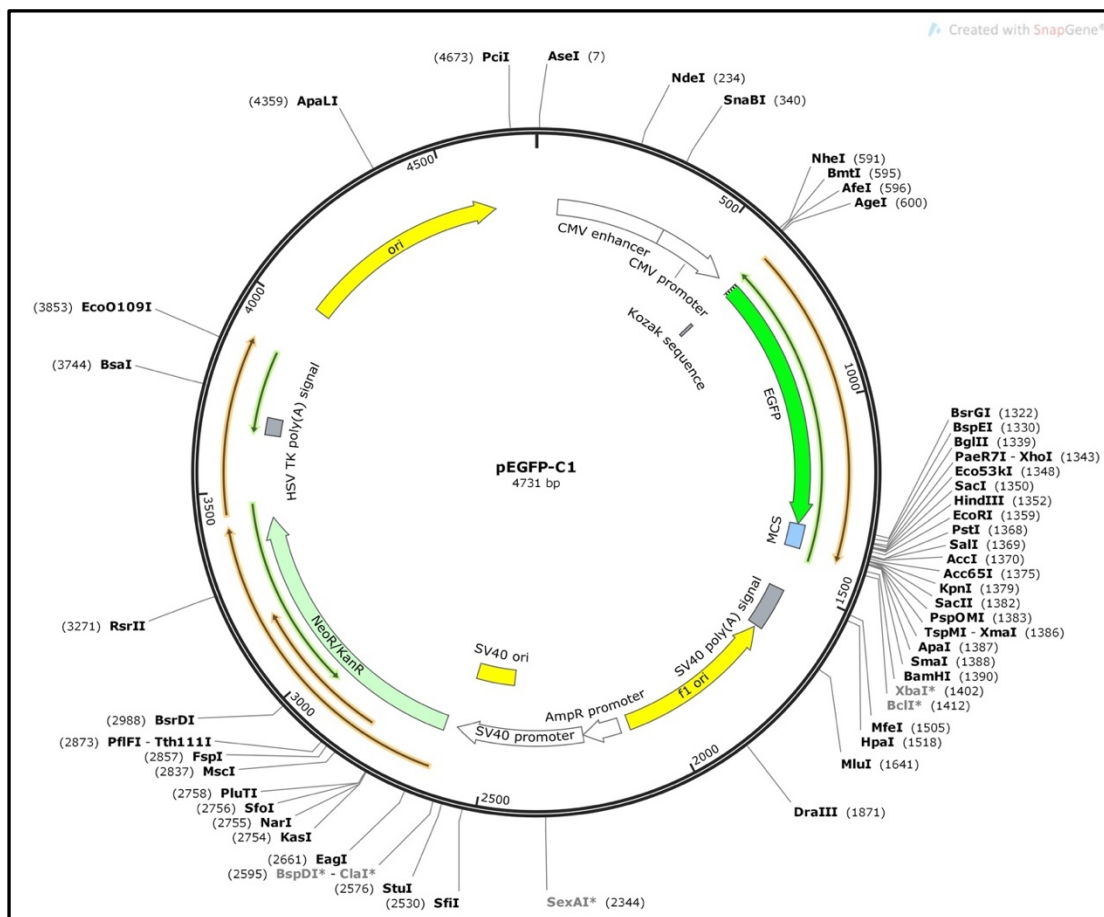


Figure 2.6 Plasmid map of pEGFP-C1 vector (designed by SnapGene software).

minutes.

Plasmid DNA was extracted using Fast Ion™ Plasmid Midi Advanced Kit (RBCBiosciences) according to manufacturer's standard protocol. DNA concentrations were measured NanoDrop® ND-1000 UV/VIS Spectrophotometer (Nanodrop, Thermo Scientific). Digested and un-digested pEGFP-C1 samples were separated on 1% agarose and were also sequenced (primers used are shown in Table 2.8), 100 ng/μl. UROS and ALDOA sequences were compared to that available in the National Centre for Biotechnology Information (NCBI).

2.10.5 DNA transient transfection of UROS and ALDOA containing pEGFP-C1 vectors into PC3 cells

TurboFect Transfection Reagent (Thermo Fisher) was used to transfect cells with plasmid DNAs. Briefly, 5×10^4 cells/well were seeded in 24 well plated and left overnight to adhere. 1 μg of the corresponding plasmid DNA was diluted in 100 μl of serum-free RPMI and 2 μl of the transfection reagent was added. They were mixed by pipetting and incubated for 20 minutes at RT. 100 μl of the transfection reagent/DNA mixture was added dropwise to each well and incubated for 24 hours. Transfection efficiency was confirmed by imaging cells using

NikonTi widefield microscope; blue light 470 nm via a CoolLED pE excitation system. For confocal microscopy, transient transfection was carried out using cells grown on glass coverslips. After 24 hours, cells were fixed with 4% paraformaldehyde (PFA) and coverslips were mounted onto glass slides in 4',6-diamidino-2-phenylindole (DAPI)-containing Vectashield mounting media. Coverslips were sealed using Marabu Fixogum rubber cement (Marabuwerke GmbH & Co.KG, Tamm, Germany) and left to dry before imaging.

2.11 Cell fixation and immunofluorescent probing

For immunofluorescence labelling, untreated PC3 cells were firstly washed 3 times with warm PBS each for 5 minutes and then fixed with 4% PFA at room temperature for 15 minutes and then with absolute ethanol for 10 minutes at -20 °C. Cells were then permeabilised for 10 minutes using 0.1% triton (x100) in PBS followed by three washes for 5 minutes with BPS. Cells were then blocked with 1% BSA in PBS-T (0.1% Tween) for 30 minutes. The fixed cells were then incubated for 1 hour with diluted primary antibody (1^o) using either anti-UROS or anti-ALDOA in 1% BSA (Table 2.6). Cells then were washed three times with PBS each for 5 minutes on a rocker to remove any excess antibody. Cells were then probed for 1 hour with a 1:1000 dilution of corresponding secondary antibody (2^o) in 1% BSA in PBS-T in dark; Goat anti-mouse IgG (Alexa Fluor® 568 or Alexa Fluor® 488; Table 2.6) (Abcam). Excess secondary antibodies were removed by washing three times with PBS and the cover slips were mounted onto glass slides in 4',6-diamidino-2-phenylindole (DAPI)-containing Vectashield mounting media and sealed using Marabu Fixogum rubber cement (Marabuwerke GmbH & Co.KG, Tamm, Germany).

2.11.1 Laser scanning confocal microscopy for proteins localization

Cells were imaged by Nikon A1R confocal microscope using an- apochromatic violet corrected (VC) 1.4 Numerical Aperture (N.A.) 60x oil- immersion objective and Nikon A1plus camera at a Refractive Index (RI) of 1.515. A laser power of 12 arbitrary units (AU) was used for the excitation of DAPI at a wavelength of 405 nm, and the emission was collected using a PMT gain of 100 AU at 450/50nm. Alexa Fluor 488 (GFP, green fluorescent protein) was excited using a laser power of 5.8 AU at 488 nm, and emission was collected using 120 AU gain at 525/50 nm. Alexa Fluor 568 (red signal) was excited at 561 nm using a laser power of 2.3 AU and signal collected at 120 AU gain at 595/50 nm. 3D images were obtained using z-

steps of 1.0 μm , and images were reconstructed by maximum intensity using NIS-Elements software (Nikon).

3 Chapter 3 Results I

3 Screening for novel therapeutic targets that regulate prostate cancer proliferation and migration

Regardless of the fact that some prostatic tumours are not AR-driven, most preserve elevated levels of AR which maintains their survival and progression into CRPC (Hodgson et al. 2012; Jernberg et al. 2017). Therefore, first line therapies, for non-organ confined disease, target this axis. Although initially successful, these therapies invariably fail, and the disease progresses to the aggressive castrate resistant stage, for which few therapeutic options exist. There is therefore a great need to identify novel therapeutic targets for the treatment of the disease. Altered metabolism is a common feature of tumorigenesis, however the metabolic changes present in prostate cancer differ to that seen in other cancers. For example, early disease does not rely on the Warburg effect or high glucose uptake as other cancers do (Eidelman et al. 2017). Prostate tumours, especially in early stages are more dependent upon other molecules such as lipids and citrate oxidation through TCA cycle for energy production (Sadeghi et al. 2015).

Generally, metabolism of malignant cells differs from that of normal cells. Cancer cells tend to not follow the orderly metabolic machinery that normal cell use, which allows a controlled proliferation that will be inhibited by cellular contact or signals of errors like DNA damage (Kalyanaraman 2017). These regulatory manners are lacked in tumours, cancer cells continuously grow regardless of the contact inhibition, poor-nutrient conditions, and other anti-proliferative factors. Therefore, they require adaptive pathways to make more energy to meet their higher demand for prolonged survival. The metabolic reprogramming has been linked to the oncogenic stimulation of key metabolic pathways (Michalopoulou et al. 2016). For example, alteration in the phosphatidylinositol-3-kinase (PI3K)/Akt and the mammalian target

of rapamycin (mTOR),PI3K/Akt/mTOR metabolic cascades result in changes that make the cell have intensified ability to uptake glucose (and other nutrients) and synthesize building blocks especially proteins (Plas et al. 2001; Thompson 2011; Pavlova & Thompson 2016). The oncogenic mutations directly and indirectly alter the metabolism of cells, which renders normal and cancer metabolic signalling to be far different from each other (Pavlova & Thompson 2016). This difference allows a therapeutic window and novel approaches to target cancer metabolism. This study was therefore designed to carry out a phenotypic screen, targeting metabolic and cell traffic signalling, in a cell line model of castrate resistant disease (PC3). The first aim of this project was to investigate the effect of siRNA depletion of metabolic and cell traffic factors upon proliferation and migration of the PC3 cell line model.

3.1 Identification of metabolic factors affecting PCa cell proliferation

3.1.1 Screening for metabolic factors that regulate PC3 proliferation

To identify novel metabolic targets involved in prostate cancer growth, a semi-high-throughput screen was carried out using an siRNA library targeting 217 metabolic and cell traffic factors. The library consists of three different siRNA oligonucleotides for each factor to reduce false-positives; which could result from the off-target effects. siRNA knockdown was performed in PC3 cell line, which is an androgen-independent cell line model that was established from a human prostatic adenocarcinoma metastatic to the bone (Kaighn et al. 1979). The screening was carried out in triplicates and the effect upon proliferation was measured using crystal violet (CV) staining on day 6 post-transfections (Figure 3.1).

The analysis identified 40 targets that significantly affected PC3 proliferation compared to NTC (Figure 3.2) ($P < 0.05$; LSD post hoc test). From the heat map, it can be seen that more factors were enhanced (26 targets) than inhibited (14 targets) PC3 proliferation. The genes found to have the most significant inhibitory effects upon proliferation following depletion were uroporphyrinogen III synthase

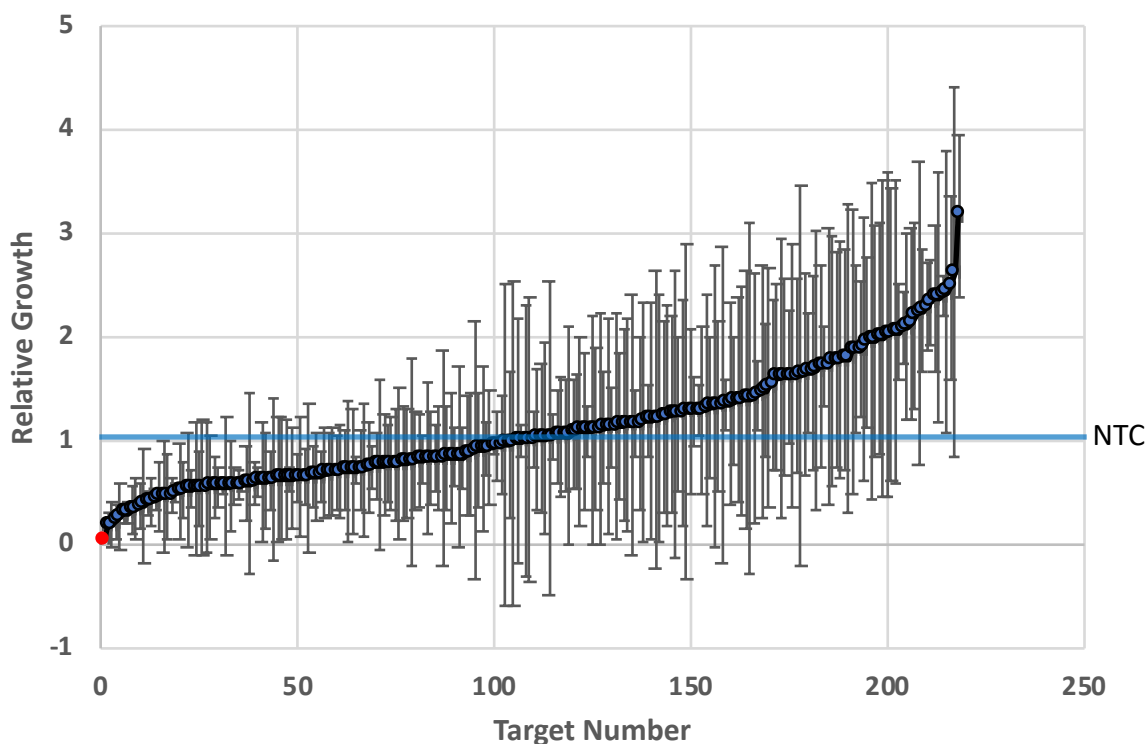


Figure 3.1 An siRNA screen to evaluate the impact of depletion of metabolic and cell traffic factors on PC3 growth.

PC3 cells were seeded at 1000 cells per well in a 96 well plates 24 hours before transfection. All siRNA transfections were performed in triplicate and all plates included the necessary controls. The medium was replaced 10-15 hours after the treatment, and cells left to grow for further 6 days. Cells were fixed, stained with crystal violet, and absorbance was read using a spectrophotometer microplate reader (FLUOstar Omega) at a wavelength of 490 nm. Each data point represents the average cell growth (three individual siRNAs per gene in triplicate) relative to non-targeting control (NTC). The blue line indicates NTC and the red circle is a positive control knockdown (polo-like kinase 1, PLK1).

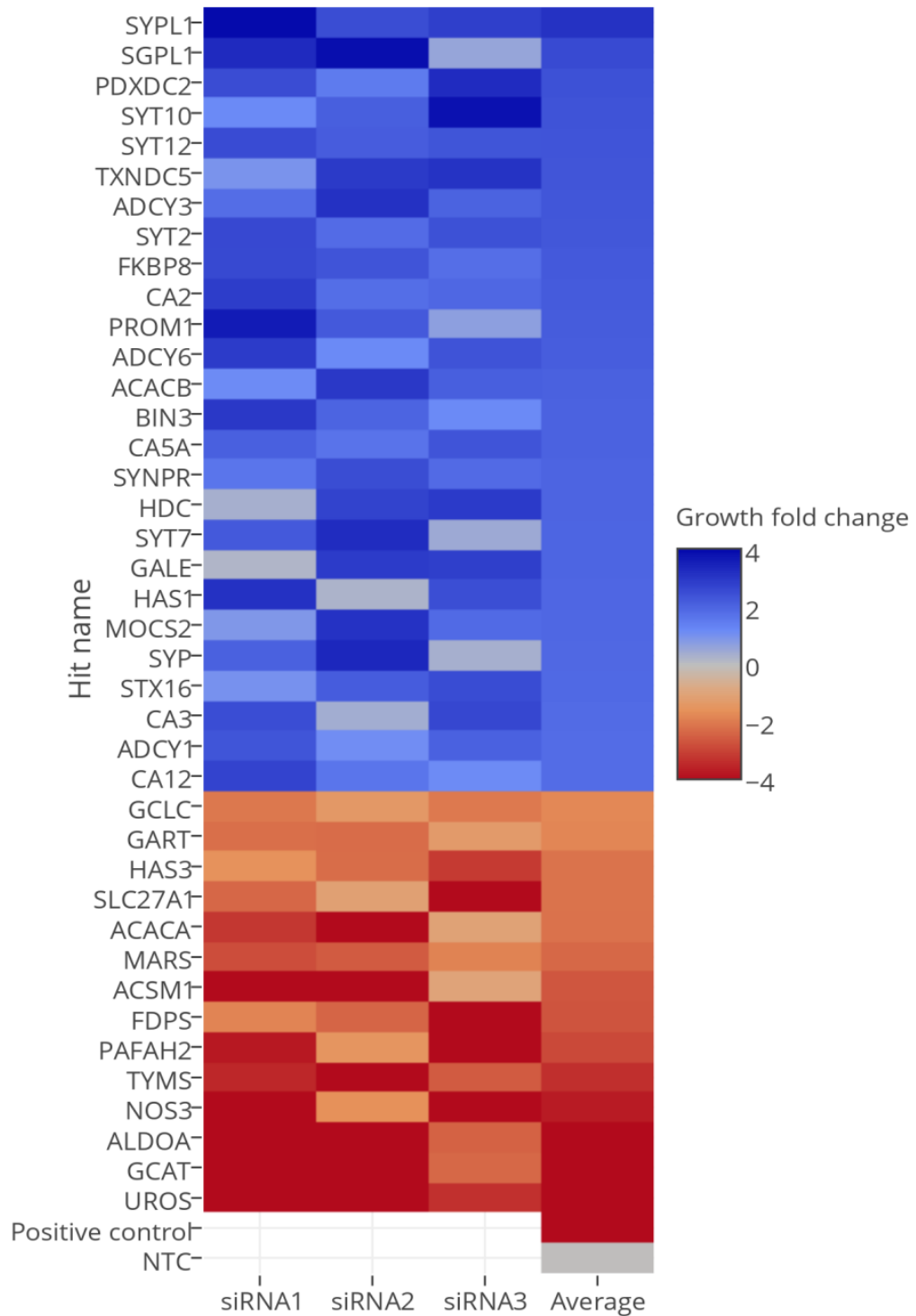


Figure 3.2 A Heat map representing the fold change of PC3 cell proliferation when transfected against 40 metabolic related factors by siRNA.

PC3 were transfected with siRNA targeting proteins involved in metabolism and cellular trafficking. 6 days after transfection, cells were fixed and stained with crystal violet. A heat map was generated for the genes found to significantly affect PC3 proliferation compared to NTC-siRNA transfection. NTC = non-targeting control. Positive control = polo-like kinase 1, PLK1.

(*UROS*), Glycine C-acetyltransferase (2-amino-3-ketobutyrate coenzyme A ligase) (*GCA*), and Aldolase A, fructose-bisphosphate A (*ALDOA*) (82, 81 and 78 % inhibition of growth compared to NTC, respectively) (Table 3.1). Table 3.1 summarises the list of lead targets, gene description, the pathways that they are involved in, and the associated inhibition of proliferation rate. Targets that significantly elevated PC3 proliferation are listed in Table 7.1 (Appendix).

3.1.2 Validation of lead targets implicated in PCa proliferation

To validate the 14 hits that showed an inhibitory effect on PCa proliferation, further proliferation assays were performed using PC3 and other PCa cell lines including LNCaP, which is a hormone-sensitive cell line that was originated from a metastatic lesion of prostatic adenocarcinoma grew in a lymph node of a patient that developed hormone-refractory disease after ADT (Horoszewicz et al. 1980; Horoszewicz et al. 1983), and DU145, which is a model of castration resistant prostate cancer (like PC3) that derived from a brain metastatic adenocarcinoma (Stone et al. 1978). The data shown represent the average effect of three siRNAs for each target, and it was made relative to NTC (non-targeting control) (Figure 3.3) ($P < 0.05$, Dunnett's comparison test). Knockdown of all of the targets resulted in a significant reduction in the proliferation of PC3 and LNCaP. siRNA depletion of the hits also significantly inhibited DU145 proliferation, with the exception of GCLC (Glutamate-cysteine ligase catalytic subunit) and MARS (Methionyl-tRNA synthetase). Data demonstrated that nearly all hits reduced proliferation to a similar level in the three PCa cell lines (Figure 3.3). The knockdown of these hits in the Benign Prostatic Hyperplasia-1 cells (BPH1), non-transformed human prostate epithelial cells derived from a patient with BPH disease (Hayward et al. 1995), demonstrated no significant changes apart from ALDOA and GCLIC knockdowns which resulted in some significant decrease in the proliferation of these cells (Figure 3.3).

Table 3.1 Summary of the lead targets identified in the siRNA screen to reduce proliferation.

Symbol (symbol in screen)	Gene Description	Pathways	Inhibition of Relative Proliferation	P-value
UROS	Uroporphyrinogen III synthase	Catalyzes the fourth step of porphyrin biosynthesis in the heme biosynthetic pathway.	82%	< 0.0001
GCAT	Glycine C-acetyltransferase (2-amino-3-ketobutyrate coenzyme A ligase)	Implicated in the degradation of L-threonine to glycine.	82%	< 0.0001
ALDOA	Aldolase A, fructose-bisphosphate A	Reversible conversion of fructose-1,6-bisphosphate to glyceraldehyde 3-phosphate and dihydroxyacetone phosphate.	78%	0.0241
NOS3	Nitric oxide synthase 3	Serves as a biologic mediator in neurotransmission and antimicrobial and anti-tumoral activities.	73%	0.0001
TYMS	Thymidylate synthetase	Catalyzes methylation of deoxyuridylate to deoxythymidylate.	70%	0.0032
PAFAH2	Platelet activating factor acetylhydrolase 2	Catalyzes the removal of the acetyl group at the SN-2 position of platelet-activating factor.	65%	0.0363
FDPS	Farnesyl diphosphate synthase	Catalyzes the production of geranyl pyrophosphate and farnesyl pyrophosphate from isopentenyl pyrophosphate.	63%	0.0036
ACSM1	Acyl-CoA synthetase medium chain family member	Unkwon.	62%	0.0227
MARS	Methionyl-tRNA synthetase	Protein biosynthesis.	57%	0.0339
ACACA	Acetyl-CoA carboxylase alpha	Fatty acid synthesis.	53%	0.0310

SLC27A1	Solute carrier family 27 member 1	Translocation of long-chain fatty acids (LFCA) across the plasma membrane.	53%	0.0037
HAS3	Hyaluronan synthase 3	Hyaluronic acid synthesis.	53%	0.0477
GART	Glycinamide ribonucleotide transformylase	Purine biosynthesis.	44%	0.0386
GCLC	Glutamate-cysteine ligase catalytic subunit, gamma-glutamylcysteine synthetase	The rate-limiting enzyme of glutathione synthesis.	42%	0.0458

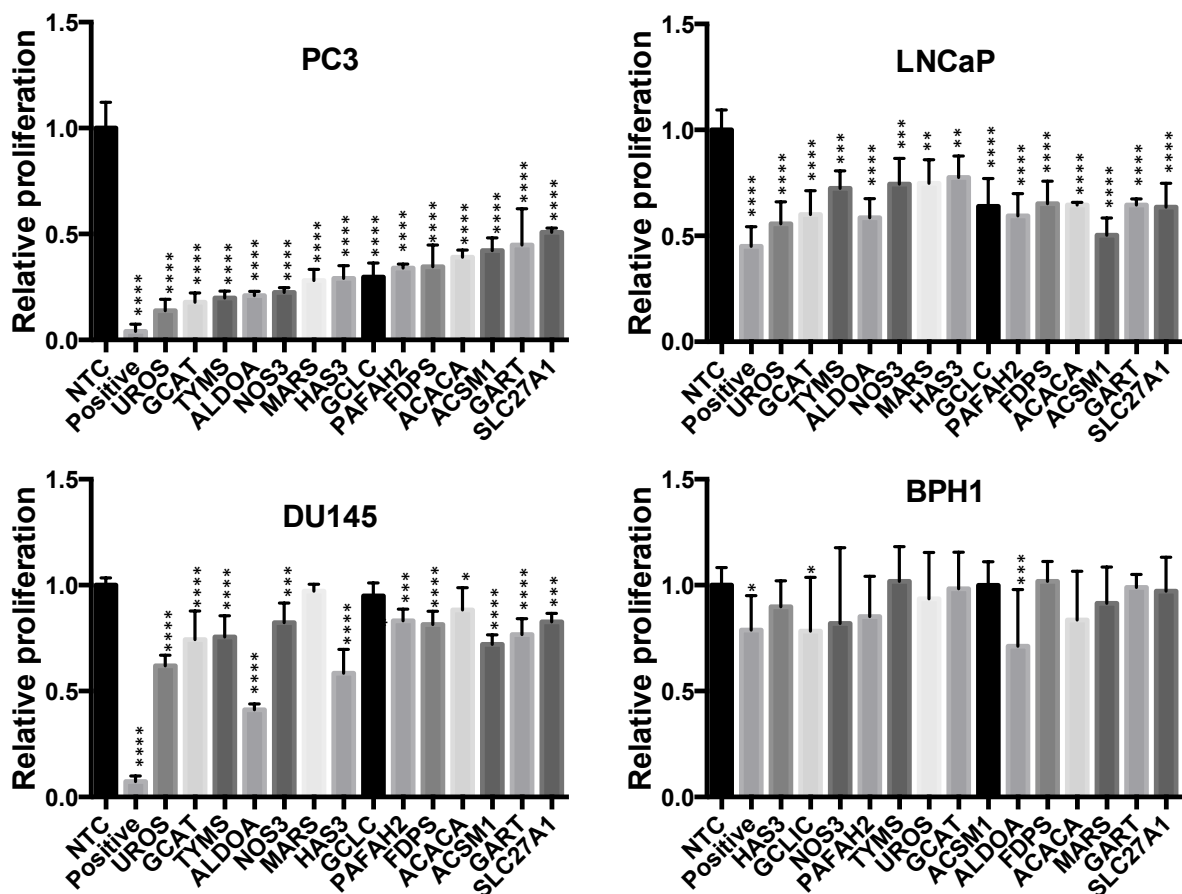


Figure 3.3 Validation growth assays of 14 hits in prostate cancer (PC) cell lines and BPH1 cells.

Cells were transfected with siRNAs against metabolic hit targets (as indicated on the graphs). Three siRNAs were used individually to knockdown every target and the effect upon proliferation was assessed using crystal violet assays. Data was made relative to the negative control (NTC) and it represents mean \pm 1SD of 3 repeats of 3 individual siRNAs. ANOVA via Dunnett's comparison test was used to quantify the statistical significance (*P < 0.05, **P < 0.01, ***P < 0.001, ****P < 0.0001).

3.2 Identification of metabolic factors affecting PCa migration

Metastasis is a hallmark of cancers. The treatment of localised prostate cancer with ADT showed good long-term clinical outcomes, although 10-50 % of patients will experience relapse and will demonstrate metastasis (Shelley et al. 2008). Prostate cancer tumours tend to spread to bones forming secondary tumours which are incurable, bony metastasis gives rise to the high rates of the disease-specific morbidity and mortality (Manca et al. 2017). The migration ability of cancer cells is an important aspect and research have focused on the alterations that could suppress the migratory potential of malignant cells. Therefore, blocking prostate cancer cell motility in respect to metabolic signalling was of interest.

The aim of this part was to screen for novel metabolic targets and pathways that contribute to migration and metastatic properties of PCa cells. Therefore, the siRNA screen was repeated in PC3-GFP cell line (PC3 cells stably transfected with empty GFP) (Chapter 2, Section 2.3.2). Changes in single cell motility (single cell speed) of siRNA-transfected PC3 cells was quantified using tracking analysis of cells that have been imaged in time-lapse image sequences. Images were acquired over 24 hours using a widefield microscope (Eclipse Ti; Nikon) equipped with a motorized stage and incubator chamber.

3.2.1 Optimization of single cell tracking

Prior to the screen, the procedure was optimised using negative (siRNA-non-targeting control, NTC) and positive controls (siRNA-radixin). Radixin is one of ezrin/radixin/moesin (ERM) family proteins that are implicated in the linkage of plasma membrane receptors and actin cytoskeleton (Tsukita & Yonemura 1997). In addition, ERM proteins function in signalling pathways that regulate cell migration and cell polarity (Fehon et al. 2010). A previous work by Valderrama et al. (2012) found that radixin regulates migration and adhesion of PC3 cells. The depletion of Radixin in by siRNA transient transfection in PC3 cells demonstrated a

significant reduction (62%) of PC3 single cell speed (Valderrama et al. 2012). Therefore, the siRNA transfection against radixin was employed as a positive control.

To confirm successful knockdown of radixin, prior to screening, GFP-PC3 cells were seeded in 6 well plates and transfected with either NTC or radixin-siRNA. Cells were incubated for 3 days, harvested and the effect upon radixin expression analysed using qPCR and immunoblotting. Figure 3.4 (a) and (b) shows that radixin knockdown was successful both at the RNA and protein levels, with expression reduced by more than 90 % compared to NTC.

3.2.2 The effect of Radixin knockdown on motility

For the screen, I developed a live cell-based semi-high throughput protocol that can be performed in 96-well plates. Cells were seeded sparsely (500-700 cell per well) to avoid cells becoming too confluent, which would have had an impact upon cell motility. Time-lapse microscopy was employed to take images of the chosen fields of view every 15 minutes, 72 hours after transfection. Before applying a tracking algorithm to follow single-cell trajectories, time-lapse images needed to be pre-processed in order to segment objects (cells in this case) from the background (Chapter 2 (2.3.2.2), Figure 2.1). Thresholding was subsequently applied to label anything above the intensity threshold as an object and the rest as background (Meijering et al. 2012). The Trackmate module in ImageJ was initially employed to analyse the tracks and cell motility (Tinevez et al. 2017). Figure 3.5 shows a graphical example of the Trackmate output of PC3-GFP cells transfected with siRNA-NTC and -radixin. 355 trajectories for each phenotype were analysed using the Trackmate algorithm and cells that appeared in less than 50 frames were excluded from the analysis for accuracy (Figure 3.6).

Radixin-depleted cells were relatively static compared to controls which appeared to be more motile, Figure 3.6 (a), and analysis confirmed that this gene knockdown significantly reduced PC3 cell speed (micron/minute) compared to NTC and mock transfected cells. Control cells demonstrated a speed of 0.48-0.58 $\mu\text{m}/\text{min}$, while radixin-siRNA transfected PC3 cells

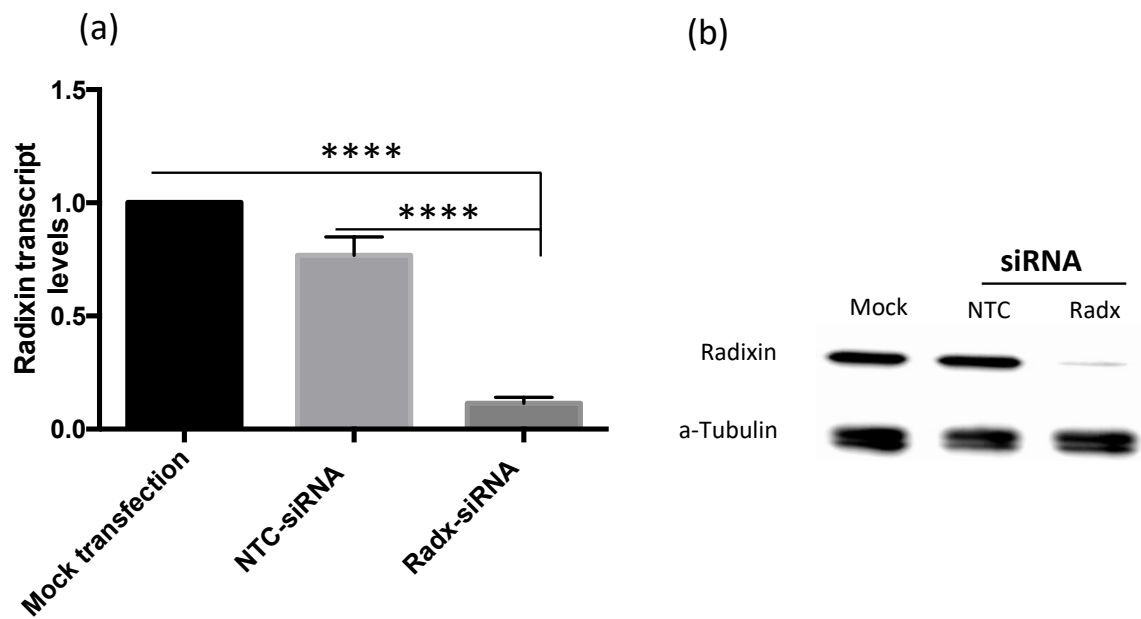


Figure 3.4 Confirmation of radixin knockdown at the RNA and protein levels.

PC3-GFP were transfected with siRNA-NTC or -radixin and incubated for 72 hours. (a): Cells were harvested, RNA extracted and cDNA synthesised. Radixin expression was subsequently quantified using qPCR. Data represent mean \pm 1SD of three independent repeats. ANOVA by Dunnett's post hoc comparison test, ****P < 0.0001. (b): Cells were harvested, and proteins separated using SDS-PAGE. Immunoblotting was subsequently performed using antibodies specific for radixin or α -tubulin (loading control).

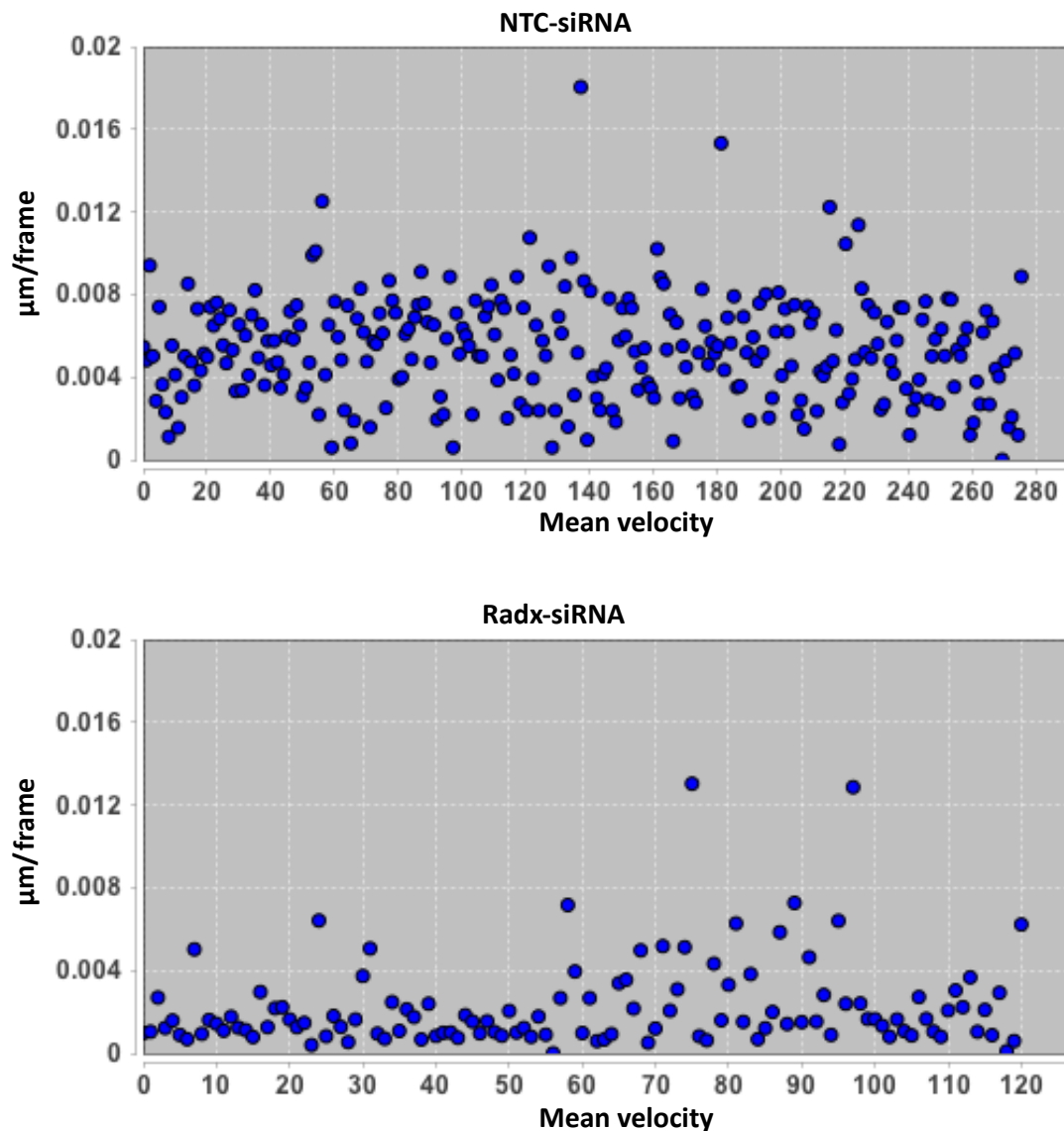


Figure 3.5 Mean velocity (micron/frame) of cells following depletion of radixin.

PC3-GFP were transfected with siRNA-NTC or -radixin and incubated for 72 hours, and on day 4 imaging was performed by widefield microscope. Images of Radixin-depleted and control cells were acquired every 15 minutes over 24 hours, time-lapse sequences were then used to calculate mean of cell speed ($\mu\text{m}/\text{frame}$) by a semi-automated method. Images show the mean speed of tracks of NTC-siRNA transfected versus Radx (Radixin)-siRNA transfected PC3 cells. These data graphs were made by Trackmate plugin in ImageJ.

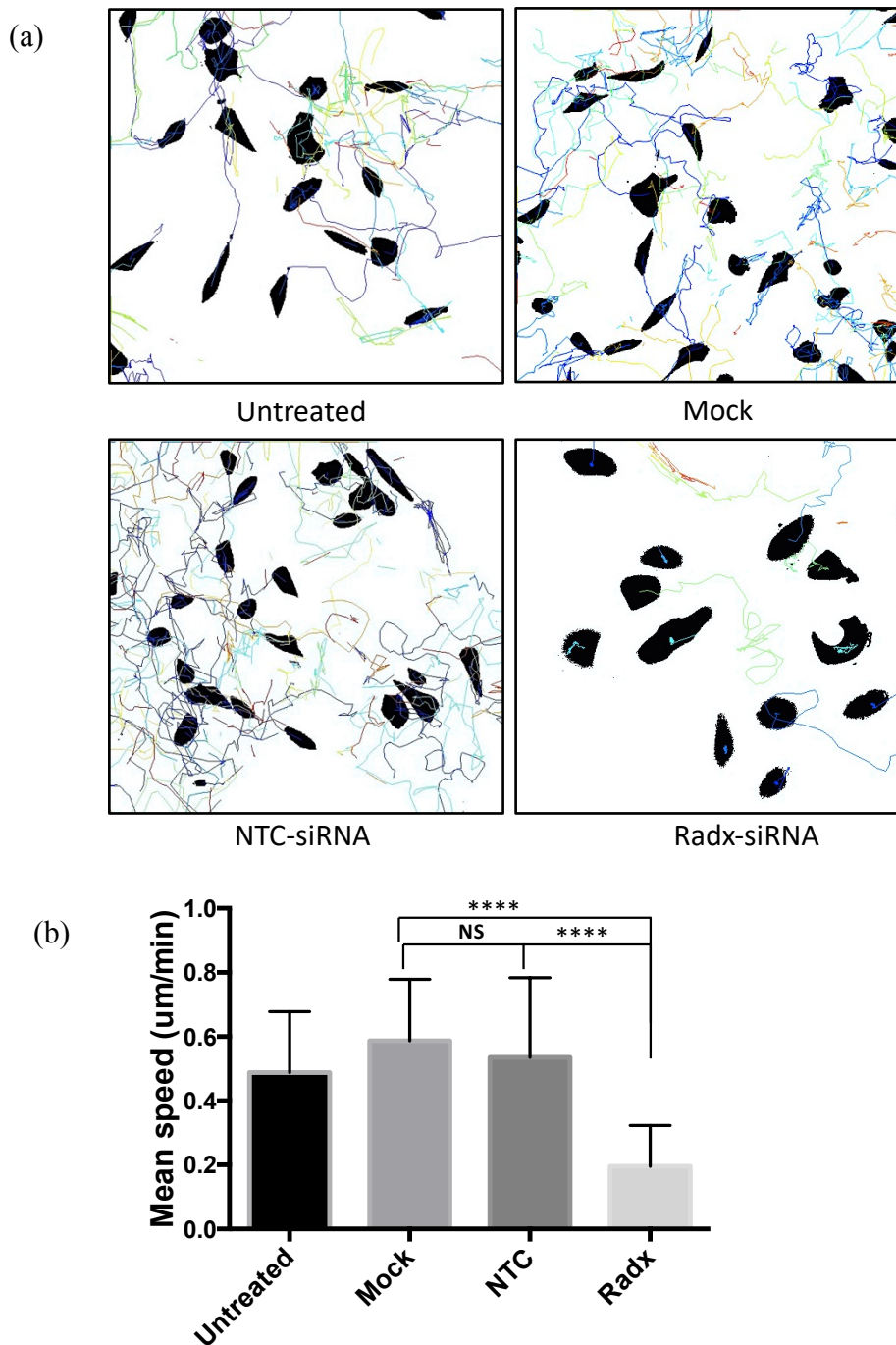


Figure 3.6 Quantification of PC3-GFP motility using a semi-automated algorithm (Trackmate).

Images of Radixin-depleted and control cells were acquired every 15 minutes over 24 hours and time-lapse sequences were used to calculate cell speed ($\mu\text{m}/\text{min}$). (a): shows images of tracks of radixin-depleted cells compared to control (NTC-transfected) cell tracks. (b): Bar chart of mean cell speed per minute (micron/minute). Data is mean \pm 1SD of more than 100 trajectories, three independent repeats. Kruskal-Wallis (Dunn's post hoc test). **** $P < 0.0001$.

migrated at a mean speed of 0.19 $\mu\text{m}/\text{min}$ or less Figure 3.6 (b).

3.2.3 Tracking analysis automation

Processing of large image-based datasets can be streamlined through the use of automation. In the case of this study, hundreds of individual transfections were performed with a minimum of 4 images per repeat. Therefore, further work was required to simplify the data analysis. Quantification of image sequences required multiple steps, including image pre-processing (background subtraction and thresholding), tracking, and statistical analysis. To streamline this process, two macros using existing ImageJ plugins were created to automatically pre-process the image sequences (Methods Chapter, Section 2.3.2.2). The first macro converted the ICS files to TIF files prior to image pre-processing. Both steps were further automated by adding a batch routine which makes the macro automatically pre-process a group of images at once by only selecting the input and output directory. Batch analysis using ADAPT plugin available in ImageJ (Barry et al. 2015) was then run automatically and data was extracted as Excel files for the rest of the analysis. This algorithm was chosen over Trackmate because the latter does not allow batch mode analysis, and it requires further processing of the output to calculate cell speed, while ADAPT automatically allows entering image parameters into the graphical user interface (GUI) and gives cell speed in micron/min. In addition, ADAPT was more efficient in cell detection and linking objects between frames. In other words, ADAPT tracks most cells to the end frame while Trackmate often loses cells between frames and detects and follows them as new objects resulting in a high number of short tracks.

The same dataset used in Figure 3.6 was reanalysed using the ADAPT algorithm (Figure 3.7). The results of the ADAPT analysis (Figure 3.7 b) gave a similar trend as when Trackmate was applied (Figure 3.7 a), with radixin knockdown significantly decreasing PC3 motility compared to controls. However, there is a slight difference in the mean speed values when comparing the two methods, and this can be explained by the mentioned drawbacks of

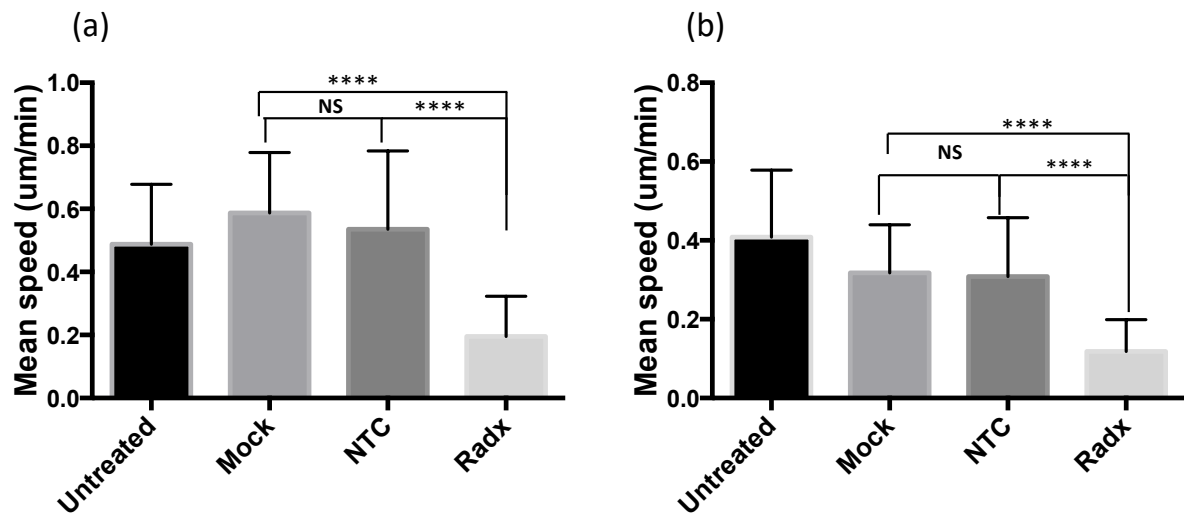


Figure 3.7 Quantification of PC3-GFP cell speed using batch mode based pre-processing macros and an automated tracking algorithm (ADAPT) versus results of the semi-automated method.

Images of Radixin-depleted and control cells were acquired every 15 minutes over 24 hours. The time-lapse sequences were used to calculate cell speed per minute. (a) cell speed was quantified by semi-automated method (Trackmate), and (b) shows cell velocity quantified using automated method (ADAPT). Data represent mean \pm 1SD of at least 100 cells for each phenotype obtained from at least 3 independent experiments. Kruskal-Wallis (Dunn's post hoc test), **** $P < 0.0001$.

Trackmate over ADAPT.

3.2.4 Screening for the identification of metabolic targets regulating prostate cancer motility

Single cell tracking analysis following siRNA knockdown of 217 targets was performed with the aim of identifying novel therapeutic targets that block cell motility (Figure 3.8). Depletion of more than 100 targets significantly affected cell motility relative to NTC control ($P < 0.05$, Dunn's test); statistical analysis performed by using all 3 siRNAs data together for each target compared to NTC. To be more stringent, a cut-off was used to reduce the list of targets. The cut-off included only targets that their knockdowns led to an average cell speed of greater than $1.25 \mu\text{m}/\text{min}$ or less than $0.65 \mu\text{m}/\text{min}$ (relative to NTC). Therefore, the resulted list included only 55 targets and 3 of which increased PC3 cell speed compared to NTC-transfection (Figure 3.9). Knockdown of UROS led to the most significant reduction in PC3 migration; 67% reduction in motility compared to NCT control data. Interestingly, knockdown of UROS resulted in a greater inhibition of PC3 motility compared to the positive control Radixin. Knockdown of other targets, including Nitric oxide synthase 3(NOS3), Ferrochelatase (FECH), scribble cell polarity complex component (LLGL2), ALDOA, and sphingomyelin synthase 2 (MGC26963) also led to a decrease in cell motility by more than 50 % (Table 3.2). Several targets identified to inhibit motility were also found to have a significant effect upon PC3 proliferation. UROS, NOS3, ALDOA, hyaluronan synthase 3 (HAS3), platelet activating factor acetylhydrolase 2 (PAFAH2), and Farnesyl diphosphate synthase (FDPS) demonstrated a considerable reduction of PC3 cell proliferation as reported previously in this work (Figure 3.3 and Table 3.1). Table 3.2 exhibits information about 18 targets of interest that demonstrated a significant effect upon PC3 motility by each of the 3 siRNAs used ($P < 0.01$, Dunn's test). The other 37 targets that were identified by the cut-off are shown in Figure 7.2 (Appendix).

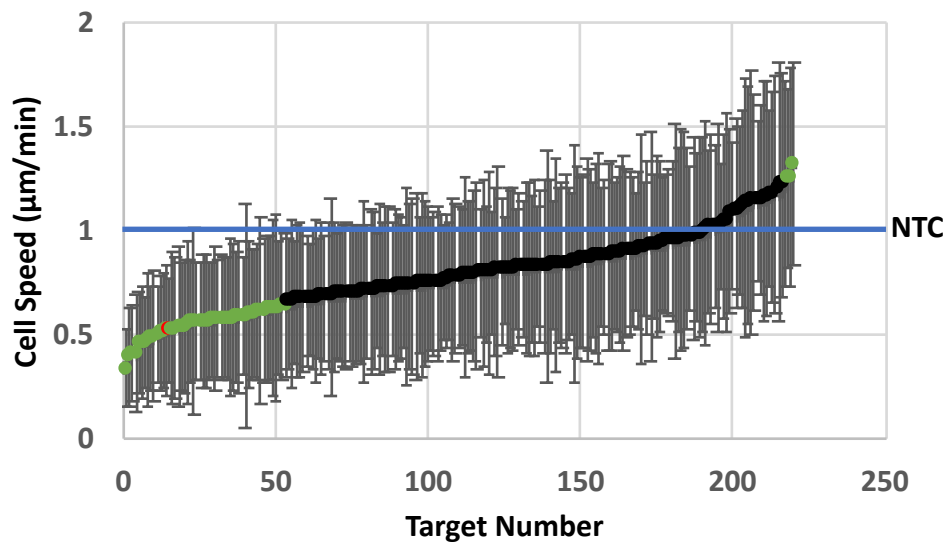


Figure 3.8 An siRNA screen to identify metabolic and cell traffic factors that affect cell motility.

PC3 were transfected with siRNA targeting 217 metabolic and cell traffic factors (3 siRNA per gene). Single cell motility was measured by automated analysis of time-lapse sequences acquired 4 days post transfection (10X objective of Nikon Eclipse Ti widefield microscope, 24 hours of imaging). The data plotted represents the average speed of three siRNA transfections of each target (each siRNA treatment included a minimum of 30 cells) and error bars are the standard deviations (SD). Data was made relative to the NTC (line) present in every run. The green circles highlight the targets' knockdowns that were chosen according to the used cut-off, $1.25 > \text{average speed } (\mu\text{m}/\text{min}) < 0.65$. The red circle represents the positive control (Radixin knockdown) and the blue line represents the speed of NTC-siRNA transfected PC3 cells.

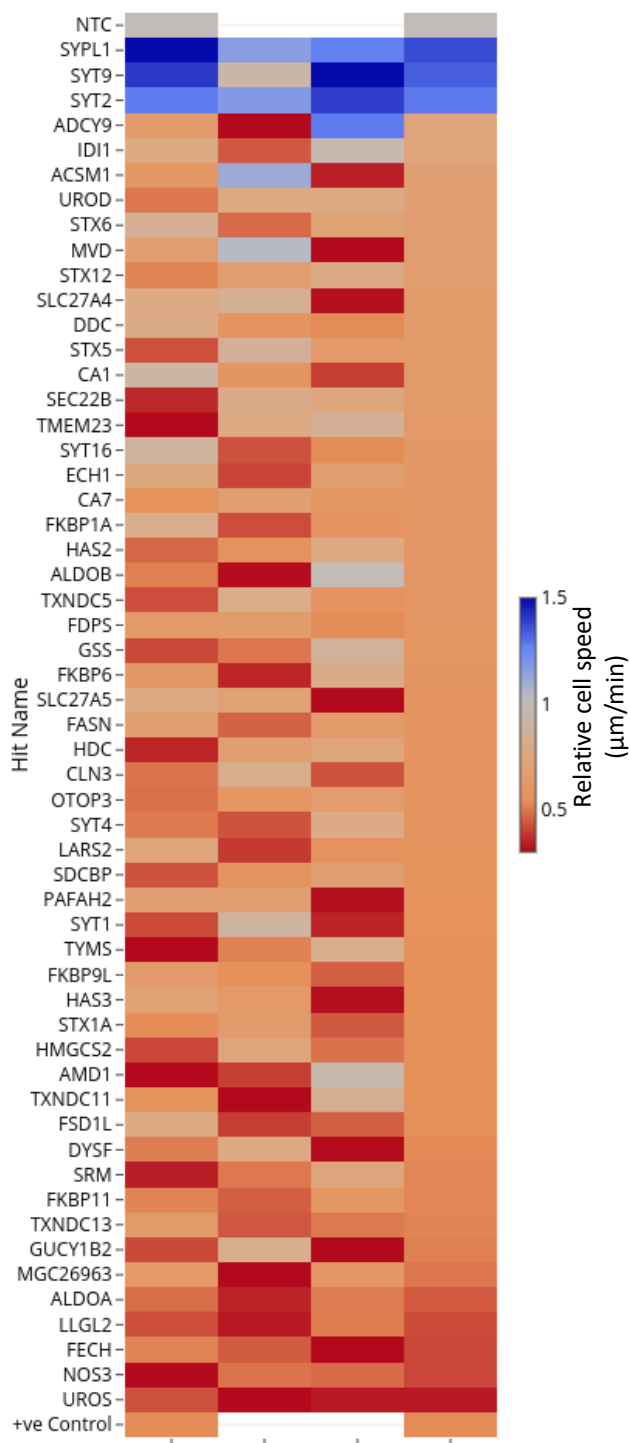


Figure 3.9 Heat map of lead targets affecting PC3 cell migration.

The heat map shows the knockdowns that led to significant reduction of PC3 cell migration ($\mu\text{m}/\text{min}$) relative to NTC according to the used cut-off of $1.25 > \text{average speed } (\mu\text{m}/\text{min}) < 0.65$. The plotted data is of 55 targets where almost each of the three siRNAs used resulted in a significant reduction of cell speed of PC3 in comparison with NTC-siRNA treated cells. The individual effect of used siRNAs is shown as well as the average effect of the three siRNAs. Positive control = RDX (Radixin).

Table 3.2 Summary of the lead targets identified in the siRNA screen to significantly reduce cell motility.

Symbol (symbol in screen)	Gene Description	Pathways	Inhibition of Motility (%)
UROS	uroporphyrinogen III synthase	Catalyzes the fourth step of porphyrin biosynthesis in the heme biosynthetic pathway.	67.3%
NOS3	Nitric oxide synthase 3	A free radical implicated in processes including neurotransmission and antimicrobial and anti-tumoral activities.	59.3%
FECH	Ferrochelatase	Catalyses the insertion of the ferrous form of iron into protoporphyrin IX in the heme synthesis pathway.	59%
LLGL2	scribble cell polarity complex component	The encoded protein is similar to the lethal (2) giant larvae of <i>Drosophila</i> , which functions in asymmetric cell division, epithelial cell polarity, and cell migration.	58%
ALDOA	Aldolase A, fructose-bisphosphate A	Reversible conversion of fructose-1,6-bisphosphate to glyceraldehyde 3-phosphate and dihydroxyacetone phosphate.	56%
	siRNA1	siRNA2	siRNA3
			Average
MGC26963	sphingomyelin synthase 2	Essential for cell growth. Catalyses the transfer of phosphocholine from phosphatidylcholine onto ceramide to make Sphingomyelin, a major component of cell and Golgi membranes.	51%

TXNDC13	TMX4, thioredoxin related transmembrane protein 4	A member of the disulfide isomerase (PDI) family of endoplasmic reticulum (ER) proteins that play roles in protein folding and thiol-disulfide interchange reactions.	48%
FKBP11	FK506 binding protein 11	Implicated in the catalysis of the folding of proline-containing polypeptides.	48%
HMGCS2	3-hydroxy-3-methylglutaryl-CoA synthase 2	It is a mitochondrial enzyme that catalyses the first reaction of ketogenesis, a metabolic pathway that makes lipid-derived energy for various organs when required.	47%
STX1A	syntaxin 1A	Syntaxins are nervous system-specific proteins which function in the docking of synaptic vesicles with the presynaptic plasma membrane.	46%
HAS3	hyaluronan synthase 3	Involved in the synthesis of the unbranched glycosaminoglycan hyaluronan, or hyaluronic acid, which is a major constituent of the extracellular matrix.	46%
FKBP9L	FK506 binding protein 9 pseudogene 1	Unknown.	46%

PAFAH2	platelet activating factor acetylhydrolase 2	The encoded enzyme catalyses the removal of the acetyl group at the SN-2 position of platelet activating factor.	45%
LARS2	leucyl-tRNA synthetase 2	This gene encodes a mitochondrial leucyl-tRNA synthetase which implicates in catalysis of the aminoacylation of a specific tRNA.	44%
OTOP3	otopetrin 3	Unknown.	42%
FASN	fatty acid synthase	The encoded enzyme mainly catalyses the synthesis of palmitate from acetyl-CoA and malonyl-CoA into long-chain saturated fatty acids.	42%
SLC27A5	solute carrier family 27 member 5	Activation of very long-chain fatty-acids containing 24- and 26-carbon.	42%
FDPS	Farnesyl diphosphate synthase	Catalyzes the production of geranyl pyrophosphate and farnesyl pyrophosphate from isopentenyl pyrophosphate.	40%

3.2.5 Validating targets that significantly affect PCa cell migration

Only 10 hits, that showed the most significant reduction of PC3 cell speed (Table 3.2), were selected for validations. As for the siRNA screen, each factor was depleted using three individual siRNAs and cells left for 72 hours prior to imaging for 24 hours. The experiments were repeated at least 3 times and 3-4 images of each siRNA transfection were acquired each time. The analysis included tracks of more than 100 cells for each siRNA and demonstrated that depletion of the majority of factors significantly reduced PC3 cells motility (Figure 3.10-3.19). The only exception was HMGCS2 which exhibited no significant change in PC3 motility for two of the siRNAs tested (Figure 3.19).

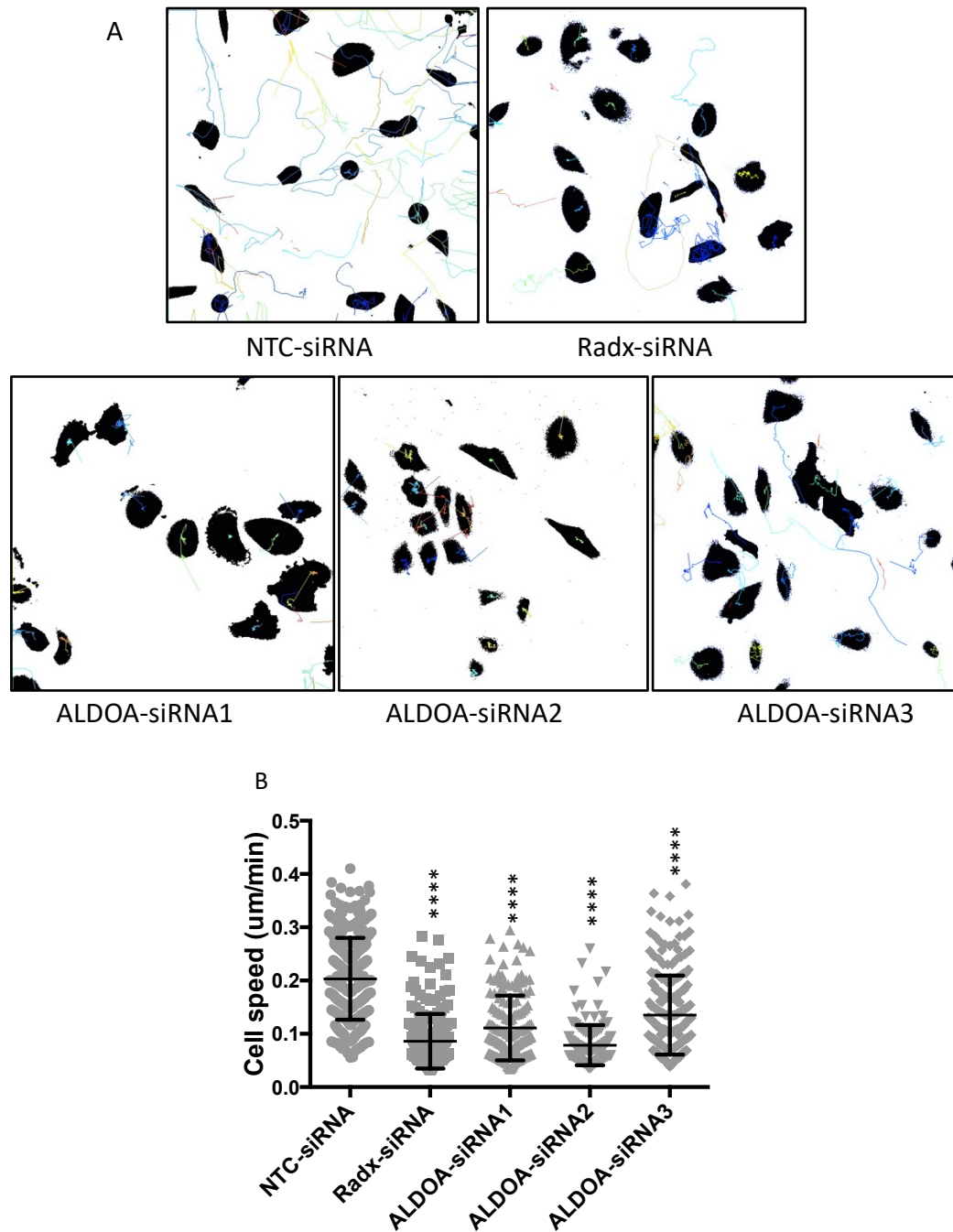


Figure 3.10 Quantification of the effect of ALDOA knockdown upon single cell tracking in GFP-PC3 cells.

Cells were transfected with 3 individual siRNAs targeting ALDOA, or positive and negative control siRNA (Radx and NTC). Images were acquired every 15 minutes using a Nikon Eclipse Ti widefield microscope. A: a panel of representative images of cell tracks after knockdowns. Images were generated using Trackmate (ImageJ) using LoG detector and nearest neighbour search tracker. B: A scatter dot plot of mean \pm 1SD of cell speed (three independent repeats, a minimum of 30 cells per mean) Kruskal-Wallis (Dunn's post hoc test), *** $P < 0.0001$.

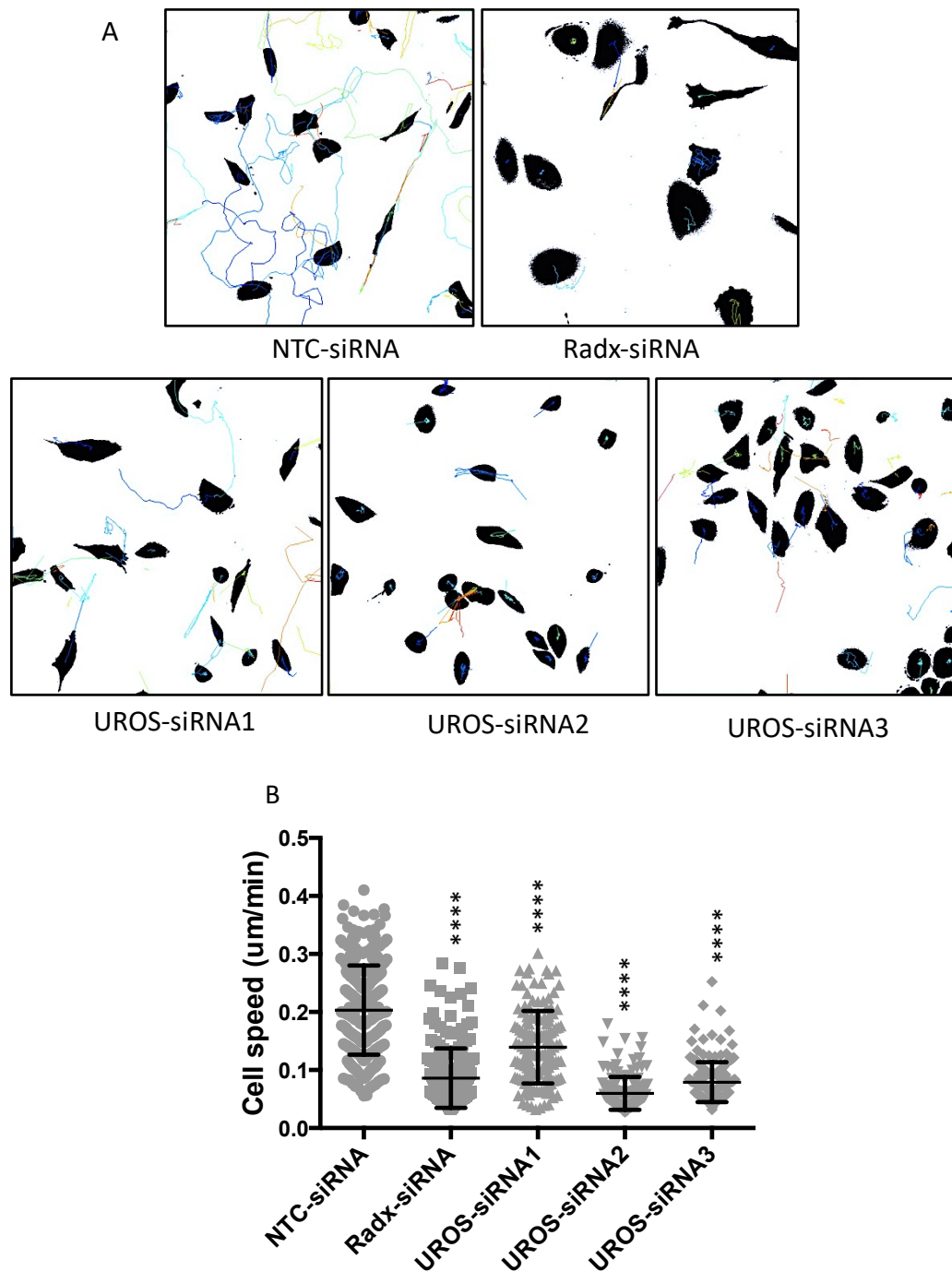


Figure 3.11 Quantification of the effect of UROS knockdown upon single cell tracking in GFP-PC3 cells.

Cells were transfected with 3 individual siRNAs targeting UROS, or positive and negative control siRNA (Radx and NTC). Images were acquired every 15 minutes using a Nikon Eclipse Ti widefield microscope. A: a panel of representative images of cell tracks after knockdowns. Images were generated using Trackmate (ImageJ) using LoG detector and nearest neighbour search tracker. B: A scatter dot plot of mean \pm 1SD of cell speed (three independent repeats, a minimum of 30 cells per mean) Kruskal-Wallis (Dunn's post hoc test), ****P < 0.0001.

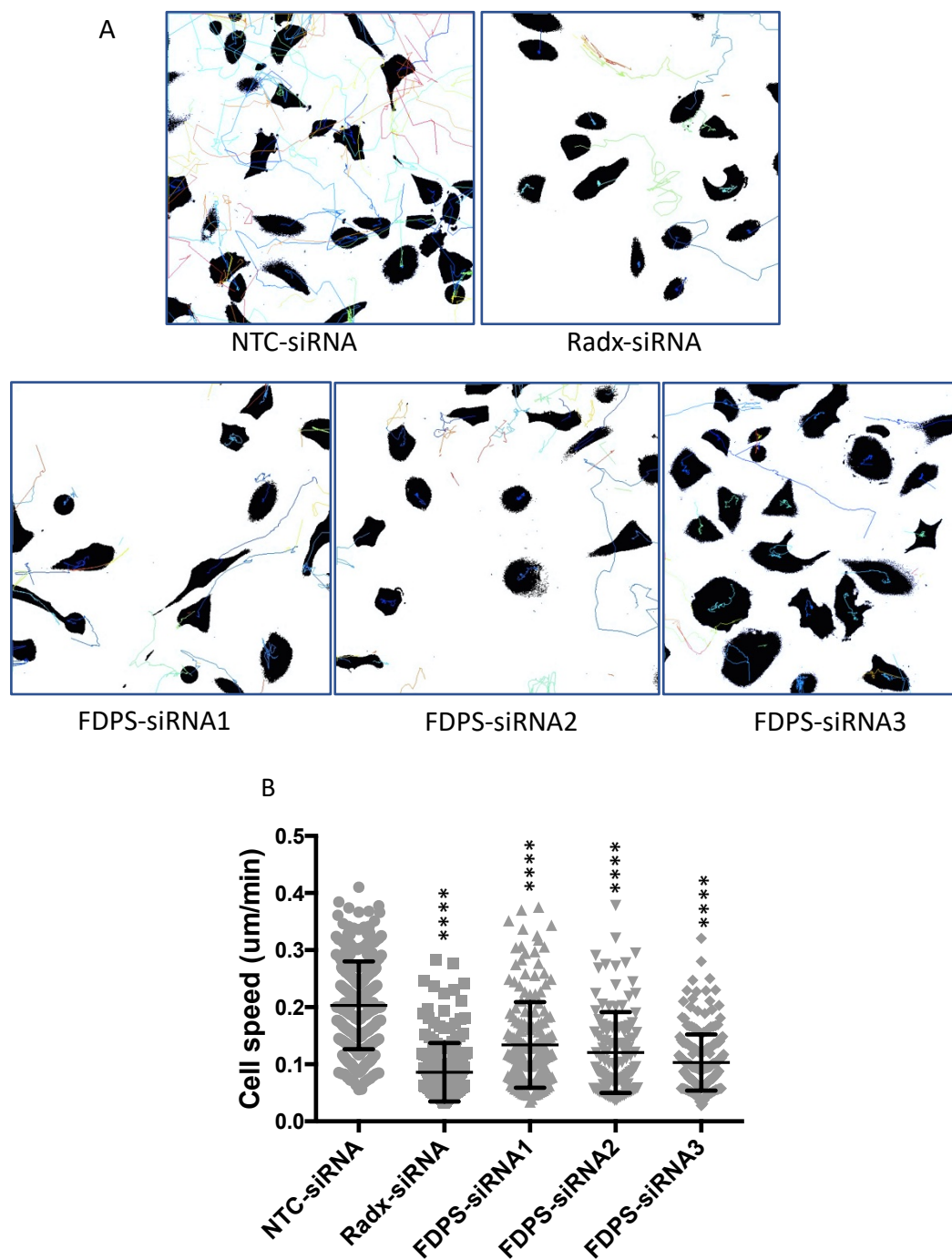


Figure 3.12 Quantification of the effect of FDPS knockdown upon single cell tracking in GFP-PC3 cells.

Cells were transfected with 3 individual siRNAs targeting FDP, or positive and negative control siRNA (Radx and NTC). Images were acquired every 15 minutes using a Nikon Eclipse Ti widefield microscope. A: a panel of representative images of cell tracks after knockdowns. Images were generated using Trackmate (ImageJ) using LoG detector and nearest neighbour search tracker. B: A scatter dot plot of mean \pm 1SD of cell speed (three independent repeats, a minimum of 30 cells per mean) Kruskal-Wallis (Dunn's post hoc test), ****P < 0.0001.

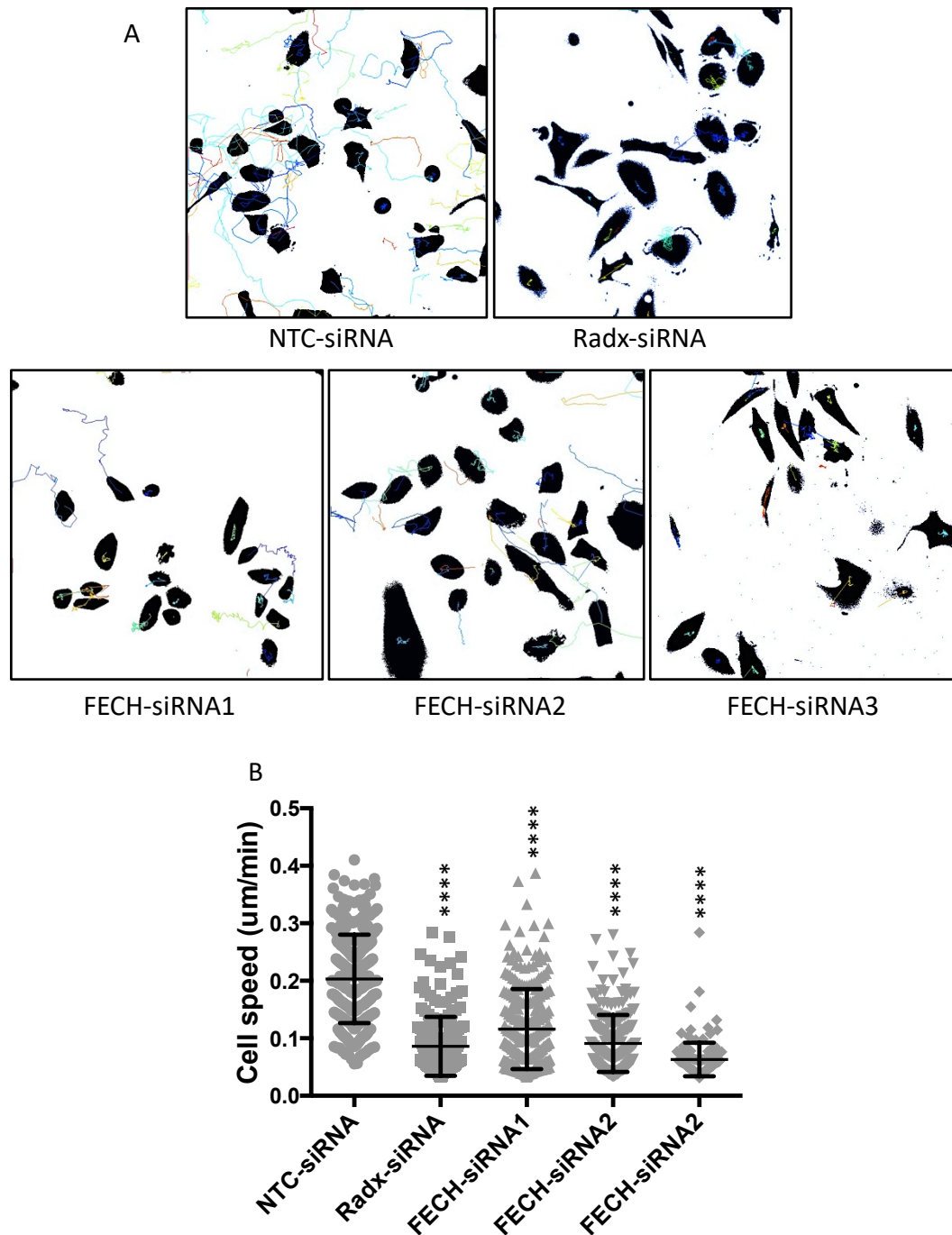


Figure 3.13 Quantification of the effect of FECH knockdown upon single cell tracking in GFP-PC3 cells.

Cells were transfected with 3 individual siRNAs targeting FECH, or positive and negative control siRNA (Radx and NTC). Images were acquired every 15 minutes using a Nikon Eclipse Ti widefield microscope. A: a panel of representative images of cell tracks after knockdowns. Images were generated using Trackmate (ImageJ) using LoG detector and nearest neighbour search tracker. B: A scatter dot plot of mean \pm 1SD of cell speed (three independent repeats, a minimum of 30 cells per mean) Kruskal-Wallis (Dunn's post hoc test), ***P < 0.0001.

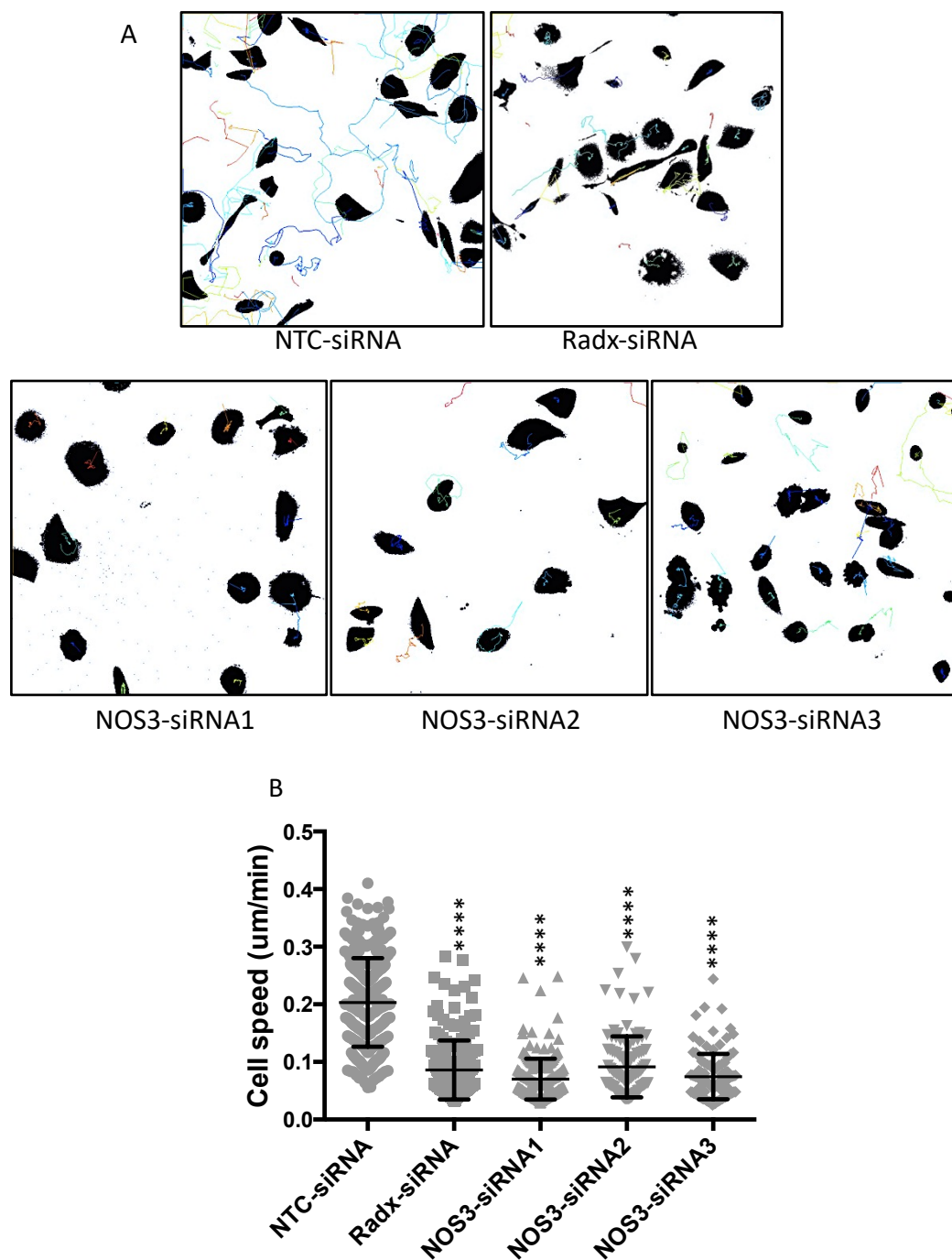


Figure 3.14 Quantification of the effect of NOS3 knockdown upon single cell tracking in GFP-PC3 cells.

Cells were transfected with 3 individual siRNAs targeting NOS3, or positive and negative control siRNA (Radx and NTC). Images were acquired every 15 minutes using a Nikon Eclipse Ti widefield microscope. A: a panel of representative images of cell tracks after knockdowns. Images were generated using Trackmate (ImageJ) using LoG detector and nearest neighbour search tracker. B: A scatter dot plot of mean \pm 1SD of cell speed (three independent repeats, a minimum of 30 cells per mean) Kruskal-Wallis (Dunn's post hoc test), ****P < 0.0001.

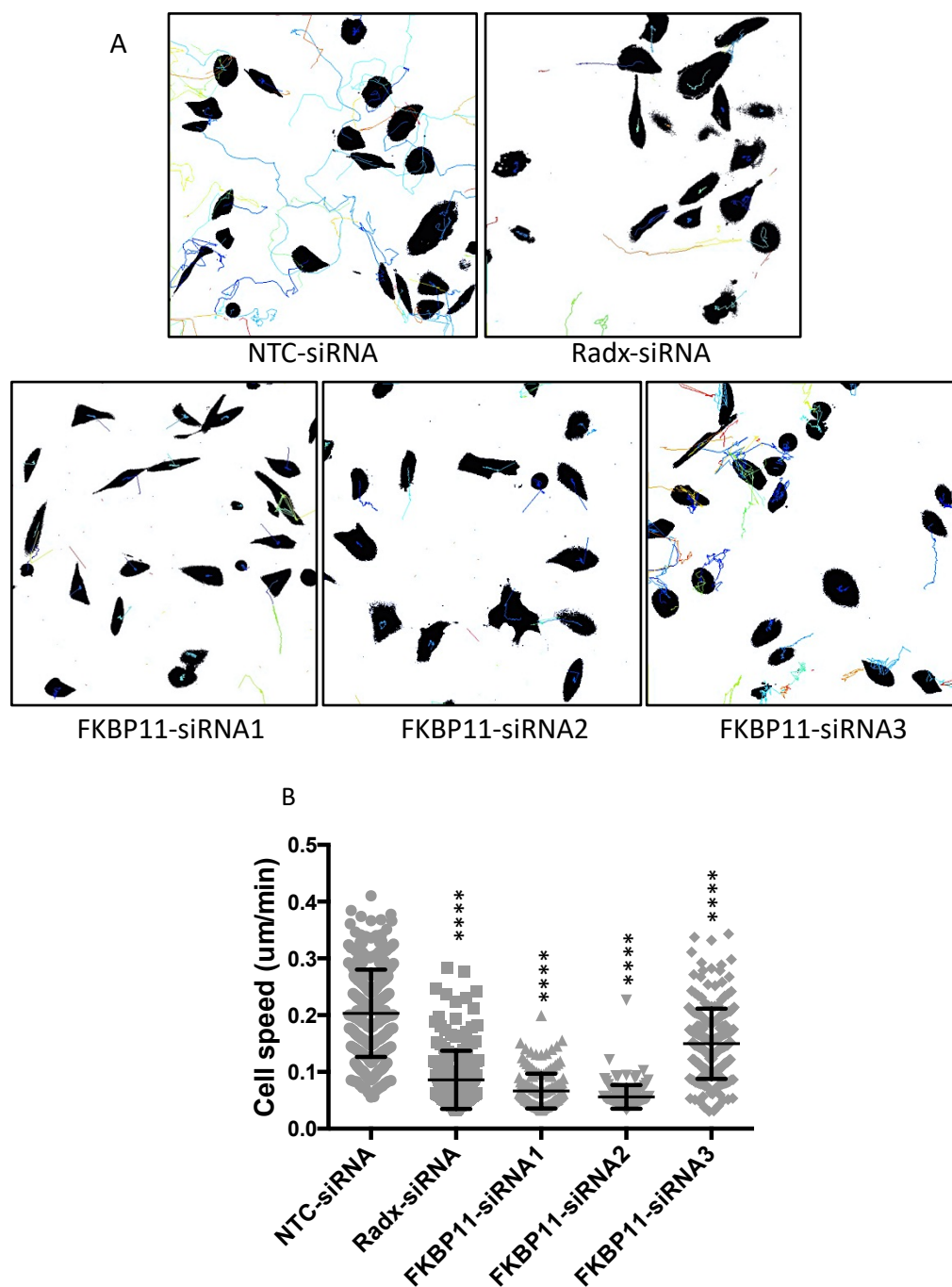


Figure 3.15 Quantification of the effect of FKBP11 knockdown upon single cell tracking in GFP-PC3 cells.

Cells were transfected with 3 individual siRNAs targeting FKBP11, or positive and negative control siRNA (Radx and NTC). Images were acquired every 15 minutes using a Nikon Eclipse Ti widefield microscope. A: a panel of representative images of cell tracks after knockdowns. Images were generated using Trackmate (ImageJ) using LoG detector and nearest neighbour search tracker. B: A scatter dot plot of mean \pm 1SD of cell speed (three independent repeats, a minimum of 30 cells per mean) Kruskal-Wallis (Dunn's post hoc test), ****P < 0.0001.

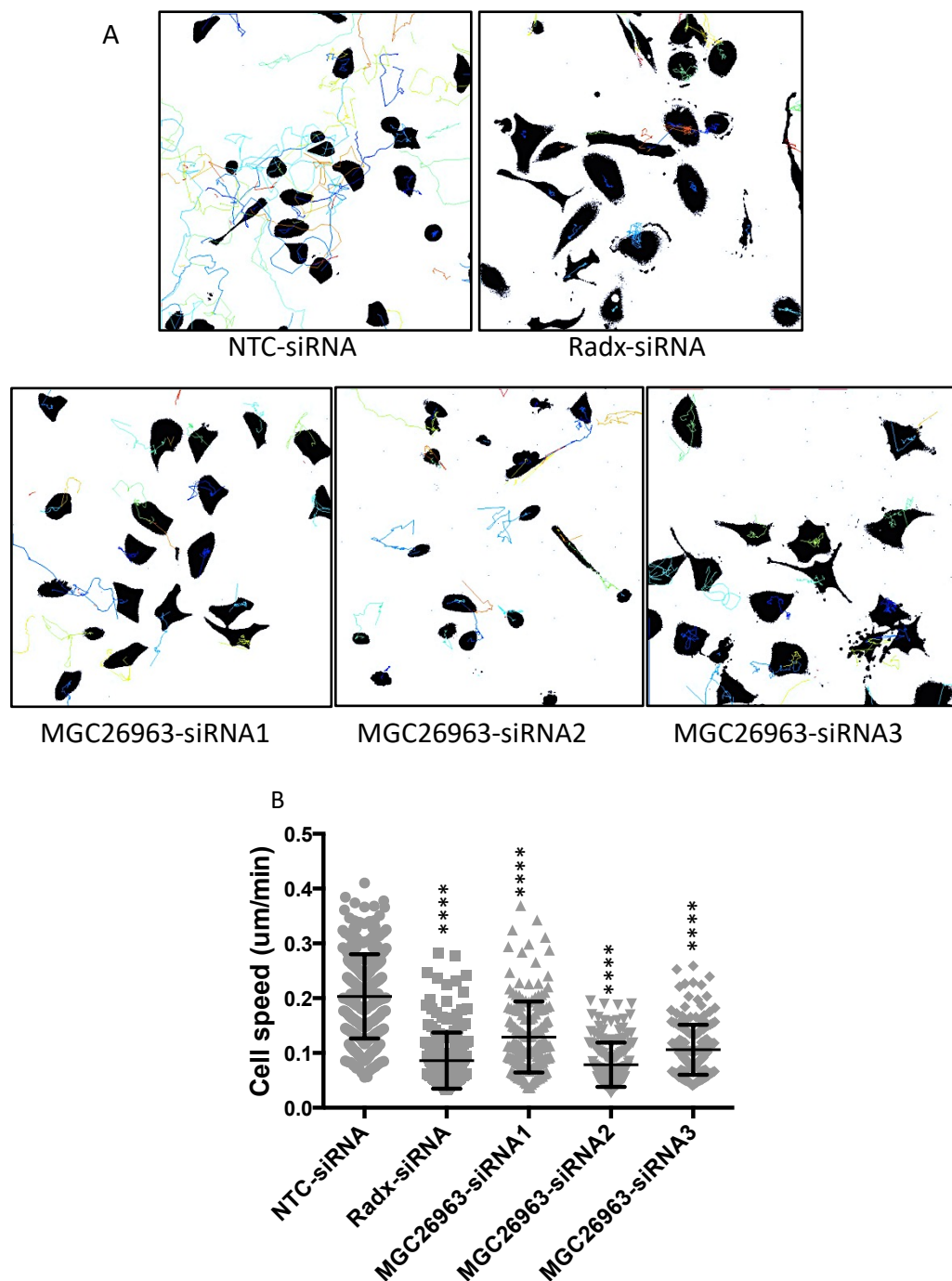


Figure 3.16 Quantification of the effect of MGC2963 knockdown upon single cell tracking in GFP-PC3 cells.

Cells were transfected with 3 individual siRNAs targeting MGC2963, or positive and negative control siRNA (Radx and NTC). Images were acquired every 15 minutes using a Nikon Eclipse Ti widefield microscope. A: a panel of representative images of cell tracks after knockdowns. Images were generated using Trackmate (ImageJ) using LoG detector and nearest neighbour search tracker. B: A scatter dot plot of mean \pm 1SD of cell speed (three independent repeats, a minimum of 30 cells per mean) Kruskal-Wallis (Dunn's post hoc test), ****P < 0.0001.

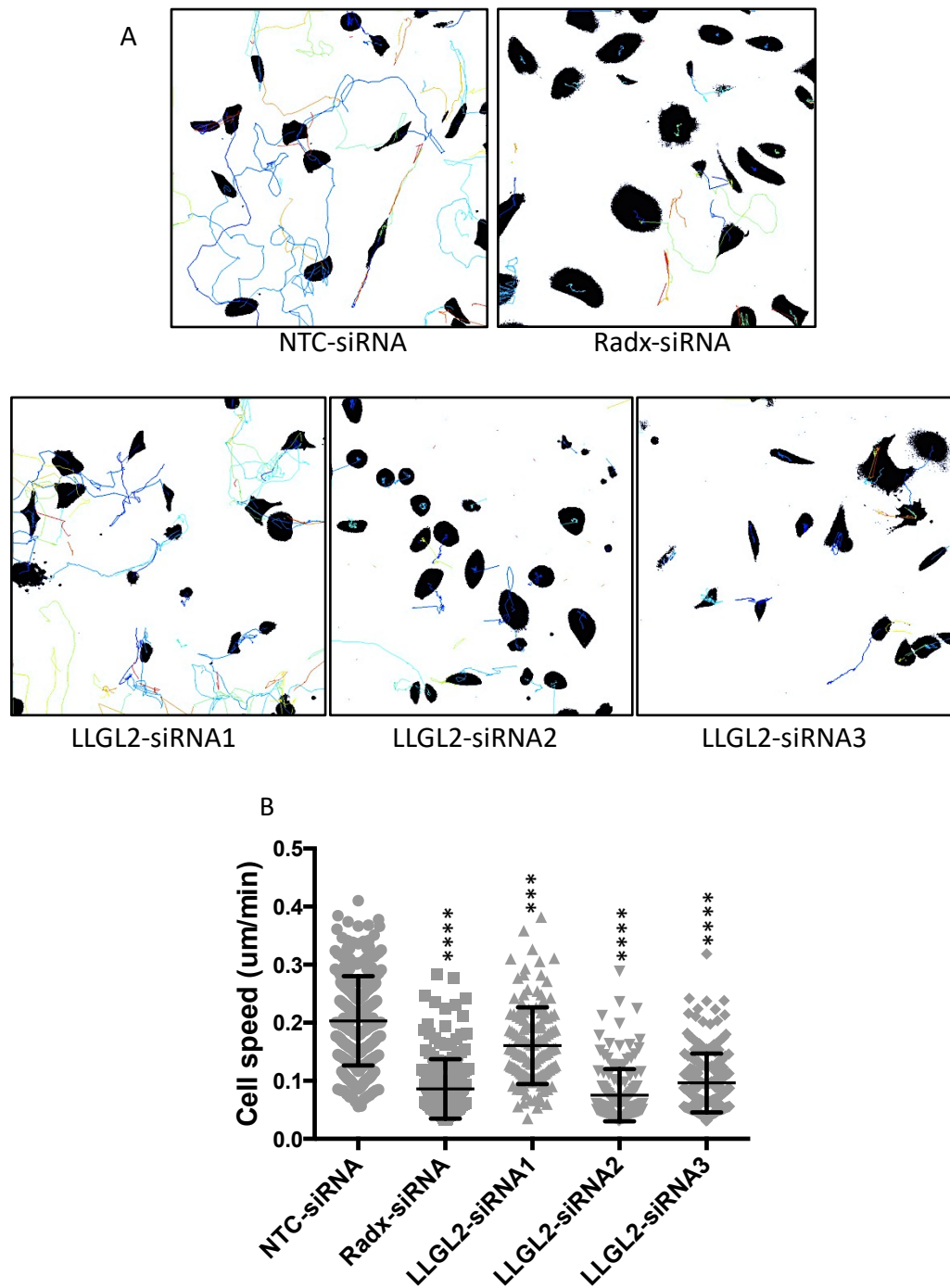


Figure 3.17 Quantification of the effect of LLGL2 knockdown upon single cell tracking in GFP-PC3 cells.

Cells were transfected with 3 individual siRNAs targeting LLGL2, or positive and negative control siRNA (Radx and NTC). Images were acquired every 15 minutes using a Nikon Eclipse Ti widefield microscope. A: a panel of representative images of cell tracks after knockdowns. Images were generated using Trackmate (ImageJ) using LoG detector and nearest neighbour search tracker. B: A scatter dot plot of mean \pm 1SD of cell speed (three independent repeats, a minimum of 30 cells per mean) Kruskal-Wallis (Dunn's post hoc test), ****P < 0.0001.

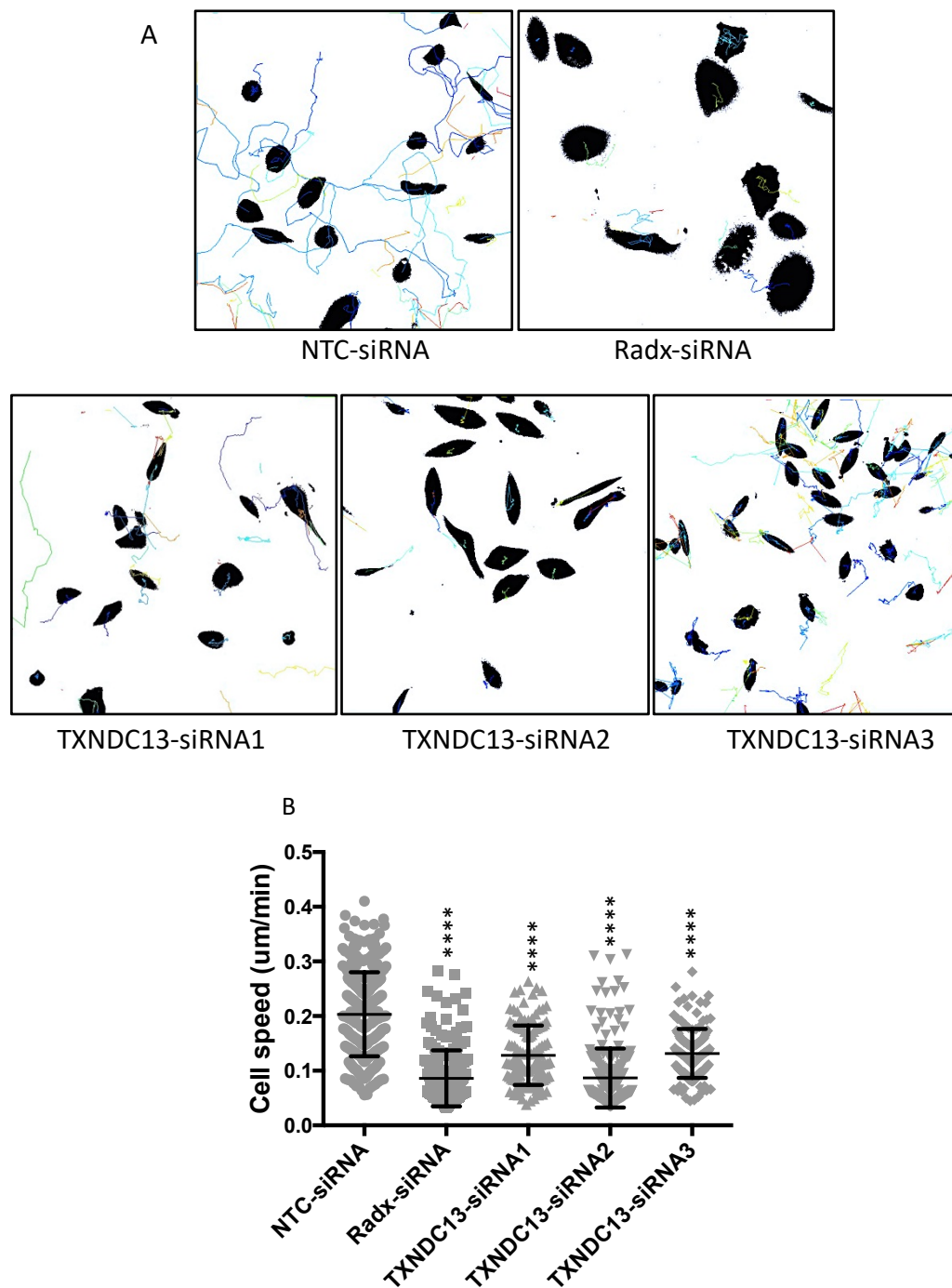


Figure 3.18 Quantification of the effect of TXNDC13 knockdown upon single cell tracking in GFP-PC3 cells.

Cells were transfected with 3 individual siRNAs targeting TXNDC13, or positive and negative control siRNA (Radx and NTC). Images were acquired every 15 minutes using a Nikon Eclipse Ti widefield microscope. A: a panel of representative images of cell tracks after knockdowns. Images were generated using Trackmate (ImageJ) using LoG detector and nearest neighbour search tracker. B: A scatter dot plot of mean \pm 1SD of cell speed (three independent repeats, a minimum of 30 cells per mean) Kruskal-Wallis (Dunn's post hoc test), ****P < 0.0001.

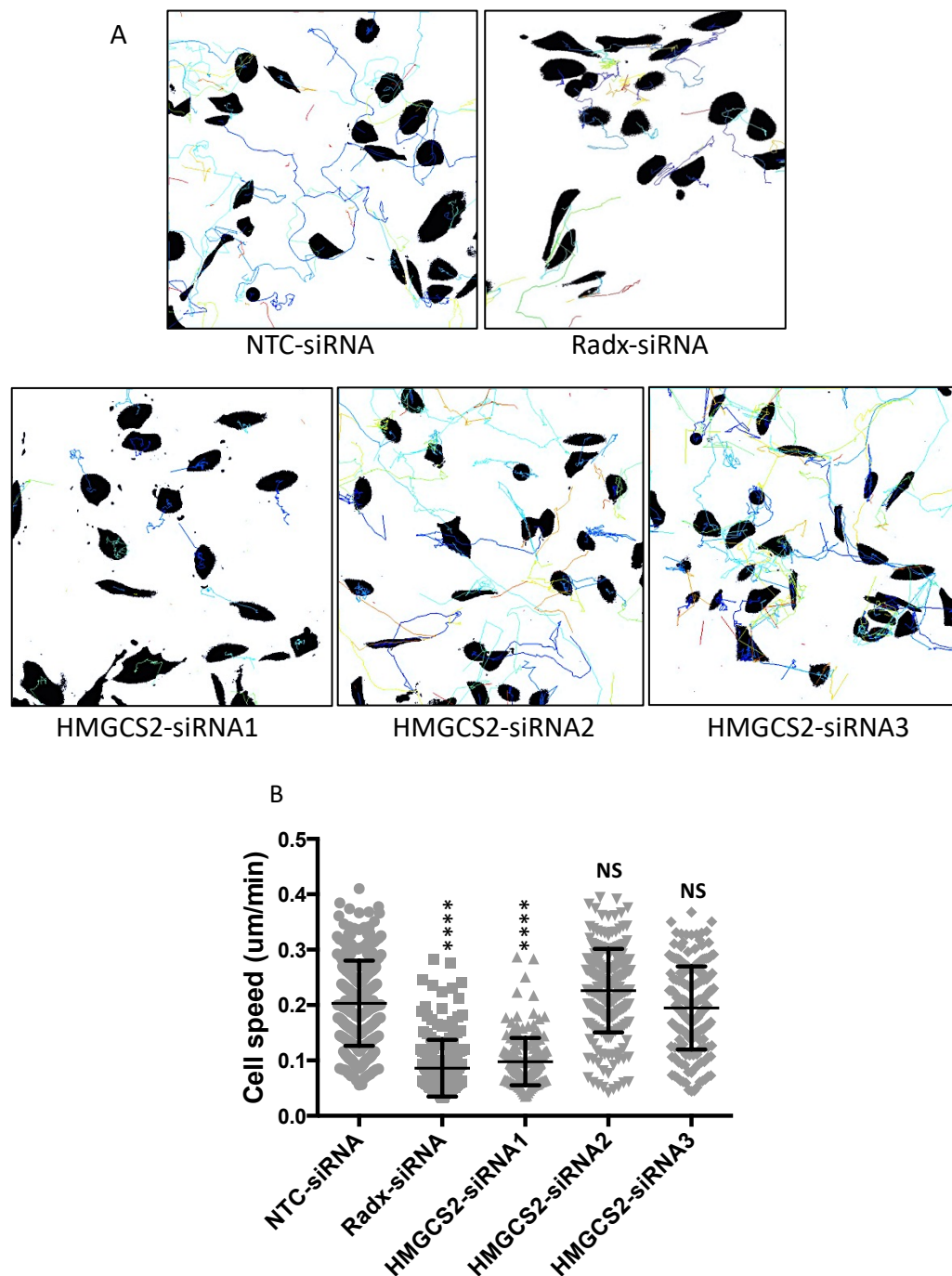


Figure 3.19 Quantification of the effect of HMGCS2 knockdown upon single cell tracking in GFP-PC3 cells.

Cells were transfected with 3 individual siRNAs targeting HMGCS2, or positive and negative control siRNA (Radx and NTC). Images were acquired every 15 minutes using a Nikon Eclipse Ti widefield microscope. A: a panel of representative images of cell tracks after knockdowns. Images were generated using Trackmate (ImageJ) using LoG detector and nearest neighbour search tracker. B: A scatter dot plot of mean \pm 1SD of cell speed (three independent repeats, a minimum of 30 cells per mean) Kruskal-Wallis (Dunn's post hoc test), ****P < 0.0001.

3.3 Bioinformatics analysis and lead targets

3.3.1 Bioinformatics analysis of hit targets

Of the 40 factors found to significantly affect PC3 growth (Figure 3.2), the 14 targets that inhibited proliferation were selected for bioinformatics analysis (Table 3.1). The Gene Expression Omnibus (GEO) (<http://www.ncbi.nlm.nih.gov/geo/profiles>) was used to access the gene expression profiles of these 14 hits in order to investigate if expression correlates with disease progression. The analysis was also performed for hits that inhibited PC3 cell migration (Table 3.2). However, no data was available for some of the hits. Results of GEO analysis (Figure 3.20-3.21) showed that the transcript levels of some of these genes, including *ALDOA*, *TYMS*, *NOS3*, *HAS3*, *GART*, and *STX1A*, tended to be higher in samples from metastatic prostate cancer compared to primary and benign tumorous. The expression of the rest of the targets seemed not too significantly altered across prostatic cancer tissues.

For further investigation, the Human Protein ATLAS (<http://www.proteinatlas.org/>) was employed to investigate changes in the protein levels in tissue samples of normal prostate and different grades of Prostate Cancer (Figure 3.22-3.23). The analysis was run for all proliferation and migration hits, however there was no data for some hits. Most hits were detected in normal and prostatic cancer tissues (Figure 3.22-3.23). Several targets including *TYMS*, *FASN*, and *PAFAH2* showed some correlation with prostate cancer progression ($P < 0.05$, Dunnett's post hoc test). Although the number of samples in available the databases is small, the expression of these hits does appear to correlate with disease progression and this warrants future investigation.

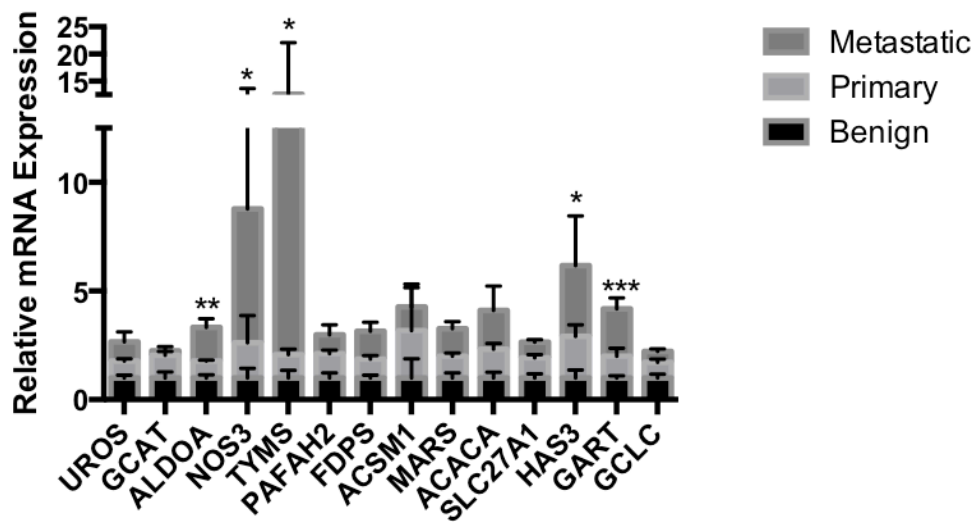


Figure 3.20 Gene expression analysis of proliferation lead targets using Gene Expression Omnibus (GEO) database.

The analysis included data on prostate cancer progression with respect to each individual target. The presented data represents mean±SD of 6-7 samples for each type and it was made relative to the Benign data average value of each target (re-scales to 1). ANOVA (Dunnett's post hoc test), *P < 0.05, **P < 0.01, ***P < 0.001.

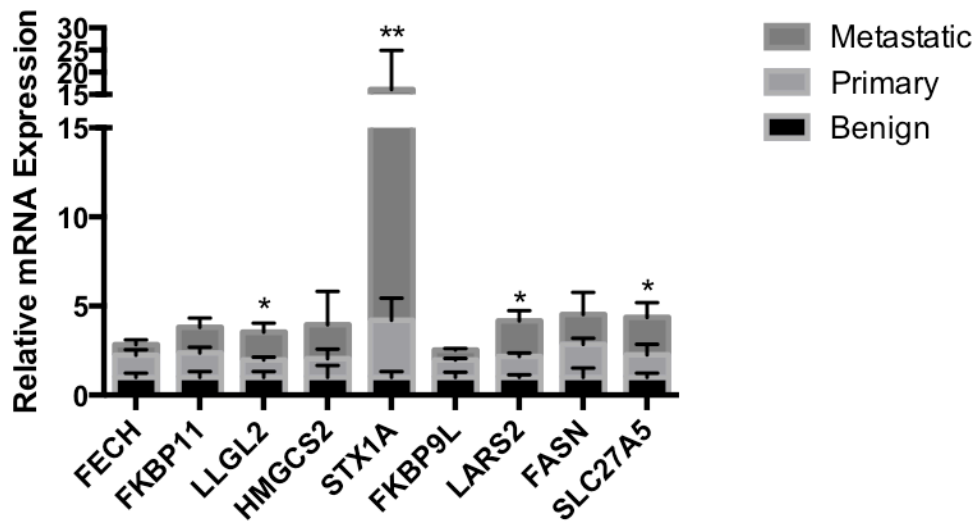
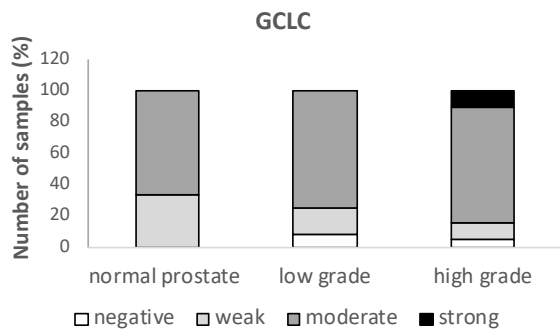
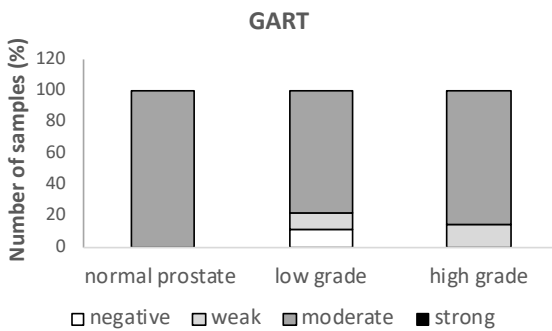
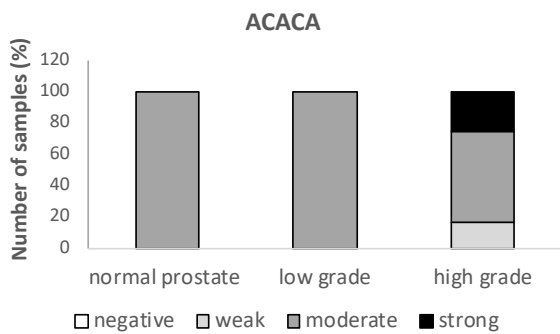
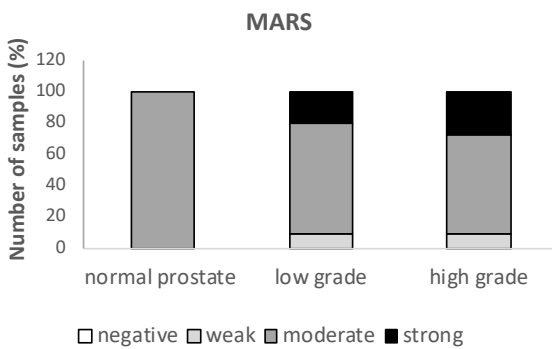
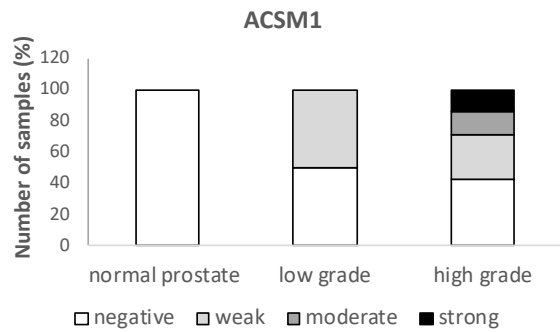
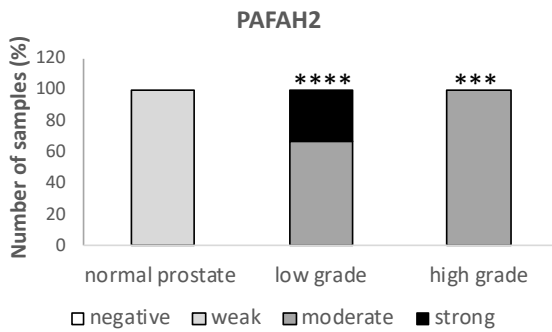
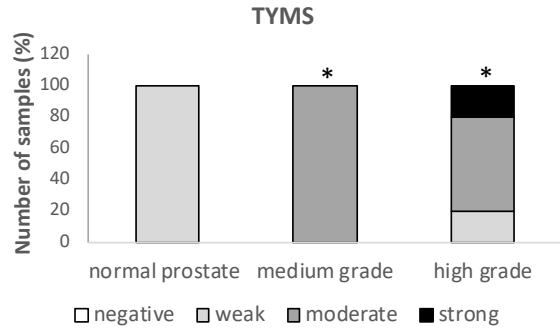
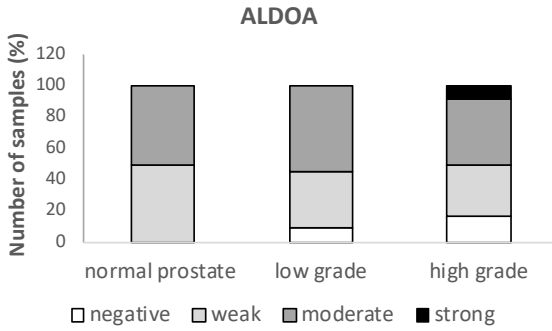
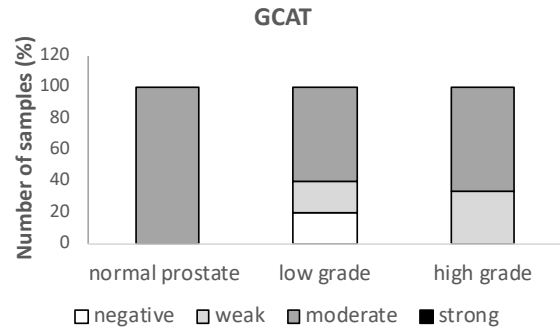
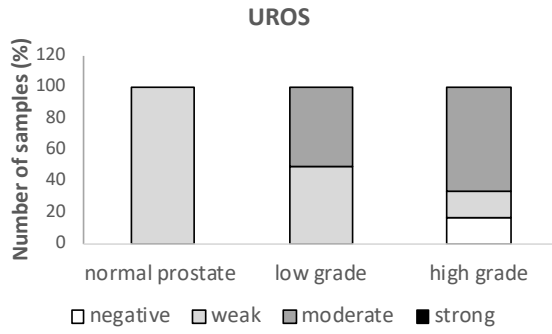


Figure 3.21 Gene expression analysis of migration lead targets using Gene Expression Omnibus (GEO) database.

The analysis included data on prostate cancer progression with respect to each individual target. The presented data is mean±SD of 6-7 samples for each type and it was made relative to the Benign average value of each target. ANOVA (Dunnett's post hoc test), *P < 0.05, **P < 0.01, ***P < 0.001.



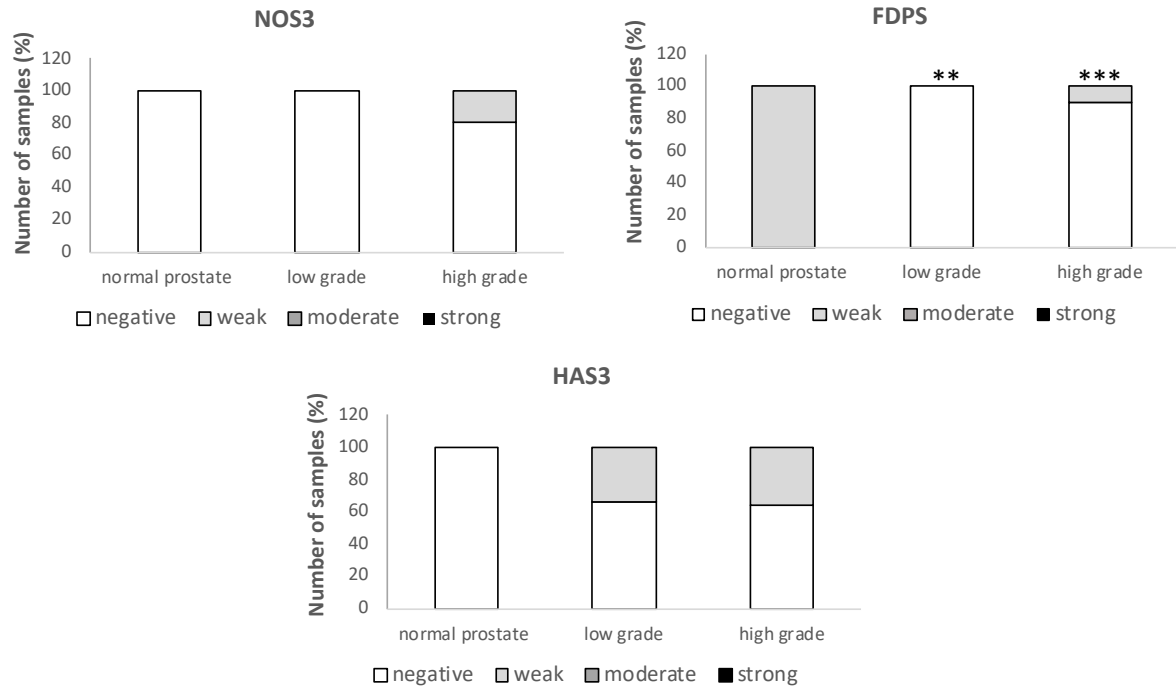


Figure 3.22 Human Protein Atlas based analysis of protein expression levels of proliferation hits in normal prostate versus low- and high-grade prostatic cancer tissues.

This dataset was made using the Human Protein Atlas database. The percentages of each staining category (negative, weak, moderate, and strong) were calculated in respect to the total number of samples in each tissue type (normal, low-grade, or high-grade). ANOVA (Dunnett's post hoc test), *P < 0.05, **P < 0.01, ***P < 0.001, ****P < 0.0001.

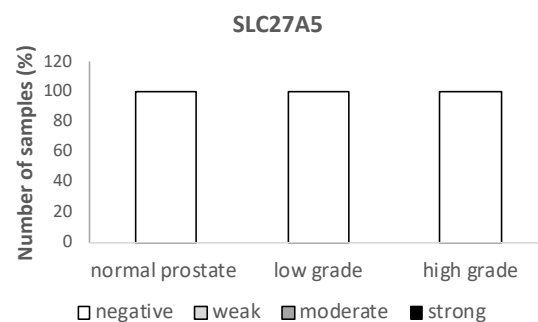
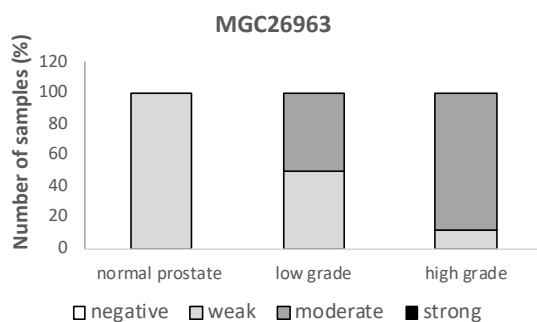
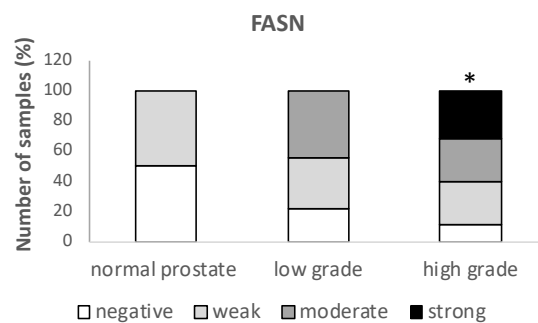
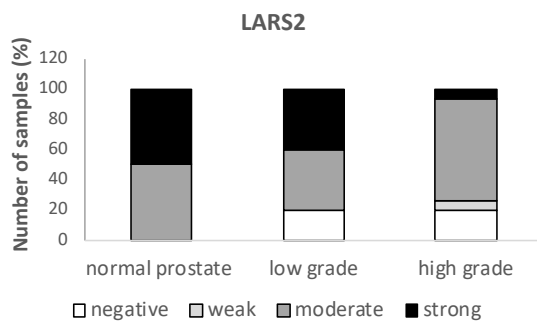
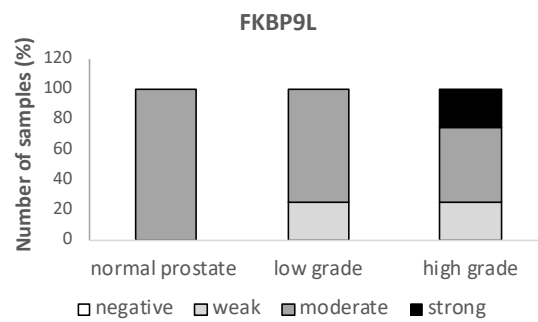
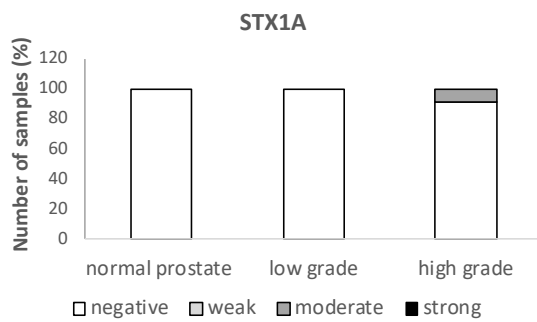
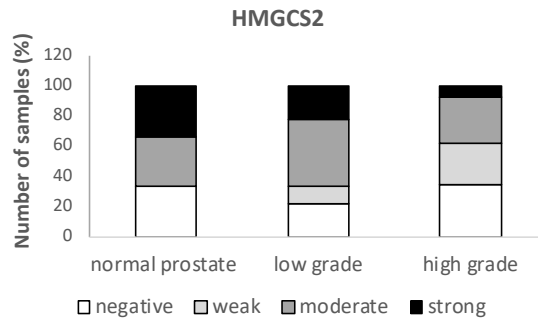
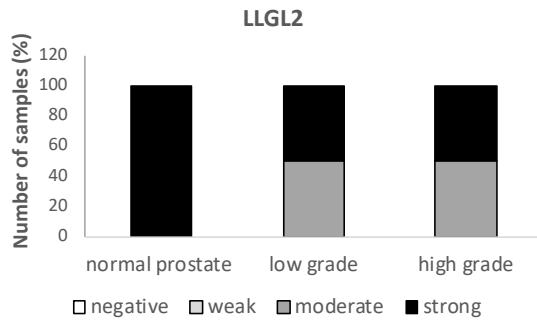
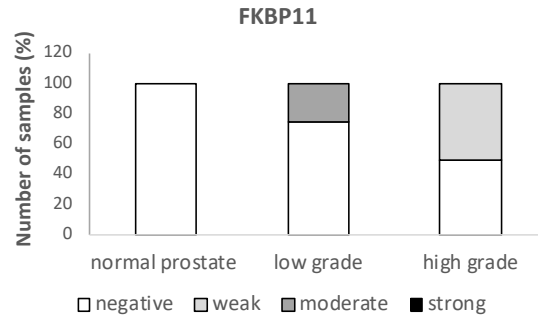
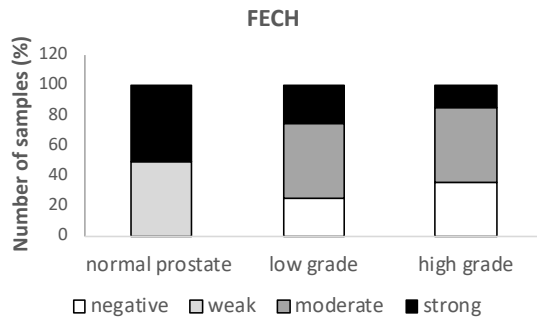


Figure 3.23 Human Protein Atlas based analysis of protein expression levels of migration hits in normal prostate versus low- and high-grade prostatic cancer tissues.

This dataset was made using the Human Protein Atlas database. The percentages of each staining category (negative, weak, moderate, and strong) were calculated in respect to the total number of samples in each tissue type (normal, low-grade, or high-grade). ANOVA (Dunnett's post hoc test), *P < 0.05.

3.3.2 Lead targets

For further work, the decisions on which targets to study was made according to several aspects but mainly dependent upon their effect on proliferation and/or motility of PC3 cells (Table 3.3). The first three hits that led to the highest anti-proliferative effect in PCa cell lines were selected. Those are UROS, GCAT, and ALDOA. UROS and ALDOA also showed high anti-migratory profiles in PC3 cells. FDPS and ACSM1 showed interesting results on cell migration of PC3 (Figure 6.4). Finally, GCLC was chosen also for further study for its affect upon proliferation and according to supporting information from literature where other groups have shown that it can promote therapy resistance in tumour cells (Mulcahy et al. 1994; Kuo et al. 1998; Oguri et al. 1998).

Table 3.3 Summary of the lead targets.

Red means that there is an effect as opposed to white which means that there was no effect. NA = information is not available +++ means a strong effect, and + is a weak effect. RNA and protein data were obtained from GEO and the Human Protein ATLAS analysis tools respectively.

Hit name	Effect on Pc3 growth	Effect on PC3 motility	Transcript upregulation	Protein staining
UROS	+++	+++		+
GCAT	+++	+		
ALDOA	+++	+++	++	
NOS3	+++	+++	++	
TYMS	+++		++	++
PAFAH2	+++	+++		+
FDPS	+++	+++		
ACSM1	+++	+		+
MARS	+++			+
ACACA	+++	+		+
SLC27A1	+++			NA
HAS3	+++	+++	+	
GART	+++		++	
GCLC	+++			
FECH		+++		
FKBP11	+	+++		+
LLGL2	+	+++	+	
HMGCS2		+++		

STX1A	+	+++		
FKBP9L	+	+++		+
LARS2		+++	+	
FASN	+	++		++
SLC27A5		++	+	
OTOP3	+	++		NA
TXNDC13		+++		NA
MGC26963	+	+++		

3.4 The effect of siRNA depletion of the lead targets upon apoptosis and cell cycle

To investigate if knockdown of the lead targets promotes apoptosis, PC3 cells transfected with the relevant pools of siRNAs were harvested and DNA hypodiploidy assays performed. Flow cytometry (Accuri C6) was used to measure the number of cells in the sub-G1 phase. Silencing of all targets (except GCLIC) resulted in some elevation in apoptosis compared to NTC control or mock-transfected cells (Figure 3.24), although this was only significant for ACSM1, UROS and ALDOA ($P < 0.05$, Dunnett's post hoc test). Noticeably, ACSM1 led to the highest rate of apoptosis in PC3, approximately 65%. Knockdown of UROS and ALDOA resulted in 30 % and 26 % apoptosis respectively.

To further determine the mechanisms behind PC3 cell proliferation inhibition, the effect of gene knockdown upon cell cycle was determined using flow cytometry analysis of DNA content (Figure 3.25). Cells were harvested on day 6 after transfection, fixed, RNA digested with RNase, and DNA stained with PI. Knockdown of ACSM1, UROS and GCAT resulted in a significant decrease in the number of cells in G1 (Figure 3.25). This may be explained by the fact that the siRNA knockdown of these genes resulted in a significant increase in the total number of cells in S phase. Additionally, transfections against UROS and GCAT also increased the number of cells in G2/M phase. It, therefore, appears that, prior to apoptosis, knockdown of ACSM1 promotes growth arrest in S phase whereas UROS and GCAT depletion caused cells to arrest in S phase and G2/M. ALDOA knockdown induced cell death as detected by the apoptosis analysis above, although it showed no significant results in respect to cell cycle progression.

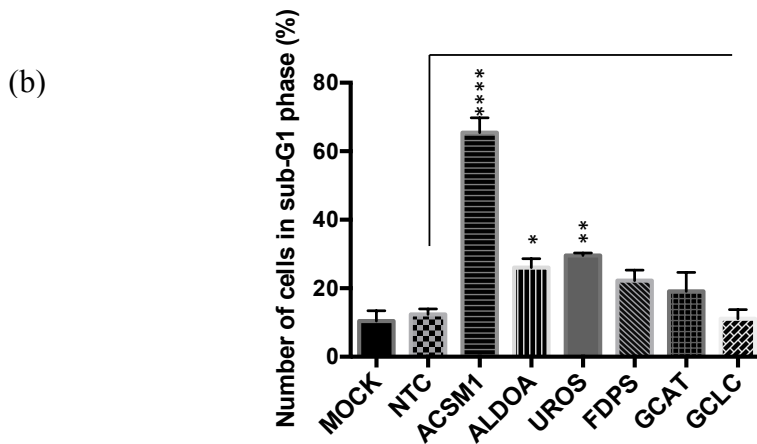
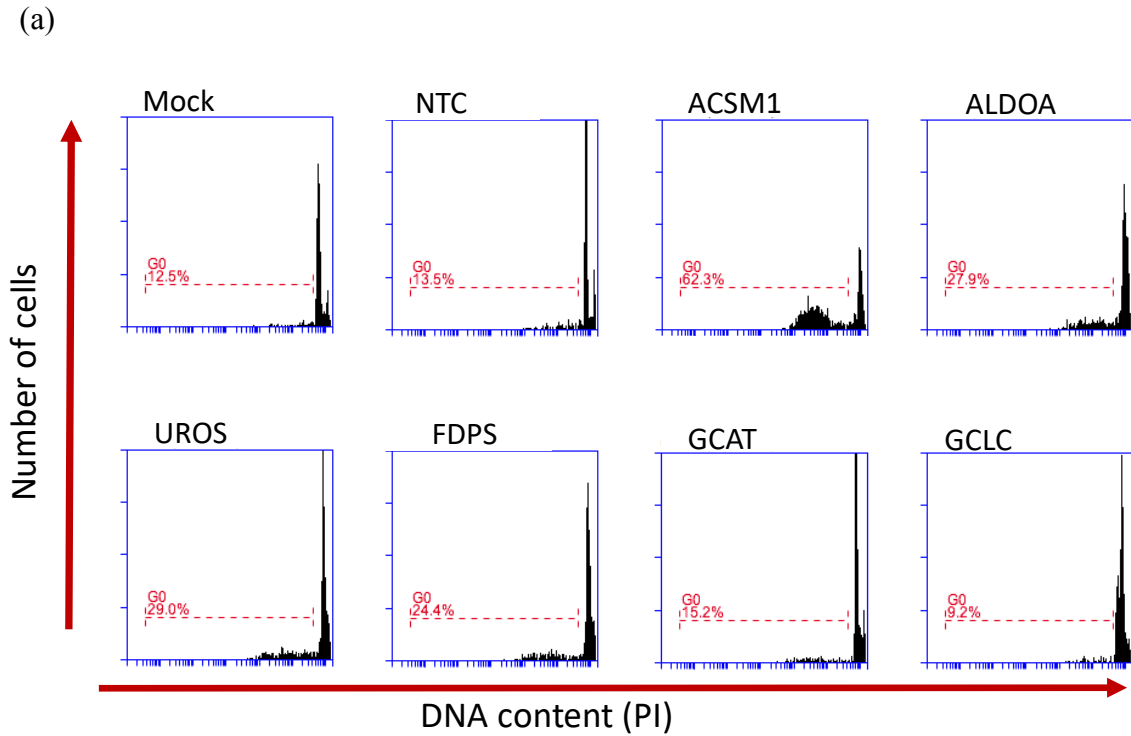


Figure 3.24 Investigation of the effects of siRNA depletion of the lead targets upon cell death.

Cells were transfected 24-hours after seeding and incubated for 7 days. Cells were harvested and PI-stained and immediately measured using FACS. (a) Shows representative images of sub-G1 profiles of controls and siRNA transfected PC3 cells; Y-axis represents the number of events or cells and the X-axis is the PI signal. (b) Graphs indicate the effect of targets knockdowns on the number of cells in sub-G1 phase. Data represent mean \pm 1SD of 3 independent repeats. ANOVA (Dunnett's post hoc test), *P < 0.05, **P < 0.01, ***P < 0.001.

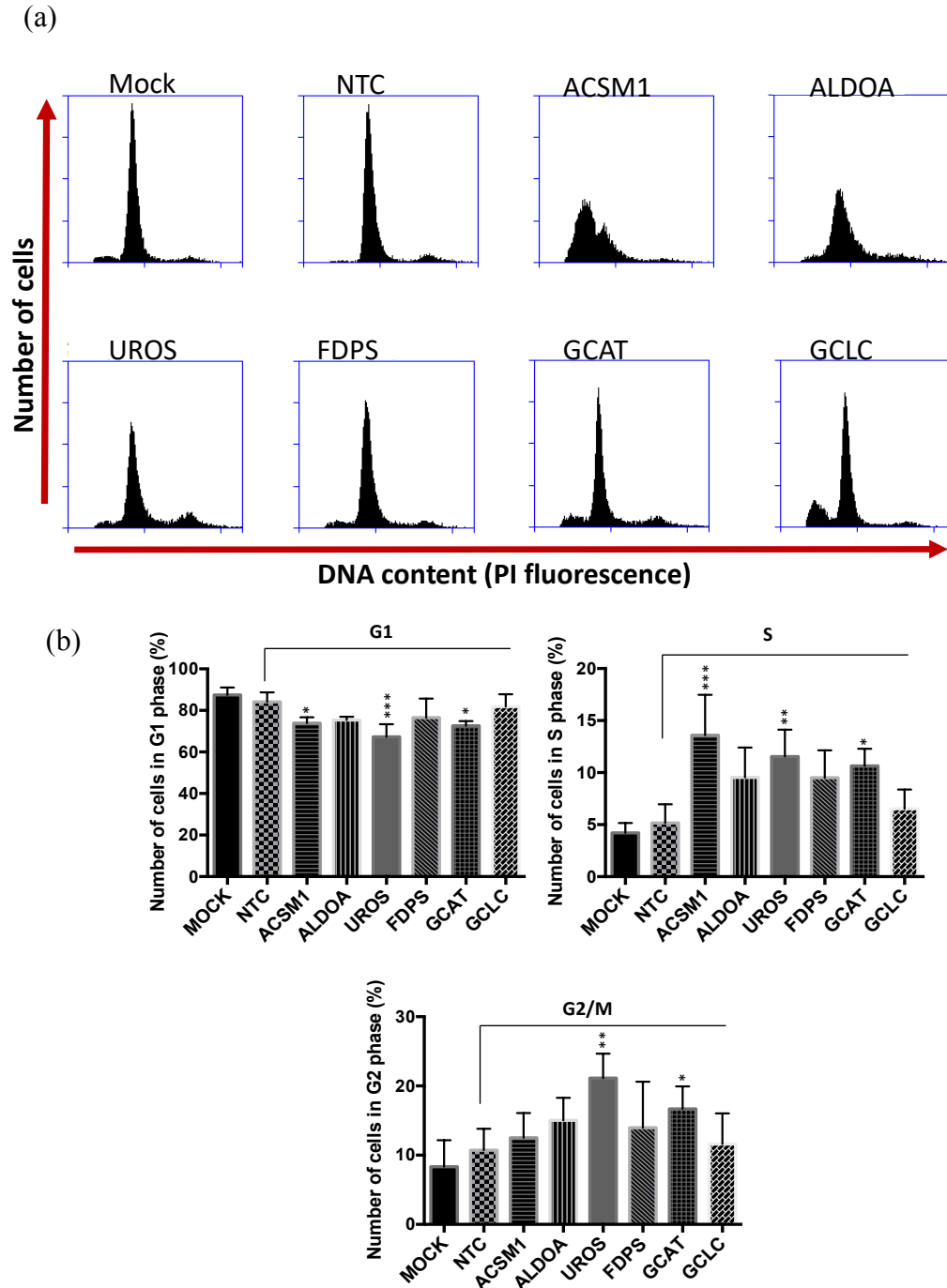


Figure 3.25 Investigation of the effects of siRNA depletion of the lead targets upon cell cycle.

Cells were transfected with a pool of 3 siRNAs against each target and incubated for 7 days. Cells were harvested, fixed and RNase treated prior to staining with PI and analysis using flow cytometry. (a) Representative cell cycle profiles of controls and siRNA transfected PC3 cells. (b) Bar graphs represent the number of cells (%) in G1, S, and G2/M phases of the cell cycle. Data presented reflects the mean \pm 1SD of at least three independent experiments. ANOVA (Dunnett's post hoc test), *P < 0.05, **P < 0.01, ***P < 0.001.

3.5 Discussion

In this study I applied a functional genetic approach to target metabolic signalling in CRPC using cell line models. The siRNA approach works on the basis of the association of the introduced siRNA with the protein components of the RNA-Induced Silencing Complex (RISC). The double stranded siRNA unwinds and its antisense strand binds to the complementary mRNA region, resulting in degradation of the bound mRNA and hence a subsequent decrease in the level of the corresponding protein (Zeng & Cullen 2002; Kroenke et al. 2004; Sledz & Williams 2005; Singh et al. 2016). Unlike in the case of overexpression studies, which might give more complex phenotypes, the siRNA-based knockdown of endogenous genes tends to give more precise phenotypes (Li et al. 2011).

One limitation of RNAi approaches is that functional redundancy with other unknown genes may lead to a lack of a knockdown phenotype (Ros et al. 2012). Functional redundancy would suggest that a particular gene is less critical for a particular cellular function or signalling than others which should be prioritized. More importantly, another RNAi limitation is the possible off-target effects. siRNA may bind to non-target mRNA due to partial complementarity, and therefore downregulate other transcripts resulting in inaccuracy (Birmingham et al. 2009). However, this depends on factors such as the specificity of the algorithms used in designing siRNA and current algorithms ensure high specificity of siRNA sequences (Filhol et al. 2012). In addition, the use of several individual siRNAs for every target (the mean effect method) further dilutes the problem of the off-target effect and increases the certainty of knockdown specificity (Riba et al. 2017).

The siRNA library utilized in this study was associated with three distinct siRNA sequences per gene and hits were prioritized according to their effect upon proliferation and motility, in comparison with non-targeting control siRNA. A gene was considered validated only when the average effect of the three siRNAs was statistically different ($P < 0.05$, LSD post

hoc test) from NTC control for the proliferation screen and only when the average effect of the three siRNAs was inside the used cut-off [$1.25 < \text{average speed } (\mu\text{m}/\text{min}) > 0.65$] for the migration screen (Figures 3.1-3.4). Therefore, false-positives should have been filtered out at this stage (Table 3.1,3-2) and in support of this, further validation studies confirmed the results of the screen.

Following a stringent selection criteria 26 potential hits were identified; 14 genes down-regulated proliferation, 18 genes significantly inhibited migration and 6 of which significantly affected both (Table 3.1,3-2). The validation experiments (Figure 3.3, Figures 3.10-3.19) led to conclude that the screening approach employed was reliable and efficient in identifying novel metabolic targets essential for prostate cancer. Importantly, several of the targets have already been identified as potential therapeutic targets for the treatment of cancer.

3.5.1 Lipogenesis and prostate cancer progression

Several of the identified targets are important factors for fatty acid and cholesterol biosynthesis. Some of those are well known enzymes such as FASN, ACACA, and FDPS (Chakravarty et al. 2004; Buhaescu & Izzedine 2007; Wang et al. 2009; Wang et al. 2010; Currie et al. 2013; Tsoumpra et al. 2015). In contrast, little is known about the role of ACSM1, SLC27A1, and SLC27A5 in metabolic signalling and cancer progression.

3.5.1.1 Fatty acid synthase (FASN)

Significant inhibition of PC3 cell migration was demonstrated by the siRNA knockdown of FASN (Figure 3.9, Table 3.2). In addition, the Human Atlas analysis suggests that FASN expression correlates with disease progression, with some high-grade tumours showing higher staining for FASN compared to low-grade tumours and normal prostatic tissues (Figure 3.23).

FASN is a large homodimeric enzyme (552-kDa) responsible for the *de novo* biosynthesis of long-chain fatty acids through the formation of palmitic acid from carbohydrates (Figure 3.26); palmitic acid is formed from acetyl-coenzyme A (acetyl-CoA) and malonyl-coenzyme A (malonyl-CoA) in the presence of NADPH (Chakravarty et al. 2004). FASN is a well-studied enzyme, and a significant volume of research has examined its biological function and validity as a potential cancer drug target. FASN was found to be over-expressed in prostate carcinomas and many other cancers (Yoshii et al. 2013), and its inhibition resulted in apoptotic cell death and proliferation inhibition of PCa tumours in a dose-dependent manner (Pflug et al. 2003).

In another study, high FASN expression was found to be significantly correlated with high Gleason scores and the development of CRPC and the expression of FASN was found to be down-regulated in response to ADT and chemotherapy (Huang et al. 2016). FASN activity suppression did not only affect cell proliferation but was also reported to halt pseudopodia formation and blocked cell adhesion, migration, and invasion (Yoshii et al. 2013). FASN inhibition also halted the expression of genes involved in the production of arachidonic acid and androgen, both of which stimulate tumour development (Yoshii et al. 2013). Because FASN upregulation positively correlated with poor prognosis and since it is expressed at low levels in normal tissues, it has been proposed as a therapeutic target (Madigan et al. 2014). Several chemical inhibitors of FASN have been developed and these have been shown to selectively kill cancer cells (Currie et al. 2013). However, severe side-effects were reported for FASN inhibitors in animal models, such as extreme weight loss (Loftus et al. 2000).

The signalling pathways activated in response to FASN overexpression are not fully understood, however, it has been suggested that the upregulation of this gene is directly linked to the activation and nuclear accumulation of Akt (Van de Sande et al. 2005). Furthermore, a recent study by Huang et al. (2016) on high-fat diet (HFD) versus low-fat diet (LFD) mice with

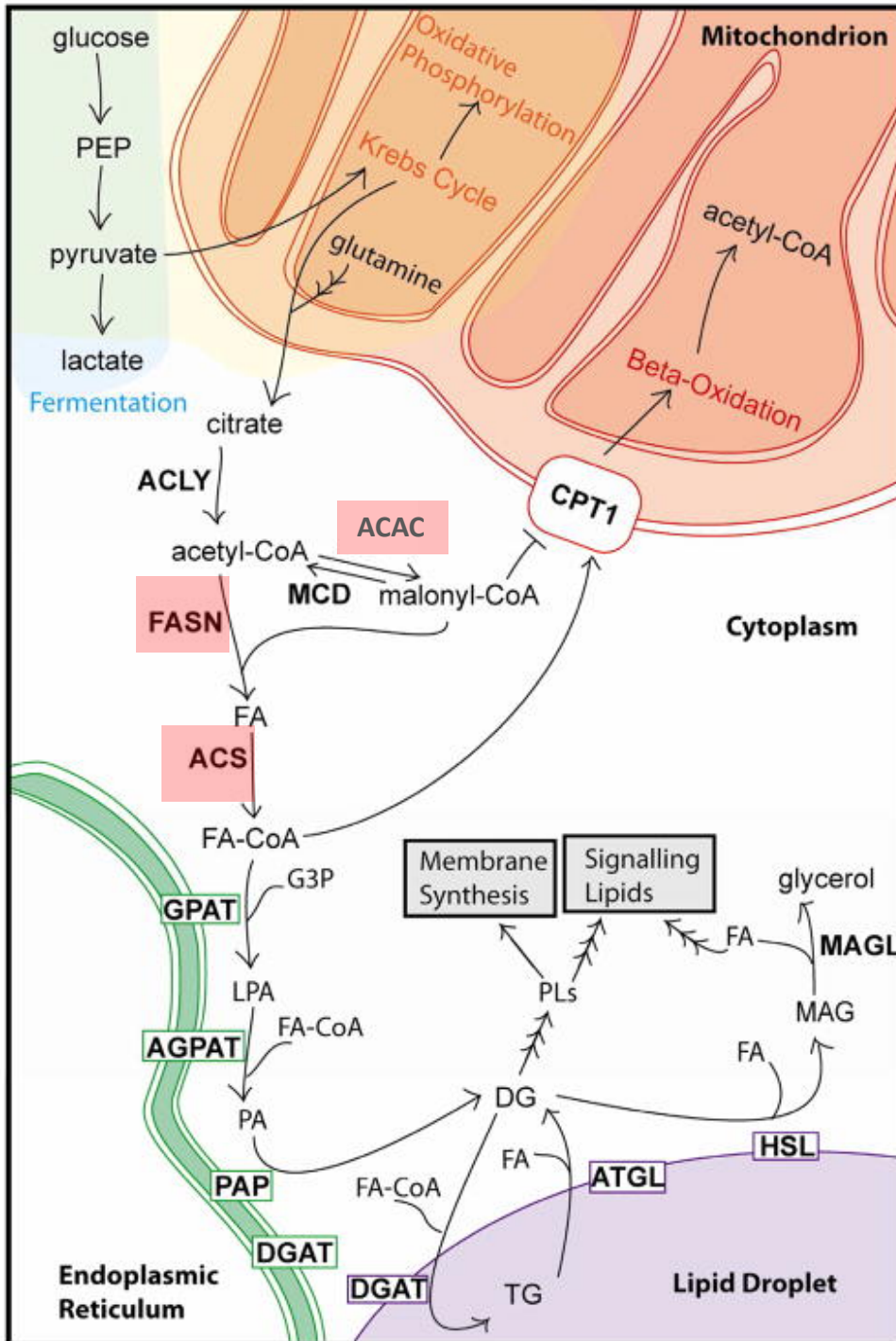


Figure 3.26 Fatty acids *de novo* biosynthesis pathway.

FASN, ACACA, and ACS (highlighted) play key roles in fatty acids biosynthesis. FASN is the key enzyme in converting citrate into active fatty acids, and ACACA is one of two enzymes of the ACAC family, which converts acetyl-CoA into malonyl-CoA. The illustration is adapted from (Currie et al. 2016).

LNCaP xenografts reported that the HFD correlated with prostate tumour progression and FASN was found to be up-regulated. The HFD resulted in Akt and extracellular signal-regulated kinase (ERK) activation and a simultaneous inactivation of 5' adenosine monophosphate-activated protein kinase (AMPK). FASN inhibition led to a reduction in PCa proliferation via PI3K/mitogen-activated protein kinase (MAPK) downregulation and AMPK activation (Huang et al. 2016).

3.5.1.2 *Acetyl-CoA carboxylase alpha (ACACA)*

Another identified target that functions in fatty acid synthesis is Acetyl-CoA carboxylase alpha (ACACA). This protein is highly involved in lipogenic and oxidative tissues (Currie et al. 2013). ACACA enhances the production of malonyl -CoA from acetyl-CoA (Figure 3.26), which is suggested to act as a substrate for fatty acid synthesis as well (Wang et al. 2009; Wang et al. 2010; Currie et al. 2013). ACACA has been found to be upregulated in several cancers, and it is believed to enhance lipogenesis and hence supports cancer cell growth and survival (Wang et al. 2015).

siRNA knockdown of ACACA was demonstrated to inhibit cell proliferation and induce apoptotic cell death in prostate (Brusselmans et al. 2005) and breast cancers (Chajès et al. 2006) and did not affect control cells. These results agree with what has been found in this study where the knockdown of this target significantly inhibited prostate cancer cell proliferation (Figure 3.3), and the analysis of tissue samples through the Human Atlas database demonstrated that this protein is upregulated in some high-grade PCa tissues (Figure 3.22). The exact molecular mechanisms of how ACACA is regulated remain unclear, however, the inactivation of these enzymes might occur downstream of kinases such as AMPK (Currie et al. 2013). Currie et al. (2013) also discussed that ACACA enzymes are positively and allosterically controlled by the availability of citrate and glutamate and negatively and allosterically by the presence of long and short-chain fatty acids.

3.5.1.3 *Acyl-CoA synthetase medium chain family member 1 (ACSM1)*

The knockdown of (ACSM1), previously known as MACS1, resulted in a significant inhibition of PCa proliferation in all cell lines tested (Figure 3.3) and suppressed PC3 cells' migration (Figure 3.9). ACSM1 is an acyl-CoA synthetase and also known as fatty acid-CoA ligase (ACS, ACSL or FAFL), which performs an essential step of fatty acid biosynthesis. Specifically, it leads to the bio-activation of fatty acids to form FA-CoA (Figure 3.26) (Mashek et al. 2007). ACSM1 is located in the mitochondrial matrix and it is believed to degrade medium-chain fatty acids to produce energy (Fujino et al. 2001). However, little is known about ACSM1 and no previous reports have linked this enzyme to cancer progression.

3.5.1.4 *Farnesyl-diphosphate synthase (FDPS)*

FDPS is another target that is involved in lipogenesis. FDPS is a key enzyme in the mevalonate metabolic pathway (Figure 3.27), which involves the synthesis of sterol and non-sterol isoprenoids such as cholesterol, heme-A, dolichol, and other essential metabolites regulating signalling and growth (Buhaescu & Izzedine 2007; Tsoumpra et al. 2015). The knockdown of this gene inhibited PCa cell lines proliferation and migration (Figure 3.3, Figure 3.9, and Figure 3.12). Interestingly, Ettinger et.al (2004) demonstrated the expression of FDPS, and FASN, increases during disease progression into CRPC and they added that FDPS and FASN are downstream of sterol response element-binding proteins (SREBPs). The latter are known to be androgen-regulated, linking AR signalling to cholesterol and fatty acid synthesis (Ettinger et al. 2004). In addition to prostate cancer, FDPS is involved in the progression of other cancers such as brain cancer (Abate et al. 2017) and colon cancer (Notarnicola et al. 2004), and in the therapy resistance in osteosarcoma (Ory et al. 2008).

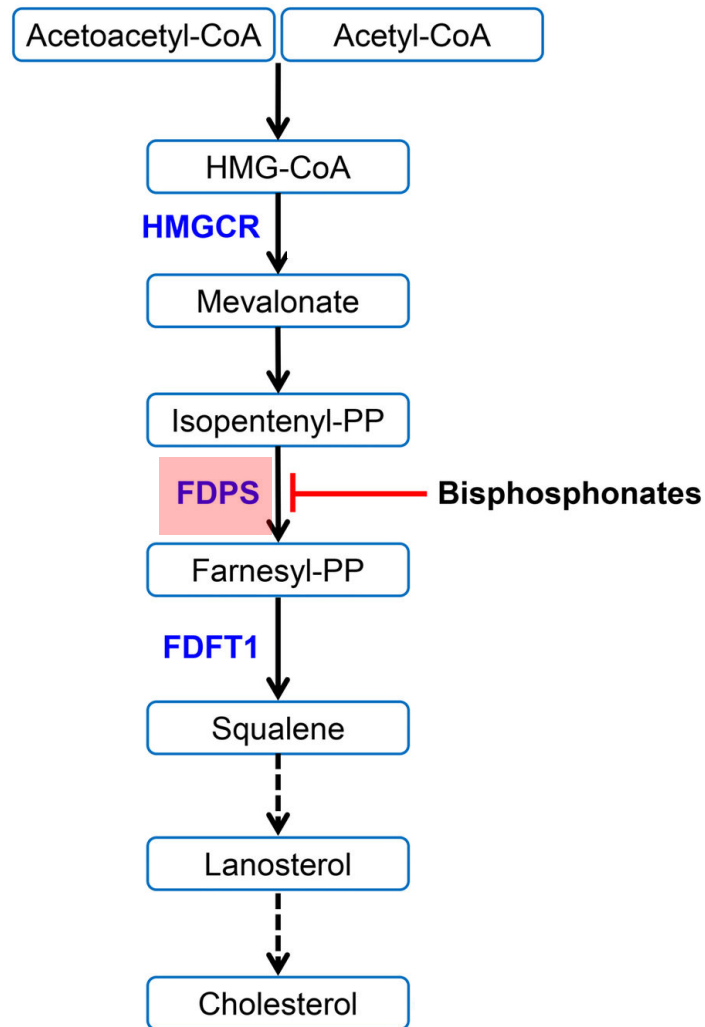


Figure 3.27 Cholesterol biosynthesis through the mevalonate pathway.

Farnesyl pyrophosphate synthase (FDPS) catalyses the conversion of isopentenyl-PP into farnesyl-PP and bisphosphonates are pyrophosphates analogues that can inhibit FDPS function. The illustration is adapted from (Griffin et al. 2017).

3.5.1.5 Fatty acids uptake and transport

Solute carrier family 27 member 1 and member 5 (SLC27A1 and SLC27A 5) are other novel therapeutic targets identified by the screening. These transporters are relatively uncharacterized, however, SLC27A1 is known to be involved in fatty acids uptake and transport (Sadowski et al. 2014). SLC27A5 may also play a role in transportation in lipogenic pathways. No work has linked those factors directly to prostate cancer development or progression. This study suggests that they might be important factors for PCa. SLC27A1 knockdown caused significant inhibition of proliferation in androgen-dependent and independent cell lines but not in the benign prostatic cell line (BPH1) (Figure 3.3), and SLC27A5 inhibited PC3 cell migration (Table 3.2) and was found to be up-regulated at the RNA levels in metastatic prostate cancer samples (Figure 3.21). All these observations suggest that the metabolic signalling of lipid biosynthesis and uptake forms an important feature of PCa progression.

3.5.2 Heme-biosynthesis and prostate cancer progression

UROS (uroporphyrinogen III synthase), whose down regulation showed interesting results in terms of cell proliferation (Figure 3.3), migration (Figure 3.11), cell death (Figure 3.24) and cell cycle (Figure 3.25), and FECH (Ferrochelatase), that resulted in a reduction in PC3 cell migration upon its knockdown (Figure 3.13), are associated with heme-biosynthesis. Importantly, this pathway has been shown to be altered in cancer (Yang et al. 2015). Heme is utilized in the formation of hemoproteins such as cytochromes and hemoglobin that store and transport oxygen, and it is an important factor in the electron transport chain (Ajioka et al. 2006).

UROS catalyses the generation of the first cyclic tetrapyrrols intermediate, Uroporphyrinogen III (UROGEN) in the fourth step of the heme-biosynthesis pathway (Figure 3.28). UROGEN is formed from a pre-uroporphyrinogen synthesized from 5-aminolevulinic

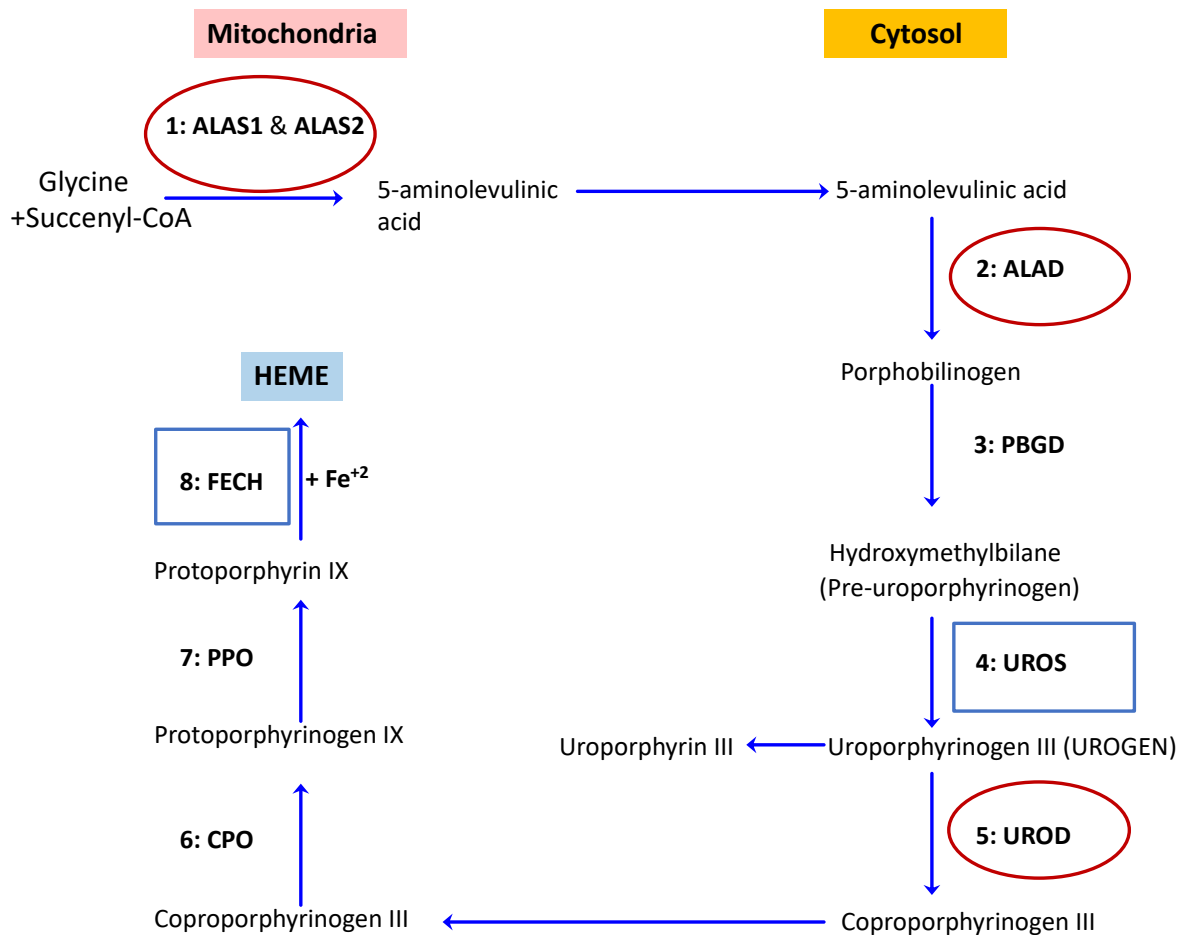


Figure 3.28 Heme-biosynthesis pathway in mammalian cells.

Heme biosynthesis pathway is initiated in the mitochondria by the formation of 5-aminolevulinic acid by ALAS enzymes, that then travels to cytosol to form porphobilinogen by the action of ALAD. Several steps then take place in cytosol, by the action of many enzymes including UROS, to form coproporphobilinogen III that travels back to mitochondria for the final steps of the process by the action of several other enzymes including FECH which inserts ferrous heme into the protoporphyrin IX to finally form heme. Several of the heme-biosynthetic factors were detected as novel targets affecting prostate cancer cell progression including UROS, which catalyse the fourth step of heme synthesis, and FECH, which catalyses the final step. Other factors such as ALAS, ALAD, and UROD (Red circles) were just below the cut off criteria but still show some significance especially on prostate cell migration.

acid (ALA; which in mammals is formed by the condensation of glycine and succinyl-CoA by the enzyme 5-aminolevulinic acid synthase, ALAS) (Hunter & Ferreira 2009). Two molecules of ALA are used to generate monopyrrole porphobilinogen (PBG) by the action of the enzyme porphobilinogen synthase (PBGS, also known as ALA dehydratase; ALAD) (Layer et al. 2010). Four of the resulting PBG molecules are linked by another enzyme called porphobilinogen deaminase (PBGD, also called hydroxymethylbilane synthase) to form the linear tetrapyrrole pre-uroporphyrinogen (Ajioka et al. 2006). The latter is finally converted to UROGEN by the action of UROS and modifications of the side chains of the macrocycle by uroporphyrinogen decarboxylase (UROD) yield coproporphyrinogen III that then catalyzes the formation of protoporphyrinogen IX by the action of oxygen-dependent coproporphyrinogen III oxidase (CPO). Protoporphyrinogen IX is oxidised by oxygen-dependent protoporphyrinogen IX oxidase (PPO) prior to insertion of ferrous iron by FECH to complete the production of heme (Layer et al. 2010).

UROS deficiency leads to a very rare autosomal recessive condition called Gunther's disease or congenital erythropoietic porphyria (CEP), which is associated with a metabolic error in heme production that leads to anemia and skin lesions due to the accumulation of porphyrins to toxic levels in the blood and skin (Shaik et al. 2012). No work has specifically investigated the role of UROS in cancer. However, this protein appears to be moderately over-expressed in high-grade prostatic tissues (Figure 3.22). Therefore, its upregulation might enhance the production of heme and hence increase oxygen consumption leading to increased cellular respiration and survival.

The final step of heme-biosynthesis, as mentioned, is performed by FECH, a mitochondrial membrane-bound enzyme, which inserts a ferrous heme into protoporphyrin (Wu et al. 2001). The inhibition of FECH has been shown to enhance ALA-photodynamic therapy (PDT)-induced cell death in PC3 cells through increasing the accumulation of protoporphyrin

IX (Fukuhara et al. 2013). ALA-PDT works on the basis of inducing the formation of the photosensitising protoporphyrin IX which accumulates in cancer tissues and absorbs a light of a particular wavelength leading to necrotic cell death of cancer cells (Zaak et al. 2004). Because protoporphyrin IX is formed in the heme synthesis cascade just before ferrous iron insertion by FECH to form heme, FECH depletion was suggested to enhance this accumulation and hence improve this therapy. The downregulation of FECH also enhanced the potency of photodynamic therapy (PDT) in glioma cells, promoting cell death and reducing proliferation (Teng et al. 2011).

Regardless of these observations, there is no work directly linking either UROS or FECH to the progression of prostate cancer. Interestingly, other heme-biosynthesis related factors including ALAS2 and ALAD, and UROD also demonstrated some significant effects on PC3 cell proliferation and migration (Figure 3.29), but these targets fell below the cut off criteria used in this work. Therefore, this pathway seems to be important for PCa growth and progression and further investigations are required to investigate if this is a viable therapeutic target. Supporting this, other studies have shown that the inhibition of heme synthesis using the ALAD inhibitor succinylacetone (SA) successfully inhibited the proliferation of non-small cell lung cancer (NSCLC) and leukemia models (Ebert et al. 1979; Weinbach & Ebert 1985; Hooda et al. 2013).

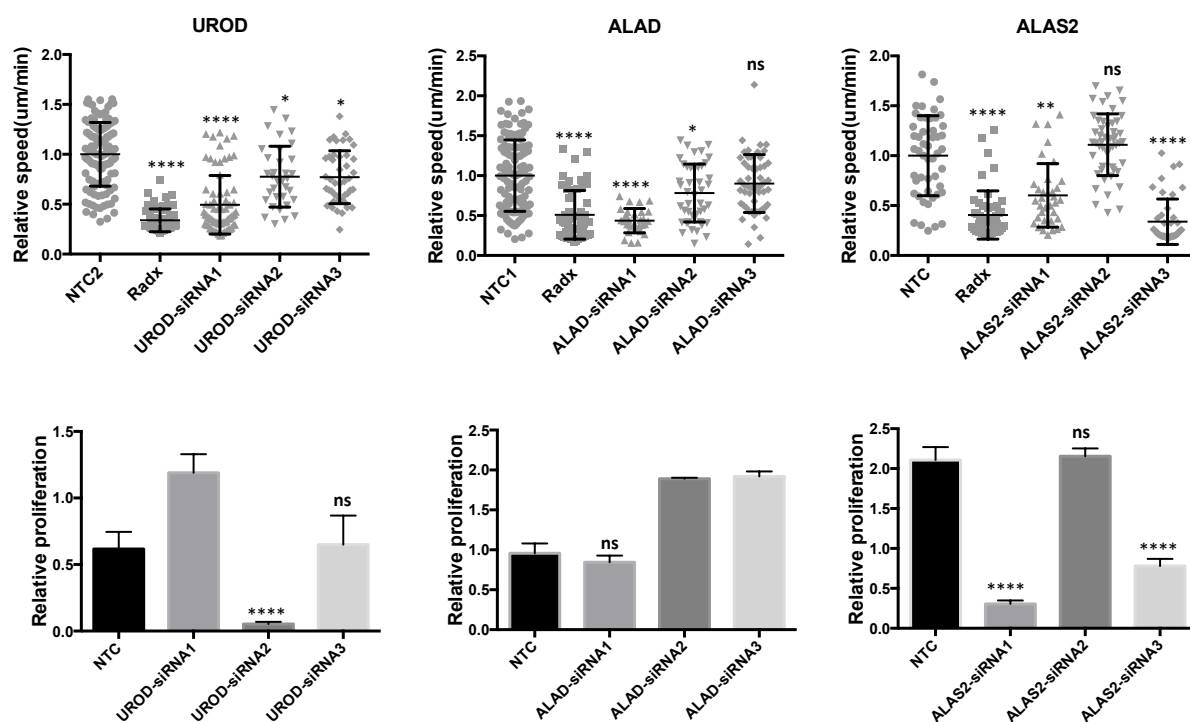


Figure 3.29 The effect of other heme-biosynthesis genes knockdowns on PC3 cell proliferation and migration.

UROD, ALDA, and ALAS2 knockdowns significantly inhibited PC3 cell migration at least by two out of three siRNAs. The effect on proliferation was less significant except for ALAS2 which showed proliferation inhibition by two siRNAs transfections. ANOVA (Dunnett's post hoc test), (ns= not significant * $P < 0.05$, ** $P < 0.01$, *** $P < 0.0001$).

3.5.3 Glycolysis-related factors in prostate cancer

Fructose biphosphate aldolase (ALDOA) is the only glycolysis-associated target identified in this study. It is one of three isozymes (aldolase A, aldolase B, and aldolase C) that are encoded by three different genes (Zhang et al. 2017). ALDOA is the most commonly expressed of the aldolase isozymes (Mamczur et al. 2013). ALDOA catalyzes the reversible conversion of fructose-1,6-bisphosphate to glyceraldehydes-3-phosphate and dihydroxyacetone phosphate (Figure 3.30) (Kajita et al. 2001). This enzyme is found to be highly expressed in early embryos and adults muscles, and it functions in several cellular processes including muscle maintenance, regulation of cell shape, cell migration, striated muscle contraction, organization of actin filament, and ATP biosynthesis (Du et al. 2014). The deficiency of this enzyme also causes an autosomal recessive disease exhibiting a hereditary hemolytic anemia (Miwa et al. 1981; Kishi et al. 1987; Yao et al. 2004). The down-regulation of this enzyme, in this study, led to significant inhibition of PCa cell line proliferation (Figure 3.3), induction of apoptosis (Figure 3.22) and impairment of PC3 cell migration (Figure 3.10).

Analysis of the transcript levels of ALDOA (Gene Ontology database) demonstrated that the enzyme is upregulated in high-grade PCa (Figure 3.20). These results suggest that ALDOA is a critical factor for PCa progression and could be a potential therapeutic target for novel therapies. Chang et al. (2017) also identified ALDOA, through proteomic screening, as a potential biomarker of prostate cancer radioresistance. They reported that combining radiotherapy with ALDOA elimination suppress survival, promote apoptosis and enhance radiosensitivity of radio-resistant PCa cells (Chang et al. 2017b). Additionally, ALDOA is also correlated with metastasis and poor prognosis in NSCLC (Chang et al. 2017a). Further, elevated expression of this enzyme was closely linked to the progression of several cancers including lung cancer (Du et al. 2014) and colon cancer (Ye et al. 2018). Furthermore, ALDOA expression was reported to correlate with the progression and treatment resistance in colorectal

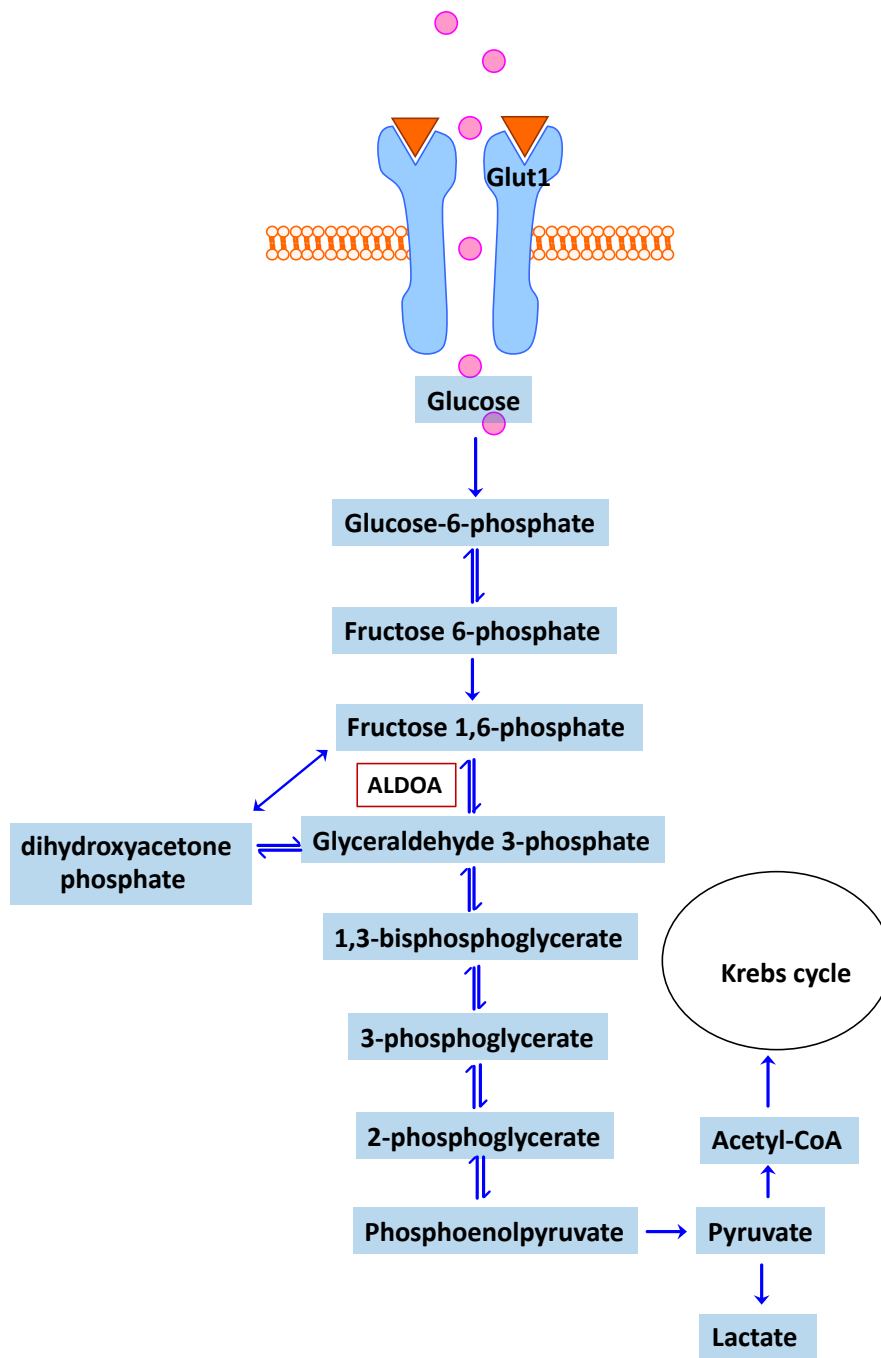


Figure 3.30 The role of ALDOA in the glycolysis pathway.

ALDOA (red box) catalyses the fourth step of glycolysis; reversibly converts fructose 1,6-phosphate to glyceraldehyde 3-phosphate and dihydroxyacetone phosphate.

cancer (CRC), and it is up-regulated in response to hypoxic conditions (Kawai et al. 2017).

These observations suggest that glucose metabolism is important in PCa progression. However, ALDOA has also been linked to pathways other than glycolysis. For example ALDOA has been linked to the HIF-1 (hypoxia-inducible factor-1) pathway and has been shown to play a role in and EMT (epithelial-mesenchymal transition) (Ye et al. 2018). In addition, a positive correlation of ALDOA with HIF-1, and downstream signalling, was reported in metastatic lung cancer. The upregulation of ALDOA expression enhanced the expression of matrix metalloproteinase-9 (MMP9) that functions downstream the HIF-1, and the inhibition of MMP9 suppressed lung cancer migration and invasion (Chang et al. 2017). Moreover, a recent microarray analysis study revealed that the transcriptional upregulation of ALDOA is co-expressed with several cell cycle-related genes in NSCLC and other solid tumours, suggesting that ALDOA might contribute to cancer progression through regulation of cell cycle factors (Zhang et al. 2017). These observations led to the hypothesis that ALDOA contributes to cancer progression by affecting several pathways, dependent upon the metabolic stress present in the tumour.

3.5.4 Amino acids and protein biosynthesis

The siRNA down regulation of several protein-synthesis related genes had a significant impact on PCa proliferation and migration; these included GCAT (glycine C acetyltransferase), Methionyl-tRNA synthetase (MARS), and Leucyl-tRNA synthetase 2 (LARS2). Little is known about the role of these factors in respect to cancer progression. The effect of these factors upon PCa suggests that the metabolic pathways related to amino acids and proteins biosynthesis are distorted perhaps to favour the rapid proliferation and survival of these cells.

3.5.4.1 GCAT (glycine C acetyltransferase)

GCAT down-regulation by siRNAs significantly inhibited PCa cell proliferation (Figure 3.3) and led to cell cycle arrest in S phase and G2/M (Figure 3.23). GCAT is involved in the mitochondrial synthesis of glycine, and the upregulation of glycine metabolism is associated with higher proliferation rates and poor prognosis in several cancers (Amelio et al. 2014). In addition, Jain et al. (2012) demonstrated that the expression of glycine biosynthetic pathway and glycine intake rates correlate with proliferation potential of cancerous cells. Moreover, elevated expression of this pathway was reported to correlate with high mortality rates in breast cancer (Jain et al. 2012). Such observations support that GCAT could be an important factor in PCa progression and targeting this pathway might be a valid approach to tumour growth.

3.5.4.2 Methionyl-tRNA synthetase (MARS)

MARS plays a vital role in protein translation and is suggested to enhance this process by transferring methionine (Met) to initiator tRNA (Kwon et al. 2011). A recent work by Kim et al. (2017) suggested that this protein protects against oxidative stress and ROS-related damage, and hence its upregulation favours cancer cell growth and drug resistance. However, no work has linked MARS to the progression of PCa. This factor has been shown to be commonly over-expressed in NSCLC and its overexpression is correlated with poor clinical results (Kim et al. 2017). The knockdown of MARS significantly reduced PCa cell proliferation (Figure 3.3) and further experiments are required to elucidate and validate its potential role in PCa.

3.5.4.3 Leucyl-tRNA synthetase 2 (LARS2)

LARS2 is a mitochondrial aminoacyl tRNA synthase that carries out aminoacylation of specific tRNAs required for accurate protein synthesis. More specifically, LARS2 carries out the aminoacylation of the human mitochondrial tRNA^{Leu(UUR)} (Sohm et al. 2004). Little is known about this target, especially in terms of cancer, and no published data is available linking

LARS2 to prostate cancer. However, LARS2 was found to be genetically and epigenetically deregulated in nasopharyngeal carcinoma. Further, 3p21.3 (where the *LARS2* gene is located) is frequently deleted in this disease (Samadder et al. 2016). siRNA-knockdown of LARS2 inhibited PC3 single cell migration across three independent siRNAs (Figure 3.9) and impaired population cell motility across two siRNAs (Figure 6.4), however more validations and are needed.

3.5.5 Nucleic acids biosynthesis

3.5.5.1 Thymidylate Synthase (TYMS)

TYMS plays a fundamental role in DNA synthesis, replication, and repair (Carreras & Santi 1995). TYMS is a target for 5-Fluorouracil (5-FU) which has been used as a palliative therapy for CRPC with or without other anti-cancer agents (Burdelski et al. 2015). The siRNA downregulation of TYMS resulted in significant inhibition of cell proliferation across three prostate cancer cell lines (Figure 3.3). Overexpression of TYMS has been shown to positively correlate with disease progression and PSA recurrence in PCa patients (Burdelski et al. 2015). This is consistent with the results of the mRNA and protein levels analyses performed here; TYMS was upregulated at the transcript and protein levels in metastatic PCa compared to primary disease and noncancerous tissues (Figure 3.20 and Figure 3.22). Moreover, TYMS knockdown significantly halted proliferation of the PCa cell lines tested (Figure 3.3). This factor has also been shown to play an essential role in chemo-resistance and its overexpression correlated with the 5-FU efficacy in breast cancer patients (Yu et al. 2005), and therapy response of NSCLC patients to pemetrexed-containing therapy regimens (Chamizo et al. 2015). Therefore, TYMS has been suggested to be a predictive biomarker for cancer therapy efficacy (Shimizu et al. 2012; Chamizo et al. 2015; Yu et al. 2005).

3.5.5.2 *Glycinamide ribonucleotide transformylase (GART)*

GART is an enzyme that functions in the third step of the purine biosynthesis pathway and it is a validated target for cancer therapy (Manieri et al. 2007). This factor has been targeted using inhibitors such as 5,10-dideazatetrahydrofolate, which has been shown to have potent anti-tumour activity (Beardsley et al. 1989). GART has not previously been described as a target in PCa, although in this study it was demonstrated that its downregulation by siRNA halted proliferation of PCa cell lines (Figure 3.3). In addition, GART upregulation correlates with the progression of other cancers such as hepatocellular carcinoma (Cong et al. 2014).

3.5.6 *Free-radicals and redox status regulators*

3.5.6.1 *Nitric oxide synthases3 (NOS3)*

The Nitric oxide synthase (NOS) family includes three enzymes NOS1, NOS2, and NOS3. These enzymes catalyse the synthesis of nitric oxide (NO) from L-arginine. NO is a reactive free-radical that plays an essential role in cell growth, apoptosis, neurotransmission, and immunological regulation (Y. Chen et al. 2014). NOS3 is predominantly expressed in endothelial cells regulating blood pressure and blood vessels dilation, and has various other vasoprotective and anti-atherosclerotic effects (Förstermann & Sessa 2012). *NOS* polymorphisms have been shown to correlate with PCa risk, pathogenesis and disease aggressiveness (Lee et al. 2009; Nikolić et al. 2015; Branković et al. 2013). However, contradictory findings are associated with this gene, as some studies found that it is anti-tumorigenic and others have described its pro-tumorigenic activity (Burke et al. 2013; Vahora et al. 2016). Therefore, the mechanism of action of this gene in cancer progression is unclear and might depend on the conditions within the tumour. The inactivation of NO occurs through its reaction with a superoxide anion ($O_2^{\cdot-}$) to form the oxidant peroxynitrite ($ONOO^-$), the latter could lead to oxidative stress, nitration, and S-nitrosylation of biomolecules including proteins,

lipids, and DNA (Förstermann & Sessa 2012). Nitrosative stress by ONOO⁻ has been linked to DNA single-strand breaks, followed by the activation of poly-ADP-ribose polymerase (PARP) (Ridnour et al. 2004).

NO enzymes have been implicated in cancer progression e.g. tumour growth, migration and invasion, survival, angiogenesis, and metastatic behaviour (Baritaki et al. 2010; Burke et al. 2013). In PCa, high expression of endothelial NOS (encoded by *NOS3*) is associated with anti-apoptotic characteristics; specifically NOS overexpression in PCa cell lines inhibited TRAIL (Tumour necrosis factor-related apoptosis-inducing ligand)-induced apoptosis (Tong & Li 2004). In a different study, that analysed patient tissues, NOS3 was found to be overexpressed in 68 % of patients and this was associated with high PSA levels (Aaltomaa et al. 2000). These observations correlate with the findings in this work regarding NOS3; the bioinformatics analysis showed that NOS3 is upregulated at the RNA level in metastatic PCa compared to primary PCa and benign prostatic tissues (Figure 3.20). Moreover, NOS3 knockdown significantly halted proliferation across three prostate cancer cell lines (Figure 3.3) and inhibited PC3 cell migration (Figure 3.14). Therefore, NOS3 might act as oncogene rather than a tumour repressor in PCa.

3.5.6.2 *Glutamate-cysteine ligase catalytic subunit (GCLC)*

GCLC or gamma-glutamylcysteine synthetase (γ -GCS) functions in glutathione biosynthesis (Lushchak 2012). The latter is a natural tripeptide found within almost all cells which is usually bound to other molecules (Balendiran et al. 2004). Glutathione forms an important mean of protection against oxidative stress (Lushchak 2012), and it is involved in other homeostatic roles such as maintenance modulation of the immune response and detoxification of xenobiotics (Balendiran et al. 2004; Lushchak 2012). Glutathione levels have been found to be raised in drug-resistant cells in cancer, including PCa (Bailey et al. 1992). This increase in glutathione was associated with elevation in the activity and the mRNA levels

of GCLC (Bailey et al. 1992; Mulcahy et al. 1994a; Mulcahy et al. 1994b; Cai et al. 1997; Kigawa et al. 1998; Tatebe et al. 2002; Li et al. 2014).

GCLC downregulation by siRNA abrogated the proliferation of PC3 and LNCaP cells but not DU145 cells (Figure 3.3). Although GCLC showed no upregulation at the RNA or protein level in this work, GCLC has been shown to be up-regulated by oxidative stress (Cai et al. 1997). Supporting this, the promoter of GCLC was found to have transcription factors sites, such as nuclear factor erythroid 2-related factor 2 (NRF2), nuclear factor (NF)- κ B and activator protein-1 (AP-1), that regulate oxidative stress mechanisms (Dequanter et al. 2016).

3.5.7 Other identified metabolic factors/pathways

3.5.7.1 Platelet activating factor acetylhydrolase 2 (PAFAH2)

PAFAH2 was identified by Marques et al. (2002) as a phospholipase enzyme that plays an important anti-inflammatory role through the conversion of pro-inflammatory autocoid (PAF) into inactive lyso-PAF by the removal of the SN-2 group of this platelet-activating factor. PAFAH enzymes also degrade the toxic poly-unsaturated-fatty-acid-containing phospholipids (Marques et al. 2002). The role of this enzyme in tumorigenesis is unknown and has not been investigated. However, it might be involved in PCa progression as its downregulation inhibited proliferation and migration (Table 3.2 and Figure 3.3).

Overexpression of PAFAH2 inhibits oxidative stress-induced cell death (Adibekian et al. 2010). These observations suggest that PCa cells might utilise this factor to suppress cell death induced by oxidative stress. In addition, the inhibition of other platelet activating factor acetylhydrolases (PAFAH1a/b) has also been shown to impair tumour cell survival (Chang et al. 2015).

3.5.7.2 *Hyaluronan Synthase 3 (HAS3)*

HAS3 is one of three enzymes that synthesise hyaluronan (HA), a polysaccharide consisting of several units of D-glucuronic acid and N-acetyl-glucosamine. HA plays a role in several cellular functions including proliferation, migration, cell adhesion, and homeostasis (Kuo et al. 2017). siRNA depletion of HAS3 significantly reduced cell proliferation and migration of PCa cells (Figure 3.3 and Table 3.2), which is consistent with previous data showing that HAS3 overexpression induced the growth of PCa cells (Liu et al. 2001). HAS3-induced overexpression of hyaluronan was demonstrated to enhance growth, extracellular matrix accumulation of HA and angiogenesis in TSU cell line (a cell line established from prostatic adenocarcinoma that has metastasised to the lymph nodes) (Itano et al. 1999). It is also postulated that the overexpression of HAS3 and other hyaluronan synthases leads to the accumulation of hyaluronan on the cell surface which is believed to enhance adhesion to bone marrow. This has been suggested as a reason as to why PCa predominantly metastasises to the bones (Simpson et al. 2001). This factor was also found to promote colon cancer progression and metastasis (Bullard et al. 2003; Teng et al. 2011; Lai et al. 2010).

3.5.7.3 *Scribble cell polarity complex component (LLGL2)*

LLGL2 protein is one of three related proteins that interact to form the Scribble complex; a highly conserved complex that is implicated in cell polarity and other cellular functions such as proliferation, cell migration and invasion, cell survival, assembly of components of adherens junctions and tight junctions that appear to act as tumour suppressors (Humbert et al. 2008; Su et al. 2012). The deregulation of the Scribble complex has been linked to the progression of several cancers (Pearson et al. 2011), although the mechanistic processes behind this complex and its components, including LLGL2 remain unclear (Humbert et al. 2008). The loss or knockdown of LLGL2 was shown to inhibit PC3 cell migration in this work (Figure 3.17), although this contradicts previous findings where loss of Scribble resulted in PCa progression, but this was in addition to an oncogenic mutation in *Kras* (Pearson et al.

2011). The results of this study and the mentioned role of this complex in cell polarity, cell migration and invasion suggest that LLGL2 may play an oncogenic role in PCa.

3.5.7.4 *FK506 binding protein member 11 (FKBP11) and member 9 (FKBP9)*

FK506 binding protein 11 (FKBP11, and named FKBP19 as well) and FK506 binding protein 9 (FKBP9) have peptidyl-prolyl cis/trans activity and assist in folding of proline-containing polypeptides (Rulten et al. 2006). The roles of those two factors in prostate and other cancers have not been elucidated, although their ligands have been suggested to be effective anticancer agents (Romano et al. 2011). FKBP9 and FKBP11 downregulation by siRNA inhibited PCa proliferation and migration, respectively (Figures 3.3 and 3.15). FKBP9 and FKBP11 have been found to be highly up-regulated in osteosarcoma tissues and hepatocellular carcinoma, respectively, compared to non-tumour tissues (Endo-Munoz et al. 2010; Lin et al. 2013). In addition, similar factors from the same family, such as FKBP51 have been found to have oncogenic activity in melanoma cells and its expression correlates with melanoma progression and aggressiveness (Romano et al. 2013). FKBP51 expression was also higher in prostatic cancer tissues compared to normal tissues, and its expression in LNCaP is elevated in response to androgen (Velasco et al. 2004).

3.5.7.5 *Syntaxin 1A (STX1A)*

STX1A belongs to a group of proteins that are involved in vesicle transport (Zhang et al. 2009), cell trafficking, cell proliferation, and exocytosis and neurotransmission (Ulloa et al. 2015). Syntaxin 1 was shown to be correlated with the progression of several cancers such as breast carcinoma (Fernández-Nogueira et al. 2015) and glioblastoma (Ulloa et al. 2015). In this study, siRNA knockdown of this gene led to a significant reduction of PC3 cell migration which agrees with previous data that has shown that it is involved in neuron migration (Cotrufo et al. 2012). These observations suggest that STX1A is a novel target that could be exploited to modulate the migratory nature PCa.

3.5.7.6 *Otopetrin3 (OTOP3)*

Otop3 belongs to a gene family called Otopetrin, which encodes multi-transmembrane domain proteins that have no homology to known transporters, channels, exchangers, or receptors (Hughes et al. 2008). The Otopetrin family includes three genes *OTOP1* and two homologues (*OTOP2* and *OTOP3*) (Hughes et al. 2008), which have unknown functions. The down-regulation of *OTOP3* led to significant reduction of PC3 cell migration (Figure 3.9), however further investigations are required to identify the functional roles of this factor in normal and cancer cells.

3.5.8 *Summary*

The screen identified several targets, such as *FASN*, *FDPS*, *ACACA*, and *ALDOA* which are already well validated as therapeutic targets and potential biomarkers for PCa and other cancers. This validates the findings of this screen. Other targets like *GCLC*, *LLGL2*, *HAS3*, and *NOS3* have been shown to be important in PCa and other cancers. However, several targets including *STXA1*, *FKBP11*, *FKBP9*, *LLGL2*, *GCLC*, *GART*, *LARS2*, *MARS*, *GCAT*, *UROS*, and *FECH* have not been linked to the progression of PCa before, although they have been found to be associated directly, or at least indirectly, with other tumour types. Some of the identified targets, such as *OTOP3*, *ACSM1*, *PAFAH2*, *LARS2*, *SLC27A1* and *SLC27A5* are novel and no work has previously linked them to cancer development/progression which highlights the need for further experimentation to characterise their roles in PCa.

The data demonstrates that a number of the targets identified are indispensable for PCa proliferation and motility. More interestingly, the benign cell line (BPH1), utilized as a noncancerous cell line control, exhibited no significant inhibition of proliferation when most of these factors were knocked down (Figure 3.3). This suggests that the signalling activity of these metabolic factors is specifically altered in PCa cells to suit metabolic demands.

Several pathways were found to be important for PCa proliferation and motility (Figure 3.31), including fatty acid/ lipid biosynthesis, heme biosynthesis, and glycolysis. It should be noted that glucose metabolism is linked to fatty acids metabolism at the point of citrate, an intermediate in the Krebs cycle (Currie et al. 2013). In addition, heme present in oxygen transporters will also provide the Krebs cycle with the required oxygen enhancing oxidative respiration and energy production.

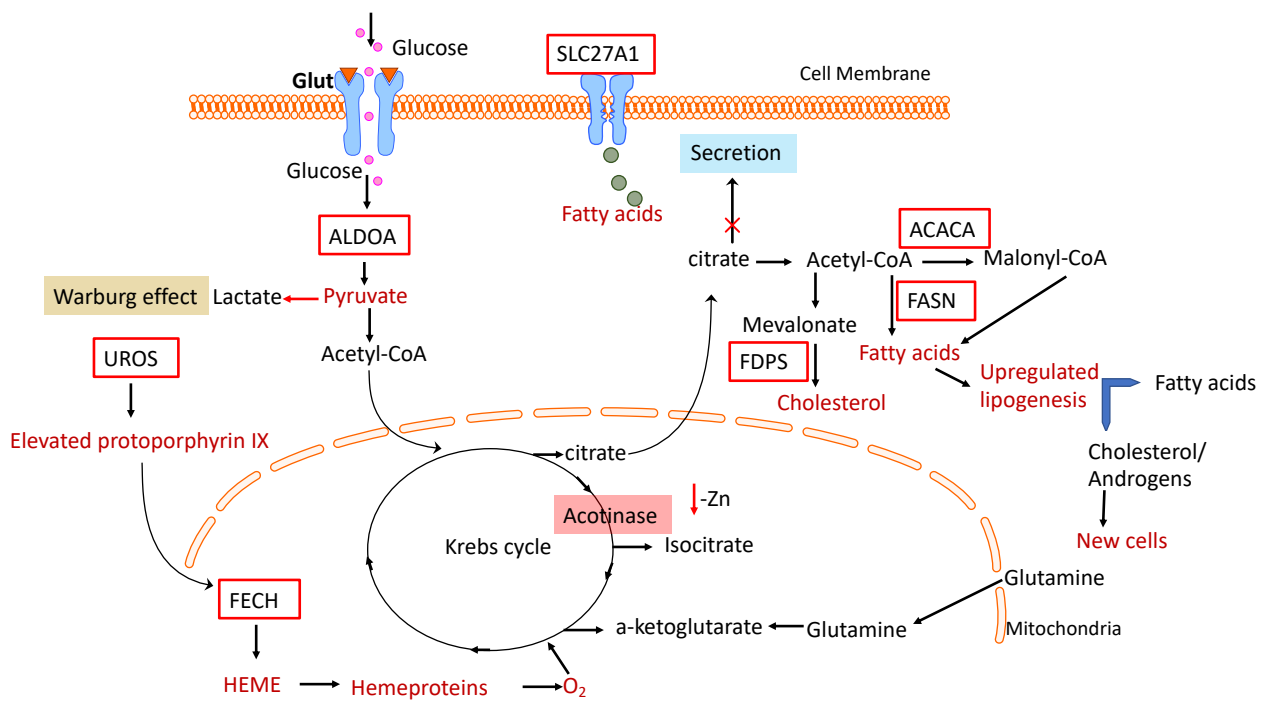


Figure 3.31 Overall key metabolic alterations and their participation in prostate cancer metabolism.

Deregulated factors (Red) and pathways identified by the siRNA screening of 217 metabolic and cell traffic factors in PCa cells. PCa cells halt the accumulation of citrate and Zn and resume the citrate oxidation through the TCA cycle. This might be accompanied by the elevation of ALDOA glycolytic activity to produce more citrate and other essential intermediates such as acetyl-CoA that is converted into lipids/fatty acids by the action of factors such as FASN and ACACA. Fatty acid uptake might be further enhanced by the upregulation of transporter proteins like SLC27A1. Heme biosynthesis enzymes (UROS and FECH) enhance the production of hemoproteins that feed the Krebs cycle with the required oxygen, enhancing the oxidative respiration and energy production. The activity of these signalling pathways and the production of energy and building macromolecules support the proliferation and survival of PCa cells.

4 Chapter 4 Results II

4 Further validations and investigation into UROS and ALDOA

The development of techniques to manipulate gene expression have greatly assisted in the identification of novel targets for the treatment of cancer (Perwitasari et al. 2013). One of these approaches is small interfering RNAs (siRNAs) (Carthew & Sontheimer 2009; Wilson & Doudna 2013; Wittrup & Lieberman 2015). I have used an siRNA screen to identify novel targets for the treatment of prostate cancer. Uroporphyrinogen III synthase (UROS) was chosen for further investigation as its knockdown showed the strongest effects on proliferation and migration in prostate cancer cells. UROS depletion also significantly inhibited cell cycle progression and induced apoptosis in PC3 cells. UROS catalyses the fourth step in heme-biosynthesis (Figure 3.28) (Aizencang et al. 2000) and deficiency in this enzyme leads to the rare autosomal recessive condition called Gunther's disease or congenital erythropoietic porphyria (CEP). This disease is associated with a metabolic error in heme synthesis that leads to anemia and skin lesions due to the accumulation of porphyrins at toxic levels in the blood and skin (Shaik et al. 2012). UROS and other heme-synthetic enzymes exist in the cytoplasm (Ajioka et al. 2006), however UROS and UROD are believed to occur in a supramolecular complex close to the mitochondrial compartment (Hamza & Dailey 2012).

UROS catalyses the generation of the first cyclic tetrapyrrols intermediate, Uroporphyrinogen III (UROGEN) (Figure 3.28). UROGEN is formed from pre-uroporphyrinogen that has been synthesized from 5-aminolevulinic acid, ALA, which in mammals is formed by the condensation of glycine and succinyl-CoA by the enzyme 5-aminolevulinic acid synthase, ALAS (Hunter & Ferreira 2009). Two molecules of ALA generate a pyrrole derivative porphobilinogen (PBG) by the action of an enzyme called porphobilinogen synthase (PBGS, also known as ALAD) (Layer et al. 2010). Then four of the

resulted PBG molecules are linked by another enzyme called porphobilinogen deaminase (PBGD, also called hydroxymethylbilane synthase) to form the linear tetrapyrrole pre-uroporphyrinogen which is finally converted to UROGEN by the action of UROS, and changes in side chains of the macrocycle occurs prior to inserting iron to complete the production of heme (Layer et al. 2010).

The second target nominated for further characterization, because of its significant effects upon PC3 proliferation is fructose-bisphosphate-aldolase A (ALDOA). ALDOA is one of three isozymes (aldolase A, aldolase B, and aldolase C) encoded by three different genes (Cibelli et al. 1996). These enzymes are involved in glycolysis, catalyzing the reversible conversion of fructose-1,6-bisphosphate to glyceraldehydes-3-phosphate and dihydroxyacetone phosphate (Figure 3.30) (Kajita et al. 2001). ALDOA is found highly expressed in early embryos and adults muscles, and it functions in several cellular processes including muscle maintenance, regulation of cell shape, cell migration, striated muscle contraction, organization of actin filament and ATP biosynthesis (Du et al. 2014). The deficiency of this enzyme also causes an autosomal recessive disease exhibiting a hereditary hemolytic anemia (Miwa et al. 1981; Kishi et al. 1987; Yao et al. 2004). Previous investigations of ALDOA demonstrated that it is involved in the progression and metastasis of lung and pancreatic cancer and is associated with poor prognosis (Ji et al. 2016; Du et al. 2014).

To date, little is known about the role of UROS or ALDOA in the progression of prostate cancer. The aim of this chapter was therefore to validate successful knockdown of UROS and ALDOA, investigate the expression of these enzymes in tumorigenic and nontumorigenic controls, determine cellular localization and confirm the effect upon cell motility using wound healing assays.

4.1 Validation of UROS and ALDOA knockdowns

To confirm successful knockdown of UROS and ALDOA, PC3 were transfected with the individual siRNAs and qPCR and western blotting conducted. UROS and ALDOA were successfully depleted by the three siRNAs with an average knockdown at the RNA level of 85% and 95 % respectively (Figure 4.1a and b). To confirm knockdown at the protein level, western blotting was also performed (Figure 4.1 c). Mock and NTC transfections were used as controls. UROS protein levels were reduced by more than 65 % while ALDOA was reduced by approximately 35% (calculated by densitometry analysis; ImageJ).

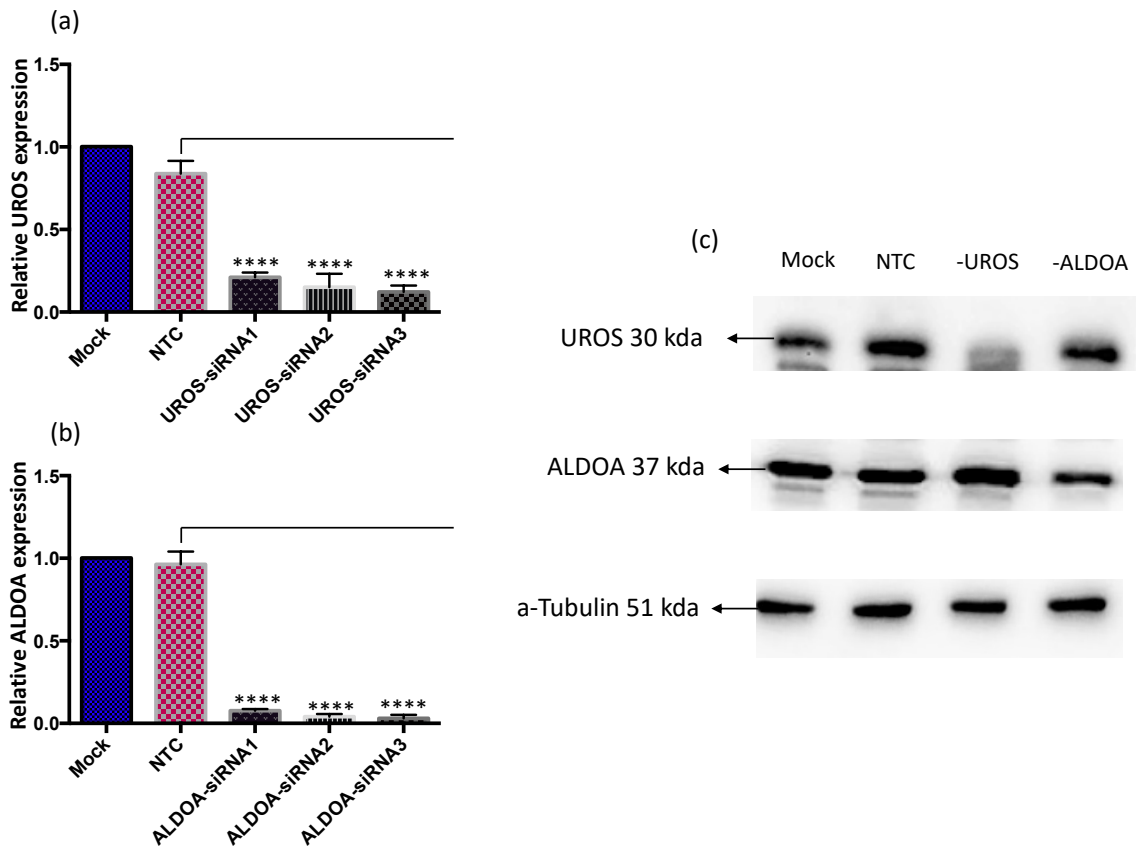


Figure 4.1 QPCR and western blotting to confirm UROS and ALDOA knockdowns.

PC3 were transfected with siRNAs and incubated for 72 hours. (a) and (b): Cells were harvested, RNA extracted and cDNA synthesised. UROS or ALDOA expression was subsequently quantified using qPCR. Data represent mean \pm 1SD of three independent repeats. ANOVA (Dunnett's post hoc test), ****P < 0.0001. (c): Cells were harvested, and proteins separated using SDS-PAGE. Immunoblotting was subsequently performed using antibodies specific for UROS, ALDOA, or α -tubulin (loading control).

4.2 Investigation of UROS and ALDOA basal levels in cancerous and noncancerous cells

To see if the expression of UROS and ALDOA is altered in prostate cancer, the transcript levels of UROS and ALDOA were measured in PC3, DU145, LNCAP, and BPH1 (Figure 4.2). *UROS* expression is significantly higher in the PCa cell lines compared to the non-tumorigenic BPH1 ($P < 0.05$, Dunnett's test) (Figure 4.2 a). Similar results were also evident for *ALDOA* (Figure 4.2. b). To investigate if these differences were also evident at the protein level, immunoblotting was performed on a range of prostate cancer and noncancerous cell lines (PC3, LNCaP, DU145, 22RV1, C42, C42B, BPH1, and PNTA1). Similar to the changes seen at the RNA level, UROS protein levels were found to be higher in the cancer cell lines compared to BPH1 and PNT1A (Figure 4.3). In contrast, the levels of ALDOA were relatively consistent in all cell lines (Figure 4.4).

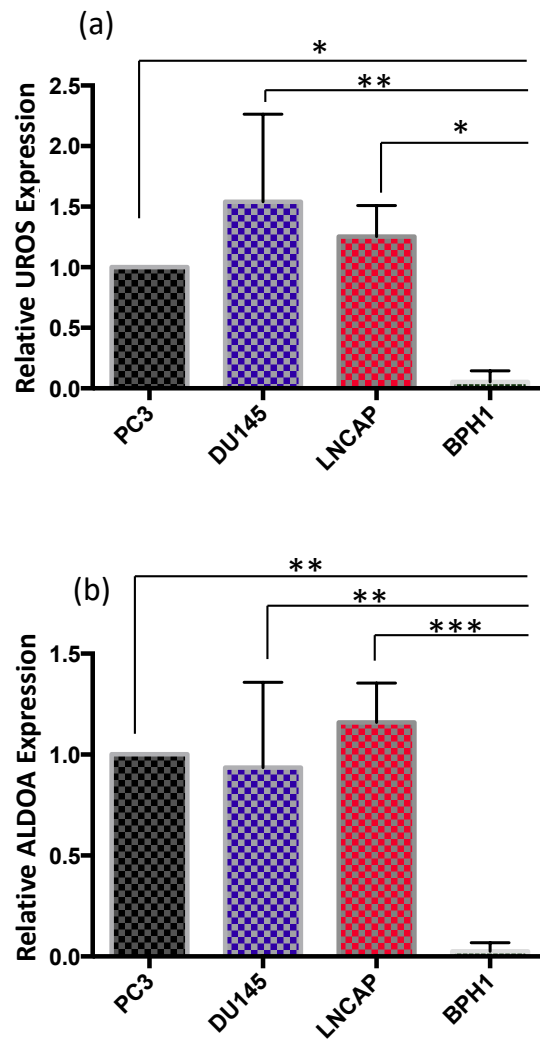


Figure 4.2 Transcript levels of UROS and ALDOA in PCa cell lines (PC3, LNCaP and DU145) and a non-cancerous cell line BPH1.

Cells were pelleted, RNA extracted, cDNA synthesised, and qPCR performed to quantify (a) *UROS* or (b) *ALDOA* expression. Data presented is the mean \pm 1SD of three repeats prepared separately with identical conditions. ANOVA (Dunnett's post hoc test), *P < 0.05, **P < 0.01, ***P < 0.001.

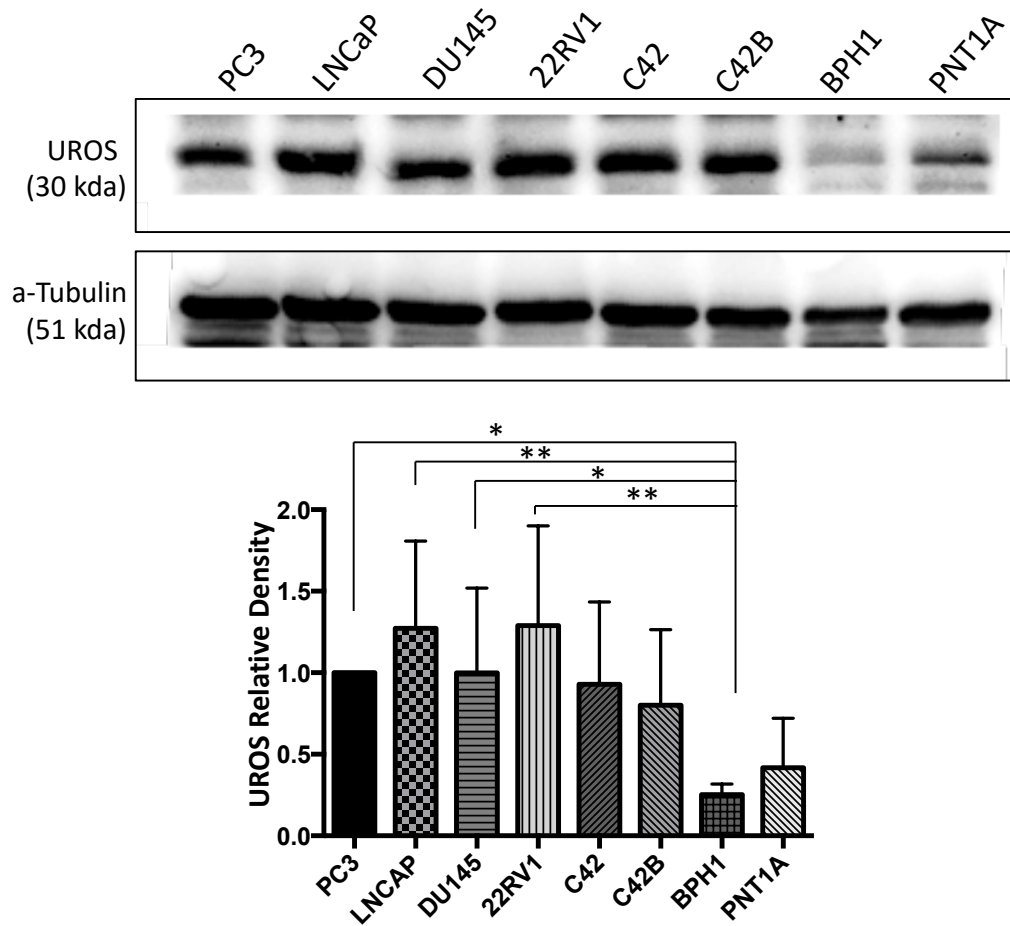


Figure 4.3 UROS protein levels in PCa cell lines and non-tumorigenic controls.

Cell pellets were lysed in RIPA buffer and protein levels quantified. Immunoblotting was subsequently performed using antibodies specific for UROS or α -tubulin (loading control). Densitometry analysis was performed using ImageJ. Data is mean \pm 1SD of three repeats. ANOVA (Dunnett's post hoc test), *P < 0.05, **P < 0.01.

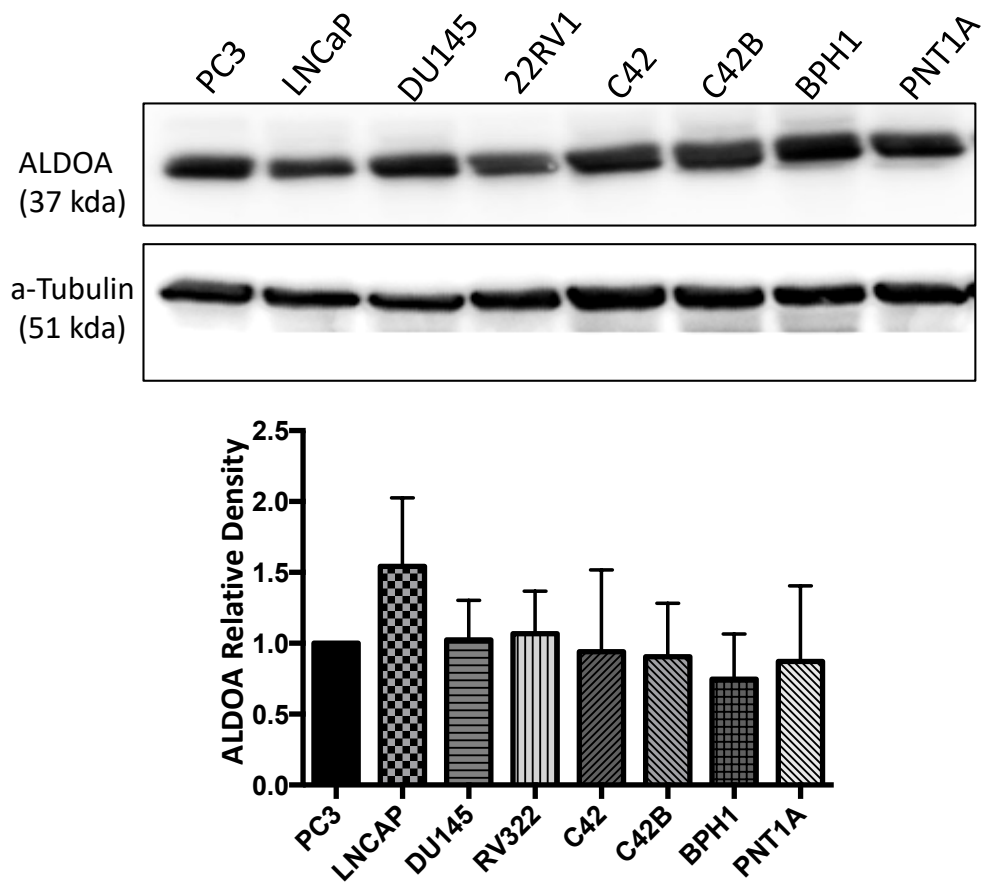


Figure 4.4 ALDOA protein levels in PCa cell lines and non-tumorigenic controls.

Cell pellets were lysed in RIPA buffer and protein levels quantified. Immunoblotting was subsequently performed using antibodies specific for ALDOA or α -tubulin (loading control). Densitometry analysis was performed using ImageJ. Data is mean \pm 1SD of three repeats. ANOVA (Dunnett's post hoc test), $P^* < 0.05$.

4.3 UROS and ALDOA localisation in PC3 cells

The localisation of UROS and ALDOA has been investigated in prostate cancer cells (PC3 cells) in order to gain insights into their cellular functions and if their localisation assists drugs' molecules accessibility. The 2 genes were PCR-cloned into pEGFP-C1. PC3 cells were transiently transfected with pEGFP-C1 Empty/UROS/ALDOA. After 24 hours, PC3 cells were fixed, stained with DAPI and visualised using laser scanning confocal microscope (Nikon Ti). In addition, immunostaining was performed using antibodies specific for UROS and ALDOA, and fluorophore conjugated secondary antibodies. Negative controls (no primary antibody) were included and cells imaged using confocal microscopy using the same parameters.

Immunostaining demonstrated that ALDOA is predominantly localised in the cytosol, however some nuclear staining is evident (Figure 4.5 a). This was further validated through imaging of GFP-ALDOA, which was also found to be predominantly localised in the cytoplasm of PC3 cells (Figure 4.5 b). UROS was localised in the nucleus and cytosol (Figure 4.6 a-b). GFP-tagged UROS showed a similar localisation to the immunostained samples, with staining being more punctate in the latter (Figure 4.6 b).

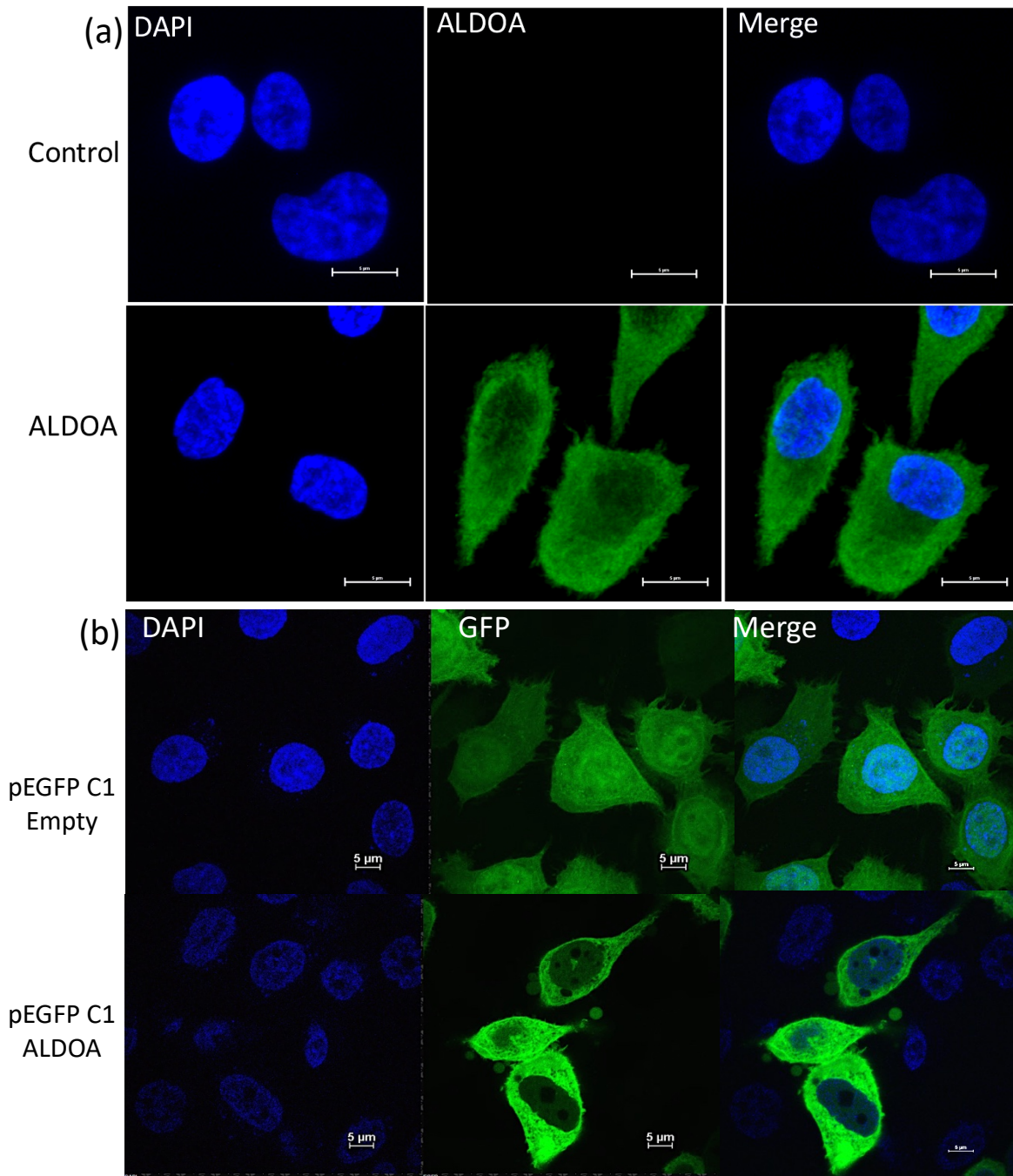


Figure 4.5 Confocal microscope images to show ALDOA localization in PC3.

(a): PC3 immuno-stained using anti-ALDOA antibody or no antibody control. (b): PC3 cells were transfected with either pEGFP C1-empty or pEGFP C1-ALDOA. Cells were fixed, stained with DAPI and imaged. All imaging was performed using 60X objective on Nikon Ti laser scanning confocal microscope. Scale bar is 5 μm.

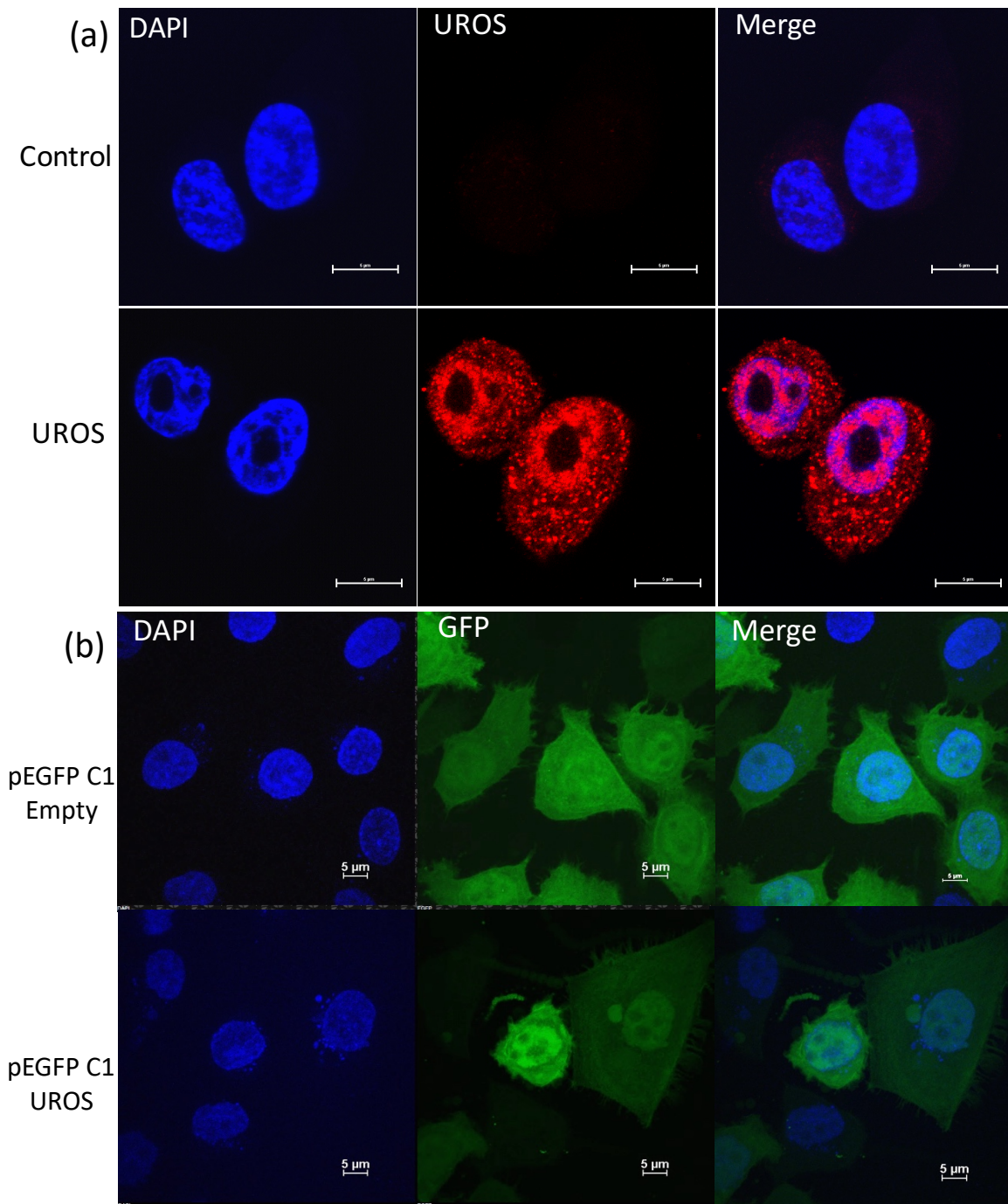


Figure 4.6 Confocal microscope images to show UROS localization in PC3.

(a): PC3 immuno-stained using anti-UROS antibody or no antibody control. (b): PC3 cells were transfected with either pEGFP C1-empty or pEGFP C1-UROS. Cells were fixed, stained with DAPI and imaged. All imaging was performed using 60X objective on Nikon *Ti* laser scanning confocal microscope. Scale bar is 5 μm.

4.4 Validation of UROS and ALDOA implication in PC3 migration by wound healing assays

4.4.1 Knockdown of Radixin reduces PC3 population cell motility

Cell migration is the movement of cells that occur to favour several physiological and pathological processes. Cancer cells metastases could occur by the dissemination of individual cells through blood or lymph nodes and/or by the movement of sheets or clusters of cells from the tumour origin into other secondary sites (Xu & Deng 2006). Therefore, wound healing assays have been performed to investigate into the relationship between lead targets and the invasive and metastatic properties of PCa cells collectively as populations. As has been stated before, radixin depletion has been shown to decrease the speed or motility of PC3 cells (Valderrama et al. 2012), and hence knockdown of this protein was used to optimise wound healing assays. PC3 were seeded in 6-well plates, transfected with siRNA (Radixin-siRNA, NTC-siRNA or mock transfected) and left 72 hours in reduced serum medium. Cell monolayers were “wounded” using a 200 µl pipette tips, and images acquired using brightfield microscopy (NikonTi widefield microscope, objective 2X). The cells were re-imaged hours after introduction of the scratches.

In order to segment scratches from the background of images, an edge detection technique was used. This technique of object segmentation is based on intensity discontinuity detection in digital images (Muthukrishnan & Radha 2011). Several edge detection algorithms are available including *Sobel* filter which simply detects horizontal and vertical edges; it detects significant changes in pixel values in the two directions and highlights them (Uchida 2013). This simple method was adequate to segment wounds from the background and precisely calculate the area. The scratch closure rate over time was then evaluated. Radixin depletion significantly decreased PC3 migratory potential (with 24 % scratch closure at 20 hours),

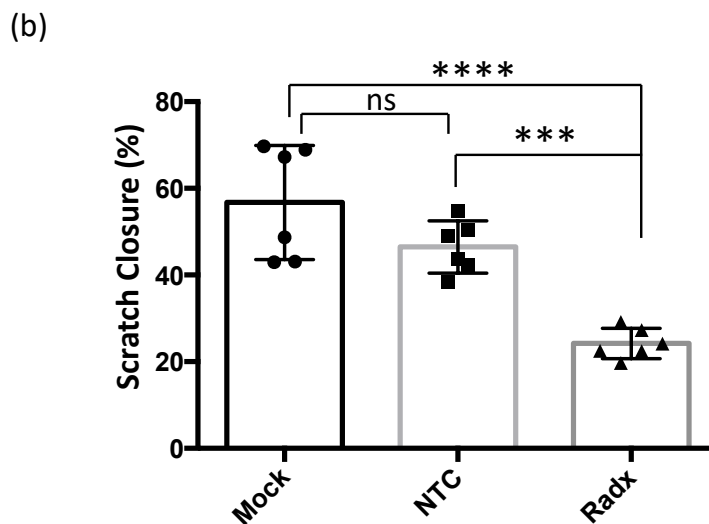
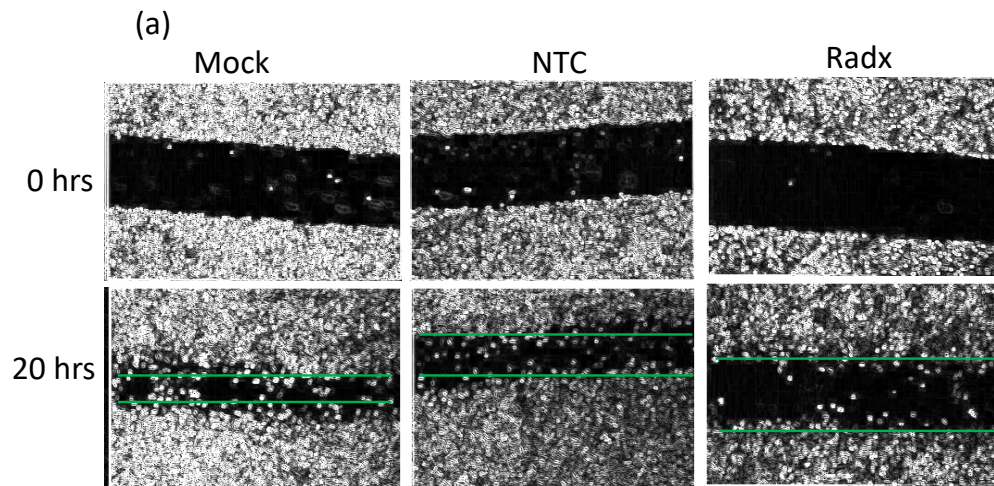


Figure 4.7 Inhibition of PC3 cell migration in response to Radixin knockdown.

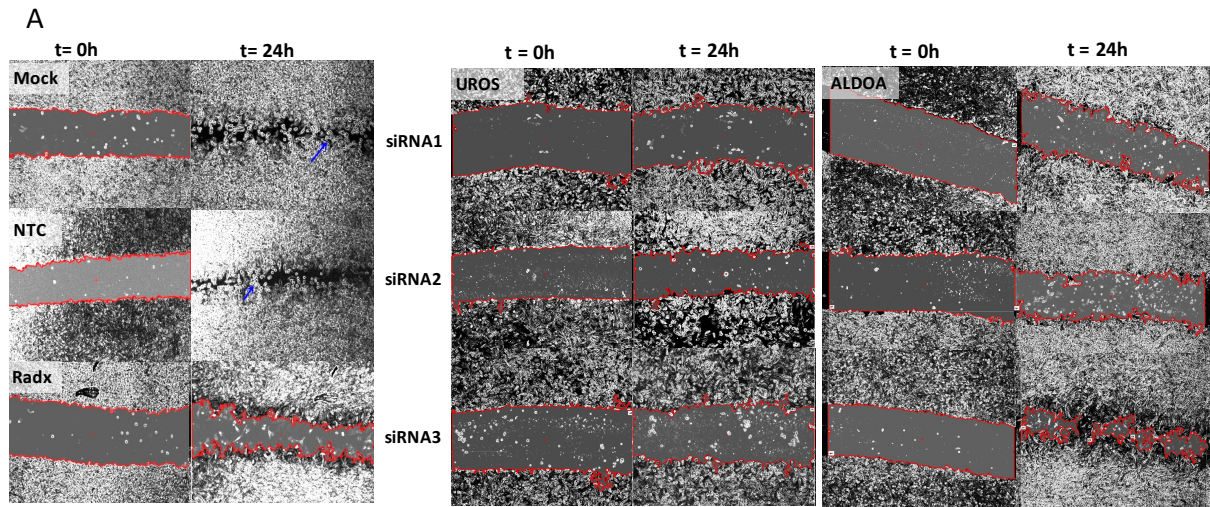
Cells were seeded in 12 well plates and transfected by radixin (Radx) or non-targeting (NTC)-siRNAs, or mock transfected control. 24 hours post-transfection, media was changed to fresh RPMI and left for 72 hours. 24 hours before introducing wounds media was changed to phenol red-free RPMI containing 5% charcoal stripped FCS. Wounds were then made, cells washed with PBS and fresh RPMI added. (a) Images were acquired using brightfield microscopy (Nikon Widefield Microscope, 2x objective) and representative images given. (b) Wounds were segmented and analysed by edge detection and automated area detection. Mean \pm 1SD of three independent repeats with at least 3 scratches quantified per experiment. ANOVA (Dunnett's post hoc test), ns= not significant, ***P < 0.001, ****P < 0.0001.

compared with mock and NTC transfections which had closure rates of 57% and 46% respectively (Figure 4.7).

4.4.2 Investigation of the effect of UROS and ALDOA knockdown upon PC3

migration

To further investigate the role of UROS and ALDOA in PC3 cell migration, wound healing assays were performed as previously described in Section (2.3.4). The results demonstrated that the scratch closure, in response to knockdown of UROS and ALDOA (average of three individual duplexes per target), was significantly decreased in comparison with NTC transfected cells. UROS knockdown reduced wound closure from 78% and 67% for the mock and NTC respectively, to < 29% for the different siRNAs used ($P < 0.05$, Dunnett's post hoc test) (Figure 4.8). For ALDOA, 2 of the siRNAs significantly reduced wound closure to 33% and 26 %, while the third siRNA showed no significant effect on the population motility of PC3 cells (Figure 4.8).



(b)

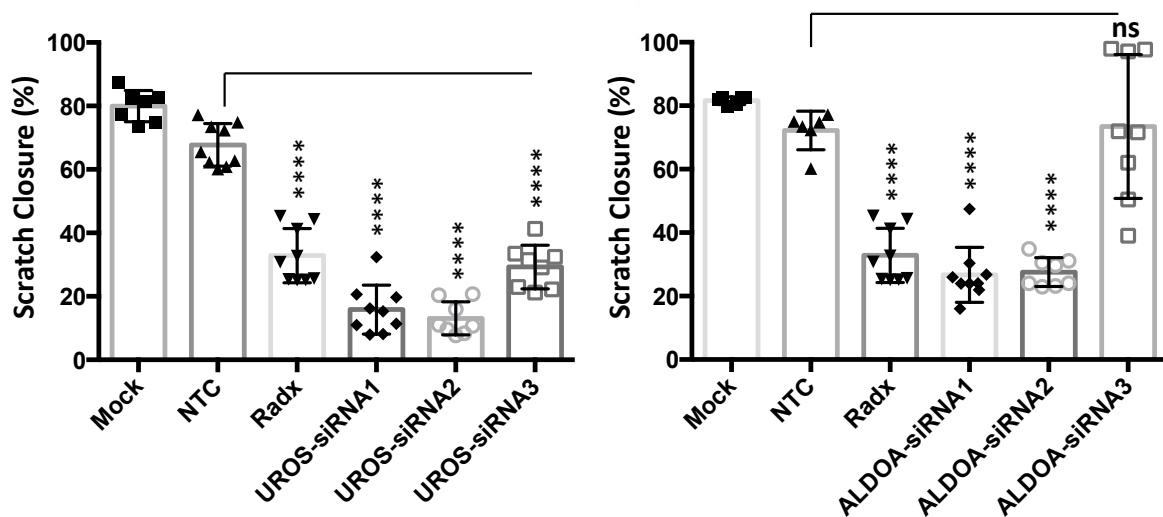


Figure 4.8 Inhibition of PC3 cell migration in response to ALDOA and UROS knockdown.

Cells were seeded in 12 well plates and transfected with siRNA (3 individual duplexes per target). siRNA Radixin (Radx) was used as a positive control and non-targeting (NTC)-siRNA and mock transfection were used as negative controls. 24 hours after transfection media was changed to fresh RPMI and cells left for 72 hours. 24 hours before introducing wounds, media was changed to phenol red- free RPMI containing 5% charcoal stripped FCS. Wounds were then made, cells washed with PBS and fresh media added. Images were captured using brightfield microscopy (Nikon Widefield microscope, 2x objective). (a) Representative images and (b) and wounds were segmented and analysed by edge detection and automated area detection. Data is mean±1SD of three independent repeats (at least 3 scratches per experiment were quantified). ANOVA (Dunnett's post hoc test), ns= not significant, ****P < 0.0001.

4.5 Discussion

4.5.1 *The effect of UROS depletion upon prostate cancer*

UROS converts the linear tetrapyrrole pre-uroporphyrinogen to a cyclic tetrapyrrole uroporphyrinogen III (UROGEN) in the heme-biosynthesis pathway (Figure 3.28) (Layer et al. 2010). UROS and other heme-synthetic enzymes exist in the cytoplasm (Ajioka et al. 2006), however UROS and UROD are believed to exist in the mitochondrial compartment as well (Hamza & Dailey 2012). This, therefore, might explain the cytoplasmic localisation of UROS obtained by immunofluorescence and transient transfections of the pEGFP C1-UROS vector. However, UROS was also found to be partially nuclear and this has not been previously described (Figure 4.6).

To date, no previous studies have linked UROS expression/activity to PCa. However, the porphyrins and heme-biosynthetic pathway intermediates have been found to be upregulated in cancers such as leukaemia and breast cancer (Navone et al. 1990; Fukuda et al. 2017). However, the mechanisms underlying heme-biosynthesis deregulation are still unknown. In this study, UROS transcript levels were shown to be significantly higher in PC3, LNCaP, and DU145 cells in comparison with BPH1 cells (Figure 4.2). In addition, the protein levels were found to be higher in several PCa cell lines compared to the noncancerous cell lines BPH1 and PNT1A (Figure 4.3). These findings suggest that UROS is over-expressed in prostate cancer cells which support the hypothesis that heme-biosynthesis is upregulated in prostate cancer. The expression of UROS mRNA was found, in a previous study, to be reduced under hypoxic conditions and this correlated with increased levels of hypoxia inducible factor 1 alpha (HIF1 α) (Vargas et al. 2008). This therefore suggests that UROS expression is regulated in response to oxidative stress.

In addition to the inhibition of proliferation, single cell migration and induction of apoptosis as demonstrated in Chapter 3, UROS downregulation resulted in reduced migration in wound healing assays (Figure 4.8). This demonstrates the role of heme biosynthesis and its key enzymes in PCa progression and suggests that the upregulation of UROS in PCa cells enhances cell survival and metastatic potential. Other heme metabolism key factors such as ALAS1 and heme uptake proteins (HCP1 and hrg-1) were also reported recently by Hooda et al. (2015) to be upregulated in NSCLC. They also found that the levels of oxygen-utilizing haemoproteins such as cytochromes and cytoglobins are elevated in NSCLC cells compared to normal cells (Hooda et al. 2015a).

Blocking heme-biosynthesis has also been reported to inhibit mitochondrial oxygen consumption and suppress proliferation, colony formation and migration in NSCLC (Hooda et al. 2013), and a similar effect was also previously demonstrated in leukaemia cells (Weinbach & Ebert 1985). These observations suggest that the upregulated factors and the increased activity of this pathway could be targeted as a novel therapeutic approach against PCa and other cancers. Inhibitors of heme-biosynthesis do exist, such as succinylacetone (SA, 4,6-dioxoheptanoic acid), which (as indicated in the last chapter) targets the activity of ALAD, the enzyme responsible for the second step of heme production (Figure 3.28). SA is a potent competitive inhibitor of ALAD that has been shown to successfully inhibit heme-biosynthesis (Sassa & Kappas 1983; Tschudy et al. 1983).

4.5.2 Investigations of ALDOA in prostate cancer

ALDOA is a key enzyme in glycolysis, catalysing the reversible conversion of fructose-1,6-bisphosphate to glyceraldehydes-3-phosphate and dihydroxyacetone phosphate (Figure 3.30) (Du et al. 2014). ALDOA was demonstrated to localize in both the cytoplasm and nucleus, however, the enzyme was found to be more abundant in the cytosol (Figure 4.5). Mamczur et al. (2013) also found ALDOA to be present in the cytosol and nucleus, and it was demonstrated

to localize preferentially into the nucleus upon stimulation of proliferation in lung cancer cells. Further, the group showed that ALDOA's nuclear localization correlated with the expression of the proliferation marker Ki-67 and that chemical inhibition of cell cycle progression resulted in the translocation of ALDOA from the nucleus to the cytosol (Mamczur et al. 2013).

As discussed in the last chapter, the upregulation of ALDOA was correlated with the progression of several cancers, however no previous studies have investigated its expression profile in relation to PCa. ALDOA was reported to be highly expressed in other cancers such as colorectal cancer, lung cancer, osteosarcoma, oral squamous cell carcinomas, and hepatocellular carcinomas (Zhang et al. 2017). Contradictory to this, the protein levels of ALDOA in prostate cancer cells was found to be similar to the levels in the noncancerous cells (Figure 4.4). However, qPCR analysis demonstrated that ALDOA mRNA levels are considerably higher in PCa cell compared to BPH1 cells (Figure 4.2). This discrepancy might be explained by differences in the stability or half-life of ALDOA between the cells. This hypothesis might be the case because when ALDOA was depleted in PC3 cells (Figure 4.1), transcript levels were efficiently down-regulated in response to the siRNA while the protein level was only reduced by approximately 35 % (Figure 4.1).

ALDOA downregulation, as shown in the Chapter 3, inhibited proliferation and single cell migration and induced apoptosis. In addition to that, wound healing assay analysis of PC3 cells transfected with siRNA targeting ALDOA showed that two siRNAs significantly inhibited cell migration (Figure 4.8). These results suggest that ALDOA is an important regulator of prostate cancer progression and motility. However, I demonstrated in the last chapter that BPH1 cells were also sensitive to ALDOA knockdown (Figure 3.3). This indicates that targeting this axis may result in toxicity in noncancerous cells and this requires further investigation.

Further investigations are also required to investigate the exact role of ALDOA in PCa as it has been demonstrated to also be involved in non-glycolytic pathways. For instance,

previous work by Lew and Tolan (2012) demonstrated that knockdown of ALDOA inhibited the proliferation of NIH-3T3 and Ras-3T3 transformed cells. Measurement of glycolytic flux (lactate levels), rate of glucose consumption and intracellular ATP levels demonstrated that ALDOA knockdown did not affect glycolysis. Further, they found that ALDOA-depleted cells had a three-fold higher number of binucleated cells compared to mock control. For this reason, the authors suggested that ALDOA knockdown impairs cancer cell proliferation via a non-glycolytic mechanisms probably as a result of disruption to the cell cycle at the cytokinesis step (Lew & Tolan 2012). Such observations highlight the need for further investigations of the role of ALDOA in PCa.

4.5.3 Summary

Depletion of UROS and ALDOA resulted in strong anti-proliferative and anti-migratory effects on PCa cells. The results of this chapter validated the previous knockdown data and the involvement of ALDOA and UROS in prostate cancer progression. However, further investigations are required to elucidate their mechanisms of action in altering the metabolic signalling of PCa. The aim of this work was to develop novel therapeutic approaches against CRPC by targeting metabolic signalling, therefore the inhibition of heme biosynthesis pathway, where UROS functions, was of interest and further work regarding this is provided in Chapter 5.

5 Chapter 5 Results III

5 Heme-biosynthesis inhibition: a therapeutic approach to inhibit prostate cancer progression

As indicated before, one of the roles that UROS plays is its function as the fourth step in heme-biosynthesis. Heme is found in all tissue types but at different levels and an alteration in heme biosynthesis is associated with several disease conditions such as anaemia, neuropathy and cancer (Hooda et al. 2015b). Further, heme forms an important factor in mitochondrial respiration and there is evidence that heme levels are elevated in cancer tissues (Alam et al. 2016). Heme forms a prosthetic group for several hemoproteins such as hemoglobin, myoglobin and cytochromes and hence it is crucial for transporting, storing, and utilizing oxygen. The increased levels of heme biosynthesis in cancer cells results in high levels of hemoproteins and therefore increased oxygen consumption (Hooda et al. 2013; Hooda et al. 2014; Hooda et al. 2015a). The latter will result in higher levels of energy generated to meet the cellular demands enabling unlimited growth and progression.

To explore if heme biosynthesis could be a valid therapeutic axis to suppress PCa proliferation, the heme synthesis inhibitor succinylacetone (SA) was used. This inhibitor works by blocking the second enzyme in the heme synthesis pathway, ALAD (δ - aminolevulinic acid dehydratase), that functions upstream of UROS (Hooda et al. 2015a). This inhibitor prevents the step when two ALA molecules are fused to form porphobilinogen (Zhang & Gerhard 2009). This chapter investigated the impact of heme synthesis inhibition on prostate cancer cell proliferation and migration. Evaluation of cell death and cell cycle analysis of heme depleted cells were followed to examine the pathways triggered upon the inhibitory effect of SA. Further, we hypothesized that combining heme synthesis inhibition with ROS will further increase PCa cell death after the prior action of SA upon cells as a result of inhibition of heme synthesis and

subsequent loss of downstream hemoproteins, which are known to protect against ROS damage. This hypothesis is based on the fact that solid tumours are usually hypoxic and maintain high levels of ROS. In addition, the presence of necrotic cells in the microenvironment of the tumour *in vivo* will facilitate damage signals (cytokines) that induce T-cells receptor (TCR) signaling, and the latter will be associated with the infiltration of immune/inflammatory cells to the tumour microenvironment (Chen et al. 2016). Immune cells, such as macrophages and neutrophils, produce high levels of ROS and hence accumulation of ROS in the tumour microenvironment will follow which leads to further cellular stress upon cancer cells (Liou & Storz 2010). Therefore, in this part different ROS sources (e.g. H₂O₂) were combined with SA treatment to explore the validity of this approach as a therapeutic strategy against prostate cancer progression.

5.1 Reduction of cellular heme content inhibits proliferation of PCa cells

Firstly, a time-course treatment with SA was performed to find the time required for the inhibitor to show its effect. Three PCa cell lines (PC3, DU145, and LNCaP) were treated with a dose range (1-1000 µM) of SA and cells left to grow for 2, 4, and 6 days. Crystal violet assays were performed to quantify proliferation and data made relative to the untreated control. Figure 5.1 shows a dose-dependent decrease in the proliferation of all cell lines starting at 4 days. The 6 days incubation demonstrated a more significant growth inhibition at the higher concentrations of SA. There was no significant effect on the growth at the 2 days treatment. Therefore 6 days treatment was selected for further experiments.

To investigate if this anti-proliferative effect of SA on PCa cell lines was specifically due to heme-synthesis reduction, PC3 cells were seeded and treated in the same manner with SA doses for 6 days. Cells were harvested, counted, and pelleted in equal numbers prior to quantification of heme content. As expected, SA significantly decreased heme levels in a dose-

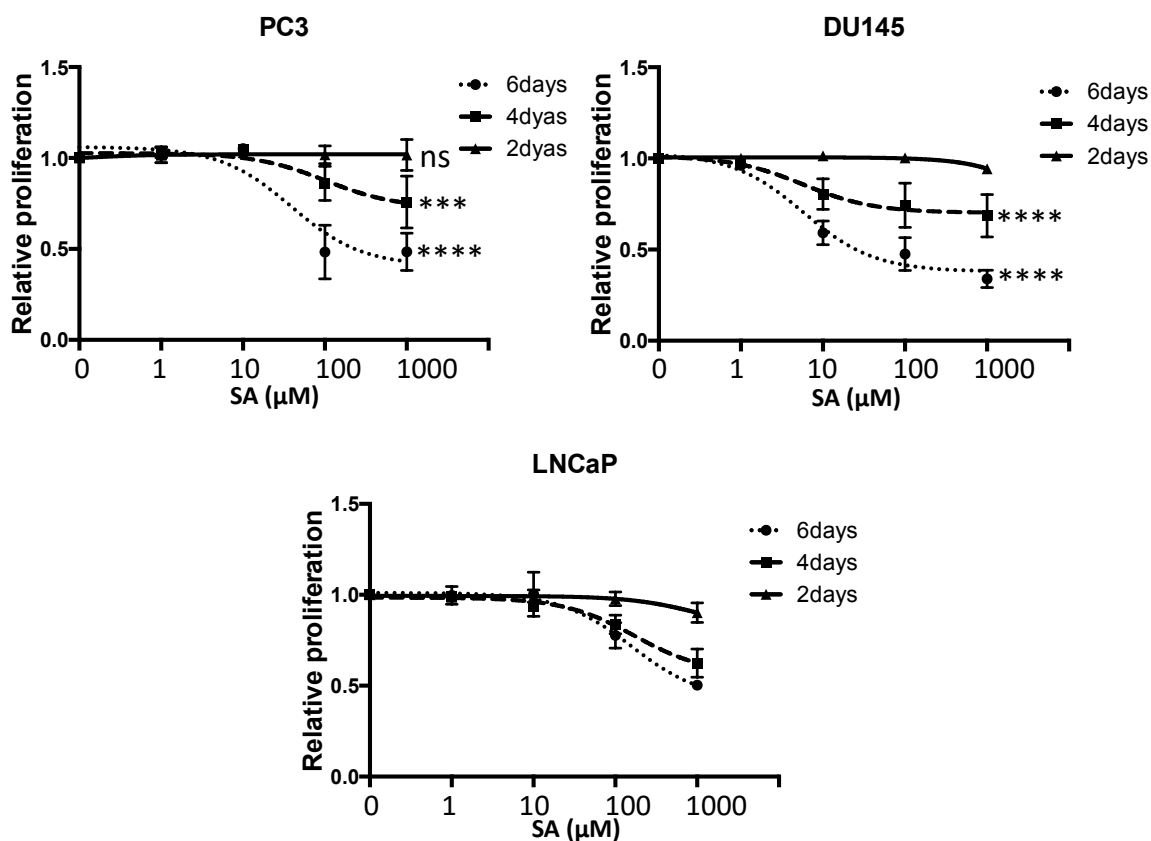


Figure 5.1 Time-course treatment of prostate cancer cell lines with succinylacetone (SA).

Cells were plated and left for 24 hours prior to treatment with SA. Cells were incubated for 2, 4, or 6 days and proliferation assessed using crystal violet (CV) assays. Data represent mean \pm 1SD of three independent repeats. ANOVA (Dunnett's post hoc test), *P < 0.05, **P < 0.01, ****P < 0.0001.

dependent manner (Figure 5.2). This decrease started at 10 μM of SA but was more considerable at 100 μM and 1000 μM .

To examine if reducing exogenous heme levels in the growth medium enhanced any the inhibitory activity of cell proliferation, cells (PC3, DU145, LNCaP and BPH1) were grown in either 5% FBS medium or 5% heme-depleted FBS medium and treated with SA doses (1-1000 μM) for 6 days. Heme-depleted medium was prepared by following a previously published protocol (Zhu et al. 2002). As before, SA was found to inhibit the proliferation of all cell lines, but heme-depleted medium did not enhance this effect (Figure 5.3). This may be because the exogenous heme level is not as critical as the endogenous heme for PCa cells' survival or that the heme depletion was sufficient to show any impact on these cells.

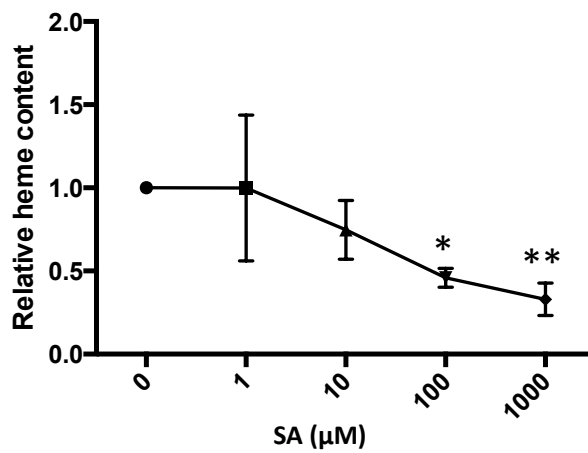


Figure 5.2 Heme content of PC3 cells treated with succinylacetone (SA).

PC3 cells were treated with SA 24 hours after seeding. Cells were left for a further 6 days, harvested, counted and pelleted. Heme was extracted by heating cells to 100 °C in a concentrated oxalic acid solution for 30 mins. Heme content was determined by measuring fluorescence of porphyrin at 400 nm excitation and 662 nm emission. Data represents mean±1SD of three independent repeats. ANOVA (Dunnett's post hoc test), *P < 0.05, **P < 0.01.

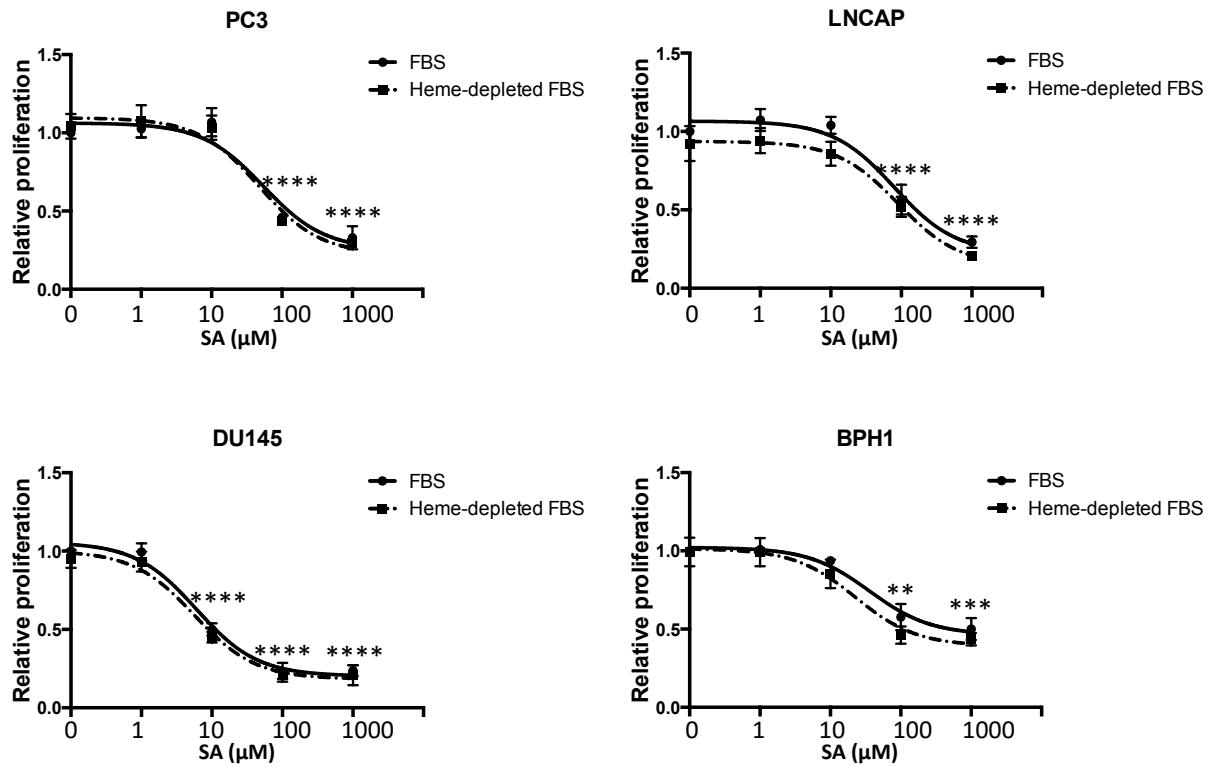


Figure 5.3 Heme-depletion and succinylacetone (SA) treatments upon the proliferation of prostate cancer cell lines and BPH1 cells.

Cells were seeded in either media containing standard FBS or in heme-depleted FBS for 24 hours prior to treatment with SA doses. Cells were left to grow for 6 days proliferation assessed using crystal violet (CV) assays. Data represent mean±1SD of three independent repeats. ANOVA (Dunnett's post hoc test), *P < 0.05, **P < 0.01, ****P < 0.0001.

5.2 Inhibition of heme synthesis reduces the metastatic potential of PCa cells

To further evaluate the effect of heme synthesis upon prostate cancer cells, the migratory potential of PC3 cells with and without SA was examined. Wound healing assays and single cell tracking experiments were performed on day 4 post SA treatment. Figure 5.4 shows that inhibition of heme synthesis significantly reduced the population motility of PC3 cells in a dose dependant manner. SA led to a more than 30 % decrease in scratch closure at 10 μ M and more than 50 % when higher concentrations were applied. These results matched the single cell tracking data where PC3 cells showed a significant decline in single cell speed in comparison with untreated controls (Figure 5.5). These findings suggest that heme biosynthesis in PCa is crucial for proliferation and the migratory potential of PCa cells.

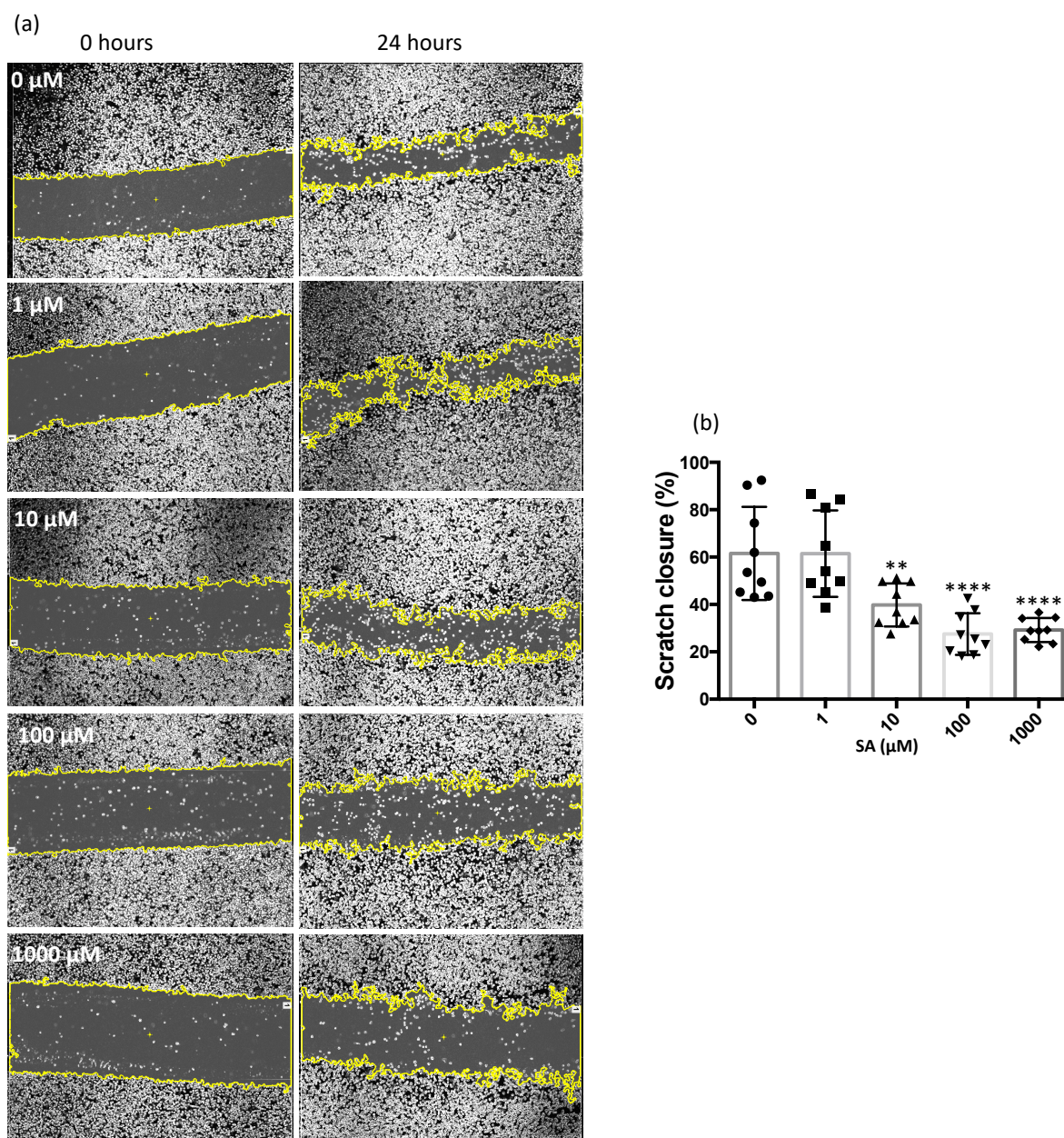


Figure 5.4 Succinylacetone (SA) inhibition of the population motility of PC3 cells.

Cells were seeded in 12 well plates and treated after 24 hours. 3 days later the media was changed to 5% hormone-depleted RPMI, retreated, and left for 6 hours. Wounds were then made, cells washed with PBS once and fresh hormone-depleted RPMI added (retreatment with SA was included). A large-scale brightfield image was captured using a Nikon widefield microscope (2x objective), and 24 hours later another image was captured. (a) Representative images were generated using Nikon NIS-elements software and wounds were segmented and analysed by edge detection and automated area detection. (b) the mean wound closure was calculated for at least 9 scratches. Data is mean \pm 1SD of three independent repeats. ANOVA (Dunnnett's post hoc test), *P < 0.05, **P < 0.01, ****P < 0.0001.

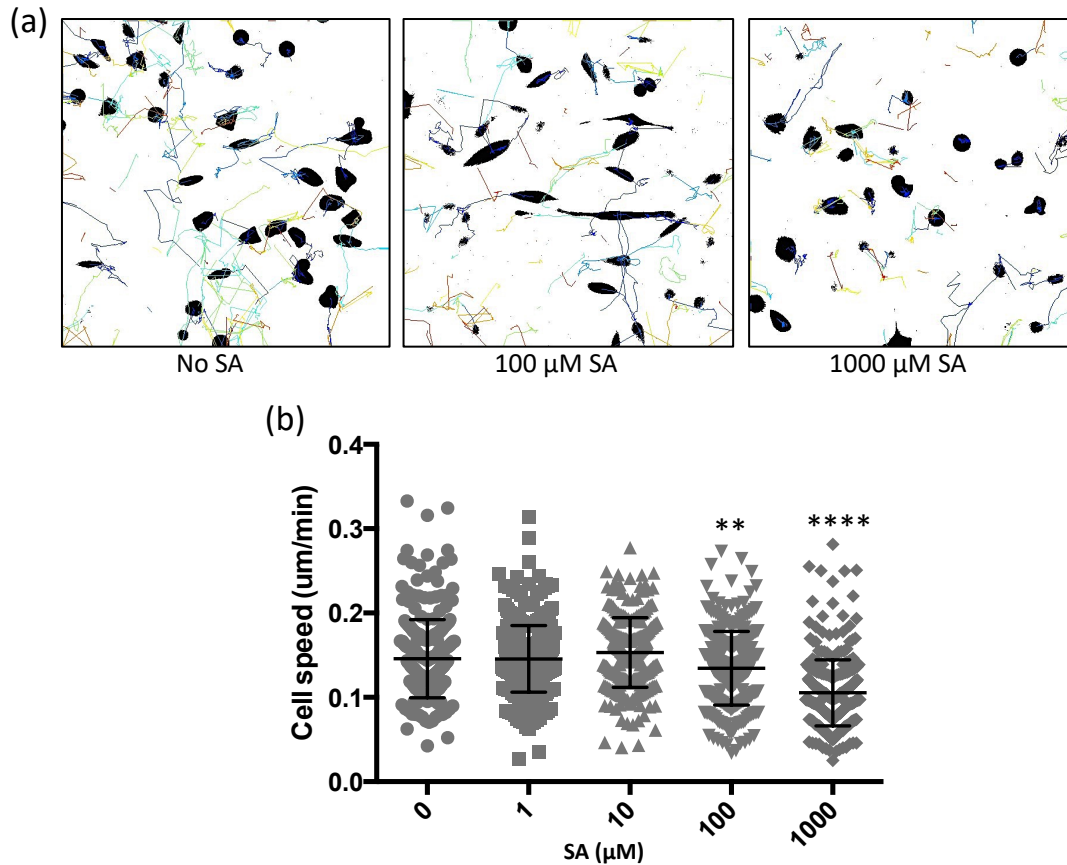


Figure 5.5 Evaluation of the effect of succinylacetone (SA) on single cell migration of PC3 cells.

PC3 were seeded sparsely, treated with SA doses 24 hours later, and left for 3 days. On day 4, images were acquired by Nikon Ti widefield microscope every 20 minutes using 10X 0.3 N.A objective lens, 20-30 % illumination, and 3-5 seconds exposure. GFP was excited using blue light 470 nm via a CoolLED pE excitation system. The time-lapse image sequences were analysed using ADAPT plugin (ImageJ). (a) Images showing tracks of untreated (no SA) versus treated (100 μM and 1000 μM SA) cells. Images were made using Trackmate plugin (ImageJ). The scatter dot plot (b) represents mean±1SD of more than 50 trajectories of three independent repeats. Kruskal-Wallis (Dunn's test) $P^{**} < 0.01$, $P^{****} < 0.0001$.

5.3 Inhibition of heme synthesis blocks cell cycle progression and enhances necrotic and apoptotic cell death in PCa cells

To investigate the mechanisms behind the reduced PCa cells' proliferation and migration induced by heme biosynthesis inhibition, cell death and cell cycle analyses using flow cytometry were performed. Briefly, PC3 cells were treated with SA as previously indicated. Cells then were pelleted and stained with propidium iodide (PI) for either cell cycle, apoptosis, or necrosis analysis (Figure 5.5a). PI staining is absorbed by cells at different extents according to cells properties, and because cells at different phases of cell cycle or when they pass through different cell death modalities exhibit different physical properties and DNA contents such type of staining is beneficial when analysed by flow cytometry. The latter is utilized to gate each population according to cells' physical characteristics and DNA content.

PC3 cells appear to be arrested in G2-phase following treatment with SA at the highest dose (Figure 5.6a and b). The number of cells in G2-phase was 50 % higher in SA-treated cells (1000 μ M) compared to the untreated control. In addition, the highest dose of SA led to a significant increase in the number of apoptotic cells compared to the control; 15 % and 5 % respectively. More interestingly, accessing the necrotic profile of the cells revealed that the SA-treatment enhanced the number of cells dying as a result of necrosis by 20 % and 15 % at the 100 μ M and 1000 μ M SA-doses respectively (Figure 5.6 c). These results suggest that heme is important for cell cycle progression in PCa cells, and that metabolic stress enhanced by heme deficiency leads to cellular arrest at G2-phase, apoptotic and necrotic cell death.

The evaluations of apoptosis and necrosis were expanded further to other prostate cancer cell lines, LNCaP and DU145 (Figure 5.7). An increase in necrosis was seen in DU145 at 100 μ M, however no elevation at the higher concentration of SA. Further, LNCaP cells demonstrated only a slight increase in necrosis upon all SA doses, however this increase was not significant.

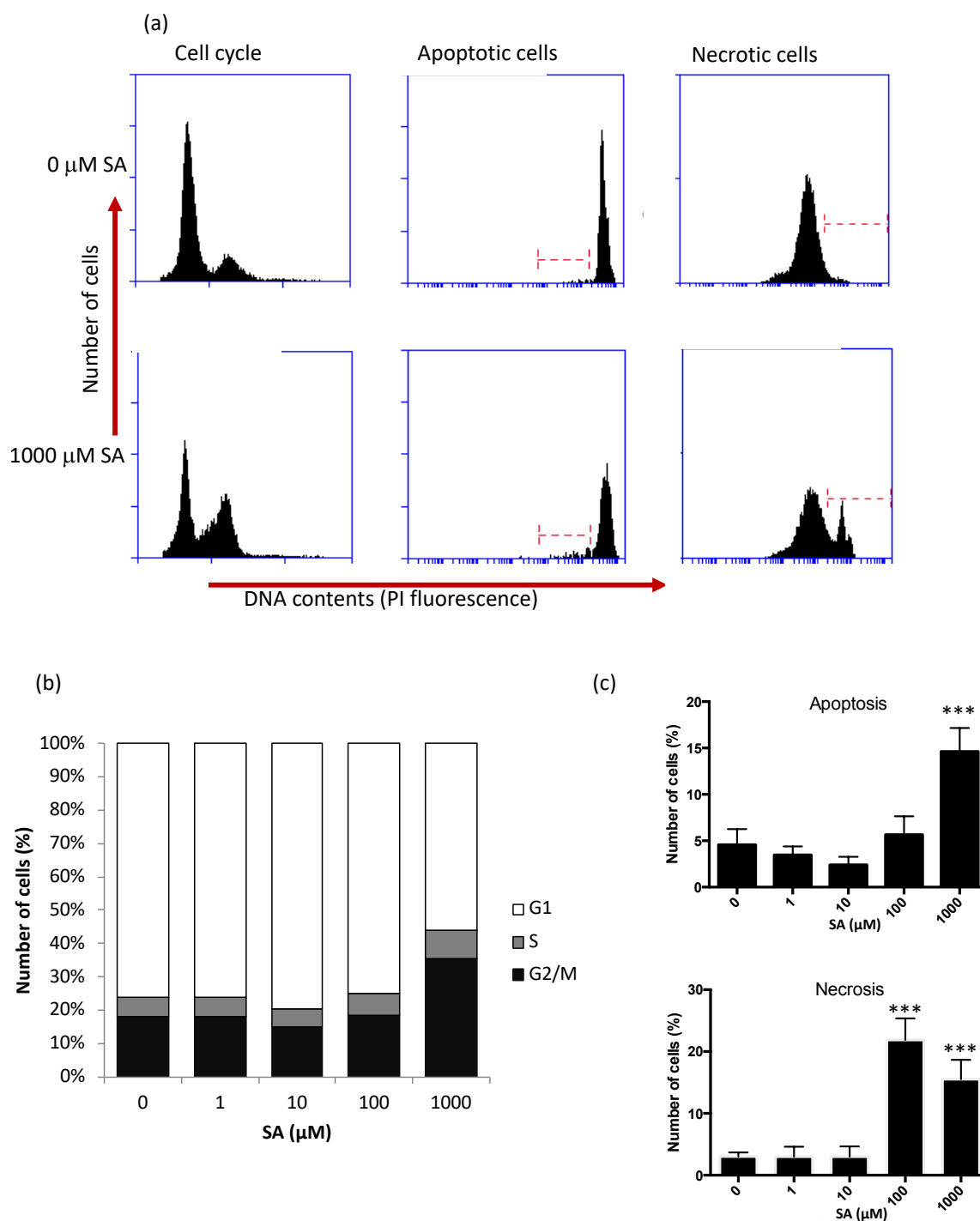


Figure 5.6 Flow cytometry analysis of PC3 cells treated with succinylacetone (SA).

Cells were treated with SA and incubated for 6 days prior to being harvested and PI stained. An Accuri C6 was used to read and analyse the samples and cells were gated to include only cells whilst debris was excluded. (a) a panel of representative of cell cycle, apoptosis, and necrosis profiles where the y axis represents the number of cells and x axis is the PI signal. (b) Cell cycle analysis exhibits the mean of three independent repeats. (c) Quantification of the number of cells undergoing apoptosis and necrosis. Data represents mean±1SD of three repeats. ANOVA (Dunnett's comparison test), ***P < 0.001.

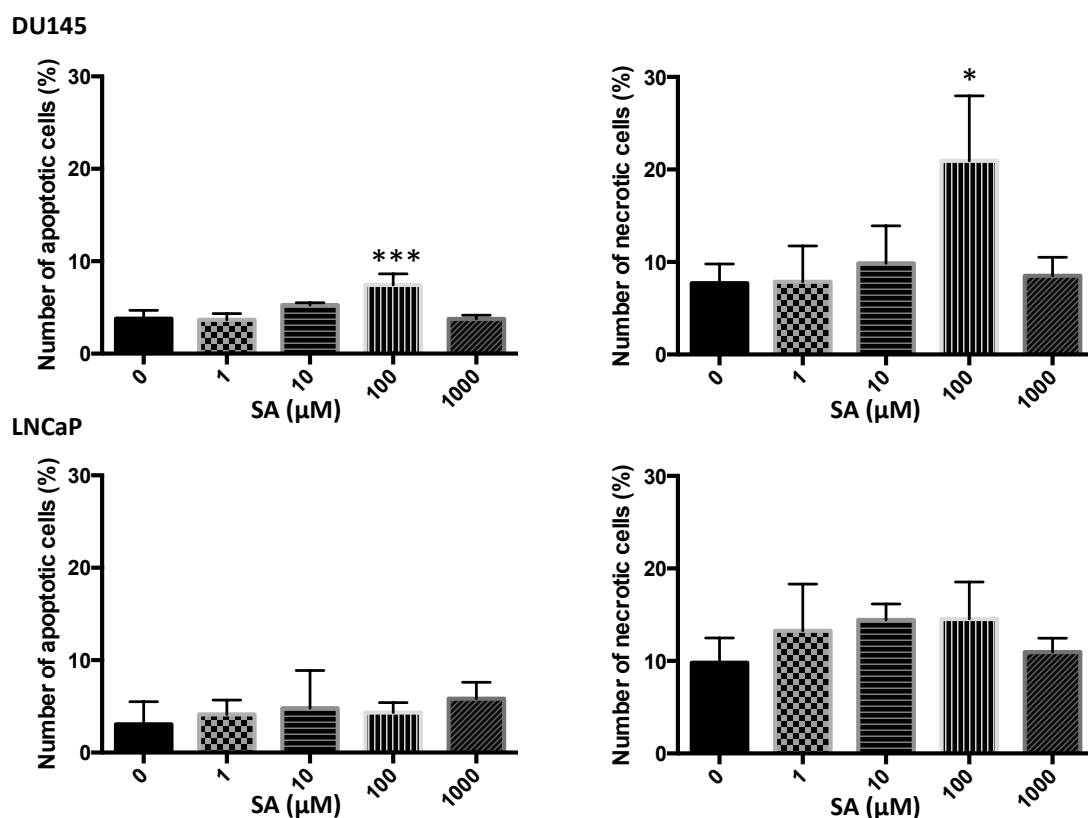


Figure 5.7 Cell death analysis by flow cytometry of succinylacetone (SA) treated DU145 and LNCaP cells.

Cells were treated with SA and incubated for 6 days prior to being harvested and PI stained. An Accuri C6 was used to read and analyse the samples and cells were gated to include only cells whilst debris was excluded. Box plots represent mean±1SD of number of cells undergoing apoptosis and necrosis (%) of at least three independent repeats. ANOVA (Dunnett's comparison test), *P < 0.05, ***P < 0.001.

5.4 Inhibition of heme synthesis sensitizes prostate cancer cells to ROS damage and enhances necrotic cell death

5.4.1 ROS potently inhibits prostate cancer proliferation following heme synthesis inhibition

To further test my hypothesis that SA inhibition of heme synthesis will make cells sensitive to ROS, H₂O₂ was applied (100-500 μM) to cells that had been treated with/without a sub-lethal dose of SA (50 μM). H₂O₂ was found to have a synergistic effect with SA in a dose-dependent manner (Figure 5.8). 50 μM of SA reduced cell viability to 28 %, 13 %, 60 %, and 28 % for PC3, LNCaP, DU145, and BPH1 respectively. H₂O₂, in contrast, exhibited no significant effect when added to the cell lines except for LNCaP. The latter showed a 44 % decrease in proliferation at 500 μM of H₂O₂, however, there was little effect on LNCaP growth for the other H₂O₂ concentrations tested. The combined treatment of, SA and H₂O₂, exhibited a significantly higher effect on PCa cells' proliferation than that of each treatment alone. A synergistic effect on PC3, LNCaP, and DU145 cells was obtained starting at 300 μM, 200 μM, and 100 μM of H₂O₂, respectively. DU145 seemed to be the most sensitive cell line to both SA alone and SA combined with H₂O₂. Interestingly, H₂O₂ doses showed no effect at all on BPH1 proliferation, alone or combined with SA.

This experiment was also repeated with a higher more toxic dose of SA, 500 μM. Similarly, combining SA with H₂O₂ led to an additive inhibition of PCa cell proliferation (Figure 5.9). The growth inhibition rate was again greater than each treatment alone, and the effect was more significant at the lower concentration of H₂O₂ than that when a sub-lethal SA dose was used (Figure 5.8). This inhibition was specific for cells treated with SA except LNCaP cells, which again showed some sensitivity to H₂O₂ dose-treatment, however, the combination was more efficacious. Additionally, as we observed in Figure 5.8, BPH1 cells were unaffected

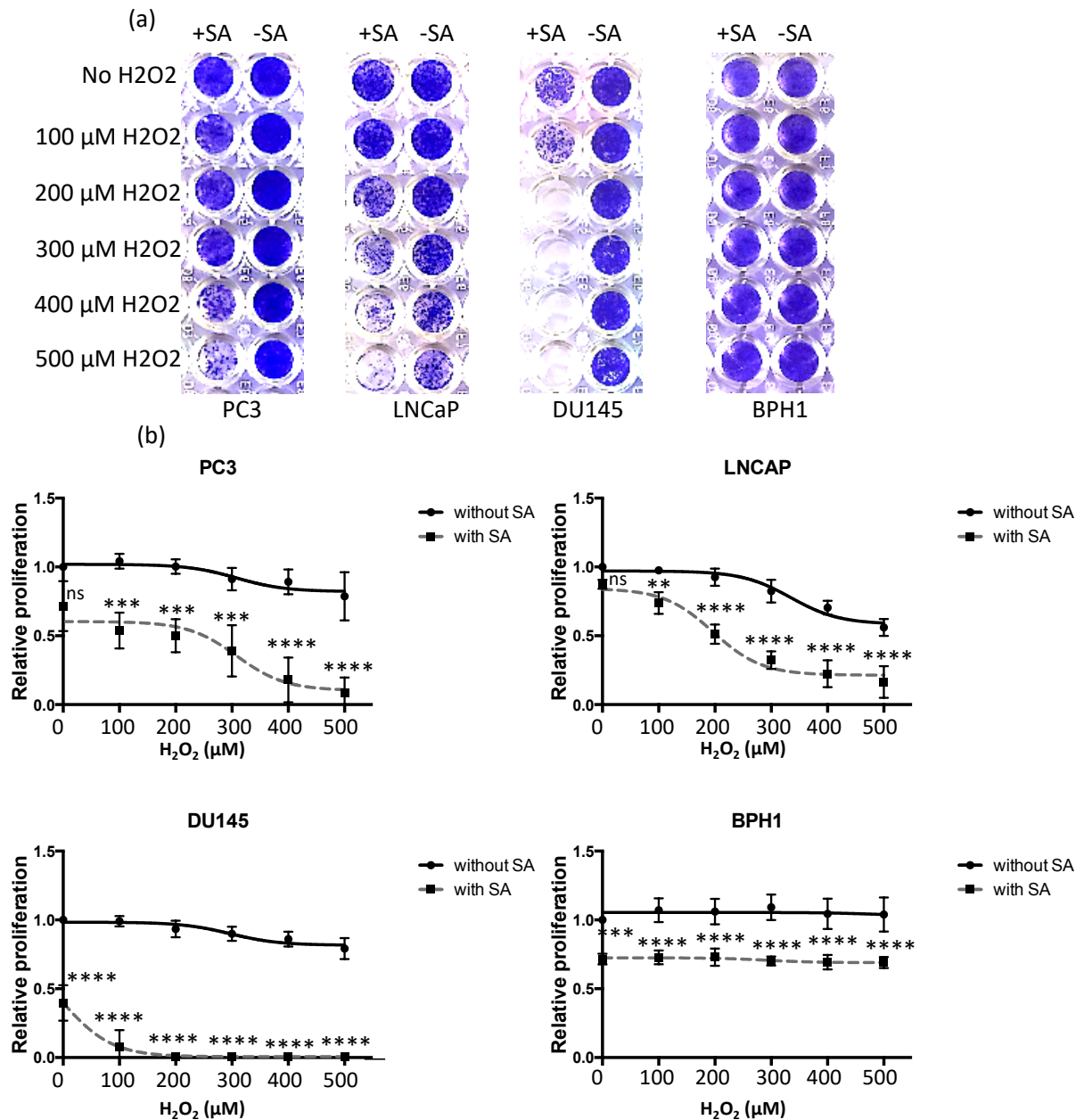


Figure 5.8 Inhibition of prostate cancer cell proliferation by succinylacetone (SA) in combination with dose-treatment of hydrogen peroxide (H₂O₂).

Prostate cancer cell lines and BPH1 cells were seeded 24 hours prior to treatment with 50 μM SA. Cells were left to grow for 5 days and then treated with H₂O₂ (0-500 μM) and left for a further 24 hours before CV staining. (a) Representative images of CV stained cells, and (b) dose-response curves of PC3, LNCaP, DU145, and BPH1 +/- SA and +/-H₂O₂. Data were normalized to untreated cells and represents mean±1SD of three independent repeats. Two-way ANOVA (Sidak's comparison test), **P < 0.01, ****P < 0.0001.

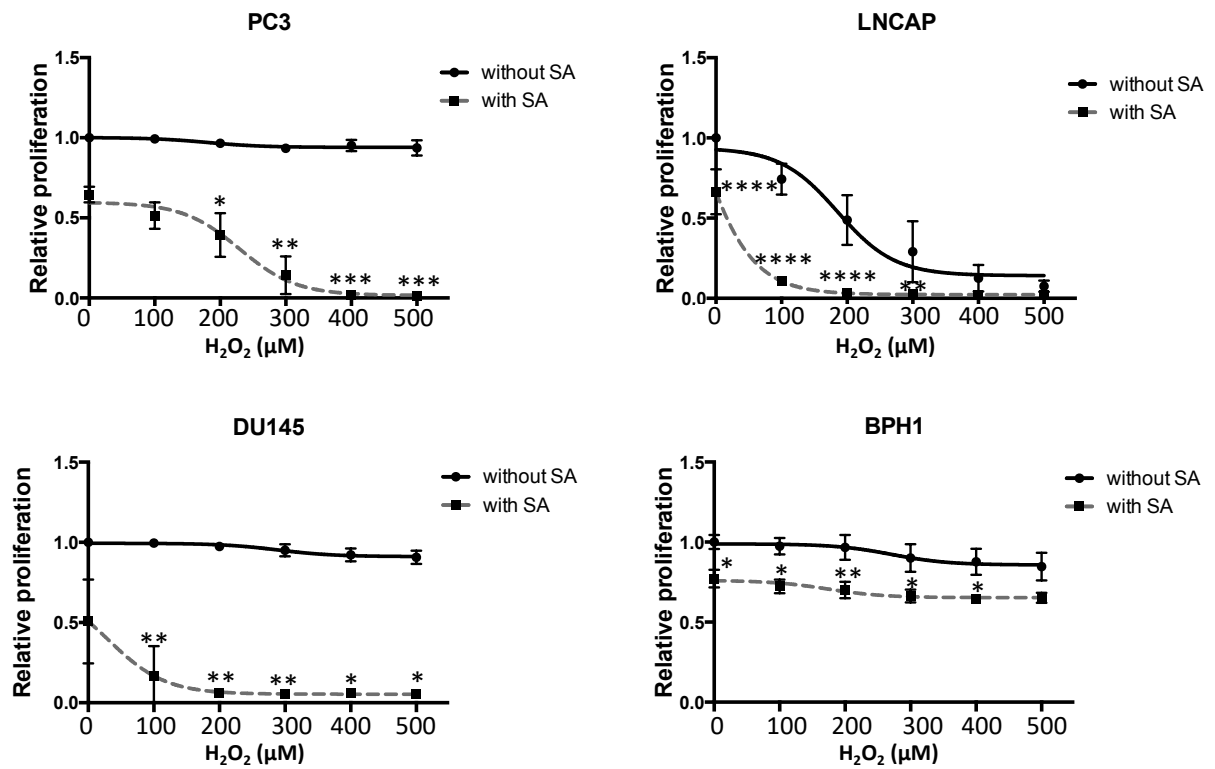


Figure 5.9 Inhibition of prostate cancer cell proliferation with a high dose of succinylacetone (SA) in combination with hydrogen peroxide (H₂O₂).

Prostate cancer cell lines and BPH1 cells were seeded 24 hours prior to treatment with 500 μM SA. Cells were left to grow for 5 days and then treated with H₂O₂ (0-500 μM) and left for a further 24 hours before CV staining. The data presented is dose-response curves of PC3, LNCaP, DU145, and BPH1 +/- SA and +/-H₂O₂. Data were normalized to untreated cells and represents mean±1SD of three independent repeats. Two-way ANOVA (Sidak's comparison test), *P < 0.05, **P < 0.01, ***P < 0.001 ****P < 0.0001.

by H₂O₂ treatment in the presence and absence of the high concentration of SA. These results suggest that exposing heme-deficient cells to ROS further initiates anti-proliferative pathways in prostatic cancer cells but not in noncancerous cells. In addition, the level of sensitivity of PCa cells to H₂O₂ is associated with the SA dose. These findings suggest that this approach represents a targeted therapeutic strategy that will have minimal cytotoxic effects upon normal cells.

5.4.2 Necrotic-like cell death of PCa cells following heme synthesis inhibition in combination with ROS

To investigate the effect of SA plus H₂O₂ upon cell death, cells were treated as for the proliferation assays (Section 2.6). DNA content was analysed using flow cytometry to assess the effect upon apoptosis and necrosis when cells were treated with a low (50 µM, Figure 5.10) and a high (500 µM, Figure 5.10) dose of SA. Both concentrations of SA ± H₂O₂ had no effect upon apoptosis for all of the cell lines tested (Figure 5.10 and 5.11). In contrast, necrosis was significantly increased in all cell lines when SA and H₂O₂ were combined ($P < 0.05$, Sidak's test). LNCaP exhibited increased levels of necrotic cell death at the higher concentrations of H₂O₂ (400 µM and 500 µM). This is consistent with the inhibition of proliferation for LNCaP which was also significant at the higher concentrations of H₂O₂. Interestingly, BPH1 cells showed no significant increase in apoptosis or necrosis in response to all treatments ($P > 0.05$, Sidak's test), which again supports the hypothesis that targeting heme synthesis, in combination with ROS damage, is more specific for PCa cells compared to non-tumorigenic controls (Figure 5.11). Figure 5.12 demonstrates the cell cycle profiles of PC3 cells upon the combination treatments of SA and H₂O₂. Cells accumulated in G₂-phase in response to heme synthesis inhibition as shown before. However, this accumulation steadily declined upon the addition of H₂O₂ with no sign of cell accumulation in either S-or G₂-phase ($P > 0.05$, Sidak's test).

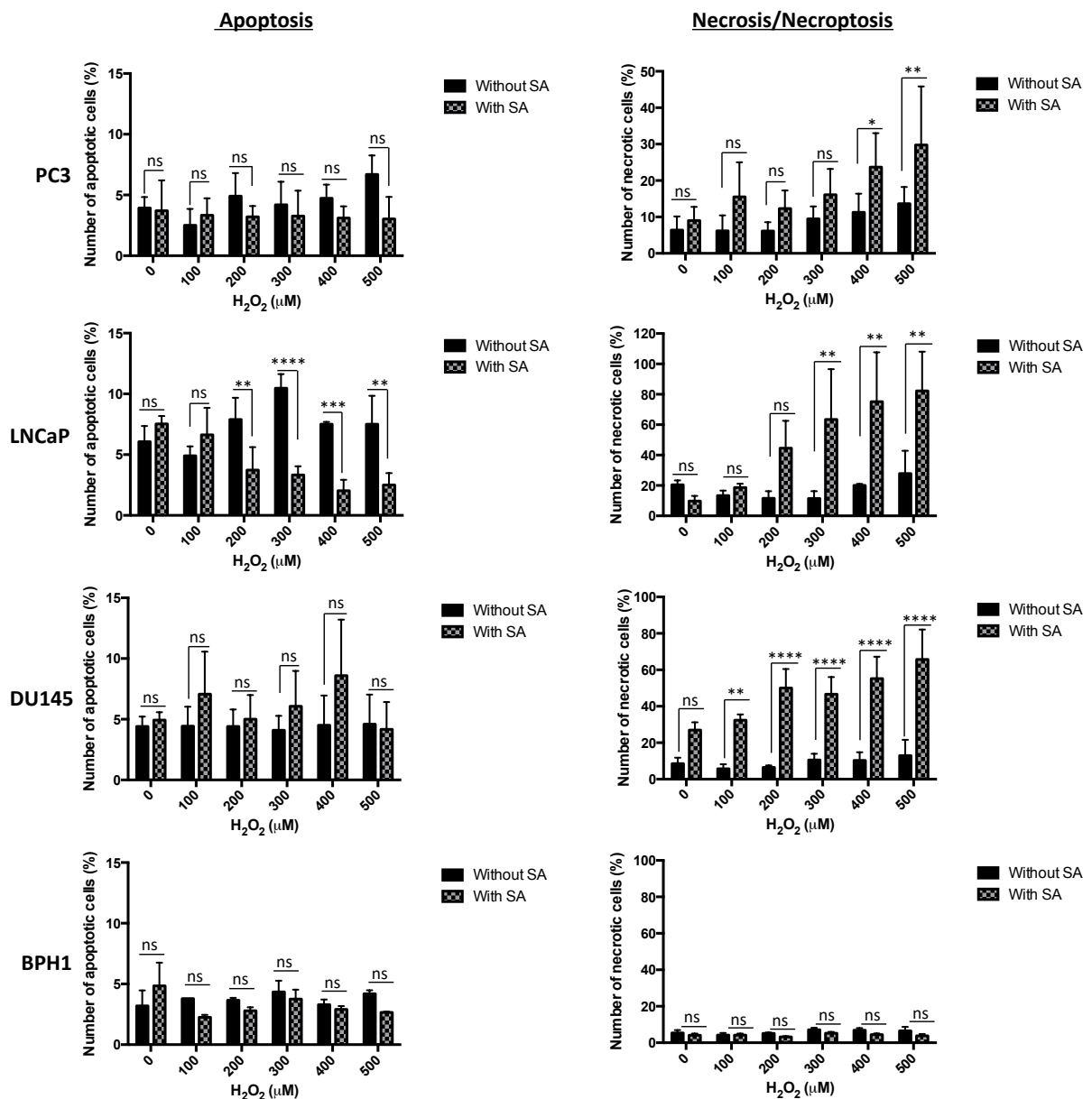


Figure 5.10 Induction of necrotic-like cell death of prostate cancer cell lines by a sub-lethal dose of succinylacetone (SA) in combination with hydrogen peroxide (H₂O₂).

Prostate cancer cell lines were seeded 24 hours prior to treatment with 50 μM SA. Cells left to grow for 5 days, treated with H₂O₂ (0-500 μM) and incubated for 24 hours before PI staining and flow cytometry analysis. Mean±1SD of at least three independent repeats. Two-way ANOVA (Sidak's comparison test), ns= not significant, *P < 0.05, **P < 0.01, ***P < 0.001, ****P < 0.0001.

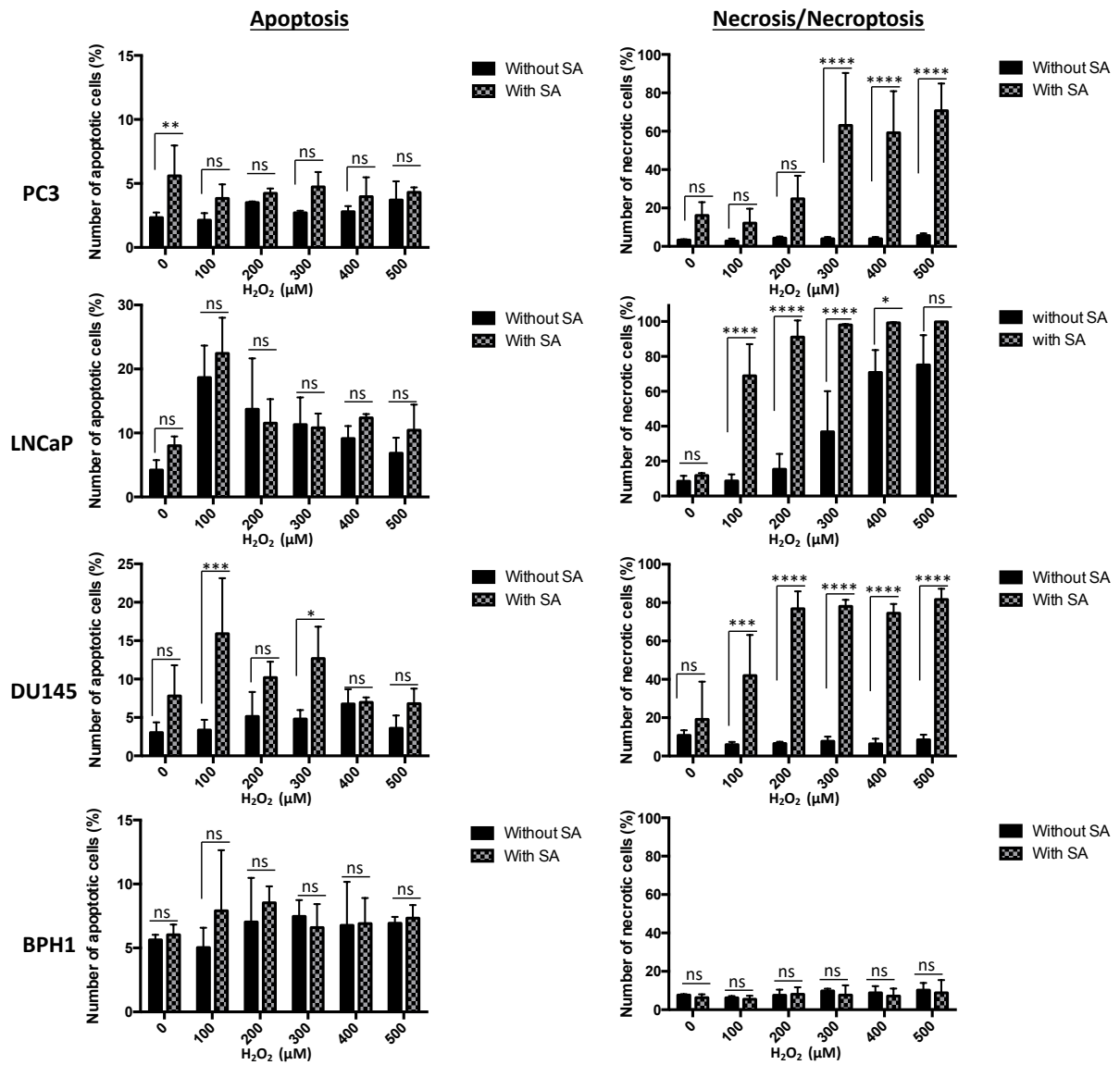


Figure 5.11 Induction of necrotic-like cell death of prostate cancer cell lines with a high dose of succinylacetone (SA) in combination with hydrogen peroxide (H₂O₂).

Prostate cancer cell lines and BPH1 cells were seeded 24 hours prior to treatment with 500 μM SA. Cells left to grow for 5 days, treated with H₂O₂ (0-500 μM) and incubated for 24 hours before PI staining and flow cytometry analysis. Mean±1SD of at least three independent repeats. Two-way ANOVA (Sidak's comparison test), ns= not significant, *P < 0.05, **P < 0.01, ***P < 0.001, ****P < 0.0001.

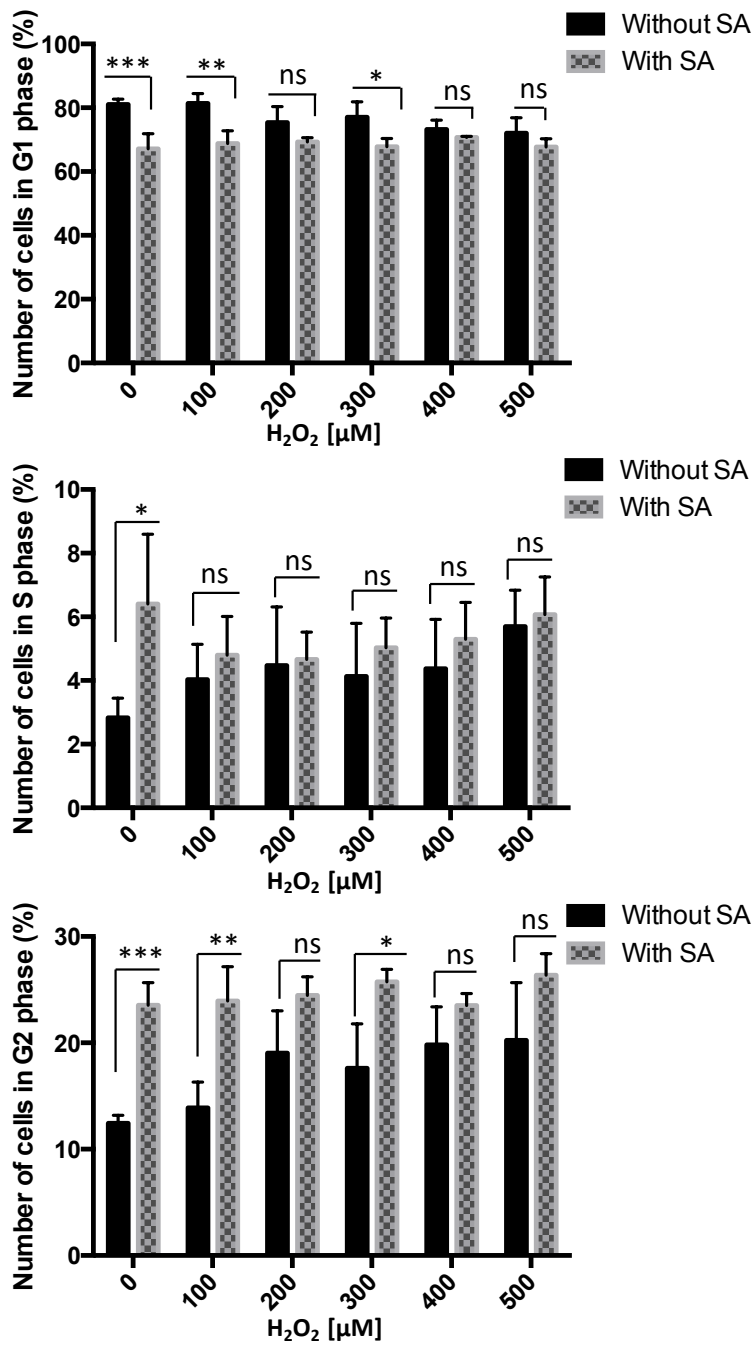


Figure 5.12 Cell cycle analysis of PC3 cells treated with succinylacetone (SA) and hydrogen peroxide (H₂O₂).

PC3 cells were treated with 50 μM SA and incubated for 5 days. H₂O₂ (0-500 μM) were added and the cells left for an additional 24 hours before they were harvested, fixed with 70% Ethanol, and PI stained. An Accuri C6 flow cytometer was used to read and analyse the samples and cells were gated to include only cells whilst debris was excluded. Cell cycle analysis included three independent repeats and data represents mean±1SD. Two-way ANOVA (Sidak's comparison test), ns= not significant, *P < 0.05, **P < 0.01, ***P < 0.001.

5.4.3 Succinylacetone induces caspase-independent cell death

The mechanism of cell death, activated in response to SA treatment, was further examined to test whether it is initiated through a caspase-independent process. ZVAD-FMK, a pan caspase inhibitor, was employed to investigate if cell death induced by SA was caspase dependent. Figure 5.13 demonstrated that ZVAD-FMK was unable to reverse the % of cells undergoing necrotic cell death following treatment with SA alone and SA+H₂O₂. This supports the hypothesis that cell death is via necrosis, which is known to be a caspase-independent mechanism of cell death (Golstein & Kroemer 2007; Ouyang et al. 2012).

Mitochondrial membrane potential (MMP) was also measured for SA alone and SA+H₂O₂ treated cells to determine if MMP is disrupted. In response to apoptotic signals, mitochondria lose membrane which coincides with release of cytochrome C, SMAC/Diablo and AIF into the cytosol apoptotic cascade (Ly et al. 2003). Therefore, loss of MMP is a hallmark of apoptotic cell death and applied as evidence for its occurrence. Cells were treated with SA, and on day 3 H₂O₂ was added and cells incubated for a further 24 hours. Cells were stained with 3,3'-dihexyloxycarbocyanine, DIOC(6)3, fluorescent dye which emits a green fluorescent signal when the molecule accumulates in the mitochondria. Disruption of MMP results in a drop in signal intensity (Mohr et al. 2008). Since loss of MMP is an early step in apoptosis, for this experiment, cells were harvested at an earlier timepoint to avoid complete cellular destruction. Figure 5.14 shows no decrease in the DIOC(6)3 signal upon the treatment with either only SA or SA+H₂O₂ in comparison with untreated control in all cell lines. This indicates that loss of MMP is not involved in SA± H₂O₂-induced death, and this supports my previous results demonstrating that cell death is via necrosis.

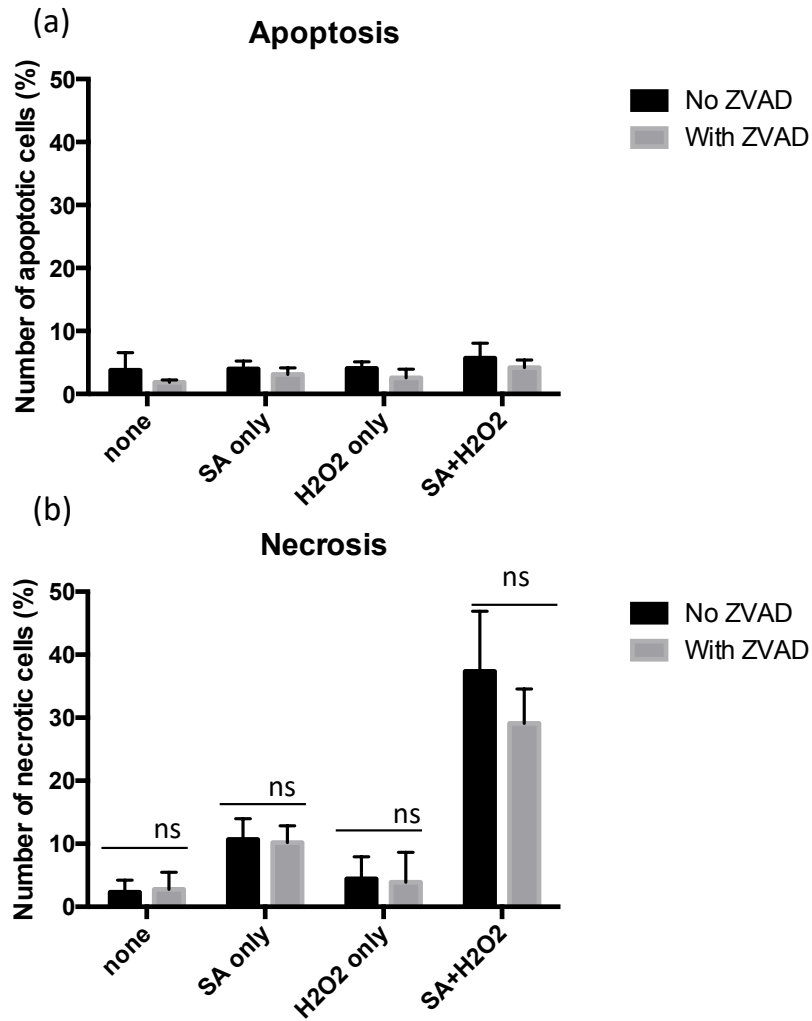
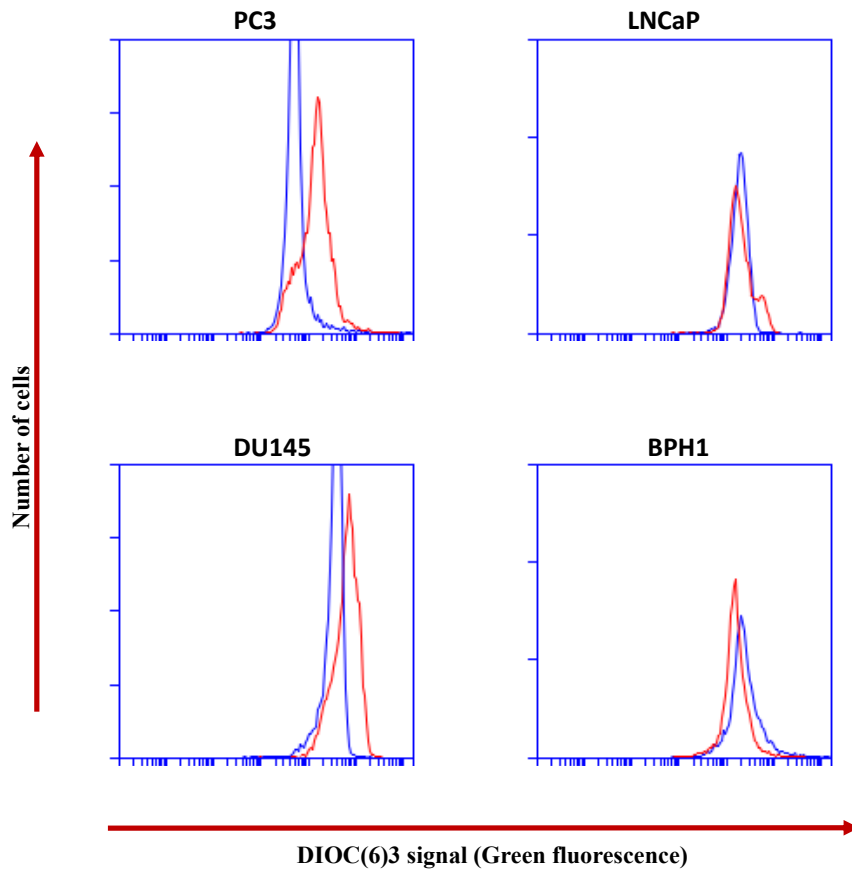


Figure 5.13 Succinylacetone (SA) and hydrogen peroxide (H₂O₂) promote caspase-independent cell death.

PC3 cells were treated with SA \pm H₂O₂ (500 μ M SA, 300 μ M H₂O₂) \pm 10 μ M the caspase inhibitor ZVAD and left 6 days prior to flow cytometric analysis. Flow cytometry analysis was performed using an Accuri C6 to evaluate the percentage of apoptotic and necrotic cells. Data presented are mean \pm 1SD of three independent repeats. Two-way ANOVA (Sidak's comparison test), ns= not significant; P-values > 0.05.

(a)



(b)

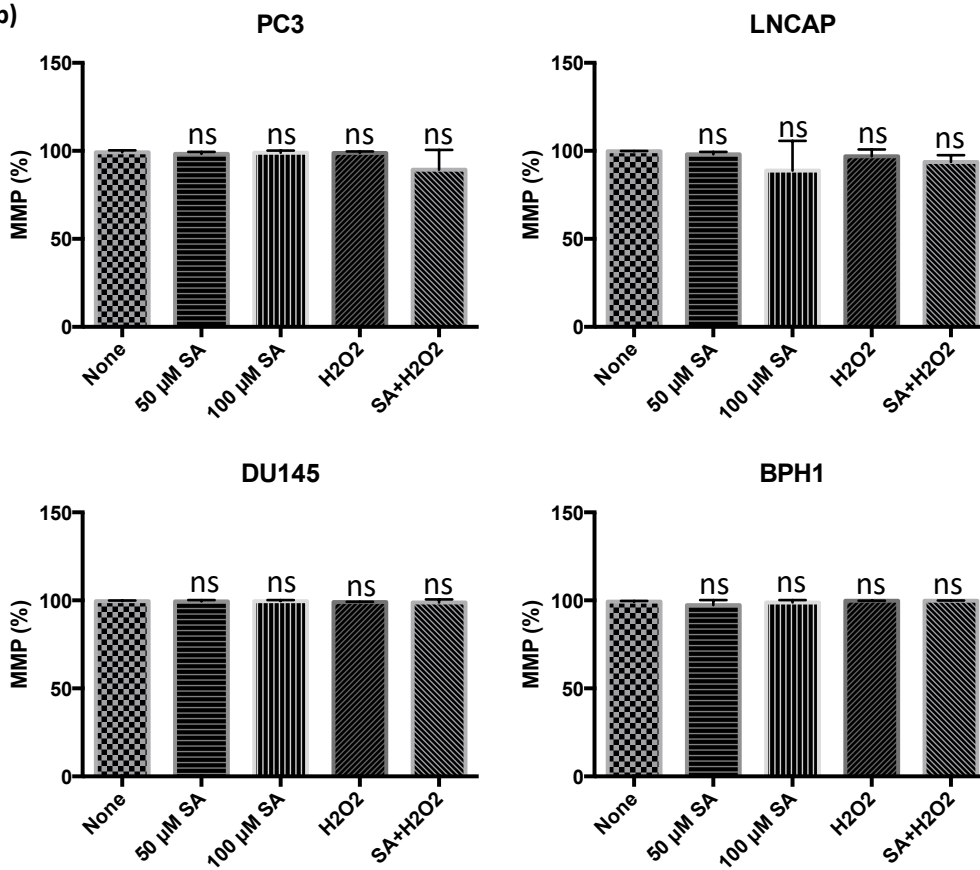


Figure 5.14 Analysis of mitochondrial membrane depolarization (MMD) of cells treated with succinylacetone (SA) and hydrogen peroxide (H₂O₂).

PC3, LNCaP, DU145, and BPH1 cells were treated with either 50 μM or 100 μM of SA and left 72 hours. On day 3, 300 μM H₂O₂ was applied to cells that has been treated with/without 50 μM SA and cells incubated for a further 24 hours. Cells were harvested, washed with PBS and resuspended in 1 ml of PBS containing the fluorescent dye DIOC(6)3. Cells were gated to exclude debris and for cells with a positive signal (green fluorescence). (a) Flow cytometric profiles show the detected DIOC(6)3 signal and the associated number of cells for control (blue) and SA+H₂O₂ treated cells (red). (b) Data is mean±1SD of three independent repeats. ANOVA (Dunnett's comparison test), ns= not significant.

5.4.4 Bleomycin shows no additive effect in combination with heme synthesis inhibition

As my results indicated that heme synthesis inhibition sensitizes PCa cells to ROS, I hypothesised that combining SA with drugs reported to induce ROS will further inhibit proliferation. Bleomycin sulfate (BLM) is a glycopeptide antibiotic produced by the fungus *Streptomyces Verticillus*, and has been clinically used as an anti-tumour drug against several cancers including head and neck cancer, Hodgkin lymphomas, and testicular cancer (Williams et al. 1987; Tobias et al. 2010; Meyer et al. 2012). This chemotherapeutic has been shown to induce apoptosis of other cancers' cells and suppress their growth, migration, and invasion partly as a result of ROS production. An example is the work of Liu and co-workers where they demonstrated that BLM promoted cell cycle arrest, induced cell death and inhibited the proliferation, migration and invasion capability of cell line models of gastric cancer (Liu et al. 2016).

BLM is activated through chelation with iron (FeII) and the following reaction with oxygen and free electrons to form activated bleomycin (ABLM), ferric hydroperoxide complex (BLM-Fe^{III}-OOH) which is the last detected complex before DNA cleavage onset (Burger et al. 1981; Hecht 1986; Chow et al. 2008). ABLM produces free radicals (ROS) which in turn breaks down the existing DNA and induces apoptosis (Wallach-Dayana et al. 2006). The mechanism of action of DNA scission by BLM action has been established *in vitro* by multiple groups (Suzuki et al. 1969; Müller et al. 1972; Caputo 1976; Hecht 1986; Stubbe & Kozarich 1987; Burger 1998). The fact that BLM utilises iron and oxygen species as well as its associated ROS release led me to propose that a joint action of this drug with heme biosynthesis inhibition might lead to enhanced anti-proliferative effects on PCa cells. Therefore, a dose treatment of BLM was applied to PC3 and BPH1 cells that were pre-treated with or without a low dose of SA (50 µM). The results showed that there is no additive effect induced by using BLM in

combination with SA, however, both reagents had an impact on proliferation separately (Figure 5.15). BLM showed a high cytotoxicity levels on both PC3 and BPH1 at concentrations as low as 0.5 nM and this was not altered by the presence and absence of SA.

5.4.5 Docetaxel shows no additive effect in combination with heme synthesis inhibition

Docetaxel forms the first-line treatment option for CRPC since it was approved by the FDA in 2004. This chemotherapy is associated with improved overall survival despite its cytotoxicity, limitations, and side effects (Hwang 2012). Docetaxel was also reported to induce ROS production through increasing phosphorylation of protein kinase C beta C (PKC β) and NADPH oxidase activity in human umbilical vein endothelial cells (HUVECs); which ultimately led to their dysfunction (Hung et al. 2015). Therefore, I examined whether combining a low dose of this agent with heme inhibition improves SA efficacy. PCa cell lines (PC3, LNCaP, and DU145) and BPH1 were treated with SA (0-1000 μ M) \pm 1 nM docetaxel. Cells were incubated for 6 days and proliferation assessed using crystal violet assays. Figure 5.16 demonstrates that docetaxel enhanced the cell death of all PCa cell lines, especially LNCaP, however an equal effect was seen in cells with or without heme synthesis inhibition. This means that no additive effect obtained of combining docetaxel to SA doses which might suggest that each of them inhibits PCa cell growth via unrelated mechanisms.

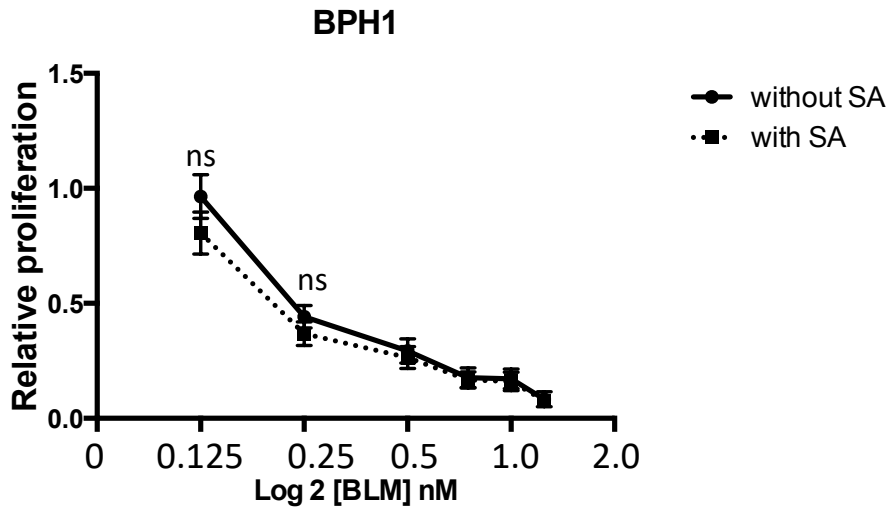
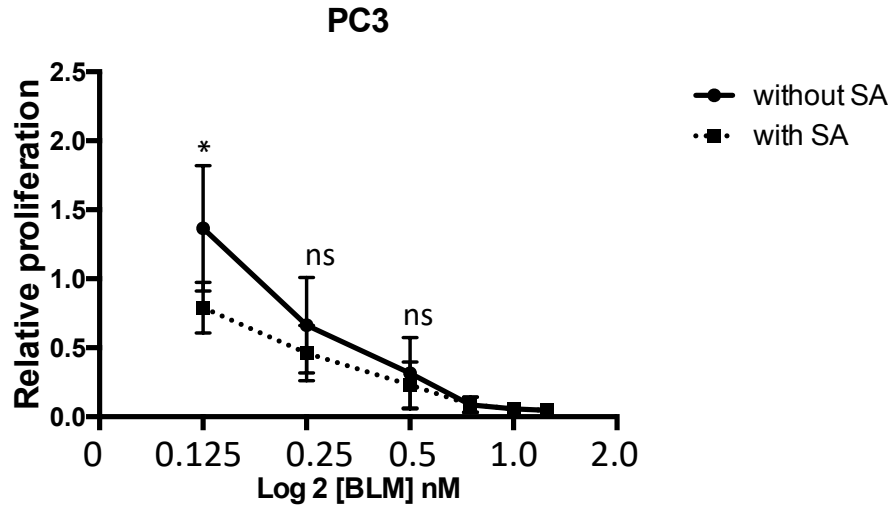


Figure 5.15 Induction of PC3 and BPH1 cell death by succinylacetone (SA) and bleomycin sulfate (BLM) combination.

Cells were treated with 50 μ M SA and BLM 24 hours post seeding. Cells were left to grow for 6 days before fixation and proliferation assessed using CV assays. Data plotted is mean \pm 1SD of three independent repeats. Two-way ANOVA (Sidak's comparison test), * $P < 0.05$, ns = not significant.

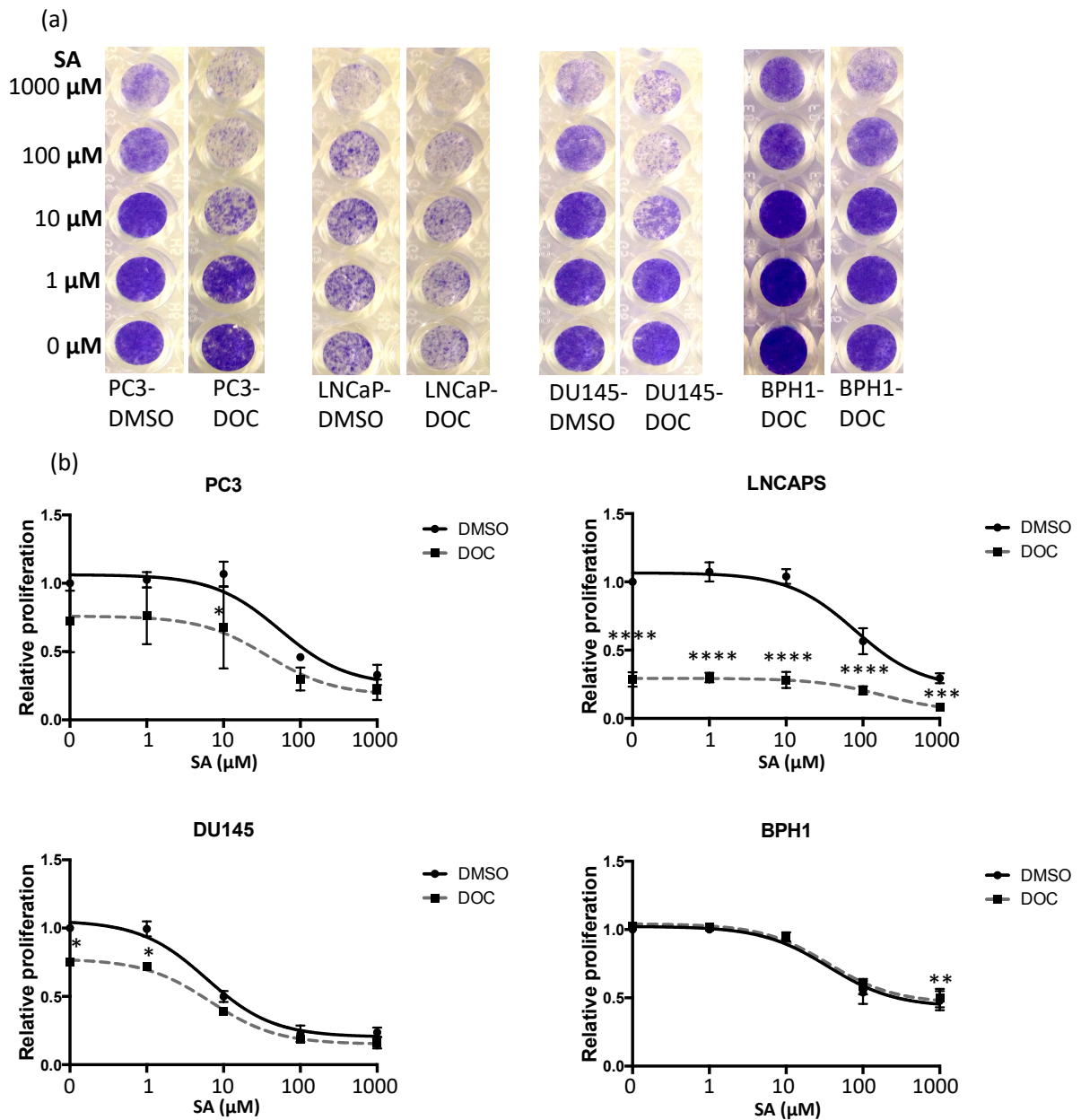


Figure 5.16 Docetaxel does not enhance the inhibitory action of Succinylacetone (SA).

Prostate cancer cell lines and BPH1 cells were seeded 24 hours prior to treatment with SA \pm 1 nM docetaxel. Cells were incubated for 6 days before proliferation was assessed using CV assays. (a) Representative images of CV stained cells, and (b) dose-response curves of PC3, LNCaP, DU145, and BPH1 \pm docetaxel. Data was normalized to untreated cells and is mean \pm 1SD of at least 3 independent repeats (each performed at least in triplicates). Two-way ANOVA (Sidak's comparison test), *P < 0.05, ***P < 0.001, ****P < 0.0001.

5.5 Discussion

5.5.1 *Heme biosynthesis inhibition impairs prostate cancer progression*

As mentioned previously, *de novo* heme biosynthesis is intensified in cancer cells and is believed to be implicated in the progression of cancers such as breast and lung (Navone et al. 1990; Hooda et al. 2013; Hooda et al. 2014; Hooda et al. 2015a). Therefore, I explored whether the inhibition of this pathway by SA would abrogate PCa progression. The results demonstrated that heme depletion by SA significantly reduced proliferation of PCa cells including PC3, DU145, and LNCaP (Figure 5.1) as well as halted PC3 cell migration (Figure 5.4 and Figure 5.5). However, heme-depletion from medium showed no enhancement of SA effect (Figure 5.3). This may suggest that *de novo* heme synthesis operates at intensified levels sufficient for PCa growth and survival regardless of the levels of extracellular heme.

The effect of SA was more significant in incubations longer than 72 hours. The latter could be explained by the postulation that the toxic effect of the inhibition of heme synthesis would eventually occur in cells as heme levels decline upon each cell division, hence the effects of heme deficiency, upon the administration of SA, occur according to the cell division speed so rapidly dividing cells or those with high intracellular heme turnover will show the effect earlier (Tschudy et al. 1983). Other studies on erythroleukemia observed similar results and the authors demonstrated that these effects could be reversed upon the addition of hematin (Tschudy et al. 1980). It has also been demonstrated that SA can be safely administered *in vivo* with minimum side-effects. For instance, a study on animal models bearing W256 tumours or Novikoff hepatoma demonstrated growth inhibition upon heme biosynthesis inhibition with no evident toxicity; the animals stayed healthy and active for 30-60 days regardless of the administration of SA (Tschudy et al. 1983).

The benign prostatic cell line BPH1 also exhibited a significant decrease in growth upon SA treatment (Figure 5.3). However, SA had a weaker effect on the proliferation of this line in

comparison to the cancer cell lines. SA led to a maximum 50 % inhibition of BPH1 proliferation at the highest concentration of SA compared to more than 70 % reduction in the PCa cell lines, PC3, DU145, and LNCaP. This suggests that PCa cells might possess more sensitivity to heme biosynthesis inhibition than noncancerous cells. This suggestion is consistent with previous data on non-small cell lung cancer (NSCLC), as demonstrated by Hooda et al. (2015), where heme synthesis inhibition by SA had more significant effects on the proliferation of HCC4017 cells (cancer cells) than HBEC30KT (normal cells). In addition, they found that oxygen-utilizing proteins such as cytoglobin and other hemoproteins levels are intensified in cancer cells compared to normal cells, and their levels declined significantly upon SA administration. Moreover, the rate of oxygen consumption was significantly higher in NSCLC cells than normal cells, and upon SA treatment oxygen consumption rates were considerably reduced and this effect was more severe in cancer cells compared to normal cells (Hooda et al. 2015a). These observations suggest that heme biosynthesis pathway is an essential metabolic pathway for cancer cells and could be a valid axis to develop novel drugs and approaches to inhibit PCa progression.

5.5.2 Intracellular heme depletion induces necrotic-like cell death

Cell death is an important mechanism for different biological events like morphogenesis, maintenance of homeostasis, and removal of harmful cells in normal tissues (Arakawa et al. 2015). This process could be induced by several regulated cell death (RCD) pathways such as apoptosis, autophagy, and regulated necrosis or recently as ‘necroptosis’ (Ashkenazi & Salvesen 2014; Ouyang et al. 2012; Tait et al. 2014). Recent accumulating evidence suggests that programmed cell death is largely associated with anti-cancer therapies and closely related to drug resistance (Sun & Peng 2009). In cancer tissues, cell death pathways, especially apoptosis, are largely distorted to facilitate uncontrolled growth and survival of cancer cells (Gerl & Vaux 2004; Su et al. 2015; Labi & Erlacher 2015). To

further assess the mechanism of cell death initiated in response to heme biosynthesis inhibition, the levels of apoptosis and necrosis were accessed. Results indicated that SA induced a G2/M arrest and resulted in apoptotic (at high concentration of SA) and necrotic-like cell death (Figure 5.6).

The occurrence of both necrosis-like cell death and apoptosis in prostate cancer cells upon SA administration may suggest that these pathways are interconnected. The interconnection between cell death pathways has been previously suggested (Conrad et al. 2016), and may be explained by TNF-induced cell death. TNF-induced cell death can induce apoptosis, through the activation of caspase-8 and other downstream proteases, or promote non-apoptotic cell death (necroptosis) upon caspase-8 failure or inhibition (Laster et al. 1988). The presence of necrotic-like cell death in response to heme biosynthesis inhibition further suggest that the cells are more sensitive to ROS damage because ROS is believed to be closely related to the initiation of necrosis (Morgan et al. 2008). Further, due to the attenuation of heme biosynthesis, intracellular iron (Fe^{+2}) may accumulate to a lethal level leading to iron-dependent ROS formation (Cao & Dixon 2016; Yang & Stockwell 2016; Altman et al. 2016). This accumulation was not reported before in cancer cells upon SA addition, however, it was demonstrated that heme biosynthesis-related alterations in autosomal anaemic conditions is associated with intracellular iron overload. For example, the sideroblastic anaemias are characterized by reduced heme biosynthesis and increased mitochondrial and cytoplasmic iron levels that leads to arrested differentiation in erythroid cells (Nakajima et al. 1999; Chiabrando et al. 2014). In addition, SA was utilized to artificially boost the cytosolic iron levels in erythroblasts differentiation studies (Schranzhofer et al. 2006). Iron is able to induce signalling pathways associated with cell death and survival as it is redox-active and hence it can form reactive oxygen species (ROS) (Figure 5.17), resulting in oxidative stress and cell death initiation (Bogdan et al. 2016).

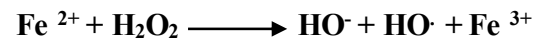


Figure 5.17 The formation of ROS species upon Fe^{+2} and hydrogen peroxide (H_2O_2) reaction (Fenton reaction).

Iron is a redox-active and hence it can form hydroxyl radicals ($\text{OH}\cdot$) and hydroxyl anion (OH^-) when it reacts with H_2O_2 , resulting in oxidative stress and cell death initiation. Adapted from: (Kalinowski & Richardson 2005)

The accumulation of cellular iron is suggested to induce a form of cell death that is distinct from apoptosis and necroptosis and is called ferroptosis (Morgan et al. 2008; Dixon et al. 2012; Bogdan et al. 2016). Ferroptosis [ferro, ‘ferrous ion’ (Fe^{2+}); ptosis, ‘fall’] means the damage caused by iron overload, with cellular iron essential to this regulated form of oxidative cell death (Yang & Stockwell 2016). This form of cell death might have occurred in PCa cell lines upon SA administration, because SA would prevent the use of ferrous iron to synthesise heme, so intracellular iron accumulation is proposed (Figure 5.18). Ferroptosis occurs as explained by recent studies on the basis of the accumulation of iron-dependent lipid-ROS (or lipid peroxidation) which can be normally alleviated by antioxidants such as iron chelators and/or glutathione peroxidase (GPX4) (Figure 5.18) (Cao & Dixon 2016). The latter have been directly linked to the process of ferroptosis, as the inhibition of GPX4 by system- X_c^- (glutamate-cystine antiporter) manipulations through cysteine depletion through the use of erastin or other glutathione synthesis inhibitors (e.g. RSL3) also induce this form of cell death (Bogdan et al. 2016; Cao & Dixon 2016; Yang & Stockwell 2016; Dixon et al. 2012). Further, cancers with distorted system- X_c^- have been reported to be more susceptible to ferroptosis. For instance, the growth of B cell lymphoma with reduced expression of SLC7A11 (a subunit in system- X_c^-) was abrogated by sulfasalazine (a system X_c^- inhibitor) (Yang & Stockwell 2016). Furthermore, *SLC7A11* expression was demonstrated to be repressed by *TP53* resulting in ferroptosis induction (Jiang et al. 2015). These insights suggest that ferroptosis is highly implicated in cell death and survival signalling pathways. However, it remains not evident whether ferroptosis is induced in response to heme synthesis inhibition. Experiments utilising the ferroptosis inhibitor ferrostatin-1 would clarify this (Dixon et al. 2012).

As mentioned, ROS is believed to induce necrotic cell death. For instance, accumulated ROS can induce necrosis in response to metabolic stress and antioxidants can shift the mechanism of cell death from necrosis to apoptosis (Lim et al. 2009). The latter might explain

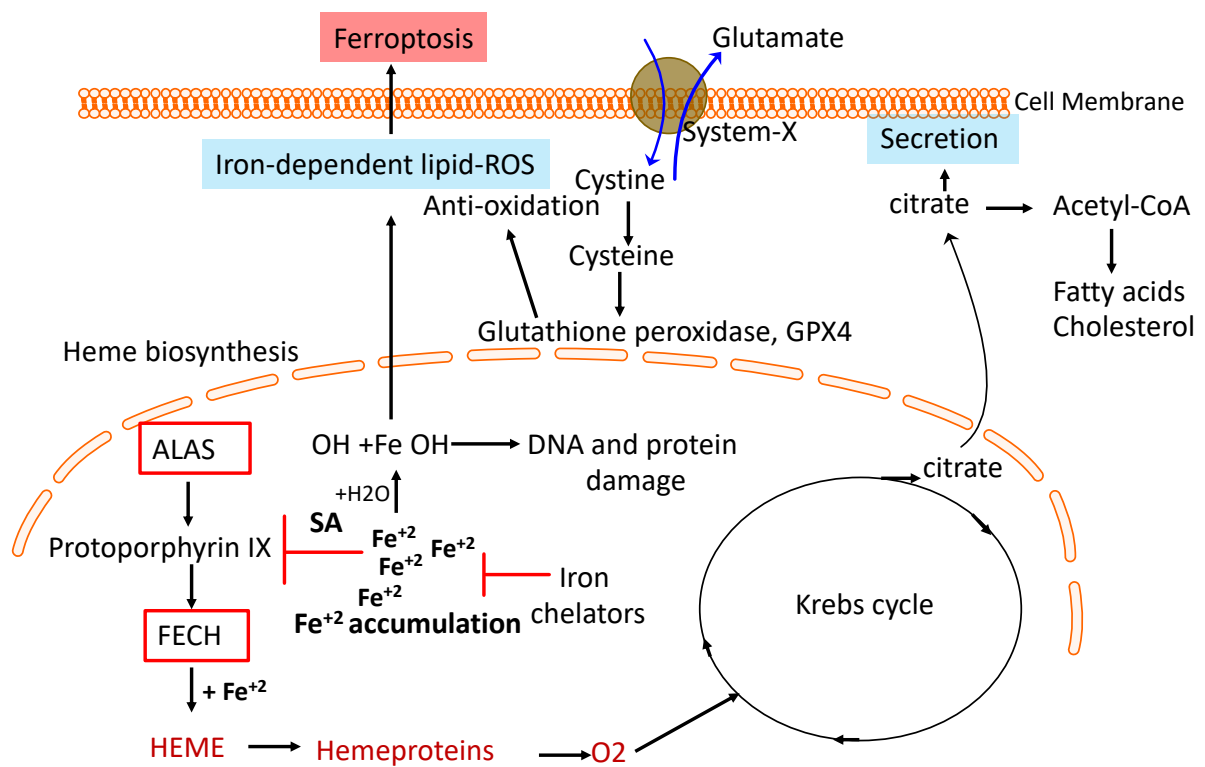


Figure 5.18 The proposed accumulation of iron due to SA inhibition of heme biosynthesis leads to accumulation of lipid-ROS and cell death by ferroptosis.

SA inhibits heme biosynthesis, which leads to the accumulation of ferrous iron (Fe^{+2}). The excess Fe^{+2} generates ROS (Fe OH) resulting in lipid peroxidation, and DNA and protein damage leading to cell death. Iron chelators and glutathione peroxidase (GPX4) reduce this effect in unstressed cells by detoxification. The process is suggested to occur due to the imbalance between iron-dependent lipid-ROS accumulation and antioxidant enzymes in prostate cancer cells.

why SA treatment induced a mixture of apoptosis and necrosis; heme biosynthesis impairment would gradually reduce heme and then steadily increase the intracellular iron amounts. Therefore, apoptosis might switch into necroptosis or ferroptosis as ROS increases. In addition to the lipid peroxidation, iron-dependant ROS might also cause DNA and protein damage leading to genome instability and cell death (Jiang et al. 2015).

5.5.3 H₂O₂ treatment of heme biosynthesis-inhibited prostate cancer cells further halted proliferation

Caspase-independent cell death has been proposed as a mechanisms to eradicate tumour cells that have established strategies to escape apoptosis (Festjens et al. 2006). Cell death by necrotic-like or other non-apoptotic pathways may form a valid strategy to overcome therapy resistance; which occur mainly through apoptotic escape and evading the immune system in malignant cells (Vinay et al. 2015). However, it is argued that necrotic cell death enhances tumour progression by inflammation and angiogenesis and correlates with poor prognosis (Vakkila & Lotze 2004; Demirag et al. 2005; Minardi et al. 2008). On the other hand, the inflammatory nature of such pathways, upon the direct release of the cellular content into the extracellular matrix, could induce the immune system to react against cancer cells and kill them (Bullough 2010).

H₂O₂ was used in this work as a method to enhance oxidative damage. H₂O₂ was applied to heme biosynthesis inhibited PCa cells, and as expected, this strategy significantly enhanced the inhibition of proliferation compared to that induced by SA only. This effect was significant using both low (50 µM) and high (500 µM) concentrations of SA (Figure 5.8 and Figure 5.9). Interestingly, the impairment of the heme metabolic cascade did not sensitize the noncancerous cells (BPH1) to H₂O₂. This might suggest that heme biosynthesis is specifically critical for prostate cancer cell survival and protection against ROS.

Some detoxification and redox status-implicated factors such as NOS3 (produces the free radical NO; that might have a dual function in inducing growth and cell death) and GCLIC (that is implicated in glutathione synthesis, an antioxidant) were found to be critical for PCa cells as siRNA knockdown of these factors halted tumour progression. In addition, normal or noncancerous cells (BPH1) might still have their ROS-regulatory signaling pathways and antioxidants defense system unmodified and functioning normally to remove any excess iron-ROS induced by SA treatment. Therefore, non-cancerous cells like BPH1 might still be able to maintain a balanced redox-status even in the presence of elevated ROS.

The specificity of SA+H₂O₂ in PCa cells highlights a potential therapeutic window. PCa cells appear to be more prone to SA-induced ROS damage because levels of ROS are known to be elevated in PCa and is known to promote an aggressiveness phenotype (Wang et al. 2018). This was supported by previous work by Kumar et al. (2008) where ROS levels were found to be specifically elevated in PC3, DU145, and LNCaP cells compared to normal prostate cell lines. They also found that the inhibition of the Nox system or extra-mitochondrial ROS production halted the aggressiveness of these cells (Kumar et al. 2008). ROS elevation in tumour cells is oncogenic and generally linked to the apoptotic signalling impairment, induction of cell cycle progression and proliferation, cell to cell adhesion, angiogenesis, migration, morphological features of cells, and metabolic alterations (Liou & Storz 2010). However, ROS levels need to remain within certain limits, since further elevation of ROS will result in oxidative stress and cell death. The latter approach has been translated into radiation therapy for the treatment of metastatic PCa (Haimovitz-Friedman 1998; Freitas et al. 2012). This was also supported by our findings that the down-regulation of a glutathione synthesis implicated factor (GCLC) inhibited prostate cancer progression (Chapter 3). In addition, to glutathione, other antioxidants like metallothionein, a cysteine-rich and heavy metal-binding protein that plays an essential role in maintaining metals homeostasis and toxic metals detoxification

(Ruttikay-Nedecky et al. 2013), were found to be upregulated in metastatic prostate cancer cells (Suzuki et al. 2000). This might further suggest that targeting glutathione and other detoxification factors might overcome resistance to such therapies.

5.5.4 *H₂O₂ enhances SA-induced caspase-independent cell death*

Succinylacetone exerted a dose-dependent cytotoxic effect across all PCa cell lines. Importantly, SA sensitized PCa cells, but not noncancerous control cells, to H₂O₂. Therefore, further investigations were undertaken to analyse the cell death mechanism induced following these treatments. The administration of H₂O₂ doses in addition to low or high doses of SA demonstrated a dose-dependent increase in the necrotic-like cell population, while H₂O₂ alone demonstrated no significant increase in the number of necrotic cells in almost all cells (Figure 5.10 and Figure 5.11). No evidence of apoptosis was found in response to these treatments. Interestingly, BPH1 cells were resistant to the combined treatment and no increase in apoptosis or necrosis was evident.

Low or sub-lethal levels of ROS have been reported to induce cellular senescence rather than apoptosis in normal fibroblast and lung cancer cells (Chen & Ames 1994; Yoshizaki et al. 2009). Therefore, it is suggested that the level of oxidative stress determines the cell fate to induce apoptosis, necrosis or growth arrest (Baigi et al. 2008). This was demonstrated by a previous work by Gardner et al. (1997) using the murine L929 fibroblast cell line. The group demonstrated that H₂O₂ concentrations of more than 10 mM induced necrotic cell death, while exposing cells to concentrations of less than 10 mM stimulated apoptotic cell death. They also showed that the apoptosis stimulated by 0.1-0.5 mM of H₂O₂ could be halted by BCL-2 overexpression but the latter had no effect when higher concentrations of H₂O₂ were applied (Gardner et al. 1997). It should be noted that these concentrations are significantly higher than the concentrations used in this study.

Cell death upon treatment of SA with or without H₂O₂ did not involve a loss of mitochondrial potential. This was evidenced by the unchanged mitochondrial membrane potential upon heme biosynthesis inhibition and H₂O₂ administration (Figure 5.14). Further, cell death was also suggested to be caspase-independent since the pan-caspase inhibitor FMK-ZVAD did not block cell death induced by these treatments (Figure 5.13). This further supports the hypothesis that inhibition of heme biosynthesis ± H₂O₂ promotes cell death via a necrotic-like mechanism.

5.5.5 Chemotherapeutic treatments did not enhance the efficacy of heme biosynthesis inhibition in prostate cancer cells

As chemotherapeutic often promote cell death in part via ROS production, I investigated if combining heme depletion with chemotherapeutics, specifically docetaxel and the DNA-damaging agent bleomycin (BLM), will enhance efficacy. Results demonstrated that no additive effect was obtained by these compounds. This might be explained by the fact that these drugs do not function primarily as inducers of ROS and instead promote cell death by alternative mechanisms. The mode of action of docetaxel depends on two major mechanisms; the first is the attenuation of microtubule depolarisation leading to G2/M cell arrest, and the second effect is its inhibition of bcl-2 and bcl-xL gene expression which results in the induction of apoptosis (Pienta 2001).

The addition of BLM to SA treated cells also failed to enhance toxicity (Figure 5.15). The action of this agent is argued to be ROS-dependant DNA damage-related. This drug is activated upon the presence of DNA, its chelating iron forms an oxygenated-iron complex (BLM-Fe^{III}-OOH) which interacts with DNA, promoting degradation (Burger et al. 1981; Hecht 1986; Chow et al. 2008). BLM-promoted DNA damage is likely to induce *TP53* activity and subsequent release of mitochondrial cell death factors. This mechanism of cell death

therefore differs to that induced by SA and may explain why these therapeutics do not have an additive effect.

As mentioned previously, cell death induced by SA and H₂O₂ may be as a result of lipid peroxidation. Peroxidation of lipids including unsaturated phospholipids, glycolipids, and cholesterol can be stimulated by free radical species (oxyl radicals, peroxy radicals, and hydroxyl radicals) as a result of iron-associated reduction of H₂O₂ or the non-radical species such as singlet oxygen, ozone, and peroxynitrite that are usually formed by superoxide and the nitric oxide reaction (Girotti 1998). It is explained by Trachootham et al. (2008) that lipid radicals, produced as a result of lipid peroxidation, could consequently damage additional lipid molecules, therefore inducing a chain reaction. This chain-reaction includes three stages: initiation, propagation, and termination (Trachootham et al. 2008). Trachootham et al. (2008) added that radicals react on different positions present on the unsaturated fatty acid residues of the phospholipid. The action can occur at one end of the fatty acid residue or at an internal position, leading to the generation of a peroxy radicals. The damage at internal positions can further facilitate the cyclisation of peroxy radicals resulting in the formation of reactive alkoxy radicals. The fatty acid can subsequently generate a hydroperoxide or experience further cyclisation resulting in the formation of aldehydes, including malondialdehyde (MDA) and 4-hydroxy-2-nonenal (HNE) (Trachootham et al. 2008). MDA and HNE can then promote DNA damage and HNE has also been shown to lead to protein damage, leading to the impairment of various signalling pathways (Vasilaki & McMillan 2011).

5.5.6 Summary

In this chapter it was shown that heme biosynthesis inhibition abrogated PCa cells progression and demonstrated less toxic effect on noncancerous cells. The cell death induced, following heme synthesis inhibition, is mitochondrial- and caspase-independent and proposed to be ferroptosis (Yang & Stockwell 2016). Ferroptosis is suggested to occur upon the

accumulation of high levels of intracellular iron (Dixon et al. 2012; Cao & Dixon 2016; Bogdan et al. 2016; Altman et al. 2016), that I suggested to occur upon heme synthesis inhibition. Iron radicals are largely associated with lipid peroxidation and membrane damage, but DNA and proteins damage has also been described. The additive toxicity of H₂O₂ to heme biosynthesis inhibition was only evident in the cancerous cell lines. This specificity demonstrates that targeting heme synthesis could be a novel targeted approach for CRPC.

6 Chapter 6 Final Discussion

6.1 Metabolic features of prostate cancer in relation to screening outcomes

Most solid tumours lack sufficient oxygen and nutrients leading them to generate in a hypoxic, nutrient-poor microenvironment (Saggar et al. 2013). These conditions cause cancer cells to adapt leading to metabolic reprogramming. This reprogramming results in alterations in pathways associated with key metabolic factors and redox homeostasis related factors (Cutruzzolà et al. 2017). The normal prostate gland exhibits specific metabolic features that cannot be found in other types of cells; prostate epithelial cells accumulate and produce citrate upon the accumulation of zinc and exhibit lower rates of oxidative phosphorylation for energy production (Zadra et al. 2013). Further, prostate epithelial cells rely on aerobic glycolysis, rather than aerobic oxidation, as a main resource of the ATP production (Wu et al. 2014). Interestingly, these secretory cells are found in the peripheral zone where prostate cancer mostly occurs (Costello et al. 2005).

Changes accompanied with the transformation of prostatic epithelial cells include a shift to citrate-oxidising cells associated with halted Zn accumulation and elevated oxygen consumption (Figure 6.1). Further, citrate re-enters the TCA cycle to produce ATP and is utilized in lipid synthesis instead of being secreted (Costello et al. 2004; Franklin et al. 2005; Franklin et al. 2005; Costello & Franklin 2006; Dakubo et al. 2006; Eidelman et al. 2017). Citrate formation through the glycolytic pathway probably remains constitutively active in cancer cells facilitating uncontrolled proliferation (Cutruzzolà et al. 2017).

In addition to the alterations in citrate-zinc metabolism, other metabolic differences have been described in PCa. For example, PCa appears to rely on citrate oxidation for ATP and macromolecule production rather than Warburg effect or increased glycolysis rates through the lactic acid pathway; however, elevated glycolysis might appear in late stages of PCa

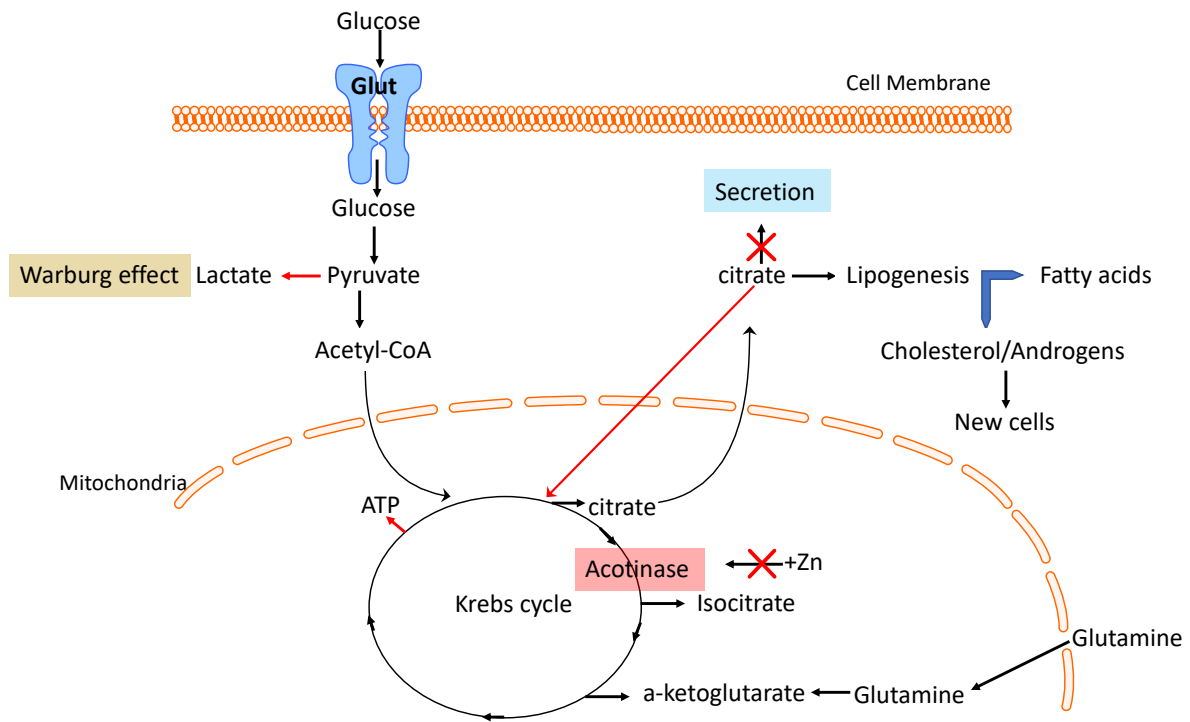


Figure 6.1 The alterations of citrate metabolism in prostate cancer cells.

Cells switch from zinc-accumulating, citrate-producing to citrate-oxidising that reactivates the Krebs cycle production of ATP. The lack of Zn accumulation leads to the reactivation of Acotinase which converts citrate to isocitrate, facilitating the completion of the TCA cycle and ATP generation.

(Eidelman et al. 2017). The general specificity of cancer cell metabolism and the unique metabolic features present in prostate cells makes targeting of metabolism a potential therapeutic option for the disease.

In this study, a screen targeting 217 metabolic and cell traffic factors was performed. The screen results depended on the phenotypic changes (proliferation and migration) upon the knockdown of different metabolic factors using siRNA. Three siRNAs were used individually against each target to reduce the risks of off-target effects/ineffective siRNA. The screen identified several factors that have already been proposed as drug targets and biomarkers for prostatic and other cancer progression (Baron et al. 2004; Ettinger et al. 2004; Notarnicola et al. 2004; Brusselmans et al. 2005; Chajès et al. 2006; Ory et al. 2008; Yoshii et al. 2013; Burdelski et al. 2015; Wang et al. 2015; Abate et al. 2017). Those included FASN, FDPS, ACACA, and TYMS. The identification of such factors is validation of the screening approach applied. Other identified factors including STXA1, FKBP11, FKBP9, GCLC, GART, MARS, GCAT, UROS, FECH, LLGL2, HAS3, and NOS3 have also been demonstrated to be important for the progression of PCa and/or other types of cancer (Beardsley et al. 1989; Bailey et al. 1992; Liu et al. 2001; Endo-Munoz et al. 2010; Pearson et al. 2011; Romano et al. 2011; Jain et al. 2012; Burke et al. 2013; Hooda et al. 2015; Hooda et al. 2013; Lin et al. 2013; Amelio et al. 2014; Cong et al. 2014; Fernández-Nogueira et al. 2015; Ulloa et al. 2015; Yang et al. 2015; Vahora et al. 2016; Kim et al. 2017). In addition, the screen identified new targets that have not previously been linked to cancer progression, including OTOP3, ACSM1, PAFAH2, LARS2, SLC27A1 and SLC27A5.

Several factors including FASN, FDPS, ACSM1, and ACACA function in lipogenesis signalling (Chakravarty et al. 2004; Buhaescu & Izzedine 2007; Mashek et al. 2007; Wang et al. 2009; Wang et al. 2010; Currie et al. 2013; Tsoumpra et al. 2015). Normal cells rely on the

uptake of exogenous fatty acids coming from diet as opposed to malignant cells that utilise endogenous biosynthesis of lipids (Wang et al. 2015). Lipogenesis is known to be deregulated in PCa and has hence been proposed as a novel therapeutic approach to selectively target cancer cells (Liang & Mulholland 2014). It is likely that lipogenesis enzymes are up-regulated in PCa to facilitate the shift from citrate-accumulation to citrate-utilisation, promoting acetyl-CoA production and the subsequent fatty acid and cholesterol biosynthesis. This hypothesis that lipogenesis is important for PCa proliferation is supported by the findings in this study that demonstrated that siRNA depletion of lipogenic factors (FASN, FDPS, ACSM1, and ACACA) halted proliferation (Chapter 3). These observations are consistent with previous studies which showed that the *in vitro* and *in vivo* down-regulation of lipogenic factors abrogates the progression of PCa (as reviewed in (Swinnen et al. 2004)).

It is indicated that factors like FDPS and FASN, and probably other lipogenesis factors, are downstream of sterol response element-binding proteins (SREBPs), which are controlled by androgen signalling. Androgen signalling therefore at least in part, regulates cholesterol and fatty acid synthesis in PCa (Ettinger et al. 2004). Lipogenesis is predominantly controlled via a feedback regulatory system mediated by SREBP transcription factors. These factors are found bound to the membranes of the endoplasmic reticulum in their inactive state and when cholesterol and fatty acids levels decrease SREBPs become active upon androgen signalling, are released from membranes and travel to the nucleus to stimulate transcription of target genes necessary for lipid synthesis and uptake (Ye & DeBose-Boyd 2011). Interestingly, SREBP transcription factors have been demonstrated to be constitutively activated in CRPC and lose their androgen dependency (Ettinger et al. 2004), and hence continued lipogenesis and the accumulation of fatty acids have been reported and regarded as hallmarks of prostatic malignancy (Ettinger et al. 2004; Swinnen, Esquenet, et al. 1997; Swinnen, Ulrix, et al. 1997).

Other factors, identified in the screen to regulate PCa proliferation, are also known to be important in fatty acid synthesis and signalling. These included ACACA, which is a lipogenesis factor that converts acetyl-CoA to the fatty acid substrate malonyl-CoA (Currie et al. 2013; Wang et al. 2010; Wang et al. 2009), and ACSM1 that is believed to be implicated in the bio-activation of fatty acids as an essential step in lipid metabolism (Mashek et al. 2007). In addition, the screening picked transporter proteins such as SLC27A1/5 that have been implicated in fatty acid uptake and transport. These findings, taken together with previous studies linking lipogenesis with androgen signalling and CRPC (Eidelman et al. 2017) suggest that targeting lipogenesis and fatty acid synthesis might be a valid axis for the development of novel therapeutic approaches to control CRPC.

In this study, few metabolic targets involved in glycolysis were found to affect proliferation or motility. The exception was Aldolase A (ALDOA), with depletion of this enzyme found to decrease proliferation and motility. The function of ALDOA is well established; it catalyses the conversion of fructose 1,6-bisphosphate into glyceraldehyde 3-phosphate and dihydroxyacetone phosphate (Kajita et al. 2001; Du et al. 2014). However, to date, no work has linked ALDOA to PCa. ALDOA might be elevated in cancer tissues to favour the upregulation of the glycolytic pathway and this warrants further investigation. In support of this, ALDOA has been identified as a novel biomarker for colorectal cancer because it was found to be highly expressed in cancer tissue samples (Yamamoto et al. 2016). Further, serum levels of ALDOA were also found to be increased in patients with lung and renal cancers (Asaka et al. 1994; Takashi et al. 1992).

Some studies have suggested that ALDOA can enhance cancer progression through non-glycolytic pathways in addition to its role in glyceraldehyde 3-phosphate production. ALDOA was reported to interact with factors that are not related to glycolysis such as the cytoskeletal proteins F-actin and tubulin (Arnold & Pette 1970; Volker & Knull 1997). In

addition, recent work demonstrated that ALDOA expression is positively correlated with increased canonical Wnt signalling (Caspi et al. 2014). Therefore, the molecular regulation of ALDOA signalling and its exact roles in cancer are still unclear and needs to be further elucidated.

In addition to lipogenesis and glycolysis, the screening identified several other pathways essential for cell proliferation/motility. These included the heme-biosynthesis pathway (UROS and FECH), amino acids and protein biosynthesis (GCAT, MARS, and LASR2), nucleic acids biosynthesis, (TYMS and GART) and factors important in the regulation of free radicals and redox status (NOS3 and GCLC). Additional experiments to validate and characterise these targets are needed. Further, elucidating the signalling functions of the identified targets might help further our understanding of the complex signalling pathways associated with metabolic alterations in PCa.

6.2 Inhibition of heme biosynthesis in combination with elevated oxidative stress as a novel approach to treat prostate cancer

The highly significant effect of UROS depletion upon cells, and the lack of knowledge of heme-biosynthesis in PCa, were the reasons that this pathway was investigated further. Heme biosynthesis inhibition has been investigated in other tumour types, including lung cancer. For example, the reduction of heme levels in response to SA resulted in significant inhibition of lung cancer progression and was associated with a reduction in oxygen consumption and in the levels of hemoproteins (Hooda et al. 2013; Hooda et al. 2015a).

Heme biosynthesis inhibition was therefore further investigated in PCa cell lines and BPH1, a noncancerous cell line. Inhibition of heme synthesis using SA led to a dose-dependent inhibition of prostate cancer cell proliferation (Figure 5.1 and 5.3) and also considerably inhibited migration of PC3 cells (Figure 5.4 and 5.5). The relation of heme-biosynthesis

inhibition to iron-overload and the subsequent iron-ROS production (Schranzhofer et al. 2006; Altman et al. 2016; Bogdan et al. 2016; Cao & Dixon 2016; Yang & Stockwell 2016) led to the hypothesis that increasing H₂O₂ levels would further enhance the oxidative stress upon cancer cells and subsequently cell death will be further promoted through ROS accumulation. This approach selectively promoted cell death in the PCa cells, but not the noncancerous cells (Figure 5.6 and 5.7).

Inhibition of heme synthesis was found to promote caspase-independent cell death. This is of particular importance, because recent work has demonstrated that cell death induced via this mechanism can enhance tumour clearance due to engagement of the hosts immune system (Giampazolias et al. 2017). It could be proposed that necrotic-like cell death of some cells upon SA administration will lead to loss of membrane integrity and release of cytosolic content with inflammatory molecules such as high mobility group box 1 (HMGB1). This will promote inflammation and result in the upregulation of NF- κ B, p38 mitogen activated protein kinase (MAPK) pathways and the elevated secretion of pro-inflammatory cytokines (Lim et al. 2009). The damage signals (cytokines) will induce T-Cell Receptor (TCR) signalling, promoting the infiltration of all types of immune/inflammatory cells to the tumour microenvironment (Chen et al. 2016).

Activated immune cells such as macrophages and neutrophils will produce high levels of ROS as a defense mechanism to kill cancer cells (Liou & Storz 2010). This ROS is mainly made through the phagocytic form of NADPH oxidase (Nox2) (Morgan *et al.*, 2008). This burst of superoxide formation by immune cells will result in ROS formation involving hydroxyl radicals and peroxynitrite radicals (ONOO⁻) (Liou & Storz 2010; Segal & Shatwell 1997). Therefore, accumulation of ROS in tumour microenvironment will follow which will lead to further cellular stress and a second wave of cell death after SA administration (Figure 6.2).

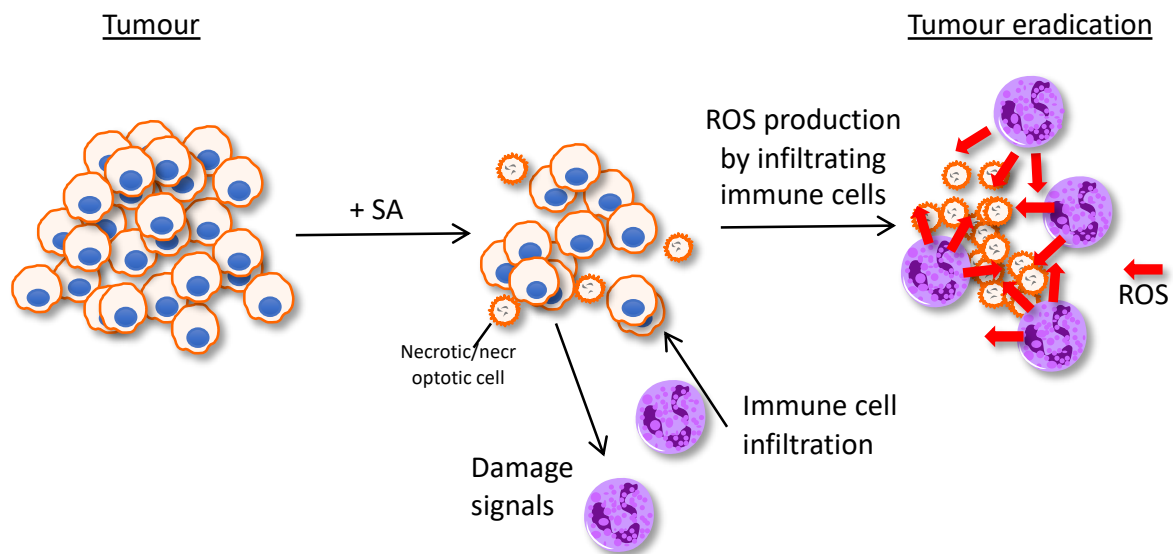


Figure 6.2 Schematic representation of the necrosis/necroptosis feed-forward mechanism.

Treatment of tumours with the heme synthesis inhibitor succinylacetone (SA) will promote necrosis/necroptosis in some cells. These cells will release damage signals (cytokines), which will promote immune cell infiltration. The infiltrating immune cells, such as neutrophils, will produce ROS leading to ROS accumulation in the microenvironment. The remaining tumour cells are sensitive to ROS damage as a result of the SA treatment and therefore a second wave of cell death is initiated, enhancing tumour death.

It is possible that immune check-point regulators could be stimulated shortly after T-cell activation through the interaction of receptors expressed on the surface of T-cells with inhibitory ligands found on malignant cells, leading to a negative regulation of their anti-tumour effect (Figure 6.3) (Śledzińska et al. 2015). For example, this could occur through the activation of T-lymphocyte antigen 4 (CTLA-4) and the programmed death 1 receptor (PD-1) and its receptor PD-L1 (Freeman et al. 2000; Walunas et al. 1994; Black et al. 2016; Buchbinder & Desai 2016). Such effect may be inhibited by combining inhibition of heme synthesis inhibition with immune check-point inhibitors. A similar strategy has been shown to enhance the efficacy of conventional PCa treatments, such as chemotherapy and radiotherapy (Finkelstein et al. 2015; Modena et al. 2016; Sharabi et al. 2015; Dewan et al. 2009; Demaria et al. 2005; Kareva 2017; Ramsay 2013).

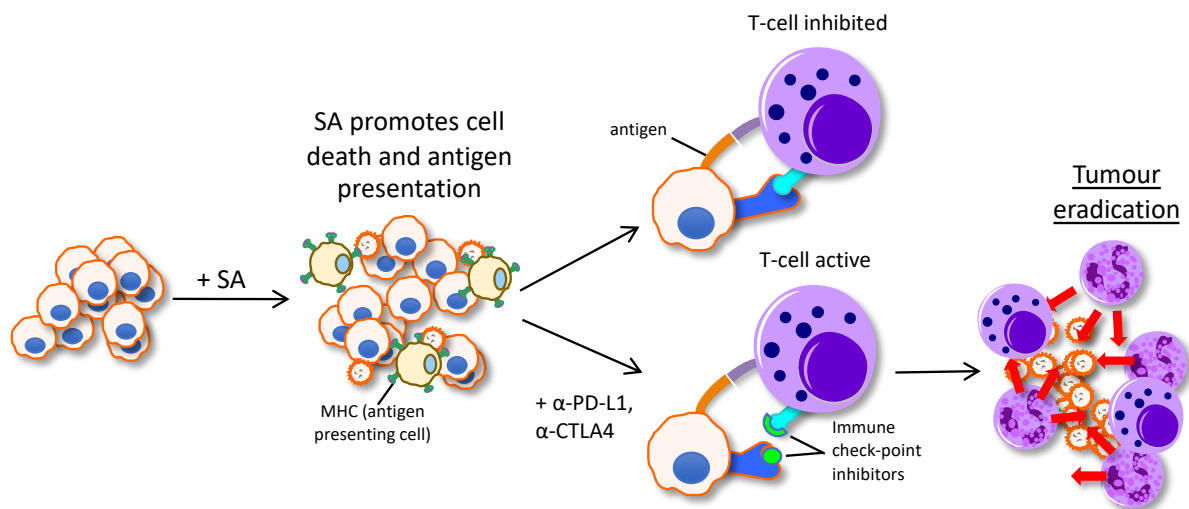


Figure 6.3 Rationale for the combination of heme synthesis inhibition with immune checkpoint inhibition.

Treatment of tumours with the heme synthesis inhibitor succinylacetone (SA) will promote cell death and tumour antigen presentation. This will activate T-cells, however, up-regulation of e.g. PD-L1, on tumour cells could block T-cell activity. The addition of immune check-point inhibitors (antibodies against PD-L1/PD-1 or CTLA4) could therefore facilitate T-cell activation ensuring that the immune response is fully utilised to promote tumour death.

6.3 Final conclusion

Non-organ confined PCa is predominantly treated with hormone therapy and such therapies are successful initially. However, remission is temporary as the disease eventually recurs into the more aggressive CRPC. The complexity of this stage of the disease limits the therapeutic options available. This thesis illustrates the power of biological techniques such as siRNA screens in the identification of novel targets for the management of prostate cancer. Metabolic specificity of cancers, especially PCa, provides potential therapeutic targets that should be specific for the disease, reducing off-target effects.

Various metabolic factors were identified in this study to be important in PCa and these were involved in pathways such as lipogenesis, glycolysis, amino acids and protein biosynthesis, heme biosynthesis, redox homeostasis, and nucleic acids synthesis. The down-regulation of these factors altered PCa proliferation and migration and hence they are suggested to be involved in the oncogenesis and progression of PCa. However, further investigations and validations are required for some of these targets. This work illustrated that potential targets belonged to several interconnected metabolic pathways, so combinational studies of inhibiting such pathways could result in more efficacious outcomes.

Depletion of UROS, the fourth step of heme biosynthesis, significantly repressed prostate cancer proliferation and migration, promoted cell cycle arrest and induced cell death. Further, inhibition of heme biosynthesis pathway where this UROS functions was found to significantly induce caspase-independent cell death and to sensitise cells to ROS. The results of heme biosynthesis inhibition and H₂O₂ administration suggest that this therapeutic approach could be of clinical significance. The apparent ROS sensitivity of PCa cells upon heme biosynthesis inhibition suggests that the redox homeostasis is not efficiently maintained in these cells as in noncancerous cells which provides a therapeutic window to target the disease. The combination of heme biosynthesis inhibition with ROS-inducing therapeutics e.g. radiotherapy

should be investigated to translate this hypothesis into a therapeutic strategy that can be used in PCa patients.

6.4 Future work

Targeting PCa metabolic signalling for novel therapeutics has been an attractive approach due to the metabolic specificity of PCa cells. However, the excessive interconnection between various metabolic signalling pathways and the commonality of metabolic pathways found in cancerous and non-cancerous cells have been problematic for researchers. Therefore, further understanding of prostate cancer metabolism will assist in finding therapeutic windows to design new agents that are highly efficacious but exert minimum side-effects upon non-cancerous tissues.

Multiple factors were found to significantly affect prostate cancer cell proliferation and migration and many of these have not been previously described to play a role in PCa. The role of these factors in PCa progression therefore requires additional studies. Preliminary assays were performed on some these targets e.g. LARS2, FDPS, and ACSM1. In agreement with the results of the screen, siRNA depletion of these factors was found to reduce PC3 cell migration in wound healing assays (Figure 6.4). Figure 6.5 is a preliminary data on siRNA knockdown validation of LARS2 and FDPS. Further, testing the effects of inhibitors of such targets upon aspects such as cell cycle, cell death, migration, invasion could follow.

The novel approach of targeting heme-biosynthesis in PCa is a promising approach, especially as it showed specificity for cancer cells when combined with elevated oxidative stress. I propose that work should continue to validate this target and a drug development project be undertaken to improve target inhibition and drug specificity. The work should also be progressed to more physiologically relevant pre-clinical models, including patient derived organoids and transgenic mouse models of PCa. This data would provide the necessary evidence to support clinical trials of this therapeutic strategy in men with PCa.

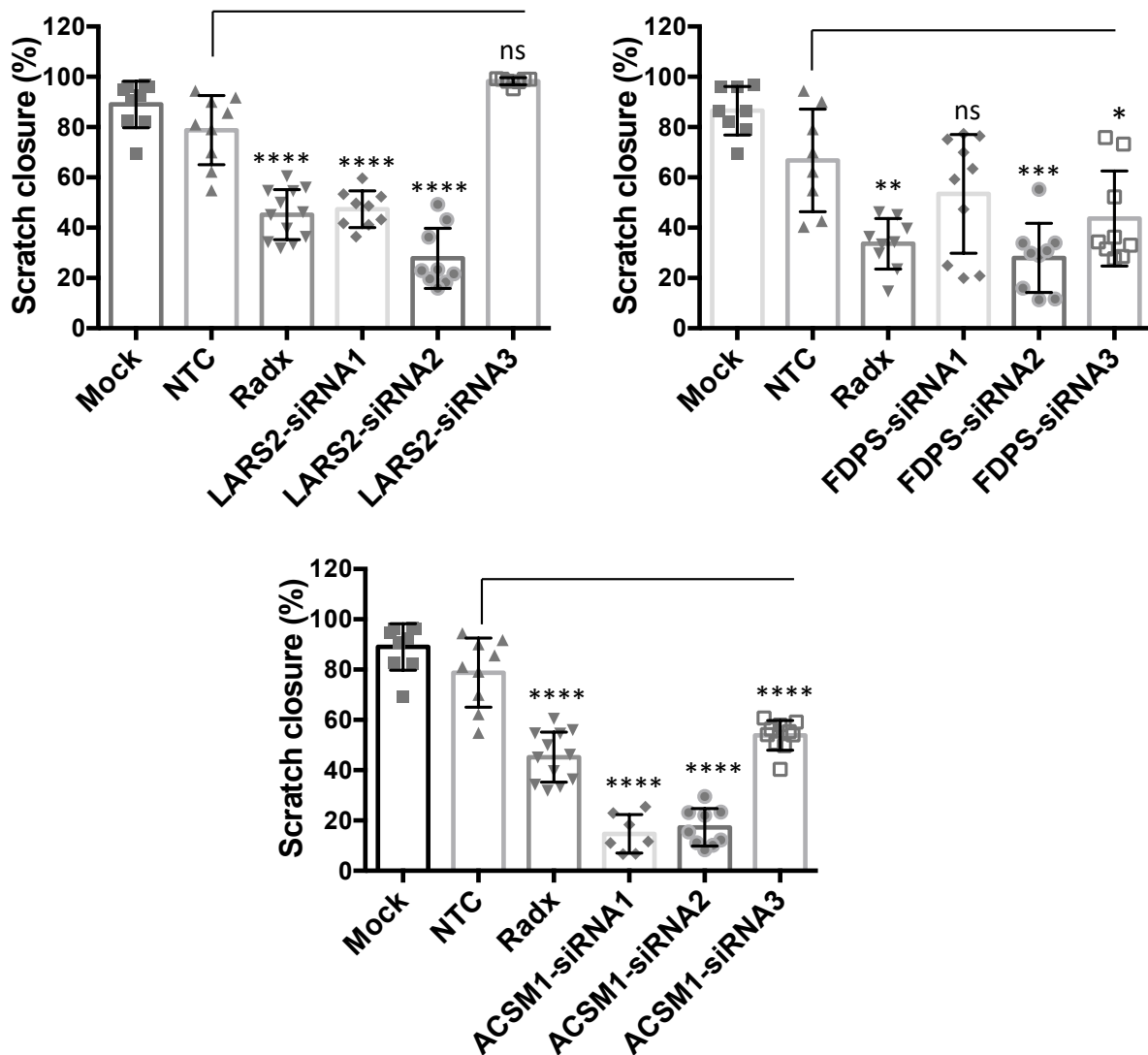


Figure 6.4 Inhibition of PC3 cell migration in response to LARS2, FDPS, and ACSM1 knockdown.

PC3 cells were seeded in 12 well plates and transfected with siRNA (3 individual duplexes per target). siRNA-Radixin (Radx) was used as a positive control and non-targeting (NTC)-siRNA and mock transfection were used as negative controls. 24 hours after transfection media was changed to fresh RPMI and cells left for 72 hours. 24 hours before introducing wounds, media was changed to phenol red-free RPMI containing 5% charcoal stripped FCS. Wounds were then made, cells washed with PBS and fresh media added. Images were captured using brightfield microscopy (Nikon Widefield microscope, 2x objective). Data is mean±1SD of three independent repeats (at least 3 scratches per experiment were quantified). ANOVA (Dunnett's post hoc test), ns= not significant, *P < 0.05, **P < 0.01, ***P < 0.001, ****P < 0.0001.

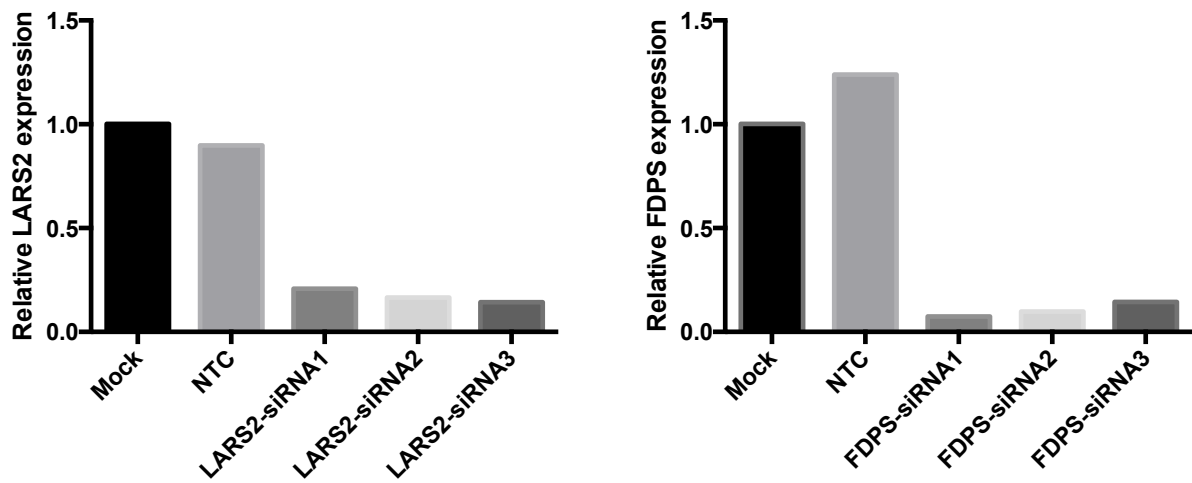


Figure 6.5 QPCR to confirm LARS2 and FDPS knockdowns.

PC3 were transfected with siRNAs and incubated for 72 hours. Cells were harvested, RNA extracted and cDNA synthesised. LARS2 or FDPS expression was subsequently quantified using qPCR. Data represent mean of one repeat.

7 References

- Aaltomaa, S. H., Lipponen, P. K., Viitanen, J., Kankkunen, J.-P., Ala-Opas, M. Y. and Kosma, V.-M. (2000). The prognostic value of inducible nitric oxide synthase in local prostate cancer. *BJU International*, 86, pp. 234–239.
- Aaron, L., Franco, O. E. and Hayward, S. W. (2016). Review of Prostate Anatomy and Embryology and the Etiology of Benign Prostatic Hyperplasia. *The Urologic clinics of North America*, 43(3), pp. 279–288.
- Abate-Shen, C. and Shen, M. M. (2000). Molecular genetics of prostate cancer. *Genes & development*, 14(19), pp. 2410–2434.
- Abate, M., Laezza, C., Pisanti, S., Torelli, G., Seneca, V., Catapano, G., Montella, F., Ranieri, R., Notarnicola, M., Gazzero, P., Bifulco, M. and Ciaglia, E. (2017). Deregulated expression and activity of Farnesyl Diphosphate Synthase (FDPS) in Glioblastoma. *Nature (Scientific reports)*, 7(1), 114123.
- Adhyam, M. and Gupta, A. K. (2012). A Review on the Clinical Utility of PSA in Cancer Prostate. *Indian journal of surgical oncology*. Springer, 3(2), pp. 120–129.
- Adibekian, A., Hsu, K.-L., Speers, A. E., Monillas, E. S., Brown, S. J., Spicer, T., Fernandez-Vega, V., Ferguson, J., Bahnson, B. J., Cravatt, B. F., Hodder, P. and Rosen, H. (2010). Optimization and characterization of a triazole urea inhibitor for platelet-activating factor acetylhydrolase type 2 (PAFAH2). *Probe Reports from the NIH Molecular Libraries Program*.
- Adigun, R. and Bhimji, S. S. (2017). Necrosis, Cell (Liquefactive, Coagulative, Caseous, Fat, Fibrinoid, and Gangrenous). *StatPearls*. Available at: <https://www.ncbi.nlm.nih.gov/books/NBK430935/>. [Accessed: 25.03.2018.]
- Adolfsson, J. (2008). Watchful waiting and active surveillance: the current position. *BJU International*, 102(1), pp. 10–14.
- Ahn, J., Kibel, A. S., Park, J. Y., Rebbeck, T. R., Rennert, H., Stanford, J. L., Ostrander, E. A., Chanock, S., Wang, M.-H., Mittal, R. D., Isaacs, W. B., Platz, E. A. and Hayes, R. B. (2011). Prostate cancer predisposition loci and risk of metastatic disease and prostate cancer recurrence. *Clinical cancer research*, 17(5), pp. 1075–1081
- Aizencang, G. I., Bishop, D. F., Forrest, D., Astrin, K. H. and Desnick, R. J. (2000). Uroporphyrinogen III synthase: An alternative promoter controls erythroid-specific expression in the murine gene. *The Journal of biological chemistry*, 275(4), pp. 2295–304.
- Ajioka, R. S., Phillips, J. D. and Kushner, J. P. (2006). Biosynthesis of heme in mammals. *Biochimica et Biophysica Acta (BBA) - Molecular Cell Research*, 1763(7), pp. 723–736.
- Akakura, K., Furuya, Y. and Ito, H. (1998). Steroidal and nonsteroidal antiandrogens: chemical structures, mechanisms of action and clinical applications. *Nihon rinsho. Japanese journal of clinical medicine*, 56(8), pp. 2124–2128.
- Alam, M. M., Lal, S., FitzGerald, K. E. and Zhang, L. (2016). A holistic view of cancer bioenergetics: mitochondrial function and respiration play fundamental roles in the development and progression of diverse tumors. *Clinical and translational medicine*, 5(3).
- Alex, A. B., Pal, S. K. and Agarwal, N. (2016). CYP17 inhibitors in prostate cancer: latest evidence and clinical potential. *Therapeutic advances in medical oncology*, 8(4), pp. 267–275.

- Altavilla, A., Iacovelli, R., Procopio, G., Alesini, D., Risi, E., Campenni, G. M., Palazzo, A. and Cortesi, E. (2012). Medical strategies for treatment of castration resistant prostate cancer (CRPC) docetaxel resistant. *Cancer biology & therapy*, 13(11), pp. 1001–1008.
- Altman, B. J., Stine, Z. E. and Dang, C. V (2016). From Krebs to clinic: glutamine metabolism to cancer therapy. *Nature reviews. Cancer*, 16(10), pp. 619–634.
- Alwarawrah, Y., Hughes, P., Loiselle, D., Carlson, D. A., Darr, D. B., Jordan, J. L., Xiong, J., Hunter, L. M., Dubois, L. G., Thompson, J. W., Kulkarni, M. M., Ratcliff, A. N., Kwiek, J. J. and Haystead, T. A. J. (2016). Fasnall, a Selective FASN Inhibitor, Shows Potent Anti-tumor Activity in the MMTV-Neu Model of HER2+ Breast Cancer. *Cell Chemical Biology*, 23(6), pp. 678–688.
- Amelio, I., Cutruzzolá, F., Antonov, A., Agostini, M. and Melino, G. (2014). Serine and glycine metabolism in cancer. *Trends in biochemical sciences*, 39(4), pp. 191–198.
- Anassi, E. and Ndefo, U. A. (2011). Sipuleucel-T (provenge) injection: the first immunotherapy agent (vaccine) for hormone-refractory prostate cancer. *P & T: a peer-reviewed journal for formulary management*. MediMedia, USA, 36(4), pp. 197–202.
- Arakawa, S., Nakanomyo, I., Kudo-Sakamoto, Y., Akazawa, H., Komuro, I. and Shimizu, S. (2015). Identification of a novel compound that inhibits both mitochondria-mediated necrosis and apoptosis. *Biochemical and Biophysical Research Communications*, 467(4), pp. 1006–1011.
- Arap, M. A. (2010). Molecular biology in prostate cancer. *Arch. Esp. Urol*, 63(1), pp. 1–9.
- Arnold, H. and Pette, D. (1970). Binding of aldolase and triosephosphate dehydrogenase to F-actin and modification of catalytic properties of aldolase. *European journal of biochemistry*, 15(2), pp. 360–366.
- Araz, M., Aras, G. and Küçük, Ö. N. (2015). The role of 18F-NaF PET/CT in metastatic bone disease. *Journal of bone oncology*, 4(3), pp. 92–97.
- Asaka, M., Kimura, T., Meguro, T., Kato, M., Kudo, M., Miyazaki, T. and Alpert, E. (1994). Alteration of aldolase isozymes in serum and tissues of patients with cancer and other diseases. *Journal of clinical laboratory analysis*, 8(3), pp. 144–148.
- Ashkenazi, A. and Salvesen, G. (2014). Regulated Cell Death: Signaling and Mechanisms. *Annual Review of Cell and Developmental Biology*, 30(1), pp. 337–356.
- Attard, G., Parker, C., Eeles, R. A., Schröder, F., Tomlins, S. A., Tannock, I., Drake, C. G. and de Bono, J. S. (2016). Prostate cancer. *The Lancet*, 387(10013), pp. 70–82.
- Baigi, M. G., Brault, L., Néguesque, A., Beley, M., Hilali, R. El, Gatüzère, F. and Bagrel, D. (2008). Apoptosis/necrosis switch in two different cancer cell lines: Influence of benzoquinone- and hydrogen peroxide-induced oxidative stress intensity, and glutathione. *Toxicology in Vitro*, 22(6), pp. 1547–1554.
- Bailey, H. H., Gipp, J. J., Ripple, M., Wilding, G. and Mulcahy, R. T. (1992). Increase in gamma-glutamylcysteine synthetase activity and steady-state messenger RNA levels in melphalan-resistant DU-145 human prostate carcinoma cells expressing elevated glutathione levels. *Cancer research*, 52(18), pp. 5115–5118.
- Balendiran, G. K., Dabur, R. and Fraser, D. (2004). The role of glutathione in cancer. *Cell Biochemistry and Function*, 22(6), pp. 343–352.
- Baritaki, S., Huerta-Yepe, S., Sahakyan, A., Karagiannides, I., Bakirtzi, K., Jazirehi, A. and Bonavida, B. (2010). Mechanisms of nitric oxide-mediated inhibition of EMT in cancer. *Cell Cycle*, 9(24), pp. 4931–4940.

Baron, A., Migita, T., Tang, D. and Loda, M. (2004). Fatty acid synthase: A metabolic oncogene in prostate cancer?. *Journal of Cellular Biochemistry*, 91(1), pp. 47–53.

Barry, D. J., Durkin, C. H., Abella, J. V. and Way, M. (2015). Open source software for quantification of cell migration, protrusions, and fluorescence intensities. *The Journal of Cell Biology*, 209(1), pp. 163–180.

Bashir, M. N. (2015). Epidemiology of Prostate Cancer. *Asian Pacific journal of cancer prevention : APJCP*, 16(13), pp. 5137–41.

Beardsley, G. P., Moroson, B. A., Taylor, E. C. and Moran, R. G. (1989). A new folate antimetabolite, 5,10-dideaza-5,6,7,8-tetrahydrofolate is a potent inhibitor of de novo purine synthesis. *The Journal of biological chemistry*, 264(1), pp. 328–33.

Beer, T. M., Kwon, E. D., Drake, C. G., Fizazi, K., Logothetis, C., Gravis, G., Ganju, V., Polikoff, J., Saad, F., Humanski, P., Piulats, J. M., Gonzalez Mella, P., Ng, S. S., Jaeger, D., Parnis, F. X., Franke, F. A., Puente, J., Carvajal, R., Sengeløv, L., McHenry, M. B., Varma, A., van den Eertwegh, A. J. and Gerritsen, W. (2017). Randomized, Double-Blind, Phase III Trial of Ipilimumab Versus Placebo in Asymptomatic or Minimally Symptomatic Patients With Metastatic Chemotherapy-Naive Castration-Resistant Prostate Cancer. *Journal of Clinical Oncology*, 35(1), pp. 40–47.

Beer, T. M., Pierce, W. C., Lowe, B. A. and Henner, W. D. (2001). Phase II study of weekly docetaxel in symptomatic androgen-independent prostate cancer. *Annals of oncology : official journal of the European Society for Medical Oncology*, 12(9), pp. 1273–1279.

Benedettini, E., Nguyen, P. and Loda, M. (2008). The pathogenesis of prostate cancer: from molecular to metabolic alterations. *Diagnostic Histopathology*, 14(5), pp. 195–201.

Berry, W., Dakhil, S., Gregurich, M. A. and Asmar, L. (2001). Phase II trial of single-agent weekly docetaxel in hormone-refractory, symptomatic, metastatic carcinoma of the prostate. *Seminars in oncology*, 28(4), pp. 8–15.

Berry, W., Dakhil, S., Modiano, M., Gregurich, M. and Asmar, L. (2002). Phase III study of mitoxantrone plus low dose prednisone versus low dose prednisone alone in patients with asymptomatic hormone refractory prostate cancer. *The Journal of urology*, 168(6), pp. 2439–2443.

Berthold, D. R., Pond, G. R., Soban, F., de Wit, R., Eisenberger, M. and Tannock, I. F. (2008). Docetaxel Plus Prednisone or Mitoxantrone Plus Prednisone for Advanced Prostate Cancer: Updated Survival in the TAX 327 Study. *Journal of Clinical Oncology*, 26(2), pp. 242–245.

Biancur, D. E., Paulo, J. A., Małachowska, B., Del Rey, M. Q., Sousa, C. M., Wang, X., Sohn, A. S. W., Chu, G. C., Gygi, S. P., Harper, J. W., Fendler, W., Mancias, J. D. and Kimmelman, A. C. (2017). Compensatory metabolic networks in pancreatic cancers upon perturbation of glutamine metabolism. *Nature Communications*, 8 (15965).

Bill-Axelsson, A., Holmberg, L., Garmo, H., Rider, J. R., Taari, K., Busch, C., Nordling, S., Häggman, M., Andersson, S.-O., Spångberg, A., Andrén, O., Palmgren, J., Steineck, G., Adami, H.-O. and Johansson, J.-E. (2014). Radical prostatectomy or watchful waiting in early prostate cancer. *The New England journal of medicine*, pp. 932–942.

Birmingham, A., Selfors, L. M., Forster, T., Wrobel, D., Kennedy, C. J., Shanks, E., Santoyo-Lopez, J., Dunican, D. J., Long, A., Kelleher, D., Smith, Q., Beijersbergen, R. L., Ghazal, P. and Shamu, C. E. (2009). Statistical methods for analysis of high-throughput RNA interference screens. *Nature Methods*, 6(8), pp. 569–575.

Bitting, R. L. and Armstrong, A. J. (2013). Targeting the PI3K/Akt/mTOR pathway in castration-resistant prostate cancer. *Endocrine Related Cancer*, 20(3), pp. R83–R99.

- Black, M., Barsoum, I. B., Truesdell, P., Cotechini, T., Macdonald-Goodfellow, S. K., Petroff, M., Siemens, D. R., Koti, M., Craig, A. W. B. and Graham, C. H. (2016). Activation of the PD-1/PD-L1 immune checkpoint confers tumor cell chemoresistance associated with increased metastasis. *Oncotarget*, 7(9), pp. 10557–10567.
- Blattner, M., Liu, D., Robinson, B. D., Chen, Y., Rubin, M. A. and Correspondence, C. E. B. (2017). SPOP Mutation Drives Prostate Tumorigenesis In Vivo through Coordinate Regulation of PI3K/mTOR and AR Signaling. *Cancer Cell*, 31, pp. 436–451.
- Boccon-Gibod, L., van der Meulen, E. and Persson, B.-E. (2011). An update on the use of gonadotropin-releasing hormone antagonists in prostate cancer. *Therapeutic advances in urology*, 3(3), pp. 127–140.
- Bogdan, A. R., Miyazawa, M., Hashimoto, K. and Tsuji, Y. (2016). Regulators of Iron Homeostasis: New Players in Metabolism, Cell Death, and Disease. *Trends in biochemical sciences*, 41(3), pp. 274–286.
- Bolte, S. and Cordelières, F. P. (2006). A guided tour into subcellular colocalization analysis in light microscopy. *Journal of microscopy*, 224(3), pp. 213–232.
- Boroughs, L. K. and DeBerardinis, R. J. (2015). Metabolic pathways promoting cancer cell survival and growth. *Nature cell biology*, 17(4), pp. 351–9.
- Bostwick, D. G., Burke, H. B., Djakiew, D., Euling, S., Ho, S., Landolph, J., Morrison, H., Sonawane, B., Shifflett, T., Waters, D. J. and Timms, B. (2004). Human prostate cancer risk factors. *Cancer*, 101(S10), pp. 2371–2490.
- Bostwick, D. G., Shan, A., Qian, J., Darson, M., Maihle, N. J., Jenkins, R. B. and Cheng, L. (1998). Independent origin of multiple foci of prostatic intraepithelial neoplasia: comparison with matched foci of prostate carcinoma. *Cancer*, 83(9), pp. 1995–2002.
- Bouman-Wammes, E. W., de Munck, L., van den Berg, H. P., Beeker, A., Smorenburg, C. H., Verheul, H. M. W., Gerritsen, W. R. and van den Eertwegh, A. J. M. (2017). A randomized phase II trial of docetaxel plus carboplatin versus docetaxel in patients with castration-resistant prostate cancer who have progressed after response to prior docetaxel chemotherapy: The RECARDO trial. *Journal of Clinical Oncology*, 35(6_suppl), pp. 166–166.
- Bowen, C., Bubendorf, L., Voeller, H. J., Slack, R., Willi, N., Sauter, G., Gasser, T. C., Koivisto, P., Lack, E. E., Kononen, J., Kallioniemi, O. P. and Gelmann, E. P. (2000). Loss of NKX3.1 expression in human prostate cancers correlates with tumor progression. *Cancer research*, 60(21), pp. 6111–6115.
- Branković, A., Brajušković, G., Nikolić, Z., Vukotić, V., Cerović, S., Savić-Pavićević, D. and Romac, S. (2013). Endothelial nitric oxide synthase gene polymorphisms and prostate cancer risk in Serbian population. *International journal of experimental pathology*, 94(6), pp. 355–361.
- Bratt, O., Häggman, M., Ahlgren, G., Nordle, Ö., Björk, A. and Damber, J.-E. (2009). Open-label, clinical phase I studies of tasquinimod in patients with castration-resistant prostate cancer. *British Journal of Cancer*, 101(8), pp. 1233–1240.
- Breast Cancer Linkage Consortium (1999) ‘Cancer risks in BRCA2 mutation carriers.’, *Journal of the National Cancer Institute*, 91(15), pp. 1310–1316.
- Brechbiel, M. W. (2007). Targeted α -therapy: past, present, future?. *Dalton Transactions*, 0(43), p. 4918.
- Bronte, V., Kasic, T., Gri, G., Gallana, K., Borsellino, G., Marigo, I., Battistini, L., Iafrate, M., Prayer-Galetti, T., Pagano, F. and Viola, A. (2005). Boosting antitumor responses of T lymphocytes infiltrating human prostate cancers. *The Journal of experimental medicine*, 201(8), pp. 1257–1268.
- Brooke, G. N. and Bevan, C. L. (2009). The role of androgen receptor mutations in prostate cancer progression. *Current genomics*, 10(1), pp. 18–25.

- Brooke, G. N., Culley, R. L., Dart, D. A., Mann, D. J., Gaughan, L., McCracken, S. R., Robson, C. N., Spencer-Dene, B., Gamble, S. C., Powell, S. M., Wait, R., Waxman, J., Walker, M. M. and Bevan, C. L. (2011). FUS/TLS is a novel mediator of androgen-dependent cell-cycle progression and prostate cancer growth. *Cancer research*, 71(3), pp. 914–924.
- Brooke, G. N., Parker, M. G. and Bevan, C. L. (2008). Mechanisms of androgen receptor activation in advanced prostate cancer: differential co-activator recruitment and gene expression. *Oncogene*, 27(21), pp. 2941–2950.
- Brooke, G. N., Powell, S. M., Lavery, D. N., Waxman, J., Buluwela, L., Ali, S. and Bevan, C. L. (2014). Engineered repressors are potent inhibitors of androgen receptor activity. *Oncotarget*, 5(4), pp. 959–69.
- Brower, V. (2016). Tasquinimod treatment for prostate cancer. *The Lancet. Oncology*, 17(8), p. e322.
- Brusselmans, K., De Schrijver, E., Verhoeven, G. and Swinnen, J. V. (2005). RNA Interference–Mediated Silencing of the *Acetyl-CoA-Carboxylase- α* Gene Induces Growth Inhibition and Apoptosis of Prostate Cancer Cells. *Cancer Research*, 65(15), pp. 6719–6725.
- Buchbinder, E. I. and Desai, A. (2016). CTLA-4 and PD-1 Pathways: Similarities, Differences, and Implications of Their Inhibition. *American journal of clinical oncology*, 39(1), pp. 98–106.
- Buhaescu, I. and Izzedine, H. (2007). Mevalonate pathway: A review of clinical and therapeutical implications. *Clinical Biochemistry*, 40(9–10), pp. 575–584.
- Buhmeida, A., Pyrhönen, S., Laato, M. and Collan, Y. (2006). Prognostic factors in prostate cancer. *Diagnostic Pathology*, 1(4).
- Bullard, K. M., Kim, H.-R., Wheeler, M. A., Wilson, C. M., Neudauer, C. L., Simpson, M. A. and McCarthy, J. B. (2003). Hyaluronan synthase-3 is upregulated in metastatic colon carcinoma cells and manipulation of expression alters matrix retention and cellular growth. *International Journal of Cancer*, 107(5), pp. 739–746.
- Bullough, P. G. (2010). Orthopaedic Pathology (Fifth Edition). *Orthopaedic Pathology*, pp. 81–108.
- Burdelski, C., Strauss, C., Tsourlakis, M. C., Kluth, M., Hube-Magg, C., Melling, N., Lebok, P., Minner, S., Koop, C., Graefen, M., Heinzer, H., Wittmer, C., Krech, T., Sauter, G., Wilczak, W., Simon, R., Schlomm, T. and Steurer, S. (2015). Overexpression of thymidylate synthase (TYMS) is associated with aggressive tumor features and early PSA recurrence in prostate cancer. *Oncotarget*, 6(10), pp. 8377–8387.
- Burger, R. M. (1998). Cleavage of Nucleic Acids by Bleomycin. *Chemical reviews*, 98(3), pp. 1153–1170.
- Burger, R. M., Peisach, J. and Horwitz, S. B. (1981). Activated bleomycin. A transient complex of drug, iron, and oxygen that degrades DNA. *The Journal of biological chemistry*, 256(22), pp. 11636–11644.
- Burke, A. J., Sullivan, F. J., Giles, F. J. and Glynn, S. A. (2013). The yin and yang of nitric oxide in cancer progression. *Carcinogenesis*, 34(3), pp. 503–512.
- Butler, L. M., Centenera, M. M. and Swinnen, J. V (2016). Androgen control of lipid metabolism in prostate cancer: novel insights and future applications. *Endocrine-related cancer*, 23(5), pp. R219-R227.
- Cai, J., Huang, Z. Z. and Lu, S. C. (1997). Differential regulation of gamma-glutamylcysteine synthetase heavy and light subunit gene expression. *The Biochemical journal*, 326, pp. 167–172.
- Campeau, E. and Gobeil, S. (2011). RNA interference in mammals: behind the screen. *Briefings in Functional Genomics*, 10(4), pp. 215–226.

- Cancer Research UK (2014) *Prostate cancer incidence and mortality statistics* | Cancer Research UK. Available at: <http://www.cancerresearchuk.org/health-professional/cancer-statistics/statistics-by-cancer-type/prostate-cancer/mortality#heading-Five> [Accessed: 13.04.2018].
- Cantor, J. R. and Sabatini, D. M. (2012). Cancer cell metabolism: one hallmark, many faces. *Cancer discovery*, 2(10), pp. 881–98.
- Cao, B., Qi, Y., Zhang, G., Xu, D., Zhan, Y. and Alvarez, X. (2014). Androgen receptor splice variants activating the full-length receptor in mediating resistance to androgen-directed therapy. *Oncotarget*, 5(6), pp. 1646–1656.
- Cao, J. Y. and Dixon, S. J. (2016). Mechanisms of ferroptosis. *Cellular and molecular life sciences*, 73(11–12), pp. 2195–209.
- Caplows, M., Shanks, J. and Ruhlen, R. (1994). How Taxol Modulates Microtubule Disassembly. *The Journal of Biological Chemistry*, 269(38), pp. 23399–23402.
- Caputo, A. (Antonio) (1976). *Biological basis of clinical effect of bleomycin*. Rome, S. Karger.
- Carreras, C. W. and Santi, D. V. (1995). The Catalytic Mechanism and Structure of Thymidylate Synthase. *Annual Review of Biochemistry*, 64(1), pp. 721–762.
- Carthew, R. W. and Sontheimer, E. J. (2009). Origins and Mechanisms of miRNAs and siRNAs. *Cell*, 136(4), pp. 642–55.
- Caspi, M., Perry, G., Skalka, N., Meisel, S., Firsow, A., Amit, M. and Rosin-Arbesfeld, R. (2014). Aldolase positively regulates of the canonical Wnt signaling pathway. *Molecular cancer*, 13(164).
- Catz, S. D. and Johnson, J. L. (2003). BCL-2 in prostate cancer: a minireview. *Apoptosis : an international journal on programmed cell death*, 8(1), pp. 29–37.
- Caubet, M., Dobi, E., Pozet, A., Almotlak, H., Montcuquet, P., Maurina, T., Mouillet, G., N'guyen, T., Stein, U., Thiery-Vuillemin, A. and Fiteni, F. (2015). Carboplatin-etoposide combination chemotherapy in metastatic castration-resistant prostate cancer: A retrospective study. *Molecular and clinical oncology*, 3(6), pp. 1208–1212.
- Cesaretti, J. A., Stone, N. N., Skouteris, V. M., Park, J. L. and Stock, R. G. (2007). Brachytherapy for the Treatment of Prostate Cancer. *The Cancer Journal*, 13(5), pp. 302–312.
- Chajès, V., Cambot, M., Moreau, K., Lenoir, G. M. and Joulin, V. (2006). Acetyl-CoA Carboxylase α Is Essential to Breast Cancer Cell Survival. *Cancer Research*, 66(10), pp. 5287–5294.
- Chakravarty, B., Gu, Z., Chirala, S. S., Wakil, S. J. and Quijcho, F. A. (2004). Human fatty acid synthase: structure and substrate selectivity of the thioesterase domain. *The National Academy of Sciences of the United States of America*, 101(44), pp. 15567–15572.
- Chamizo, C., Zazo, S., Dómine, M., Cristóbal, I., García-Foncillas, J., Rojo, F. and Madoz-Gúrpide, J. (2015). Thymidylate synthase expression as a predictive biomarker of pemetrexed sensitivity in advanced non-small cell lung cancer. *BMC pulmonary medicine*, 15 (132), pp. 2-7.
- Chang, J. W., Zuhl, A. M., Speers, A. E., Niessen, S., Brown, S. J., Mulvihill, M. M., Fan, Y. C., Spicer, T. P., Southern, M., Scampavia, L., Fernandez-Vega, V., Dix, M. M., Cameron, M. D., Hodder, P. S., Rosen, H., Nomura, D. K., Kwon, O., Hsu, K.-L. and Cravatt, B. F. (2015). Selective Inhibitor of Platelet-Activating Factor Acetylhydrolases 1b2 and 1b3 That Impairs Cancer Cell Survival. *ACS Chemical Biology*, 10(4), pp. 925–932.

- Chang, L., Graham, P. H., Ni, J., Hao, J., Bucci, J., Cozzi, P. J. and Li, Y. (2015). Targeting PI3K/Akt/mTOR signaling pathway in the treatment of prostate cancer radioresistance. *Critical Reviews in Oncology/Hematology*, 96(3), pp. 507–517.
- Chang, L., Ni, J., Beretov, J., Wasinger, V. C., Hao, J., Bucci, J., Malouf, D., Gillatt, D., Graham, P. H. and Li, Y. (2017). Identification of protein biomarkers and signaling pathways associated with prostate cancer radioresistance using label-free LC-MS/MS proteomic approach. *Nature Publishing Group*, 7(41834).
- Chang, S. S. (2007). Androgen -Independent Prostate Cancer Treatment Options for Hormone- Refractory Prostate Cancer. *Reveiwrs in urology*, 9, pp. 13–18.
- Chang, Y.-C., Chan, Y.-C., Chang, W.-M., Lin, Y.-F., Yang, C.-J., Su, C.-Y., Huang, M.-S., Wu, A. T. H. and Hsiao, M. (2017). Feedback regulation of ALDOA activates the HIF-1 α /MMP9 axis to promote lung cancer progression. *Cancer Letters*, 403, pp. 28–36.
- Chappell, W. H., Lehmann, B. D., Terrian, D. M., Abrams, S. L., Steelman, L. S. and McCubrey, J. A. (2012). p53 expression controls prostate cancer sensitivity to chemotherapy and the MDM2 inhibitor Nutlin-3. *Cell cycle*, 11(24), pp. 4579–4588.
- Chen, G.-X., Zhang, S., He, X.-H., Liu, S.-Y., Ma, C. and Zou, X.-P. (2014). Clinical utility of recombinant adenoviral human p53 gene therapy: current perspectives. *OncoTargets and therapy*. Dove Press, 7, pp. 1901–1909.
- Chen, Q. and Ames, B. N. (1994). Senescence-like growth arrest induced by hydrogen peroxide in human diploid fibroblast F65 cells. *Proceedings of the National Academy of Sciences of the United States of America*, 91(10), pp. 4130–4134.
- Chen, R. C., Rumble, R. B., Loblaw, D. A., Finelli, A., Ehdaie, B., Cooperberg, M. R., Morgan, S. C., Tyldesley, S., Haluschak, J. J., Tan, W., Justman, S. and Jain, S. (2016). Active Surveillance for the Management of Localized Prostate Cancer (Cancer Care Ontario Guideline): American Society of Clinical Oncology Clinical Practice Guideline Endorsement. *official journal of the American Society of Clinical Oncology*, 34(18), pp. 2182–2190.
- Chen, X., Li, L., Guan, Y., Yang, J. and Cheng, Y. (2016). Anticancer strategies based on the metabolic profile of tumor cells: therapeutic targeting of the Warburg effect. *Acta Pharmacologica Sinica*, 37(8), pp. 1013–1019.
- Chen, X. P. and Du, G. H. (2007). Target validation: A door to drug discovery. *Drug discoveries & therapeutics*, 1(1), pp. 23–29.
- Chen, X., Song, M., Zhang, B. and Zhang, Y. (2016). Reactive Oxygen Species Regulate T Cell Immune Response in the Tumor Microenvironment. *Oxidative medicine and cellular longevity*, 2016, pp. 1-10.
- Chen, Y., Clegg, N. J. and Scher, H. I. (2009). Anti-androgens and androgen-depleting therapies in prostate cancer: novel agents for an established target. *The Lancet. Oncology*, 10(10), pp. 981–991.
- Chen, Y., Li, J., Guo, Y. and Guo, X.-Y. (2014). Nitric oxide synthase 3 gene variants and colorectal cancer: a meta-analysis. *Asian Pacific journal of cancer prevention : APJCP*, 15(8), pp. 3811–3815.
- Chiabrando, D., Mercurio, S. and Tolosano, E. (2014). Heme and erythropoiesis: more than a structural role. *Haematologica*. Ferrata Storti Foundation, 99(6), pp. 973–983.
- Chittoor, S., Berry, W., Loesch, D., Logie, K., Fleagle, J., Mull, S., Boehm, K. A., Zhan, F. and Asmar, L. (2006). Phase II Study of Low-Dose Docetaxel/Estramustine in Elderly Patients or Patients Aged 18-74 Years with Hormone-Refractory Prostate Cancer. *Clinical Genitourinary Cancer*, 5(3), pp. 212–218.

- Chow, H., Ghosh, P., D'Abronzio, L. S., de Vere White, R., Dall'Era, M., Evans, C. P., Yap, S. A., Lara, P. and Pan, C.-X. (2015). Everolimus plus bicalutamide for castration resistant prostate cancer (CRPC): Bench to bedside and back. *Journal of Clinical Oncology*, 33.
- Chow, H., Ghosh, P. M., deVere White, R., Evans, C. P., Dall'Era, M. A., Yap, S. A., Li, Y., Beckett, L. A., Lara, P. N., Pan, C.-X. and Pan, C. (2016). A phase 2 clinical trial of everolimus plus bicalutamide for castration-resistant prostate cancer. *Cancer*, 122(12), pp. 1897–1904.
- Chow, M. S., Liu, L. V and Solomon, E. I. (2008). Further insights into the mechanism of the reaction of activated bleomycin with DNA. *Proceedings of the National Academy of Sciences of the United States of America*, 105(36), pp. 13241–13245.
- Cibelli, G., Schoch, S., Pajunk, H., Brand, I. A. and Thiel, G. (1996). A (G+C)-rich motif in the aldolase C promoter functions as a constitutive transcriptional enhancer element. *Eur. J. Biochem*, 237, pp. 311–317.
- Ciccarese, C., Santoni, M., Massari, F., Modena, A., Piva, F., Conti, A., Mazzucchelli, R., Cheng, L., Lopez-Beltran, A., Scarpelli, M., Tortora, G. and Montironi, R. (2016). Metabolic Alterations in Renal and Prostate Cancer. *Current drug metabolism*, 17(2), pp. 150–155.
- Clavell, L. A., Gelber, R. D., Cohen, H. J., Hitchcock-Bryan, S., Cassady, J. R., Tarbell, N. J., Blattner, S. R., Tantravahi, R., Leavitt, P. and Sallan, S. E. (1986). Four-Agent Induction and Intensive Asparaginase Therapy for Treatment of Childhood Acute Lymphoblastic Leukemia. *New England Journal of Medicine*, 315(11), pp. 657–663.
- Cong, X., Lu, C., Huang, X., Yang, D., Cui, X., Cai, J., Lv, L., He, S., Zhang, Y. and Ni, R. (2014). Increased expression of glycinamide ribonucleotide transformylase is associated with a poor prognosis in hepatocellular carcinoma, and it promotes liver cancer cell proliferation. *Human Pathology*, 45(7), pp. 1370–1378.
- Conrad, M., Angeli, J. P. F., Vandenabeele, P. and Stockwell, B. R. (2016). Regulated necrosis: disease relevance and therapeutic opportunities. *Nature Reviews Drug Discovery*, 15(5), pp. 348–366.
- Cook, T. and Sheridan, W. P. (2000). Development of GnRH antagonists for prostate cancer: new approaches to treatment. *The oncologist*, 5(2), pp. 162–168.
- Cooperberg, M. R., Carroll, P. R. and Klotz, L. (2011). Active Surveillance for Prostate Cancer: Progress and Promise. *Journal of Clinical Oncology*, 29(27), pp. 3669–3676.
- Corcoran, A. T., Peele, P. B. and Benoit, R. M. (2010). Cost Comparison Between Watchful Waiting With Active Surveillance and Active Treatment of Clinically Localized Prostate Cancer. *Urology*, 76(3), pp. 703–707.
- Costello, L. C., Feng, P., Milon, B., Tan, M. and Franklin, R. B. (2004). Role of zinc in the pathogenesis and treatment of prostate cancer: critical issues to resolve. *Prostate Cancer and Prostatic Diseases*, 7(2), pp. 111–117.
- Costello, L. C. and Franklin, R. B. (2000). The intermediary metabolism of the prostate: a key to understanding the pathogenesis and progression of prostate malignancy. *Oncology*, 59(4), pp. 269–282.
- Costello, L. C. and Franklin, R. B. (2006). The clinical relevance of the metabolism of prostate cancer; zinc and tumor suppression: connecting the dots. *Molecular cancer*, 5 (17), pp. 17.
- Costello, L. C. and Franklin, R. B. (2016). A comprehensive review of the role of zinc in normal prostate function and metabolism; and its implications in prostate cancer. *Archives of Biochemistry and Biophysics*, 611, pp. 100–112.
- Costello, L. C., Franklin, R. B. and Feng, P. (2005). Mitochondrial function, zinc, and intermediary metabolism relationships in normal prostate and prostate cancer. *Mitochondrion*, 5(3), pp. 143–153.

- Costello, L.C., Franklin, R. B., Zou, J., Feng, P., Bok, R., Swanson, M. G. and Kurhanewicz, J. (2011). Human prostate cancer ZIP1/zinc/citrate genetic/metabolic relationship in the TRAMP prostate cancer animal model. *Cancer Biology & Therapy*, 12(12), pp. 1078–1084.
- Cote, R. J., Shi, Y., Groshen, S., Feng, A.-C., Skinner, D., Lieskovosky, G. and Cordon-Cardo, C. (1998). Association of p27Kipl Levels With Recurrence and Survival in Patients With Stage C Prostate Carcinoma. *JNCI Journal of the National Cancer Institute*, 90(12), pp. 916–920.
- Cotrufo, T., Andrés, R. M., Ros, O., Pérez-Brangulí, F., Muhaisen, A., Fuschini, G., Martínez, R., Pascual, M., Comella, J. X. and Soriano, E. (2012). Syntaxin 1 is required for DCC/Netrin-1-dependent chemoattraction of migrating neurons from the lower rhombic lip. *European Journal of Neuroscience*, 36(9), pp. 3152–3164.
- Coutinho, I., Day, T. K., Tilley, W. D. and Selth, L. A. (2016). Androgen receptor signaling in castration-resistant prostate cancer: a lesson in persistence. *Endocrine-related cancer*, 23(12), pp. T179–T197.
- Covey, S.N., Al-Kaff, N. S., Lángara, A. and Turner, D. S. (1997). Plants combat infection by gene silencing. *Nature*, 385(6619), pp. 781–782.
- Crawford, E. D. (2004). Hormonal therapy in prostate cancer: historical approaches. *Reviews in urology*, LLC, 6(Suppl 7), pp. S3–S11.
- Crocetti, E. (2015). Epidemiology of prostate cancer in Europe - European Commission. *Centre for Parliamentary Studies*. Available at: <https://ec.europa.eu/jrc/en/publication/epidemiology-prostate-cancer-europe>. [Accessed: 25.03.2018].
- Cunha, G. R. (1975). Age-Dependent Loss of Sensitivity of Female Urogenital Sinus to Androgenic Conditions as a Function of the Epithelial-Stromal Interaction in Mice. *Endocrinology*, 97(3), pp. 665–673.
- Cunha, G. R. (1994). Role of mesenchymal-epithelial interactions in normal and abnormal development of the mammary gland and prostate. *Cancer*, 74(3 Suppl), pp. 1030–1044.
- Currie, E., Schulze, A., Zechner, R., Walther, T. C., Farese, R. V and Jr. (2013). Cellular fatty acid metabolism and cancer. *Cell metabolism*, 18(2), pp. 153–161.
- Cutruzzola, F., Giardina, G., Marani, M., Macone, A., Paiardini, A., Rinaldo, S. and Paone, A. (2017). Glucose Metabolism in the Progression of Prostate Cancer. *Frontiers in physiology*, 8(97).
- Cyll, K., Ersvær, E., Vlatkovic, L., Pradhan, M., Kildal, W., Avranden Kjær, M., Kleppe, A., Hveem, T. S., Carlsen, B., Gill, S., Löffeler, S., Haug, E. S., Wæhre, H., Sooriakumaran, P. and Danielsen, H. E. (2017). Tumour heterogeneity poses a significant challenge to cancer biomarker research. *British journal of cancer*, 117(3), pp. 367–375.
- Dakubo, G. D., Parr, R. L., Costello, L. C., Franklin, R. B. and Thayer, R. E. (2006). Altered metabolism and mitochondrial genome in prostate cancer. *Journal of Clinical Pathology*, 59(1), pp. 10–16.
- Damber, J.-E. (2005). Endocrine therapy for prostate cancer. *Acta Oncologica*, 44(6), pp. 605–609.
- Damber, J.-E. and Khatami, A. (2005). Surgical treatment of localized prostate cancer. *Acta Oncologica*, 44(6), pp. 599–604.
- Dang, C. V (2012). Links between metabolism and cancer. *Genes & development*, 26(9), pp. 877–890.
- Das, U. N. (2011). Essential fatty acids enhance free radical generation and lipid peroxidation to induce apoptosis of tumor cells. *Clinical Lipidology*, 6(4), pp. 463–489.

Dasari, S. and Tchounwou, P. B. (2014). Cisplatin in cancer therapy: molecular mechanisms of action. *European journal of pharmacology*, 740, pp. 364–378.

Dayyani, F., Gallick, G. E., Logothetis, C. J. and Corn, P. G. (2011). Novel therapies for metastatic castrate-resistant prostate cancer. *Journal of the National Cancer Institute*, 103(22), pp. 1665–1675.

de Bono, J. S., Logothetis, C. J., Molina, A., Fizazi, K., North, S., Chu, L., Chi, K. N., Jones, R. J., Goodman, O. B., Saad, F., Staffurth, J. N., Mainwaring, P., Harland, S., Flaig, T. W., Hutson, T. E., Cheng, T., Patterson, H., Hainsworth, J. D., Ryan, C. J., Sternberg, C. N., Ellard, S. L., Fléchon, A., Saleh, M., Scholz, M., Efstathiou, E., Zivi, A., Bianchini, D., Loriot, Y., Chieffo, N., Kheoh, T., Haqq, C. M., and Scher, H. I. (2011). Abiraterone and increased survival in metastatic prostate cancer. *The New England journal of medicine*, 364(21), pp. 1995–2005.

de Bono, J. S., Oudard, S., Ozguroglu, M., Hansen, S., Machiels, J.-P., Kocak, I., Gravis, G., Bodrogi, I., Mackenzie, M. J., Shen, L., Roessner, M., Gupta, S., and Sartor, A. O. (2010). Prednisone plus cabazitaxel or mitoxantrone for metastatic castration-resistant prostate cancer progressing after docetaxel treatment: a randomised open-label trial. *The Lancet*, 376(9747), pp. 1147–1154.

Deberardinis, R. J. (2014). Q&A: Targeting metabolism to diagnose and treat cancer. *Cancer & metabolism*, 2(5).

DeBerardinis, R. J. and Chandel, N. S. (2016). Fundamentals of cancer metabolism. *Science Advances*, 2(5), pp. e1600200–e1600200.

DeBerardinis, R. J. and Cheng, T. (2010). Q's next: the diverse functions of glutamine in metabolism, cell biology and cancer. *Oncogene*, 29(3), pp. 313–324.

DeBerardinis, R. J., Mancuso, A., Daikhin, E., Nissim, I., Yudkoff, M., Wehrli, S. and Thompson, C. B. (2007). Beyond aerobic glycolysis: Transformed cells can engage in glutamine metabolism that exceeds the requirement for protein and nucleotide synthesis. *The National Academy of Sciences of the United States of America*, 104(49), pp. 19345- 19350.

Deberardinis, R. J., Sayed, N., Ditsworth, D. and Thompson, C. B. (2008). Brick by brick: metabolism and tumor cell growth. *Current opinion in genetics & development*, 18(1), pp. 54-61.

Debruyne, F. M. J. (2004). Gonadotropin-releasing hormone antagonist in the management of prostate cancer. *Reviews in urology*, 6(Suppl 7), pp. S25-S32.

Delongchamps, N. B. (2014). Prostate cancer: Review in 2014 Detection and characterization: new RNA markers. *Diagnostic and Interventional Imaging*, 95, pp. 739–742.

Demaria, S., Kawashima, N., Yang, A. M., Devitt, M. L., Babb, J. S., Allison, J. P. and Formenti, S. C. (2005). Immune-mediated inhibition of metastases after treatment with local radiation and CTLA-4 blockade in a mouse model of breast cancer. *The American Association for Cancer Research*, 11(2), pp. 728–734.

Demirag, F., Ünsal, E., Yilmaz, A. and çağlar, A. (2005). Prognostic Significance of Vascular Endothelial Growth Factor, Tumor Necrosis, and Mitotic Activity Index in Malignant Pleural Mesothelioma. *Chest*, 128(5), pp. 3382–3387.

Denis, L. J. and Griffiths, K. (2000). Endocrine treatment in prostate cancer. *Seminars in surgical oncology*, 18(1), pp. 52–74.

Dequanter, D., VAN DE Velde, M., Bar, I., Nuyens, V., Rousseau, A., Nagy, N., Vanhamme, L., Vanhaeverbeek, M., Brohée, D., Delrée, P., Boudjeltia, K., Lothaire, P. and Uzureau, P. (2016). Nuclear localization of glutamate-cysteine ligase is associated with proliferation in head and neck squamous cell carcinoma. *Oncology letters*, 11(6), pp. 3660–3668.

- Deshayes, E., Roumiguie, M., Thibault, C., Beuzeboc, P., Cachin, F., Hennequin, C., Huglo, D., Rozet, F., Kassab-Chahmi, D., Rebillard, X. and Houédé, N. (2017). Radium 223 dichloride for prostate cancer treatment. *Drug design, development and therapy*, 11, pp. 2643–2651.
- Desselberger, U. (2017). Reverse genetics of rotavirus. *The National Academy of Sciences of the United States of America*, 114(9), pp. 2106–2108.
- Dewan, M. Z., Galloway, A. E., Kawashima, N., Dewyngaert, J. K., Babb, J. S., Formenti, S. C. and Demaria, S. (2009). Fractionated but Not Single-Dose Radiotherapy Induces an Immune-Mediated Abscopal Effect when Combined with Anti-CTLA-4 Antibody. *Clinical Cancer Research*, 15(17), pp. 5379–5388.
- Dhingra, R., Sharma, T., Singh, S., Sharma, S., Tomar, P., Malhotra, M. and Bhardwaj, T. R. (2013). Enzalutamide: a novel anti-androgen with prolonged survival rate in CRPC patients. *Mini reviews in medicinal chemistry*, 13(10), pp. 1475–1486.
- Dibble, C. C. and Manning, B. D. (2013). Signal integration by mTORC1 coordinates nutrient input with biosynthetic output. *Nature Cell Biology*, 15(6), pp. 555–564.
- Dienstmann, R., Rodon, J., Serra, V. and Tabernero, J. (2014). Picking the Point of Inhibition: A Comparative Review of PI3K/AKT/mTOR Pathway Inhibitors. *Molecular Cancer Therapeutics*, 13(5), pp. 1021–1031.
- Dixon, S. J., Lemberg, K. M., Lamprecht, M. R., Skouta, R., Zaitsev, E. M., Gleason, C. E., Patel, D. N., Bauer, A. J., Cantley, A. M., Yang, W. S., Morrison, B., Stockwell, B. R. and Stockwell, B. R. (2012). Ferroptosis: an iron-dependent form of nonapoptotic cell death. *Cell*, 149(5), pp. 1060–1072.
- Djulgovic, M., Beyth, R. J., Neuberger, M. M., Stoffs, T. L., Vieweg, J., Djulgovic, B. and Dahm, P. (2010). Screening for prostate cancer: systematic review and meta-analysis of randomised controlled trials. *BMJ*, 341, p. c4543.
- Donkena, K. V., Young, C. Y. F. and Tindall, D. J. (2010). Oxidative stress and DNA methylation in prostate cancer. *Obstetrics and gynecology international*, 2010 (ID:302051) pp. 1-14.
- Doskey, C. M., Buranasudja, V., Wagner, B. A., Wilkes, J. G., Du, J., Cullen, J. J. and Buettner, G. R. (2016). Tumor cells have decreased ability to metabolize H₂O₂: Implications for pharmacological ascorbate in cancer therapy. *Redox Biology*, 10, pp. 274–284.
- Du, S., Guan, Z., Hao, L., Song, Y., Wang, L., Gong, L., Liu, L., Qi, X., Hou, Z. and Shao, S. (2014). Fructose-bisphosphate aldolase a is a potential metastasis-associated marker of lung squamous cell carcinoma and promotes lung cell tumorigenesis and migration. *PloS one*, 9(1), pp. e85804.
- Dubrovskaya, A., Kim, S., Salamone, R. J., Walker, J. R., Maira, S.-M., Garcia-Echeverria, C., Schultz, P. G. and Reddy, V. A. (2009). The role of PTEN/Akt/PI3K signaling in the maintenance and viability of prostate cancer stem-like cell populations. *The National Academy of Sciences*, 106(1), pp. 268–273.
- Duchesne, G. (2011). Localised prostate cancer - current treatment options. *Australian family physician*, 40(10), pp. 768–771.
- Duncan, R., Gannavaram, S., Dey, R., Debrabant, A., Lakhali-Naouar, I. and Nakhasi, H. L. (2011). Identification and characterization of genes involved in leishmania pathogenesis: the potential for drug target selection. *Molecular biology international*, 2011, 428486, pp.1-10.
- Ebert, P. S., Hess, R. A., Frykholm, B. C. and Tschudy, D. P. (1979). Succinylacetone, a potent inhibitor of heme biosynthesis: effect on cell growth, heme content and delta-aminolevulinic acid dehydratase activity of malignant murine erythroleukemia cells. *Biochemical and biophysical research communications*, 88(4), pp. 1382–1390.

- Ecke, T. H., Schlechte, H. H., Schiemenz, K., Sachs, M. D., Lenk, S. V., Rudolph, B. D. and Loening, S. A. (2010). TP53 gene mutations in prostate cancer progression. *Anticancer research*, 30(5), pp. 1579–1586.
- Eidelman, E., Twum-Ampofo, J., Ansari, J. and Siddiqui, M. M. (2017). The Metabolic Phenotype of Prostate Cancer. *Frontiers in Oncology*, 7 (131).
- Eisermann, K., Wang, D., Jing, Y., Pascal, L. E. and Wang, Z. (2013). Androgen receptor gene mutation, rearrangement, polymorphism. *Translational andrology and urology*, 2(3), pp. 137–147.
- Elmore, S. (2007). Apoptosis: a review of programmed cell death. *Toxicologic pathology*, 35(4), pp. 495–516.
- Elstrom, R. L., Bauer, D. E., Buzzai, M., Karnauskas, R., Harris, M. H., Plas, D. R., Zhuang, H., Cinalli, R. M., Alavi, A., Rudin, C. M. and Thompson, C. B. (2004). Akt Stimulates Aerobic Glycolysis in Cancer Cells. *Cancer Research*, 64(11), pp. 3892–3899.
- Emilien, G., Ponchon, M., Caldas, C., Isacson, O. and Maloteaux, J. M. (2000). Impact of genomics on drug discovery and clinical medicine. *QJM: monthly journal of the Association of Physicians*, 93(7), pp. 391–423.
- Endo-Munoz, L., Cumming, A., Sommerville, S., Dickinson, I. and Saunders, N. (2010). Osteosarcoma is characterised by reduced expression of markers of osteoclastogenesis and antigen presentation compared with normal bone. *British Journal of Cancer*, 103, pp. 73–81.
- Engelman, J. A., Luo, J. and Cantley, L. C. (2006). The evolution of phosphatidylinositol 3-kinases as regulators of growth and metabolism. *Nature Reviews Genetics*, 7(8), pp. 606–619.
- Epstein, J. I., Egevad, L., Amin, M. B., Delahunt, B., Srigley, J. R., Humphrey, P. A. and Grading Committee (2016). The 2014 International Society of Urological Pathology (ISUP) Consensus Conference on Gleason Grading of Prostatic Carcinoma. *The American Journal of Surgical Pathology*, 40(2), pp. 244–252.
- Epstein, J. I., Zelefsky, M. J., Sjoberg, D. D., Nelson, J. B., Egevad, L., Magi-Galluzzi, C., Vickers, A. J., Parwani, A. V., Reuter, V. E., Fine, S. W., Eastham, J. A., Wiklund, P., Han, M., Reddy, C. A., Ciezki, J. P., Nyberg, T. and Klein, E. A. (2016). A Contemporary Prostate Cancer Grading System: A Validated Alternative to the Gleason Score. *European urology*, 69(3), pp. 428–435.
- Ettinger, S. L., Sobel, R., Whitmore, T. G., Akbari, M., Bradley, D. R., Gleave, M. E. and Nelson, C. C. (2004). Dysregulation of sterol response element-binding proteins and downstream effectors in prostate cancer during progression to androgen independence. *Cancer research*, 64(6), pp. 2212–2221.
- Euling, S. Y. and Kimmel, C. A. (2001). Developmental stage sensitivity and mode of action information for androgen agonists and antagonists. *The Science of the total environment*, 274(1–3), pp. 103–113.
- Farber, S., Diamond, L. K., Mercer, R. D., Sylvester, R. F. and Wolff, J. A. (1948). Temporary Remissions in Acute Leukemia in Children Produced by Folic Acid Antagonist, 4-Aminopteroyl-Glutamic Acid (Aminopterin). *New England Journal of Medicine*, 238(23), pp. 787–793.
- Fay, A. P., Albiges, L. and Bellmunt, J. (2015). Current role of cabozantinib in metastatic castration-resistant prostate cancer. *Expert Review of Anticancer Therapy*. Informa Healthcare, 15(2), pp. 151–156.
- Fehon, R. G., McClatchey, A. I. and Bretscher, A. (2010). Organizing the cell cortex: the role of ERM proteins. *Nature Reviews Molecular Cell Biology*, 11(4), pp. 276–287.
- Feoktistova, M., Geserick, P. and Leverkus, M. (2016). Crystal Violet Assay for Determining Viability of Cultured Cells. *Cold Spring Harbor protocols*, pp. 343-346.

- Ferlay, J., Shin, H.-R., Bray, F., Forman, D., Mathers, C. and Parkin, D. M. (2010). Estimates of worldwide burden of cancer in 2008: GLOBOCAN 2008. *International Journal of Cancer*, 127(12), pp. 2893–2917.
- Fernald, K. and Kurokawa, M. (2013). Evading apoptosis in cancer. *Trends in cell biology*, 23(12), pp. 620–633.
- Fernández-Nogueira, P., Bragado, P., Almendro, V., Ametller, E., Rios, J., Choudhury, S., Mancino, M. and Gascón, P. (2015). Differential expression of neurogenes among breast cancer subtypes identifies high risk patients. *Oncotarget*, 7(5).pp. 5313-5326.
- Festino, L., Vanella, V., Strudel, M. and Ascierto, P. A. (2018). Molecular Mechanisms Underlying the Action of Ipilimumab Against Metastatic Melanoma. *Immunology*, pp. 85–96.
- Festjens, N., Vanden Berghe, T. and Vandenabeele, P. (2006). Necrosis, a well-orchestrated form of cell demise: Signalling cascades, important mediators and concomitant immune response. *Biochimica et Biophysica Acta (BBA) - Bioenergetics*, 1757(9–10), pp. 1371–1387.
- Feun, L., You, M., Wu, C. J., Kuo, M. T., Wangpaichitr, M., Spector, S. and Savaraj, N. (2008). Arginine deprivation as a targeted therapy for cancer. *Current pharmaceutical design*, 14(11), pp. 1049–1057.
- Filhol, O., Ciais, D., Lajaunie, C., Charbonnier, P., Foveau, N., Vert, J.-P. and Vandenbrouck, Y. (2012). DSIR: Assessing the Design of Highly Potent siRNA by Testing a Set of Cancer-Relevant Target Genes. *PLoS ONE*, 7(10), e48057.
- Finkelstein, S. E., Salenius, S., Mantz, C. A., Shore, N. D., Fernandez, E. B., Shulman, J., Myslicki, F. A., Agassi, A. M., Rotterman, Y., DeVries, T. and Sims, R. (2015). Combining Immunotherapy and Radiation for Prostate Cancer. *Clinical Genitourinary Cancer*, 13(1), pp. 1–9.
- Fire, A., Xu, S., Montgomery, M. K., Kostas, S. A., Driver, S. E. and Mello, C. C. (1998). Potent and specific genetic interference by double-stranded RNA in *Caenorhabditis elegans*. *Nature*, 391(6669), pp. 806–811.
- Fitzpatrick, J. M. and de Wit, R. (2014). Taxane Mechanisms of Action: Potential Implications for Treatment Sequencing in Metastatic Castration-resistant Prostate Cancer. *European Urology*, 65(6), pp. 1198–1204.
- Fizazi, K., Jones, R., Oudard, S., Efstathiou, E., Saad, F., de Wit, R., De Bono, J., Cruz, F. M., Fountzilas, G., Ulys, A., Carcano, F., Agarwal, N., Agus, D., Bellmunt, J., Petrylak, D. P., Lee, S.-Y., Webb, I. J., Tejura, B., Borgstein, N. and Dreicer, R. (2015). Phase III, Randomized, Double-Blind, Multicenter Trial Comparing Orteronel (TAK-700) Plus Prednisone With Placebo Plus Prednisone in Patients With Metastatic Castration-Resistant Prostate Cancer That Has Progressed During or After Docetaxel-Based Therapy: ELM-PC 5. *Journal of Clinical Oncology*, 33(7), pp. 723–731.
- Fizazi, K., Ulys, A., Sengeløv, L., Moe, M., Ladoire, S., Thiery-Vuillemin, A., Flechon, A., Guida, A., Bellmunt, J., Climent, M. A., Chowdhury, S., Dumez, H., Matouskova, M., Penel, N., Liutkauskienė, S., Stachurski, L., Sternberg, C. N., Baton, F., Germann, N. and Daugaard, G. (2017). A randomized, double-blind, placebo-controlled phase II study of maintenance therapy with tasquinimod in patients with metastatic castration-resistant prostate cancer responsive to or stabilized during first-line docetaxel chemotherapy. *Annals of Oncology*, 28(11), pp. 2741–2746.
- Flaherty, A. L., Teer, J. and Zhang, J. (2014). IDH1 mutation in prostate cancer: R132H and beyond. *Journal of Clinical Oncology*, 32(4_suppl), pp. 213–213.
- Flaveny, C. A., Griffett, K., El-Dien, B., El-Gendy, M., Solt, L. A., Kamenecka, T. M., Burris, T. P., Kazantzis, M., Sengupta, M., Amelio, A. L., Chatterjee, A. and Walker, J. (2015). Broad Anti-tumor Activity of a Small Molecule that Selectively Targets the Warburg Effect and Lipogenesis. *Cancer cell*, 28, pp. 42–56.

- Flavin, R., Zadra, G. and Loda, M. (2011). Metabolic alterations and targeted therapies in prostate cancer. *The Journal of pathology*, 223(2), pp. 283–294.
- Foley, C. and Mitsiades, N. (2016). Moving Beyond the Androgen Receptor (AR): Targeting AR-Interacting Proteins to Treat Prostate Cancer. *Hormones & cancer*, 7(2), pp. 84–103.
- Förstermann, U. and Sessa, W. C. (2012). Nitric oxide synthases: regulation and function. *European heart journal*, 33(7), p. 829–37, 837a–837d.
- Fox, J. L. and MacFarlane, M. (2016). Targeting cell death signalling in cancer: minimising “Collateral damage”. *British Journal of Cancer*, 115(1), pp. 5–11.
- Franklin, R. B., Feng, P., Milon, B., Desouki, M. M., Singh, K. K., Kajdacsy-Balla, A., Bagasra, O. and Costello, L. C. (2005). hZIP1 zinc uptake transporter down regulation and zinc depletion in prostate cancer. *Molecular cancer*, 4(1), 32.
- Franklin, R. B., Milon, B., Feng, P. and Costello, L. C. (2005). Zinc and zinc transporters in normal prostate and the pathogenesis of prostate cancer. *Frontiers in bioscience : a journal and virtual library*, 10, pp. 2230–2239.
- Franz, M.-C., Anderle, P., Bürzle, M., Suzuki, Y., Freeman, M. R., Hediger, M. A. and Kovacs, G. (2013). Zinc transporters in prostate cancer. *Molecular aspects of medicine*, 34, pp. 735–741.
- Freeman, G. J., Long, A. J., Iwai, Y., Bourque, K., Chernova, T., Nishimura, H., Fitz, L. J., Malenkovich, N., Okazaki, T., Byrne, M. C., Horton, H. F., Fouser, L., Carter, L., Ling, V., Bowman, M. R., Carreno, B. M., Collins, M., Wood, C. R. and Honjo, T. (2000). Engagement of the PD-1 immunoinhibitory receptor by a novel B7 family member leads to negative regulation of lymphocyte activation. *The Journal of experimental medicine*, 192(7), pp. 1027–1034.
- Freitas, M., Baldeiras, I., Proença, T., Alves, V., Mota-Pinto, A. and Sarmento-Ribeiro, A. (2012). Oxidative stress adaptation in aggressive prostate cancer may be counteracted by the reduction of glutathione reductase. *FEBS Open Bio*, 2, pp. 119–128.
- Fridman, J. S. and Lowe, S. W. (2003). Control of apoptosis by p53. *Oncogene*. Nature Publishing Group, 22(56), pp. 9030–9040.
- Friedland, D., Cohen, J., Miller, R., Voloshin, M., Gluckman, R., Lembersky, B., Zidar, B., Keating, M., Reilly, N. and Dimitt, B. (1999). A phase II trial of docetaxel (Taxotere) in hormone-refractory prostate cancer: correlation of antitumor effect to phosphorylation of Bcl-2. *Seminars in oncology*, 26(5 Suppl 17), pp. 19–23.
- Fritz, V. and Fajas, L. (2010). Metabolism and proliferation share common regulatory pathways in cancer cells. *Oncogene*. Inserm, 29(31), pp. 4369–4377.
- Fujino, T., Takei, Y. A., Sone, H., Ioka, R. X., Kamataki, A., Magoori, K., Takahashi, S., Sakai, J. and Yamamoto, T. T. (2001). Molecular identification and characterization of two medium-chain acyl-CoA synthetases, MACS1 and the Sa gene product. *The Journal of biological chemistry*, 276(38), pp. 35961–35966.
- Fukuda, Y., Wang, Y., Lian, S., Lynch, J., Nagai, S., Fanshawe, B., Kandilci, A., Janke, L. J., Neale, G., Fan, Y., Sorrentino, B. P., Roussel, M. F., Grosveld, G. and Schuetz, J. D. (2017). Upregulated heme biosynthesis, an exploitable vulnerability in MYCN-driven leukemogenesis. *JCI insight*, 2(15).
- Fukuhara, H., Inoue, K., Kurabayashi, A., Furihata, M., Fujita, H., Utsumi, K., Sasaki, J. and Shuin, T. (2013). The inhibition of ferrochelatase enhances 5-aminolevulinic acid-based photodynamic action for prostate cancer. *Photodiagnosis and Photodynamic Therapy*, 10(4), pp. 399–409.

- Fulda, S. and Debatin, K.-M. (2006). Extrinsic versus intrinsic apoptosis pathways in anticancer chemotherapy. *Oncogene*, 25(34), pp. 4798–4811.
- Fung, M. K. L. and Chan, G. C.-F. (2017). Drug-induced amino acid deprivation as strategy for cancer therapy. *Journal of Hematology & Oncology*, 10(1), pp. 144.
- Ganapathy-Kanniappan, S. and Geschwind, J.-F. H. (2013). Tumor glycolysis as a target for cancer therapy: progress and prospects. *Molecular cancer*, 12, 152.
- Gardner, A. M., Xu, F. H., Fady, C., Jacoby, F. J., Duffey, D. C., Tu, Y. and Lichtenstein, A. (1997). Apoptotic vs. nonapoptotic cytotoxicity induced by hydrogen peroxide. *Free radical biology & medicine*. 22(1–2), pp. 73–83.
- Gerl, R. and Vaux, D. L. (2004). Apoptosis in the development and treatment of cancer. *Carcinogenesis*, 26(2), pp. 263–270.
- Geybels, M. S., Fang, M., Wright, J. L., Qu, X., Bibikova, M., Klotzle, B., Fan, J.-B., Feng, Z., Ostrander, E. A., Nelson, P. S. and Stanford, J. L. (2017). PTEN loss is associated with prostate cancer recurrence and alterations in tumor DNA methylation profiles. *Oncotarget*, 8(48), pp. 84338–84348.
- Giampazolias, E., Zunino, B., Dhayade, S., Bock, F., Cloix, C., Cao, K., Roca, A., Lopez, J., Ichim, G., Proïcs, E., Rubio-Patiño, C., Fort, L., Yatim, N., Woodham, E., Orozco, S., Taraborrelli, L., Peltzer, N., Lecis, D., Machesky, L., Walczak, H., Albert, M. L., Milling, S., Oberst, A., Ricci, J.-E., Ryan, K. M., Blyth, K. and Tait, S. W. G. (2017). Mitochondrial permeabilization engages NF-κB-dependent anti-tumour activity under caspase deficiency. *Nature Cell Biology*, 19(9), pp. 1116–1129.
- Girotti, A. W. (1998). Lipid hydroperoxide generation, turnover, and effector action in biological systems. *Journal of lipid research*, 39(8), pp. 1529–1542.
- Gleason, D. F. (1992). Histologic grading of prostate cancer: a perspective. *Human pathology*, 23(3), pp. 273–279.
- Gleason, D. F. and Mellinger, G. T. (1974). Prediction of prognosis for prostatic adenocarcinoma by combined histological grading and clinical staging. *The Journal of urology*, 111(1), pp. 58–64.
- Goa, K. L. and Spencer, C. M. (1998). Bicalutamide in advanced prostate cancer. A review. *Drugs & aging*, 12(5), pp. 401–422.
- Goldenberg, S. L. and Bruchofsky, N. (1991). Use of cyproterone acetate in prostate cancer. *The Urologic clinics of North America*, 18(1), pp. 111–122.
- Goldspiel, B. R. and Kohler, D. R. (1990) ‘Flutamide: an antiandrogen for advanced prostate cancer.’, *DICP : the annals of pharmacotherapy*, 24(6), pp. 616–623.
- Gomella, L. G. (2009). Effective testosterone suppression for prostate cancer: is there a best castration therapy?. *Reviews in urology*, 11(2), pp. 52–60.
- Goodspeed, A., Heiser, L. M., Gray, J. W. and Costello, J. C. (2016). Tumor-Derived Cell Lines as Molecular Models of Cancer Pharmacogenomics. *Molecular cancer research : MCR*, 14(1), pp. 3–13.
- Gordetsky, J. and Epstein, J. (2016). Grading of prostatic adenocarcinoma: current state and prognostic implications. *Diagnostic Pathology*, 11, 25.
- Gravis, G., Bladou, F., Salem, N., Macquart-Moulin, G., Serment, G., Camerlo, J., Genre, D., Bardou, V.-J., Maraninchi, D. and Viens, P. (2003). Weekly administration of docetaxel for symptomatic metastatic hormone-refractory prostate carcinoma. *Cancer*, 98(8), pp. 1627–1634.

- Griffin, S., Preta, G. and Sheldon, I. M. (2017). Inhibiting mevalonate pathway enzymes increases stromal cell resilience to a cholesterol-dependent cytotoxin. *Scientific Reports*, 7, 17050.
- Grönberg, H., Damber, L. and Damber, J. E. (1994). Studies of genetic factors in prostate cancer in a twin population. *The Journal of urology*, 152(5 Pt 1), pp. 1484-1487.
- Gross, M. E., Dorff, T. B., Quinn, D. I., Diaz, P. M., Castellanos, O. O. and Agus, D. B. (2018). Safety and Efficacy of Docetaxel, Bevacizumab, and Everolimus for Castration-resistant Prostate Cancer (CRPC). *Clinical Genitourinary Cancer*, 16(1), pp. e11–e21.
- Gross, M. I., Demo, S. D., Dennison, J. B., Chen, L., Chernov-Rogan, T., Goyal, B., Janes, J. R., Laidig, G. J., Lewis, E. R., Li, J., MacKinnon, A. L., Parlati, F., Rodriguez, M. L. M., Shwonek, P. J., Sjogren, E. B., Stanton, T. F., Wang, T., Yang, J., Zhao, F. and Bennett, M. K. (2014). Antitumor Activity of the Glutaminase Inhibitor CB-839 in Triple-Negative Breast Cancer. *Molecular Cancer Therapeutics*, 13(4), pp. 890–901.
- Grossmann, M. E., Huang, H. and Tindall, D. J. (2001). Androgen Receptor Signaling in Androgen-Refractory Prostate Cancer. *JNCI Journal of the National Cancer Institute*, 93(22), pp. 1687–1697.
- Guo, Y., Sklar, G. N., Borkowski, A. and Kyprianou, N. (1997). Loss of the cyclin-dependent kinase inhibitor p27(Kip1) protein in human prostate cancer correlates with tumor grade. *Clinical cancer research*, 3, pp. 2269–2274.
- Gupta, N., Al Ustwani, O., Shen, L. and Pili, R. (2014). Mechanism of action and clinical activity of tasquinimod in castrate-resistant prostate cancer. *OncoTargets and therapy*, 7, pp. 223–234.
- Haas, N., Roth, B., Garay, C., Yeslow, G., Entmacher, M., Weinstein, A., Rogatko, A., Babb, J., Minniti, C., Flinker, D., Gillon, T. and Hudes, G. (2001). Phase I trial of weekly paclitaxel plus oral estramustine phosphate in patients with hormone-refractory prostate cancer. *Urology*, 58(1), pp. 59–64.
- Hadjipavlou, M., Promponas, J. and Madaan, S. (2015). Active surveillance for low-risk prostate cancer. *Journal of Clinical Urology*, 8(6), pp. 420–428.
- Hager, S., Ackermann, C. J., Joerger, M., Gillessen, S. and Omlin, A. (2016). Anti-tumour activity of platinum compounds in advanced prostate cancer—a systematic literature review. *Annals of Oncology*, 27, pp. 975–984.
- Haimovitz-Friedman, A. (1998). Radiation-induced signal transduction and stress response. *Radiation research*, 150(5 Suppl), pp. S102-S108.
- Halliwell, B. and Gutteridge, J. M. (1990). Role of free radicals and catalytic metal ions in human disease: an overview. *Methods in enzymology*, 186, pp. 1–85.
- Hamza, I. and Dailey, H. A. (2012). One ring to rule them all: Trafficking of heme and heme synthesis intermediates in the metazoans. *Biochimica et Biophysica Acta (BBA) - Molecular Cell Research*, 1823(9), pp. 1617–1632.
- Hamilton, W. and Sharp, D. (2004). Symptomatic diagnosis of prostate cancer in primary care: a structured review. *The British journal of general practice : the journal of the Royal College of General Practitioners*, 54(505), pp. 617–621.
- Han, W., Gao, S., Barrett, D., Ahmed, M., Han, D., Macoska, J. A., He, H. H. and Cai, C. (2018). Reactivation of androgen receptor-regulated lipid biosynthesis drives the progression of castration-resistant prostate cancer. *Oncogene*, 37(6), pp. 710–721.
- Hanahan, D. and Weinberg, R. A. (2011). Hallmarks of Cancer: The Next Generation. *Cell*, 144(5), pp. 646–674.

- Harmon, S. A., Bergvall, E., Mena, E., Shih, J. H., Adler, S., McKinney, Y., Mehralivand, S., Citrin, D. E., Couvillon, A., Madan, R., Gulley, J., Mease, R. C., Jacobs, P. M., Pomper, M. G., Turkbey, B., Choyke, P. L. and Lindenberg, M. L. (2018). A Prospective Comparison of ¹⁸F-Sodium Fluoride PET/CT and PSMA-targeted ¹⁸F-DCFBC PET/CT in Metastatic Prostate Cancer. *Journal of Nuclear Medicine*.
- Harvey, H. and deSouza, N. M. (2016). The role of imaging in the diagnosis of primary prostate cancer. *Journal of clinical urology*, 9(2 Suppl), pp. 11–17.
- Hayward, S. W., Dahiya, R., Cunha, G. R., Bartek, J., Deshpande, N. and Narayan, P. (1995). Establishment and characterization of an immortalized but non-transformed human prostate epithelial cell line: BPH-1. *In Vitro Cellular & Developmental Biology - Animal*, 31(1), pp. 14–24.
- Hazra, B. G. and Pore, V. S. (2001). Mifepristone (RU-486), the recently developed antiprogestosterone drug and its analogues. *J. Indian Inst. Sci*, 81, pp. 287–298.
- Hecht, S. M. (1986). The chemistry of activated bleomycin. *Accounts of Chemical Research*. American Chemical Society, 19(12), pp. 383–391.
- Hernandez, D. J., Nielsen, M. E., Han, M. and Partin, A. W. (2007). Contemporary Evaluation of the D'Amico Risk Classification of Prostate Cancer. *Urology*, 70(5), pp. 931–935.
- Heidenberg, H. B., Sesterhenn, I. A., Gaddipati, J. P., Weghorst, C. M., Buzard, G. S., Moul, J. W. and Srivastava, S. (1995). Alteration of the tumor suppressor gene p53 in a high fraction of hormone refractory prostate cancer. *The Journal of urology*, 154(2 Pt 1), pp. 414–421.
- Heinlein, C. a and Chang, C. (2004). Androgen receptor in prostate cancer. *Endocrine reviews*, 25(2), pp. 276–308.
- Helsen, C., Van den Broeck, T., Voet, A., Prekovic, S., Van Poppel, H., Joniau, S. and Claessens, F. (2014). Androgen receptor antagonists for prostate cancer therapy. *Endocrine-related cancer*. BioScientifica, 21(4), pp. T105-T118.
- Hemminki, K. and Vaittinen, P. (1998). Familial breast cancer in the family-cancer database. *International journal of cancer*, 77(3), pp. 386–391.
- Heuer, T. S., Ventura, R., Mordec, K., Lai, J., Fridlib, M., Buckley, D. and Kemble, G. (2017). FASN Inhibition and Taxane Treatment Combine to Enhance Anti-tumor Efficacy in Diverse Xenograft Tumor Models through Disruption of Tubulin Palmitoylation and Microtubule Organization and FASN Inhibition-Mediated Effects on Oncogenic Signaling and Gene Expression. *EBioMedicine*, 16, pp. 51–62.
- Hinsch, A., Brolund, M., Hube-Magg, C., Kluth, M., Simon, R., Möller-Koop, C., Sauter, G., Steurer, S., Luebke, A., Angerer, A., Wittmer, C., Neubauer, E., Göbel, C., Büscheck, F., Minner, S., Wilczak, W., Schlomm, T., Jacobsen, F., Clauditz, T. S., Krech, T., Tsourlakis, M. C. and Schroeder, C. (2018). Immunohistochemically detected IDH1R132H mutation is rare and mostly heterogeneous in prostate cancer. *World Journal of Urology*, 36(6), pp. 877–882.
- Hirawat, S., Budman, D. R. and Kreis, W. (2003). The Androgen Receptor: Structure, Mutations, and Antiandrogens. *Cancer Investigation*, 21(3), pp. 400–417.
- Ho, C. K. M. and Habib, F. K. (2011). Estrogen and androgen signaling in the pathogenesis of BPH. *Nature Reviews Urology*, 8(1), pp. 29–41.
- Hoang, D. T., Iczkowski, K. A., Kilari, D., See, W. and Nevalainen, M. T. (2017). Androgen receptor-dependent and -independent mechanisms driving prostate cancer progression: Opportunities for therapeutic targeting from multiple angles. *Oncotarget*, 8(2), pp. 3724–3745.

- Hodgson, M. C., Bowden, W. A. and Agoulnik, I. U. (2012). Androgen receptor footprint on the way to prostate cancer progression. *World journal of urology*, 30(3), pp. 279–285.
- Homma, Y., Gotoh, M., Yokoyama, O., Masumori, N., Kawachi, A., Yamanishi, T., Ishizuka, O., Seki, N., Kamoto, T., Nagai, A., Ozono, S. and Japanese Urological Association (2011). Outline of JUA clinical guidelines for benign prostatic hyperplasia. *International Journal of Urology*, 18(11), pp. 741–756.
- Hong, S.-W., Shin, J.-S., Moon, J.-H., Kim, Y.-S., Lee, J., Choi, E. K., Ha, S.-H., Lee, D. H., Chung, H. N., Kim, J. E., Kim, K., Hong, Y. S., Lee, J.-L., Lee, W.-J., Choi, E. K., Lee, J. S., Jin, D.-H. and Kim, T. W. (2014). NVP-BEZ235, a dual PI3K/mTOR inhibitor, induces cell death through alternate routes in prostate cancer cells depending on the PTEN genotype. *Apoptosis*, 19(5), pp. 895–904.
- Hooda, J., Alam, M. M. and Zhang, L. (2015a). Evaluating the Association of Heme and Heme Metabolites with Lung Cancer Bioenergetics and Progression. *Postgenomics Drug & Biomarker Development*, 5(3).
- Hooda, J., Alam, M. M. and Zhang, L. (2015b). Measurement of Heme Synthesis Levels in Mammalian Cells. *Journal of Visualized Experiments*, (101), e51579.
- Hooda, J., Cadinu, D., Maksudul Alam, M., Shah, A., Cao, T. M., Sullivan, L. A., Brekken, R. and Zhang, L. (2013). Enhanced Heme Function and Mitochondrial Respiration Promote the Progression of Lung Cancer Cells. *PLoS ONE*, 8(5), e63402.
- Hooda, J., Shah, A. and Zhang, L. (2014). Heme, an Essential Nutrient from Dietary Proteins, Critically Impacts Diverse Physiological and Pathological Processes. *Nutrients*, 6(3), pp. 1080–1102.
- Hoover, P. and Naz, R. K. (2012). Do men with prostate abnormalities (prostatitis/benign prostatic hyperplasia/prostate cancer) develop immunity to spermatozoa or seminal plasma?. *International Journal of Andrology*, 35(4), pp. 608–615.
- Horning, A. M., Wang, Y., Lin, C.-K., Louie, A. D., Jadhav, R. R., Hung, C.-N., Wang, C.-M., Lin, C.-L., Kirma, N. B., Liss, M. A., Kumar, A. P., Sun, L., Liu, Z., Chao, W.-T., Wang, Q., Jin, V. X., Chen, C.-L. and Huang, T. H.-M. (2018). Single-Cell RNA-seq Reveals a Subpopulation of Prostate Cancer Cells with Enhanced Cell-Cycle-Related Transcription and Attenuated Androgen Response. *Cancer research*, 78(4), pp. 853–864.
- Horoszewicz, J. S., Leong, S. S., Chu, T. M., Wajzman, Z. L., Friedman, M., Papsidero, L., Kim, U., Chai, L. S., Kakati, S., Arya, S. K. and Sandberg, A. A. (1980). The LNCaP cell line--a new model for studies on human prostatic carcinoma. *Progress in clinical and biological research*, 37, pp. 115–132.
- Horoszewicz, J. S., Leong, S. S., Kawinski, E., Karr, J. P., Rosenthal, H., Chu, T. M., Mirand, E. A. and Murphy, G. P. (1983). LNCaP model of human prostatic carcinoma. *Cancer research*, 43(4), pp. 1809–1818.
- Hoskin, P., Sartor, O., O’Sullivan, J. M., Johannessen, D. C., Helle, S. I., Logue, J., Bottomley, D., Nilsson, S., Vogelzang, N. J., Fang, F., Wahba, M., Aksnes, A.-K. and Parker, C. (2014). Efficacy and safety of radium-223 dichloride in patients with castration-resistant prostate cancer and symptomatic bone metastases, with or without previous docetaxel use: a prespecified subgroup analysis from the randomised, double-blind, phase 3 ALSYMPCA trial. *The Lancet Oncology*, 15(12), pp. 1397–1406.
- Hotte, S. J. and Saad, F. (2010). Current management of castrate-resistant prostate cancer. *Current oncology*, 17 (Suppl 2), pp. S72-S79.
- Howlader, N., Noone, A., Krapcho, M., Miller, D., Bishop, K., Kosary, C., Yu, M., Ruhl, J., Tatalovich, Z., Mariotto, A., Lewis, D., Chen, H., Feuer, E. and Cronin, K. (2014). Browse the SEER Cancer Statistics Review 1975-2014. *National Cancer Institute. Bethesda*.

- Hsueh, E. C., Knebel, S. M., Lo, W. H., Leung, Y. C., Cheng, P. N. M. and Hsueh, C. T. (2012). Deprivation of arginine by recombinant human arginase in prostate cancer cells. *Journal of hematology & oncology*, 5 (17).
- Huang, M., Koizumi, A., Narita, S., Inoue, T., Tsuchiya, N., Nakanishi, H., Numakura, K., Tsuruta, H., Saito, M., Satoh, S., Nanjo, H., Sasaki, T. and Habuchi, T. (2016). Diet-induced alteration of fatty acid synthase in prostate cancer progression. *Oncogenesis*, 5(2), pp. e195–e195.
- Hudes, G. R., Nathan, F., Khater, C., Haas, N., Cornfield, M., Giantonio, B., Greenberg, R., Gomella, L., Litwin, S., Ross, E., Roethke, S. and McAleer, C. (1997). Phase II trial of 96-hour paclitaxel plus oral estramustine phosphate in metastatic hormone-refractory prostate cancer. *Journal of Clinical Oncology*, 15(9), pp. 3156–3163.
- Hughes, I., Binkley, J., Hurlle, B., Green, E. D., Comparative, N., Program, S., Sidow, A. and Ornitz, D. M. (2008). Identification of the Otopetrin Domain, a conserved domain in vertebrate otopetrins and invertebrate otopetrin-like family members. *BMC Evolutionary Biology*, 8,41.
- Hughes, J. P., Rees, S., Kalindjian, S. B. and Philpott, K. L. (2011). Principles of early drug discovery. *British journal of pharmacology*, 162(6), pp. 1239–1249.
- Hugosson, J., Stranne, J. and Carlsson, S. V. (2011). Radical retropubic prostatectomy: A review of outcomes and side-effects. *Acta Oncologica*, 50(sup1), pp. 92–97.
- Humbert, P. O., Grzeschik, N. A., Brumby, A. M., Galea, R., Elsum, I. and Richardson, H. E. (2008). Control of tumourigenesis by the Scribble/Dlg/Lgl polarity module. *Oncogene*, 27(55), pp. 6888–6907.
- Humphrey, P. A. (2004). Gleason grading and prognostic factors in carcinoma of the prostate. *Modern Pathology*, 17(3), pp. 292–306.
- Hung, C. H., Chan, S. H., Chu, P. M. and Tsai, K. L. (2015). Docetaxel facilitates endothelial dysfunction through oxidative stress via modulation of protein kinase C beta: The protective effects of sotrastaurin. *Toxicological Sciences* 145(1), pp. 59–67.
- Hunter, G. A. and Ferreira, G. C. (2009). 5-aminolevulinic acid synthase: catalysis of the first step of heme biosynthesis. *Cellular and molecular biology*, 55(1), pp. 102–110.
- Hwang, C. (2012). Overcoming docetaxel resistance in prostate cancer: a perspective review. *Therapeutic advances in medical oncology*. SAGE Publications, 4(6), pp. 329–340.
- Imamura, Y. and Sadar, M. D. (2016). Androgen receptor targeted therapies in castration-resistant prostate cancer: Bench to clinic. *International Journal of Urology*, 23(8), pp. 654–665.
- Imamura, Y., Sakamoto, S., Endo, T., Utsumi, T., Fuse, M., Suyama, T., Kawamura, K., Imamoto, T., Yano, K., Uzawa, K., Nihei, N., Suzuki, H., Mizokami, A., Ueda, T., Seki, N., Tanzawa, H. and Ichikawa, T. (2012). FOXA1 Promotes Tumor Progression in Prostate Cancer via the Insulin-Like Growth Factor Binding Protein 3 Pathway. *PLoS ONE*, 7(8), p. e42456.
- Ionov, Y., Yamamoto, H., Krajewski, S., Reed, J. C. and Perucho, M. (2000). Mutational inactivation of the proapoptotic gene BAX confers selective advantage during tumor clonal evolution. *The National Academy of Sciences*, 97(20), pp. 10872–10877.
- Isbarn, H., Boccon-Gibod, L., Carroll, P. R., Montorsi, F., Schulman, C., Smith, M. R., Sternberg, C. N. and Studer, U. E. (2009). Androgen deprivation therapy for the treatment of prostate cancer: consider both benefits and risks. *European urology*, 55(1), pp. 62–75.

- Itano, N., Sawai, T., Miyaishi, O., Kimata, K., Underhill, C. B. and Zhang, L. (1999). Relationship between hyaluronan production and metastatic potential of mouse mammary carcinoma cells. *Cancer research*, 59(10), pp. 2499–2504.
- Jacque, N., Ronchetti, A. M., Larrue, C., Meunier, G., Birsén, R., Willems, L., Saland, E., Decroocq, J., Maciel, T. T., Lambert, M., Poulain, L., Hospital, M. A., Sujobert, P., Joseph, L., Chapuis, N., Lacombe, C., Moura, I. C., Demo, S., Sarry, J. E., Recher, C., Mayeux, P., Tamburini, J. and Bouscary, D. (2015). Targeting glutaminolysis has antileukemic activity in acute myeloid leukemia and synergizes with BCL-2 inhibition. *Blood*, 126(11), pp. 1346–1356.
- Jain, M., Nilsson, R., Sharma, S., Madhusudhan, N., Kitami, T., Souza, A. L., Kafri, R., Kirschner, M. W., Clish, C. B. and Mootha, V. K. (2012). Metabolite Profiling Identifies a Key Role for Glycine in Rapid Cancer Cell Proliferation. *Science*, 336(6084), pp. 1040–1044.
- Jao, S. W., Beart, R. W., Reiman, H. M., Gunderson, L. L. and Ilstrup, D. M. (1987). Colon and anorectal cancer after pelvic irradiation. *Diseases of the colon and rectum*, 30(12), pp. 953–958.
- Jarrard, D. F., Kinoshita, H., Shi, Y., Sandefur, C., Hoff, D., Meisner, L. F., Chang, C., Herman, J. G., Isaacs, W. B. and Nassif, N. (1998). Methylation of the androgen receptor promoter CpG island is associated with loss of androgen receptor expression in prostate cancer cells. *Cancer research*, 58(23), pp. 5310–5314.
- Jeon, J. Nim, S., Teyra, J., Datti, A., Wrana, J. L., Sidhu, S.S., Moffat, J., and Kim, P. M. (2014). A systematic approach to identify novel cancer drug targets using machine learning, inhibitor design and high-throughput screening. *Genome medicine*, 6(7), 57.
- Jernberg, E., Bergh, A. and Wikström, P. (2017). Clinical relevance of androgen receptor alterations in prostate cancer. *Endocrine connections*, 6(8), pp. R146–R161.
- Ji, S., Zhang, B., Liu, J., Qin, Y., Liang, C., Shi, S., Jin, K., Liang, D., Xu, W., Xu, H., Wang, W., Wu, C., Liu, L., Liu, C., Xu, J., Ni, Q. and Yu, X. (2016). ALDOA functions as an oncogene in the highly metastatic pancreatic cancer. *Cancer Letters*, 374(1), pp. 127–135.
- Jiang, L., Kon, N., Li, T., Wang, S.-J., Su, T., Hibshoosh, H., Baer, R. and Gu, W. (2015). Ferroptosis as a p53-mediated activity during tumour suppression. *Nature*, 520(7545), pp. 57–62.
- Jin, S., DiPaola, R. S., Mathew, R. and White, E. (2007). Metabolic catastrophe as a means to cancer cell death. *Journal of cell science*, 120(Pt 3), pp. 379–383.
- Johns, L. E. and Houlston, R. S. (2003). A systematic review and meta-analysis of familial prostate cancer risk. *BJU international*, 91(9), pp. 789–794.
- Johnson, M. H., Ross, A. E., Alshalalfā, M., Erho, N., Yousefi, K., Glavaris, S., Fedor, H., Han, M., Faraj, S. F., Bezerra, S. M., Netto, G., Partin, A. W., Trock, B. J., Davicioni, E. and Schaeffer, E. M. (2016). SPINK1 Defines a Molecular Subtype of Prostate Cancer in Men with More Rapid Progression in an at Risk, Natural History Radical Prostatectomy Cohort. *The Journal of Urology*, 196(5), pp. 1436–1444.
- Jones, C. U., Hunt, D., McGowan, D. G., Amin, M. B., Chetner, M. P., Bruner, D. W., Leibenhaut, M. H., Husain, S. M., Rotman, M., Souhami, L., Sandler, H. M. and Shipley, W. U. (2011). Radiotherapy and Short-Term Androgen Deprivation for Localized Prostate Cancer. *New England Journal of Medicine*, 365(2), pp. 107–118.
- Jones, L. H. (2016). An industry perspective on drug target validation. *Expert Opinion on Drug Discovery*. Taylor & Francis, 11(7), pp. 623–625.
- Kaighn, M. E., Narayan, K. S., Ohnuki, Y., Lechner, J. F. and Jones, L. W. (1979). Establishment and characterization of a human prostatic carcinoma cell line (PC-3). *Investigative urology*, 17(1), pp. 16–23.

- Kajita, E., Moriwaki, J., Yatsuki, H., Hori, K., Miura, K., Hirai, M. and Shiokawa, K. (2001). Quantitative expression studies of aldolase A, B and C genes in developing embryos and adult tissues of *Xenopus laevis*. *Mechanisms of development*, 102(2001), pp. 283–287.
- Takehi, Y. (2003). Watchful Waiting as a Treatment Option for Localized Prostate Cancer in the PSA Era. *Japanese Journal of Clinical Oncology*, 33(1), pp. 1–5.
- Kalinowski, D. S. and Richardson, D. R. (2005). The evolution of iron chelators for the treatment of iron overload disease and cancer. *Pharmacological reviews*, 57(4), pp. 547–583.
- Kalyanaraman, B. (2017). Teaching the basics of cancer metabolism: Developing antitumor strategies by exploiting the differences between normal and cancer cell metabolism. *Redox Biology*, 12, pp. 833–842.
- Kan, Z., Jaiswal, B. S., Stinson, J., Janakiraman, V., Bhatt, D., Stern, H. M., Yue, P., Haverty, P. M., Bourgon, R., Zheng, J., Moorhead, M., Chaudhuri, S., Tomsho, L. P., Peters, B. A., Pujara, K., Cordes, S., Davis, D. P., Carlton, V. E. H., Yuan, W., Li, L., Wang, W., Eigenbrot, C., Kaminker, J. S., Eberhard, D. A., Waring, P., Schuster, S. C., Modrusan, Z., Zhang, Z., Stokoe, D., de Sauvage, F. J., Faham, M. and Seshagiri, S. (2010). Diverse somatic mutation patterns and pathway alterations in human cancers. *Nature*, 466(7308), pp. 869–873.
- Kanade, T., Yin, Z., Bise, R., Huh, S., Eom, S., Sandbothe, M. F. and Chen, M. (2011). Cell image analysis: Algorithms, system and applications. *Institute of Electrical and Electronics Engineers (IEEE)*, pp. 374–381.
- Kanduc, D., Mittelman, A., Serpico, R., Sinigaglia, E., Sinha, A., Natale, C., Santacroce, R., Di Corcia, M., Lucchese, A., Dini, L., Pani, P., Santacroce, S., Simone, S., Bucci, R. and Farber, E. (2002). Cell death: Apoptosis versus necrosis (Review). *International Journal of Oncology*, 21(1), pp. 165–170.
- Kang, C. B., Hong, Y., Dhe-Paganon, S. and Yoon, H. S. (2008). FKBP Family Proteins: Immunophilins with Versatile Biological Functions. *Neurosignals*, 16(4), pp. 318–325.
- Kang, S. W., Kang, H., Park, I. S., Choi, S. H., Shin, K. H., Chun, Y. S., Chun, B. G. and Min, B. H. (2000). Cytoprotective effect of arginine deiminase on taxol-induced apoptosis in DU145 human prostate cancer cells. *Molecules and cells*, 10(3), pp. 331–337.
- Kantoff, P. W., Halabi, S., Conaway, M., Picus, J., Kirshner, J., Hars, V., Trump, D., Winer, E. P. and Vogelzang, N. J. (1999). Hydrocortisone With or Without Mitoxantrone in Men With Hormone-Refractory Prostate Cancer: Results of the Cancer and Leukemia Group B 9182 Study. *Journal of Clinical Oncology*, 17(8), pp. 2506–2506.
- Karantanos, T., Corn, P. G. and Thompson, T. C. (2013). Prostate cancer progression after androgen deprivation therapy: mechanisms of castrate resistance and novel therapeutic approaches. *Oncogene*, 32(49), pp. 5501–5511.
- Kareva, I. (2017). A Combination of Immune Checkpoint Inhibition with Metronomic Chemotherapy as a Way of Targeting Therapy-Resistant Cancer Cells. *International journal of molecular sciences*, 18(10).
- Karl, A. and Konety, B. (2009). Androgen deprivation therapy for prostate cancer: indications, contraindications and possible consequences. *F1000 medicine reports*, 2(1).
- Kassouf, W., Tanguay, S. and Aprikian, A. (2003). Nilutamide as Second Line Hormone Therapy for Prostate Cancer After Androgen Ablation Fails. *The Journal of Urology*, 169(5), pp. 1742–1744.
- Kaur, A. and Sharma, S. (2017). Mammalian target of rapamycin (mTOR) as a potential therapeutic target in various diseases. *Inflammopharmacology*, 25(3), pp. 293–312.
- Kawahara, A., Ohsawa, Y., Matsumura, H., Uchiyama, Y. and Nagata, S. (1998). Caspase-independent cell killing by Fas-associated protein with death domain. *The Journal of cell biology*, 143(5), pp. 1353–1360.

- Kawai, K., Uemura, M., Munakata, K., Takahashi, H., Haraguchi, N., Nishimura, J., Hata, T., Matsuda, C., Ikenaga, M., Murata, K., Mizushima, T., Yamamoto, H., Doki, Y. and Mori, M. (2017). Fructose-bisphosphate aldolase A is a key regulator of hypoxic adaptation in colorectal cancer cells and involved in treatment resistance and poor prognosis. *International Journal of Oncology*, 50(2), pp. 525–534.
- Kelly, W. K., Curley, T., Slovin, S., Heller, G., McCaffrey, J., Bajorin, D., Ciolino, A., Regan, K., Schwartz, M., Kantoff, P., George, D., Oh, W., Smith, M., Kaufman, D., Small, E. J., Schwartz, L., Larson, S., Tong, W. and Scher, H. (2001). Paclitaxel, Estramustine Phosphate, and Carboplatin in Patients With Advanced Prostate Cancer. *Journal of Clinical Oncology*, 19(1), pp. 44–53.
- Kemmner, W., Wan, K., Rüttinger, S., Ebert, B., Macdonald, R., Klamm, U. and Moesta, K. T. (2008). Silencing of human ferrochelatase causes abundant protoporphyrin-IX accumulation in colon cancer. *The FASEB Journal*, 22(2), pp. 500–509.
- Keyes, M., Crook, J., Morton, G., Vigneault, E., Usmani, N. and Morris, W. J. (2013). Treatment options for localized prostate cancer. *Canadian family physician Medecin de famille canadien*, 59(12), pp. 1269–1274.
- Kigawa, J., Minagawa, Y., Cheng, X. and Terakawa, N. (1998). Gamma-glutamyl cysteine synthetase up-regulates glutathione and multidrug resistance-associated protein in patients with chemoresistant epithelial ovarian cancer. *Clinical cancer research*, 4(7), pp. 1737–1741.
- Kim, E. Y., Jung, J. Y., Kim, A., Kim, K. and Chang, Y. S. (2017). Methionyl-tRNA synthetase overexpression is associated with poor clinical outcomes in non-small cell lung cancer. *BMC cancer*. BioMed Central, 17(1), 467.
- Kim, G., Ison, G., McKee, A. E., Zhang, H., Tang, S., Gwise, T., Sridhara, R., Lee, E., Tzou, A., Philip, R., Chiu, H.-J., Ricks, T. K., Palmby, T., Russell, A. M., Ladouceur, G., Pfuma, E., Li, H., Zhao, L., Liu, Q., Venugopal, R., Ibrahim, A. and Pazdur, R. (2015). FDA Approval Summary: Olaparib Monotherapy in Patients with Deleterious Germline BRCA-Mutated Advanced Ovarian Cancer Treated with Three or More Lines of Chemotherapy. *Clinical cancer research*, 21(19), pp. 4257–4261.
- Kirby, R. S., Fitzpatrick, J. M. and Clarke, N. (2009). Abarelix and other gonadotrophin-releasing hormone antagonists in prostate cancer. *BJU International*, 104(11), pp. 1580–1584.
- Kishi, H., Mukai, T., Hirono, A., Fujii, H., Miwa, S. and Hori, K. (1987). Human aldolase A deficiency associated with a hemolytic anemia: thermolabile aldolase due to a single base mutation. *The National Academy of Sciences of the United States of America*, 84(23), pp. 8623–8627.
- Kishton, R. J. and Rathmell, J. C. (2015). Novel therapeutic targets of tumor metabolism. *Cancer journal*, 21(2), pp. 62–69.
- Klotz, L. (2008). Maximal androgen blockade for advanced prostate cancer. *Best Practice & Research Clinical Endocrinology & Metabolism*, 22(2), pp. 331–340.
- Kluth, M., Harasimowicz, S., Burkhardt, L., Grupp, K., Krohn, A., Prien, K., Gjoni, J., Haß, T., Galal, R., Graefen, M., Haese, A., Simon, R., He Uhne-Simon, J., Koop, C., Korb, J., Weischenfeld, J., Huland, H., Sauter, G., Quaas, A., Wilczak, W., Tsourlakakis, M.-C., Minner, S. and Schlomm, T. (2014). Clinical significance of different types of p53 gene alteration in surgically treated prostate cancer. *International Journal of Cancer*, 135, pp. 1369–1380.
- Knudsen, K. E. and Penning, T. M. (2010). Partners in crime: deregulation of AR activity and androgen synthesis in prostate cancer. *Trends in Endocrinology & Metabolism*, 21(5), pp. 315–324.
- Koivisto, P., Kononen, J., Palmberg, C., Tammela, T., Hyytinen, E., Isola, J., Trapman, J., Cleutjens, K., Noordzij, A., Visakorpi, T. and Kallioniemi, O. P. (1997). Androgen receptor gene amplification: a possible molecular mechanism for androgen deprivation therapy failure in prostate cancer. *Cancer research*, 57(2), pp. 314–319.

- Kolvenbag, G. J. C. M. and Furr, B. J. A. (2009). Nonsteroidal Antiandrogens. in *Hormone Therapy in Breast and Prostate Cancer*. pp. 347–368.
- Koppenol, W. H., Bounds, P. L. and Dang, C. V. (2011). Otto Warburg's contributions to current concepts of cancer metabolism. *Nature reviews*, 11(5), pp. 325–37.
- Kozempel, J., Mokhodoeva, O. and Vlk, M. (2018). Progress in Targeted Alpha-Particle Therapy. What We Learned about Recoils Release from In Vivo Generators. *Molecules*, 23(3), p. 581.
- Kreis, W., Budman, D. R. and Calabro, A. (1997). Unique synergism or antagonism of combinations of chemotherapeutic and hormonal agents in human prostate cancer cell lines. *British journal of urology*, 79(2), pp. 196–202.
- Kreis, W., Budman, D. R., Fetten, J., Gonzales, A. L., Barile, B. and Vinciguerra, V. (1999). Phase I trial of the combination of daily estramustine phosphate and intermittent docetaxel in patients with metastatic hormone refractory prostate carcinoma. *Annals of oncology*, 10(1), pp. 33–38.
- Kridel, S. J., Axelrod, F., Rozenkrantz, N. and Smith, J. W. (2004). Orlistat is a novel inhibitor of fatty acid synthase with antitumor activity. *Cancer research*, 64(6), pp. 2070–2075.
- Kroemer, G. and Pouyssegur, J. (2008). Tumor cell metabolism: cancer's Achilles' heel. *Cancer cell*, 13(6), pp. 472–482.
- Kroenke, B. A., Grabner, A., Hannus, M., Sachse, C. and Dorris, D. (2004). Using RNAi to identify and validate novel drug targets-targeting human kinases with an siRNA library. *Drug Discovery World*, pp. 53–62.
- Kumar, B., Koul, S., Khandrika, L., Meacham, R. B. and Koul, H. K. (2008). Oxidative Stress Is Inherent in Prostate Cancer Cells and Is Required for Aggressive Phenotype. *Cancer Research*, 68(6), pp. 1777–1785.
- Kumar, B. and Lupold, S. E. (2016). MicroRNA expression and function in prostate cancer: a review of current knowledge and opportunities for discovery. *Asian journal of andrology*, 18(4), pp. 559–567.
- Kumar, R., Srivastava, R. and Srivastava, S. (2015). Detection and Classification of Cancer from Microscopic Biopsy Images Using Clinically Significant and Biologically Interpretable Features. *Journal of Medical Engineering*, 2015, 457906.
- Kumar, S., Shelley, M., Harrison, C., Coles, B., Wilt, T. J. and Mason, M. (2006). Neo-adjuvant and adjuvant hormone therapy for localised and locally advanced prostate cancer. *Cochrane Database of Systematic Reviews*, (4), CD006019.
- Kumar, V. L. and Majumder, P. K. (1995). Prostate gland: structure, functions and regulation. *International urology and nephrology*, 27(3), pp. 231–243.
- Kuo, M. T., Bao, J., Furuichi, M., Yamane, Y., Gomi, A., Savaraj, N., Masuzawa, T. and Ishikawa, T. (1998). Frequent coexpression of MRP/GS-X pump and γ -glutamylcysteine synthetase mRNA in drug-resistant cells, untreated tumor cells, and normal mouse tissues. *Biochemical Pharmacology*, 55(5), pp. 605–615.
- Kuo, Y.-Z., Fang, W.-Y., Huang, C.-C., Tsai, S.-T., Wang, Y.-C., Yang, C.-L. and Wu, L.-W. (2017). Hyaluronan synthase 3 mediated oncogenic action through forming inter-regulation loop with tumor necrosis factor alpha in oral cancer. *Oncotarget*, 8(9), pp. 15563–15583.
- Kusmartsev, S., Nefedova, Y., Yoder, D. and Gabrilovich, D. I. (2004). Antigen-specific inhibition of CD8+ T cell response by immature myeloid cells in cancer is mediated by reactive oxygen species. *Journal of immunology (Baltimore, Md. : 1950)*, 172(2), pp. 989–999.

- Kwon, N. H., Kang, T., Lee, J. Y., Kim, H. H., Kim, H. R., Hong, J., Oh, Y. S., Han, J. M., Ku, M. J., Lee, S. Y. and Kim, S. (2011). Dual role of methionyl-tRNA synthetase in the regulation of translation and tumor suppressor activity of aminoacyl-tRNA synthetase-interacting multifunctional protein-3. *The National Academy of Sciences*, 108(49), pp. 19635–19640.
- Labi, V. and Erlacher, M. (2015). How cell death shapes cancer. *Cell Death and Disease*, 6(3), e1675.
- Lai, E., Singh, R., Teng, B., Zhao, Y., Sharratt, E., Howell, G., Rajput, A. and Bullard Dunn, K. (2010) 'Inhibition of Hyaluronan Synthase-3 Decreases Subcutaneous Colon Cancer Growth in Mice', *Diseases of the Colon & Rectum*, 53(4), pp. 475–482.
- Laplanche, M. and Sabatini, D. M. (2012). mTOR signaling in growth control and disease. *Cell*, 149(2), pp. 274–293.
- Laster, S. M., Wood, J. G. and Gooding, L. R. (1988). Tumor necrosis factor can induce both apoptic and necrotic forms of cell lysis. *Journal of immunology*, 141(8), pp. 2629–1634.
- Layer, G., Reichelt, J., Jahn, D. and Heinz, D. W. (2010). Structure and function of enzymes in heme biosynthesis. *Protein science*, 19(6), pp. 1137–61.
- Le, A., Lane, A. N., Hamaker, M., Bose, S., Gouw, A., Barbi, J., Tsukamoto, T., Rojas, C. J., Slusher, B. S., Zhang, H., Zimmerman, L. J., Liebler, D. C., Slebos, R. J. C., Lorkiewicz, P. K., Higashi, R. M., Fan, T. W. M. and Dang, C. V. (2012). Glucose-Independent Glutamine Metabolism via TCA Cycling for Proliferation and Survival in B Cells. *Cell Metabolism*, 15(1), pp. 110–121.
- Lee, K.-M., Kang, D., Park, S. K., Berndt, S. I., Reding, D., Chatterjee, N., Chanock, S., Huang, W.-Y. and Hayes, R. B. (2009). Nitric oxide synthase gene polymorphisms and prostate cancer risk. *Carcinogenesis*, 30(4), pp. 621–625.
- Leong, F. J. W.-M., Brady, M. and McGee, J. O. (2003). Correction of uneven illumination (vignetting) in digital microscopy images. *Journal of clinical pathology*, 56(8), pp. 619–621.
- Lepor, H. (2000). Selecting candidates for radical prostatectomy. *Reviews in urology*, 2(3), pp. 182–189.
- Lepor, H. and Shore, N. D. (2012). LHRH Agonists for the Treatment of Prostate Cancer: 2012. *Reviews in urology*, 14(1–2), pp. 1–12.
- Lessner, H. E., Valenstein, S., Kaplan, R., DeSimone, P. and Yunis, A. (1980). Phase II study of L-asparaginase in the treatment of pancreatic carcinoma. *Cancer treatment reports*, 64(12), pp. 1359–1361.
- Lew, C. R. and Tolan, D. R. (2012). Targeting of Several Glycolytic Enzymes Using RNA Interference Reveals Aldolase Affects Cancer Cell Proliferation through a Non-glycolytic Mechanism. *Journal of Biological Chemistry*, 287(51), pp. 42554–42563.
- Li, J., Jiang, D., Zhou, H., Li, F., Yang, J., Hong, L., Fu, X., Li, Z., Liu, Z., Li, J. and Zhuang, C. (2011). Expression of RNA-Interference/Antisense Transgenes by the Cognate Promoters of Target Genes Is a Better Gene-Silencing Strategy to Study Gene Functions in Rice. *PLoS ONE*, 6(3), e17444.
- Li, J., Yen, C., Liaw, D., Podsypanina, K., Bose, S., Wang, S. I., Puc, J., Miliareis, C., Rodgers, L., McCombie, R., Bigner, S. H., Giovanella, B. C., Ittmann, M., Tycko, B., Hibshoosh, H., Wigler, M. H. and Parsons, R. (1997). PTEN, a putative protein tyrosine phosphatase gene mutated in human brain, breast, and prostate cancer. *Science (New York, N.Y.)*, 275(5308), pp. 1943–1947.
- Li, M., Zhang, Z., Yuan, J., Zhang, Y. and Jin, X. (2014). Altered glutamate cysteine ligase expression and activity in renal cell carcinoma. *Biomedical reports*, 2(6), pp. 831–834.

- Li, R., Ravizzini, G. C., Gorin, M. A., Maurer, T., Eiber, M., Cooperberg, M. R., Alemozzaffar, M., Tollefson, M. K., Delacroix, S. E. and Chapin, B. F. (2018). The use of PET/CT in prostate cancer. *Prostate Cancer and Prostatic Diseases*, 21(1), pp. 4–21.
- Li, Y., Li, X., Hussain, M. and Sarkar, F. H. (2004). Regulation of Microtubule, Apoptosis, and Cell Cycle-Related Genes by Taxotere in Prostate Cancer Cells Analyzed by Microarray 1. *Neoplasia*, 6, pp. 158–167.
- Liang, M. and Mulholland, D. J. (2014). Lipogenic metabolism: a viable target for prostate cancer treatment?. *Asian journal of andrology*, 16(5), pp. 661–663.
- Lim, K. Bin (2017). Epidemiology of clinical benign prostatic hyperplasia. *Asian journal of urology*, 4(3), pp. 148–151.
- Lim, S.-C., Choi, J. E., Kang, H. S. and Si, H. (2009). Ursodeoxycholic acid switches oxaliplatin-induced necrosis to apoptosis by inhibiting reactive oxygen species production and activating p53-caspase 8 pathway in HepG2 hepatocellular carcinoma. *Int. J. Cancer*, 126, pp. 1582–1595.
- Lin, I. Y., Yen, C. H., Liao, Y. J., Lin, S. E., Ma, H. P., Chan, Y.-. and Chen, Y. M. A. (2013). Identification of FKBP11 as a biomarker for hepatocellular carcinoma. *Anticancer research*, 33(6), pp. 2763–2769.
- Lin, Y., Choksi, S., Shen, H.-M., Yang, Q.-F., Hur, G. M., Kim, Y. S., Tran, J. H., Nedospasov, S. A. and Liu, Z. (2004). Tumor Necrosis Factor-induced Nonapoptotic Cell Death Requires Receptor-interacting Protein-mediated Cellular Reactive Oxygen Species Accumulation. *Journal of Biological Chemistry*, 279(11), pp. 10822–10828.
- Lin, Y., Fukuchi, J., Hiipakka, R. A., Kokontis, J. M. and Xiang, J. (2007). Up-regulation of Bcl-2 is required for the progression of prostate cancer cells from an androgen-dependent to an androgen-independent growth stage. *Cell Research*, 17(6), pp. 531–536.
- Lindsay, M. a (2003). Target discovery. *Nature reviews. Drug discovery*, 2(10), pp. 831–838.
- Linja, M. J., Savinainen, K. J., Saramäki, O. R., Tammela, T. L., Vessella, R. L. and Visakorpi, T. (2001). Amplification and overexpression of androgen receptor gene in hormone-refractory prostate cancer. *Cancer research*, 61(9), pp. 3550–3555.
- Liou, G.-Y. and Storz, P. (2010). Reactive oxygen species in cancer. *Free radical research*, 44(5), pp. 479–496.
- Litwin, M. S. and Tan, H.-J. (2017). The Diagnosis and Treatment of Prostate Cancer. *JAMA*, 317(24), p. 2532.
- Liu, B., Ezeogu, L., Zellmer, L., Yu, B., Xu, N. and Joshua Liao, D. (2015). Protecting the normal in order to better kill the cancer. *Cancer medicine*, 4(9), pp. 1394–1403.
- Liu, J. F., Nie, X. C., Shao, Y. C., Su, W.-H., Ma, H. Y. and Xu, X. Y. (2016). Bleomycin Suppresses the Proliferation and the Mobility of Human Gastric Cancer Cells Through the Smad Signaling Pathway. *Cellular physiology and biochemistry*, 40(6), pp. 1401–1409.
- Liu, N., Gao, F., Han, Z., Xu, X., Underhill, C. B. and Zhang, L. (2001). Hyaluronan synthase 3 overexpression promotes the growth of TSU prostate cancer cells. *Cancer research*, 61(13), pp. 5207–14.
- Liu, T., Kishton, R. J., Macintyre, A. N., Gerriets, V. A., Xiang, H., Liu, X., Abel, E. D., Rizzieri, D., Locasale, J. W. and Rathmell, J. C. (2014). Glucose transporter 1-mediated glucose uptake is limiting for B-cell acute lymphoblastic leukemia anabolic metabolism and resistance to apoptosis. *Cell Death & Disease*, 5(10), e1470.

Liu, Y. (2006). Fatty acid oxidation is a dominant bioenergetic pathway in prostate cancer', *Prostate Cancer and Prostatic Diseases*, 9(3), pp. 230–234.

Liu, Y., Cao, Y., Zhang, W., Bergmeier, S., Qian, Y., Akbar, H., Colvin, R., Ding, J., Tong, L., Wu, S., Hines, J. and Chen, X. (2012). A Small-Molecule Inhibitor of Glucose Transporter 1 Downregulates Glycolysis, Induces Cell-Cycle Arrest, and Inhibits Cancer Cell Growth In Vitro and In Vivo. *Molecular Cancer Therapeutics*, 11(8), pp. 1672–1682.

Loeb, S., Zhou, Q., Siebert, U., Rochau, U., Jahn, B., Mühlberger, N., Carter, H. B., Lepor, H. and Braithwaite, R. S. (2017) 'Active Surveillance Versus Watchful Waiting for Localized Prostate Cancer: A Model to Inform Decisions', *European Urology*, 72(6), pp. 899–907.

Loftus, T. M., Jaworsky, D. E., Frehywot, G. L., Townsend, C. A., Ronnett, G. V, Lane, M. D. and Kuhajda, F. P. (2000). Reduced food intake and body weight in mice treated with fatty acid synthase inhibitors. *Science (New York, N.Y.)*, 288(5475), pp. 2379–2381.

Logothetis, C. J. and Lin, S.-H. (2005). Osteoblasts in prostate cancer metastasis to bone. *Nature Reviews Cancer*, 5(1), pp. 21–28.

Lowe, S. W. and Lin, A. W. (2000). Apoptosis in cancer. *Carcinogenesis. Oxford University Press*, 21(3), pp. 485–495.

Lu, T., Ramakrishnan, R., Altiok, S., Youn, J.-I., Cheng, P., Celis, E., Pisarev, V., Sherman, S., Sporn, M. B. and Gabilovich, D. (2011). Tumor-infiltrating myeloid cells induce tumor cell resistance to cytotoxic T cells in mice. *The Journal of clinical investigation*, 121(10), pp. 4015–4029.

Luengo, A., Gui, D. Y. and Vander Heiden, M. G. (2017). Targeting Metabolism for Cancer Therapy. *Cell Chemical Biology*, 24(9), pp. 1161–1180.

Lund, L., Svolgaard, N. and Poulsen, M. H. (2014). Prostate cancer: a review of active surveillance. *Research and reports in urology*, 6, pp. 107–112.

Lundström, E. A., Rencken, R. K., van Wyk, J. H., Coetzee, L. J. E., Bahlmann, J. C. M., Reif, S., Strasheim, E. A., Bigalke, M. C., Pontin, A. R., Goedhals, L., Steyn, D. G., Heyns, C. F., Aldera, L. A., Mackenzie, T. M., Purcea, D., Groscurin, P. Y. and Porchet, H. C. (2009). Triptorelin 6-Month Formulation in the Management of Patients with Locally Advanced and Metastatic Prostate Cancer. *Clinical Drug Investigation*, 29(12), pp. 757–765.

Lunt, S. Y. and Vander Heiden, M. G. (2011). Aerobic Glycolysis: Meeting the Metabolic Requirements of Cell Proliferation. *Annual Review of Cell and Developmental Biology*, 27(1), pp. 441–464.

Lushchak, V. I. (2012). Glutathione Homeostasis and Functions: Potential Targets for Medical Interventions. *Journal of Amino Acids*, 2012, pp. 1–26.

Ly, J. D., Grubb, D. R. and Lawen, A. (2003). The mitochondrial membrane potential ($\Delta\psi(m)$) in apoptosis; an update. *Apoptosis: an international journal on programmed cell death*, 8(2), pp. 115–128.

Macfarlane, R. J. and Chi, K. N. (2010). Novel Targeted Therapies for Prostate Cancer. *Urologic Clinics of North America*, 37(1), pp. 105–119.

Macintosh, C. A., Stower, M., Reid, N. and Maitland, N. J. (1998). Precise microdissection of human prostate cancers reveals genotypic heterogeneity. *Cancer research*, 58(1), pp. 23–28.

Madan, R. A., Pal, S. K., Sartor, O. and Dahut, W. L. (2011). Overcoming chemotherapy resistance in prostate cancer. *Clinical cancer research: an official journal of the American Association for Cancer Research*, 17(12), pp. 3892–3902.

- Madigan, A. A., Rycyna, K. J., Parwani, A. V., Datiri, Y. J., Basudan, A. M., Sobek, K. M., Cummings, J. L., Basse, P. H., Bacich, D. J. and O'Keefe, D. S. (2014). Novel Nuclear Localization of Fatty Acid Synthase Correlates with Prostate Cancer Aggressiveness. *The American Journal of Pathology*, 184(8), pp. 2156–62.
- Mamczur, P., Gamian, A., Kolodziej, J., Dziegiel, P. and Rakus, D. (2013). Nuclear localization of aldolase A correlates with cell proliferation. *Biochimica et Biophysica Acta (BBA) - Molecular Cell Research*, 1833(12), pp. 2812–2822.
- Manca, P., Pantano, F., Iuliani, M., Ribelli, G., De Lisi, D., Danesi, R., Del Re, M., Vincenzi, B., Tonini, G. and Santini, D. (2017). Determinants of bone specific metastasis in prostate cancer. *Critical reviews in oncology/hematology*, 112, pp. 59–66.
- Manieri, W., Moore, M. E., Soellner, M. B., Tsang, P. and Caperelli, C. A. (2007). Human glycinamide ribonucleotide transformylase: active site mutants as mechanistic probes. *Biochemistry*, 46(1), pp. 156–163.
- Mapelli, P. and Picchio, M. (2015). Initial prostate cancer diagnosis and disease staging—the role of choline-PET–CT. *Nature Reviews Urology*, 12(9), pp. 510–518.
- Marín de Mas, I., Aguilar, E., Zodda, E., Balcells, C., Marin, S., Dallmann, G., Thomson, T. M., Papp, B. and Cascante, M. (2018). Model-driven discovery of long-chain fatty acid metabolic reprogramming in heterogeneous prostate cancer cells. *PLoS Computational Biology*, 14(1), e1005914.
- Marker, P. C., Donjacour, A. A., Dahiya, R. and Cunha, G. R. (2003). Hormonal, cellular, and molecular control of prostatic development. *Developmental biology*, 253(2), pp. 165–74.
- Marques, M., Pei, Y., Southall, M. D., Johnston, J. M., Arai, H., Aoki, J., Inoue, T., Seltsmann, H., Zouboulis, C. C. and Travers, J. B. (2002). Identification of Platelet-Activating Factor Acetylhydrolase II in Human Skin. *Journal of Investigative Dermatology*, 119(4), pp. 913–919.
- Martinez, J. D. (2010). Restoring p53 tumor suppressor activity as an anticancer therapeutic strategy. *Future oncology*, 6(12), pp. 1857–1862.
- Mashek, D. G., Li, L. O. and Coleman, R. A. (2007). Long-chain acyl-CoA synthetases and fatty acid channeling. *Future lipidology*, 2(4), pp. 465–476.
- Masko, E. M., Allott, E. H. and Freedland, S. J. (2013). The relationship between nutrition and prostate cancer: is more always better?. *European urology*, 63(5), pp. 810–820.
- Massard, C., Mateo, J., Lorient, Y., Pezaro, C., Albiges, L., Mehra, N., Varga, A., Bianchini, D., Ryan, C. J., Petrylak, D. P., Attard, G., Shen, L., Fizazi, K. and de Bono, J. (2017). Phase I/II trial of cabazitaxel plus abiraterone in patients with metastatic castration-resistant prostate cancer (mCRPC) progressing after docetaxel and abiraterone. *Annals of Oncology*, 28(1), pp. 90-95.
- Mateo, J., Carreira, S., Sandhu, S., Miranda, S., Mossop, H., Perez-Lopez, R., Nava Rodrigues, D., Robinson, D., Omlin, A., Tunariu, N., Boysen, G., Porta, N., Flohr, P., Gillman, A., Figueiredo, I., Paulding, C., Seed, G., Jain, S., Ralph, C., Protheroe, A., Hussain, S., Jones, R., Elliott, T., McGovern, U., Bianchini, D., Goodall, J., Zafeiriou, Z., Williamson, C. T., Ferraldeschi, R., Riisnaes, R., Ebbs, B., Fowler, G., Roda, D., Yuan, W., Wu, Y.-M., Cao, X., Brough, R., Pemberton, H., A'Hern, R., Swain, A., Kunju, L. P., Eeles, R., Attard, G., Lord, C. J., Ashworth, A., Rubin, M. A., Knudsen, K. E., Feng, F. Y., Chinnaiyan, A. M., Hall, E. and de Bono, J. S. (2015). DNA-Repair Defects and Olaparib in Metastatic Prostate Cancer. *New England Journal of Medicine*, 373(18), pp. 1697–1708.
- Maycotte, P., Blancas, S. and Morán, J. (2008). Role of Inhibitor of Apoptosis Proteins and Smac/DIABLO in Staurosporine-induced Cerebellar Granule Neurons Death. *Neurochemical Research*, 33(8), pp. 1534–1540.

- Mayers, J. R., Wu, C., Clish, C. B., Kraft, P., Torrence, M. E., Fiske, B. P., Yuan, C., Bao, Y., Townsend, M. K., Tworoger, S. S., Davidson, S. M., Papagiannakopoulos, T., Yang, A., Dayton, T. L., Ogino, S., Stampfer, M. J., Giovannucci, E. L., Qian, Z. R., Rubinson, D. A., Ma, J., Sesso, H. D., Gaziano, J. M., Cochrane, B. B., Liu, S., Wactawski-Wende, J., Manson, J. E., Pollak, M. N., Kimmelman, A. C., Souza, A., Pierce, K., Wang, T. J., Gerszten, R. E., Fuchs, C. S., Vander Heiden, M. G. and Wolpin, B. M. (2014). Elevation of circulating branched-chain amino acids is an early event in human pancreatic adenocarcinoma development. *Nature Medicine*, 20(10), pp. 1193–1198.
- McCullough, A. R. (2005). Sexual dysfunction after radical prostatectomy. *Reviews in urology*, 7 (Suppl 2), pp. S3–S10.
- McLeod, D. G. (1997). Tolerability of Nonsteroidal Antiandrogens in the Treatment of Advanced Prostate Cancer. *The oncologist*, 2(1), pp. 18–27.
- Medrano, A., Fernández-Novell, J. M., Ramió, L., Alvarez, J., Goldberg, E., Montserrat Rivera, M., Guinovart, J. J., Rigau, T. and Rodríguez-Gil, J. E. (2006). Utilization of citrate and lactate through a lactate dehydrogenase and ATP-regulated pathway in boar spermatozoa. *Molecular Reproduction and Development*, 73(3), pp. 369–378.
- Meeks, J. J. and Schaeffer, E. M. (2011). Genetic Regulation of Prostate Development. *Journal of Andrology*, 32(3), pp. 210–217.
- Mehta, A. and Armstrong, A. (2016). Tasquinimod in the treatment of castrate-resistant prostate cancer – current status and future prospects. *Therapeutic Advances in Urology*, 8(1), pp. 9–18.
- Meijering, E., Dzyubachyk, O. and Smal, I. (2012) *Methods for Cell and Particle Tracking, Imaging and Spectroscopic Analysis of Living Cells*. Available at: <http://smal.ws/pdf/mie2012.pdf>. [Accessed: 29.08.2015].
- Merson, S., Yang, Z. H., Brewer, D., Olmos, D., Eichholz, A., McCarthy, F., Fisher, G., Kovacs, G., Berney, D. M., Foster, C. S., Møller, H., Scardino, P., Cuzick, J., Cooper, C. S. and Clark, J. P. (2014). Focal amplification of the androgen receptor gene in hormone-naïve human prostate cancer. *British Journal of Cancer*, 110(6), pp. 1655–1662.
- Meyer, R. M., Gospodarowicz, M. K., Connors, J. M., Pearcey, R. G., Wells, W. A., Winter, J. N., Horning, S. J., Dar, A. R., Shustik, C., Stewart, D. A., Crump, M., Djurfeldt, M. S., Chen, B. E. and Shepherd, L. E. (2012). ABVD Alone versus Radiation-Based Therapy in Limited-Stage Hodgkin's Lymphoma. *New England Journal of Medicine*, 366(5), pp. 399–408.
- Michalopoulou, E., Bulusu, V. and Kamphorst, J. J. (2016). Metabolic scavenging by cancer cells: when the going gets tough, the tough keep eating. *British journal of cancer*, 115(6), pp. 635–640.
- Micheau, O. and Tschopp, J. (2003). Induction of TNF receptor I-mediated apoptosis via two sequential signaling complexes. *Cell*, 114(2), pp. 181–190.
- Miller, K. D., Siegel, R. L., Lin, C. C., Mariotto, A. B., Kramer, J. L., Rowland, J. H., Stein, K. D., Alteri, R. and Jemal, A. (2016). Cancer treatment and survivorship statistics, 2016. *CA: A Cancer Journal for Clinicians*, 66(4), pp. 271–289.
- Minardi, D., Lucarini, G., Filosa, A., Milanese, G., Zizzi, A., Di Primio, R., Montironi, R. and Muzzonigro, G. (2008). Prognostic Role of Tumor Necrosis, Microvessel Density, Vascular Endothelial Growth Factor and Hypoxia Inducible Factor-1 α in Patients with Clear Cell Renal Carcinoma after Radical Nephrectomy in a Long Term Follow-up. *International Journal of Immunopathology and Pharmacology*, 21(2), pp. 447–455.

- Mita, A. C., Denis, L. J., Rowinsky, E. K., DeBono, J. S., Goetz, A. D., Ochoa, L., Forouzesh, B., Beeram, M., Patnaik, A., Molpus, K., Semiond, D., Besenval, M. and Tolcher, A. W. (2009). Phase I and Pharmacokinetic Study of XRP6258 (RPR 116258A), a Novel Taxane, Administered as a 1-Hour Infusion Every 3 Weeks in Patients with Advanced Solid Tumors. *Clinical Cancer Research*, 15(2), pp. 723–730.
- Miwa, S., Fujii, H., Tani, K., Takahashi, K., Takegawa, S., Fujinami, N., Sakurai, M., Kubo, M., Tanimoto, Y., Kato, T. and Matsumoto, N. (1981). Two cases of red cell aldolase deficiency associated with hereditary hemolytic anemia in a Japanese family. *American journal of hematology*, 11(4), pp. 425–437.
- Miyashita, T., Krajewski, S., Krajewska, M., Wang, H. G., Lin, H. K., Liebermann, D. A., Hoffman, B. and Reed, J. C. (1994). Tumor suppressor p53 is a regulator of bcl-2 and bax gene expression in vitro and in vivo. *Oncogene*, 9(6), pp. 1799–1805.
- Modena, A., Ciccicarese, C., Iacovelli, R., Brunelli, M., Montironi, R., Fiorentino, M., Tortora, G. and Massari, F. (2016). Immune checkpoint inhibitors and prostate cancer: a new frontier?. *Oncology Reviews*, 10(1), 293.
- Mohile, S. G., Mustian, K., Bylow, K., Hall, W. and Dale, W. (2009). Management of complications of androgen deprivation therapy in the older man. *Critical reviews in oncology/hematology*, 70(3), pp. 235–255.
- Mohr, A., Büneker, C., Gough, R. P. and Zwacka, R. M. (2008). MnSOD protects colorectal cancer cells from TRAIL-induced apoptosis by inhibition of Smac/DIABLO release. *Oncogene*, 27(6), pp. 763–774.
- Moore, K. and Rees, S. (2001). Cell-Based Versus Isolated Target Screening: How Lucky Do You Feel?. *Journal of Biomolecular Screening*, 6(2), pp. 69–74.
- Morgan, M. J., Kim, Y.-S. and Liu, Z. (2008). TNF α and reactive oxygen species in necrotic cell death. *Cell Research*, 18(3), pp. 343–349.
- Moscat, J., Richardson, A. and Diaz-Meco, M. T. (2015). Nutrient stress revamps cancer cell metabolism. *Cell Research*. Nature Publishing Group, 25(5), pp. 537–538.
- Mostaghel, E. A., Montgomery, B. and Nelson, P. S. (2010). Castration-resistant prostate cancer: targeting androgen metabolic pathways in recurrent disease. *Urologic oncology*, 27(3), pp. 251–257.
- Mulcahy, R. T., Bailey, H. H. and Gipp, J. J. (1994). Up-regulation of gamma-glutamylcysteine synthetase activity in melphalan-resistant human multiple myeloma cells expressing increased glutathione levels. *Cancer chemotherapy and pharmacology*, 34(1), pp. 67–71.
- Mulcahy, R., Untawale, S. and Gipp, J. (1994). Transcriptional up-regulation of gamma-glutamylcysteine synthetase gene expression in melphalan-resistant human prostate carcinoma cells. *Mol. Pharmacol.*, 46(5), pp. 909–914.
- Müller, W. E., Yamazaki, Z., Breter, H. J. and Zahn, R. K. (1972). Action of bleomycin on DNA and RNA. *European journal of biochemistry*, 31(3), pp. 518–525.
- Muñoz-Pinedo, C., El Mjiyad, N. and Ricci, J.-E. (2012). Cancer metabolism: current perspectives and future directions. *Cell Death & Disease*, 3(1), pp. e248–e248.
- Muthukrishnan, R. and Radha, M. (2011). EDGE DETECTION TECHNIQUES FOR FOR IMAGE SEGMENTATION. *International Journal of Computer Science & Information Technology (IJCSIT)*, 3(6), pp. 259–267.
- Naji, L., Randhawa, H., Sohani, Z., Dennis, B., Lautenbach, D., Kavanagh, O., Bawor, M., Banfield, L. and Profetto, J. (2018). Digital Rectal Examination for Prostate Cancer Screening in Primary Care: A Systematic Review and Meta-Analysis. *The Annals of Family Medicine*, 16(2), pp. 149–154.

- Nakajima, O., Takahashi, S., Harigae, H., Furuyama, K., Hayashi, N., Sassa, S. and Yamamoto, M. (1999). Heme deficiency in erythroid lineage causes differentiation arrest and cytoplasmic iron overload. *The EMBO Journal*, 18(22), pp. 6282–6289.
- Nakouzi, N. Al, Le Moulec, S., Albigès, L., Wang, C., Beuzeboc, P., Gross-Goupil, M., De, T., Motte Rouge, L., Guillot, A., Gajda, D., Massard, C., Gleave, M., Fizazi, K. and Lorient, Y. (2015). Platinum Priority – Prostate Cancer Cabazitaxel Remains Active in Patients Progressing After Docetaxel Followed by Novel Androgen Receptor Pathway Targeted Therapies. *European Urology*, 68(2), pp. 228–235.
- Narla, G., Heath, K. E., Reeves, H. L., Li, D., Giono, L. E., Kimmelman, A. C., Glucksman, M. J., Narla, J., Eng, F. J., Chan, A. M., Ferrari, A. C., Martignetti, J. A. and Friedman, S. L. (2001). KLF6, a candidate tumor suppressor gene mutated in prostate cancer. *Science (New York, N.Y.)*, 294(5551), pp. 2563–2566.
- Narod, S. A., Seth, A. and Nam, R. (2008). Fusion in the ETS gene family and prostate cancer. *British journal of cancer*, 99(6), pp. 847–851.
- Navone, N. M., Polo, C. F., Frisardi, A. L., Andrade, N. E. and Battle, A. M. (1990). Heme biosynthesis in human breast cancer--mimetic 'in vitro' studies and some heme enzymic activity levels. *The International journal of biochemistry*, 22(12), pp. 1407–1411.
- Neugut, A. I., Ahsan, H., Robinson, E. and Ennis, R. D. (1997). Bladder carcinoma and other second malignancies after radiotherapy for prostate carcinoma. *Cancer*, 79(8), pp. 1600–1604.
- Nieto, C. M., Rider, L. C. and Cramer, S. D. (2014). Influence of stromal-epithelial interactions on androgen action. *Endocrine Related Cancer*, 21(4), pp. T147–T160.
- Niklas, C., Saar, M., Berg, B., Steiner, K., Janssen, M., Siemer, S., Stöckle, M. and Ohlmann, C.-H. (2016). da Vinci and Open Radical Prostatectomy: Comparison of Clinical Outcomes and Analysis of Insurance Costs. *Urologia Internationalis*, 96(3), pp. 287–294.
- Nikoletopoulou, V., Markaki, M., Palikaras, K. and Tavernarakis, N. (2013). Crosstalk between apoptosis, necrosis and autophagy. *Biochimica et Biophysica Acta (BBA) - Molecular Cell Research*, 1833(12), pp. 3448–3459.
- Nikolić, Z. Z., Pavićević, D. L. S., Romac, S. P. and Brajušković, G. N. (2015). Genetic Variants within Endothelial Nitric Oxide Synthase Gene and Prostate Cancer: A Meta-Analysis. *Clinical and Translational Science*, 8(1), pp. 23–31.
- Nishi, K., Kenta, S., Sawamoto, J., Tokizawa, Y., Iwase, Y., Yumita, N. and Ikeda, T. (2016). Inhibition of Fatty Acid Synthesis Induces Apoptosis of Human Pancreatic Cancer Cells. *Anticancer Research*, 36(9), pp. 4655–4660.
- Njar, V. C. O. and Brodie, A. M. H. (2015). Discovery and Development of Galeterone (TOK-001 or VN/124-1) for the Treatment of All Stages of Prostate Cancer. *Journal of Medicinal Chemistry*, 58(5), pp. 2077–2087.
- Notarnicola, M., Messa, C., Cavallini, A., Bifulco, M., Tecce, M. F., Eletto, D., Di Leo, A., Montemurro, S., Laezza, C. and Caruso, M. G. (2004) 'Higher farnesyl diphosphate synthase activity in human colorectal cancer inhibition of cellular apoptosis.', *Oncology*. Karger Publishers, 67(5–6), pp. 351–358.
- Nussbaum, N., George, D. J., Abernethy, A. P., Dolan, C. M., Oestreicher, N., Flanders, S. and Dorff, T. B. (2016). Patient experience in the treatment of metastatic castration-resistant prostate cancer: state of the science. *Prostate Cancer and Prostatic Diseases*, 19(2), pp. 111–121.

- Oguri, T., Fujiwara, Y., Isobe, T., Katoh, O., Watanabe, H. and Yamakido, M. (1998). Expression of gamma-glutamylcysteine synthetase (gamma-GCS) and multidrug resistance-associated protein (MRP), but not human canalicular multispecific organic anion transporter (cMOAT), genes correlates with exposure of human lung cancers to platinum drug. *British journal of cancer*, 77(7), pp. 1089–1096.
- Oh, W. K., Haggmann, E., Manola, J., George, D. J., Gilligan, T. D., Jacobson, J. O., Smith, M. R., Kaufman, D. S. and Kantoff, P. W. (2005). A phase I study of estramustine, weekly docetaxel, and carboplatin chemotherapy in patients with hormone-refractory prostate cancer. *Clinical cancer research: an official journal of the American Association for Cancer Research*, 11(1), pp. 284–289.
- Okada, H. and Mak, T. W. (2004). Pathways of apoptotic and non-apoptotic death in tumour cells. *Nature Reviews Cancer*, 4(8), pp. 592–603.
- Oldan, J. D., Hawkins, A. S. and Chin, B. B. (2016). (18)F Sodium Fluoride PET/CT in Patients with Prostate Cancer: Quantification of Normal Tissues, Benign Degenerative Lesions, and Malignant Lesions. *World journal of nuclear medicine*, 15(2), pp. 102–108.
- Omlin, A., Pezaro, C. and Gillessen Sommer, S. (2014). Sequential use of novel therapeutics in advanced prostate cancer following docetaxel chemotherapy. *Therapeutic advances in urology*, 6(1), pp. 3–14.
- Ory, B., Moriceau, G., Trichet, V., Blanchard, F., Berreur, M., Rédini, F., Rogers, M. and Heymann, D. (2008). Farnesyl diphosphate synthase is involved in the resistance to zoledronic acid of osteosarcoma cells. *Journal of Cellular and Molecular Medicine*, 12(3), pp. 928–941.
- Osanto, S. and Van Poppel, H. (2012). Emerging novel therapies for advanced prostate cancer. *Therapeutic advances in urology*, 4(1), pp. 3–12.
- Ouyang, L., Shi, Z., Zhao, S., Wang, F.-T., Zhou, T.-T., Liu, B. and Bao, J.-K. (2012). Programmed cell death pathways in cancer: a review of apoptosis, autophagy and programmed necrosis. *Cell Proliferation*, 45(6), pp. 487–498.
- Paller, C. J. and Antonarakis, E. S. (2011). Cabazitaxel: a novel second-line treatment for metastatic castration-resistant prostate cancer. *Drug design, development and therapy*, 5, pp. 117–124.
- Palmberg, C., Koivisto, P., Visakorpi, T. and Tammela, T. L. (1999). PSA decline is an independent prognostic marker in hormonally treated prostate cancer. *European urology*, 36(3), pp. 191–196.
- Pan, C., Ghosh, P., Lara, P., Robles, D., Beckett, L. and de Vere White, R. (2011). Encouraging activity of bicalutamide and everolimus in castration-resistant prostate cancer (CRPC): Early results from a phase II clinical trial. *Journal of Clinical Oncology*, 29(7_suppl), pp. 157–157.
- Pan, T., Gao, L., Wu, G., Shen, G., Xie, S., Wen, H., Yang, J., Zhou, Y., Tu, Z. and Qian, W. (2015). Elevated expression of glutaminase confers glucose utilization via glutaminolysis in prostate cancer. *Biochemical and Biophysical Research Communications*, 456(1), pp. 452–458.
- Pasparakis, M. and Vandenabeele, P. (2015). Necroptosis and its role in inflammation. *Nature*, 517(7534), pp. 311–320.
- Patel, P., Ashdown, D. and James, N. (2004). Is gene therapy the answer for prostate cancer?. *Prostate Cancer and Prostatic Diseases*, 7(S1), pp. S14–S19.
- Patnaik, A., Swanson, K. D., Csizmadia, E., Solanki, A., Landon-Brace, N., Gehring, M. P., Helenius, K., Olson, B. M., Pyzer, A. R., Wang, L. C., Elemento, O., Novak, J., Thornley, T. B., Asara, J. M., Montaser, L., Timmons, J. J., Morgan, T. M., Wang, Y., Levantini, E., Clohessy, J. G., Kelly, K., Pandolfi, P. P., Rosenblatt, J. M., Avigan, D. E., Ye, H., Karp, J. M., Signoretti, S., Balk, S. P. and Cantley, L. C. (2017). Cabozantinib Eradicates Advanced Murine Prostate Cancer by Activating Antitumor Innate Immunity. *Cancer Discovery*, 7(7), pp. 750–765.

- Paul, A., Krelin, Y., Arif, T., Jeger, R. and Shoshan-Barmatz, V. (2017). A New Role for the Mitochondrial Pro-apoptotic Protein SMAC/Diablo in Phospholipid Synthesis Associated with Tumorigenesis. *Molecular Therapy*, 26(3), pp. 680–694.
- Paulo, P., Barros-Silva, J. D., Ribeiro, F. R., Ramalho-Carvalho, J., Jerónimo, C., Henrique, R., Lind, G. E., Skotheim, R. I., Lothe, R. A. and Teixeira, M. R. (2012). FLI1 is a novel ETS transcription factor involved in gene fusions in prostate cancer. *Genes, Chromosomes and Cancer*, 51(3), pp. 240–249.
- Pavlova, N. N. and Thompson, C. B. (2016). The Emerging Hallmarks of Cancer Metabolism. *Cell metabolism*, 23(1), pp. 27–47.
- Payne, H. and Mason, M. (2011). Androgen deprivation therapy as adjuvant/neoadjuvant to radiotherapy for high-risk localised and locally advanced prostate cancer: recent developments. *British journal of cancer*, 105(11), pp. 1628–1634.
- Pearson, H. B., Perez-Mancera, P. A., Dow, L. E., Ryan, A., Tennstedt, P., Bogani, D., Elsum, I., Greenfield, A., Tuveson, D. A., Simon, R. and Humbert, P. O. (2011). SCRIB expression is deregulated in human prostate cancer, and its deficiency in mice promotes prostate neoplasia. *The Journal of clinical investigation*, 121(11), pp. 4257–4267.
- Pelicano, H., Martin, D. S., Xu, R.-H. and Huang, P. (2006). Glycolysis inhibition for anticancer treatment. *Oncogene*, 25(34), pp. 4633–4646.
- Pelton, K., Freeman, M. R. and Solomon, K. R. (2012). Cholesterol and prostate cancer. *Current Opinion in Pharmacology*, 12(6), pp. 751–759.
- Peng, Y.-C. and Joyner, A. L. (2015). Hedgehog signaling in prostate epithelial-mesenchymal growth regulation. *Developmental biology*, 400(1), pp. 94–104.
- Pentyala, S., Whyard, T., Pentyala, S., Muller, J., Pfail, J., Parmar, S., Helguero, C. G. and Khan, S. (2016). Prostate cancer markers: An update (Review). *Biomedical Reports*, 4(3), pp. 263-268.
- Perrimon, N., Ni, J.-Q. and Perkins, L. (2010). In vivo RNAi: today and tomorrow. *Cold Spring Harbor perspectives in biology*, 2(8), a003640.
- Perwitasari, O., Bakre, A., Tompkins, S. M. and Tripp, R. A. (2013). siRNA Genome Screening Approaches to Therapeutic Drug Repositioning. *Pharmaceuticals (Basel, Switzerland)*, 6(2), pp. 124–160.
- Petrylak, D. P., Macarthur, R. B., O'Connor, J., Shelton, G., Judge, T., Balog, J., Pfaff, C., Bagiella, E., Heitjan, D., Fine, R., Zuech, N., Sawczuk, I., Benson, M. and Olsson, C. A. (1999). Phase I Trial of Docetaxel With Estramustine in Androgen-Independent Prostate Cancer. *Journal of Clinical Oncology*, 17(3), pp. 958–958.
- Pflug, B. R., Pecher, S. M., Brink, A. W., Nelson, J. B. and Foster, B. A. (2003). Increased fatty acid synthase expression and activity during progression of prostate cancer in the TRAMP model. *The Prostate*, 57(3), pp. 245–254.
- Phin, S., Moore, M. W. and Cotter, P. D. (2013). Genomic Rearrangements of PTEN in Prostate Cancer. *Frontiers in oncology*, 3, 240.
- Picus, J. and Schultz, M. (1999). Docetaxel (Taxotere) as monotherapy in the treatment of hormone-refractory prostate cancer: preliminary results. *Seminars in oncology*, 26(5 Suppl 17), pp. 14–18.
- Pienta, K. J. (2001). Preclinical mechanisms of action of docetaxel and docetaxel combinations in prostate cancer. *Seminars in oncology*, 28(4 Suppl 15), pp. 3–7.

- Pierorazio, P. M., Walsh, P. C., Partin, A. W. and Epstein, J. I. (2013). Prognostic Gleason grade grouping: data based on the modified Gleason scoring system. *BJU International*, 111(5), pp. 753–760.
- Pili, R., Häggman, M., Stadler, W. M., Gingrich, J. R., Assikis, V. J., Björk, A., Nordle, Ö., Forsberg, G., Carducci, M. A. and Armstrong, A. J. (2011). Phase II Randomized, Double-Blind, Placebo-Controlled Study of Tasquinimod in Men With Minimally Symptomatic Metastatic Castrate-Resistant Prostate Cancer. *Journal of Clinical Oncology*, 29(30), pp. 4022–4028.
- Pivot, X., Koralewski, P., Hidalgo, J. L., Chan, A., Goncalves, A., Schwartzmann, G., Assadourian, S. and Lotz, J. P. (2008). A multicenter phase II study of XRP6258 administered as a 1-h i.v. infusion every 3 weeks in taxane-resistant metastatic breast cancer patients. *Annals of Oncology*, 19(9), pp. 1547–1552.
- Placzek, W. J., Wei, J., Kitada, S., Zhai, D., Reed, J. C. and Pellecchia, M. (2010). A survey of the anti-apoptotic Bcl-2 subfamily expression in cancer types provides a platform to predict the efficacy of Bcl-2 antagonists in cancer therapy. *Cell Death & Disease*, 1(5), e40.
- Plas, D. R., Talapatra, S., Edinger, A. L., Rathmell, J. C. and Thompson, C. B. (2001). Akt and Bcl-x_L Promote Growth Factor-independent Survival through Distinct Effects on Mitochondrial Physiology. *Journal of Biological Chemistry*, 276(15), pp. 12041–12048.
- Ploussard, G. and Mongiat-Artus, P. (2013). Triptorelin in the management of prostate cancer. *Future Oncology*, 9(1), pp. 93–102.
- Pope, A. J. and Abel, P. D. (2010). Androgen deprivation therapy for prostate cancer and its complications. *Trends in Urology Gynaecology & Sexual Health May*, pp. 33-37.
- Porta, C., Paglino, C. and Mosca, A. (2014). Targeting PI3K/Akt/mTOR Signaling in Cancer. *Frontiers in oncology*, 4, 64.
- Potosky, A. L., Davis, W. W., Hoffman, R. M., Stanford, J. L., Stephenson, R. A., Penson, D. F. and Harlan, L. C. (2004). Five-Year Outcomes After Prostatectomy or Radiotherapy for Prostate Cancer: The Prostate Cancer Outcomes Study. *JNCI Journal of the National Cancer Institute*, 96(18), pp. 1358–1367.
- Potter, G. A., Barrie, S. E., Jarman, M. and Rowlands, M. G. (1995). Novel Steroidal Inhibitors of Human Cytochrome P45017.alpha.-Hydroxylase-C17,20-lyase): Potential Agents for the Treatment of Prostatic Cancer. *Journal of Medicinal Chemistry*, 38(13), pp. 2463–2471.
- Prins, G. S. and Putz, O. (2008). Molecular signaling pathways that regulate prostate gland development. *Differentiation; research in biological diversity*, 76(6), pp. 641–659.
- Puente, J., Grande, E., Medina, A., Maroto, P., Lainez, N. and Arranz, J. A. (2017). Docetaxel in prostate cancer: a familiar face as the new standard in a hormone-sensitive setting *Therapeutic Advances in Medical Oncology*, 9(5), pp. 307–318.
- Ramsay, A. G. (2013). Immune checkpoint blockade immunotherapy to activate anti-tumour T-cell immunity. *British Journal of Haematology*, 162(3), pp. 313–325.
- Rastogi, R. P., Sinha, R. P. and Sinha, R. (2009). Apoptosis: Molecular Mechanisms and Pathogenicity. *EXCLI Journal*, 8, pp. 155–181.
- Ratcliff, F., Harrison, B. D. and Baulcombe, D. C. (1997). A similarity between viral defense and gene silencing in plants. *Science (New York, N.Y.)*, 276(5318), pp. 1558–1560.
- Raymond, E., Dalgleish, A., Damber, J.-E., Smith, M. and Pili, R. (2014). Mechanisms of action of tasquinimod on the tumour microenvironment. *Cancer chemotherapy and pharmacology*, 73(1), pp. 1–8.

- Rehman, Y. and Rosenberg, J. E. (2012). Abiraterone acetate: oral androgen biosynthesis inhibitor for treatment of castration-resistant prostate cancer. *Drug design, development and therapy*. Dove Press, 6, pp. 13–18.
- Riba, A., Emmenlauer, M., Chen, A., Sigoillot, F., Cong, F., Dehio, C., Jenkins, J. and Zavolan, M. (2017). Explicit Modeling of siRNA-Dependent On- and Off-Target Repression Improves the Interpretation of Screening Results. *Cell Systems*, 4(2), p. 182–193.
- Ricci, M. S. and Zong, W.-X. (2006). Chemotherapeutic Approaches for Targeting Cell Death Pathways. *The Oncologist*, 11(4), pp. 342–357.
- Ridnour, L. A., Thomas, D. D., Mancardi, D., Espey, M. G., Miranda, K. M., Paolocci, N., Feelisch, M., Fukuto, J. and Wink, D. A. (2004). The chemistry of nitrosative stress induced by nitric oxide and reactive nitrogen oxide species. Putting perspective on stressful biological situations. *Biological Chemistry*, 385(1), pp. 1–10.
- Rivera, M., Ramos, Y., Rodríguez-Valentín, M., López-Acevedo, S., Cubano, L. A., Zou, J., Zhang, Q., Wang, G. and Boukli, N. M. (2017). Targeting multiple pro-apoptotic signaling pathways with curcumin in prostate cancer cells. *PLOS ONE*, 12(6), e0179587.
- Robbins, C. M., Tembe, W. A., Baker, A., Sinari, S., Moses, T. Y., Beckstrom-Sternberg, S., Beckstrom-Sternberg, J., Barrett, M., Long, J., Chinnaiyan, A., Lowey, J., Suh, E., Pearson, J. V., Craig, D. W., Agus, D. B., Pienta, K. J. and Carpten, J. D. (2011). Copy number and targeted mutational analysis reveals novel somatic events in metastatic prostate tumors. *Genome Research*, 21(1), pp. 47–55.
- Roberts, R. O., Lieber, M. M., Bostwick, D. G. and Jacobsen, S. J. (1997). A review of clinical and pathological prostatitis syndromes. *Urology*, 49(6), pp. 809–21.
- Robson, M., Im, S.-A., Senkus, E., Xu, B., Domchek, S. M., Masuda, N., Delaloge, S., Li, W., Tung, N., Armstrong, A., Wu, W., Goessl, C., Runswick, S. and Conte, P. (2017). Olaparib for Metastatic Breast Cancer in Patients with a Germline *BRCA* Mutation. *New England Journal of Medicine*, 377(6), pp. 523–533.
- Rodrigues, G., Warde, P., Pickles, T., Crook, J., Brundage, M., Souhami, L., Lukka, H. and Genitourinary Radiation Oncologists of Canada (2012). Pre-treatment risk stratification of prostate cancer patients: A critical review. *Canadian Urological Association journal*, 6(2), pp. 121–127.
- Romano, S., Sorrentino, A., Di Pace, A. L., Nappo, G., Mercogliano, C. and Romano, M. F. (2011). The emerging role of large immunophilin FK506 binding protein 51 in cancer. *Current medicinal chemistry*, 18(35), pp. 5424–5429.
- Romano, S., Staibano, S., Greco, A., Brunetti, A., Nappo, G., Ilardi, G., Martinelli, R., Sorrentino, A., Di Pace, A., Mascolo, M., Bisogni, R., Scalvenzi, M., Alfano, B. and Romano, M. F. (2013). FK506 binding protein 51 positively regulates melanoma stemness and metastatic potential. *Cell Death & Disease*, 4(4), e578.
- Romero-Garcia, S., Lopez-Gonzalez, J. S., Báez-Viveros, J. L., Aguilar-Cazares, D. and Prado-Garcia, H. (2011). Tumor cell metabolism: an integral view. *Cancer biology & therapy*, 12(11), pp. 939–948.
- Ros, S., Santos, C. R., Moco, S., Baenke, F., Kelly, G., Howell, M., Zamboni, N. and Schulze, A. (2012). Functional metabolic screen identifies 6-phosphofructo-2-kinase/fructose-2,6-biphosphatase 4 as an important regulator of prostate cancer cell survival. *Cancer discovery*, 2(4), pp. 328–343.
- Ross, R. W., Beer, T. M., Jacobus, S., Bublely, G. J., Taplin, M.-E., Ryan, C. W., Huang, J. and Oh, W. K. (2007). A phase 2 study of carboplatin plus docetaxel in men with metastatic hormone-refractory prostate cancer who are refractory to docetaxel. *Cancer*, 112(3), pp. 521–526.

- Roth, B. J., Yeap, B. Y., Wilding, G., Kasimis, B., McLeod, D. and Loehrer, P. J. (1993). Taxol in advanced, hormone-refractory carcinoma of the prostate. A phase II trial of the Eastern Cooperative Oncology Group. *Cancer*, 72(8), pp. 2457–2460.
- Rulten, S. L., Kinloch, R. A., Tateossian, H., Robinson, C., Gettins, L. and Kay, J. E. (2006). The human FK506-binding proteins: characterization of human FKBP19. *Mammalian Genome*, 17(4), pp. 322–331.
- Ruttkay-Nedecky, B., Nejdil, L., Gumulec, J., Zitka, O., Masarik, M., Eckschlager, T., Stiborova, M., Adam, V. and Kizek, R. (2013). The role of metallothionein in oxidative stress. *International journal of molecular sciences*, 14(3), pp. 6044–6066.
- Sadeghi, M., Enferadi, M. and Shirazi, A. (2010). External and internal radiation therapy: past and future directions. *Journal of cancer research and therapeutics*, 6(3), pp. 239–248.
- Sadeghi, R. N., Karami-Tehrani, F. and Salami, S. (2015). Targeting prostate cancer cell metabolism: impact of hexokinase and CPT-1 enzymes. *Tumor Biology*, 36(4), pp. 2893–2905.
- Sadowski, M. C., Pouwer, R. H., Gunter, J. H., Lubik, A. A., Quinn, R. J. and Nelson, C. C. (2014). The fatty acid synthase inhibitor triclosan: repurposing an anti- microbial agent for targeting prostate cancer. *Oncotarget*, 5(19) pp: 9362-9381
- Saelens, X., Festjens, N., Walle, L. Vande, Gulp, M. van, Loo, G. van and Vandenberghe, P. (2004). Toxic proteins released from mitochondria in cell death. *Oncogene*, 23(16), pp. 2861–2874.
- Saggari, J. K., Yu, M., Tan, Q. and Tannock, I. F. (2013). The tumor microenvironment and strategies to improve drug distribution. *Frontiers in oncology*. Frontiers Media SA, 3, 154.
- Sakr, W. A., Haas, G. P., Cassin, B. F., Pontes, J. E. and Crissman, J. D. (1993). The frequency of carcinoma and intraepithelial neoplasia of the prostate in young male patients. *The Journal of urology*, 150(2 Pt 1), pp. 379–385.
- Salomon, L., Sebe, P., De la Taille, A., Vordos, D., Hoznek, A., Yiou, R., Chopin, D. and Abbou, C. C. (2004). Open versus laparoscopic radical prostatectomy: Part I. *BJU International*, 94(2), pp. 238–243.
- Salzer, W., Bostrom, B., Messinger, Y., Perissinotti, A. J. and Marini, B. (2017). Asparaginase activity levels and monitoring in patients with acute lymphoblastic leukemia. *Leukemia & Lymphoma*, pp. 1–10.
- Samadder, A., Mitra, S. and Chakrabarti, B. C. and J. (2016). tRN-A-RS Acts As Biomarker for Cancer and Other Diseases. *Journal of Molecular Biomarkers & Diagnosis*, s2.
- Sarkar, S. and Das, S. (2016). A Review of Imaging Methods for Prostate Cancer Detection', *Biomedical Engineering and Computational Biology*, 7s1, p.S34255.
- Sassa, S. and Kappas, A. (1983). Hereditary tyrosinemia and the heme biosynthetic pathway. Profound inhibition of delta-aminolevulinic acid dehydratase activity by succinylacetone. *The Journal of clinical investigation*, 71(3), pp. 625–634.
- Savarese, D. M., Halabi, S., Hars, V., Akerley, W. L., Taplin, M. E., Godley, P. A., Hussain, A., Small, E. J. and Vogelzang, N. J. (2001). Phase II study of docetaxel, estramustine, and low-dose hydrocortisone in men with hormone-refractory prostate cancer: a final report of CALGB 9780. Cancer and Leukemia Group B. *Journal of clinical oncology : official journal of the American Society of Clinical Oncology*, 19(9), pp. 2509–2516.
- Scannell, J. W., Blanckley, A., Boldon, H. and Warrington, B. (2012). Diagnosing the decline in pharmaceutical R&D efficiency. *Nature Reviews Drug Discovery*, 11(3), pp. 191–200.

Schaeffer, E. M., Marchionni, L., Huang, Z., Simons, B., Blackman, A., Yu, W., Parmigiani, G. and Berman, D. M. (2008). Androgen-induced programs for prostate epithelial growth and invasion arise in embryogenesis and are reactivated in cancer. *Oncogene*, 27(57), pp.7180–91.

Scher, H. I., Beer, T. M., Higano, C. S., Anand, A., Taplin, M.-E., Efstathiou, E., Rathkopf, D., Shelkey, J., Yu, E. Y., Alumkal, J., Hung, D., Hirmand, M., Seely, L., Morris, M. J., Danila, D. C., Humm, J., Larson, S., Fleisher, M. and Sawyers, C. L (2010). Antitumour activity of MDV3100 in castration-resistant prostate cancer: a phase 1–2 study. *The Lancet*, 375(9724), pp. 1437–1446.

Scher, H. I., Fizazi, K., Saad, F., Taplin, M.-E., Sternberg, C. N., Miller, K., de Wit, R., Mulders, P., Chi, K. N., Shore, N. D., Armstrong, A. J., Flaig, T. W., Fléchon, A., Mainwaring, P., Fleming, M., Hainsworth, J. D., Hirmand, M., Selby, B., Seely, L. and de Bono, J. S. (2012). Increased Survival with Enzalutamide in Prostate Cancer after Chemotherapy. Edited by R. C. Cabot, N. L. Harris, E. S. Rosenberg, J.-A. O. Shepard, A. M. Cort, S. H. Ebeling, and E. K. McDonald. *New England Journal of Medicine*, 367(13), pp. 1187–1197.

Schiff, P. B. and Horwitz, S. B. (1980). Taxol stabilizes microtubules in mouse fibroblast cells. *Proceedings of the National Academy of Sciences of the United States of America*, 77(3), pp. 1561–1565.

Schranzhofer, M., Schifrer, M., Cabrera, J. A., Kopp, S., Chiba, P., Beug, H. and Mü, E. W. (2006). Remodeling the regulation of iron metabolism during erythroid differentiation to ensure efficient heme biosynthesis. *Blood*, 107(10), pp. 4159–4167.

Schulz, W. A., Burchardt, M. and Cronauer, M. V. (2003). Molecular biology of prostate cancer. *Molecular Human Reproduction*, 9(8), pp. 437–448.

Schweizer, M. T. and Drake, C. G. (2014). Immunotherapy for prostate cancer: recent developments and future challenges. *Cancer metastasis reviews*, 33(2–3), pp. 641–655.

SEER Cancer Statistics Review 1975-2014 (no date). Available at: https://seer.cancer.gov/csr/1975_2014/browse_csr.php [Accessed: 15.10. 2017]

Segal, A. W. and Shatwell, K. P. (1997). The NADPH oxidase of phagocytic leukocytes. *Annals of the New York Academy of Sciences*, 832, pp. 215–22.

Seo, H. J., Lee, N. R., Son, S. K., Kim, D. K., Rha, K. H. and Lee, S. H. (2016). Comparison of Robot-Assisted Radical Prostatectomy and Open Radical Prostatectomy Outcomes: A Systematic Review and Meta-Analysis. *Yonsei medical journal*, 57(5), pp. 1165–1177.

Sever, R. and Brugge, J. S. (2015). Signal transduction in cancer.?, *Cold Spring Harbor perspectives in medicine*, 5(4).

Shah, S., Carriveau, W. J., Li, J., Campbell, S. L., Kopinski, P. K., Lim, H.-W., Daurio, N., Trefely, S., Won, K.-J., Wallace, D. C., Koumenis, C., Mancuso, A. and Wellen, K. E. (2016). Targeting ACLY sensitizes castration-resistant prostate cancer cells to AR antagonism by impinging on an ACLY-AMPK-AR feedback mechanism. *Oncotarget*, 7(28), pp. 43713–43730.

Shaik, A. P., Alsaeed, A. H. and Sultana, A. (2012). Phylogenetic analysis of uroporphyrinogen III synthase (UROS) gene. *Bioinformation*, 8(25), pp. 1265–1270.

Shand, R. L. and Gelmann, E. P. (2006). Molecular biology of prostate-cancer pathogenesis. *Current Opinion in Urology*, 16(3), pp. 123–131.

Sharabi, A. B., Lim, M., DeWeese, T. L. and Drake, C. G. (2015). Radiation and checkpoint blockade immunotherapy: radiosensitisation and potential mechanisms of synergy. *The Lancet Oncology*, 16(13), pp. e498–e509.

- Shelley, M., Harrison, C., Coles, B., Stafforth, J., Wilt, T. and Mason, M. (2008). Chemotherapy for hormone-refractory prostate cancer (Review). *John Wiley & Sons*, (4), pp. 1-68.
- Shimizu, T., Nakanishi, Y., Nakagawa, Y., Tsujino, I., Takahashi, N., Nemoto, N. and Hashimoto, S. (2012). Association between expression of thymidylate synthase, dihydrofolate reductase, and glycinamide ribonucleotide formyltransferase and efficacy of pemetrexed in advanced non-small cell lung cancer. *Anticancer research*, 32(10), pp. 4589–4596.
- Shoag, J. and Barbieri, C. E. (2016). Clinical variability and molecular heterogeneity in prostate cancer. *Asian journal of andrology*, 18(4), pp. 543–548.
- Shore, N. D. (2013). Experience with degarelix in the treatment of prostate cancer. *Therapeutic advances in urology*, 5(1), pp. 11–24.
- Shore, N. D. (2017). Darolutamide (ODM-201) for the treatment of prostate cancer. *Expert Opinion on Pharmacotherapy*, 18(9), pp. 945–952.
- Shuvalov, O., Petukhov, A., Daks, A., Fedorova, O., Vasileva, E. and Barlev, N. A. (2017). One-carbon metabolism and nucleotide biosynthesis as attractive targets for anticancer therapy. *Oncotarget*, 8(14), pp. 23955–23977.
- Siegel, R. L., Miller, K. D. and Jemal, A. (2016). Cancer statistics, 2016. *CA: A Cancer Journal for Clinicians*, 66(1), pp. 7–30.
- Simpson, M. A., Reiland, J., Burger, S. R., Furcht, L. T., Spicer, A. P., Oegema, T. R. and McCarthy, J. B. (2001). Hyaluronan synthase elevation in metastatic prostate carcinoma cells correlates with hyaluronan surface retention, a prerequisite for rapid adhesion to bone marrow endothelial cells. *The Journal of biological chemistry*, 276(21), pp. 17949–17957.
- Sinclair, P. R., Gorman, N. and Jacobs, J. M. (2001). Measurement of Heme Concentration, in *Current Protocols in Toxicology*. Hoboken, NJ, USA: John Wiley & Sons.
- Singh, D., Chaudhary, S., Kumar, R., Sirohi, P., Mehla, K., Sirohi, A., Kumar, S., Chand, P. and Singh, P. K. (2016). RNA Interference Technology — Applications and Limitations, in *RNA Interference*. New Delhi, India, InTech.
- Singh, P., Pal, S. K., Alex, A. and Agarwal, N. (2015). Development of PROSTVAC immunotherapy in prostate cancer. *Future oncology*, 11(15), pp. 2137–2148.
- Sinibaldi, V. J., Carducci, M. A., Moore-Cooper, S., Laufer, M., Zahurak, M. and Eisenberger, M. A. (2002). Phase II evaluation of docetaxel plus one-day oral estramustine phosphate in the treatment of patients with androgen independent prostate carcinoma. *Cancer*, 94(5), pp. 1457–1465.
- Sinnott, J. A., Rider, J. R., Carlsson, J., Gerke, T., Tyekucheva, S., Penney, K. L., Sesso, H. D., Loda, M., Fall, K., Stampfer, M. J., Mucci, L. A., Pawitan, Y., Andersson, S.-O. and Andren, O. (2015). Molecular differences in transition zone and peripheral zone prostate tumors. *Carcinogenesis*, 36(6), pp. 632–638.
- Sioud, M. (2007). Main Approaches to Target Discovery and Validation, in *Target Discovery and Validation Reviews and Protocols*, New Jersey, Humana Press, pp. 1–12.
- Skinder, D., Zacharia, I., Studin, J. and Covino, J. (2016). Benign prostatic hyperplasia. *Journal of the American Academy of Physician Assistants*, 29(8), pp. 19–23.
- Skowronek, J. (2013). Low-dose-rate or high-dose-rate brachytherapy in treatment of prostate cancer - between options. *Journal of contemporary brachytherapy*, 5(1), pp. 33–41.

Sledz, C. A. and Williams, B. R. G. (2005). RNA interference in biology and disease. *Blood*, 106(3), pp. 787–794.

Śledzińska, A., Menger, L., Bergerhoff, K., Peggs, K. S. and Quezada, S. A. (2015). Negative immune checkpoints on T lymphocytes and their relevance to cancer immunotherapy. *Molecular Oncology*, 9(10), pp. 1936–1965.

Smith, D. C., Esper, P., Strawderman, M., Redman, B. and Pienta, K. J. (1999). Phase II Trial of Oral Estramustine, Oral Etoposide, and Intravenous Paclitaxel in Hormone-Refractory Prostate Cancer. *Journal of Clinical Oncology*, 17(6), pp. 1664–1664.

Smith, D. C., Smith, M. R., Sweeney, C., Elfiky, A. A., Logothetis, C., Corn, P. G., Vogelzang, N. J., Small, E. J., Harzstark, A. L., Gordon, M. S., Vaishampayan, U. N., Haas, N. B., Spira, A. I., Lara, P. N., Lin, C.-C., Srinivas, S., Sella, A., Schöffski, P., Scheffold, C., Weitzman, A. L. and Hussain, M. (2013). Cabozantinib in patients with advanced prostate cancer: results of a phase II randomized discontinuation trial. *Journal of clinical oncology : official journal of the American Society of Clinical Oncology*, 31(4), pp. 412–419.

Smith, M., De Bono, J., Sternberg, C., Le Moulec, S., Oudard, S., De Giorgi, U., Krainer, M., Bergman, A., Hoelzer, W., De Wit, R., Bögemann, M., Saad, F., Cruciani, G., Thierry-Vuillemin, A., Feyerabend, S., Miller, K., Houédé, N., Hussain, S., Lam, E., Polikoff, J., Stenzl, A., Mainwaring, P., Ramies, D., Hessel, C., Weitzman, A. and Fizazi, K. (2016). Phase III Study of Cabozantinib in Previously Treated Metastatic Castration-Resistant Prostate Cancer: COMET-1. *Journal of clinical oncology : official journal of the American Society of Clinical Oncology*, 34(25), pp. 3005–3013.

Smith, M. R., Antonarakis, E. S., Ryan, C. J., Berry, W. R., Shore, N. D., Liu, G., Alumkal, J. J., Higano, C. S., Chow Maneval, E., Bandekar, R., de Boer, C. J., Yu, M. K. and Rathkopf, D. E. (2016). Phase 2 Study of the Safety and Antitumor Activity of Apalutamide (ARN-509), a Potent Androgen Receptor Antagonist, in the High-risk Nonmetastatic Castration-resistant Prostate Cancer Cohort. *European Urology*, 70(6), pp. 963–970.

Smith, M. R., Sweeney, C. J., Corn, P. G., Rathkopf, D. E., Smith, D. C., Hussain, M., George, D. J., Higano, C. S., Harzstark, A. L., Sartor, A. O., Vogelzang, N. J., Gordon, M. S., de Bono, J. S., Haas, N. B., Logothetis, C. J., Elfiky, A., Scheffold, C., Laird, A. D., Schimmoller, F., Basch, E. M. and Scher, H. I. (2014). Cabozantinib in Chemotherapy-Pretreated Metastatic Castration-Resistant Prostate Cancer: Results of a Phase II Nonrandomized Expansion Study. *Journal of Clinical Oncology*, 32(30), pp. 3391–3399.

Sohm, B., Sissler, M., Park, H., King, M. P. and Florentz, C. (2004). Recognition of Human Mitochondrial tRNA^{Leu(UUR)} by its Cognate Leucyl-tRNA Synthetase. *Journal of Molecular Biology*, 339(1), pp. 17–29.

Soliman, G. A. (2013). The role of mechanistic target of rapamycin (mTOR) complexes signaling in the immune responses. *Nutrients*, 5(6), pp. 2231–57.

Soloway, M. S. (1988). Efficacy of buserelin in advanced prostate cancer and comparison with historical controls. *American journal of clinical oncology*, 11 Suppl 1, pp. S29-S32.

Sonpavde, G., Bhor, M., Hennessy, D., Bhowmik, D., Shen, L., Nicacio, L., Rembert, D., Yap, M. and Schnadig, I. (2015). Sequencing of Cabazitaxel and Abiraterone Acetate After Docetaxel in Metastatic Castration-Resistant Prostate Cancer: Treatment Patterns and Clinical Outcomes in Multicenter Community-Based US Oncology Practices. *Clinical Genitourinary Cancer*, 13(4), pp. 309–318.

Sountoulides, P., Koletsas, N., Kikidakis, D., Paschalidis, K. and Sofikitis, N. (2010). Secondary malignancies following radiotherapy for prostate cancer. *Therapeutic advances in urology*, 2(3), pp. 119–25.

Stacey, D. W. and Hitomi, M. (2008). Cell cycle studies based upon quantitative image analysis. *Cytometry. Part A*, 73(4), pp. 270–278.

Stein, M. E., Boehmer, D. and Kuten, A. (2007). Radiation Therapy in Prostate Cancer, in *Prostate Cancer*. Berlin, Heidelberg: Springer Berlin Heidelberg, pp. 179–199.

Stephan, C., Rittenhouse, H., Hu, X., Cammann, H. and Jung, K. (2014). Prostate-Specific Antigen (PSA) Screening and New Biomarkers for Prostate Cancer (PCa). *EJIFCC*, 25(1), pp. 55–78.

Sternberg, C., Armstrong, A., Pili, R., Ng, S., Huddart, R., Agarwal, N., Khvorostenko, D., Lyulko, O., Brize, A., Vogelzang, N., Delva, R., Harza, M., Thanos, A., James, N., Werbrouck, P., Bögemann, M., Hutson, T., Milecki, P., Chowdhury, S., Gallardo, E., Schwartzmann, G., Pouget, J.-C., Baton, F., Nederman, T., Tuvesson, H. and Carducci, M. (2016). Randomized, Double-Blind, Placebo-Controlled Phase III Study of Tasquinimod in Men With Metastatic Castration-Resistant Prostate Cancer. *Journal of clinical oncology : official journal of the American Society of Clinical Oncology*, 34(22), pp. 2636–43.

Sternberg, C. N. (2012). Novel hormonal therapy for castration-resistant prostate cancer. *Annals of Oncology*, 23(suppl 10), pp. x259–x263.

Stone, K. R., Mickey, D. D., Wunderli, H., Mickey, G. H. and Paulson, D. F. (1978). Isolation of a human prostate carcinoma cell line (DU 145). *International Journal of Cancer*, 21(3), pp. 274–281.

Storz, P. (2005) ‘Reactive oxygen species in tumor progression. *Frontiers in bioscience : a journal and virtual library*, 10, pp. 1881–1896.

Strief, D. M. (2007). An Overview of Prostate Cancer: Diagnosis and Treatment. *UROLOGIC NURSING*, 27(6), pp. 475–479.

Stubbe, J. and Kozarich, J. W. (1987). Mechanisms of bleomycin-induced DNA degradation. *Chemical Reviews*, 87(5), pp. 1107–1136.

Studer, U. E., Whelan, P., Albrecht, W., Casselman, J., de Reijke, T., Hauri, D., Loidl, W., Isorna, S., Sundaram, S. K., Debois, M. and Collette, L. (2006). Immediate or Deferred Androgen Deprivation for Patients With Prostate Cancer Not Suitable for Local Treatment With Curative Intent: European Organisation for Research and Treatment of Cancer (EORTC) Trial 30891. *Journal of Clinical Oncology*, 24(12), pp. 1868–1876.

Su, W.-H., Mruk, D. D., Wong, E. W. P., Lui, W.-Y. and Cheng, C. Y. (2012). Polarity protein complex Scribble/Lgl/Dlg and epithelial cell barriers. *Advances in experimental medicine and biology*, 763, pp. 149–170.

Su, Z., Yang, Z., Xu, Y., Chen, Y. and Yu, Q. (2015). Apoptosis, autophagy, necroptosis, and cancer metastasis. *Molecular cancer*, 14, 48.

Sun, X., Frierson, H. F., Chen, C., Li, C., Ran, Q., Otto, K. B., Cantarel, B. M., Vessella, R. L., Gao, A. C., Petros, J., Miura, Y., Simons, J. W., Dong, J.-T. and Dong, J.-T. (2005). Frequent somatic mutations of the transcription factor ATBF1 in human prostate cancer. *Nature Genetics*, 37(4), pp. 407–412.

Sun, Y. and Peng, Z.-L. (2009). Programmed cell death and cancer. *Postgraduate Medical Journal*, 85(1001), pp. 134–140.

Sundar, S. and Dickinson, P. D. (2012). Spironolactone, a possible selective androgen receptor modulator, should be used with caution in patients with metastatic carcinoma of the prostate. *BMJ Case Reports*, 2012.

Sundararajan, S. and Vogelzang, N. (2014). Chemotherapy in the Treatment of Prostate Cancer -- The Past, the Present, and the Future. *American Journal of Hematology / Oncology*, 10(6).

Suzuki, H., Nagai, K., Yamaki, H., Tanaka, N. and Umezawa, H. (1969). On the mechanism of action of bleomycin: scission of DNA strands in vitro and in vivo. *The Journal of antibiotics*, 22(9), pp. 446–448.

- Suzuki, H., Okihara, K., Miyake, H., Fujisawa, M., Miyoshi, S., Matsumoto, T., Fujii, M., Takihana, Y., Usui, T., Matsuda, T., Ozono, S., Kumon, H., Ichikawa, T., Miki, T. and Nonsteroidal Antiandrogen Sequential Alternation for Prostate Cancer Study Group (2008). Alternative Nonsteroidal Antiandrogen Therapy for Advanced Prostate Cancer That Relapsed After Initial Maximum Androgen Blockade. *The Journal of Urology*, 180(3), pp. 921–927.
- Suzuki, Y., Kondo, Y., Himeno, S., Nemoto, K., Akimoto, M. and Imura, N. (2000). Role of antioxidant systems in human androgen-independent prostate cancer cells. *The Prostate*, 43(2), pp. 144–149.
- Sweeney, C. J., Chen, Y.-H., Carducci, M., Liu, G., Jarrard, D. F., Eisenberger, M., Wong, Y.-N., Hahn, N., Kohli, M., Cooney, M. M., Dreicer, R., Vogelzang, N. J., Picus, J., Shevrin, D., Hussain, M., Garcia, J. A. and DiPaola, R. S. (2015). Chemohormonal Therapy in Metastatic Hormone-Sensitive Prostate Cancer. *New England Journal of Medicine*, 373(8), pp. 737–746.
- Swinnen, J. V., Heemers, H., de Sande, T. Van, Schrijver, E. De, Brusselmans, K., Heyns, W. and Verhoeven, G. (2004). Androgens, lipogenesis and prostate cancer. *The Journal of Steroid Biochemistry and Molecular Biology*, 92(4), pp. 273–279.
- Swinnen, J. V., Esquenet, M., Goossens, K., Heyns, W. and Verhoeven, G. (1997). Androgens stimulate fatty acid synthase in the human prostate cancer cell line LNCaP. *Cancer research*, 57(6), pp. 1086–1090.
- Swinnen, J. V., Ulixir, W., Heyns, W. and Verhoeven, G. (1997). Coordinate regulation of lipogenic gene expression by androgens: evidence for a cascade mechanism involving sterol regulatory element binding proteins. *Proceedings of the National Academy of Sciences of the United States of America*, 94(24), pp. 12975–12980.
- Swinnen, J. V. and Verhoeven, G. (1998). Androgens and the control of lipid metabolism in human prostate cancer cells. *The Journal of Steroid Biochemistry and Molecular Biology*, 65(1–6), pp. 191–198.
- Tafani, M., Sansone, L., Limana, F., Arcangeli, T., De Santis, E., Polese, M., Fini, M. and Russo, M. A. (2016). The Interplay of Reactive Oxygen Species, Hypoxia, Inflammation, and Sirtuins in Cancer Initiation and Progression. *Oxidative Medicine and Cellular Longevity*, 2016, pp. 1–18.
- Tait, S. W. G., Ichim, G. and Green, D. R. (2014). Die another way--non-apoptotic mechanisms of cell death. *Journal of cell science*, 127(Pt 10), pp. 2135–2144.
- Takashi, M., Zhu, Y., Nakano, Y., Miyake, K. and Kato, K. (1992). Elevated levels of serum aldolase A in patients with renal cell carcinoma. *Urological research*, 20(4), pp. 307–311.
- Tannock, I. F., de Wit, R., Berry, W. R., Horti, J., Pluzanska, A., Chi, K. N., Oudard, S., Théodore, C., James, N. D., Turesson, I., Rosenthal, M. A. and Eisenberger, M. A. (2004). Docetaxel plus Prednisone or Mitoxantrone plus Prednisone for Advanced Prostate Cancer. *New England Journal of Medicine*, 351(15), pp. 1502–1512.
- Tannock, I. F., Osoba, D., Stockler, M. R., Ernst, D. S., Neville, A. J., Moore, M. J., Armitage, G. R., Wilson, J. J., Venner, P. M., Coppin, C. M. and Murphy, K. C. (1996). Chemotherapy with mitoxantrone plus prednisone or prednisone alone for symptomatic hormone-resistant prostate cancer: a Canadian randomized trial with palliative end points. *Journal of Clinical Oncology*, 14(6), pp. 1756–1764.
- Tatebe, S., Sinicrope, F. A. and Tien Kuo, M. (2002). Induction of Multidrug Resistance Proteins MRP1 and MRP3 and γ -Glutamylcysteine Synthetase Gene Expression by Nonsteroidal Anti-inflammatory Drugs in Human Colon Cancer Cells. *Biochemical and Biophysical Research Communications*, 290(5), pp. 1427–1433.

- Taylor, B. S., Schultz, N., Hieronymus, H., Gopalan, A., Xiao, Y., Carver, B. S., Arora, V. K., Kaushik, P., Cerami, E., Reva, B., Antipin, Y., Mitsiades, N., Landers, T., Dolgalev, I., Major, J. E., Wilson, M., Socci, N. D., Lash, A. E., Heguy, A., Eastham, J. A., Scher, H. I., Reuter, V. E., Scardino, P. T., Sander, C., Sawyers, C. L. and Gerald, W. L. (2010). Integrative Genomic Profiling of Human Prostate Cancer. *Cancer Cell*, 18(1), pp. 11–22.
- Templeton, A. J., Dutoit, V., Cathomas, R., Rothermundt, C., Bärtschi, D., Dröge, C., Gautschi, O., Borner, M., Fechter, E., Stenner, F., Winterhalder, R., Müller, B., Schiess, R., Wild, P. J., Rüschoff, J. H., Thalmann, G., Dietrich, P.-Y., Aebbersold, R., Klingbiel, D. and Gillessen, S. (2013). Phase 2 Trial of Single-agent Everolimus in Chemotherapy-naive Patients with Castration-resistant Prostate Cancer (SAKK 08/08). *European Urology*, 64(1), pp. 150–158.
- Teng, B. P., Heffler, M. D., Lai, E. C., Zhao, Y.-L., LeVea, C. M., Golubovskaya, V. M. and Bullarddunn, K. M. (2011). Inhibition of hyaluronan synthase-3 decreases subcutaneous colon cancer growth by increasing apoptosis. *Anti-cancer agents in medicinal chemistry*, 11(7), pp. 620–628.
- Teng, L., Nakada, M., Zhao, S.-G., Endo, Y., Furuyama, N., Nambu, E., Pyko, I. V., Hayashi, Y. and Hamada, J.-I. (2011). Silencing of ferrochelatase enhances 5-aminolevulinic acid-based fluorescence and photodynamic therapy efficacy. *British Journal of Cancer*, 104(5), pp. 798–807.
- Terakawa, N., Shimizu, I., Tanizawa, O. and Matsumoto, K. (1988). RU486, a progestin antagonist, binds to progesterone receptors in a human endometrial cancer cell line and reverses the growth inhibition by progestins. *Journal of steroid biochemistry*, 31(2), pp. 161–166.
- Thellenberg-Karlsson, C., Nyman, C., Nilsson, S., Blom, R., Márquez, M., Castellanos, E. and Holmberg, A. R. (2016). Bone-targeted Novel Cytotoxic Polybisphosphonate Conjugate in Castration-resistant Prostate Cancer: A Multicenter Phase 1 Study. *Anticancer research*, 36(12), pp. 6499–6504.
- Thompson, C. B. (2011). Rethinking the Regulation of Cellular Metabolism. *Cold Spring Harbor Symposia on Quantitative Biology*, 76(0), pp. 23–29.
- Thompson, D., Easton, D. and Breast Cancer Linkage Consortium (2001). Variation in Cancer Risks, by Mutation Position, in BRCA2 Mutation Carriers. *The American Journal of Human Genetics*, 68(2), pp. 410–419.
- Thompson, E. D., Enriquez, H. L., Fu, Y.-X. and Engelhard, V. H. (2010). Tumor masses support naive T cell infiltration, activation, and differentiation into effectors. *The Journal of experimental medicine*, 207(8), pp. 1791–804.
- Thompson, I. M., Ankerst, D. P., Chi, C., Goodman, P. J., Tangen, C. M., Lucia, M. S., Feng, Z., Parnes, H. L. and Coltman, C. A. (2006). Assessing Prostate Cancer Risk: Results from the Prostate Cancer Prevention Trial. *JNCI: Journal of the National Cancer Institute*, 98(8), pp. 529–534.
- Tinevez, J.-Y., Perry, N., Schindelin, J., Hoopes, G. M., Reynolds, G. D., Laplantine, E., Bednarek, S. Y., Shorte, S. L. and Eliceiri, K. W. (2017). TrackMate: An open and extensible platform for single-particle tracking. *Methods*, 115, pp. 80–90.
- Tobias, J. S., Monson, K., Gupta, N., MacDougall, H., Glaholm, J., Hutchison, I., Kadalayil, L., Hackshaw, A. and UK Head and Neck Cancer Trialists' Group (2010). Chemoradiotherapy for locally advanced head and neck cancer: 10-year follow-up of the UK Head and Neck (UKHAN1) trial. *The Lancet Oncology*, 11(1), pp. 66–74.
- Tolkach, Y. and Kristiansen, G. (2018). The Heterogeneity of Prostate Cancer: A Practical Approach. *Pathobiology : journal of immunopathology, molecular and cellular biology*, 85(1–2).

- Tomlins, S. A., Laxman, B., Varambally, S., Cao, X., Yu, J., Helgeson, B. E., Cao, Q., Prensner, J. R., Rubin, M. A., Shah, R. B., Mehra, R. and Chinnaiyan, A. M. (2008). Role of the TMPRSS2-ERG gene fusion in prostate cancer. *Neoplasia*, 10(2), pp. 177–188.
- Tomlins, S. A., Rhodes, D. R., Perner, S., Dhanasekaran, S. M., Mehra, R., Sun, X.-W., Varambally, S., Cao, X., Tchinda, J., Kuefer, R., Lee, C., Montie, J. E., Shah, R. B., Pienta, K. J., Rubin, M. A. and Chinnaiyan, A. M. (2005). Recurrent Fusion of TMPRSS2 and ETS Transcription Factor Genes in Prostate Cancer. *Science*, 310(5748), pp. 644–648.
- Tong, X. and Li, H. (2004). eNOS protects prostate cancer cells from TRAIL-induced apoptosis. *Cancer Letters*, 210(1), pp. 63–71.
- Tosoian, J. J. and Antonarakis, E. S. (2017). Molecular heterogeneity of localized prostate cancer: more different than alike. *Translational cancer research*, 6(Suppl 1), pp. S47–S50.
- Tosoian, J. J., Carter, H. B., Lopor, A. and Loeb, S. (2016). Active surveillance for prostate cancer: Current evidence and contemporary state of practice. *Nature Reviews Urology*, 13(4), pp. 205–215.
- Trachootham, D., Lu, W., Ogasawara, M. A., Nilsa, R.-D. V. and Huang, P. (2008). Redox regulation of cell survival. *Antioxidants & redox signaling*, 10(8), pp. 1343–1374.
- Treloar, K. K. and Simpson, M. J. (2013). Sensitivity of edge detection methods for quantifying cell migration assays. *PloS one*, 8(6), e67389.
- Trivedi, C., Redman, B., Flaherty, L. E., Kucuk, O., Du, W., Heilbrun, L. K. and Hussain, M. (2000). Weekly 1-hour infusion of paclitaxel. Clinical feasibility and efficacy in patients with hormone-refractory prostate carcinoma. *Cancer*, 89(2), pp. 431–436.
- Tsao, C.-K., Cutting, E., Martin, J. and Oh, W. K. (2014). The role of cabazitaxel in the treatment of metastatic castration-resistant prostate cancer. *Therapeutic advances in urology*, 6(3), pp. 97–104.
- Tschudy, D. P., Ebert, P. S., Hess, R. A., Frykholm, B. C. and Atsmon, A. (1983). Growth inhibitory activity of succinylacetone: studies with Walker 256 carcinosarcoma, Novikoff hepatoma and L1210 leukemia. *Oncology*, 40(2), pp. 148–154.
- Tschudy, D. P., Elbert, P., Hess, R. A., Frekholm, B. and Weinbach, E. C. (1980). The effect of heme depletion on growth, protein synthesis, and respiration of murine erythroleukemia cells. *Biochem.Pharmac*, 29, pp. 1825–1831.
- Tsoumpra, M. K., Muniz, J. R., Barnett, B. L., Kwaasi, A. A., Pilka, E. S., Kavanagh, K. L., Evdokimov, A., Walter, R. L., Von Delft, F., Ebetino, F. H., Oppermann, U., Russell, R. G. G. and Dunford, J. E. (2015). The inhibition of human farnesyl pyrophosphate synthase by nitrogen-containing bisphosphonates. Elucidating the role of active site threonine 201 and tyrosine 204 residues using enzyme mutants. *Bone*, 81, pp. 478–486.
- Tsukita, S. and Yonemura, S. (1997). ERM (ezrin/radixin/moesin) family: from cytoskeleton to signal transduction. *Current opinion in cell biology*, 9(1), pp. 70–75.
- Tunn, U. W., Gruca, D. and Bacher, P. (2013). Six-month leuprorelin acetate depot formulations in advanced prostate cancer: a clinical evaluation. *Clinical interventions in aging*, 8, pp. 457–464.
- Twum-Ampofo, J., Fu, D.-X., Passaniti, A., Hussain, A. and Siddiqui, M. M. (2016). Metabolic targets for potential prostate cancer therapeutics. *Current Opinion in Oncology*, 28(3), pp. 241–247.
- Uchida, S. (2013). Image processing and recognition for biological images. *Development, growth & differentiation*, 55(4), pp. 523–549.

Ulloa, F., González-Juncà, A., Meffre, D., Barrecheguren, P. J., Martínez-Mármol, R., Pazos, I., Olivé, N., Cotrufo, T., Seoane, J. and Soriano, E. (2015). Blockade of the SNARE Protein Syntaxin 1 Inhibits Glioblastoma Tumor Growth. *PLOS ONE*, 10(3), e0119707.

Urruticoechea, a, Alemany, R., Balart, J., Villanueva, a, Viñals, F. and Capellá, G. (2010). Recent advances in cancer therapy: an overview. *Current pharmaceutical design*, 16(1), pp. 3–10.

U.S. Food and Drug Administration (2017) *Drug Innovation - Novel Drug Approvals*. Center for Drug Evaluation and Research. Available at: <https://www.fda.gov/Drugs/DevelopmentApprovalProcess/DrugInnovation/ucm537040.htm> [Accessed: 15.04.2018].

Vahora, H., Khan, M. A., Alalami, U. and Hussain, A. (2016). The Potential Role of Nitric Oxide in Halting Cancer Progression Through Chemoprevention. *Journal of Cancer Prevention*, 21(1), pp. 1–12.

Vaishampayan, U. N. (2014). Development of cabozantinib for the treatment of prostate cancer. *Core evidence*, 9, pp. 61–67.

Vaishampayan, U., Shevrin, D., Stein, M., Heilbrun, L., Land, S., Stark, K., Li, J., Dickow, B., Heath, E., Smith, D. and Fontana, J. (2015). Phase II Trial of Carboplatin, Everolimus, and Prednisone in Metastatic Castration-resistant Prostate Cancer Pretreated With Docetaxel Chemotherapy: A Prostate Cancer Clinical Trial Consortium Study. *Urology*, 86(6), pp. 1206–1211.

Vakkila, J. and Lotze, M. T. (2004). Opinion: Inflammation and necrosis promote tumour growth. *Nature Reviews Immunology*, 4(8), pp. 641–648.

Valderrama, F., Thevapala, S. and Ridley, A. J. (2012). Radixin regulates cell migration and cell-cell adhesion through Rac1. *Journal of cell science*, 125(Pt 14), pp. 3310–3319.

Valvona, C. J., Fillmore, H. L., Nunn, P. B. and Pilkington, G. J. (2016). The Regulation and Function of Lactate Dehydrogenase A: Therapeutic Potential in Brain Tumor. *Brain Pathology*, 26(1), pp. 3–17.

Van de Sande, T., Roskams, T., Lerut, E., Joniau, S., Van Poppel, H., Verhoeven, G. and Swinnen, J. V. (2005). High-level expression of fatty acid synthase in human prostate cancer tissues is linked to activation and nuclear localization of Akt/PKB. *The Journal of Pathology*, 206(2), pp. 214–219.

Vander Heiden, M. G. (2011). Targeting cancer metabolism: a therapeutic window opens. *Nature reviews. Drug discovery*, 10(9), pp. 671–684.

Vander Heiden, M. G. (2013). Exploiting tumor metabolism: challenges for clinical translation. *Journal of Clinical Investigation*, 123(9), pp. 3648–3651.

Vander Heiden, M. G., Cantley, L. C. and Thompson, C. B. (2009). Understanding the Warburg Effect: The Metabolic Requirements of Cell Proliferation. *Science*, 324(5930), pp. 1029–1033.

Van Hook, K., Huang, T. and Alumkal, J. J. (2014). Orteronel for the treatment of prostate cancer. *Future oncology*, 10(5), pp. 803–811.

Vanhoefer, U., Cao, S., Harstrick, A., Seeber, S. and Rustum, Y. M. (1997). Comparative antitumor efficacy of docetaxel and paclitaxel in nude mice bearing human tumor xenografts that overexpress the multidrug resistance protein (MRP). *Annals of oncology: official journal of the European Society for Medical Oncology*, 8(12), pp. 1221–1228.

Vanlangenakker, N., Bertrand, M. J. M., Bogaert, P., Vandenabeele, P. and Vanden Berghe, T. (2011). TNF-induced necroptosis in L929 cells is tightly regulated by multiple TNFR1 complex I and II members. *Cell death & disease*, 2(11), e230.

Vargas, P. D., Furuyama, K., Sassa, S. and Shibahara, S. (2008). Hypoxia decreases the expression of the two enzymes responsible for producing linear and cyclic tetrapyrroles in the heme biosynthetic pathway. *FEBS Journal*, 275(23), pp. 5947–5959.

Vasilaki, A. T. and McMillan, D. C. (2011). Lipid Peroxidation, in *Encyclopedia of Cancer*. Berlin, Heidelberg: Springer Berlin Heidelberg, pp. 2054–2055.

Velasco, A. M., Gillis, K. A., Li, Y., Brown, E. L., Sadler, T. M., Achilleos, M., Greenberger, L. M., Frost, P., Bai, W. and Zhang, Y. (2004). Identification and Validation of Novel Androgen-Regulated Genes in Prostate Cancer. *Endocrinology*, 145(8), pp. 3913–3924.

Veldscholte, J., Ris-Stalpers, C., Kuiper, G. G., Jenster, G., Berrevoets, C., Claassen, E., van Rooij, H. C., Trapman, J., Brinkmann, A. O. and Mulder, E. (1990). A mutation in the ligand binding domain of the androgen receptor of human LNCaP cells affects steroid binding characteristics and response to anti-androgens. *Biochemical and biophysical research communications*, 173(2), pp. 534–540.

Vercammen, D., Beyaert, R., Denecker, G., Goossens, V., Van Loo, G., Declercq, W., Grooten, J., Fiers, W. and Vandenabeele, P. (1998). Inhibition of caspases increases the sensitivity of L929 cells to necrosis mediated by tumor necrosis factor. *The Journal of experimental medicine*, 187(9), pp. 1477–1485.

Verze, P., Cai, T. and Lorenzetti, S. (2016). The role of the prostate in male fertility, health and disease. *Nature Reviews Urology*, 13(7), pp. 379–386.

Vinay, D. S., Ryan, E. P., Pawelec, G., Talib, W. H., Stagg, J., Elkord, E., Lichtor, T., Decker, W. K., Whelan, R. L., Kumara, H. M. C. S., Signori, E., Honoki, K., Georgakilas, A. G., Amin, A., Helferich, W. G., Boosani, C. S., Guha, G., Ciriolo, M. R., Chen, S., Mohammed, S. I., Azmi, A. S., Keith, W. N., Bilsland, A., Bhakta, D., Halicka, D., Fujii, H., Aquilano, K., Ashraf, S. S., Newsheem, S., Yang, X., Choi, B. K. and Kwon, B. S. (2015). Immune evasion in cancer: Mechanistic basis and therapeutic strategies. *Seminars in Cancer Biology*, 35, pp. S185–S198.

Vincent, F., Loria, P., Pregel, M., Stanton, R., Kitching, L., Nocka, K., Doyonnas, R., Steppan, C., Gilbert, A., Schroeter, T. and Peakman, M.-C. (2015). Developing predictive assays: The phenotypic screening “rule of 3”. *Science Translational Medicine*, 7(293).

Vogel, C. and Marcotte, E. M. (2012). Insights into the regulation of protein abundance from proteomic and transcriptomic analyses. *Nature reviews*, 13(4), pp. 227–232.

Vogelzang, N. J. (2017). Radium-223 dichloride for the treatment of castration-resistant prostate cancer with symptomatic bone metastases. *Expert Review of Clinical Pharmacology*, 10(8), pp. 809–819.

Volker, K. W. and Knull, H. r (1997). A glycolytic enzyme binding domain on tubulin. *Archives of biochemistry and biophysics*, 338(2), pp. 237–243.

Wagenlehner, F., Pilatz, A., Linn, T., Diemer, T., Schuppe, H. C., Schagdarsurengin, U., Hossain, H., Meinhardt, A., Ellem, S., Risbridger, G. and Weidner, W. (2013). Prostatitis and andrological implications. *Minerva urologica e nefrologica = The Italian journal of urology and nephrology*, 65(2), pp. 117–123.

Waldmann, T. (2003). ABCs of radioisotopes used for radioimmunotherapy: alpha- and beta-emitters. *Leukemia & lymphoma*, 44 Suppl 3, pp. S107–113.

Wallach-Dayana, S. B., Izbicki, G., Cohen, P. Y., Gerstl-Golan, R., Fine, A. and Breuer, R. (2006). Bleomycin initiates apoptosis of lung epithelial cells by ROS but not by Fas/FasL pathway. *American Journal of Physiology-Lung Cellular and Molecular Physiology*, 290(4), pp. L790–L796.

Wallis, C. J. D. and Nam, R. K. (2015). Prostate Cancer Genetics: A Review. *EJIFCC*, 26(2), pp. 79–91.

- Wallis, C. J. D., Mahar, A. L., Choo, R., Herschorn, S., Kodama, R. T., Shah, P. S., Danjoux, C., Narod, S. A. and Nam, R. K. (2016). Second malignancies after radiotherapy for prostate cancer: systematic review and meta-analysis. *BMJ (Clinical research ed)*, 352, i851.
- Wallis, C. J. D., Saskin, R., Choo, R., Herschorn, S., Kodama, R. T., Satkunasivam, R., Shah, P. S., Danjoux, C. and Nam, R. K. (2016). Surgery Versus Radiotherapy for Clinically-localized Prostate Cancer: A Systematic Review and Meta-analysis. *European Urology*, 70(1), pp. 21–30.
- Walsh, P. C. (2000). Radical prostatectomy for localized prostate cancer provides durable cancer control with excellent quality of life: a structured debate. *The Journal of Urology*, 163(6), pp. 1802–1807.
- Walsh, P. C. and Siiteri, P. K. (1975). Suppression of plasma androgens by spironolactone in castrated men with carcinoma of the prostate. *The Journal of urology*, 114(2), pp. 254–256.
- Walunas, T. L., Lenschow, D. J., Bakker, C. Y., Linsley, P. S., Freeman, G. J., Green, J. M., Thompson, C. B. and Bluestone, J. A. (1994). CTLA-4 can function as a negative regulator of T cell activation. *Immunity*, 1(5), pp. 405–413.
- Wang, C., Ma, J., Zhang, N., Yang, Q., Jin, Y. and Wang, Y. (2015). The acetyl-CoA carboxylase enzyme: a target for cancer therapy?. *Expert Review of Anticancer Therapy*, 15(6), pp. 667–676.
- Wang, C., Rajput, S., Watabe, K., Liao, D.-F. and Cao, D. (2010). Acetyl-CoA carboxylase-a as a novel target for cancer therapy. *Frontiers in bioscience (Scholar edition)*, 2, pp. 515–526.
- Wang, C., Xu, C., Sun, M., Luo, D., Liao, D.-F. and Cao, D. (2009). Acetyl-CoA carboxylase-alpha inhibitor TOFA induces human cancer cell apoptosis. *Biochemical and biophysical research communications*, 385(3), pp. 302–306.
- Wang, E. S., Frankfurt, O., Orford, K. W., Bennett, M., Flinn, I. W., Maris, M. and Konopleva, M. (2015). Phase 1 Study of CB-839, a First-in-Class, Orally Administered Small Molecule Inhibitor of Glutaminase in Patients with Relapsed/Refractory Leukemia. *Blood*, 126(23).
- Wang, J., Xiao, Q., Chen, X., Tong, S., Sun, J., Lv, R., Wang, S., Gou, Y., Tan, L., Xu, J., Fan, C. and Ding, G. (2018). LanCL1 protects prostate cancer cells from oxidative stress via suppression of JNK pathway. *Cell Death & Disease*, 9(2), 197.
- Wang, M. C., Papsidero, L. D., Kuriyama, M., Valenzuela, L. A., Murphy, G. P. and Chu, T. M. (1981). Prostate antigen: a new potential marker for prostatic cancer. *The Prostate*, 2(1), pp. 89–96.
- Wang, Q., Hardie, R.-A., Balaban, S., Schreuder, M., Hoy, A., van Geldermalsen, M., Fazli, L., Nagarajah, R., Bailey, C., Rasko, J. and Holst, J. (2014). Inhibition of glutamine uptake regulates mTORC1, glutamine metabolism and cell growth in prostate cancer. *Cancer & Metabolism*, 2(Suppl 1), P27.
- Wang, Q., Hardie, R.-A., Hoy, A. J., van Geldermalsen, M., Gao, D., Fazli, L., Sadowski, M. C., Balaban, S., Schreuder, M., Nagarajah, R., Wong, J. J.-L., Metierre, C., Pinello, N., Otte, N. J., Lehman, M. L., Gleave, M., Nelson, C. C., Bailey, C. G., Ritchie, W., Rasko, J. E. J. and Holst, J. (2015). Targeting ASCT2-mediated glutamine uptake blocks prostate cancer growth and tumour development. *The Journal of pathology*, 236(3), pp. 278–289.
- Wang, Q., Tiffen, J., Bailey, C. G., Lehman, M. L., Ritchie, W., Fazli, L., Metierre, C., Feng, Y. (Julie), Li, E., Gleave, M., Buchanan, G., Nelson, C. C., Rasko, J. E. J. and Holst, J. (2013). Targeting Amino Acid Transport in Metastatic Castration-Resistant Prostate Cancer: Effects on Cell Cycle, Cell Growth, and Tumor Development. *JNCI: Journal of the National Cancer Institute*, 105(19), pp. 1463–1473.
- Wang, S. I., Parsons, R. and Ittmann, M. (1998). Homozygous deletion of the PTEN tumor suppressor gene in a subset of prostate adenocarcinomas. *Clinical cancer research: an official journal of the American Association for Cancer Research*, 4(3), pp. 811–815.

Wang, Y., Mikhailova, M., Bose, S., Pan, C.-X., White, R. W. deVere and Ghosh, P. M. (2008). Regulation of androgen receptor transcriptional activity by rapamycin in prostate cancer cell proliferation and survival. *Oncogene*, 27(56), pp. 7106–7117.

Warburg, O. (1956). On respiratory impairment in cancer cells. *Science (New York, N.Y.)*, 124(3215), pp. 269–270.

Ward, P. S. and Thompson, C. B. (2012). Metabolic reprogramming: a cancer hallmark even warburg did not anticipate. *Cancer cell*. Elsevier, 21(3), pp. 297–308.

Wasserman, N. F., Aneas, I. and Nobrega, M. A. (2010). An 8q24 gene desert variant associated with prostate cancer risk confers differential in vivo activity to a MYC enhancer. *Genome research*, 20(9), pp. 1191–1197.

Watson, P. A., Chen, Y. F., Balbas, M. D., Wongvipat, J., Socci, N. D., Viale, A., Kim, K. and Sawyers, C. L. (2010). Constitutively active androgen receptor splice variants expressed in castration-resistant prostate cancer require full-length androgen receptor. *Proceedings of the National Academy of Sciences of the United States of America*, 107(39), pp. 16759–16765.

Wedge, D. C., Gundem, G., Mitchell, T., Woodcock, D. J., Martincorena, I., Ghori, M., Zamora, J., Butler, A., Whitaker, H., Kote-Jarai, Z., Alexandrov, L. B., Van Loo, P., Massie, C. E., Dentre, S., Warren, A. Y., Verrill, C., Berney, D. M., Dennis, N., Merson, S., Hawkins, S., Howat, W., Lu, Y.-J., Lambert, A., Kay, J., Kremeyer, B., Karaszi, K., Luxton, H., Camacho, N., Marsden, L., Edwards, S., Matthews, L., Bo, V., Leongamornlert, D., McLaren, S., Ng, A., Yu, Y., Zhang, H., Dadaev, T., Thomas, S., Easton, D. F., Ahmed, M., Bancroft, E., Fisher, C., Livni, N., Nicol, D., Tavaré, S., Gill, P., Greenman, C., Khoo, V., Van As, N., Kumar, P., Ogden, C., Cahill, D., Thompson, A., Mayer, E., Rowe, E., Dudderidge, T., Gnanapragasam, V., Shah, N. C., Raine, K., Jones, D., Menzies, A., Stebbings, L., Teague, J., Hazell, S., Corbishley, C., CAMCAP Study Group, J., de Bono, J., Attard, G., Isaacs, W., Visakorpi, T., Fraser, M., Boutros, P. C., Bristow, R. G., Workman, P., Sander, C., TCGA Consortium, A., Hamdy, F. C., Futreal, A., McDermott, U., Al-Lazikani, B., Lynch, A. G., Bova, G. S., Foster, C. S., Brewer, D. S., Neal, D. E., Cooper, C. S. and Eeles, R. A. (2018). Sequencing of prostate cancers identifies new cancer genes, routes of progression and drug targets. *Nature genetics*, 50(5), pp. 682–692.

Wei, X. X., Fong, L. and Small, E. J. (2015). Prostate Cancer Immunotherapy with Sipuleucel-T: Current Standards and Future Directions. *Expert Review of Vaccines*, 14(12), pp. 1529–1541.

Weinbach, E. C. and Ebert, P. S. (1985). Effects of succinylacetone on growth and respiration of L1210 leukemia cells. *Cancer letters*, 26(3), pp. 253–259.

Wernert, N., Lindstrot, A., Ellinger, J., Rogenhofer, S., Buettner, R., Perner, S. and Wernert, N. (2011). The peripheral zone of the prostate is more prone to tumor development than the transitional zone: Is the ETS family the key?. *Molecular Medicine Reports*, 5(2), pp. 313–316.

Wieman, H. L., Wofford, J. A. and Rathmell, J. C. (2007). Cytokine Stimulation Promotes Glucose Uptake via Phosphatidylinositol-3 Kinase/Akt Regulation of Glut1 Activity and Trafficking. *Molecular Biology of the Cell*, 18(4), pp. 1437–1446.

Wild, D., Frischknecht, M., Zhang, H., Morgenstern, A., Bruchertseifer, F., Boisclair, J., Provencher-Bolliger, A., Reubi, J.-C. and Maecke, H. R. (2011), Alpha- versus Beta-Particle Radiopeptide Therapy in a Human Prostate Cancer Model (213Bi-DOTA-PESIN and 213Bi-AMBA versus 177Lu-DOTA-PESIN). *Cancer Research*, 71(3), pp. 1009–1018.

Williams, J. F., Muenchen, H. J., Kamradt, J. M., Korenchuk, S. and Pienta, K. J. (2000). Treatment of Androgen-Independent Prostate Cancer Using Antimicrotubule Agents Docetaxel and Estramustine in Combination: An Experimental Study. *Prostate*, 44, pp. 275–278.

Williams, R. M. and Naz, R. K. (2010). Novel biomarkers and therapeutic targets for prostate cancer. *Frontiers in bioscience (Scholar edition)*, 2, pp. 677–684.

- Williams, S. D., Birch, R., Einhorn, L. H., Irwin, L., Greco, F. A. and Loehrer, P. J. (1987). Treatment of Disseminated Germ-Cell Tumors with Cisplatin, Bleomycin, and either Vinblastine or Etoposide. *New England Journal of Medicine*, 316(23), pp. 1435–1440.
- Wilson, R. C. and Doudna, J. A. (2013). Molecular Mechanisms of RNA Interference. *Annual Review of Biophysics*, 42(1), pp. 217–239.
- Wise, D. R. and Thompson, C. B. (2010). Glutamine addiction: a new therapeutic target in cancer. *Trends in biochemical sciences*, 35(8), pp. 427–433.
- Wittrup, A. and Lieberman, J. (2015). Knocking down disease: a progress report on siRNA therapeutics. *Nature Reviews Genetics*, 16(9), pp. 543–552.
- Woo, S., Kim, S. Y., Kim, S. H. and Cho, J. Y. (2016). Identification of Bone Metastasis With Routine Prostate MRI: A Study of Patients With Newly Diagnosed Prostate Cancer. *American Journal of Roentgenology*, 206(6), pp. 1156–1163.
- Woodson, K., Hayes, R., Wideroff, L., Villaruz, L. and Tangrea, J. (2003). Hypermethylation of GSTP1, CD44, and E-cadherin genes in prostate cancer among US Blacks and Whites. *The Prostate*, 55(3), pp. 199–205.
- Wright, M. E., Chang, S.-C., Schatzkin, A., Albanes, D., Kipnis, V., Mouw, T., Hurwitz, P., Hollenbeck, A. and Leitzmann, M. F. (2007). Prospective study of adiposity and weight change in relation to prostate cancer incidence and mortality. *Cancer*, 109(4), pp. 675–684.
- Wu, C.-K., Dailey, H. A., Rose, J. P., Burden, A., Sellers, V. M. and Wang, B.-C. (2001). The 2.0 Å structure of human ferrochelatase, the terminal enzyme of heme biosynthesis. *Nature Structural Biology*, 8(2), pp. 156–160.
- Wu, S., Yin, X., Fang, X., Zheng, J., Li, L., Liu, X. and Chu, L. (2015). c-MYC responds to glucose deprivation in a cell-type-dependent manner. *Cell Death Discovery*, 1(1), 15057.
- Wu, X., Daniels, G., Lee, P. and Monaco, M. E. (2014). Lipid metabolism in prostate cancer. *American journal of clinical and experimental urology*, 2(2), pp. 111–120.
- Xu, J., Neale, A. V., Dailey, R. K., Eggly, S. and Schwartz, K. L. (2012). Patient perspective on watchful waiting/active surveillance for localized prostate cancer. *Journal of the American Board of Family Medicine : JABFM*, 25(6), pp. 763–770.
- Xu, L. & Deng, X. (2006). Suppression of Cancer Cell Migration and Invasion by Protein Phosphatase 2A through Dephosphorylation of μ - and m-Calpains. *Journal of Biological Chemistry*, 281(46), pp.35567–35575.
- Yamamoto, T., Kudo, M., Peng, W.-X., Takata, H., Takakura, H., Teduka, K., Fujii, T., Mitamura, K., Taga, A., Uchida, E. and Naito, Z. (2016). Identification of aldolase A as a potential diagnostic biomarker for colorectal cancer based on proteomic analysis using formalin-fixed paraffin-embedded tissue. *Tumour biology : the journal of the International Society for Oncodevelopmental Biology and Medicine*, 37(10), pp. 13595–13606.
- Yang, R. M., Naitoh, J., Murphy, M., Wang, H. J., Phillipson, J., deKernion, J. B., Loda, M. and Reiter, R. E. (1998). Low p27 expression predicts poor disease-free survival in patients with prostate cancer. *The Journal of urology*, 159(3), pp. 941–945.
- Yang, W. S. and Stockwell, B. R. (2016). Ferroptosis: Death by Lipid Peroxidation. *Trends in cell biology*. Elsevier, 26(3), pp. 165–176.

- Yang, X., Palasuberniam, P., Kraus, D. and Chen, B. (2015). Aminolevulinic Acid-Based Tumor Detection and Therapy: Molecular Mechanisms and Strategies for Enhancement. *International Journal of Molecular Sciences*, 16(12), pp. 25865–25880.
- Yang, Y. A. and Yu, J. (2015). Current perspectives on FOXA1 regulation of androgen receptor signaling and prostate cancer. *Genes & diseases*, 2(2), pp. 144–151.
- Yao, D. C., Tolan, D. R., Murray, M. F., Harris, D. J., Darras, B. T., Geva, A. and Neufeld, E. J. (2004). Hemolytic anemia and severe rhabdomyolysis caused by compound heterozygous mutations of the gene for erythrocyte/muscle isozyme of aldolase, ALDOA(Arg303X/Cys338Tyr). *Blood*, 103(6), pp. 2401–2403.
- Ye, F., Chen, Y., Xia, L., Lian, J. and Yang, S. (2018). Aldolase A overexpression is associated with poor prognosis and promotes tumor progression by the epithelial-mesenchymal transition in colon cancer. *Biochemical and Biophysical Research Communications*, 497(2), pp. 639–645.
- Ye, J. and DeBose-Boyd, R. A. (2011). Regulation of cholesterol and fatty acid synthesis. *Cold Spring Harbor perspectives in biology*, 3(7).
- Yi, R., Chen, B., Duan, P., Zheng, C., Shen, H., Liu, Q., Yuan, C., Ou, W. and Zhou, Z. (2016). Sipuleucel-T and Androgen Receptor-Directed Therapy for Castration-Resistant Prostate Cancer: A Meta-Analysis. *Journal of immunology research*, 2016, 4543861.
- Yizhak, K., Le Dévédec, S. E., Rogkoti, V. M., Baenke, F., de Boer, V. C., Frezza, C., Schulze, A., van de Water, B. and Ruppin, E. (2014). A computational study of the Warburg effect identifies metabolic targets inhibiting cancer migration. *Molecular systems biology*, 10(8), 744.
- Yokoyama, A., Shao, N., Hoang, S., Yokoyama, N. N., Shao, S., Hoang, B. H., Mercola, D. and Zi, X. (2014). Wnt signaling in castration-resistant prostate cancer: implications for therapy. *American journal of clinical and experimental urology*, 2(1).
- Yoo, S., Choi, S. Y., You, D. and Kim, C.-S. (2016). New drugs in prostate cancer. *Prostate International*, 4(2), pp. 37–42.
- Yoshii, Y., Furukawa, T., Oyama, N., Hasegawa, Y., Kiyono, Y., Nishii, R., Waki, A., Tsuji, A. B., Sogawa, C., Wakizaka, H., Fukumura, T., Yoshii, H., Fujibayashi, Y., Lewis, J. S. and Saga, T. (2013). Fatty Acid Synthase Is a Key Target in Multiple Essential Tumor Functions of Prostate Cancer: Uptake of Radiolabeled Acetate as a Predictor of the Targeted Therapy Outcome. *PLoS ONE*, 8(5), e64570.
- Yoshizaki, K., Fujiki, T., Tsunematsu, T., Yamashita, M., Udono, M., Shirahata, S. and Katakura, Y. (2009). Pro-Senescent Effect of Hydrogen Peroxide on Cancer Cells and Its Possible Application to Tumor Suppression. *Biosci. Biotechnol. Biochem.*, 73(2), pp. 311–315.
- Young, S.-M., Bansal, P., Vella, E. T., Finelli, A., Levitt, C. and Loblaw, A. (2015). Systematic review of clinical features of suspected prostate cancer in primary care. *Canadian family physician Medecin de famille canadien*, 61(1), pp. e26-35.
- Yu, Z., Sun, J., Zhen, J., Zhang, Q. and Yang, Q. (2005). Thymidylate synthase predicts for clinical outcome in invasive breast cancer. *Histology and histopathology*, 20(3), pp. 871–878.
- Yue, S., Li, J., Lee, S.-Y., Lee, H. J., Shao, T., Song, B., Cheng, L., Masterson, T. A., Liu, X., Ratliff, T. L. and Cheng, J.-X. (2014). Cholesteryl Ester Accumulation Induced by PTEN Loss and PI3K/AKT Activation Underlies Human Prostate Cancer Aggressiveness. *Cell Metabolism*, 19(3), pp. 393–406.

- Zaak, D., Sroka, R., Stocker, S., Bise, K., Lein, M., Höppner, M., Frimberger, D., Schneede, P., Reich, O., Kriegmair, M., Knüchel, R., Baumgartner, R. and Hofstetter, A. (2004). Photodynamic Therapy of Prostate Cancer by Means of 5-Aminolevulinic Acid-Induced Protoporphyrin IX – In vivo Experiments on the Dunning Rat Tumor Model. *Urologia Internationalis*, 72(3), pp. 196–202.
- Zadra, G., Photopoulos, C. and Loda, M. (2013). The fat side of prostate cancer. *Biochimica et Biophysica Acta (BBA) - Molecular and Cell Biology of Lipids*, 1831(10), pp. 1518–1532.
- Zeigler-Johnson, C. M., Rennert, H., Mittal, R. D., Jalloh, M., Sachdeva, R., Malkowicz, S. B., Mandhani, A., Mittal, B., Gueye, S. M. and Rebbeck, T. R. (2008). Evaluation of prostate cancer characteristics in four populations worldwide. *The Canadian journal of urology*, 15(3), pp. 4056–4064.
- Zeng, Y. and Cullen, B. R. (2002). RNA interference in human cells is restricted to the cytoplasm. *RNA (New York, N.Y.)*, 8(7), pp. 855–860.
- Zhang, F., Lin, J.-D., Zuo, X.-Y., Zhuang, Y.-X., Hong, C.-Q., Zhang, G.-J., Cui, X.-J. and Cui, Y.-K. (2017). Elevated transcriptional levels of aldolase A (ALDOA) associates with cell cycle-related genes in patients with NSCLC and several solid tumors. *BioData Mining*, 10(1), 6.
- Zhang, L., Kang, L., Bond, W. and Zhang, N. (2009). Interaction Between Syntaxin 8 and HECTd3, a HECT Domain Ligase. *Cellular and Molecular Neurobiology*, 29(1), pp. 115–121.
- Zhang, S. and Gerhard, G. S. (2009). Heme mediates cytotoxicity from artemisinin and serves as a general anti-proliferation target. *PloS one*, 4(10), e7472.
- Zhao, Y., Butler, E. B. and Tan, M. (2013). Targeting cellular metabolism to improve cancer therapeutics. *Cell Death & Disease*, 4(3), e532.
- Zheng, J. (2012). Energy metabolism of cancer: Glycolysis versus oxidative phosphorylation (Review). *Oncology letters*, 4(6), pp. 1151–1157.
- Zhu, Y., Hon, T., Ye, W. and Zhang, L. (2002). Heme deficiency interferes with the Ras-mitogen-activated protein kinase signaling pathway and expression of a subset of neuronal genes. *Cell growth & differentiation : the molecular biology journal of the American Association for Cancer Research*, 13(9), pp. 431–439.
- Zhu, Y., Li, T., Ramos da Silva, S., Lee, J.-J., Lu, C., Eoh, H., Jung, J. U. and Gao, S.-J. (2017). A Critical Role of Glutamine and Asparagine γ -Nitrogen in Nucleotide Biosynthesis in Cancer Cells Hijacked by an Oncogenic Virus. *mBio*, 8(4), pp. e01179-17.
- Zinner, N. R., Bidair, M., Centeno, A. and Tomera, K. (2004). Similar frequency of testosterone surge after repeat injections of goserelin (Zoladex) 3.6 mg and 10.8 mg: Results of a randomized open-label trial. *Urology*, 64(6), pp. 1177–1181.

8 Appendix

Table 8.1 Summary of the targets identified in the siRNA screen to elevate PC3 proliferation.

Symbol (symbol in screen)	Gene Description	Pathways	Elevation of Relative Proliferation	P-value
CA12	Carbonic anhydrase 12	A member of zinc metalloenzymes that catalyse the reversible hydration of carbon dioxide.	88%	0.0112
ADCY1	Adenylate cyclase 1	Encodes a member of the of adenylate cyclase gene family that is primarily expressed in the brain.	88%	0.0338
CA3	Carbonic anhydrase 3	A member of a multigene family that encodes carbonic anhydrase isozymes.	89%	0.0335
STX16	Syntaxin 16	This gene encodes a member of the syntaxin or t-SNARE (target-SNAP receptor) protein family which present on cell membranes and serve as the targets for V-SNARES.	95%	0.0191
SYP	Synaptophysin	This gene encodes an integral membrane protein of small synaptic vesicles in brain and endocrine cells.	97%	0.0114
MOCS2	Molybdenum cofactor synthesis 2	A unique molybdenum cofactor (MoCo) consisting of a pterin, termed molybdopterin, and the catalytically active metal molybdenum.	100%	0.0116
HAS1	Hyaluronan synthase 1	Hyaluronan or hyaluronic acid (HA) is a high molecular weight unbranched polysaccharide and is a constituent of the extracellular matrix.	100%	0.0094
GALE	UDP-galactose-4-epimerase	Encodes UDP-galactose-4-epimerase which catalyses the epimerization of UDP-	103%	0.0289

		glucose to UDP-galactose, and the epimerization of UDP-N-acetylglucosamine to UDP-N-acetylgalactosamine.		
SYT7	Synaptotagmin 7	Encodes a protein similar to other family members that mediate calcium-dependent regulation of membrane trafficking in synaptic transmission.	103%	0.0188
HDC	Histidine decarboxylase	Encodes a member of the group II decarboxylase family and forms a homodimer that converts L-histidine to histamine.	105%	0.0104
SYNPR	Synaptoporin	Unknown.	105%	0.0070
CA5A	Carbonic anhydrase 5A	Encodes a member of zinc metalloenzymes that catalyse the reversible hydration of carbon dioxide.	108%	0.0112
BIN3	Bridging integrator 3	This gene encodes a member of the BAR domain protein family.	110%	0.0075
ACACB	Acetyl-CoA carboxylase beta	A member of ACC family which catalyse the carboxylation of acetyl-CoA to malonyl-CoA, the rate-limiting step in fatty acid synthesis.	112%	0.0253
ADCY6	Adenylate cyclase 6	This gene encodes a member of the adenylyl cyclase family of proteins, which catalyse the synthesis of cyclic AMP.	120%	0.0241
PROM1	Prominin 1	This gene encodes a protein which localises to membrane protrusions and is often expressed on adult stem cells to halt their differentiation.	123%	0.0228
CA2	Carbonic anhydrase 2	The encoded protein catalyses reversible hydration of carbon dioxide.	125%	0.0038

FKBP8	FK506 binding protein 8	The encoded protein is a member of the immunophilin protein family, which play a role in immunoregulation, protein folding, and trafficking.	129%	0.0009
SYT2	Synaptotagmin 2	The encoded protein is thought to function as a calcium sensor in vesicular trafficking and exocytosis.	134%	0.0030
ADCY3	Adenylate cyclase 3	The encoded protein catalyses the formation of the secondary messenger cyclic adenosine monophosphate (cAMP).	137%	0.0105
TXNDC5	Thioredoxin domain containing 5	This gene encodes one of the endoplasmic reticulum (ER) proteins that catalyse protein folding and thiol-disulfide interchange reactions.	138%	0.0067
SYT12	Synaptotagmin 12	This gene encodes a protein similar to other family members that mediate calcium-dependent regulation of membrane trafficking in synaptic transmission.	140%	0.0004
SYT10	Synaptotagmin 10	This gene encodes a protein similar to other family members that mediate calcium-dependent regulation of membrane trafficking in synaptic transmission.	143%	0.0004
PDXDC2	Pyridoxal dependent decarboxylase domain containing 2	Unknown.	148%	0.0017
SGPL1	Sphingosine-1-phosphate lyase 1	Unknown.	163%	0.0007
SYPL1	Synaptophysin like 1	Unknown.	217%	< 0.0001

Table 8.2 Summary of extra 37 targets identified in the siRNA screen to significantly reduce cell motility.

Symbol (symbol in screen)	Gene Description	Pathways	Inhibition/Elevation of Motility (%)
GUCY1B2	Guanylate cyclase 1 soluble subunit beta 2	Unknown.	49%
SRM	Spermidine synthase	Carries out the final step of spermidine biosynthesis.	48%
DYSF	Dysferlin	Implicated in muscle contraction and contains C2 domains that play a role in calcium-mediated membrane fusion events.	47%
FSD1L	Fibronectin type III and SPRY domain containing 1 like	Unknown.	46%
TXNDC11	Thioredoxin domain containing 11	Unknown.	46%
AMD1	Adenosylmethionine decarboxylase 1	Polyamine biosynthesis.	46%
TYMS	Thymidylate synthetase	Catalyzes methylation of deoxyuridylate to deoxythymidylate.	46%

SYT1	Synaptotagmin 1	A membrane protein of synaptic vesicles thought to act as Ca ²⁺ sensors in the process of vesicular trafficking and exocytosis.	45%
SDCBP	Syndecan binding protein	Linking syndecan-mediated signalling to the cytoskeleton.	44%
SYT4	Synaptotagmin 4	Unknown.	43%
CLN3	CLN3, battenin	Lysosomal function.	42%
HDC	histidine decarboxylase	Conversion of L-histidine to histamine in a pyridoxal phosphate dependent manner.	42%
FKBP6	FK506 binding protein 6	May be involved in immunoregulation and basic cellular processes involving protein folding and trafficking.	41%
GSS	Glutathione synthetase	Protection of cells from oxidative damage by free radicals, detoxification of xenobiotics, and membrane transport.	41%
TXNDC5	Thioredoxin domain containing 5	Protein folding and thiol-disulfide interchange reactions.	40%

ALDOB	Aldolase, fructose-bisphosphate B	Conversion of fructose-1,6-bisphosphate to glyceraldehyde 3-phosphate and dihydroxyacetone phosphate.	40%
HAS2	Hyaluronan synthase 2	Constitutes the extracellular matrix.	40%
FKBP1A	FK506 binding protein 1A	A member of the immunophilin protein family, which play a role in immunoregulation and basic cellular processes involving protein folding and trafficking.	40%
CA7	carbonic anhydrase 7	Reversible hydration of carbon dioxide.	40%
ECH1	enoyl-CoA hydratase 1	Functions in the auxiliary step of the fatty acid beta-oxidation pathway.	40%
SYT16	Synaptotagmin 16	Unknown.	38%
TMEM23	Sphingomyelin synthase 1 (SGMS1)	Predicted to be a five-pass transmembrane protein.	38%
SEC22B	SEC22 homolog B, vesicle trafficking protein (gene/pseudogene).	A vesicle trafficking protein.	37%

CA1	Carbonic anhydrase 1	Catalysation of the reversible hydration of carbon dioxide.	37%
STX5	Syntaxin 5	A member of membrane proteins that serve as the targets for v-SNAREs (vesicle-SNAP receptors), permitting specific synaptic vesicle docking and fusion.	37%
DDC	Dopa decarboxylase	Decarboxylation of L-3,4-dihydroxyphenylalanine (DOPA) to dopamine.	37%
SLC27A4	Solute carrier family 27 member 4	Fatty acid transport.	36%
STX12	Syntaxin 12	Unknown.	35%
MVD	Mevalonate diphosphate decarboxylase	Conversion of mevalonate pyrophosphate into isopentenyl pyrophosphate in cholesterol biosynthesis.	34%
STX6	Syntaxin 6	Unknown	33%
UROD	Uroporphyrinogen decarboxylase	Heme biosynthetic pathway.	32%

ACSM1	Acyl-CoA synthetase medium chain family member	Fatty acid biosynthesis.	32%
IDI1	Isopentenyl-diphosphate delta isomerase 1	Interconversion of isopentenyl diphosphate (IPP) to its highly electrophilic isomer, dimethylallyl diphosphate (DMAPP).	28%
ADCY9	Adenylate cyclase 9	Formation of cyclic AMP from ATP.	27%
SYT2	Synaptotagmin 2	A vesicle membrane and cell trafficking protein.	29%
SYT9	Synaptotagmin 9	A vesicle membrane and cell trafficking protein.	34%
SYPL1	Synaptophysin like 1	Unknown.	38%
